



**DESIGN AND CHARACTERIZATION OF A SPACE BASED
CHROMOTOMOGRAPHIC HYPERSPECTRAL
IMAGING EXPERIMENT**

THESIS

Jason D. Niederhauser, Captain, USAF

AFIT/GA/ENY/11-J02

**DEPARTMENT OF THE AIR FORCE
AIR UNIVERSITY**

AIR FORCE INSTITUTE OF TECHNOLOGY

Wright-Patterson Air Force Base, Ohio

APPROVED FOR PUBLIC RELEASE; DISTRIBUTION UNLIMITED

The views expressed in this thesis are those of the author and do not reflect the official policy or position of the United States Air Force, the Department of Defense, or the United States Government. This material is declared a work of the U.S. Government and is not subject to copyright protection in the United States.

AFIT/GA/ENY/11-J02

**DESIGN AND CHARACTERIZATION OF A SPACE BASED
CHROMOTOMOGRAPHIC HYPERSPECTRAL IMAGING EXPERIMENT**

THESIS

Presented to the Faculty

Department of Aeronautics and Astronautics

Graduate School of Engineering and Management

Air Force Institute of Technology

Air University

Air Education and Training Command

In Partial Fulfillment of the Requirements for the
Degree of Master of Science in Astronautical Engineering

Jason D. Niederhauser, BSME

Captain, USAF

June 2011

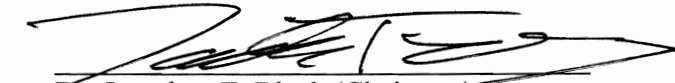
APPROVED FOR PUBLIC RELEASE; DISTRIBUTION UNLIMITED

**DESIGN AND CHARACTERIZATION OF A SPACE BASED
CHROMOTOMOGRAPHIC HYPERSPECTRAL IMAGING EXPERIMENT**

Jason D. Niederhauser, BSME

Captain, USAF

Approved:



Dr. Jonathan T. Black (Chairman)

1 Jun 11
Date



Michael R. Hawks, Lt Col, USAF (Member)

1 Jun 11
Date



Dr. Eric Swenson (Member)

1 June 11
Date

Abstract

This research focuses upon the design, analysis and characterization of several systems related to a space-based chromotomographic experiment (CTEx), a hyperspectral imager, currently in development at the Air Force Institute of Technology. Three interrelated subject-areas were developed.

The initial focal point was a generic, system-level mechanical layout and integration analysis of the space-based instrument. The scope of this work was intended to baseline the space-based system design in order to allow for further trade-space refinement and requirements development.

Second, development of an iteration upon the ground-based version of CTEx was accomplished in an effort to support higher-fidelity field data-collection. This effort encompassed both the engineering design process as well as a system-level characterization test series to validate the enhancements to deviation angle, image quality, and alignment characterization methodologies.

Finally, the third effort in this thesis related to the design, analysis, and characterization test campaign encompassing the space-based CTEx instrument computer unit (ICU). This activity produced an experimentally validated thermal mathematical model supporting further trade-space refinement and operational planning aspects for this device.

Results from all three of the above focus areas support the transition of this next-generation technology from the laboratory to a fully-realized, space-readied platform achieving intelligence preparation of the battlespace for the warfighter.

To My Father

Acknowledgments

First and foremost, I would like to express my humble appreciation to my faculty committee (Dr. Jonathan Black, Chairman; Lt Col Michael Hawks, Member; and Dr. Eric Swenson, Member) for their guidance and support throughout the course of this thesis effort. Thanks also go to the remaining CTEEx faculty and staff team, including: Dr. Brad Ayres, Dr. Richard Cobb, and Lt. Col. Carl Hartsfield. The experimental effort in this thesis could never have happened without the diehard dedication of the technician and support crew – to say I had a tremendous amount of help from these individuals is an understatement (as their support was absolutely critical). These unsung heroes include: Jay Anderson, Brian Crabtree, Chris Harkless, John Hixenbaugh, Jeremy Kaczmarek, Wilbur Lacy, Jan LeValley, Sean Miller, Barry Page, Mike Ranft, Dan Ryan, Greg Smith, and Chris Zickefoose. Additionally, the assembly, test and evaluation campaign could never have been successfully accomplished without the help of Aaron Dugger, Kimberly Gresham, Capt Mark Lesar, Peter Mage, and Capt Chad Su'e. All of your efforts are building toward another outstanding space mission for AFIT. Keep up the great work!

Finally, last but not least, is the gratitude I have toward my wife and family. You have carried me through these last several years with your love, encouragement and support – I am eternally in your debt for the opportunity to chase my dreams. Thank you.

Jason D. Niederhauser

Table of Contents

	Page
Abstract.....	iv
Table of Contents.....	vii
List of Figures.....	ix
List of Tables.....	xii
I. Introduction.....	1
1.1 <i>Motivation</i>	1
1.1.1. <i>Spectroscopy</i>	2
1.1.2. <i>Hyperspectral Imaging</i>	5
1.1.3. <i>CTEx</i>	7
1.2 <i>Research Objectives</i>	10
1.3 <i>Organization</i>	12
II. Background.....	15
2.1 <i>Literature Review</i>	15
2.1.1. <i>EO-1 (Hyperion)</i>	15
2.1.2. <i>TACSAT-3 (ARTEMIS)</i>	18
2.1.3. <i>HREP (HICO)</i>	21
2.2 <i>CTEx Background</i>	23
2.2.1. <i>Anthony J. Dearing (2004)</i>	27
2.2.2. <i>Kevin C. Gustke (2004)</i>	28
2.2.3. <i>Daniel A. LeMaster (2004)</i>	28
2.2.4. <i>Malcolm G. Gould (2005)</i>	29
2.2.5. <i>Randall L. Bostick (2008-2011)</i>	29
2.2.6. <i>Phillip Sheirich (2009)</i>	30
2.2.7. <i>Todd A. Book (2010)</i>	31
2.2.8. <i>Steven D. Miller (2010)</i>	32
2.2.9. <i>Arthur L. Morse (2010)</i>	32
2.2.10. <i>Daniel O'Dell (2010)</i>	33
2.2.11. <i>William J. Starr (2010)</i>	33
2.3 <i>International Space Station Experimental Platforms</i>	34
2.4 <i>Background Summary</i>	37
III. Space-Based CTEx Design.....	38
3.1 <i>Design Requirements</i>	38
3.2 <i>Design Concept Methodology</i>	41
3.3 <i>Results</i>	53
3.3.1. <i>Mass Properties</i>	53
3.3.2. <i>Breadboard Lightweighting</i>	58
3.4 <i>Space-Based CTEx Design Summary</i>	62

IV. Ground-Based CTE _x Design/Characterization.....	63
4.1 <i>Design Requirements</i>	63
4.2 <i>Design and Validation Methodology</i>	67
4.2.1. <i>Ground-Based CTE_x Design Development.</i>	67
4.2.2. <i>Validation Methodology.</i>	77
4.3 <i>Results</i>	84
4.3.1. <i>Deviation Angle Results.</i>	84
4.3.2. <i>Image Quality Results.</i>	88
4.3.3. <i>Alignment Characterization Results.</i>	90
4.4 <i>GCTE_x Revision Summary</i>	96
V. Space-Based CTE _x Instrument Computer Unit Design/Characterization	97
5.1 <i>Design Requirements</i>	97
5.2 <i>Thermal Modeling Methodology</i>	98
5.3 <i>Model Characterization Methodology Through Design and Test</i>	108
5.3.1. <i>Model Design Methodology.</i>	108
5.3.1. <i>Test Campaign Methodology.</i>	116
5.4 <i>Results</i>	121
5.4.1. <i>Modeling Expectations.</i>	121
5.4.2. <i>Test Campaign Outcome.</i>	127
5.4.3. <i>On-Orbit Predictions.</i>	137
5.5 <i>ICU Design Summary</i>	139
VI. Conclusions and Recommendations	140
6.1 <i>SCTE_x Design Conclusions</i>	140
6.2 <i>GCTE_x Design/Characterization Conclusions</i>	141
6.3 <i>SCTE_x ICU Design/Characterization Conclusions</i>	143
6.4 <i>Proposed Future Work</i>	145
6.5 <i>Final Conclusions</i>	149
Appendix A: MATLAB Analysis Code	150
Appendix A.1: Isogrid FEM Dat-file Rapid-Generation	150
Appendix A.2: GCTE _x Alignment Characterization.....	154
Appendix A.3: SCTE _x ICU Thermal Modeling Code.....	159
Appendix B: Mechanical Drawing Packages	162
Appendix C: Procedures	205
Bibliography	363
Vita.....	376

List of Figures

Figure 1.1: Electromagnetic Spectrum [4].....	3
Figure 1.2: Absorption and Emission Spectroscopy [4]	4
Figure 1.3: Refractive Dispersion [5]	5
Figure 1.4: Multispectral, Hyperspectral, and Ultraspectral Imaging Differences [5]	6
Figure 1.5: Representative Spectral Response from an Explosive Scene [9]	8
Figure 1.6: CTE _x Optical Layout [9].....	9
Figure 1.7: ISS Exposed Facilities (EF) (Credit: NASA) [12]	10
Figure 1.8: CTE _x Program Road Map.....	12
Figure 2.1: EO-1 (Credit: NASA) [14]	16
Figure 2.2: TacSat-3 (Credit: AFRL) [22].....	19
Figure 2.3: HREP JEM-EF ISS Configuration (Credit: NRL) [27].....	22
Figure 2.5: ISS External Research Facilities [38].....	34
Figure 2.6: CEF Configuration [38].....	35
Figure 2.7: JEM-EF Configuration [38]	36
Figure 3.1: Required Telescope Configuration with ExPA (Concept).....	41
Figure 3.2: Utilization of the ExPA Fastener Configuration	42
Figure 3.3: Utilization of the TCU/ICU as Strong-Back Members (Concept).....	44
Figure 3.4: TCU Configuration (Concept).....	45
Figure 3.5: Strong-Back Configuration (Concept)	46
Figure 3.6: RCOS Telescope Configuration.....	47
Figure 3.7: Ejection Release Configuration (Concept).....	48
Figure 3.8: Aperture Configuration (Concept)	49
Figure 3.9: Aperture Mechanism Operation (Notional Concept)	50
Figure 3.10: Isogrid Parameters.....	52
Figure 3.11: Space-Based CTE _x CG and Configuration	58
Figure 3.12: Isogrid Mesh Density Validation (Compared Against Test Data)	59
Figure 3.13: Typical Breadboard Isogrid Mode Shapes	60
Figure 4.1: GCTE _x , Newtonian Telescope Configuration	63
Figure 4.2: Original DVP (Dimensions in Millimeters) [6]	64
Figure 4.3: Updated DVP (Dimensions in Inches)	65
Figure 4.4: GCTE _x Section-View, Previous DVP Holder Design	68
Figure 4.5: GCTE _x Section-View, Updated DVP Holder Design.....	69
Figure 4.6: Updated GCTE _x Pin-into-Socket DVP Holder & Motor/Encoder	70
Figure 4.7: GCTE _x Linear System Concept.....	71
Figure 4.8: GCTE _x Section-View, L3 Interface Block	72
Figure 4.9: GCTE _x Section-View, L2 Interface Block	73
Figure 4.10: L2 Configuration	74
Figure 4.11: GCTE _x Linear System Structure.....	75
Figure 4.12: Portable Rack-Mounted Electronics Configured with Instrument	76
Figure 4.13: GCTE _x Linear Instrument Configured with Newtonian Telescope.....	77
Figure 4.14: Theoretical DVP Deviation Angle vs. Wavelength	78
Figure 4.15: Mercury Pen Lamp Source Configured with Pin-hole.....	79
Figure 4.16: Unilamp Source Configured with T-22 / USAF-1951 Target [50].....	80

Figure 4.17: Theoretical MTF for a Newtonian System (Notional)	81
Figure 4.18: GCTEx Aperture Cover Laser Characterization System	82
Figure 4.19: GCTEx Monochrometer Test Setup.....	83
Figure 4.20: Mercury Pen-Lamp Pin-hole Source, Instrument View	84
Figure 4.21: Convolved Mercury Pen-Lamp Captures for Instrument Configurations....	85
Figure 4.22: Newtonian System, Deviation Vs. Wavelength	86
Figure 4.23: “Misaligned” Newtonian System, Deviation Vs. Wavelength.....	87
Figure 4.24: Linear System, Deviation Vs. Wavelength	87
Figure 4.25: Image Quality Development	88
Figure 4.26: USAF-1951/T22 Target, Raw Data.....	89
Figure 4.27: MTF Comparison, Newtonian Vs. Linear Systems	89
Figure 4.28: Alignment Characterization, Image Construction.....	91
Figure 4.29: Alignment Characterization, Circle Data Determination	92
Figure 4.30: “Pinwheel” Offset.....	93
Figure 4.31: Alignment, Deviation Vs. Wavelength (Uncorrected).....	94
Figure 4.32: Alignment Characterization, Deviation Vs. Wavelength (Corrected)	95
Figure 5.1: Heat Transfer Control Volume Concept	98
Figure 5.2: ICU Lumped Capacitance Thermal Circuit Model	100
Figure 5.3: Earth View Factor Geometry Parameters.....	103
Figure 5.4 Heat Sink Geometrical Parameters.....	105
Figure 5.5 Space-Based CTE _x Instrument Layout	109
Figure 5.6: ICU Thermal Dissipation, Surface Temp vs Input (Generation)	110
Figure 5.7: ICU PC/104 Card Cage Configuration.....	111
Figure 5.8: ICU Convective-Flow Fan Assembly	112
Figure 5.9: ICU Electrical Feedthrough.....	113
Figure 5.10: Swagelok SS-4BW Purge/Fill Hand Valve.....	114
Figure 5.11: ICU O-Ring Gasket Face-Seal	115
Figure 5.12: ICU Housing and Final Assembly.....	116
Figure 5.13 ICU Leak-Check, Process and Identification Diagram	117
Figure 5.14: ICU Purge & Fill, Process and Identification Diagram.....	118
Figure 5.15: TVAC Special Test Equipment Configuration, Block Diagram	121
Figure 5.16: ICU MATLAB Simulink ® mathematical model.....	122
Figure 5.17: ICU Thermal Trending, TVAC Simulation (13W, -40C, $\epsilon = 0.09$).....	123
Figure 5.18: ICU FEM, Max Displacement (in), Internal Pressure Load Case, 35 psia	126
Figure 5.19: ICU FEM, Max Displacement (in), Ext Pressure Case, 14.7 psia	127
Figure 5.20: Parvus Card Cage Reconfiguration	128
Figure 5.21: ICU Assembly	129
Figure 5.22: SCTEx ICU, 0.25g Sine-Sweep, X-Axis	130
Figure 5.23: SCTEx ICU, 0.25g Sine-Sweep, Y-Axis	131
Figure 5.24: SCTEx ICU, 0.25g Sine-Sweep, Z-Axis.....	131
Figure 5.25: SCTEx ICU Temperature Profile, Measured Vs. Simulated, 13W/-40C...	133
Figure 5.26: SCTEx ICU Error Profile, Measured Vs. Simulated, 13W/-40C.....	134
Figure 5.27: SCTEx ICU Temperature Profile, Measured Vs. Simulated, 13W/20C	135
Figure 5.28: SCTEx ICU Error Profile, Measured Vs. Simulated, 13W/20C	135
Figure 5.29: SCTEx ICU Temperature Profile, Measured Vs. Simulated, 27W/20C	136

Figure 5.30: SCTEx ICU Error Profile, Measured Vs. Simulated, 27W/20C	137
Figure 5.31: SCTEx ICU, Simulated On-Orbit Behavior (13W, Emissivity=.91)	138
Figure 5.32: SCTEx ICU, Simulated On-Orbit Behavior (25W, Emissivity=.91)	139
Figure 6.1: GCTEx Linear System	142
Figure 6.2: SCTEx ICU, Housing Apart (Left) and Assembled (Right)	144

List of Tables

Table 2.1: Effects of Error (“X”: Effect Observed; “-“: Effect Not Observed) [31]	30
Table 3.3: JEM vs. ExPA, Generic Mechanical Differences [38]	39
Table 3.4: Structure / Strong-Back Mass	54
Table 3.5: RCOS Telescope Mass	55
Table 3.6: TCU & ICU Mass	56
Table 3.7: Miscellaneous Subsystem Mass	57
Table 3.8: Optical Breadboard Isogrid Process Results.....	61
Table 4.9: GCTEEx Linear System Curve-Fit Parameters (from corrected data)	95
Table 5.10: ICU Mathematical Model, Thermal Behavior Predictions.....	124

DESIGN AND CHARACTERIZATION OF A SPACE BASED CHROMOTOMOGRAPHIC HYPERSPECTRAL IMAGING EXPERIMENT

I. Introduction

This thesis presents an engineering analysis for systems related to the space-based chromotomographic experiment (CTEx) led by the Air Force Institute of Technology (AFIT). The overall program is broken into three overlapping experimental phases: laboratory, ground, and space. The intent behind the phased approach relates to mitigating technology risk prior to space-flight operations. The program is currently in the ground-based experimental phase and deemed a Technology Readiness Level (TRL) of three. The TRL will increase to six upon successful completion of the space-based experimental phase.

The objectives of this thesis research are threefold and focus primarily on the ground- and space-based phases of the program. The three specific research areas include: development of the space-based experiment mechanical layout, designing/characterizing a linear revision to the ground-based experiment, and designing/characterizing the Instrument Computer Unit (ICU) intended for the space-based experiment. We will now discuss the program motivation, thesis research objectives and organization.

1.1 Motivation

Remote sensing, a fundamental underpinning of the CTEx program, is related to gathering information about a source without making physical contact with it. [1]

Hyperspectral imaging (HSI), composing a segment of the remote sensing field, began in the late 1970's and is a powerful tool enabling many cutting-edge military and civilian applications currently in use today. [2] Examples include: gathering information about the battlespace, defeating camouflage, missile early warning, environmental monitoring, vegetation analysis, monitoring of coastal environments, and disaster assessment (only naming a few). Given these varied uses for HSI, a current drawback relating to this type of imager is that it can provide data for only static or slowly-evolving scenes. A chromographic HSI provides the ability to collect spatial, spectral, and temporal measurements enabling short-duration event location and classification (e.g., explosive device stoichiometry determination, missile plumes detection/classification, forest fire characterization, etc.). These aforementioned CT HSI abilities present strong rationale for further development (hence, the previous and current space-mission research thrust). The following subsections develop the framework for this program further.

1.1.1. Spectroscopy. Spectroscopy is typically classified as the “study of the absorption and emission of light and other radiation by matter, as related to the dependence of these processes on the wavelength of the radiation.” [2] Based on these ideas, it is possible to determine one material from another when reviewing the differences in spectral responses or “spectral signature matching.” [1] [3] Spectroscopic techniques have been utilized in a wide array of applications ranging from assessing the internal structure of atomic nuclei, medical assessments (e.g., magnetic resonance imaging in order to visualize soft tissue in the body), and determination of distant-star constituents, only naming a few. Due to this ever-expanding utilization of the field,

spectroscopy makes use of a large portion of the electromagnetic (EM) spectrum to accomplish specific missions in wavelength regions ranging over 16 orders of magnitude.

[2] EM radiation, made up of electric and magnetic fields having the ability to transfer energy through space, propagates as a wave and travels according to Equation (1),

$$v\lambda = c \tag{1}$$

Where v is the EM frequency (Hz), λ is the wavelength (nm) and c is the speed of light (299,792,458 m/s in vacuum). Decomposition of EM radiation into component wavelengths is critical to the study of spectroscopy (the frequency the EM wave oscillates is used to characterize the radiation). Figure 1.1 details the EM spectrum broken up into its constituents. [2]

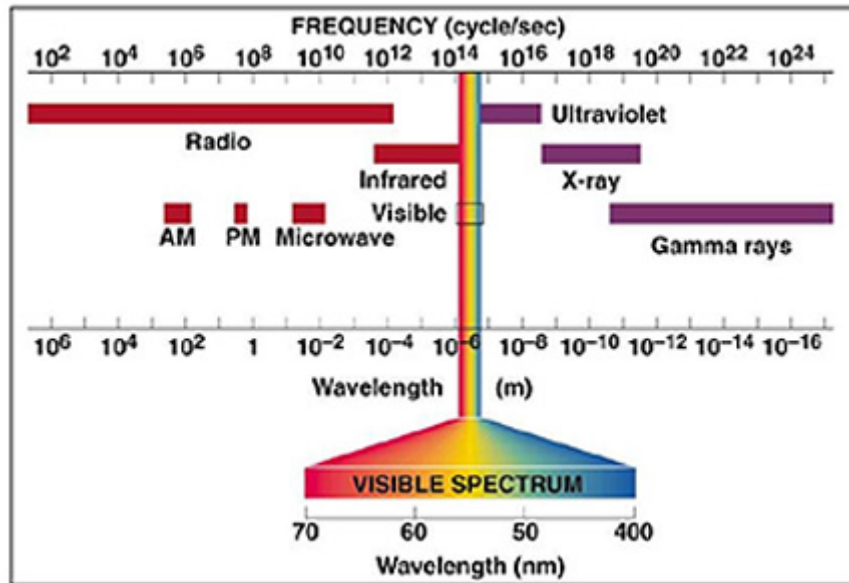


Figure 1.1: Electromagnetic Spectrum [4]

In order to perform production and assessments upon a spectrum, the following three components are required: an EM source, a device to disperse the incident EM

radiation into component wavelengths, and a detector to sense the dispersed EM radiation. The latter two elements noted above are collectively called a spectrometer and typically fall into two applications, measuring either absorption or emission spectra. Absorption spectroscopy presents a continuously bright background with dark lines measuring the loss of EM energy after illumination. Emission spectroscopy excites a sample of interest and shows one or more lines (bands) on a dark backdrop. Figure 1.2 details the differences between resulting absorptive and emissive plots. [2]

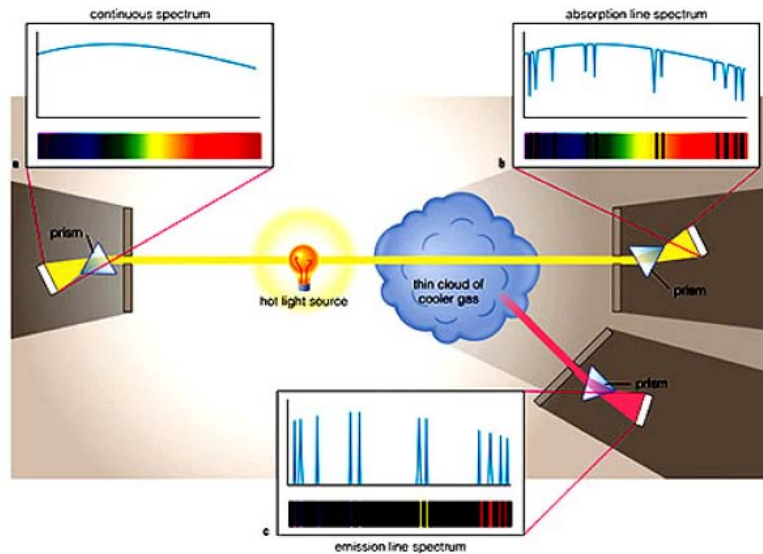


Figure 1.2: Absorption and Emission Spectroscopy [4]

Further categorization for spectrometers focus upon the dispersing element in the device as either based on diffraction or refraction. Diffraction dispersing elements have a periodic structure (e.g., grating), which splits and diffracts light into several beams travelling in different directions (dependent upon the spacing of the grating and the wavelength of the light). [2] Refractive-based instruments make use of Snell's Law to accomplish their mission, Equation (2):

$$n_1 \sin i = n_2 \sin r \quad (2)$$

Where n_i is the refractive index (unitless), i and r are the incident and resultant EM radiation vector paths of the light entering and leaving an optical surface (degrees), respectively. These devices are able to determine the wavelength of EM radiation based on the resulting angle through this component. Figure 1.3 details this methodology.

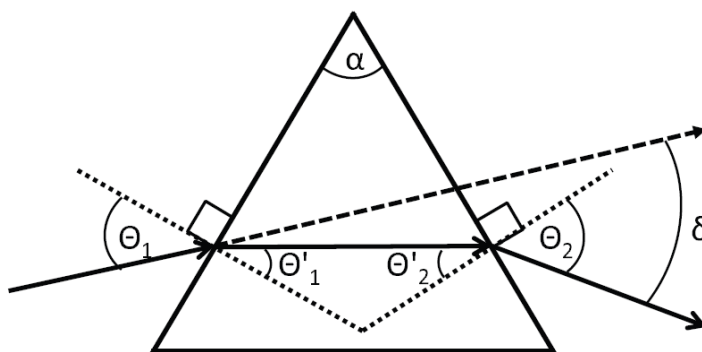


Figure 1.3: Refractive Dispersion [5]

1.1.2. *Hyperspectral Imaging.* Spectral imaging combines spectroscopy with traditional imaging to accomplish missions that each could not perform independently. Resulting data from this technique yields a “stack” of images wherein each is at a particular wavelength for the same scene. [4] While spectral imaging is typically thought to capture data in a limited region of the EM spectrum, it is further broken up into three categories, including: multispectral, hyperspectral, and ultraspectral imaging.

Multispectral imaging (MSI) deals with data collected simultaneously from several discrete and broad bands (i.e., a contiguous region of the spectrum over which a sensor detects and measures reflections or emissions). Typical MSI data products are based on three-color composites, similar to the human eye (which is itself a three-band sensor). In

contrast, HSI sensors are those collecting narrow bandwidth and “hundreds” of bands while ultraspectral sensors have a very narrow bandwidth and “thousands” of bands. While the advantage to hyperspectral and ultraspectral is increased spectral resolution, ultraspectral imaging is still an area of development specifically sensitive to discriminating specific materials (e.g., identification of aerosols, gas plumes, and effluents). [5] Figure 1.4 shows an example of the differences between multispectral, hyperspectral, and ultraspectral imaging.

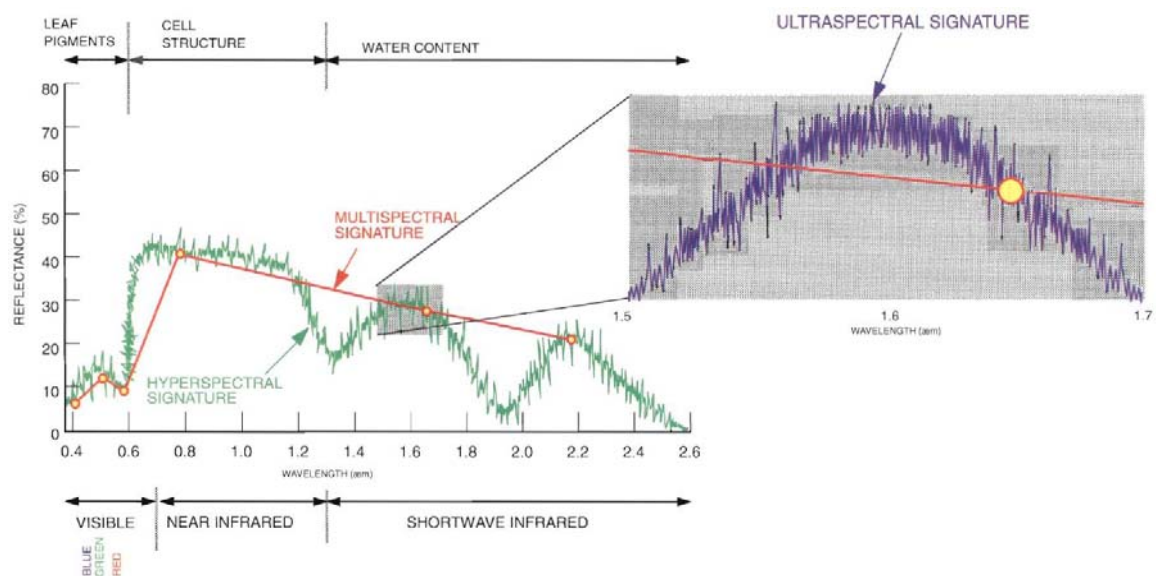


Figure 1.4: Multispectral, Hyperspectral, and Ultraspectral Imaging Differences [5]

Due to the fact that HSI sensors provide higher spectral resolution over a contiguous region of the spectrum, they allow for “spectral fingerprinting” of particular scenes due to the increase in information acquired. [6] A HSI sensor builds a four-dimensional data cube consisting of two spatial, a spectral and a temporal component typically requiring scanning in either the spectral or spatial domains. HSI technology first began to be implemented in the early 1980’s with the development of NASA’s

Airborne Visible / Infrared Imaging Spectrometer (AVIRIS) which took advantage of advancements in detector technology allowing their use on a moving platform. This development enabled practical and rigorous assessments of surfaces at remote distances and large areas. It should also be noted that the processing of HSI data is different from that of MSI wherein “spectra matching” is conducted to detect and classify targets (for HSI scenes due to the increase in resolution). With the aid of Fourier procedures, mixtures of two or three different materials may also be identified as constituents of a compound spectral curve. [7]

1.1.3. CTE_x. With the inherent advantages that HSI provides (listed earlier), a limitation of this technology relates to the capture speed (i.e., acquisition of spectral, spatial and temporal data). Current capabilities only allow for collection upon scenes with slowly changing features (i.e., in the realm of minutes duration). The current AFIT-led project technology-push is to enable the collection of “fast” transient spectral and temporal data while balancing spatial resolution. For military exploitation, CTE_x is being developed to aid in the study of bomb phenomenology (where the majority of useful data occurs in 0.1 sec and the entire event is over within 1.0 sec). Figure 1.5 details notional data from such an event and the response expected.

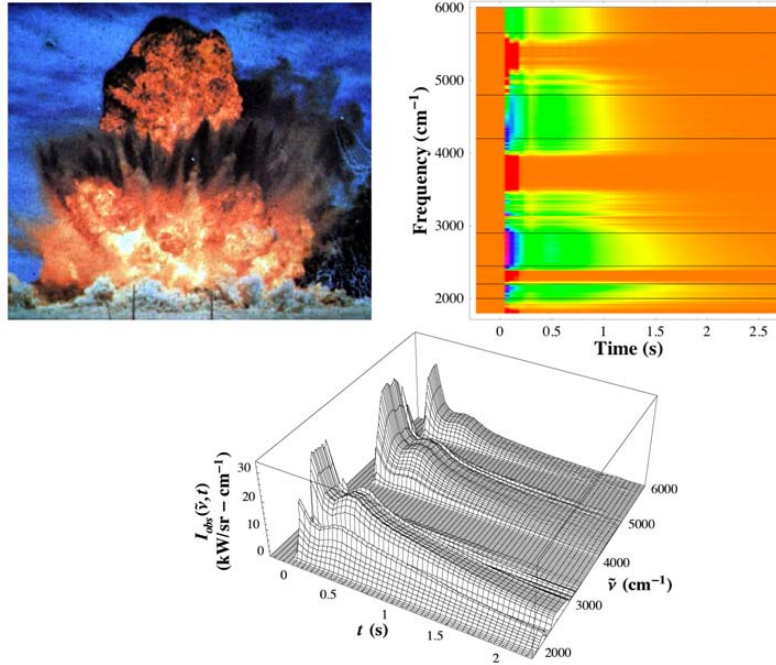


Figure 1.5: Representative Spectral Response from an Explosive Scene [9]

Chromotomographic (CT) imaging is one area of remote sensing which holds the potential to resolve the issues noted earlier to enable a fast-transient HSI capability. CT imaging is a process of convolving spectral and spatial information to later build the HSI hypercube from transform algorithms (similar to those found in medical tomography).

[10] The AFIT-led experiment, CTE_x, is a configuration which is being investigated as a CT platform to accomplish this mission area from the perspective of space.

Fundamentally, CTE_x utilizes a rotating direct vision prism (DVP) as the dispersing element of the device coupled with a high-speed camera and an optical system, including: field stop (FS), and three lenses (aperture, L₁; re-collimating, L₂; and focusing, L₃). A software algorithm then transforms the raw data into a reconstructed scene. Figure 1.6 details the generic layout for the instrument.

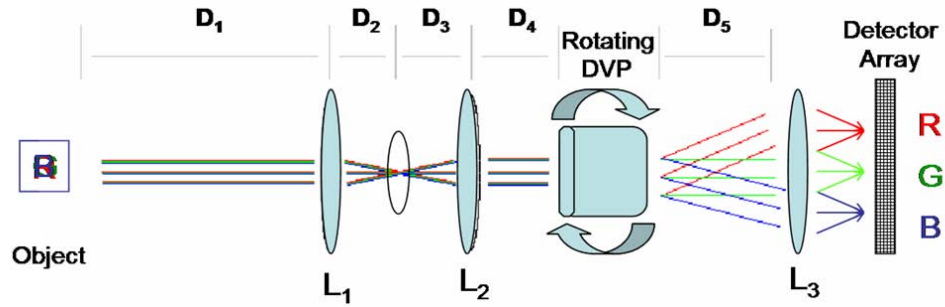


Figure 1.6: CTEEx Optical Layout [9]

The CTEEx program has been broken into three phases in order to further develop the technology and mitigate risk prior to on-orbit operations. The three phases include laboratory, ground-based, and space-based experimental efforts. The laboratory phase was accomplished by Bostick and Peram and deemed successfully completed, reported in references [8] and [9]. The ground-based phase was begun by Book and O'Dell (references [13] and [6]) with the objective of building a field-deployable instrument in order to acquire transient scenes of interest. Although this work was successful, further work was necessary to accomplish project goals and develop the basic science.

Finally, the space instrument demonstration is the current end-phase for this program. The intent is to fly aboard the International Space Station (ISS), likely assigned to an ELC docking location (i.e., the US controlled side of the station), depicted in Figure 1.7. Three on-orbit demonstrations are planned, including: static-scene hyperspectral scene (e.g., validate the instrument can discern between a man-made object and the surrounding environment), point-source transient event (e.g., demonstrate determination of combustion constituents), and a large-scale transient event (e.g., assess wide-area scenes to determine combustion constituents, such as a forest fire).

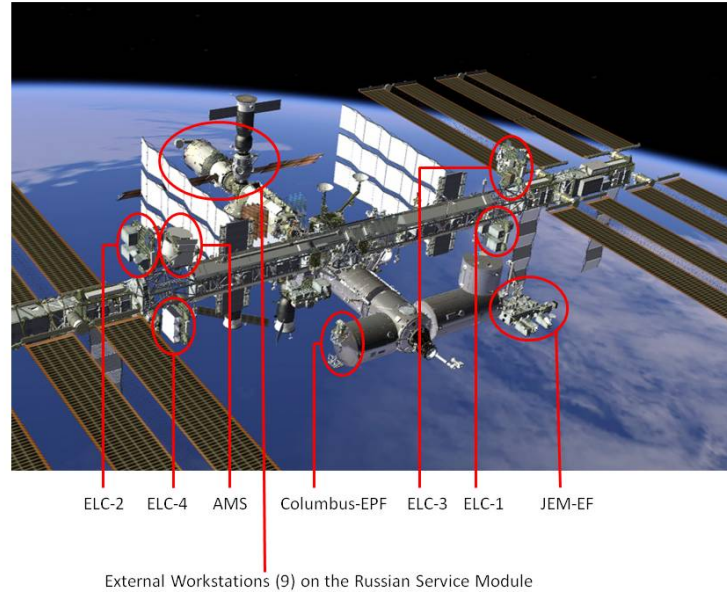


Figure 1.7: ISS Exposed Facilities (EF) (Credit: NASA) [12]

1.2 *Research Objectives*

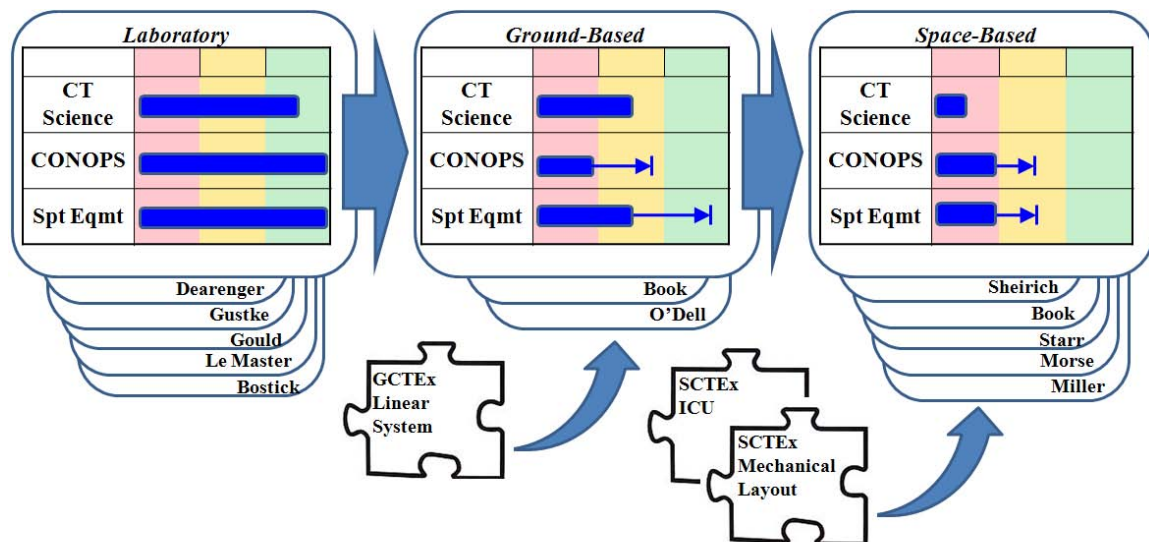
Since the beginning of the CTE_x program, the overall motivation and research objective is to, “conduct a space experiment to demonstrate a novel low-cost multifunctional chromotographic (CT) imaging spectrometer that will provide VIS-IR hyperspectral imaging for transient combustion event classification.” To accomplish this stated objective, three primary areas of effort constitute each program phase (i.e., laboratory, ground-based, and space-based), including: chromotomography optical science and algorithm transform development (“CT Science”), concept of operations maturing (“CONOPS”), and support equipment engineering (“Spt Eqmt”). “CT Science” incorporates the algorithm and physics development of the core technology. “CONOPS” are related to the requirements, mission constraints, collection event plans, alignment/calibration methods, and ancillary ground/space processing operations.

Finally, “Support Equipment” includes the mechanical and electrical engineering tasks related to each mission phase (e.g., structure, mechanisms, control electronics, software, etc.).

While the aforementioned mission objectives motivated CTE_x as a whole, this thesis research is an incremental step in the overall program development effort composed of three interrelated tasks, including:

- Design of the space-based experiment mechanical layout to integrate components, determine mass properties and explore trade-space options
- Design and characterize a linear revision to the ground-based experiment in order to acquire higher-fidelity data and assess on-orbit calibration schemas
- Design and characterize the space-based experiment Instrument Computer Unit (ICU) in order to validate modeling and predict on-orbit performance

These above topics continue to build upon previous work conducted at AFIT and are a logical stepping stone to a fully-realized space-based experiment. Figure 1.8 depicts the current level of development for the mission (indicated by a blue bar), where previous research efforts apply and how this thesis supports the overall mission progression (shown by an arrow extending from the blue status bar).



- **Chromotomography Science: Algorithm & Physics Development**
- **Concept of Operations: Req'ts, Calibration, Collection Plans, Ground/Space Ops**
- **Support Equipment: Structure, Mechanisms, Electronics, Software**

Figure 1.8: CTEEx Program Road Map

1.3 Organization

This effort is composed of three primary areas of research and therefore is logically organized within this document in a similar fashion. The three abovementioned areas are further developed within each chapter, divided into a construct which supports the overall objective.

Chapter II lays an initial framework in the science and developmental status of the program. CTEEx is discussed starting from the early laboratory efforts conducted and continues through specific research performed by various personnel at AFIT. Next, a brief literature review describes similar programs and their relevance to this mission. Finally, a synopsis of the proposed space-based platform, the Expedite the Processing of Experiments for the Space Station (EXPRESS) Logistics Carrier (ELC) aboard the

International Space Station (ISS) is presented. All of these sections have relevance in the research found in the subsequent chapters.

Chapter III details the Space-based CTE_x (SCTE_x) design. The first section details overarching threshold and objective requirements. Next, the design methodology is stepped through one functional area at a time (to include trade space setup for the breadboard isogrid analysis performed). Finally, results are presented for the design specifying the overall mass, center of gravity and recommended parameters for a breadboard constructed with an aluminum isogrid structure.

Chapter IV discusses the Ground-based CTE_x (GCTE_x) linear design and characterization. The first section lays out the overall intent and design objectives. The next section reviews the specific component design and validation methodologies to include procedures for prism deviation angle, image quality, and alignment characterization. Finally, results are reviewed with lessons learned from this exploration.

Chapter V gets into the SCTE_x Instrument Computer Unit (ICU) design and characterization effort. Again, the first two sections walk through the design requirements followed with the thermal modeling philosophy, respectively. The third section discusses component design and test campaign methodologies. Finally, the last section presents results encompassing: modeling expectations, test campaign outcome and on-orbit predictions.

Chapter VI is the basis for follow-on research from the work accomplished herein. The first, second and third sections discuss conclusions from the SCTEx, GCTEx, and ICU design and characterization studies, respectively. The final two sections discuss future work recommendation and a wrap-up of the collective research campaign.

II. Background

Prior to discussion of the specific focus areas covered in this thesis, it is prudent to discuss previous and current research related to space-based hyperspectral imaging. To aid in placing the CTE_x mission into context, the first section details similar technology and its applicability. Next, the evolution of CTE_x is described beginning in the early AFRL developments and evolving to specific research accomplished by AFIT personnel (including the relation to this thesis work). Finally, ISS experimental platforms and integration details are addressed.

2.1 Literature Review

Crucial to understanding the state of the art in spectral imagers and the niche CTE_x will fill, it is necessary to perform a review of past and present systems. This section reviews three different HSI sensors employed over the last decade, including Earth Observing-One (EO-1/Hyperion), TacSat-3 (ARTEMIS) and HREP (HICO).

2.1.1. EO-1 (Hyperion). EO-1 was launched on November 20, 2000 with the intent to validate new technology enhancements to Earth observation and refine specifications for future Landsat missions. The space vehicle flew in formation with Landsat-7, roughly one-minute behind so-as to enable comparison of remote sensing data products. [10] Three primary payloads were integrated into this satellite and include: the Advanced Land Imager (ALI), the Hyperion Imaging Spectrometer, and the Linear Etalon Imaging Spectral Array (LEISA) Atmospheric Corrector (LAC). [11] ALI, a prototype Landsat Thematic Mapper (MSI sensor), uses a 15-degree wide-field telescope

allowing for a 37 km ground swath width. [10] Hyperion was the first earth-orbiting high-spatial and high-spectral resolution imaging spectrometer. LAC was designed to measure water vapor content in a wedge-spectrometer package allowing for high spectral resolution. [11] Figure 2.1 details the EO-1 spacecraft.

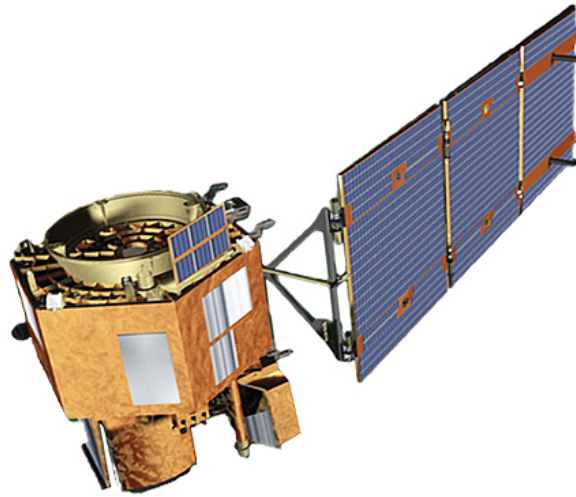


Figure 2.1: EO-1 (Credit: NASA) [14]

Hyperion, a grating spectrometer, provided a new class of Earth observation data and was used to generate a comprehensive space-based hyperspectral imaging archive. [12] [13] The sensor has a 30-meter ground sample distance, 7.5 kilometer swath width and supports up to 10 nm spectral resolution in the band from 400-2500 nm. [10] The aforementioned performance characteristics enable more accurate land asset classification in areas including mineral exploration, crop yield predictions, and containment mapping (to name only a few). [12] Additionally, several quoted notable firsts for this mission include:

- Acquisition of space-based hyperspectral observations with Landsat spatial (30 m) and AVIRIS spectral (10 nm) resolution
- Accurate space-based characterization of temperature gradients in lava flows and forest fires
- Tracking Amazon forest drought-stress and re-growth in logged areas
- Validation in the identification of vegetation species, nitrogen concentration levels and mineral deposits from space [13]

The Hyperion sensor payload is equipped with a 12.5 cm diameter aperture, is 49 kg in mass and consumes 78 watts of power (orbital average). [10] It is composed of three devices, including: the Hyperion Electronics Assembly (HEA), the Cryocooler Electronics Assembly (CEA) and the Hyperion Sensor Assembly (HSA). The HEA provides the interface/control electronics while CEA controls the cryocooler sub-system. The HSA contains the telescope, two grating spectrometers and focal plane array. The telescope is a three-mirror astigmat design with an effective f-number of 11 while the imaging slit, oriented perpendicular to space-vehicle motion, corresponds to a 7.7 km wide by 30 m (along track) area on the ground at an average orbit altitude of 705 km. [11] Two spectrometers utilize the incident beam (broken into two bands with the aid of a dichroic filter) in the Visible/Near-Infrared (VNIR; 400-1000 nm) and Short-Wave Infrared (SWIR; 900-2500 nm) bands. The overlap at 900-1000 nm allow for cross calibration between the devices. [14] To maintain alignment and imaging precision, the HSA housing was thermally controlled by the CEA to 293 +/- 2 K. The VNIR

spectrometer FPA was passively cooled through a radiator (operating at 283 K) while the SWIR spectrometer was actively cooled to 110 K. [14]

Due to the fact Hyperion was a technology demonstrator, deliberate focus was placed on the characterization and calibration of the instrument. As an important design feature in the calibration process, the motorized HSA cover was placed into three different orientations in order to characterize the instrument (including: open, closed and calibration). While in the calibration position, solar irradiance reflects off of a silicone thermal control paint and is utilized for radiometric calibration. In the closed position, internal lamps were used to spectrally calibrate the instrument. Both of these techniques required characterizing the paint reflectivity (based off of incidence angle). [14] While on the ground, the calibration lamps were characterized and found to be stable; however, on-orbit operations revealed as much as a 30% change, attributable to the microgravity environment. Thus, lamps could not be used for absolute radiometry. After a single year of operations, calibration data from vicarious, lunar and solar collections were used to adjust the radiometric coefficients, wherein the instrument was found to be very stable (1% variation found in VNIR and 3% in SWIR data). [14] The Hyperion sensor calibration scheme was utilized in this thesis research as a reference during the characterization test series development.

2.1.2. TACSAT-3 (ARTEMIS). A new development within DoD began in 2003 interested in Operationally Responsive Space (ORS) experimentation. One of the advanced concept demonstrators from this focused interest was the TacSat-3 satellite, a system initiated through new joint processes for mission selection, where the payload was

a hyperspectral imager. [15] Launched in 2009, the space vehicle features an on-board real-time processor enabling data dissemination to combatant commanders in 10 minutes from collection. Three payloads were integrated, including the Advanced Responsive Tactically-Effective Military Imaging Spectrometer (ARTEMIS), the Satellite Communications Package, and the Space Avionics Experiment. [16]

ARTEMIS, the primary payload for TacSat-3, rapidly disseminates target detection and identification data as well as battlespace preparation and damage assessment information directly to the warfighter. [16] [17] As part of the new ORS paradigm, the design, characterization, and operation of the sensor represents a shift in thinking from other similar payloads. Designed by Raytheon Space and Airborne Systems, constrained cost and schedule budgets directly impacted decisions from program inception to characterization and in-flight calibration methodologies. [18] Figure 2.2 presents the TacSat-3 spacecraft.

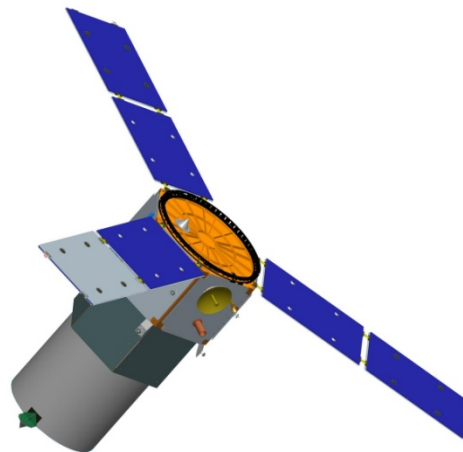


Figure 2.2: TacSat-3 (Credit: AFRL) [22]

To begin, the TacSat-3 mission orbit was mid-inclination allowing for a narrow swath and high spatial resolution. [18] A Ritchey-Chrétien sub-meter telescope was selected to both optimize the spectrometer performance as well as fit inside an ORS launch vehicle fairing (although launched on an OSC Minotaur I, a Space-X Falcon-1 was used as baseline). [17] To simplify ground testing, a mechanism was built into the secondary mirror to perform on-orbit optimization of the focus settings (while on the ground, gravity and thermal compensation analysis was purposely not performed, only focus range was validated during pre-launch). [19] Finally, the spectrometer is an Offner-form composed of primary and tertiary reflecting surfaces (both powered) while the secondary is the curved grating element. Sampling is at 5 nm increments. Modeling of the system was accomplished in detail in order to permit rapid evaluation of sensor design decisions. [17]

The characterization and calibration scheme for both ground processing and on-orbit checkout was also centered around ORS mantras. As discussed earlier, best-focus was determined on-orbit by collecting an image with high-spatial frequency and stepping the focus mechanism through the entire range of settings. Software image processing was then used to assess the spatial frequency for each image at its associated focus, and determine optimal response. [19] Spectral calibration was handled through the use of two panels illuminated by the sun (while on the ground) and an on-board health monitor (OBHM) in flight. Pre-launch ground processing focused on sensor characterization which could not be determined easily on-orbit, including spectral response for channels, linearity of the detector and reproducibility of the data (at operational settings). The two

panels used to assess these metrics were large enough to cover the entire aperture and included a special coating to provide known absorption features (designed to provide a large number of spectral lines) while the other panel contained a flat spectral reflectance (used for absolute radiometric calibration). [18] The OBHM was utilized while in-flight in lieu of an onboard calibration lamp (another departure from conventional scheme). [18] Used for spectral trending, the OBHM is composed of a blackbody source (color temperature of about 2200 K), an elliptical reflector, and a spectral filter. [17] Overall, the radiometric calibration uncertainty was assessed at less than 3% (for most spectral bands). [18] For this thesis, ARTEMIS provided useful concepts in the ground-based CTE_x characterization campaign.

2.1.3. *HREP (HICO)*. The Office of Naval Research, in conjunction with the Naval Research Laboratory, began a mission in 2005 to develop a spectral imager optimized for the ocean coasts. [20] In late 2009, the Hyperspectral Imager for the Coastal Ocean (HICO) and the Remote Atmospheric and Ionospheric Detection System (RAIDS) Experiment Payload (HREP) was launched from Tanegashima Island, Japan, and was integrated to the Japanese Experimental Module Exposed Facility (JEM-EF) aboard the ISS. [21] [22] RAIDS is designed to investigate the upper atmosphere (75-750 km altitude) and will be used to develop next-generation techniques to perform remote sensing upon the neutral atmosphere and ionosphere. [29] HICO is a pathfinder mission utilized as a technology demonstrator toward a future free-flying spacecraft. Data acquired from HICO includes bathymetry, optical/biological properties and bottom-characterization of coastal scenes as monitored from space. Derived data products from

HICO include honed calibration (currently a very complex process), atmospheric correction, and in-water transform procedures (all in the effort of exploiting the HSI signatures). [22] Figure 2.3 displays the HREP payload.

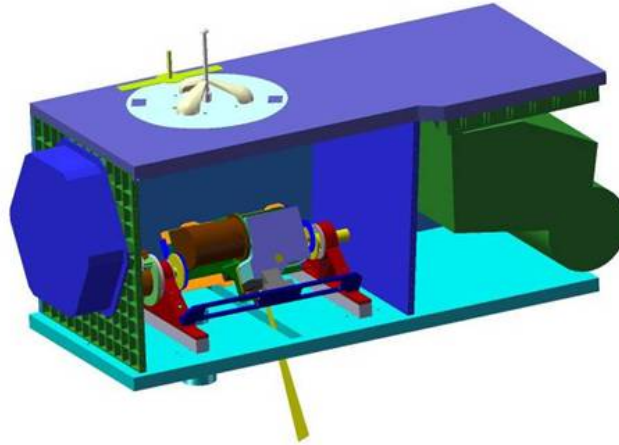


Figure 2.3: HREP JEM-EF ISS Configuration (Credit: NRL) [27]

The overall design of HICO is centered on the subject of interest (i.e., coastal scenes). Three overarching ideas laid the framework for the mission, including: a high signal-to-noise ratio (SNR), high sensitivity in the “blue” wavelengths and a large ground sample distance (GSD). [21] A high SNR is required due to the fact that coastal ocean scenes are “dark” (albedo is only a few percent) and compounded by the fact that this mission will view these scenes through the “bright” atmosphere (i.e., scattered sunlight). Additionally, VNIR wavelengths are the only portion of the EM spectrum to penetrate the water column. [20] High sensitivity in the shorter visible wavelengths is critical to discern dissolved and suspended matter. [21] Finally, a large GSD is specified due to the size required to adequately characterize and classify coastal environments. Typically, for many HSI sensors, meter-class GSD is required to distinguish man-made objects;

however, tens-of-meters was more appropriate for this mission (as harbor charts are typically at this scale). Therefore, HICO was designed to the following specifications: 100 m GSD, 350-1070 nm spectral range (10 nm spectral resolution), 200:1 SNR, 5% radiometric accuracy, 50x200 km scene size (nominal) and 15 scene collections per day (maximum). [20] [21] [22]

One important, yet not as overt, mission requirement for HICO was to “demonstrate new and innovative ways to develop and build the imaging payload” in order to reduce cost and schedule. [21] To accomplish this objective, use of COTS and hermetic enclosures were employed throughout the design, including the camera, computer and rotation stage. The benefit this provides to the HICO mission is in opening the door to the use of aircraft-grade components and computers which may not be available in a space-qualified form for years. [20] The spectrometer, camera and rotation stage were all commercially available, reducing the cost and time to complete the instrument package. [Note: the remainder of this section has been redacted; requests for these omitted sections shall be referred to AFIT/ENY, Dr. Jonathan T. Black, 2950 HOBSON WAY, WPAFB, OH 45433-7765]

2.2 CTE_x Background

Chromotomography technology first began to be investigated in the mid-1990’s as HSI data products were realized along with computer processing advancements. As discussed within Section 1.1, spectral imagers utilize a series of two-dimensional images to create the three-dimensional data cube. Most of these imagers operate in one of two different configurations: scanning-slit and filter-based. [25] Scanning-slit HSI

technology is well understood and has been used on both satellite and aircraft systems. Capture operations are accomplished through dispersing the light through a slit to a focal-plane-array where high spectral resolution is achieved by making the slit narrow (typically the width of a column of pixels). A narrow slit causes a loss in the amount of light allowed to pass, therein reducing the signal-to-noise ratio; however, designs typically accommodate this through increasing exposure time. Thus, scanning-slit HSI sensors are limited both in the amount of coverage area as well as the exposure time necessary to witness an event. Filter-based sensors are those which obtain a HSI scene through sweeping a resonant cavity or spectral filter. These sensors have good coverage area; however, their throughput and synchronization of the event spectrum and sensor spectral bandpass (at the moment desired) are limitations in application. [26]

Two HSI configurations which take exception to the efficiency and/or resolution degradation limitations addressed above include a cascade of beam splitters and Fourier Transform spectroscopy. The former utilizes a separate imaging plane for each spectral band (where efficiency can be maximized in each color); however, in practice this application would limit the device to only a few bands. The latter, a Fourier Transform spectrometer, multiplexes spectral information through the use of either a lateral shear or longitudinal displacement interferometer. Lateral shear interferometers multiplex spatial and spectral data, are insensitive to vibration, have the same efficiency limit as scanning-slit spectrometers, and are typically used in the field. Conversely, longitudinal displacement interferometers multiplex spectral data through time, have high efficiency but are susceptible to vibration, and consequently are used in laboratory settings

(normally). All of these Fourier Transform techniques are examples of tomographic imaging, allowing for both a wide area of coverage and wide spectral bandwidth. [25] [26]

In practice, tomographic signals are complex, requiring a substantial investment in understanding both the image and signal processing methodology. [26] Amid these complexities, the medical community has enjoyed products from tomographic imagers for the human body for some time now. Medical imagers employ computers to acquire the highest signal-to-noise ratio for the fewest photons as possible (x-rays); thus, due to the fact the spectral imaging problem shares commonality, it was logical to assess these techniques for military and scientific application. [25] Early review of medical tomographic technology showed that these techniques would need to be modified in order for spectral imaging to become a reality in the collection of transient events and evolving scenarios (e.g., measurement of lightning activity, detection of forest fire initiation, bomb detonations, muzzle flashes, and other combustion events). [27] [26] [9] Nevertheless, the term Chromotomography was coined and refers to “use of a dispersive element which convolves spatial and spectral information that can be reconstructed using the same transforms employed in medical tomography.” [9]

Chromotomographic imagers constructed in recent years consist of a telescope, dispersive element, and camera. [26] A critical feature in the telescope relates to the field-stop which reduces ill-conditioned regions of the scene by limiting the field of view (taking into consideration the size of the detector array, spectral dispersion and magnification of the system). [25] [9] The dispersive element typically is a rotated direct

vision prism (DVP) due to the greater potential in acquired spectral response versus that of grating-based systems (e.g., detonation events demand high spectral resolution capabilities). [8] As the DVP is rotated about the instrument optical axis, the image is broken into component wavelengths wherein point sources create circles (the radii for each circle is dependent upon wavelength). [26] Each image is a linear superposition of spectral information for a unique point spread function (i.e., wavelength information has been multiplexed over successive video frames). [25] The inversion algorithm uses the sequence of images, tracing circular paths corresponding to chromatic bands, to return a data cube of useful information from the scene witnessed (i.e., rotating the DVP obtains a sequence of two-dimensional images used to reconstruct the three-dimensional hypercube). [27] This allows determination of four data products, including: the individual pixel spectrum, primary spectral component mixture, spectral slices, and spectral signature matching for object determination (or other similar analysis, as discussed in Section 1.1.2). [26]

Early AFRL research conducted by Mooney in the mid-1990's ([25], [27]) demonstrated the fundamental operation as well as complications of the CT technique. One of the first instruments developed was the Angularly Multiplexed Spectral Imager (AMSI), consisting of an infrared camera and DVP. AMSI demonstrated that spectral imaging could be possible and likely applicable to any band (given the proper DVP and focal plane array). As an early complicating observation, AMSI resulted with lost scene information (low spatial and high spectral frequency) yielding image quality degradation. Thus, this early research recommended that application be limited to sensors requiring

multiband spectral imagery over wide fields of view that do not require radiometric information. [25]

As tomographic HSI techniques matured, several other configurations of instruments were developed by the turn of the century to include a medium-wave infrared (MWIR) and VNIR Chromotomographic Hyperspectral Imaging Sensor (CTHIS). Again, these instruments had the goal of capturing all available light and eliminating/reducing the amount of scanning required. [28] Demonstration that CT designs could be applied to any spectral band was bolstered through operating successfully in the VNIR band. Additionally, the fact that the envelope of this instrument could be minimized significantly implied that many air and space platforms could potentially incorporate this sensor. The VNIR CTHIS sensor delivered 64 spectral bands at frame rates up to 955 Hz, weighing 6 lbs, occupied a 4x12x6 inch envelope, and required 20 W electrical power. [26]

From the early AFRL research accomplished, we will next step through various efforts accomplished by AFIT personnel. The discussion provided is generic (not exhaustive); nevertheless, it will provide context and applicability to further development efforts pursued in this thesis.

2.2.1. Anthony J. Dearing (2004). Dearing developed chromotomographic software models to simulate unit impulse response of the sensor resulting with point spread functions for the system (based upon geometric Fourier and wave optics propagation principles). The rationale herein was due to the fact that a transient event (e.g., explosion) assumes the radiant energy from this source is dominant within the scene

during the collection period. His goal was to enable further investigation into CT trade-space development as well as future reconstruction techniques. [29] While not wholly applicable, his research and mapping of various components (e.g., field stop, DVP, etc.) was assessed for application of efficiencies in this thesis work.

2.2.2. *Kevin C. Gustke (2004)*. Gustke pursued trending associated with infrared hyperspectral chromotomographic reconstruction wherein his work assessed the pseudo-inverse singular matrix problem in an effort to reduce error. Synthetic data was produced in order to approximate gathered collection events. His results indicated that absolute radiometry was impractical; nevertheless, several lessons were learned, including: the number of spectral bands required relates directly to the number of frames recorded, spectral resolution increases if a smaller region of the scene is utilized for reconstruction, and several observations associated with the infrared setup. [30] Gustke's work, while not used directly in this thesis, was assessed for implications for the CTE_x mission and this specific research.

2.2.3. *Daniel A. LeMaster (2004)*. LeMaster's research involved assessing and developing point spread functions (PSF) for an infrared chromotomographic imaging system (as HSI reconstruction depends upon accurate knowledge of these PSF's for each wavelength). PSF's were determined through utilizing phase screens (the Gerchberg-Saxton algorithm was used for phase retrieval whereas the Richardson-Lucy algorithm enabled extraction of the point spread functions). Validation of this methodology was accomplished through collection of blackbody source data in the laboratory. [33]

LeMaster's work contributes to this thesis in the concept that prism alignment and rotation errors need to be minimized as much as possible throughout the design of all ground- and space-based systems.

2.2.4. *Malcolm G. Gould (2005)*. Gould developed estimation-theory algorithms promoting higher-fidelity hyperspectral reconstruction for infrared scenes. Two algorithms were developed. The first reconstructed the entire hyperspectral scene data cube whereas the second allowed for reconstruction of a single spectral dimension and one compound spatial dimension. Gould also discusses correction methods for atmospheric attenuation. From testing he conducted, 4-6% radiometry error was concluded from reconstructed data cubes. [34] Malcolm's work, while important in the overall progression of the CTE_x program, was not used directly in this thesis.

2.2.5. *Randall L. Bostick (2008-2011)*. Bostick empirically mapped the fundamental CT science through characterizing the spectral/spatial resolution as well as introduced error into the system in order to assess the impact. His work is considered to be the conclusion to the CTE_x laboratory phase as discussed earlier. He designed and built a VNIR Chromotomographic hyperspectral imager (CTI) wherein his DVP was a two-prism set (Schott SFL6 and LaSF N30 glass) with an undeviated wavelength designed at 548 nm. Results from his initial studies showed that spatial and spectral resolution for CT reconstructed objects were no better or worse than those acquired using a prism spectrometer. [8] Additionally, he found the spectral resolution of these systems to range from 0.5 nm at shorter wavelengths (400 nm) and 7 nm at longer wavelengths

(750 nm). [9] The latter work Bostick accomplished was in assessing the impact of error in the CTI system, attributable from prism alignment, detector array position and prism rotation angle. Results from this effort showed that the most significant impact to the HSI data was in misalignment of the prism rotation mount (spectral resolution was degraded by 50-100% with 1° total angular error). [31] Other impacts are summarized in Table 2.1.

Table 2.1: Effects of Error (“X”: Effect Observed; “-“: Effect Not Observed) [31]

Systematic Error	Spectral Resolution	Spatial Resolution	Spectral Peak Shift	Spatial Peak Shift
Tile of Detector Array	-	-	-	X
Estimation of Prism Angular Dispersion	-	-	X	-
Prism Misalignment in Mount	-	-	X	-
Prism Mount Misalignment	X	X	X	X
Estimation of Prism Rotation Angle	-	X	-	-

Bostick’s research was pivotal in this thesis in assessing the predominant issues with the previous CTE_x ground instrument. Maintaining a high-precision instrument centerline through the linear revision is critical in acquiring a high-fidelity HSI hypercube. Additionally, his designed DVP was utilized as the baseline for characterization testing.

2.2.6. *Phillip Sheirich (2009)*. Sheirich performed the first engineering trade study assessment upon the space-based version of CTE_x to determine an initial notional payload, concept of operations and orbital requirement in order to properly demonstrate this technology. Sheirich defined general instrument requirements and reviewed primary

instrument components, to include: optics, prism, focal-plane array, early on-orbit calibration, and data handling. [32] His efforts afforded this research the early confidence in feasibility that an on-orbit CTE_x sensor is viable.

2.2.7. *Todd A. Book (2010)*. Book's work attacked several issues, including: developing the first ground-based version of CTE_x as risk-reduction, assessing a contractor's design for an off-axis Mersenne telescope (intended for use as the telescope for the space-based instrument), and developing a methodology for on-orbit focus, alignment and calibration. The structural assembly provided to the AFIT Engineering Physics department was largely successful and enabled ground-based CTE_x goals to be met. The design review for the off-axis Mersenne telescope was also conducted and deemed successful at the time. Book recommended several mechanisms to achieve proper focus, alignment and calibration while on-orbit. For focus, sodium street lamps were recommended to be imaged at night as the instrument steps through various focus settings (as sodium spectral response is nearly monochromatic and the sharpest image will be deemed optimal). Additionally, a focus target should be placed in the aperture cover for another focus mode. Next, alignment concerns were discussed relating to the collimated optical beam wherein the recommendation was to ensure the primary and secondary off-axis parabolic mirrors remain parallel (through maintaining tight tolerances during fabrication/mounting). Finally, Book recommended using three separate sources, including: (1) a laser diode system in the aperture cover for initial calibration and troubleshooting, (2) atmospheric oxygen A and B bands will be utilized for absolute (primary) spectral calibration, and (3) radiometric calibration will use two targets, green

LED's in the aperture cover (for pixel characterization) and a filter wheel while the aperture cover is open on-orbit (for spectral calibration trending and further troubleshooting). [33] His design and procedures from these schemas were further developed in this research in order to acquire higher-fidelity data as well as reduce risk in CONOPS for the space-based mission.

2.2.8. *Steven D. Miller (2010)*. Miller's thesis research focused on developing a passive vibration isolation system in order to mitigate jitter concerns. His design was intended to reduce excitation inputs to the optical breadboard structure from both internal and external sources (i.e., the rotating prism and ISS loading). While results from this design and test series were not acceptable for the final CTE_x flight configuration (due to premature ISS configuration assumptions and further development on damping mechanisms) his design was a nominal baseline for a six degree of freedom compact isolator and was utilized in the mechanical layout analysis as a notional design for further review. [34]

2.2.9. *Arthur L. Morse (2010)*. Morse, an electrical engineer, designed the first avionics layout for the CTE_x instrument (both hardware and software). His design balanced the high resource demands this imager will need (due to the level of angular precision and data from each capture event) with the limitations of the space environment. Morse also laid the groundwork for the software development to begin to take shape, providing a flow-path architecture to both operate quickly while also enabling real-time feedback for targeting. Finally, recommendations were provided for the AFIT

satellite ground system (modeled after the United States Air Force Academy's ground station). [35] His efforts were crucial to understand for the grouping and packaging of essential avionic components in the space-based instrument mechanical layout in this thesis.

2.2.10. Daniel O'Dell (2010). O'Dell assessed the ground-based CTE_x design, provided by Book, into a characterization study for the new instrument. Utilizing a simplistic shift-and-add algorithm, he was able to show that the instrument had the ability to capture spectral data of both static and fast-transient scenes. O'Dell's research also provided discussion on concern areas for hyperspectral reconstruction, including the need for precise angular position knowledge as well as misalignment errors (attributable to less-than-desirable results). Additionally, he noted that an algorithm which has the ability to better locate the center of dispersion would allow for more confidence and resolution in the spectral and spatial domains. [36] This thesis research made use of these observations to both update the instrument to account for the high-degree of alignment required as well as in developing algorithms and in calibration schemas to better locate the center of dispersion.

2.2.11. William J. Starr (2010). Starr answered fundamental space-based experiment questions and provided requirements definition for instrument slewing, attitude knowledge and a concept of operations for CTE_x. It was shown that +/- 8 degrees slewing is necessary to allow for a 10 second on-orbit access and collect aboard the ISS. Additionally, his research has shown that given the ISS attitude measurement

inaccuracy (+/- 3 degrees), it is critical for CTE_x to incorporate a star tracker with better than 90 arcsecond accuracy (1 arcsecond was recommended). [3] These components were integrated from his recommendations into the mechanical layout of the space-based experiment.

2.3 *International Space Station Experimental Platforms*

In 1998, on-orbit assembly began on the most complex technological endeavor ever undertaken, the International Space Station (ISS). Collaborating the efforts of 16 countries, the ISS is a test bed and laboratory for next-generation technology in materials, communications, medical, remote sensing and other research. [37] For purposes of external accommodations (i.e., exposed facilities to the space environment), three overall integration platforms are available to the scientific community, including: ESA's Columbus External Facility (CEF), JAXA's Japanese Experiment Module-Exposed Facility (JEM-EF), and NASA's EXPRESS Logistics Carrier (ELC) which is the planned location for CTE_x. [38] Figure 2.4 details the external research facilities and their locations.

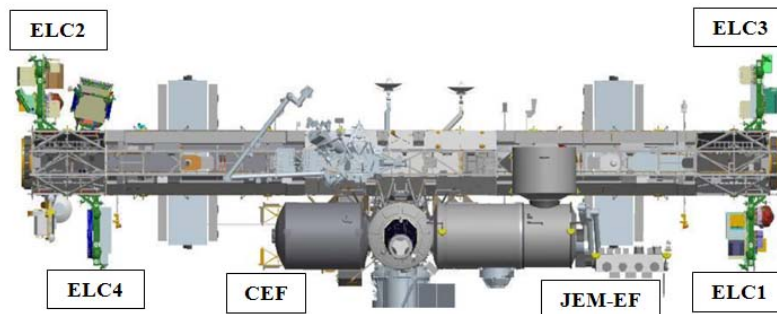


Figure 2.4: ISS External Research Facilities [38]

The CEF accommodates four different experiments (two sites are available to NASA) at varying mass capacities, including 230, 550 and 2250 kg (depending upon the allocation). Palletized payloads must fit volume constraints of 86.3 cm x 124.4 cm x 116.8 cm (34 in x 49 in x 46 in), 120 Vdc (1.25 kW) and be passively cooled. Low- and medium-rate data transfer is provided at these sites at 1 Mbps (per two-way MIL-STD-1553) and 2 Mbps (shared, two-way), respectively. [38] Figure 2.5 details the CEF overview.

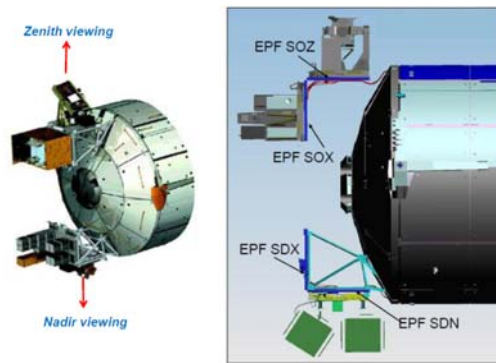


Figure 2.5: CEF Configuration [38]

Next, the JEM-EF offers 10 experiment sites (five dedicated to NASA) at two varying mass capacities of 550 and 2250 kg. The largest volume payload accommodations are offered on this platform (in comparison with the other two) at roughly 1.5 m³ with dimensions at 80 cm x 100 cm x 185 cm (31.5 in x 39.4 in x 72.8 in). Active cooling as well as 113-126 Vdc (3-6 kW) is provided along with low-, medium-, and high-rate data transfer capabilities (1 Mbps, IEEE-802.3 and 43 Mbps, respectively). [53] Figure 2.6 depicts JEM-EF integration accommodations.

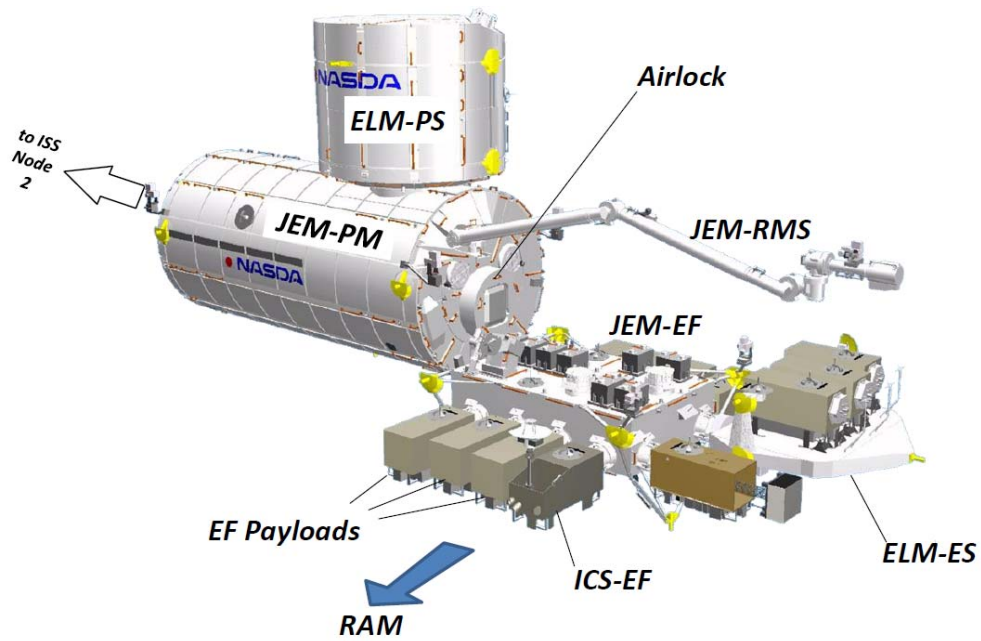


Figure 2.6: JEM-EF Configuration [38]

Finally, two external experimental sites are available per ELC, enabling a total of eight potential attachment allocations on the four carriers (note that half of these sites are nadir facing while the others are zenith oriented). Experimental payloads are constrained to one mass specification, 226 kg, and volume at roughly 1 m³ with dimensions at 86.3 cm x 124.4 cm x 116.8 cm (34 in x 49 in x 46 in). Active heating (with passive cooling) is provided with 113-126 Vdc (750 W) electrical power. Low- and medium-rate data transfer is accommodated at 1 Mbps (MIL-STD-1553) and 6 Mbps, respectively. [38]

[Note: the remainder of this section has been redacted; requests for these omitted sections shall be referred to AFIT/ENY, Dr. Jonathan T. Black, 2950 HOBSON WAY, WPAFB, OH 45433-7765]

2.4 Background Summary

This chapter provided details associated with HSI sensor state of the art, the development of the CTE_x program and ISS considerations to provide context and rationale for further design work. Three different HSI sensors were discussed in Section 2.1 wherein the design, operation and characterization/calibration campaign was focused upon in each program. Section 2.2 detailed specific efforts of early AFRL and AFIT researchers for the CTE_x program. Section 2.3 outlined ISS platform details. This background work will be tied into the overall program progressive research associated with development of the space-based experimental payload (as well as devices associated herein).

III. Space-Based CTE_x Design

This chapter pertains to the space-based CTE_x layout development and integration design covering the relevant background requirements, design concepts and results. The overarching goal herein is to baseline a potential solution for launch and on-orbit operations which meet fundamental requirements (note, this is not an optimization study). Conclusions to this research are captured in Section 6.1 with recommendations for future work contained in Section 6.4.

3.1 Design Requirements

The objective in this study was to assess an initial mechanical layout for the space-based CTE_x instrument. This layout is intended to be a baseline effort for further iteration refinement; nevertheless, it allows future researchers to begin trade-space mapping given this first concept. Optimization was not pursued at this time due to other elements and requirements of the payload still in relative flux.

As background, it needs to be understood up front that the solutions obtained made use of design efforts performed by previous AFIT research personnel; however, a major departure occurred early in the design relating to integration requirements to the International Space Station (ISS). This change was due to the interest and likelihood that the CTE_x program would be allocated to an “Expedite the Processing of Experiments to the Space Station” (ExPRESS) Logistics Carrier (ELC) payload assignment position versus earlier efforts which focused on integrating the system to a Japanese Experiment Module, Exposed Facility (JEM/EF) slot. This redirection caused the AFIT team to reevaluate envelope, orientation, mass properties, and other issues critical to mission

accomplishment. Table 3.2 reviews some of the generic differences in these mechanical requirements.

Table 3.2: JEM vs. ExPA, Generic Mechanical Differences [38]

Platform	JEM/EF	ExPA
Mass	1100-5500 lbm (500-2500 kg)	500 lbm (226 kg)
Envelope (LxWxH)	78 in x 32 in x 40 in (198 cm x 81 cm x 101 cm)	34 in x 46 in x 49 in (86 cm x 116 cm x 124 cm)

Independent of this major departure in overall integration, the launch and on-orbit planning efforts have otherwise been unchanged in that the payload, now aboard an ExPRESS Pallet Adapter (ExPA), will reach orbit via a Japanese H-IIB Transfer Vehicle (HTV). Additionally, due to the fact that funding for this mission is constrained (as it is a graduate-school mission), the ability to maximize flying commercial, off-the-shelf (COTS) hardware is critical and was a large driver in early decision making (similar to the HREP design, discussed in Section 2.1.3).

With the above concepts in mind, the following requirements (thresholds) were established to guide and constrain this early layout assessment.

- Meet all requirements for mechanical layout associated with mission operations, to include: integration of the telescope, motor/encoder, direct vision prism (DVP), camera, lens system, control electronics
- Meet all ELC / ExPA requirements per ExPRESS Payload Adapter (ExPA) Interface Definition Document (IDD), D683-97497-01, Revision C

- Meet all HTV requirements per HTV Cargo Standard Interface Requirements Document, NASDA-ESPC-2857 Rev.C
- Integrate the currently contracted telescope into the system (provided by RC Optical Systems, Inc.)
- Make use of COTS equipment as much as possible
- Reduce the number of fastener sizes to no more than three (for ease of future bolt analysis, fabrication and assembly)

Additionally, as a potential to expand the operational utility and interest in this instrument, a list of desired secondary goals (objectives) were presented, listed below:

- Utilize the high-speed camera as a stand-alone unit to observe fast events (e.g., lightning strikes, fireworks, automobile traffic, etc.)
- Utilize the high-speed camera as a stand-alone unit at night to image city lights and other phenomena (e.g., quickly assess power-outages, assess the phase of electric illumination networks, etc.)
- Configure the instrument with a mechanism to amplify the signal at night to enable night-vision (e.g., micro-channel plate between the telescope and detector array)
- Enable the DVP to be replaced by a polarizer or diffraction grating filter to generate polarimetric data and/or multi/hyper-spectral data without the adverse effects of the chromotomography system

We will now explore the design concept methodology leading to the convergence of this baseline system.

3.2 Design Concept Methodology

The design methodology begins first in terms of the orientation of the primary optic (the telescope) aboard the ISS payload integration carrier, the ExPA. As identified in the previous section, the payload envelope which must be maintained is 34" (L) x 46" (W) x 49" (H). Therefore, to accommodate the current telescope design, provided through a contract with RC Optical Systems, Inc, the telescope must be erected lengthwise in a perpendicular arrangement to the ExPA. See Figure 3.1 for further detail.

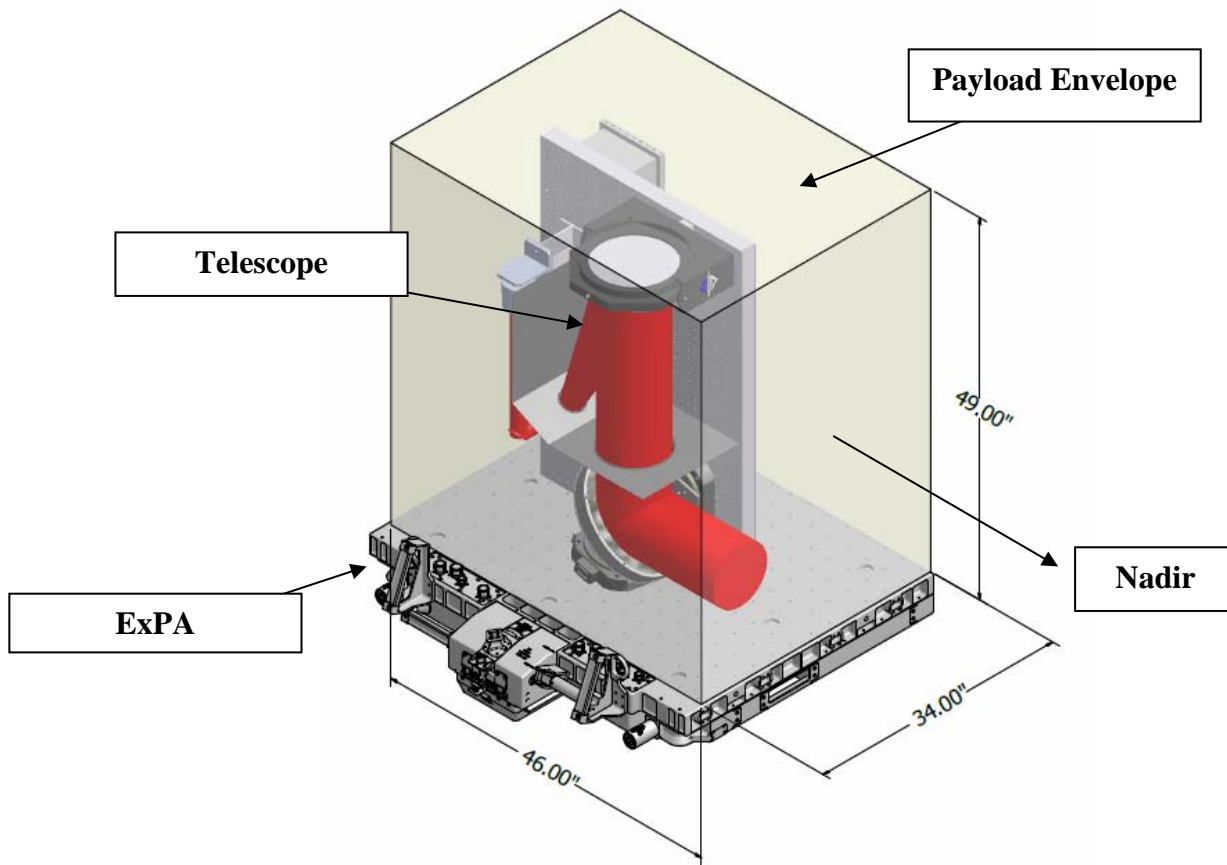


Figure 3.1: Required Telescope Configuration with ExPA (Concept)

With this configuration, a “strong-back” structure is necessitated to support the instrument. This structure needs to be a strong, stiff and lightweight design in order to meet launch and on-orbit requirements. To enable the strong-back to achieve threshold requirements, a lattice-arrangement of 0.5-inch plate 6061-T6 aluminum is designed to be milled into struts, ribs and brackets. To minimize the bolt analysis in a later phase of development, bolt sizes selected as a nominal standard around the instrument included ¼-28 UNF-3B, 8-32 UNC-2B, and 4-40 UNF-2B. Additionally, a strong-back support baseplate was designed to directly fasten to the ExPA and utilize its integrated 70 x 70 mm arrangement of ¼-28 UNF-3B threaded holes as common attachment points for the structure assembly. Figure 3.2 details the fasteners connection through the strong-back structure into the ExPA.

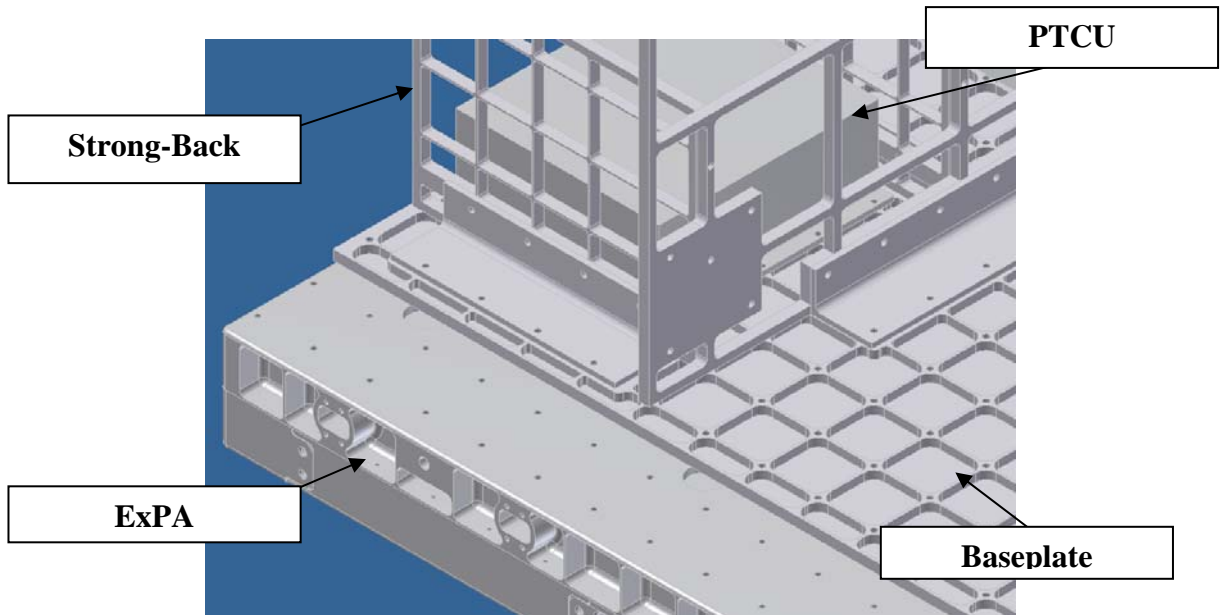


Figure 3.2: Utilization of the ExPA Fastener Configuration

Due to a lack of knowledge concerning final orientation of the payload (as the nadir direction is critical), it was deemed important to enable the design to be able to rotate about the Z-axis of the ExPA (i.e., outward from the integrating face-plate; thus, the baseplate needs to be no larger than 34-inches in the length or width directions; refer to Figure 2.10 for the ExPA associated coordinate system). The baseplate is also configured to accommodate shear boss pins in order to prevent fastener single-point-of-failure.

In an effort to light-weight the payload, another design feature in the instrument was to integrate the strong-back with the instrument computer unit (ICU) and telescope control unit (TCU) into the structural framework. This concept provided a unique challenge as these elements are hermetically-sealed enclosures intended to fly at pressure (~18 psia). The design calls for bolting the framework directly to a 0.5-inch rib around both the ICU and TCU which has vented threaded-holes integrated for securing the structure. Note, if an issue arises in the future of these devices with their face-seal, a potential solution is to integrate a male industrial static-seal gland design per Parker O-Ring handbook, ORD-5700 (versus the current face-seal design). [43] Figure 3.3 details the integrated design of the ICU/TCU with the strong-back structure.

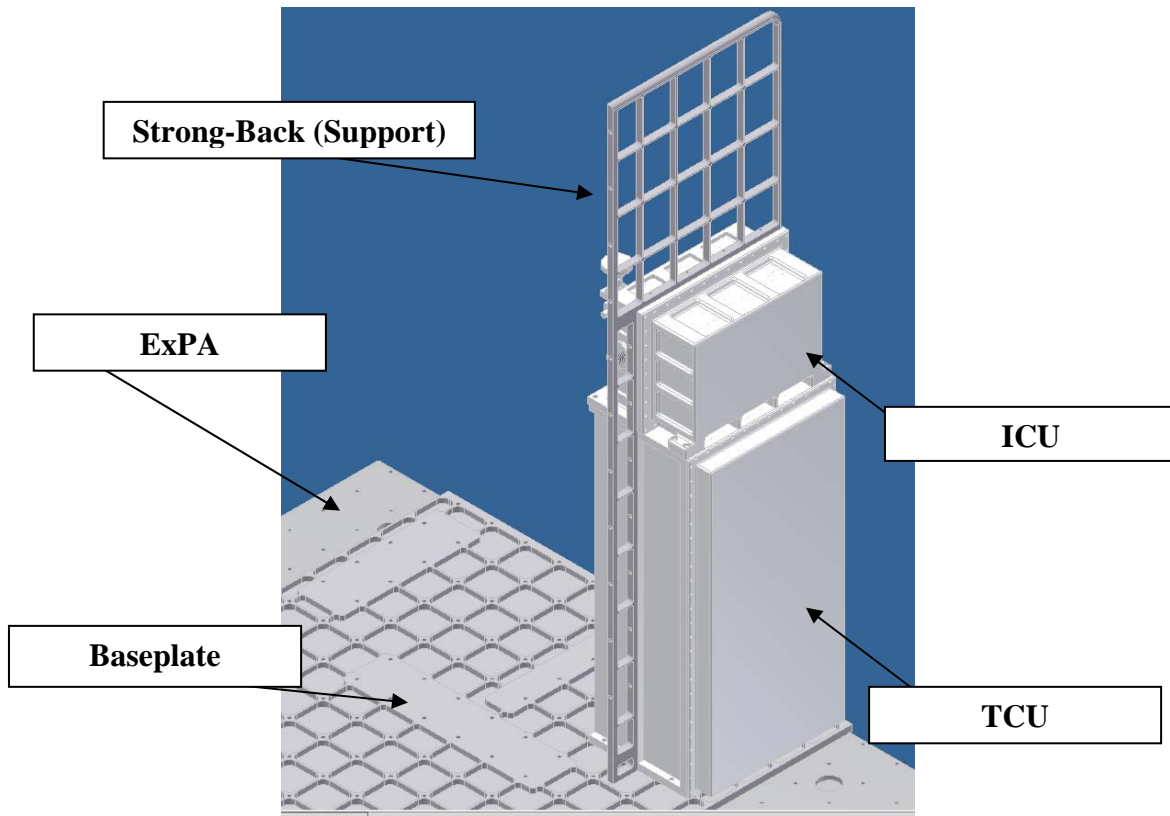


Figure 3.3: Utilization of the TCU/ICU as Strong-Back Members (Concept)

It should be noted that the TCU envelope was determined based on the intent to fly COTS electronics (e.g., motor/actuator controllers which are not space-rated). To enable operation of COTS electronics in the space-environment, a similar concept to the ICU was developed (i.e., hermetically sealed enclosure with internal convective cooling); however, to accommodate the size of the components of interest, a much larger scale was required (as a baseline, the housing is milled from a 6061-T6 aluminum billet at the dimensions of 8" x 12" x 24"). Figure 3.4 details a conceptual layout for this housing and the devices it will likely contain.

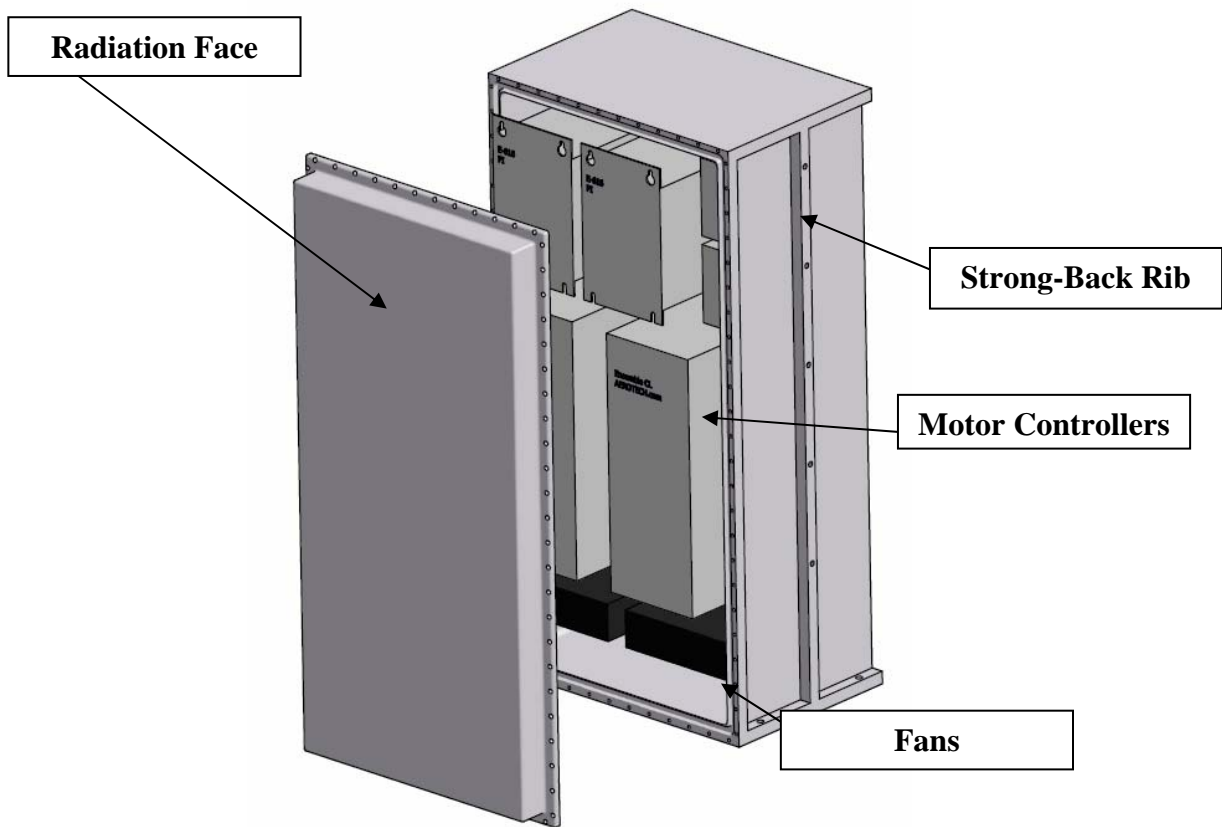


Figure 3.4: TCU Configuration (Concept)

The optical system, including the telescope, DVP/motor and camera, are all configured upon a breadboard optimized for this mission. In turn, this breadboard is affixed to a passive, compact, six degree of freedom (6DOF) vibration isolation system (based on Miller and attachment points known as the “Jewel”) and the strong-back integration baseplate. [44] Again, this baseplate is designed to be lightweight and mount directly to the structural frame members and ExPA baseplate. Four of Miller’s isolators were configured into this design with modifications being made to use ¼-28 UNF-3B fasteners versus the metric bolts originally called for. [38] Figure 3.5 shows the strong-back integration backplane.

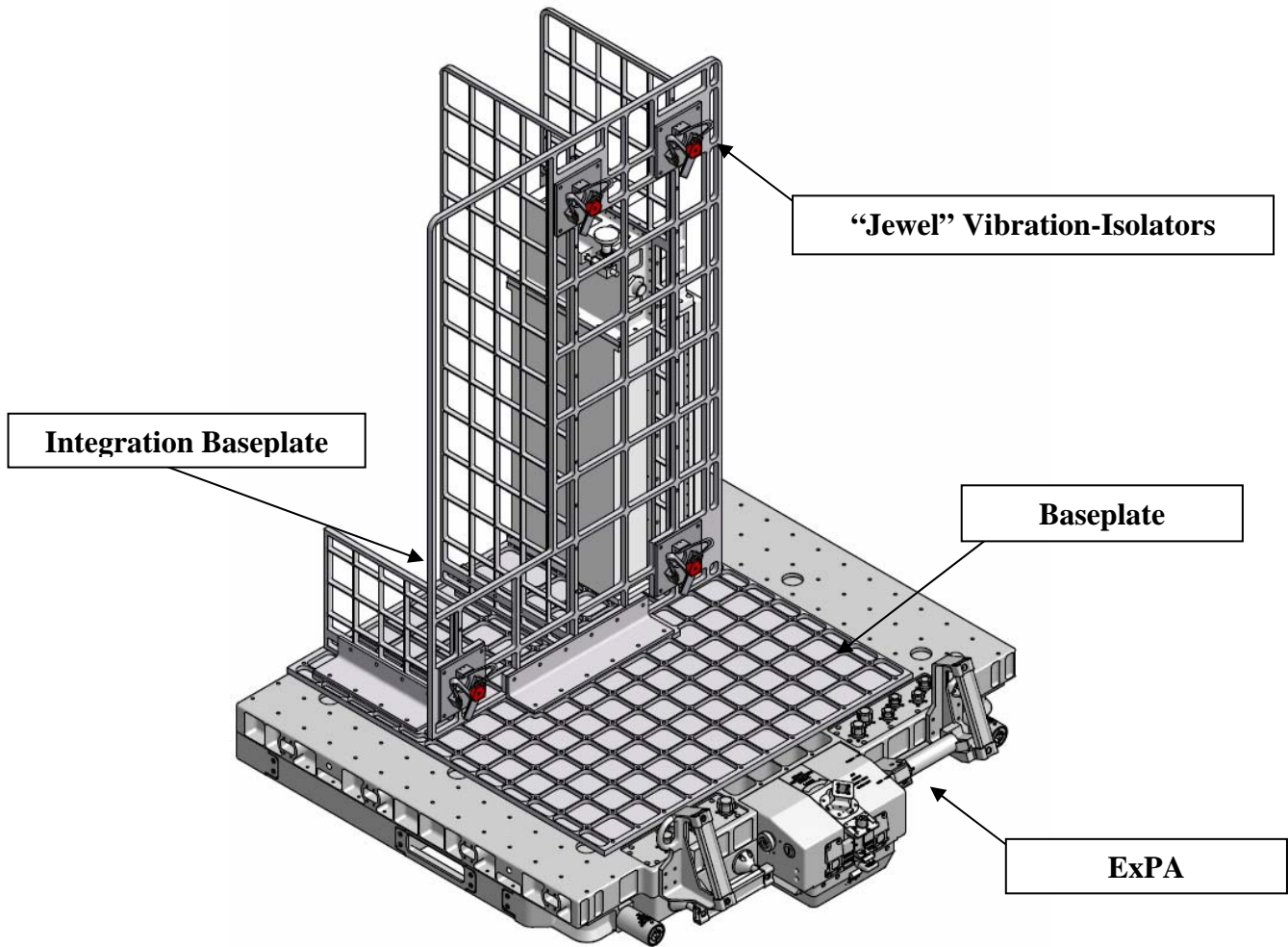


Figure 3.5: Strong-Back Configuration (Concept)

The telescope is largely unchanged from the discussion presented in Book’s review. [37] RC Optical Systems, Inc. is providing the initial design and is composed of a slew/dwell mirror, primary/secondary off-axis parabolic (OAP) mirrors, a fast-steering mirror (FSM), breadboard, baffling and control electronics (placed into the TCU). AFIT is expected to provide a field stop assembly as well as the remaining imager components (to include DVP, motor/encoder, camera and turning-mirrors/corrective optics downstream of the telescope). [44] Because this configuration places the breadboard

perpendicular to the ExPA, it was deemed necessary to wrap the optical beam through the breadboard for the motor and camera to be affixed to the rear of the instrument (mainly to reduce the overall length of the breadboard and alleviate center-of-gravity issues). To accommodate this configuration, the strong-back integration backplane was altered to allow for these features. A star-tracker will also be integrated to the optical breadboard in order to have precise attitude knowledge for instrument pointing. Figure 3.6 details the telescope and imaging unit layout.

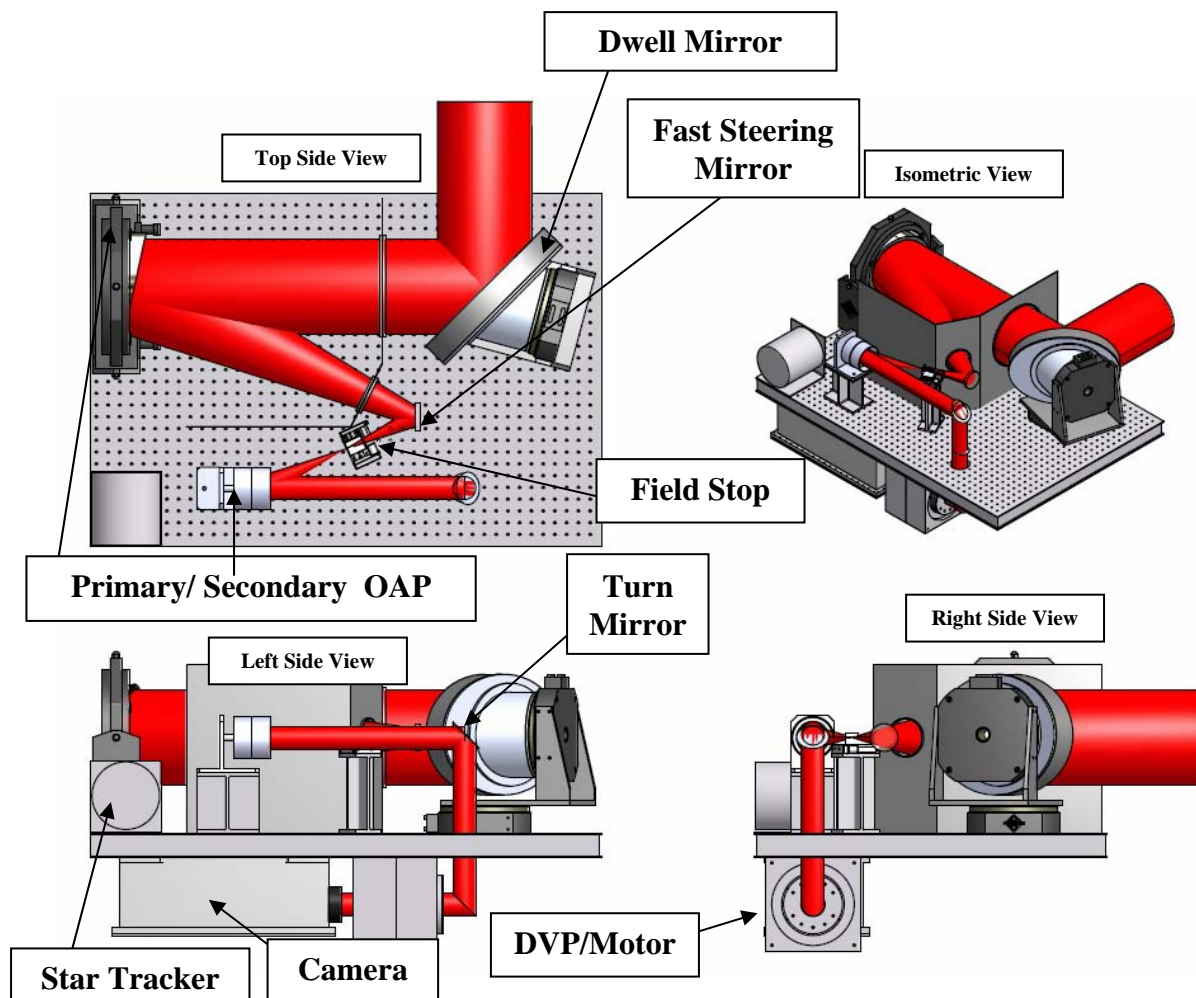


Figure 3.6: RCOS Telescope Configuration

For launch vibrational loading, a system of pinpuller and ejection release mechanisms (ERM) will be integrated into the design. Pinpullers will be applied to the slew mirror (two required, one for each actuator), FSM, and aperture mechanism. To restrain the optical breadboard, two ERM devices are intended to be mounted to the instrument baseplate. These devices will mate with a bracket and spring-loaded fastening device to “pull” the breadboard assembly down in order to stiffen the entire structure for launch. Once on-orbit, the ERMs will be commanded to release the fasteners, wherein the breadboard will slowly be released and supported solely by the 6DOF Jewel mounting system. The spring-loading on the fasteners allows the threaded portion of the system to be retracted into the bracket to mitigate issues relating to interference with the ERM devices. [45] Figure 3.7 details the concept design.

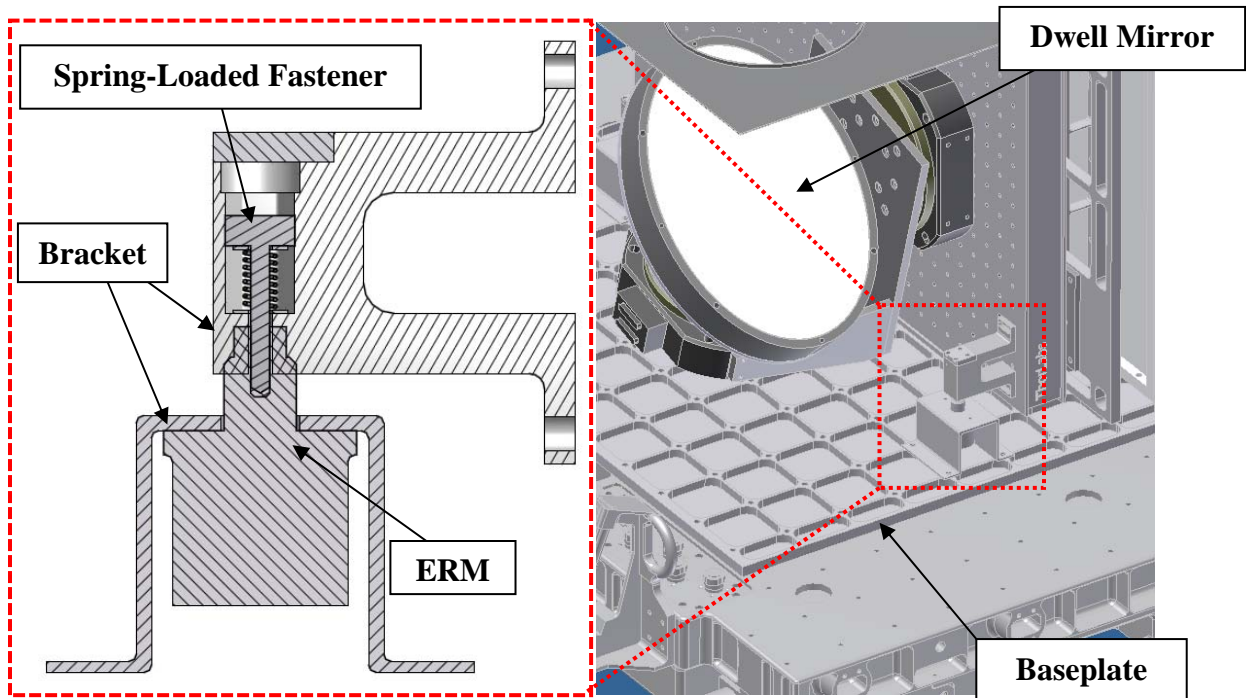


Figure 3.7: Ejection Release Configuration (Concept)

The aperture sub-system is composed of both a device to open and close the door allowing incident electromagnetic radiation to enter the instrument as well as an alignment/calibration suite of sensors to permit characterization of the system. The door mechanism is a standard four-bar link mechanism driven by a Physik Instrumente, LP S340 linear actuator capable of 50mm travel (see Figure 3.8 for detail).

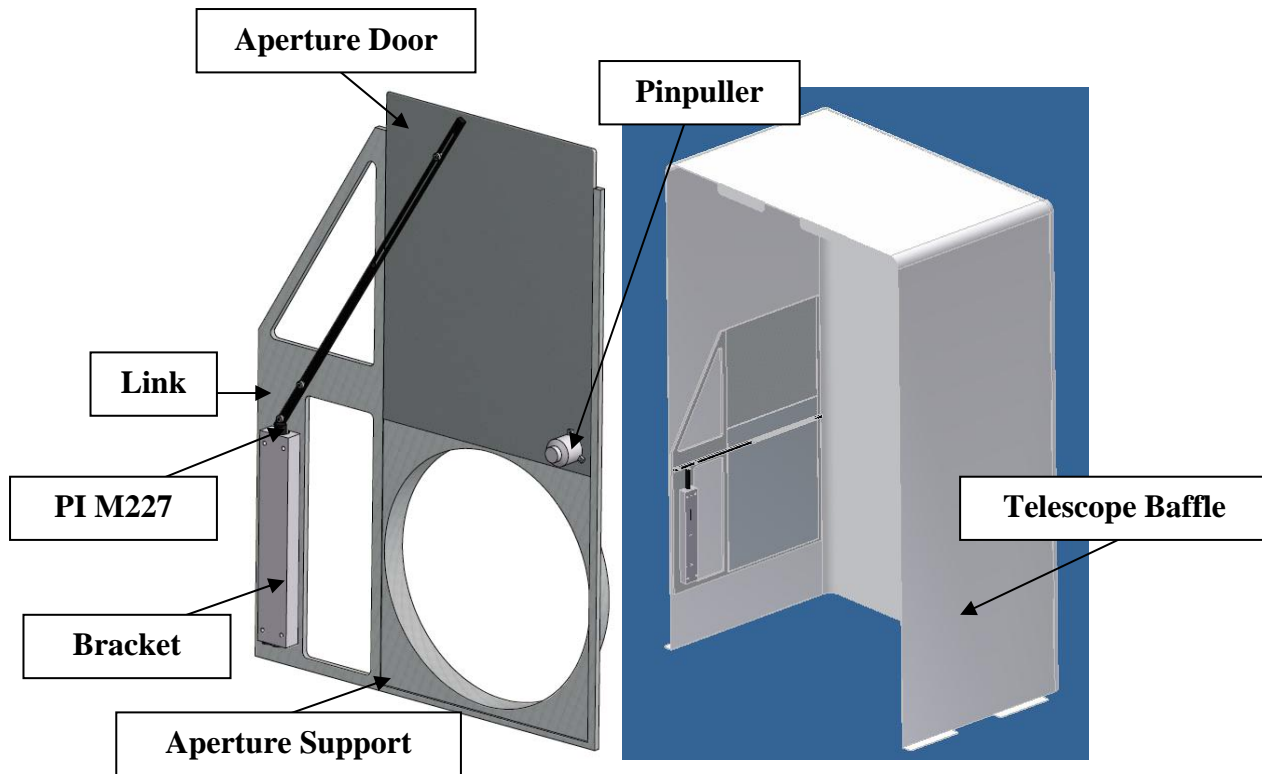


Figure 3.8: Aperture Configuration (Concept)

Because the dwell mirror is capable of +/- 8 degrees of slew, and is situated 8.5-inches from the exterior baffle, an aperture window of 11-inches diameter is required. Therefore, to open/close the aperture door, 15 inches of travel in the link arm was required to support this design. In order to prevent binding of this mechanism, a highly-toleranced shoulder-screw was utilized as the rotation pin while it will be operationally practical to ensure an optical and vacuum-compatible grease is selected for lubrication of

this link mechanism. The alignment/calibration design is still in development; however, it is anticipated that both lasers and light-emitting-diodes will be integrated into the aperture door at wavelengths throughout the spectral measurement region of the instrument to perform troubleshooting as well as trend the instrument over time. Figure 3.9 details the aperture mechanism operation.

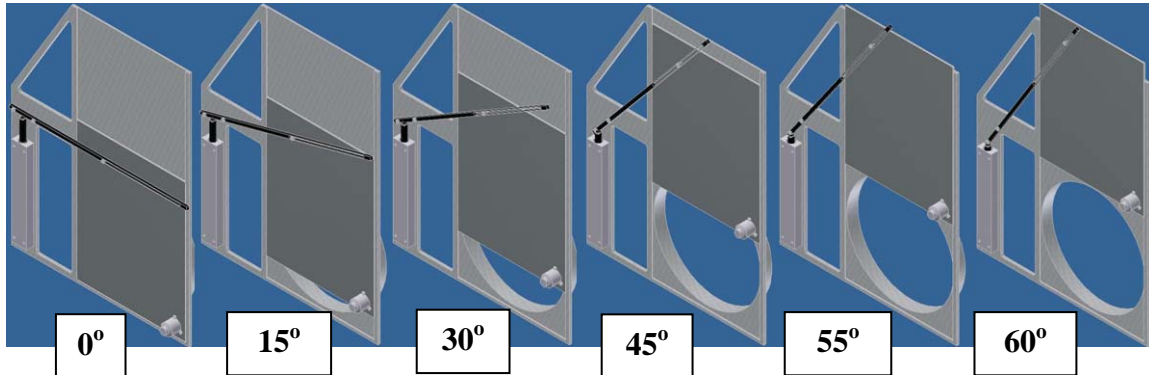


Figure 3.9: Aperture Mechanism Operation (Notional Concept)

As the most massive single component on-board this payload was anticipated to be the optical breadboard, it was a major area of attention during the design development. Initial assessments performed by RC Optical Systems, Inc called for use of an invar-style design in order to mitigate coefficient of thermal expansion (CTE) issues. [44] This decision, at the time, was deemed acceptable as the platform to integrate the instrument (i.e., the JEM/EF) allowed for higher masses in comparison with the ELC. The move to the ELC necessitated a lower mass solution for on-orbit operation, meaning that heaters needed to be implemented to maintain a constant breadboard temperature to support optical alignment. A typical aerospace component to reduce mass while upholding rigidity is an isogrid structure (“iso” meaning the plate behaves like an isotropic material and “grid” referring to the stiffener and sheet structure). [46] In this arrangement, a

material has pockets cut to retain stiffness; thus, also working well to meet mass constraints.

To perform this isogrid analysis, a process was developed to rapidly produce various breadboard configurations from a software script to then inject the outputs into a finite element modeling program to assess mass and modal properties. The code developed was produced in MATLAB and was setup to output different meshed geometries (.dat files) ready for FEMAP to perform further meshing, analysis and reporting upon each design. To validate and add confidence to the process, a similar-style isogrid 6061-T6 aluminum panel, originally intended to launch as part of the FalconSat-5 program, was acquired and tested by AFIT personnel. These test results could be compared against the model to determine appropriate mesh densities and relative error. Note that the analysis performed was a “Free-Free” type as a first-order understanding for mass properties and modal characteristics (requiring additional future analysis as this design is integrated with the remaining payload assembly).

For modeling purposes, simplifying assumptions needed to be applied and included that these plates were constructed of the same homogeneous, isotropic material and that they behave with linear properties. Because this analysis focused on a strictly modal analysis of these breadboards, no boundary conditions or static loads were applied. Additionally, the code did not include minor features such as bolt holes or milling radii which should only alter results by a small amount (in many cases, it will stiffen the breadboard to a higher level).

For this analysis, given the breadboard overall length and width (at 43.5 x 30-inches), it was determined that the four most important design variables include: breadboard thickness, pocket size, rib thickness, and pocket thickness. With these parameters, the following values were allocated and deemed appropriate initial design points for this effort (detailed in Figure 3.10):

- Plate Thickness: 0.5, 1.0, 1.5, 2.0, and 2.5 inches
- Pocket Size: 4.0, and 6.0 inches (square)
- Rib Thickness: 0.1, and 0.25 inches
- Pocket Thickness: 0.375, and 0.25 inches (depth)

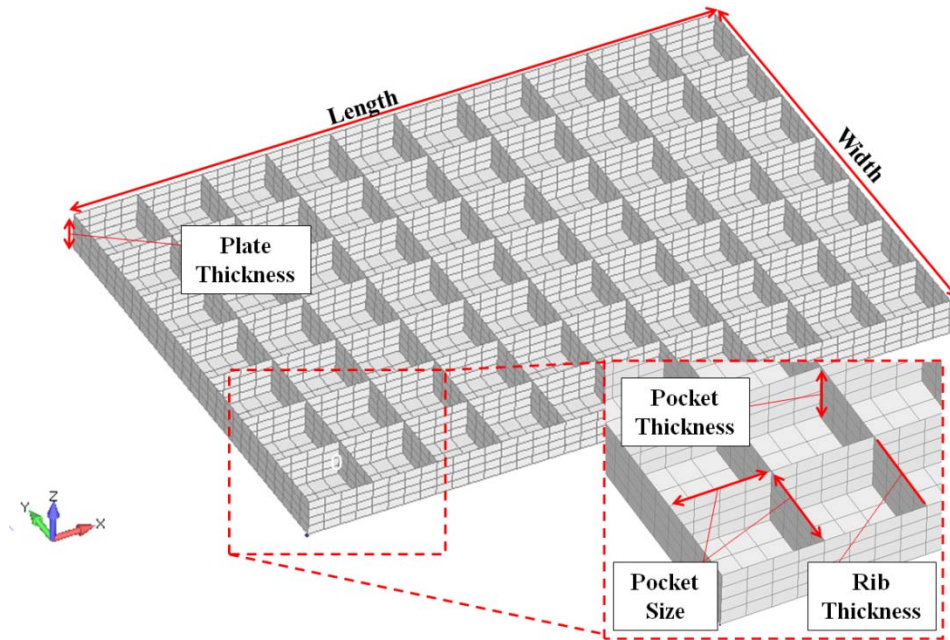


Figure 3.10: Isogrid Parameters

The primary output from this analysis was the mass of each breadboard and the first four structural natural frequencies for that design. Selection of the final

configuration will be based upon mission requirements, honed as further jitter assessments are performed. Initially, the configuration with the lowest mass and most attractive modal attributes will be selected as a potential candidate for further analysis.

The next section will detail the overarching results from the design developed and discussed within this section. Details relating to the mass, center-of-gravity, breadboard light-weighting analysis and initial finite-element stress results will be presented.

3.3 Results

From the design discussed in Section 3.2, mechanical assessments were derived from the overall layout developed for the space-based CTE_x system. These assessments include the overall mass-breakout/allocation, center-of-gravity (CG) determination, secondary payload cursory assessment, and an early light-weighting effort for the optical breadboard associated with the telescope.

3.3.1. Mass Properties. The mass breakout constitutes an important milestone in mission development as it will allow future research personnel the ability to possess constraints and objectives in final design work leading to designs for launch and on-orbit operations. In some cases, the mass determined for a sub-system is approximate and should be utilized as a future constraint (with the intent to minimize, where possible).

To begin, we start with the overall structure and strong-back mass. The strong-back structure and related mechanisms include: payload baseplate, vibration isolators, strongback supports, ejection release mechanisms and instrument external baffle. These items account for roughly 43.5 kg of the instrument. Table 3.3 details these components.

Table 3.3: Structure / Strong-Back Mass

<u>Description</u>	<u>Qty</u>	<u>Vendor</u>	<u>Model</u>	<u>Mass (EA)</u>	<u>Total Mass</u>
<i>(Name)</i>	<i>(#)</i>	<i>(Name)</i>	<i>(Name)</i>	<i>(Kg)</i>	<i>(Kg)</i>
Structure / Strong-Back					
Baseplate Payload (AL)	1	TBD	TBD	7.46	7.46
Isolator Vibe Telescope	4	AFIT (Miller)	NA	0.27	1.10
Strongback Support	1	TBD	TBD	13.19	13.19
Baffle Instrument	1	NA	NA	21.32	21.32
Ejection Release Mechanism & Bracket	2	TiNi	ERM-1000	0.27	0.53

Next, the telescope, currently provided by RC Optical Systems, Inc, constitutes roughly 98 kg of the instrument mass and includes: the breadboard, mirrors, actuators, brackets, internal baffle, star tracker and pinpuller mechanisms. Note that the breadboard currently selected is a lightweight COTS aluminum variant with excessive areas truncated to reduce mass as much as possible. This is an initial solution (expected as part of the delivery for the qualification model of the instrument); nevertheless, further discussion for mass reduction of the breadboard will be included in the next subsection. Table 3.5 details the mass from this subsystem.

Table 3.4: RCOS Telescope Mass

<u>Description</u>	<u>Qty</u>	<u>Vendor</u>	<u>Model</u>	<u>Mass (EA)</u>	<u>Total Mass</u>
<i>(Name)</i>	<i>(#)</i>	<i>(Name)</i>	<i>(Name)</i>	<i>(Kg)</i>	<i>(Kg)</i>
Telescope					
Breadboard	1	TBD	-	43.50	43.50
Mirror Slew/Dwell	1	RCOS	NA	8.11	8.11
Mirror Primary OAP	1	RCOS	NA	6.34	6.34
Mirror Fast Steering	1	RCOS	NA	0.07	0.07
Mirror Secondary OAP	1	RCOS	NA	0.20	0.20
Actuator Aperature	1	PI	M-227	0.26	0.26
Actuator FS	1	PI	PI M-122	0.22	0.22
Actuator Slew/Dwell	2	ADRS	200	7.60	15.20
Actuator FSM	1	PI	PI S340	0.34	0.34
Bracket/Mount Slew/Dwell	1	RCOS	NA	5.519	5.519
Bracket/Mount Primary OAP	1	Aerotech	AOM-110	11.213	11.213
Bracket/Mount FSM	1	RCOS	NA	0.565	0.565
Bracket/Mount FS	1	AFIT	NA	0.565	0.565
Bracket/Aperature	1	AFIT	NA	3.14	3.14
Bracket/Mount Secondary OAP	1	RCOS	NA	2.189	2.189
Bracket/Mount 90-degree Turn Mirror	1	TBD	NA	0.565	0.565
Baffle Internal	1	RCOS	NA	1.27	1.27
Pinpuller (Launch Restraints)	4	TiNi	P10-STD	0.05	0.18
Star Tracker	1	Microcosm	RadMak	1.5	1.5

The instrument computer unit (ICU) and telescope control unit (TCU) will be detailed next. The ICU (discussed further in Chapter 5) contributes roughly 10 kg and consists of the housing, fan, bracketry, PC/104 system, electrical feed-through and valve components. In a similar fashion, the TCU contributes 26 kg mass and contains the majority of the components listed for the ICU with the exception that it holds the motor controllers (instead of the PC/104 components). Table 3.5 details the mass breakout for the ICU and TCU.

Table 3.5: TCU & ICU Mass

<u>Description</u>	<u>Qty</u>	<u>Vendor</u>	<u>Model</u>	<u>Mass (EA)</u>	<u>Total Mass</u>
<i>(Name)</i>	<i>(#)</i>	<i>(Name)</i>	<i>(Name)</i>	<i>(Kg)</i>	<i>(Kg)</i>
Telescope Control Unit (TCU)					
Controller FS & AP	2	PI	C-863	0.30	0.60
Controller FSM	1	PI	E-616	0.70	0.70
Controller Slew/Dwell	2	Aerotech	Ensemble CL	3.80	7.60
Controller Motor/Encoder	1	TBD	TBD	5.00	5.00
Motor Amplifier (Required?)	1	TBD	TBD	0.50	0.50
Bracket Fan ICU R0 100929	2	NA	NA	0.1	0.3
Fan Orion OD1248-24HB	2	Orion	OD1247-24HB	0.5	1.1
Feedthru Pave Tech Co PN-1649 12-Wire	2	Pave Technology	1649	0.3	0.6
Purge Valve Assy	1	Swagelok	SS-4BW	0.9	0.9
Housing Lower TCU R0 101007	1	NA	NA	8.2	8.2
Housing Upper TCU R0 101007	1	NA	NA	1.4	1.4
Instrument Computer Unit (ICU)					
Housing Lower ICU R0b 101007	1	NA	NA	3.3	3.3
Housing Upper ICU R0b 101007	1	NA	NA	3.9	3.9
Bracket Fan ICU R0 100929	1	NA	NA	0.1	0.1
Fan Orion OD1248-24HB	1	Orion	OD1247-24HB	0.5	0.5
Plate Thermal Baffle ICU R0 101004	1	NA	NA	0.2	0.2
Parvus Cage w/ Shock Rocks	1	Parvus	PC/104 Card Cage	0.4	0.4
Printed Circuit Boards	1	TBD	TBD	0.6	0.6
Feedthru Pave Tech Co PN-1649 12-Wire	1	Pave Technology	1649	0.3	0.3
Purge Valve Assy	1	Swagelok	SS-4BW	0.9	0.9

As the final designs for the chromotomography imaging unit (CIU) and the power-thermal control unit (PTCU) are still in development, relative mass assignments were placed upon these sub-assemblies (referencing current expectations from similar ground-based CTE_x designs). Thus, the CIU accounts for 30 kg and is composed of the hermetically-sealed high-speed camera as well as the motor/encoder assembly. The PTCU will include overvoltage protection, power conditioning, and thermal control subsystems and is assigned to 10 kg mass.

Finally, we must account for a space GPS receiver, heater sub-assemblies (throughout the instrument), and miscellaneous hardware/wiring (e.g., fasteners, spacers, lock-washers, various gauge wiring, etc.). For hardware and wiring, we assume a gross

nominal mass of 10% above the summation of all other subsystems and components (for initial rough-order-of-magnitude estimation). Additionally, although a very small portion of the overall mass, the electrical heater subsystem will require four-to-five unique survival sub-systems (including: during launch, on-orbit rendezvous, and on-orbit processing) as well as for operational/alignment purposes. These miscellaneous systems account for roughly 29 kg of the overall mass and are detailed in Table 3.6.

Table 3.6: Miscellaneous Subsystem Mass

<u>Description</u> <i>(Name)</i>	<u>Qty</u> <i>(#)</i>	<u>Vendor</u> <i>(Name)</i>	<u>Model</u> <i>(Name)</i>	<u>Mass (EA)</u> <i>(Kg)</i>	<u>Total Mass</u> <i>(Kg)</i>
Misc.					
Heater Assembly	5	TBD	TBD	1.00	5.00
Space GPS Receiver	1	Surrey	SGR-07	0.45	0.45
Hardware & Wiring (Assume 10% Add'l)	1	TBD	NA	23.84	23.84

Altogether, the instrument currently comes in at ~250 kg mass. At this mass, the payload is certainly over the mass constraint levied by the ExPA requirement. Light-weighting will be discussed further in the next subsection where the mass could be dropped in the breadboard down to roughly 10 kg, equating to an instrument at ~216 kg.

Next, the CG for the CTEx instrument affixed to the ExPA pallet meets the requirement of being +/- 7.5 inches deviation from the geometric center in the X-Y payload plane and at a maximum height of 19.5 inches in the Z-payload above the ExPA plate mounting-plane. The current design comes in at 1.18 inches and 0.364 inches deviation in the X and Y payload axes, respectively. The payload height CG is at 11.565 inches overall. Figure 3.11 details the location of the CG as well as the internal aspects of the payload.

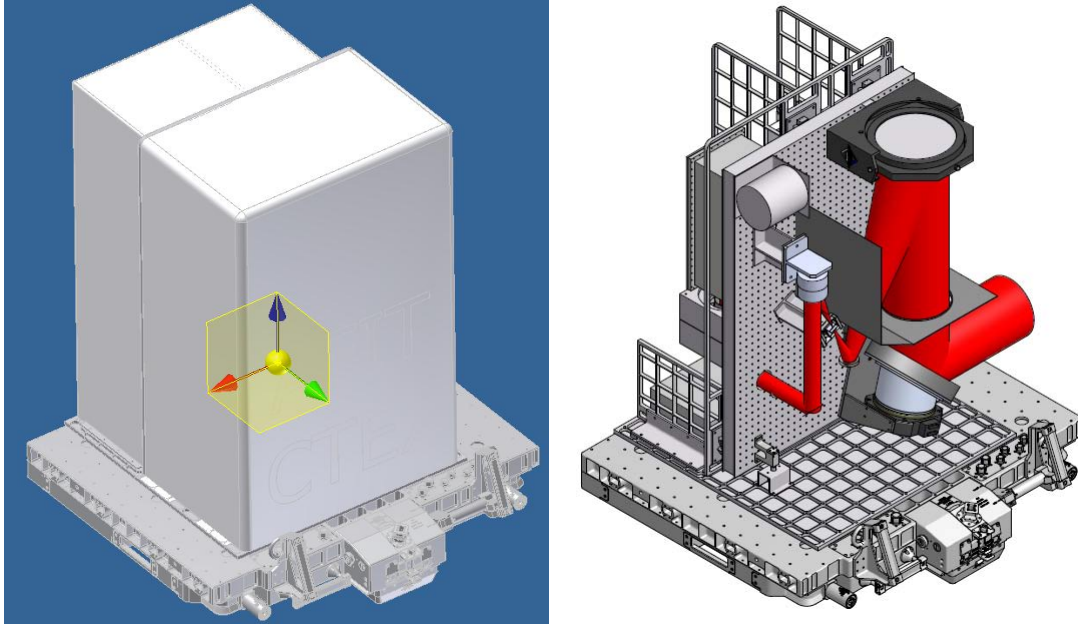


Figure 3.11: Space-Based CTEEx CG and Configuration

As a very cursory review of the secondary payload options for incorporation into the CTEEx platform, it currently does not seem feasible to add additional hardware to the design as there is little mass budget to allow for these additional mission requirements. Options to add a camera or remove the DVP will likely add more mass than can be afforded currently. Application of other options such as a micro-channel plate between the detector plane and the telescope to acquire “night-vision” may be a minimal effort which could be accomplished for minimal mass; however, further investigation will be needed here and will be discussed further in Section 6.1 and 6.4, conclusions and future work, respectively.

3.3.2. Breadboard Lightweighting. As discussed earlier, the single-most massive component currently on-board the experiment is the optical breadboard. To enable this design to meet launch and on-orbit requirements, mass must be reduced as

much as possible. Following the methodology discussed in Section 3.2, an iterative design process was performed in order to determine a possible solution for further development.

To begin, a validation of the analysis process had to be accomplished to assess the mesh density and associated error. Utilizing the FalconSat-5 isogrid as a baseline to provide confidence in this process, mesh sizes of 4.0, 2.0, 1.0, 0.5 and 0.25 inches (square) were assessed to determine the effect to mode 7 (initial bending mode, after the initial six rigid-body modes). Figure 3.12 details the results from this validation effort.

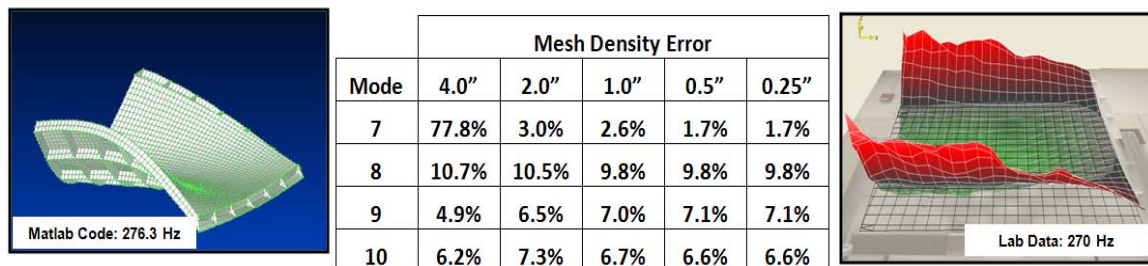


Figure 3.12: Isogrid Mesh Density Validation (Compared Against Test Data)

From this assessment, it was deemed that a 1.0-inch mesh density resulted with an acceptable level of error while balancing the processing time required. With that information in hand, the isogrid rapid-generation script was populated with the parameters required for analysis (specific values indicated previously in Section 3.2), and each finite element data file was imported, refined and analyzed. Figure 3.13 details the mode shapes acquired and Table 3.6 reports the results from this effort.

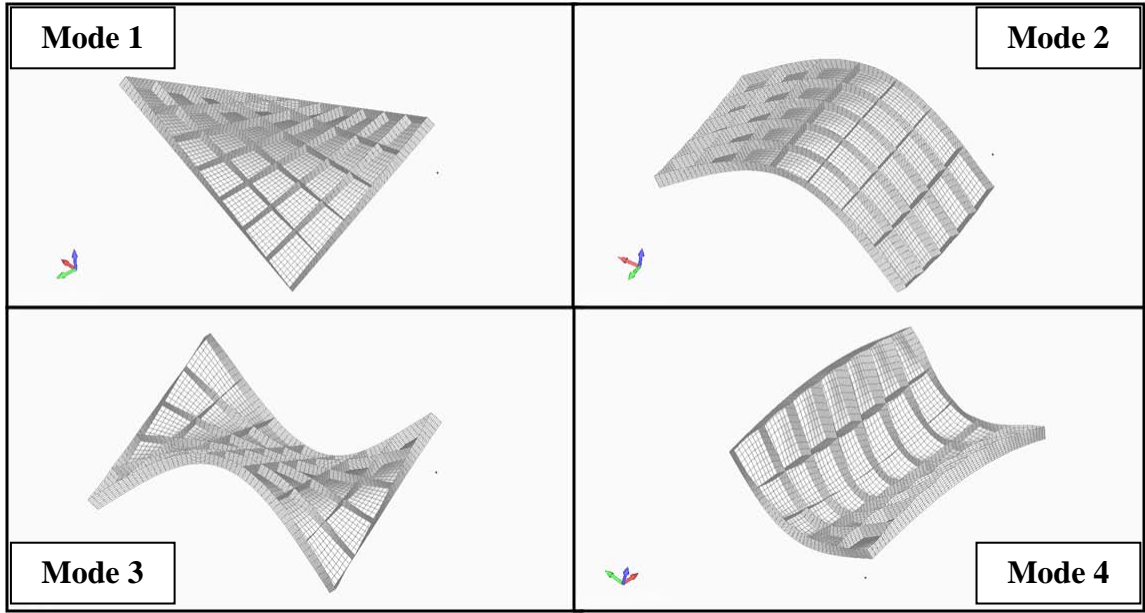


Figure 3.13: Typical Breadboard Isogrid Mode Shapes

Table 3.7: Optical Breadboard Isogrid Process Results

Case No.	Description				Mass Properties		Modal Properties			
	Plate Thickness	Pocket Size (LxW)	Rib Thickness (t)	Pocket Thickness (D)	Mass	Mass	Mode 1	Mode 2	Mode 3	Mode 4
Units	(in)	(in)	(in)	(in)	(lbm)	(Kg)	(Hz)	(Hz)	(Hz)	(Hz)
1	0.5	Solid Board, 0.5-inch Thickness (No Isogrid)			62.04	28.17	87.70	89.31	143.09	170.95
2	0.25	Solid Board, 0.25-inch Thickness (No Isogrid)			31.02	14.08	44.42	45.61	72.57	87.14
3	0.5	4	0.1	0.375	48.74	22.13	34.99	43.57	84.05	93.61
4	0.5	4	0.1	0.25	33.60	15.25	23.26	34.65	59.58	72.74
5	0.5	4	0.25	0.375	49.95	22.68	33.85	46.89	84.13	98.94
6	0.5	4	0.25	0.25	36.01	16.35	22.81	40.81	63.24	84.07
7	0.5	6	0.1	0.375	48.82	22.16	35.17	42.70	83.86	91.76
8	0.5	6	0.1	0.25	33.76	15.33	23.41	32.99	58.91	69.15
9	0.5	6	0.25	0.375	49.08	22.28	34.13	45.45	83.83	95.78
10	0.5	6	0.25	0.25	34.28	15.56	22.79	38.45	61.89	78.54
11	1	4	0.1	0.1	19.34	8.77	9.97	80.30	89.17	159.94
12	1	4	0.1	0.25	38.44	17.43	22.85	65.34	84.65	132.23
13	1	4	0.25	0.1	29.26	13.27	18.07	92.51	103.85	184.56
14	1	4	0.25	0.25	48.36	21.93	23.90	82.95	101.20	166.44
15	1	6	0.1	0.1	17.62	7.99	9.74	73.50	84.87	142.35
16	1	6	0.1	0.25	36.71	16.65	23.18	59.50	81.33	118.59
17	1	6	0.25	0.1	24.95	11.32	16.65	88.23	101.24	170.88
18	1	6	0.25	0.25	44.04	19.98	23.73	76.78	97.56	150.81
19	1.5	4	0.1	0.1	22.65	10.27	10.47	129.64	139.90	256.33
20	1.5	4	0.1	0.25	41.74	18.93	22.23	106.14	123.99	211.49
21	1.5	4	0.25	0.1	37.53	17.02	21.90	140.17	151.75	278.28
22	1.5	4	0.25	0.25	56.62	25.68	25.35	131.12	148.48	260.50
23	1.5	6	0.1	0.1	20.06	9.10	9.98	120.44	134.66	230.34
24	1.5	6	0.1	0.25	39.15	17.76	22.63	96.12	117.75	187.37
25	1.5	6	0.25	0.1	31.06	14.09	19.47	135.90	149.68	261.19
26	1.5	6	0.25	0.25	50.15	22.75	24.41	122.50	143.44	237.09
27	2	4	0.1	0.1	20.06	9.10	9.98	120.40	134.66	230.38
28	2	4	0.1	0.25	45.05	20.43	21.69	150.85	169.13	297.30
29	2	4	0.25	0.1	45.80	20.77	25.21	185.14	196.01	365.51
30	2	4	0.25	0.25	64.89	29.43	27.15	179.72	196.50	354.23
31	2	6	0.1	0.1	25.96	11.77	11.13	178.63	189.41	350.40
32	2	6	0.1	0.25	41.60	18.87	22.06	137.21	160.70	263.70
33	2	6	0.25	0.1	37.16	16.86	21.73	181.30	194.80	345.60
34	2	6	0.25	0.25	56.26	25.52	25.25	169.75	191.29	325.15
35	2.5	4	0.1	0.1	29.26	13.27	11.96	226.13	236.24	439.60
36	2.5	4	0.1	0.25	48.36	21.93	21.32	196.94	215.88	384.09
37	2.5	4	0.25	0.1	54.06	24.52	28.41	227.72	236.81	446.66
38	2.5	4	0.25	0.25	73.16	33.18	29.29	227.13	242.93	444.11
39	2.5	6	0.1	0.1	24.95	11.32	10.67	214.24	230.91	397.41
40	2.5	6	0.1	0.25	44.04	19.98	21.56	180.27	205.95	341.99
41	2.5	6	0.25	0.1	43.27	19.63	23.79	224.36	236.48	423.72
42	2.5	6	0.25	0.25	62.37	28.29	26.26	216.53	238.03	410.73

From a preliminary assessment, the final breadboard mass might be reduced by nearly 75%, depending upon the extent stiffening occurs as other elements of the system are assembled (resulting with an overall payload mass of 216 kg, down from 250 kg). A minimum requirement for the ExPA is to achieve greater than 35 Hz as a fundamental

frequency for the payload, thus a more likely reduction may be in the realm of 50% (~20 kg total mass).

3.4 Space-Based CTE_x Design Summary

This chapter covered the space-based CTE_x overarching mechanical requirements, design methodology and results for early assessments in determining the instrument mass properties. Overall, it was determined that the design can meet minimum requirements; however, further work is warranted to better map the trade space. Conclusions from this work will be identified in Section 6.1 and future work contained in Section 6.4.

IV. Ground-Based CTE_x Design/Characterization

This chapter discusses the requirements, design philosophy, validation methodology and results from a developmental iteration of the ground-based CTE_x hardware. The intent of this effort is focused upon supporting the acquisition of higher-fidelity field data as well as incorporating on-orbit alignment and calibration schemes into the ground-based instrument design. Conclusions from this effort are indicated in Section 6.2 with recommendations for future work in Section 6.4.

4.1 Design Requirements

As discussed in Section 2.1, AFIT research personnel (Book, O'Dell, et al.) designed, fabricated and characterized an initial ground-based instrument to support the CTE_x science and algorithm development. This work was largely successful; however, three factors attributed to revising this instrument, including: design changes in fundamental aspects of the device (e.g., prism and motor), new-information about the on-orbit concept of operations, and lessons learned while in the field. Figure 4.1 details the original/previous design iteration of the ground-based CTE_x (GCTE_x) instrument.

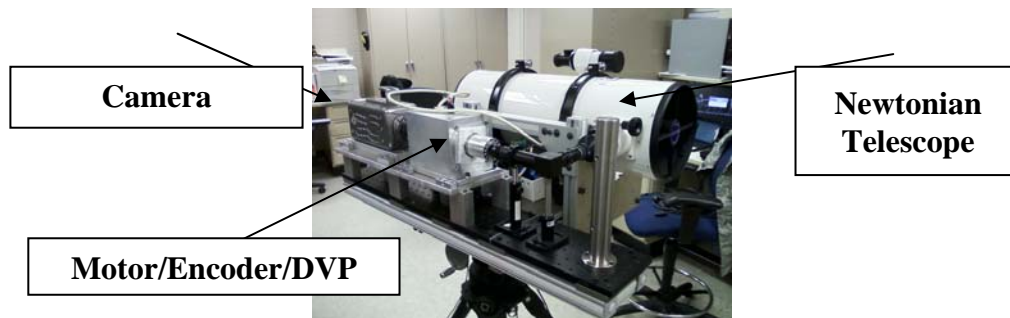


Figure 4.1: GCTE_x, Newtonian Telescope Configuration

Regarding fundamental changes in the instrument, the most notable change is to the direct vision prism (DVP). The current design (an octangular 1.5”(L) x 0.825” (W) geometry constructed of optically-bonded Schott LaSF N30 and SFL6 glass 8) will grow in size and complexity. The intent is to validate the intended on-orbit configuration DVP (which will receive a two-inch diameter incident electromagnetic (EM) radiation beam from the telescope, currently on contract). Therefore, to account for this increase in incident beam width from that of the ground-instrument, a 2.26-inch diameter DVP is in development. Additionally, to account for internal reflection concerns, three-to-four individual constituent prisms will compose the updated DVP design. The surfaces of the different prisms may or may not be in optical contact with each other; nevertheless, a 60-degree angle is currently planned at each interface. See Figure 4.2 and Figure 4.3 for further detail.

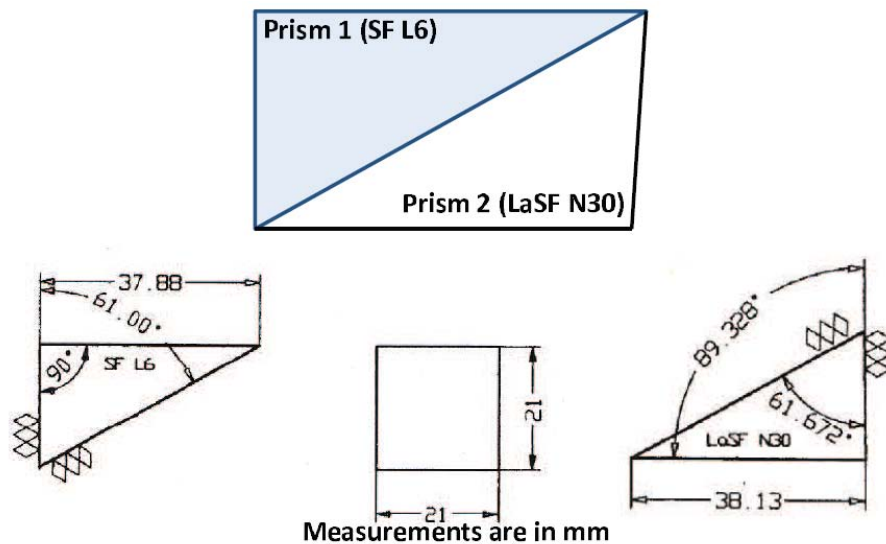


Figure 4.2: Original DVP (Dimensions in Millimeters) [6]

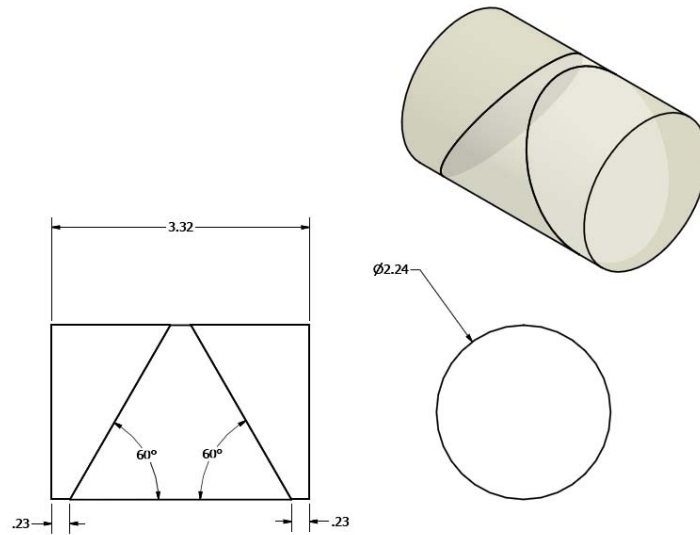


Figure 4.3: Updated DVP (Dimensions in Inches)

The result of this reconfiguration impacts the size of the ground-based CTE_x mounting shaft, motor/encoder and many other upstream/downstream components within the system. Therefore, an updated motor/encoder design had to be developed to accommodate this redirection.

Next, a portion of the on-orbit alignment and calibration methodology calls for placement of a suite of lasers and light-emitting-diodes (all at different wavelengths) within the aperture cover. The overall intent is to continually track alignment trending as well as account for deviation in calibration in order to better apply corrections to data collected. To validate these methodologies on the ground first, the current configuration CTE_x (designed around a Newtonian telescope) was not best suited for the alignment and calibration schemes currently in work. Thus, an alternate design needed to allow for process validation efforts.

Finally, lessons learned from field collection events proved the device needed design improvements in order to alleviate anomalies as well as missed collection opportunities. These issues witnessed in the field included: alignment, stray-light, ruggedization, wiring, electrical power, lifting points, screen visibility and training concerns.

Therefore, in an effort to mitigate the above issues while capitalizing on improvements to validate the science and on-orbit operations, the following requirements were established.

- Incorporate updated DVP designs into the configuration (encompassing all necessary up- and down-stream effects)
- Implement alignment / calibration methodologies to simulate on-orbit operations
- Correct known issues: alignment, stray-light, ruggedization, wiring/electrical power, lifting points, screen visibility and training
- Reduce turns in the optical path
- Utilize commercial, off-the-shelf (COTS) lens systems and other hardware components as much as possible
- Make use of current hardware as much as possible
- Incorporate lessons learned from previous iterations of the instrument
- Create standard operating procedures for instrument field collection and operations/maintenance
- Retain the ability to revert back to the Newtonian telescope, if desired

We will now discuss the design philosophy and validation behind accomplishing the above requirements.

4.2 *Design and Validation Methodology*

This section is broken into two sub-sections, including the ground-based CTE_x design development and the validation methodology. Results will be reported in the following section covering the performance and comparison to the previous version of this instrument.

4.2.1. Ground-Based CTE_x Design Development. As indicated in the previous section, the overall design and validation objective is to continue the development effort to acquire high-fidelity data while characterizing operational elements of the future space-based design. It is therefore critical to scale fundamental components (e.g., DVP) to the intended flight specifications in order to learn as much as possible and mitigate major on-orbit issues. Starting with the updated prism design specifications, we begin by assessing the assembly to constrain this device. The previous versions of the DVP holder was a cylindrical design that contained two separate restraints, one custom internal holder interfacing with the octangular DVP and another external housing which clamped the internal subassembly with nylon spacers and set-screws. There is the ability in this configuration for adjustment; however, it comes at the cost of potential issues in acquiring high-precision alignment (e.g., potential alignment issues upon rotation of the DVP). While some of this design works very well, those aspects which seemed beneficial were carried over to the updated design (e.g., nylon compression retainers,

cylindrical holder design, and alignment pins, etc.). One aspect which was modified slightly from the previous design was that of the holder which had been cantilevered over the end of the motor (attached at the end of the AISI 1018 steel shaft). It will now be internally mounted and reconfigured as a “pin-into-socket” style interface. The advantage here again relates to the overall alignment (especially as the size and mass grow, cantilevering this new prism will likely negatively affect other performance aspects such as bearing life). To accommodate this larger prism, a collar diameter of three-inches was selected as a standard size interface, providing the ability of this new holder design to be balanced through removing material in the wall. Figure 4.4 and 4.5 detail the old and new configuration of these DVP holders.

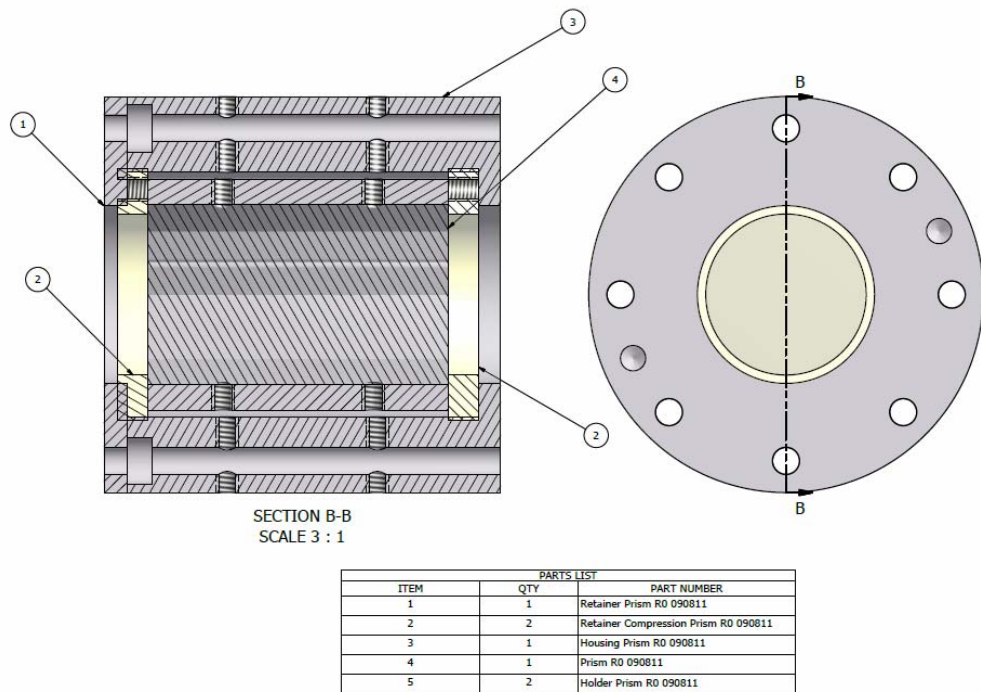


Figure 4.4: GCTEx Section-View, Previous DVP Holder Design

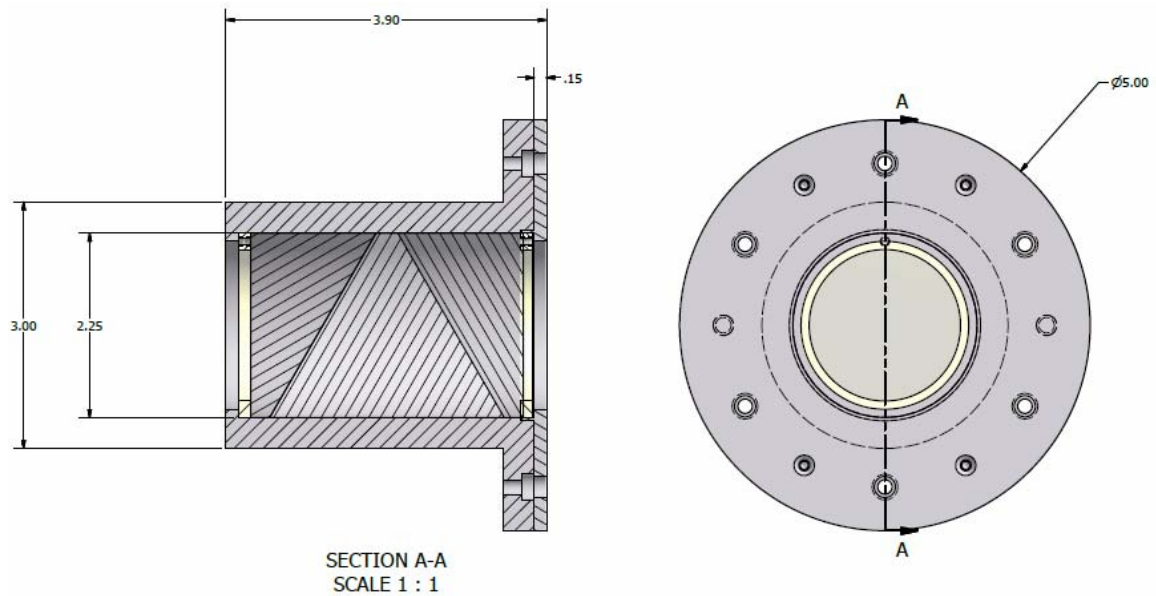


Figure 4.5: GCTEx Section-View, Updated DVP Holder Design

The next interface to this design comes at the motor/encoder shaft. It was decided, after review of several concepts, that a hollow-shaft with a concentric motor/encoder would provide optimal results relating to alignment and vibrational loading (as opposed to an off- or parallel-axis motor with a belt/chain power-transfer assembly to the DVP). Thus, to accommodate such a large diameter hollow-shaft and concentric motor/encoder that a 6061-T6 aluminum housing measuring roughly 8" x 8" x 8" would be necessary. This spatial dimension would now drive many other factors related to the remaining instrument integration; nevertheless, it meets the design intent to incorporate the new DVP into the design. Figure 4.6 details the generics of this updated motor/encoder assembly.

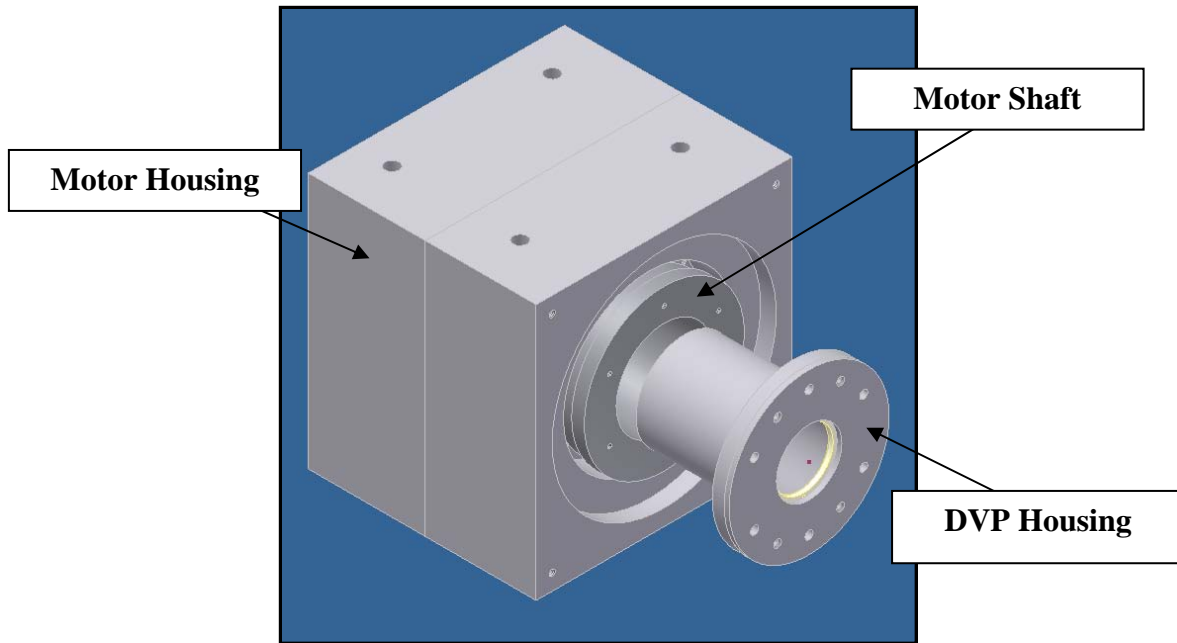


Figure 4.6: Updated GCTEx Pin-into-Socket DVP Holder & Motor/Encoder

In order to alleviate the issues and satisfy design requirements (noted in Section 4.1), a “linear” approach was offered as a potential solution. This linear-style ground-instrument would focus on maintaining a constant centerline through the entire device via specifying high geometric and dimensional tolerances on all interfaces. Additionally, a 400 mm focal length telephoto lens (Nikon AF-5 Nikkor) was allocated to the program to replace the Newtonian telescope (Vixen R200SS). Optical components on the instrument to be maintained, include: high-speed camera, COTS lens systems (lens two, Tamron 75mm; and lens three, Nikon AF Nikkor 85 mm), field stop adjustable orifice, as well as the majority of the control electronics. The electronics would be relocated from on-board the instrument to a portable rack-mount container for ease of handling and ruggedization. In effect, this concept satisfies the requirements to reduce optical turns, implement

lessons learned, and use current hardware/COTS lens systems. Figure 4.7 is an early concept drawing for this development.

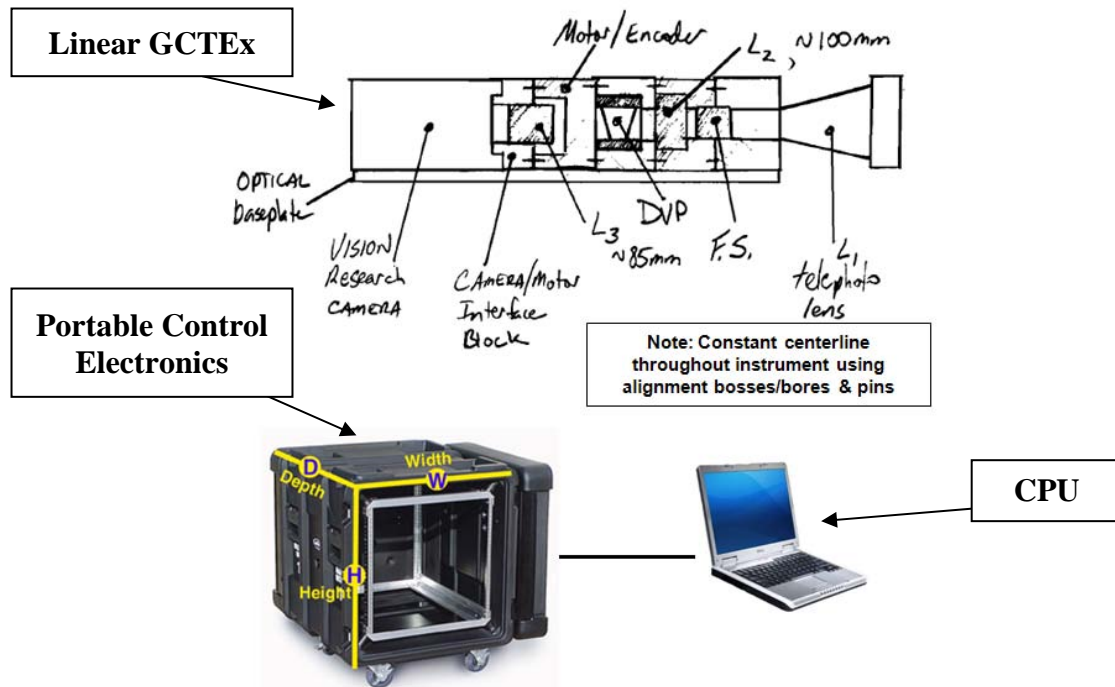


Figure 4.7: GCTEx Linear System Concept

Next, we will discuss the elements of this design providing the high-degree of tolerance to the instrument alignment. In essence, components fore and aft of the prism need to be kept in close alignment with one another, both in terms of the final two-dimensional target position as well as the angle of incident rays as they traverse to the detector plane. The components which must be kept in this alignment to the DVP include: the primary aperture optic (telephoto lens), field stop, re-collimating lens (L2), focusing/detector lens (L3) and the camera. To accomplish this, high-tolerance interfacing blocks were determined to be a solution to this problem (two, in all, one each up- and down-stream of the motor/encoder block). Each block is meant to contain

features which allow concentricity to be held through bores, bosses and alignment pins. Due to the fact that COTS lens systems were used, standard F-mount receivers were procured and modified to allow for this design philosophy. Additionally, utilizing the ThorLabs, Inc. Cage Mounting scheme (a laboratory-standard optical configuration) allowed components to easily align and configure together. Finally, camera mounting was performed in a similar manner through applying a special boss into its integration block and supporting it with a structural shim at a specified height. These alignment features are detailed in Figure 4.8 and Figure 4.9.

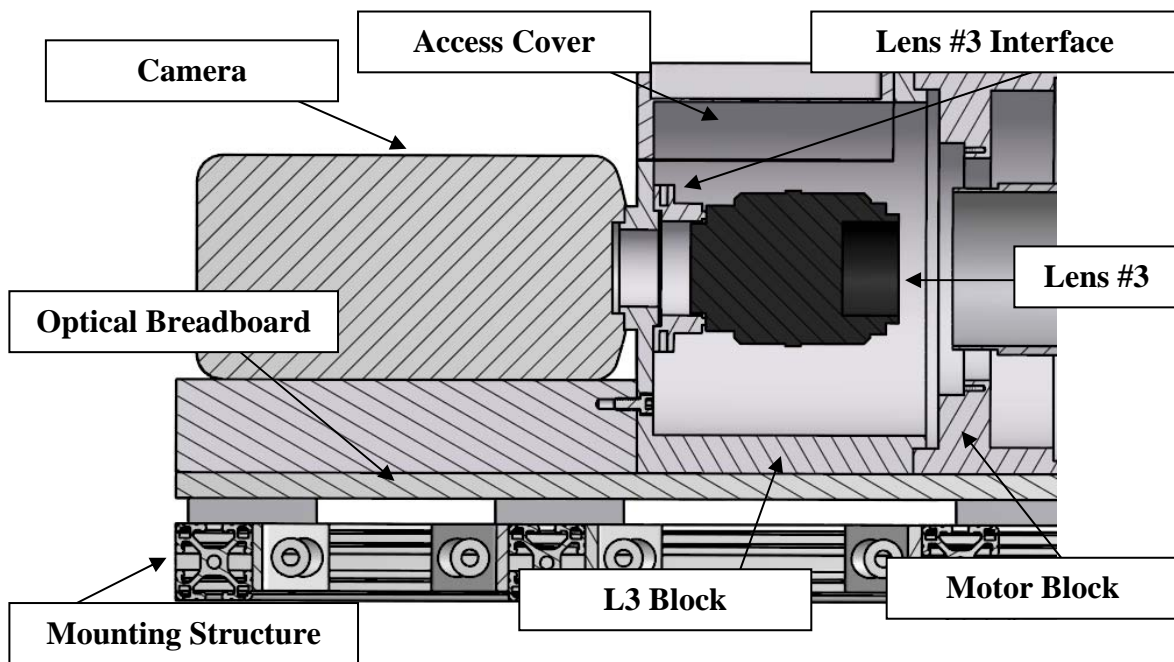


Figure 4.8: GCTEx Section-View, L3 Interface Block

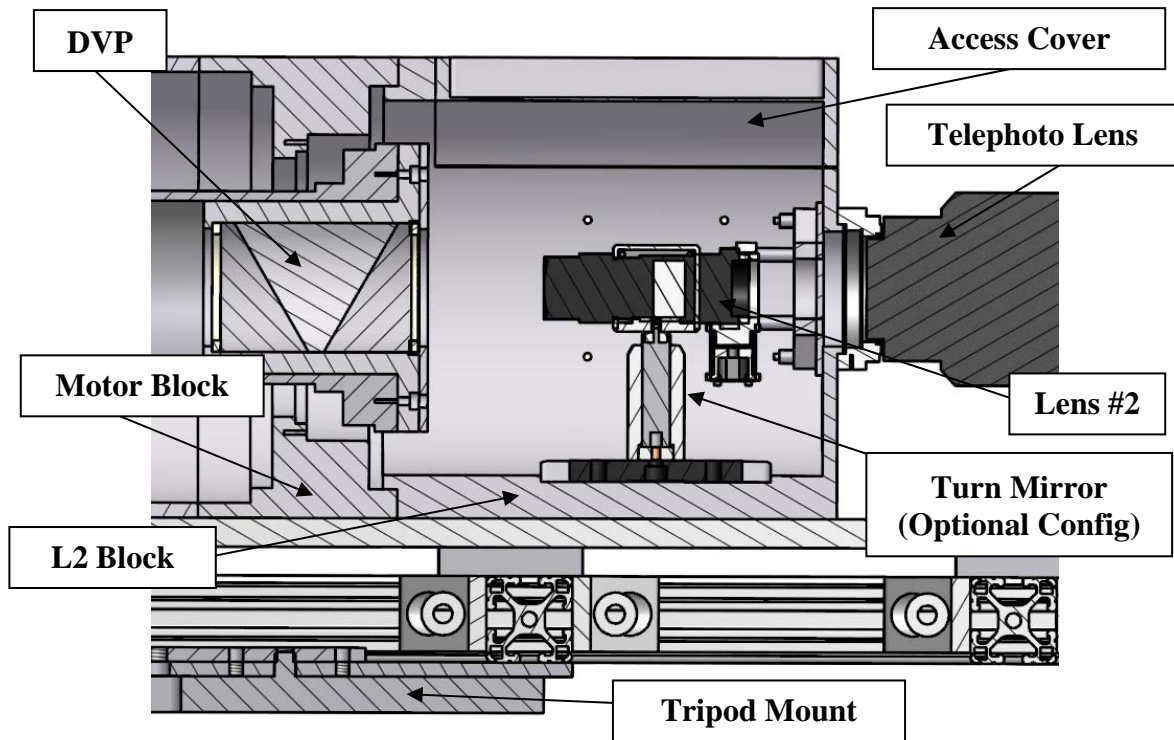


Figure 4.9: GCTEx Section-View, L2 Interface Block

A linear translator was used to ensure the proper focus. The Flange Focal Distance (FFD) is the distance between a lens mounting surface (i.e., the flange) and the image focusing point. [47] It is critical that this distance be exacting in order to achieve good image quality (as reference, the F-mount FFD is 46.50 mm whereas the C-mount is 17.52 mm). [47] Another element placed in the optics train to support this proper alignment is a linear translator (ThorLabs, Inc. SM1Z). The intent here is to provide the ability to set a crisp focus setting for the recollimating lens. Figure 4.10 presents this configuration.

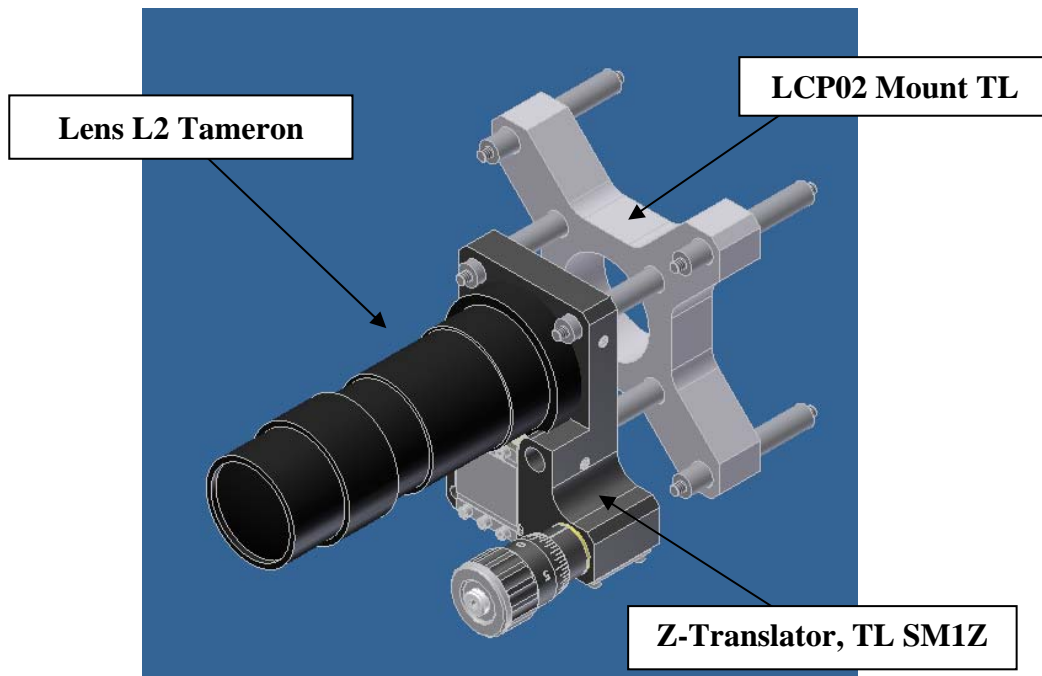


Figure 4.10: L2 Configuration

The structure which supports the optical components is composed of a COTS 36" (L) x 6" (W) optical breadboard (for alignment purposes) coupled with a frame consisting of an 80/20®, Inc. commercial-grade extruded aluminum truss. As there were concerns identified with the previous version of the instrument relating to lifting points, handles were integrated at convenient positions on the structure permitting easier two-person lifts. Spacers and integration plates allow for mounting to a Moog Hercules tripod (capable of supporting up to 150 pounds). [49] With the overall mass of the instrument at approximately 100 pounds, the center of gravity (CG) was critical to assess for the safety of the test team and instrument. Thus, the CG was placed directly over the baseplate of the instrument which interfaces to the tripod. Figure 4.11 details the structure of the instrument.

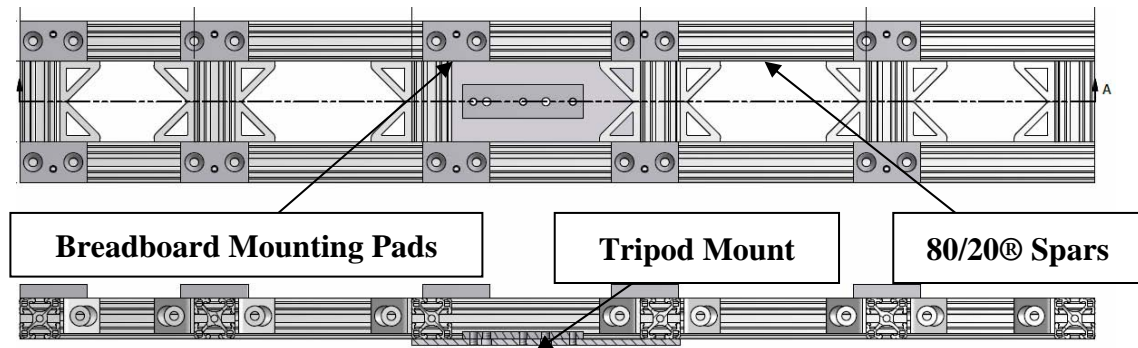


Figure 4.11: GCTEx Linear System Structure

Additional features of the instrument to improve issues witnessed in the field include access-covers, relocating the electronics off of the instrument (to a portable rack-mounted structure), and ruggedizing the electronics as much as possible. The access covers are meant to prevent stray-light and contaminants from entering the system while allowing test personnel the ability to manipulate the optics. Due to the frequent occurrence of wiring issues both in the laboratory and the field, it was also prudent to rewire the instrument and ruggedize the electrical connections to mitigate future issues (e.g., strain-relief, heavier-duty gauge wire, and mil-spec pin-and-socket style connections applied to the electronics to allow ease to setup and securing). Screen visibility was corrected through allocation of an updated computer with contrast and brightness settings which far exceed the previous unit. The rack-mounted electronics box also served as a platform to expand the device functionality as future racks may be integrated to support further in-the-field science research (e.g., the upgraded motor/encoder device controllers and Vision Research Signal Acquisition Module-3 may easily be integrated within the system). Figure 4.12 depicts the portable rack mount control box.

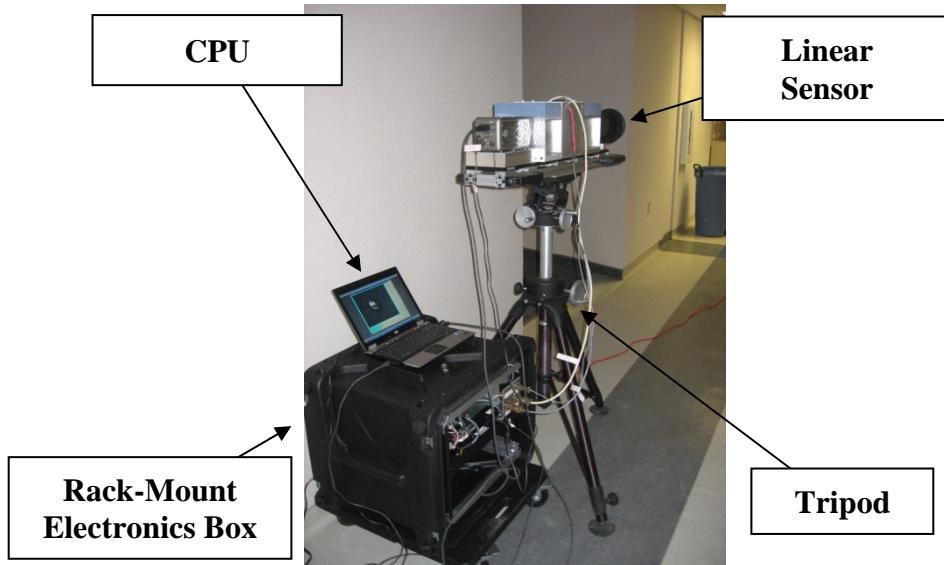


Figure 4.12: Portable Rack-Mounted Electronics Configured with Instrument

Finally, one last feature of the instrument is the capability to integrate with the previous system (i.e., the Newtonian telescope, Vixen R200SS), if deemed necessary. The capability was retained in the scenario where chromatic aberrations or other significant issues related from use of the telephoto lens causing the system to perform in a less-than-desirable fashion. The L2 integration block was specified with a port to accommodate an incident beam at 90-degrees from that of the remaining components downstream, utilizing a turning mirror with a standard optical support bracket. A cover is used over the port allocated for the telephoto mount. Personnel interested in utilizing this configuration should note that a significant issue with this configuration relates to the center of gravity. It is recommended that if this setup is desired, that the instrument be taken off of the tripod and placed on another suitable mounting point to account for this offset (e.g., cart, table, or a uniquely-designed 80/20 ® structure). Figure 4.13 shows the Newtonian telescope configuration.

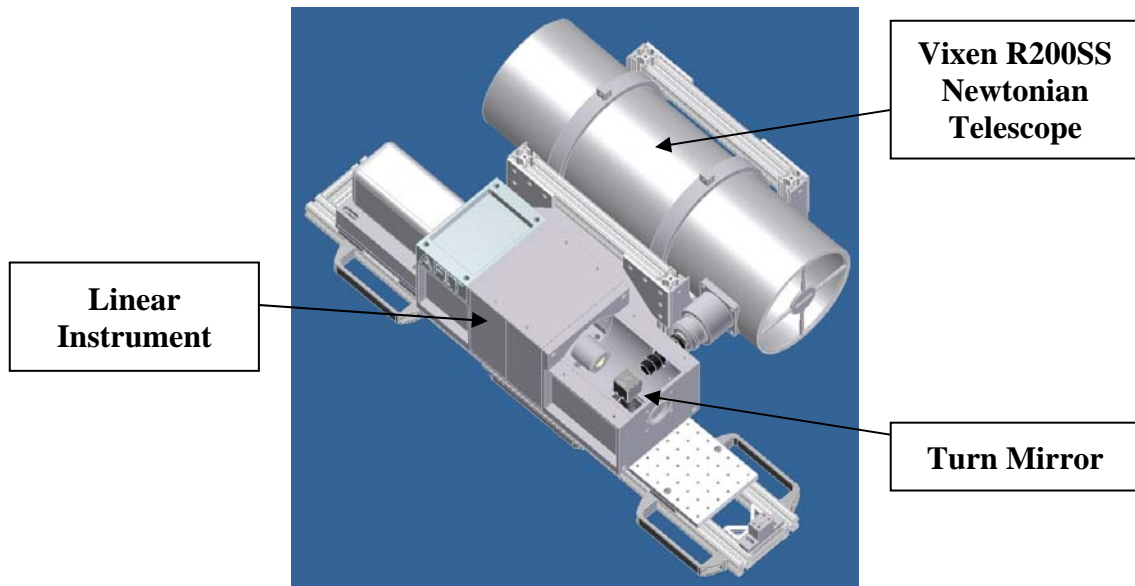


Figure 4.13: GCTEx Linear Instrument Configured with Newtonian Telescope

4.2.2. *Validation Methodology.* As a means to characterizing the overall effectiveness of the iterated ground instrument, a test series was developed incorporating DVP deviation angle, image quality and alignment characterization. Test operations were documented and conducted per TOP-GCTEX-0002 (included in Appendix C for reference). The intent was to detail pre-launch and on-orbit alignment/calibration processes as well as compare differences from the new to the old instrument.

The initial test related to DVP deviation angle characterization. Due to the fact that all prisms (and any translucent medium for that matter) deviates incident rays dependent upon wavelength, it is critical for our system to be well understood to enable proper hypercube data post-processing. Figure 4.14 depicts the expected deviation based on the current design DVP.

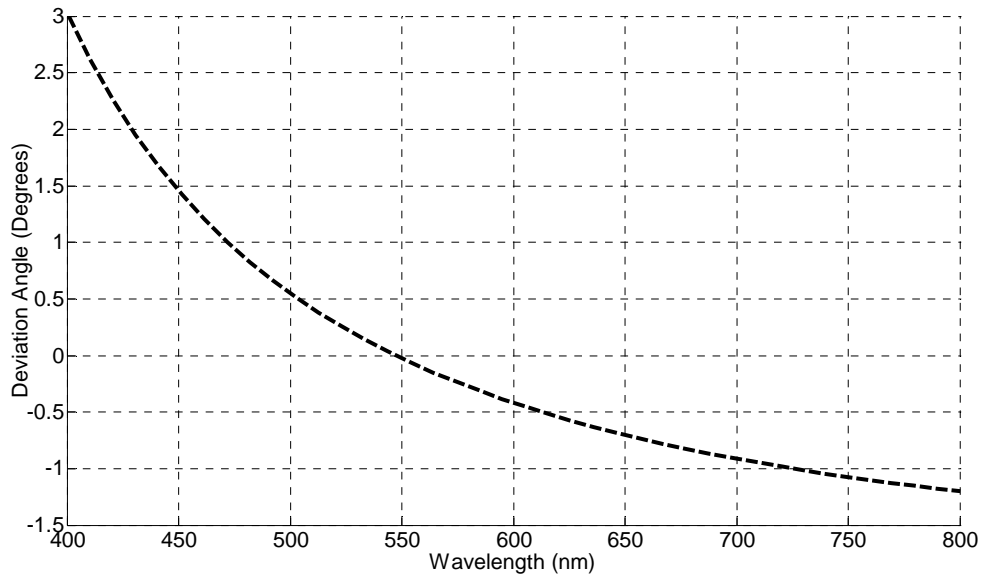


Figure 4.14: Theoretical DVP Deviation Angle vs. Wavelength

The rationale for performing this activity with the ground instrument encompasses the concept that this test will be performed on subsequent qualification and space flight-hardware designs in the future. Failing to perform this test will lead to a system which cannot accurately sense collection events of interest. The test methodology includes setup of a point-source at an approximate focus range for the instrument (greater than four meters for the updated system). For the tests conducted during this series, a mercury pen lamp was selected with a pin-hole aperture (to only allow a point-source to be witnessed). Figure 4.15 depicts the source for this particular test.

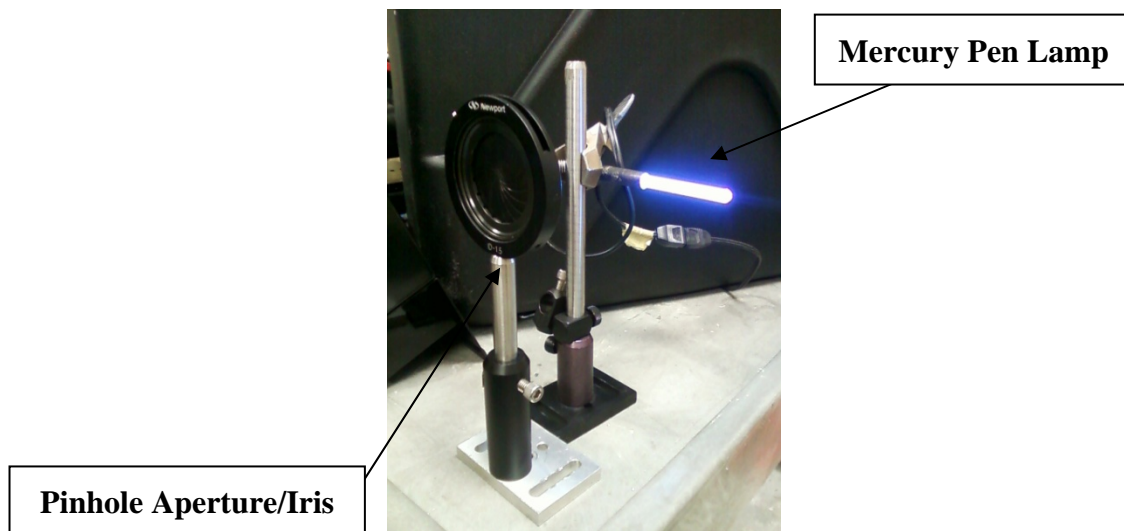


Figure 4.15: Mercury Pen Lamp Source Configured with Pin-hole

This test configuration will allow the incident mercury rays to enter the system and break into their constituent peak wavelengths (for the current instrument, primarily sensed at 435.8, 546.07, and 576.96 nm). In effect, the point-source will be broken up into several points on the camera. Additionally, the prism is rotated in this test in order to characterize the difference that this source has as the DVP is at 0, 90, 180 and 270 degrees of rotation. The final product of this data will be in characterizing how close to the predicted deviation angle the system is (enabling comparison and alignment metrics to be performed). This process and test was developed in order to prove the concept for further development to continue (i.e., other sources at varying wavelengths).

The next activity conducted was the image quality characterization. Again, a known source was setup at an approximate distance from the ground instrument for comparison and further analysis (note, measurement between the source and instrument was critical to ensure both the previous and updated design were the same). In this test

series, the object is a standard reference target from Mil-Std-150A known as a USAF-1951/T22. [50] This object was illuminated with a Unilamp source (allowing only 546.1 nm light to be emitted) with the object affixed to the front. Again, the prism was rotated by hand to four different position (0, 90, 180, and 270 degrees). Figure 4.16 depicts this setup.

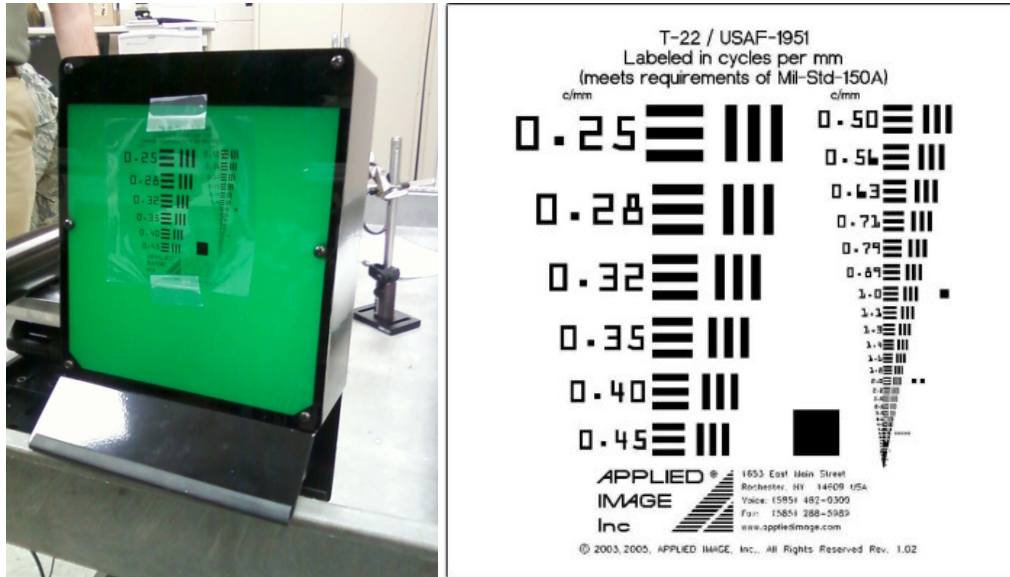


Figure 4.16: Unilamp Source Configured with T-22 / USAF-1951 Target [50]

The results from this effort are attributable to characterizing the overall optical system performance between the two systems. Post-processing of the data yields a modulation transfer function (MTF) and overall instrument magnification which is useful in evaluating the system contrast through assessment of maximum and minimum intensity. Equation (3) and (4) detail the evaluation for the MTF and magnification, respectively. [51]

$$MTF = \frac{[I_{max} - I_{min}]_{object}}{[I_{max} + I_{min}]_{image}} \quad (3)$$

$$M = \frac{y_{image}}{y_{object}} \quad (4)$$

Where, MTF is the modulation transfer function, I_{max} is the maximum intensity, I_{min} is the minimum intensity, M is the magnification (unitless), y_{image} is the image height (mm), and y_{object} is the object height (mm). Figure 4.17 depicts a notional MTF for a Newtonian system as reference.

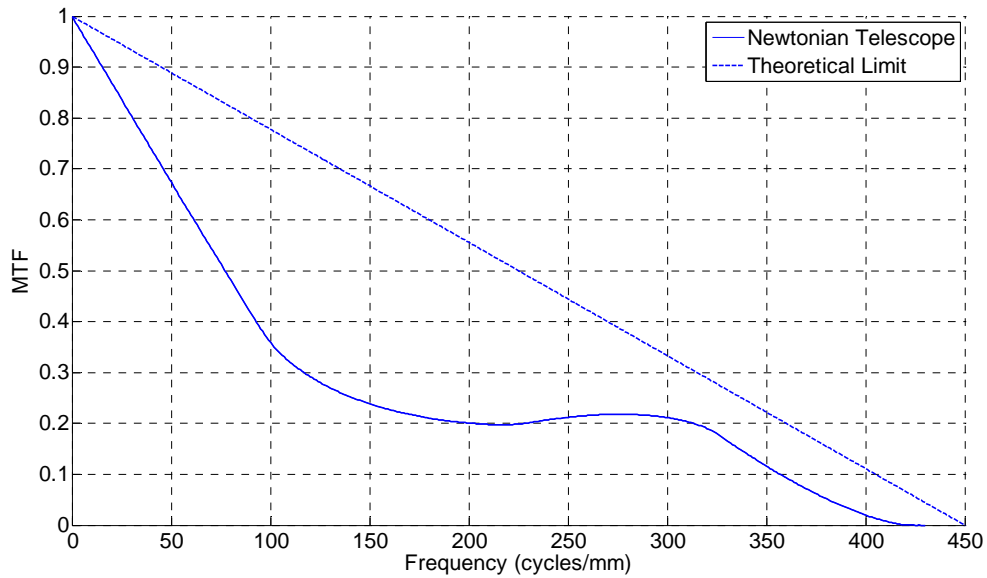


Figure 4.17: Theoretical MTF for a Newtonian System (Notional)

Finally, the last test accomplished was the alignment characterization. An apparatus was devised to cover the aperture of the linear system and provide an incident laser emission into the instrument. The rationale for performing this test series relates to the on-orbit strategy for assessing alignment which Book described. [13] Figure 4.18 details the aperture cover laser system.

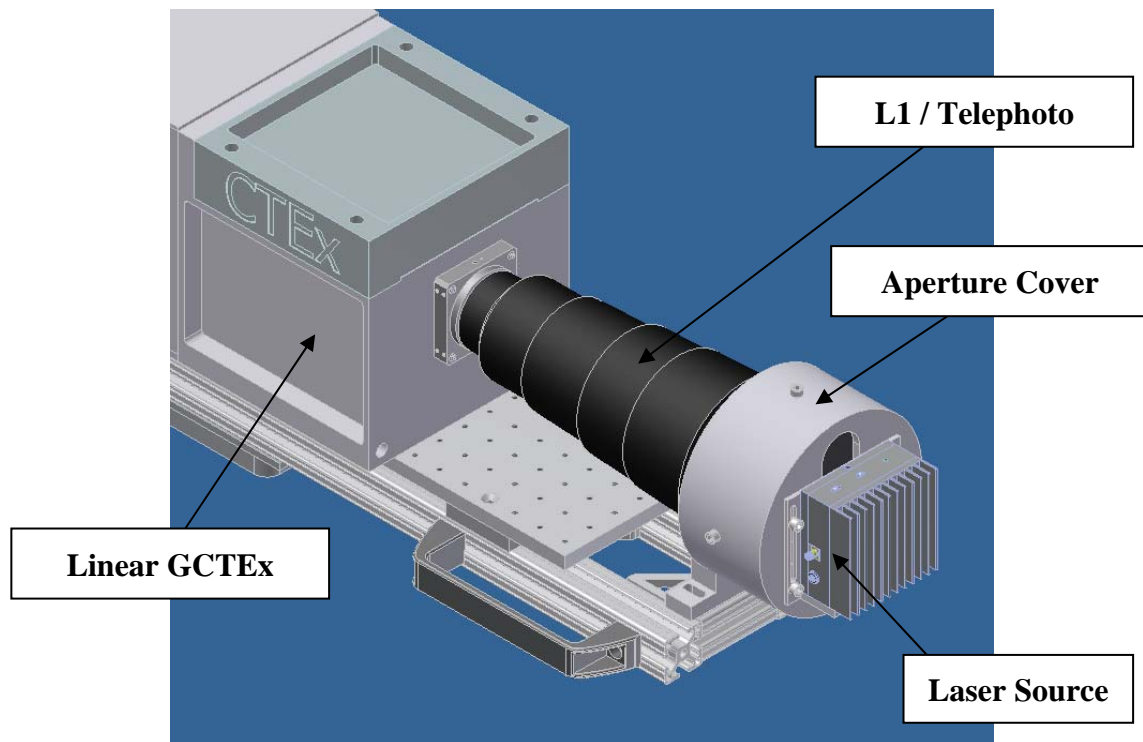


Figure 4.18: GCTEx Aperture Cover Laser Characterization System

In the test series, it is important to realize that placing a laser dot (or traced circle) at the center of the focal plane array is not as important as characterizing how close the circle is to perfectly round. This relates to the fact that angular incidence to the instrument is critical to providing good data for post-processing. Previous test efforts with the previous system have demonstrated issues here witnessing oblong/oval circular traces (attributable to improper alignment of the incident beam as it traverses through the instrument). Again, on-orbit, the intent would be to have a suite of lasers and LEDs at varying wavelengths to trace circles of varying diameters (due to the deviation angle differences at various wavelengths, discussed earlier). Note that the lasers and LED's

alignment would not be overtly critical as they only need to lie in the field of view of the instrument during calibration.

It should be noted that a similar test configuration to the aperture cover laser characterization system was also setup with a monochromator and white light source. In this setup, the intent is to incrementally step through specific wavelengths of incident light to enable the generation of the deviation angle versus wavelength plot (in an effort to assess system response for future hypercube processing). Figure 4.19 details this monochromator setup. In the next section, we will review the results obtained from this test campaign.

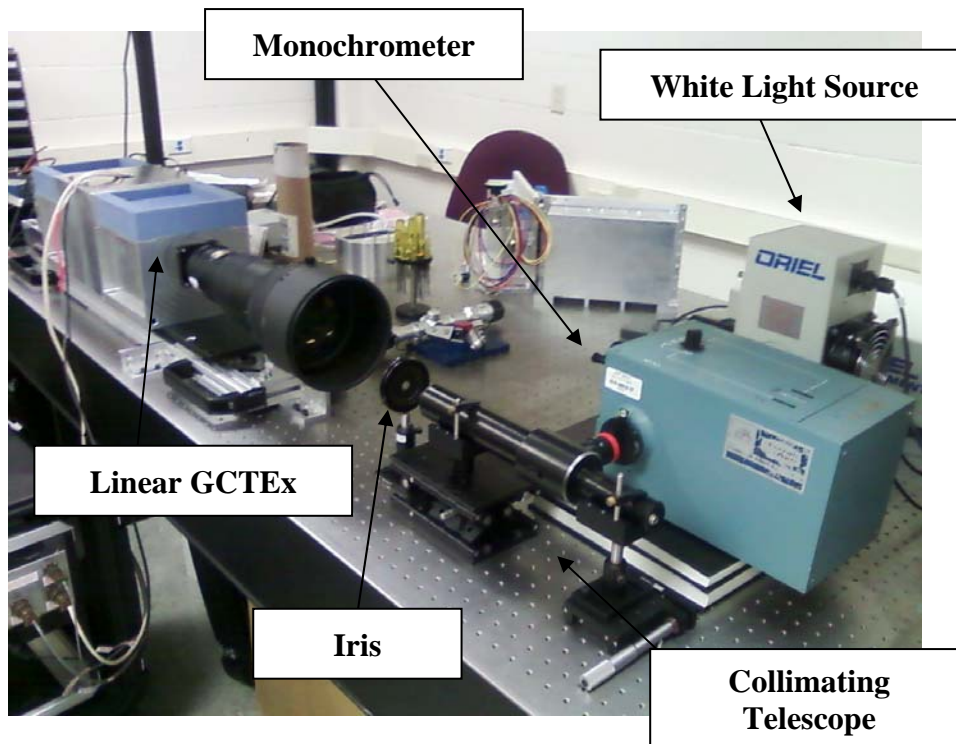


Figure 4.19: GCTEx Monochromator Test Setup

4.3 Results

This section presents the results obtained from the developmental research efforts relating to the ground based instrument. It is broken up into three subsections including deviation angle, image quality and alignment characterization results. Conclusions and recommendations for future work are captured in Section 6.2 and 6.4, respectively.

4.3.1. Deviation Angle Results. The overarching goal for this portion of the test series related to comparing the Newtonian and linear systems against theoretical predictions. As described in Section 4.2.2, the generic process involved acquiring point-source data (a mercury pen lamp viewed through an iris), capturing measurements through rotating the prism between 0, 90, 180, 270 degrees, and post-processing the data to acquire corresponding curves for DVP deviation angle versus wavelength.

To begin, each instrument was setup at roughly 133.5 ft distance from the source. A sample of the raw data through the instrument is depicted in Figure 4.20 where the mercury pen-lamp source is broken into constituent primary wavelengths.

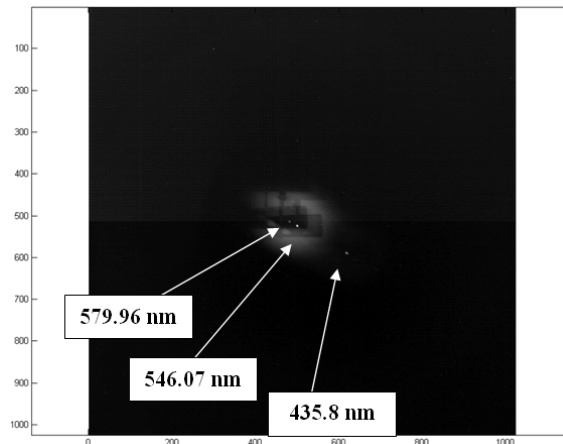


Figure 4.20: Mercury Pen-Lamp Pin-hole Source, Instrument View

The general processing flow involved identifying an appropriate point-source center at each wavelength, determining a circle and center of rotation data (from measurements acquired), finding the DVP offset (“pinwheel”) to allocate the true center of rotation and output the associated deviation angle. Figure 4.21 depicts the circle and center of rotation for the Newtonian system, “Misaligned DVP” Newtonian system, and the linear revision. It can qualitatively be seen that the concentricity of the circles developed from point-source data clearly improved with the linear revision. The “misaligned” DVP Newtonian configuration was a physical manipulation in an effort to align the system through unbolting and skewing the motor assembly (i.e., the motor assembly was unbolted and shifted in orientation to try and manually correct for witnessed alignment issues), wherein concentricity still was not completely obtained.

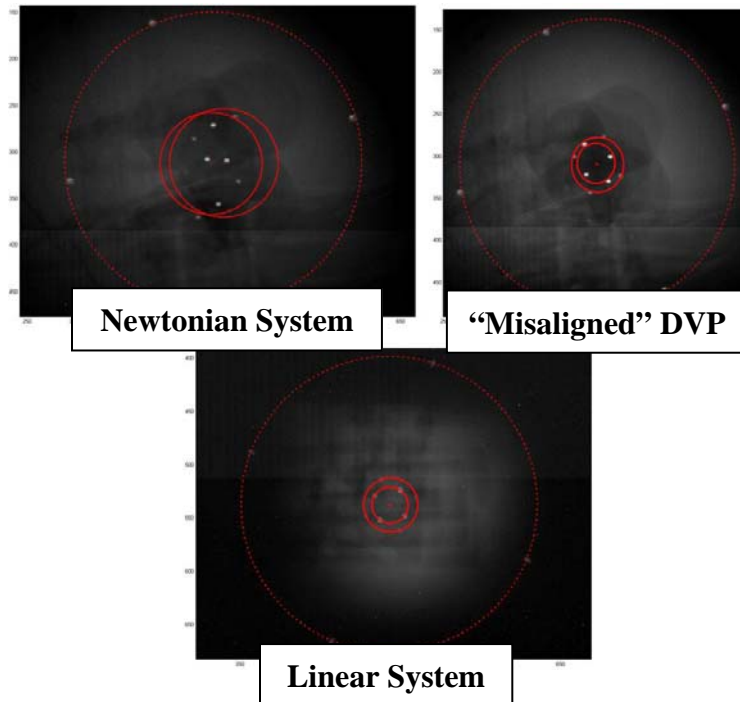


Figure 4.21: Convolved Mercury Pen-Lamp Captures for Instrument Configurations

The importance of these qualitative concentricity plots can be seen in the quantitative curves generated from this acquired data. Figure 4.22, Figure 4.23 and Figure 4.24 present the deviation angle versus wavelength for each instrument configuration (with standard deviation error bars included) compared against the theoretical predication assessed through a Zemax simulation. Clearly, the associated error and standard deviation is significantly reduced with the linear revision as compared with the Newtonian system (from 15% to 1%). This is attributable to a +/- 50 nm error down to +/- 2 nm overall, based on the incident deviation angle.

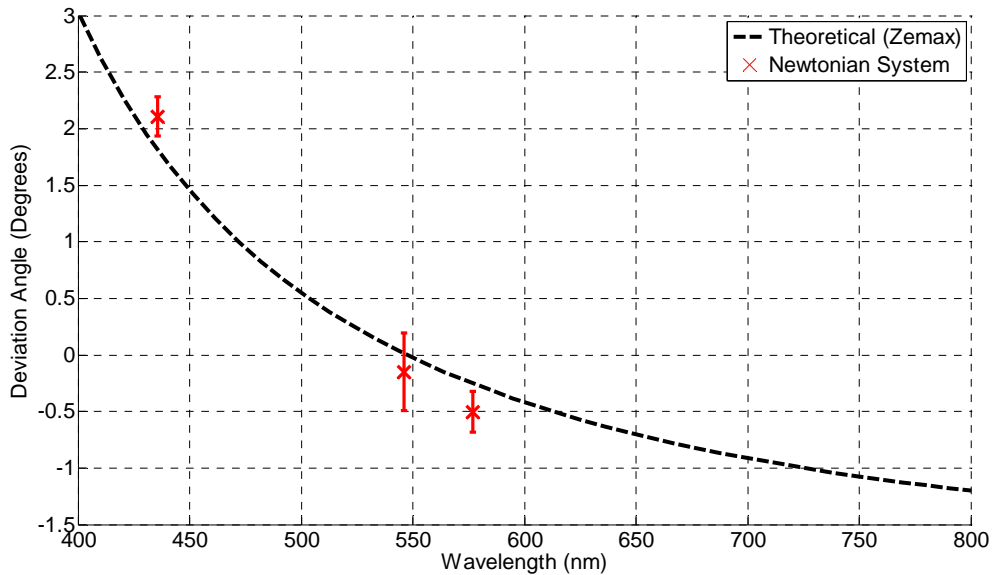


Figure 4.22: Newtonian System, Deviation Vs. Wavelength

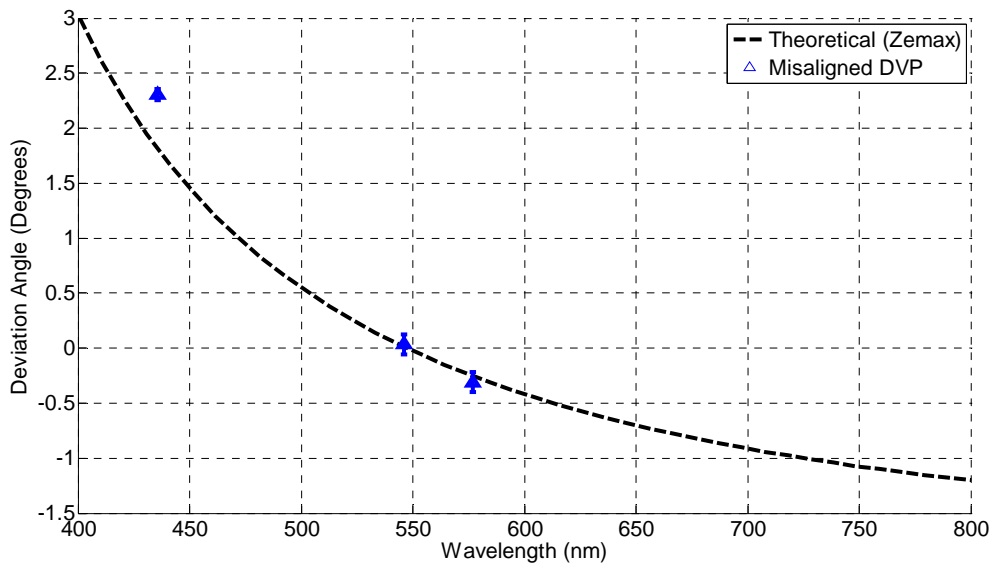


Figure 4.23: "Misaligned" Newtonian System, Deviation Vs. Wavelength

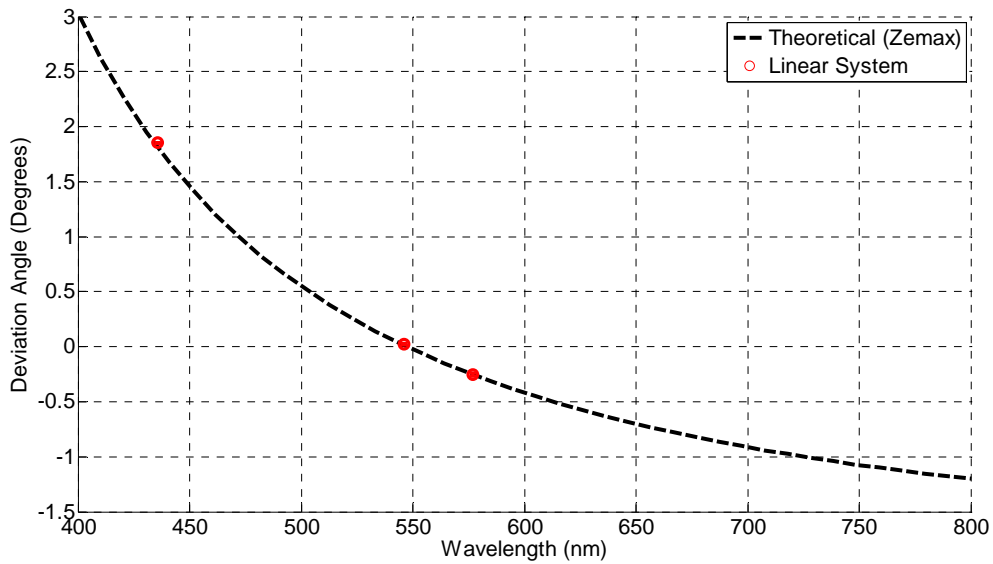


Figure 4.24: Linear System, Deviation Vs. Wavelength

Overall, these results are incredibly important in image reconstruction. The above plots increase confidence in the ability for the linear hardware to accurately capture

scenes and acquire higher-fidelity data. The next subsection will discuss image quality comparisons of the two instruments.

4.3.2. Image Quality Results. As previously discussed in Section 4.2.2, the intent in this series of tests was again to compare the image quality of the Newtonian and linear instruments. Image quality was assessed through qualitative measures as well as the more quantitative modulation transfer function. From a qualitative standpoint, and without the DVP in the optical path, Figure 4.25 depicts the difference in image quality through recent iterations of this instrument. It can be witnessed that the magnification of the linear instrument is not the same as the Newtonian due to the fact the primary optic focal length is lower in comparison (specific magnification results will be followed shortly).



Figure 4.25: Image Quality Development

Determination of the MTF was accomplished through collecting USAF-1951/T22 target source data (wherein the DVP was rotated between 0, 90, 180, and 270 degree set points). This collection was followed by post-processing, wherein determination of the

maximum and minimum intensity at each spatial frequency was assessed. Additionally, an overall magnification for this instrument could be assessed from the resolving power to discern horizontal/vertical target bar-patterns. Figure 4.26 represents the raw data for the target source.

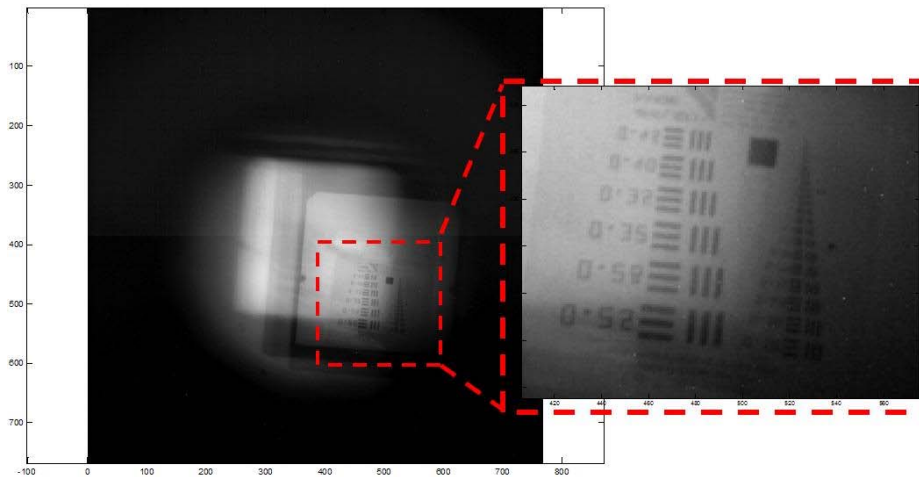


Figure 4.26: USAF-1951/T22 Target, Raw Data

Averages were applied across each DVP rotation orientation to determine the final curve. Figure 4.27 details the MTF for both the Newtonian and linear systems.

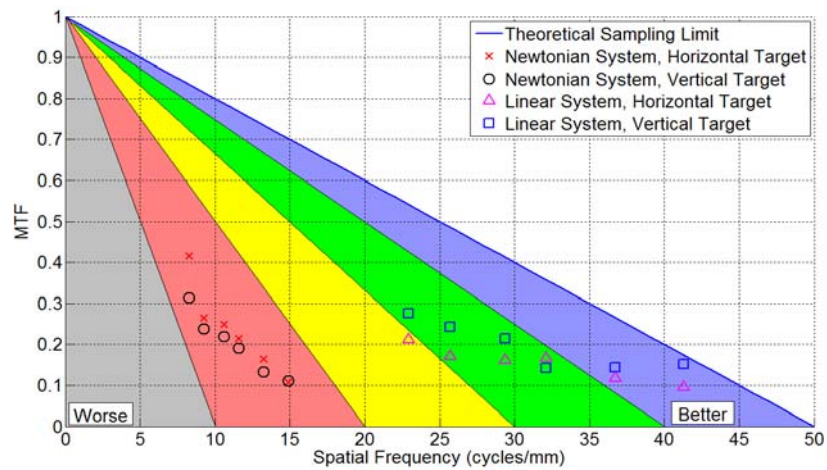


Figure 4.27: MTF Comparison, Newtonian Vs. Linear Systems

From these above data, several resulting assessments can be attributed. First, the MTF shows that the linear system approaches the sampling limits of the system in the image domain better than that of the Newtonian system (note the sample limit is 50 cycles/mm due to the camera pixel size of 20×10^{-6} m). [52] The impact is that the linear system is able to discern spatial features and contrasts of a scene to a higher degree than that of the Newtonian system. Second, from this data, overall magnification can be assessed for each system. The Newtonian system resulted with an overall magnification of 0.030 while the linear system was found to magnify at 0.010. Note that these quantities are low due to the fact we are trying to take a large object and fit it into our overall detector FPA, based on Equation (4).

4.3.3. Alignment Characterization Results. The objective in this effort related to developing characterization methodologies which could be directly applied to the space-based version of this experiment. The idea is that the space instrument will be outfitted with a set of lasers and LED lamps which will be coupled into the aperture assembly. Thus, this effort is an initial step in assessing the instrument alignment and ability to return the correct wavelength according to DVP deviation angle curves. The first step in this process was collecting incident laser data. Figure 4.28 presents this raw data including an individual frame (i.e., laser point), images added over three rotations, and a scaled image showing relative intensities. Due to the intensity of this incident beam, internal reflections (ghosting) can be seen as a result of the compound COTS lens systems utilized.

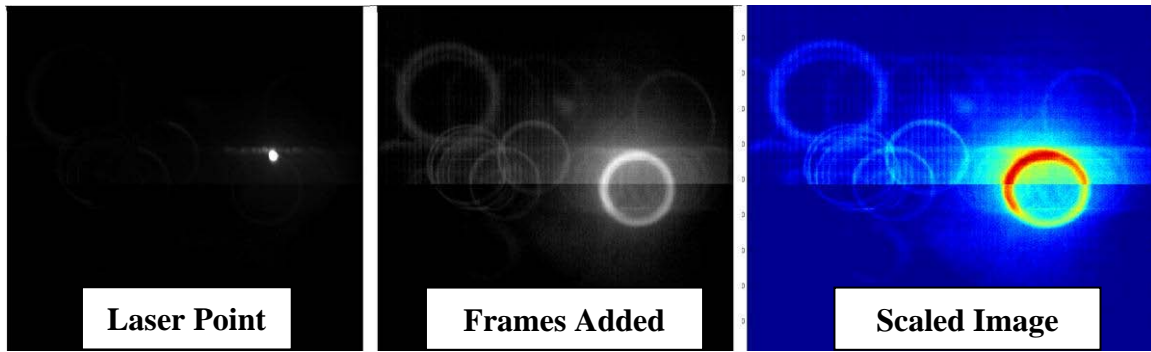


Figure 4.28: Alignment Characterization, Image Construction

Upon acquiring the necessary data, a MATLAB post-processing script was generated and executed to acquire optical metrics. The script performed several operations and functions to acquire circle/center-of-rotation, eccentricity, and resulting deviation angle/sensed wavelength. To begin, the location of the laser point centroid needed to be found for each frame of data and saved as an array of coordinates (Matlab's tutorial "Identifying Round Objects" was utilized as a baseline and edited accordingly to support this effort). [53] This initial subroutine performs a number of image processing operations, including: reading in individual images, converting to black & white (to allow boundary tracing), removing noise (stray pixels), determination of boundaries, finding which object is round and logging the centroid coordinates for each frame. Next, the array of coordinates were processed through two functions in order to trace the circle center, radius, eccentricity, and other statistical data from these points. Note, this circle center is not the DVP deviation center of rotation. Use of the functions "try_circ_fit.m" (to fit a circle based on x and y column vectors of centroid coordinates) and "fit_ellipse.m" (to determine the best fit to an ellipse based on the same centroid

coordinates indicated earlier) were used and edited for purposes here. [54] [55] Figure 4.29 presents a graphical depiction of the image processing described above.

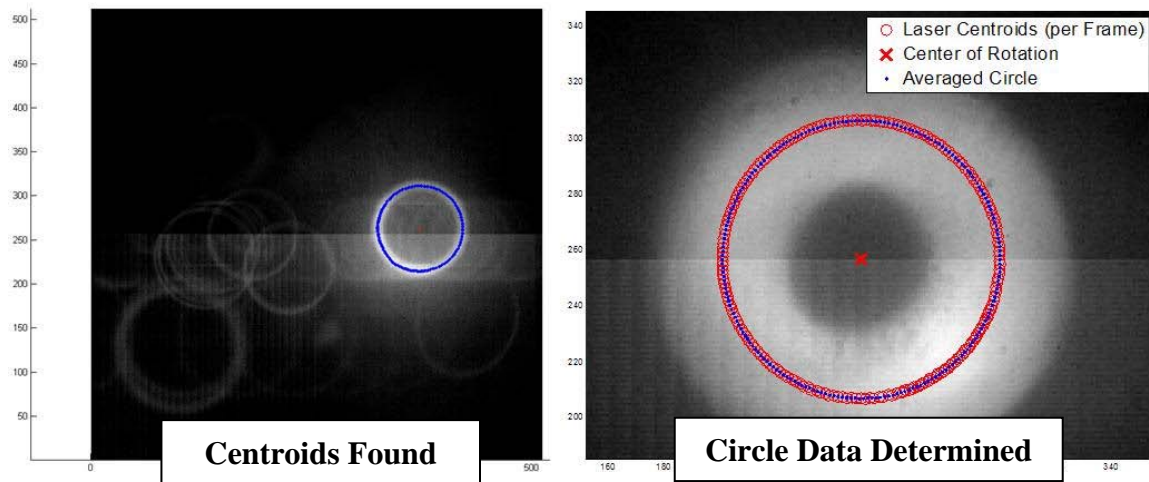


Figure 4.29: Alignment Characterization, Circle Data Determination

Finally, after some data cleaning (truncated FPA window region is utilized, versus the entire array), determination of the deviation angle and associated wavelength could be determined. However, prior to assessing the final solution, an offset value needs to be incorporated to allow for the “pinwheel” phenomena noted earlier (i.e., the center of rotation offset due to misalignments within the instrument). Figure 4.30 details this pinwheel offset from the deviation angle (shown with the mercury pen-lamp for ease of interpretation).

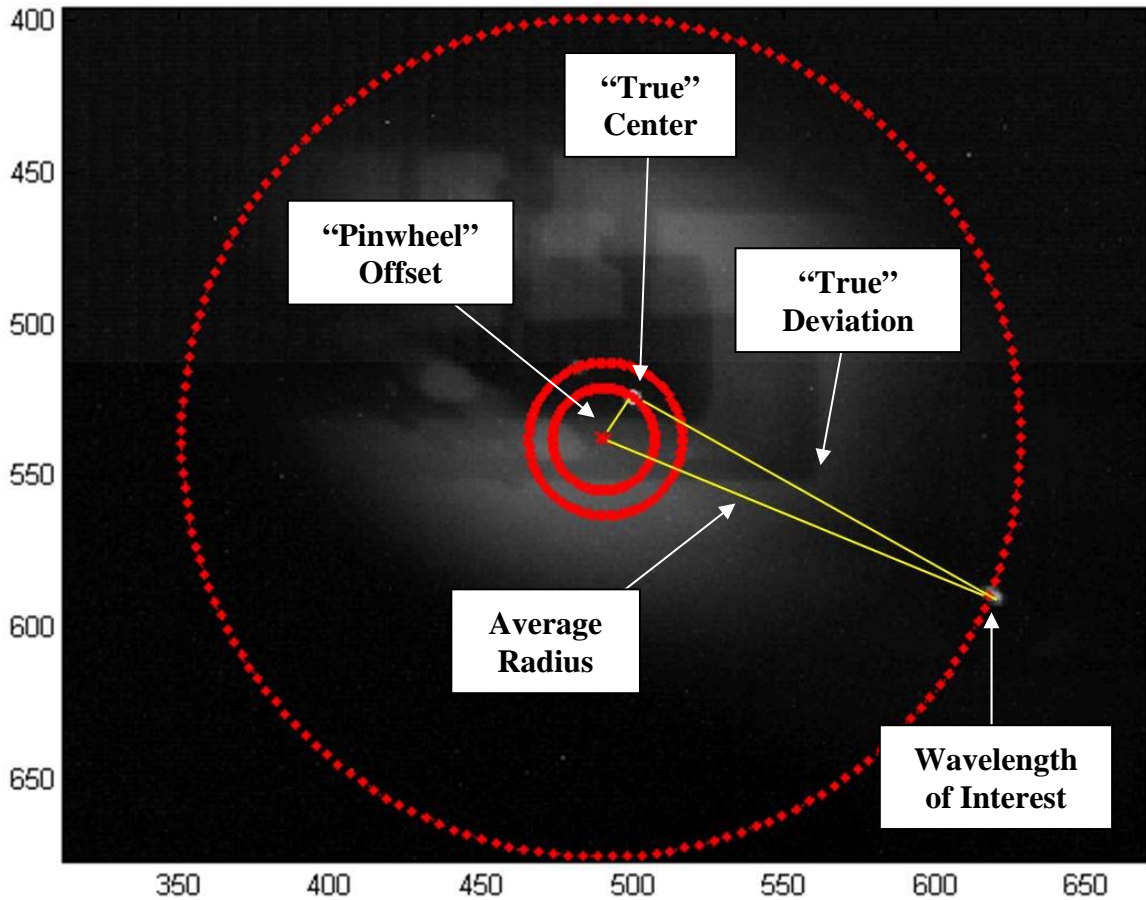


Figure 4.30: “Pinwheel” Offset

Determination of this offset can be performed by several different methods; however, the approach utilized in this research was by review of the raw deviation angle data and assessing the discontinuity at the 548 nm crossover point. The distance (in degrees) from zero-deviation should be attributed to this offset parameter (upon performing the proper curve fit). Figure 4.31 presents the deviation angle versus wavelength plot without application of this offset parameter. Note that this plot shows the discontinuity utilized for the offset determination.

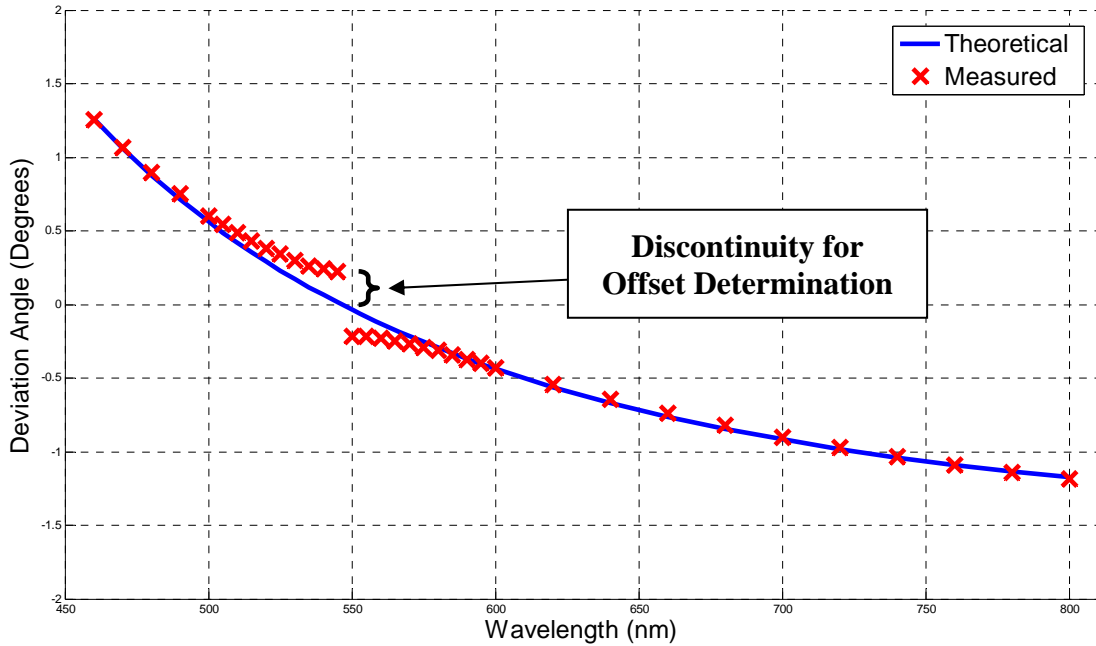


Figure 4.31: Alignment, Deviation Vs. Wavelength (Uncorrected)

Review of this data indicates that the offset is only of importance in the region of 548 +/- 25 nm. With the exception of this area, the linear instrument acquires nearly +/- 4 nm (0.26% error throughout) accuracy through the remaining sensing range in comparison with theoretical predictions. To determine this offset, trigonometry is used to find the chord length where the offset is assessed to be roughly .217324 degrees. Incorporating this into the data yields the plot seen below in Figure 4.32.

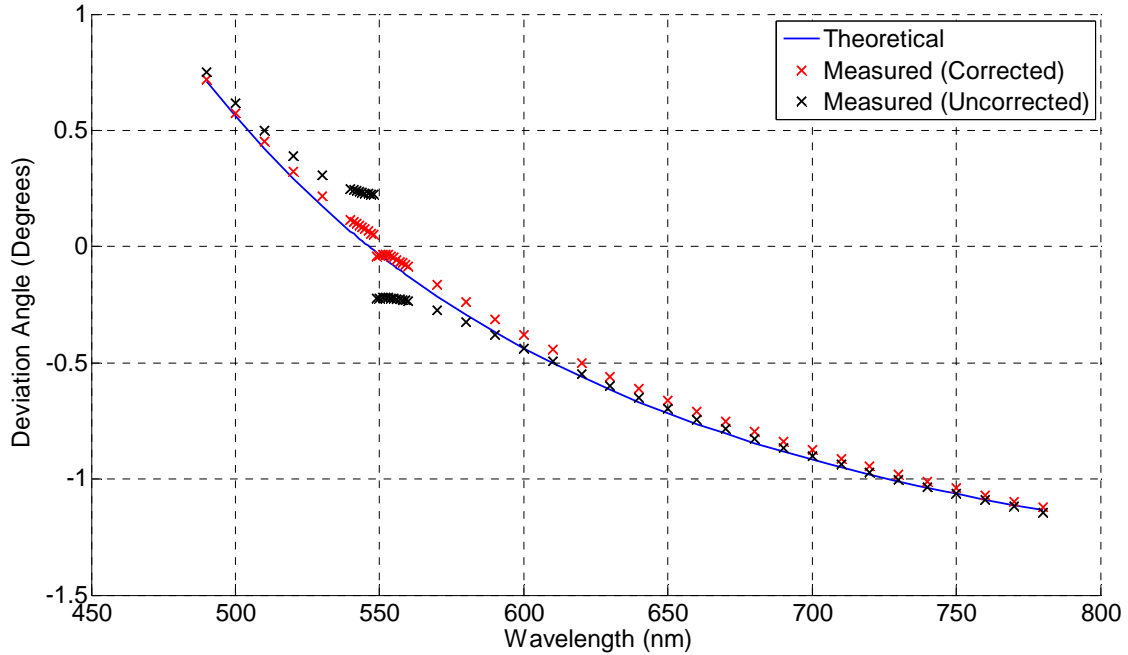


Figure 4.32: Alignment Characterization, Deviation Vs. Wavelength (Corrected)

While the discontinuity is somewhat removed, the remaining error in the instrument averages to +/- 12 nm (1.6%) offset across the region after the crossover point (greater than 548 nm). The curve fit for this characterization is a power function of the form in Equation (5).

$$\delta = a\lambda^b + c \quad (5)$$

Where δ is the deviation angle (degrees), λ is the wavelength (nm) and a, b and c are the power curve-fit parameters. Parameter for this curve fit are listed in Table 4.8.

Table 4.8: GCTEx Linear System Curve-Fit Parameters (from corrected data)

a	2.043e+008
b	-2.944
c	-1.737
R^2	0.9989

4.4 *GCTEx Revision Summary*

This chapter discussed the ground-based CTE_x linear revision requirements, design/characterization philosophy, and results from the associated test series. In all, it was assessed that the revision to the instrument met the fundamental requirements which it set out to solve. Further characterization and field collection will be necessary to completely map this design and properly apply lessons learned to the space instrument. Conclusions from this effort are identified in Section 6.2 and future work indicated in Section 6.4.

V. Space-Based CTE_x Instrument Computer Unit Design/Characterization

This chapter covers the relevant requirements, thermal model analysis, design and test methodology and the results from the development and characterization of the Instrument Computer Unit (ICU). This effort is intended to support the space-based CTE_x development campaign. Conclusions from this work will be identified in Section 6.3 and future work contained in Section 6.4.

5.1 Design Requirements

The design of the ICU had to meet several requirements, providing a baseline for this design development. These baseline requirements are listed below.

- Utilize commercial, off-the-shelf (COTS) electronics and mechanical hardware as much as possible
- Minimize mass to 10 kg, or less
- Ensure the fundamental frequency is above 35 Hertz in all axes
- Ensure the design will survive normal operations in a high vacuum/space environment
- Meet all regulatory requirements associated with HTV, EXPA and ISS
- Do not dissipate excess thermal loading to the ISS (or surrounding structure/devices)
- Review the HREP ICU for design efficiencies and applications to CTE_x

Due to the fact that the PC/104 configuration is a relatively wide-spread form-factor in ruggedized military applications, utilization in the CTE_x program as an avionics

platform made practical sense from a design standpoint. Thus, the next preliminary assessment pertains to what is anticipated for the CTE_x ICU PC/104 stack. At a minimum, the following items will need to be accounted for: CPU, solid-state drive, internal I/O (e.g., Ethernet, SATA, and/or RAID cards for high throughput data transfer to/from the high-speed camera), and external I/O (e.g., 1553 for communication with the ISS). As an option, a pressure/temperature card (for health monitoring) and universal power supply may also be required. If a similar PC/104 stack to HREP is assembled, we can expect a stack power usage of roughly 25 watts. Thus, this power level will also be factored into the design requirement trade-space as the design progresses. Next, we will explore the mathematical thermal model developed to assess this input to the system.

5.2 Thermal Modeling Methodology

As an initial characterization for the ICU thermal environment, a one-dimensional lumped-capacitance model was developed for predictive purposes. This model, upon validation through testing, will be utilized to map the design trade-space. Figure 5.1 is the general control volume concept for this model development

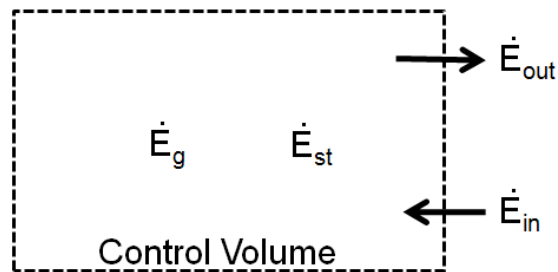


Figure 5.1: Heat Transfer Control Volume Concept

This control volume theory can be related to the first law of thermodynamics, Equation (6) [56]:

$$\dot{E}_{st} = \frac{dE_{st}}{dt} = \dot{E}_{in} + \dot{E}_g - \dot{E}_{out} \quad (6)$$

Where \dot{E}_{st} is the energy stored within a control volume changing with time (W), \dot{E}_{in} is input energy changing with time (W; e.g., albedo, Earth infrared, etc.), \dot{E}_g is the rate of generated energy (W; e.g., PC/104 electrical input power, fan and other sources) and \dot{E}_{out} is the rate of output energy (W). Moreover, Equation (6) is the conservation of energy, in that no additional energy will enter or leave the system unless an equal or opposite change is experienced elsewhere in the model.

More specifically, we will now assess the particulars of our situation through breaking up the constituents of routine, nominal on-orbit operations. The ICU is initially viewed as an independent unit, passively cooled, and thermally isolated. From a simplistic perspective, the highest temperature found within the device will likely be that of the CPU. The cooling circuit will consist of using a fan to circulate a pure and dry gaseous-nitrogen atmosphere in the unit to cooling fins, built into the aluminum housing, where radiation will transfer the excess thermal energy to the Earth and deep-space. Therefore, with that given concept-of-operations, a general lumped capacitance thermal circuit can be realized, depicted in Figure 5.2

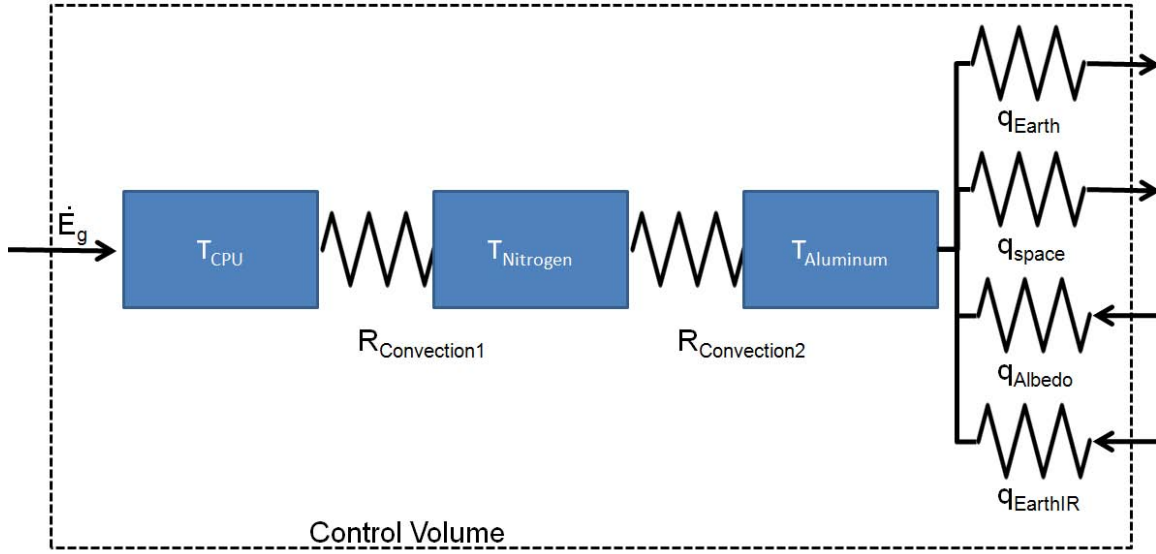


Figure 5.2: ICU Lumped Capacitance Thermal Circuit Model

Note that albedo is related to the sunlight reflected off of the planet/moon, while Earth infrared (IR) is related to incident sunlight absorbed by the Earth and re-emitted as IR energy (or blackbody radiation). Each block in Figure 5.2 represents a lumped capacitance energy balance per Equation (6). Additionally, we can re-write E_{st} to Equation (7) [56]:

$$\dot{E}_{st} = \rho V C_p \frac{dT}{dt} \quad (7)$$

Where ρ is the mass density (kg/m^3), V is the spatial volume of the thermal material (m^3), C_p is the specific heat at constant pressure for a material ($\text{J}/\text{kg K}$) and $\frac{dT}{dt}$ is the change in temperature with respect to time (K/s). It should be noted that \dot{E}_{st} can be rewritten as [56]:

$$\dot{E}_{st} = M C_i \frac{dT}{dt} \quad (8)$$

Where MC_i is the product of mass density, ρ , volume, V , and the specific heat of the thermal material under analysis. In all, MC_i becomes a simplification term when processing transient and steady-state solutions. Equation (8) is utilized in the context of the overall system model wherein each thermal element is linked by a heat transfer mode (i.e., the PC/104 cards and the bulk nitrogen gas are linked by convection, external ICU aluminum housing and the environment are linked via radiative cooling/heating, etc.).

Other terms in the model also need to be broken down as well, including the first convection term, rewritten in Equation (9). [56]

$$\dot{E}_1 = h_1 A_1 (T_{CPU} - T_{GN2}) \quad (9)$$

Where h_1 is the convection coefficient with respect to the PC/104 stack ($\text{W}/\text{m}^2 \text{K}$), A_1 is the convection flow surface-area (m^2 ; again, over the PC/104 stack), and T_{CPU} / T_{GN2} are the temperatures of the CPU and nitrogen (K), respectively. Likewise, the second convection term can be broken out to Equation (10). [56]

$$\dot{E}_2 = h_2 A_2 (T_{GN2} - T_{AL}) \quad (10)$$

Where h_2 is the convection coefficient with respect to the aluminum housing heat-sink cooling fins ($\text{W}/\text{m}^2 \text{K}$), A_2 is the convection flow surface-area (m^2 ; again, over the cooling fins), and T_{GN2} / T_{AL} are the temperatures of the nitrogen and aluminum housing (K), respectively.

Heat transfer exiting from the ICU can only, as assumed earlier, be conducted through radiation. Additionally, a small input to the thermal energy load will come from solar irradiance (i.e., albedo), and Earth infrared inputs. Therefore, because radiation is

our primary mode of heat transfer out of the system, the analysis must begin by assessing the physical phenomena in that region (i.e., radiative heat transfer surface) first, and then work backwards toward the primary heat-generation source (e.g., the CPU). These inputs and outputs can be broken up as laid out in Equations (11) through (14). [56] [57]

$$q_{space} = \varepsilon A \sigma (1 - f) (T_{AL}^4 - T_{space}^4) \quad (11)$$

$$q_{earth} = \varepsilon A \sigma (f) (T_{AL}^4 - T_{earth}^4) \quad (12)$$

$$q_{albedo} = \alpha I_{solar} \rho_{albedo} F_{albedo} \quad (13)$$

$$q_{space} = \varepsilon I_{EIR} F_{EIR} \quad (14)$$

Where ε is the emissivity of the radiative surface (unitless), f is the view factor (unitless), σ is the steffan-boltzman constant, A is the radiation surface area (m^2), T_{AL} is the aluminum temperature (K), T_{space} is the temperature of empty-space (typically 3 K), T_{earth} is the temperature of Earth (typically 293 K), α is the absorptivity factor (unitless), I_{solar} is the solar flux (W/m^2), I_{EIR} is the Earth IR flux (W/m^2), ρ_{albedo} is the Earth's albedo, and F_{albedo} / F_{EIR} are geometrical terms, based on the angle of the face to the sun and Earth (unitless).

The nadir view factor, f , is calculated according to the spherical geometry, associated with Figure 5.3.

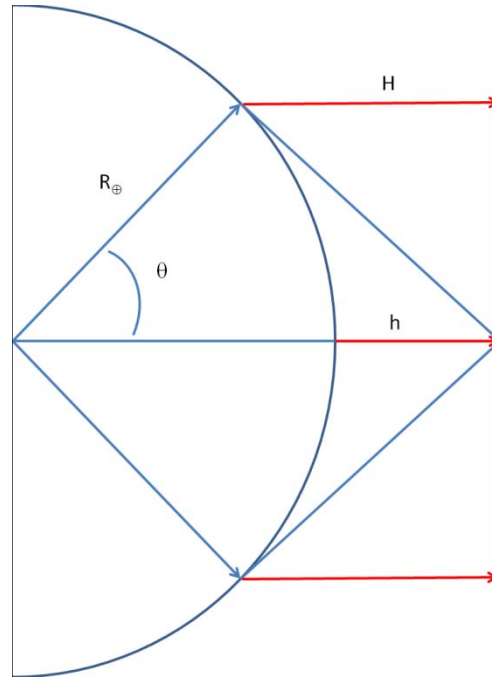


Figure 5.3: Earth View Factor Geometry Parameters

The geometrical calculations which relate to Figure 5.3 are found below in Equations (15) to (19).

$$R_{satellite} = R_{earth} + h \quad (15)$$

$$\theta = \sin^{-1} \frac{R_{earth}}{R_{satellite}} \quad (16)$$

$$r = R_{earth} \cos \theta \quad (17)$$

$$H = \frac{r}{\tan \theta} \quad (18)$$

$$f_{earth} = \frac{\pi r^2}{\pi r^2 + 2\pi r H} \quad (19)$$

Where R_{earth} is the radius of the Earth (km), h is the altitude of the satellite (km), θ is the half-angle horizon view point from the sensor (degrees), H is the maximum height

from the orbit altitude to the earth-tangent point (km), r is the radius of the cylinder created with H as the cylinder length (km), and f_{earth} is the earth-facing view-factor (unitless). Note that the space-facing view factor can be related by Equation (20).

$$f_{space} = 1 - f_{earth} \quad (20)$$

Continuing to work backwards to the thermal source, the next step in the thermal circuit is that of the conduction through the aluminum wall from the thermal transport fluid (dry nitrogen) to the radiative wall. Equation (21) is used to calculate that conduction thermal resistance. [56]

$$R_{conduction} = \frac{L_{wall}}{k_{AL}A_2} \quad (21)$$

Where L_{wall} is the thickness of the thermal barrier (m; aluminum housing), k_{al} is the thermal conductivity (W/m K) and A_2 is the conduction surface area (m²).

Next, we need to assess the convection coefficient for the heat transfer from the thermal fluid (nitrogen) to the aluminum housing, or h_i from Equation (9) or (10). For maximum thermal pickup at this interface, it was prudent to design a heat-sink into the aluminum housing via cooling fins (allowing for a higher surface area for this transfer to take place). Initially, we must identify the geometry parameters for modeling purposes, depicted in Figure 5.4 (the general layout for the heat-sink modeling layout).

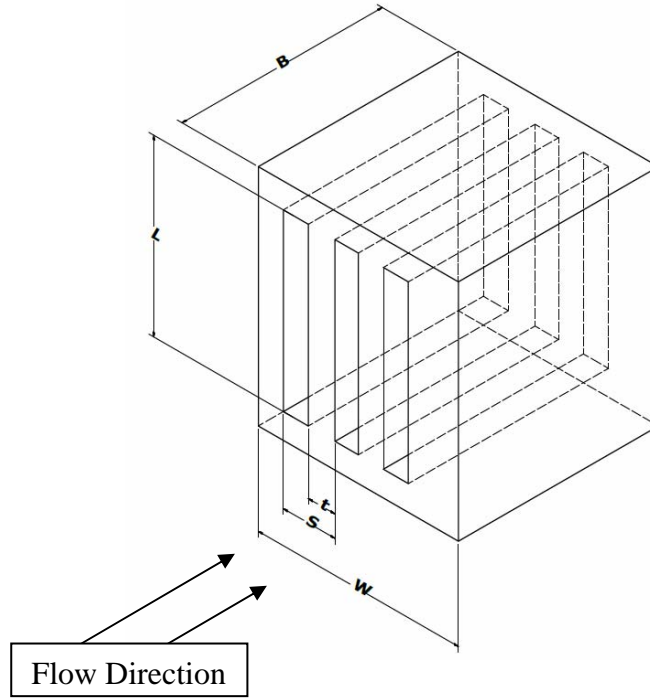


Figure 5.4 Heat Sink Geometrical Parameters

Where B is the length of the heat sink (m), L is the channel depth (m), t is the fin thickness (m), W is the heat sink width (m), and S is the combined channel width and fin thickness (m). From the above parameters, the following process is followed to determining the convection through the heat-sink. The number of channels is calculated from Equation (22). [56]

$$N = \text{round} \left[\frac{W}{S} \right] \quad (22)$$

Next, the surface area of the base and fin area along the wall can be attained from Equation (23) through (26). [56]

$$A_{base} = (W - Nt)B \quad (23)$$

$$A_{fin} = 2 \left[\frac{L}{2} \right] B \quad (24)$$

$$A_{total} = NA_{fin} + A_{base} \quad (25)$$

$$A_{channel} = L[S - t] \quad (26)$$

Also important to this assessment will be the perimeter, hydraulic diameter and overall area, calculated by equating Equation (27) through (29). [56]

$$P = 2(L + S - t) \quad (27)$$

$$D_h = \frac{4A_{channel}}{P} \quad (28)$$

$$A = 2NLB \quad (29)$$

Now that we have the needed geometry, we begin the fluid-flow heat-transfer calculations, all utilizing thermophysical properties of nitrogen (assumed at 20 degrees Celsius and 18 psia). The mass flow rate is determined via Equation (30). [56]

$$\dot{m} = \frac{\rho \dot{V}}{N} \quad (30)$$

Where ρ is the mass density of the nitrogen (kg/m^3), \dot{V} is the volumetric flow rate of the fluid (m^3/s) and N is the number of channels within the heat sink (unitless). Note that an assumption made regarding the volumetric flow rate in this analysis was that constant flow was assumed throughout the interior of the ICU at steady-state conditions. Additionally, without the aid of a detailed computational fluid dynamic analysis, an assumption of 40% of the volumetric flow rate from the DC fan can be expected within

the ICU. A suitable approximation for the mass density, ρ , can be found using the ideal gas law in Equation (31). [56]

$$\rho = \frac{P}{RT} \quad (31)$$

Where P is the absolute pressure (Pa), R is the universal gas constant and T is the fluid absolute temperature (K).

Upon determining the mass flow rate, the Reynolds number may subsequently be found for an internal flow-field in order to determine whether we are dealing with a laminar ($Re < 2300$) or turbulent ($Re > 2300$) flow. Equation (32) calculates this parameter. [56]

$$Re_D = \frac{\dot{m}D_h}{\mu A_{channel}} \quad (32)$$

Where \dot{m} is the mass flow rate of the fluid (kg/m^3), D_h is the hydraulic diameter (m), $A_{channel}$ is the frontal area of the channel (m^2) and μ is the fluid viscosity ($\text{kg}/\text{s m}$). The final step prior to determination of the convection coefficient is to ascertain the value of the Nusselt number, which can be found utilizing Equation (33). [56]

$$Nu_D = .023Re_D^{4/5}Pr^n \quad (33)$$

Where Re_D is the hydraulic diameter variant of the Reynolds number (unitless), Pr is the Prandtl number based on thermophysical property data of the fluid (unitless) and n is a correction power based on whether the fluid is being heated ($n=.4$) or cooled ($n=.3$). Also, it should be noted the Equation (33) is strictly utilized for a turbulent flow situation. Finally, Equation (34) can be used to determine the convection coefficient. [56]

$$h = \frac{k}{D_h} Nu_D \quad (34)$$

Where k is the thermal conductivity of the fluid based on thermophysical material properties (W/m K), D_h is the hydraulic diameter (m) and Nu_D is the Nusselt number (unitless). Additionally, note that this process can be utilized for both the design of the aluminum housing cooling fins as well as for the PC/104 computer stack as the nitrogen passes over each.

In conclusion, these equations are used to balance and build the thermal model in order to characterize the system behavior over time from an initial state.

5.3 *Model Characterization Methodology Through Design and Test*

5.3.1. Model Design Methodology. Validation of the mathematical model required careful consideration of the maximum predicted environments as well as the design constraints due to the mission. First and foremost, assessment of the orientation of the device upon this instrument is critical to developing a successful mission payload. From preliminary concept modeling of the space-based CTEx imaging platform, as discussed in chapter 3, it was decided that the ICU will currently be oriented in a nadir-facing orientation along with the TCU due to the higher-level of confidence that this will be an unobstructed radiation emission path (as ISS requirements dictate that conduction into the structure and radiation to another device on-board the ISS is strictly prohibited). Figure 5.5 depicts the intended orientation of the ICU.

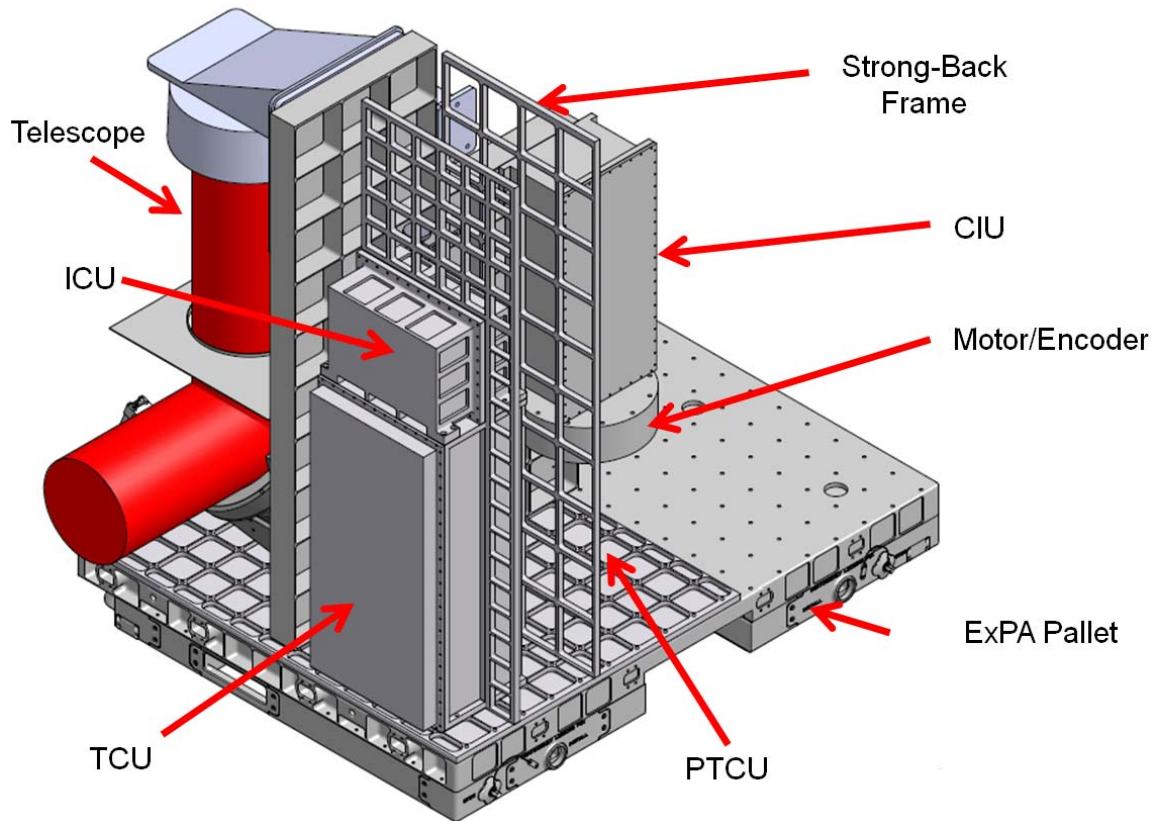


Figure 5.5 Space-Based CTE Instrument Layout

Because of this configuration, it is intentional that the ICU be designed as a stand-alone unit, meaning that upon applying power to the device, it will perform its mission (accepting commands, commanding the instrument, and saving/transmitting mission data as necessary) and it will be passively cooled via radiation. Therefore, one face will need to be purposely designed as a radiation surface to support the design intent (i.e., high emissivity with low absorptivity). Note that, even with a high emissivity, the radiation heat transfer is governed by the exterior surface temperature, per Equation (11) and (12), wherein it follows a profile similar to Figure 5.6

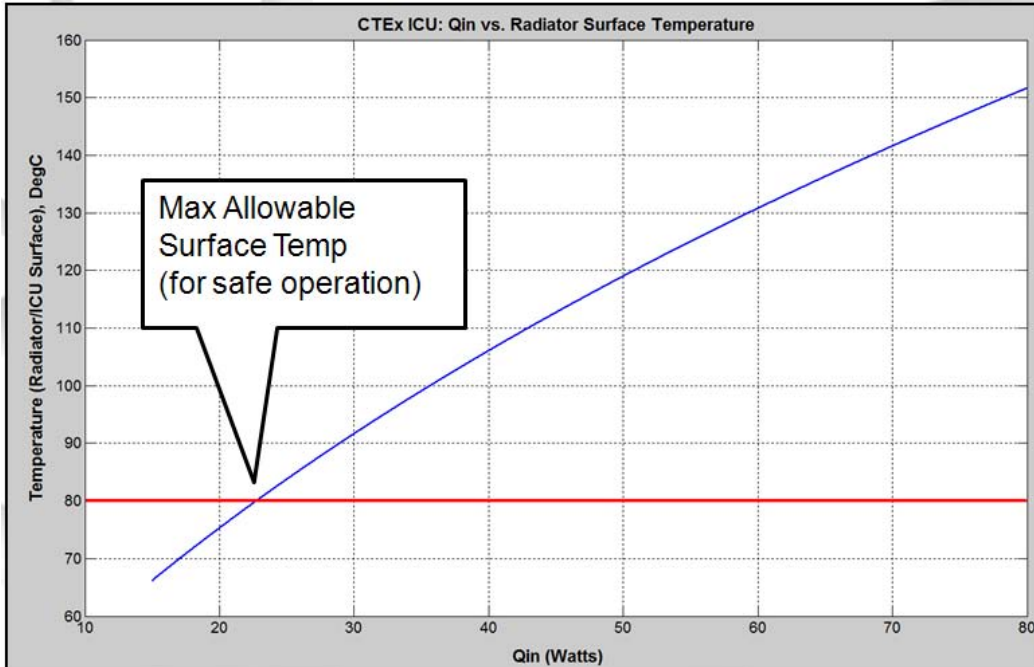


Figure 5.6: ICU Thermal Dissipation, Surface Temp vs Input (Generation)

Note that the higher the temperature, the better the heat dissipation; however, most COTS hardware and electronics have a maximum service operating temperature in the neighborhood of 70-85 degrees Celsius, thus a cutoff temperature is required for this design. Power levels over this threshold will likely mandate other means to successfully cool the device.

Next, we will discuss the design features throughout the ICU assembly. As part of the listed requirements, detailed in Section 5.1, this design process was intended to assess the HREP design to apply lessons learned and efficiencies as much as possible. From that review, it was noted that much of their design could be utilized for the CTEx mission. Commonalities include the selection of PC/104 board restraint structure and

vibration isolation system, cooling fan, purge/fill valve (and associated hardware) as well as features in the aluminum housing.

The PC/104 card cage and vibration isolation system is a COTS item procured from Parvus Corporation and is called their PC/104 Card Cage with Shock Rocks®. [58] This system is rated for military applications and utilized a novel securing mechanism to hold the PC/104 cards in place (through squeezing an elastomeric material in its corner). The Shock Rocks isolate the system from vibration by acting as a low-pass filter and are fastened directly to the card cage. Securing this system into the housing is accomplished through strategic placement of translation isolators (toleranced boss features in the housing to prevent motion). These translation isolators compress the Shock Rocks by approximately 2% in order to assure a positive compression upon these components (however, this internal compression does not affect the PC/104 card cage stack/structure and electronic components). Figure 5.7 depicts this arrangement.

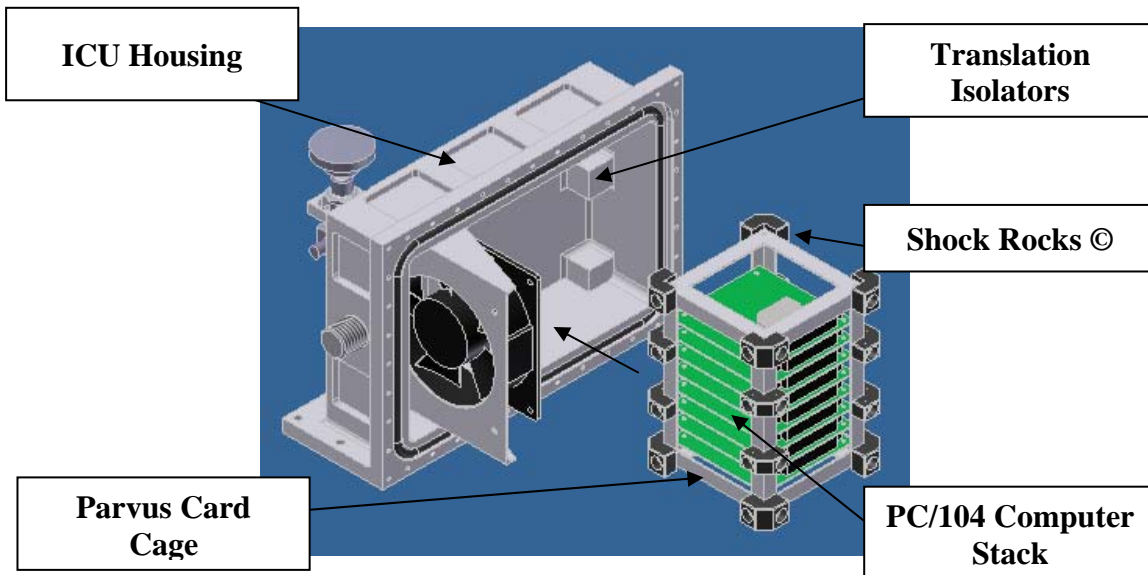


Figure 5.7: ICU PC/104 Card Cage Configuration

The next feature of interest is the forced-convection fan which circulates the dry nitrogen atmosphere within the ICU at 18 psia. The Orion OD1238-24HB direct-current fan was selected for the high-level of throughput it produces while consuming minimal electrical power. Operating between 24 to 28 volts DC and roughly 4.8 watts, this device outputs 226 cubic feet per minute airflow at a nominal 65,000 lifetime-hours (at 45 °C). Note that its temperature operating range is between -10 and 70 °C. [59] A support bracket was designed for the fan from aluminum 6061-T6 which fastens directly to the aluminum housing with spring washers (for mitigation against fastener-loosening via vibrational loading). Figure 5.8 presents the aforementioned components.

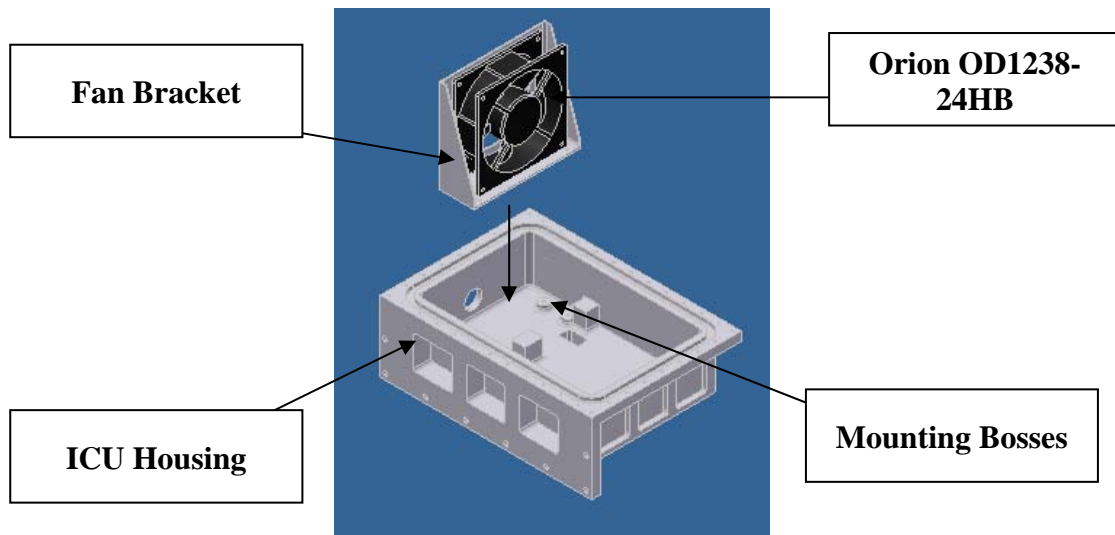


Figure 5.8: ICU Convective-Flow Fan Assembly

The hermetically sealed electrical feedthrough is a face-seal, o-ring assembly supporting 12 pins at 20 AWG. This component was acquired through Pave Technology, Co. wherein each are delivered sealed with accompanying data specification documentation (required for space-traceability). Helium leak checks as well as Hypot

electrical testing is accomplished upon each of these devices at the factory providing confidence to end-users of their pedigree for operations. [60] Figure 5.9 presents the feedthrough configured within the ICU -- note the direction of assembly is critical for proper, long-term, on-orbit operations (specified in assembly procedures).

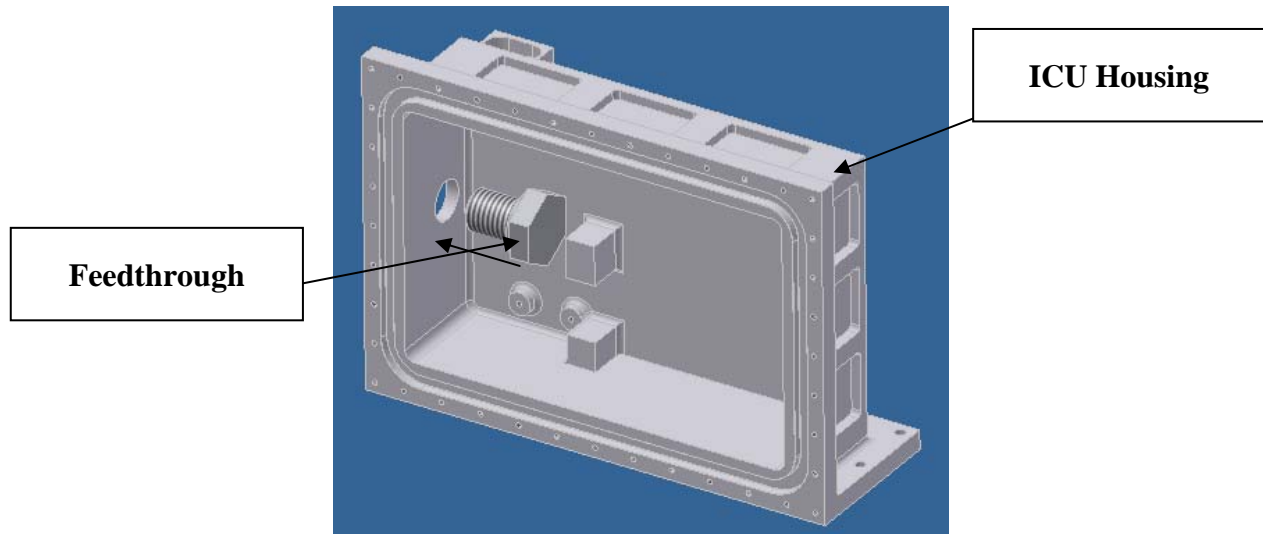


Figure 5.9: ICU Electrical Feedthrough

The fill/purge hand valve is a Swagelok SS-4BW stainless steel bellows valve rated to above 200 °C and 500 psig (note this design is not intended to attain these high levels of operation). It was selected for its compact size, durability and ability to perform pressure and vacuum service in both directions of flow (required for our concept of operations). The valve connects to the ICU via a welded VCR fitting to a 1/8-inch National Pipe Thread bore in a special feature designed into the aluminum housing known as a “doghouse.” [61] A custom mounting bracket was designed directly into the housing to secure the device. After assembly of the ICU, this valve is operated to allow leak check and purge operations to be performed (to remove air containing oxygen,

moisture, carbon dioxide and other contaminants) through connecting a vacuum pump for purge cycles to be completed. Roughly 10 purge cycles are acceptable for space-flight operations (pressurize to 30 psig followed by venting and vacuum-pumping down to 26 inches of mercury). Once the above-stated operations are completed, the valve handle may be removed and lock-wire shut as pre-launch operations continue. Figure 5.10 displays the purge/fill valve.

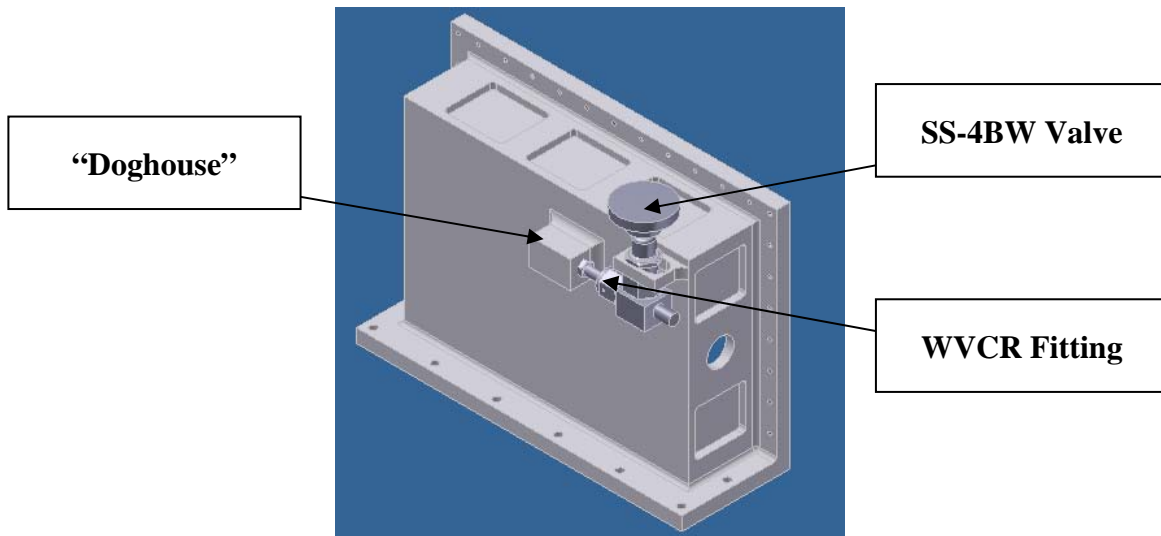


Figure 5.10: Swagelok SS-4BW Purge/Fill Hand Valve

The o-ring seal is a viton (fluorocarbon) seal, compatible for space-flight operations. This component was designed to integrate directly with the aluminum housing as a static face-seal gland wherein sizing and tolerance specifications were supported through manufacturer guidelines. Gland dimensions were set and adjusted to ensure that a 5-8% face squeeze is applied to the seal and a circumferential 2% squeeze is allowed (on the inner diameter of the o-ring) to support proper assembly. [43]

Additionally, a very thin layer of vacuum compatible grease was selected to be applied to

the o-ring to support the seal at the temperature range expected (Castrol Braycote[®] 600EF). [62] Figure 5.11 details the o-ring assembly.

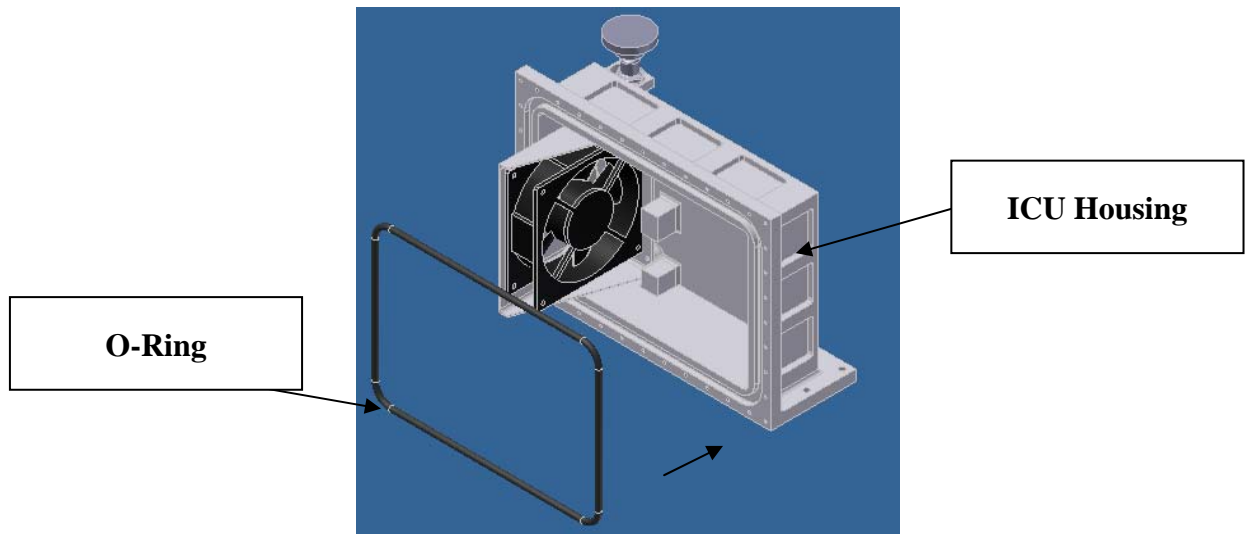


Figure 5.11: ICU O-Ring Gasket Face-Seal

The aluminum housing is the most critical element in this assembly as it both supports all of the structural aspects of the device as well as promotes the proper thermal dissipation for normal operations. The housing front face is integrated with cooling fins and a thermal baffle which supports positive-compression of the PC/104 vibration isolation system as well as ensures proper thermal loop flow direction. The positive-compression on the PC/104 stack is critical to ensure that the structure does not translate or rotate within the device. Moreover, a proper thermal loop flow direction is crucial so as not to develop “hot-spots” (i.e., pockets of stagnated flow). It should be noted that design of the cooling fins was not optimized due to the fact that the final PC/104 stack composition (and thermal load) was not known at the time of design. Light-weighting was performed on the unit to acquire mass figures as low as possible while retaining

structural safety margins. The housing elements are secured with 40 individual fasteners spread out at one-inch intervals due to the fact this is a low-pressure pressure vessel (18 psia). Maintaining this device as an “ambient-pressure” device is critical for the CTE_x program in order to reduce prelaunch and on-orbit safety documentation requirements.

Figure 5.12 details these components.

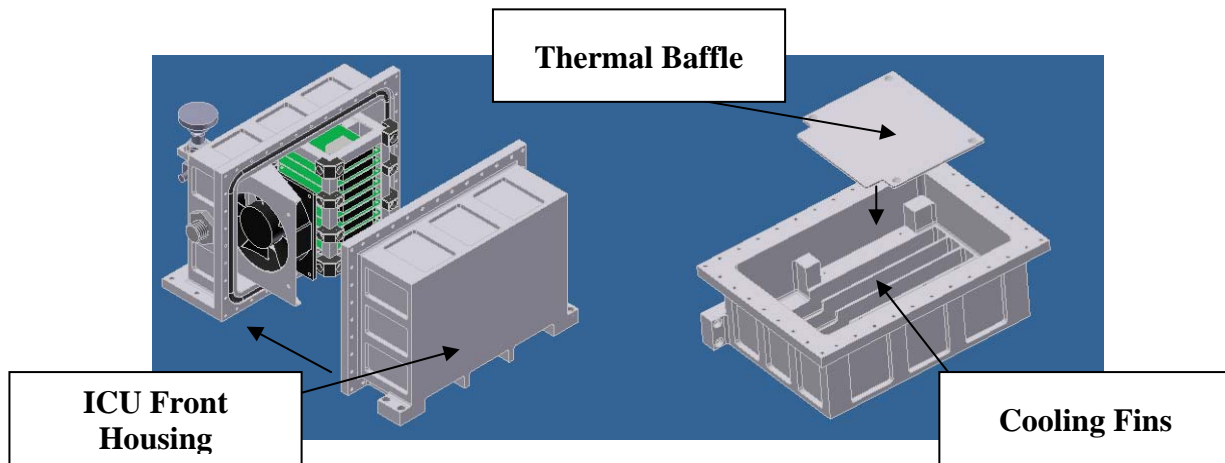


Figure 5.12: ICU Housing and Final Assembly

5.3.1. *Test Campaign Methodology.* The test campaign, to characterize nominal ICU operations, consisted of three primary phases, including: assembly/checkout, vibration and thermal-vacuum (TVAC) environmental loading. Each phase was intended to validate preliminary expectations for the performance of the device in order to provide confidence in the design as-built. Modifications to this design and lessons learned are identified in the results, Section 5.4 while conclusions and future work are indicated in Sections 6.3 and 6.4, respectively.

The assembly and checkout operations are critical in validating the basic mechanical and electrical functionality of the ICU. Detailed procedures for this phase

were established per SOP-SCTEX-0001 (and provided as reference in Appendix C). This procedure has two overarching efforts, including the proper assembly and construction process, as well as leak check, purge and fill operations. Assembly is straight-forward per the steps listed within the procedure requiring all components listed in the equipment requirements (to be built to specification per the technical drawings). Upon successful assembly, the device must be assessed for its leak rate. The leak-rate test is accomplished through setting up the configuration detailed below, wherein the ICU is connected to a pressure source (gaseous, dry nitrogen; i.e., GN2 K-Bottle), GN2 regulator, pressure gauge (PG-1) and valves (HV-1, HV-2, HV-3, GN2 Isolation HV). See Figure 5.13 for further detail.

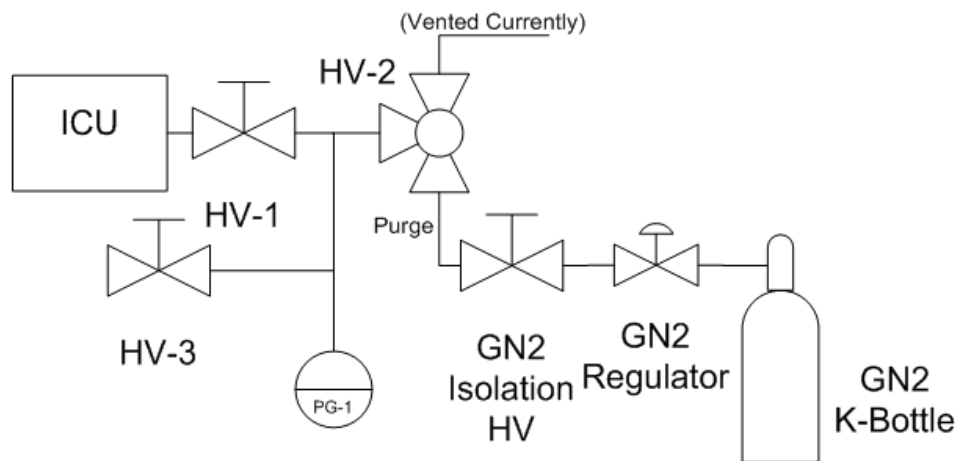


Figure 5.13 ICU Leak-Check, Process and Identification Diagram

The leak check is conducted through slowly increasing the pressure at 10 psig increments from 0 to 35 psig (isolating the source pressure through closing the tank valve or regulator), holding each pressure-level for one minute, then elevating to the next set point, and holding the final test pressure (35 psig) for five minutes. Leak test solution is

utilized to determine locations of spot leaks. If found, the system must be depressurized and the issue resolved prior to continuing. Upon witnessing no leaks and the process is accomplished satisfactorily, the test team may proceed.

The next operation which must be executed is the purge and fill of the ICU. The intent here is to ensure a high-purity thermal convective fluid exists within the device, allowing for low levels of contaminants (e.g., humidity, oxygen, carbon dioxide, etc.) as well as assisting in the designer's ability to better predict the behavior of the unit. To execute the purge/fill, the previous apparatus setup is reconfigured with a vacuum pump (for this operation, an Edwards two-stage pump was selected, capable of .005 torr vacuum levels) and a three-way valve flow valve to be placed in line (in order to enable selection of purge or vacuum operations). Note that the earlier system for leak check may be setup into this final configuration in order to save time. Figure 5.14 depicts this updated configuration.

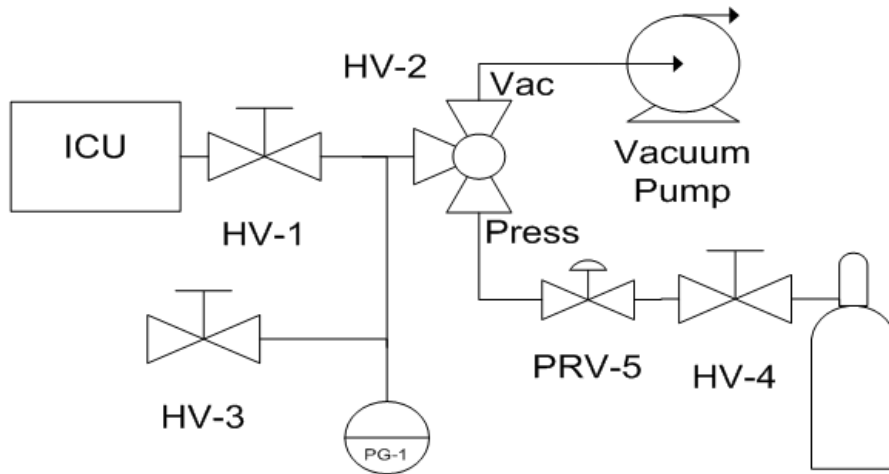


Figure 5.14: ICU Purge & Fill, Process and Identification Diagram

A minimum of ten vacuum/pressure cycles were conducted from 26-28 inches of mercury to 30 psig, respectively, to ensure the proper purge levels have been attained. Upon completion of the final fill cycle to 30 psig, the source valving (tank valve and regulator) will be closed followed by the remaining downstream system vented down to roughly 3-4 psig (~18-19 psia), leaving a low “pad-purge” on the system. This pad-pressure continues to keep internal positive pressure on the system while at ambient conditions as well as enabling users to witness leaks, should they occur during pre-launch and on-orbit operations. Completion of this set of operations allows for final electrical checkout, upon closeout of mechanical validation, prior to further integration of this device into the larger CTE_x instrument assembly.

The second phase of this test campaign is that of maximum predicted environmental loading (MPEL) beginning with vibrational testing. The ICU sub-system was characterized utilizing the H-IIB Transfer Vehicle (HTV) Cargo Standard Interface Requirements Document (NASDA-ESPC-2857 Rev.C). [69] The primary goals of this phase were to understand the modal properties of the ICU (natural resonances) and validate functionality after the test run had been conducted. Test operations were accomplished per TOP-SC_{TE}X-0001 (provided in Appendix C). All three axes of the ICU were excited following a pattern of sine-sweep (.25g level), random vibration (three minutes duration per the ISS Qualification and Acceptance Environmental Test Requirements, SSP 41172 Revision U, and HTV Cargo Standard Interface Requirements Document, NASDA-ESPC-2857 Rev. C), final sine-sweep (.25g level, to assess changes from the initial) and a functionality test (cycling power, assessing all electrical/sensor

functionality, and mechanical pressure is held). [63] [64] After all portions of this phase were complete, the ICU was opened to assess internal issues (visual inspection).

Finally, the last portion of the ICU test campaign consisted of the TVAC operations to both assess the ability to operate in a vacuum environment as well as to characterize thermal behavior (while cycling and controlling the environmental temperature it operates within). Test operations for this phase were accomplished per TOP-SCTEX-0002 (included in Appendix C as reference). The intent of this effort was to acquire actual thermal behavior while adjusting the input parameters (TVAC temperature and ICU electrical power). Vacuum levels are set to those witnessed during nominal, space-flight operations ($\sim 1\text{E-}6$ torr). Set points were determined through assessing low-, mid-, and high-range expectations for operational scenarios. Regarding electrical input power, these parameter set points were 13 watts (low), 25 watts (mid) and 40 watts (high). TVAC thermal-environment loading was characterized at $-40\text{ }^{\circ}\text{C}$ (low), $20\text{ }^{\circ}\text{C}$ (mid) and $40\text{ }^{\circ}\text{C}$ (high) levels. Test operations were executed by allowing the system to start at an initial (cool) state, then applying power and temperature set points to monitor the transient reaction of the device. After an adequate period of time or a threshold temperature was attained (e.g., CPU temperature at $85\text{ }^{\circ}\text{C}$), the power was disabled for cooling operations to begin in order to recycle to the next set point. Within the TVAC chamber, the ICU was setup to only allow radiation as the means for thermal dissipation (through insulating the bottom of the unit from the TVAC platen with a sheet of one-inch delrin). TVAC electrical feed-throughs allow for independent power to be connected to the CPU, fan and resistive heater-patch (enabling selective control over the

operations of this phase of the characterization), as well as, external thermocouples to monitor thermal flux and internal temperature levels. Figure 5.15 depicts the TVAC test setup

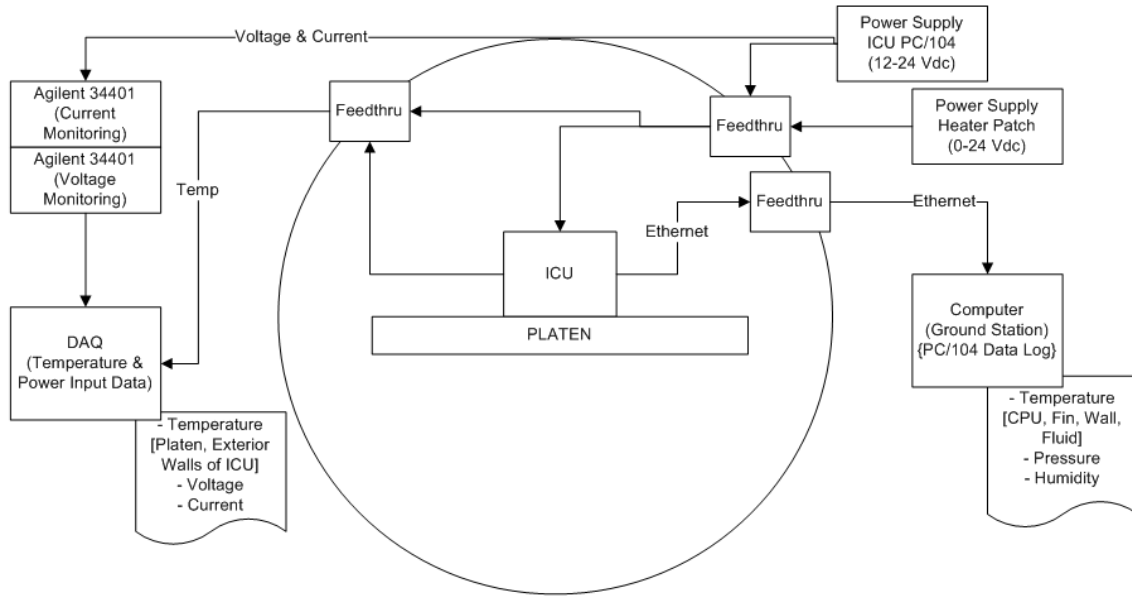


Figure 5.15: TVAC Special Test Equipment Configuration, Block Diagram

5.4 Results

ICU data resulting from the design, analysis and test campaign is broken into three segments including: modeling expectations, test campaign products and on-orbit predictions. Conclusions from information gathered can be found in Section 6.3 with recommendations for future work found in Section 6.4

5.4.1. Modeling Expectations. Due to the fact that this developmental work is centered around a model validation focus, a moderate amount of research effort was expended determining a suitable model to meet early trade-space requirements. From the

methodology setup in Section 5.2, a MATLAB Simulink [®] mathematical model was developed to study the transient and steady-state effects of various set point conditions for the ICU. See Figure 5.16 presenting the Simulink model.

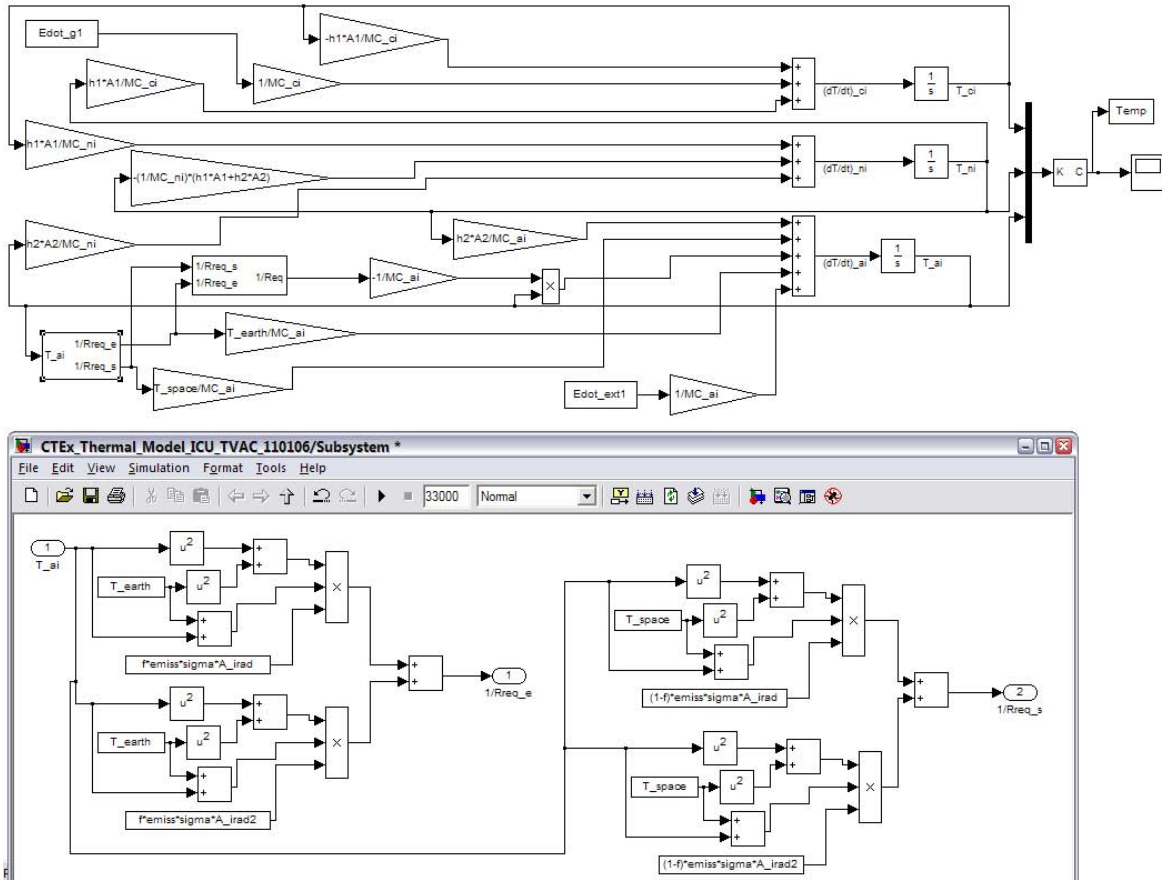


Figure 5.16: ICU MATLAB Simulink [®] mathematical model

From an early point in the design, it was understood that even moderate power levels will cause high thermal conditions, likely exceeding thresholds deemed as “safe” (through assessment of manufacturer technical data). Nevertheless, the primary input parameters for the thermal model include the external thermal environmental conditions (Earth, deep-space, or TVAC temperature), electrical power level input, and emissivity.

Results from a representative run (ICU power at 13 W, TVAC temperature at -40°C and surface finish is machined aluminum, $\epsilon = 0.09$) are shown in Figure 5.17.

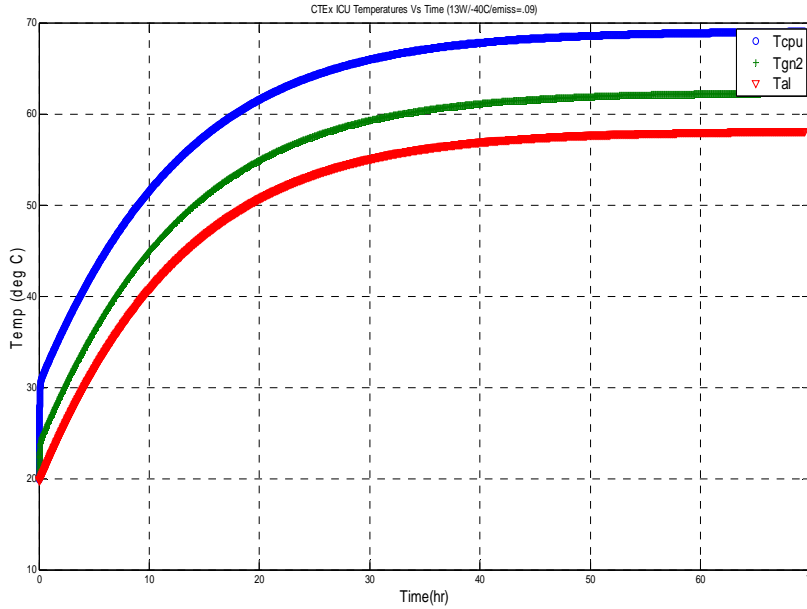


Figure 5.17: ICU Thermal Trending, TVAC Simulation (13W, -40°C , $\epsilon = 0.09$)

Results from a select number of runs are tabulated below in Table 5.9. It should be noted that these early results presented from this model are for the ICU testing within the TVAC chamber, radiating all energy off of five of its surfaces (i.e., a “best-case” scenario; versus on orbit, where likely only 2-3 surfaces will be permitted to dissipate excess energy through radiation).

Table 5.9: ICU Mathematical Model, Thermal Behavior Predictions

Surface Finish	Machined Aluminum ($\epsilon=0.09$)						Black Paint, Chemglaze Z306 ($\epsilon=0.90$)						Units
	13			25			13			25			
Power	13			25			13			25			(Watts)
Temp (TVAC)	-40	20	40	-40	20	40	-40	20	40	-40	20	40	(deg C)
Temp_CPU(Steady-State)	68.7	95.9	107.5	125.9	144.9	153.5	28.1	39.5	58.0	37.9	56.9	74.3	(deg C)
Temp_GN2(Steady-State)	62.1	89.2	100.8	113.0	132.1	140.7	21.8	32.8	51.4	25.3	44.1	61.5	(deg C)
Temp_AL(Steady-State)	57.9	85.0	96.6	104.9	124.0	132.6	19.9	28.6	47.2	19.9	36.0	53.4	(deg C)
Time (to Steady-State)	39.7	38.3	36.9	35.7	32.9	31.6	0.1	3.4	4.3	0.1	4.0	4.4	(Hr)
Time (CPU to 85C)	NA	18.0	11.9	7.1	5.0	4.3	NA	NA	NA	NA	NA	NA	(Hrs)

The information that Table 5.9 supports is some of the early trade-space analysis needed to better define more rigorous design (as further requirements are refined) as well as provide for an early operational picture (i.e., how long we can execute operations at peak electrical load conditions). From this data, it can be witnessed that a surface treatment will be necessary if this design is utilized for on-orbit operations. Additionally, peak power consumption will be limited to 25 watts for limited periods of time (after which will need to be periods of cooling).

The next assessment performed was a cursory review of stress and modal properties associated with operational conditions. This activity focused on the ICU housing internal pressure, external pressure and modal analysis load cases, analyzed with the help of finite element modeling (FEM) wherein ANSYS® was utilized. Note that this analysis was intended to verify, after significant light-weighting of the ICU assembly, that significant structural issues had not resulted, possibly causing failure under load (and to mitigate those, if found). Therefore, best-practice methodologies were utilized in this portion of the effort; however, an optimization and refinement of the results was not conducted (nor was it the goal to closely match the model to gathered laboratory results).

It was found that, after feature reduction of the CAD model to only the most critical aspects (primarily the housing elements and fan bracketry, removing holes and other non-essential geometry for modeling purposes), that a mesh size of 0.1 inch cubes (solids) was acceptable to converge to a solution. Load cases for the internal and external pressure were meant to assess the operational set points expected; however, additional pressure was added to the internal pressure load case to account for the purge and pressurization pre-launch operations. The external pressure load case was also meant to simulate the purge and pressurization load case in the scenario of vacuum operations (and a higher external pressure is witnessed). Thus, the internal pressure load case was set to 35 psia and external pressure load case was set to 14.7 psia. The modal analysis collected the first six non-rigid body modes.

Overall, results from this modeling effort were favorable. Worst-case loading in the internal pressure scenario accounted for a 12.64 ksi maximum stress and 0.0048 inch displacement at the rear-side of the ICU housing. The selected material (aluminum 6061-T6) was deemed acceptable as yield strength is 45 ksi (roughly a 3.5 safety factor). See Figure 5.18 for the post-processed plot for this load case. The external pressure load case (during pressure/vacuum purge cycling) was significantly lower at 5.755 ksi and maximum displacement at 0.002 inches predicted (again, acceptable in light of the previous discussion). Figure 5.19 details the post-processed results from this operational analysis. Finally, an eigenvalue analysis was performed to determine the modal response of the ICU structure. From this analysis it was determined that the first structural natural frequency is expected to be at 386.2 Hz. These results are acceptable as the initial natural

resonance mode needs to be greater than 35 Hz to meet specifications for launch. Note that this requirement is for the assembly in the Z-direction; however, due to the fact the orientation of the ICU could be different from current plans (due to ISS ELC slot assignments), it is prudent to ensure that the device can be flexible (in order to meet requirements in any orientation).

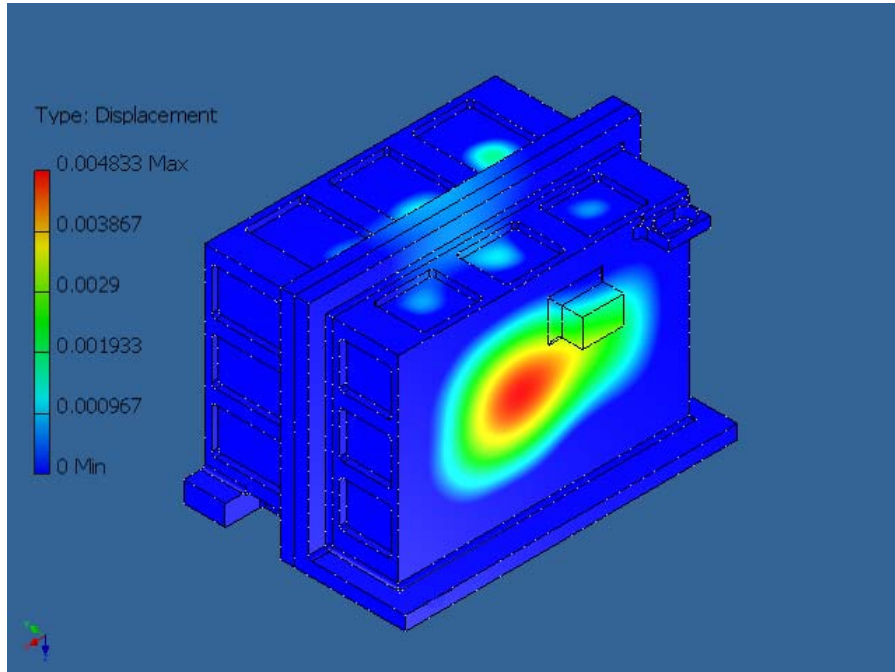


Figure 5.18: ICU FEM, Max Displacement (in), Internal Pressure Load Case, 35 psia

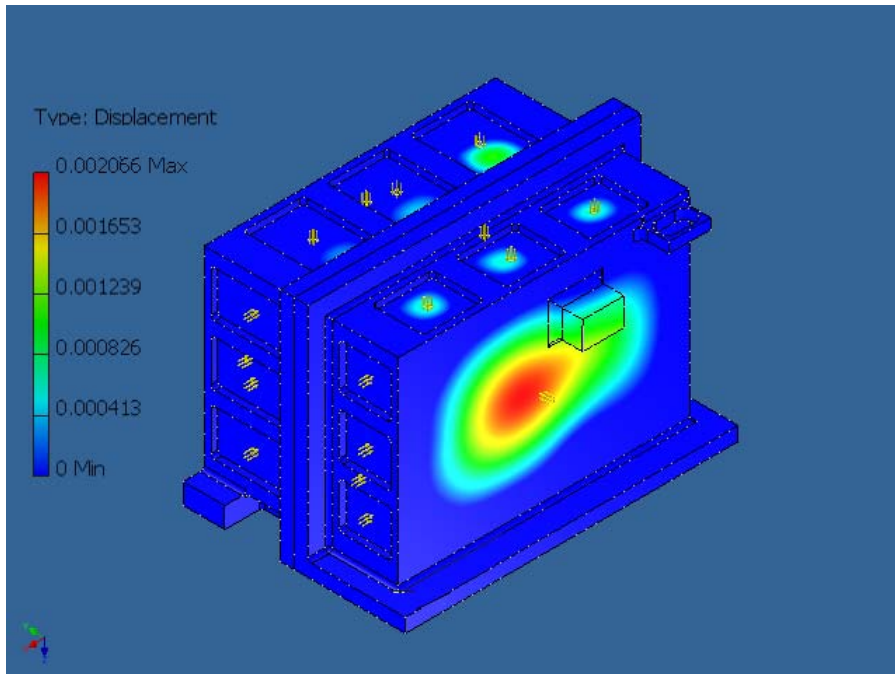


Figure 5.19: ICU FEM, Max Displacement (in), Ext Pressure Case, 14.7 psia

Overall, the stress and modal FEM analysis results were favorable allowing the design to proceed to fabrication and characterization testing for validation of the mathematical model. The next subsection will discuss these results wherein these modeling results were confirmed.

5.4.2. Test Campaign Outcome. As discussed in Section 5.3, the intent of the test campaign was to validate the mathematical thermal model as well as assess whether the design met feasibility thresholds for expected operational mission constraints. The initial qualitative results acquired from the test campaign were in the assembly process. Through only minor corrections in the mechanical design, the most major issue resulted from a convenience in the fabrication process of the ICU housing. Due to the geometry of the Parvus Shock Rocks ®, the translation isolators in the ICU aluminum housing

originally called for a non-radius/square corner; however, a simple solution was found to modify the Shock Rocks through allowing the housing machine radius and adding a 1/8 inch chamfer to the shock rocks. See Figure 5.20 for further detail.

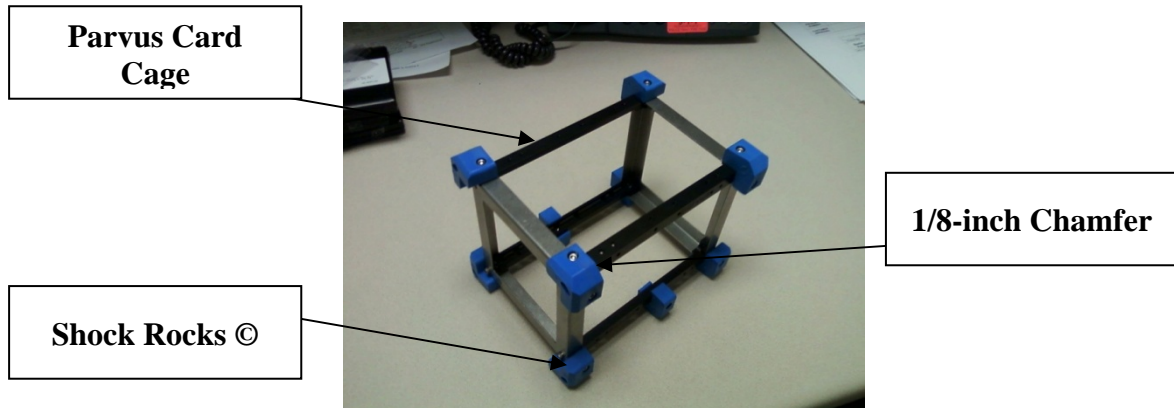


Figure 5.20: Parvus Card Cage Reconfiguration

Overall, SOP-SCTEX-0001, ICU Assembly and Checkout procedures, were seamless and provide an outstanding baseline for further development upon this design. Upon successful assembly, mass was determined to be 9.98 kg, meeting the requirements that it must fall under 10 kg. Figure 5.21 depicts the assembly processing.

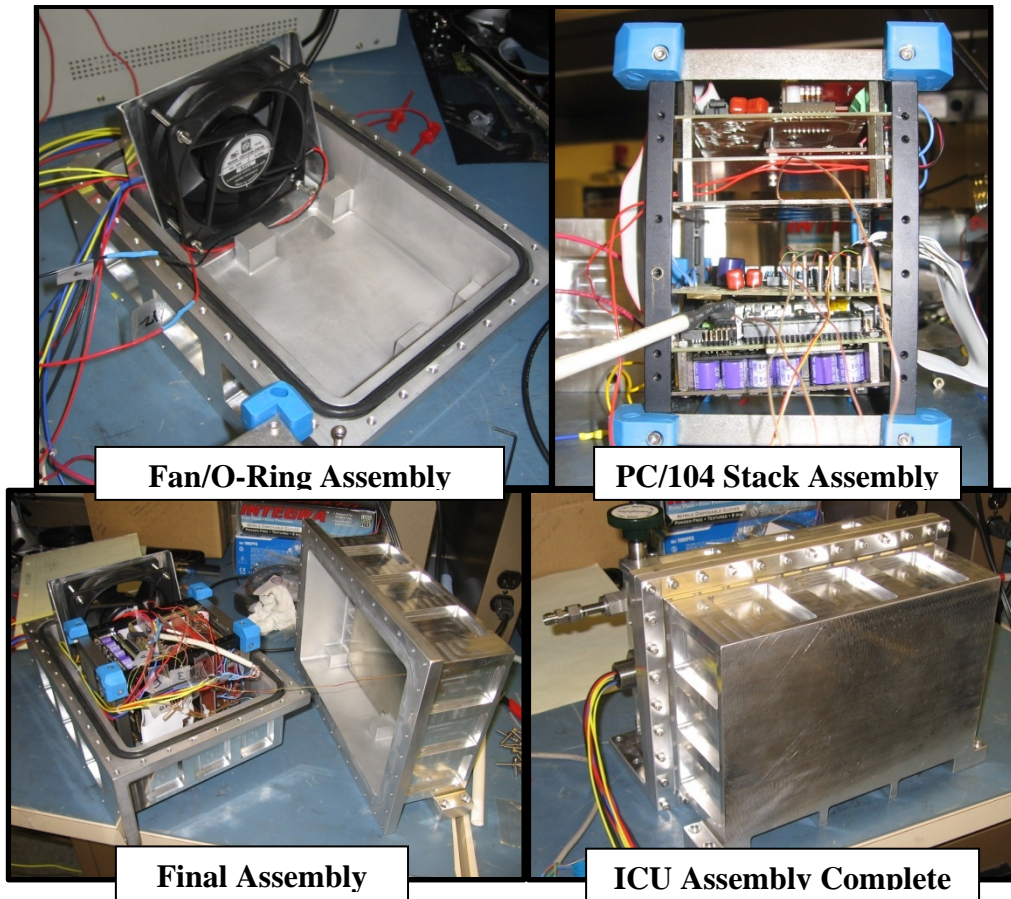


Figure 5.21: ICU Assembly

The vibration phase of the test campaign resulted in positive results as well. The fundamental frequency resulted at 376 Hz, roughly 2.7% from the FEM predictions (386.2 Hz – due to excitation of the fan/bracket assembly). This also surpasses the modal requirement to ensure the fundamental frequency is above 35 Hz (in all directions for this design). The functionality of the electronics and the ability to mechanically retain pressure also passed successfully without any issue to report. One primary issue experienced was that of fasteners loosening during random vibration testing, especially at metal/plastic interfaces, such as the fan bracket (even though locking spring-washers

were used throughout the design). This issue could be resolved through application of a vacuum-compatible thread-locking fluid to fasteners. Figure 5.22, Figure 5.23, and Figure 5.24 details the modal testing for the X, Y and Z axes under test, respectively.

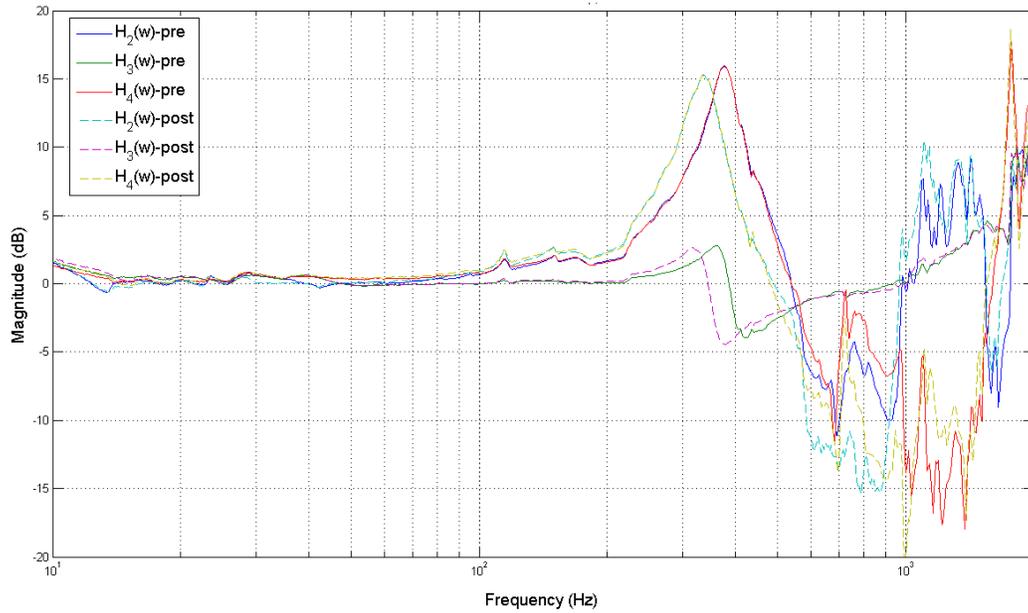


Figure 5.22: SCTEx ICU, 0.25g Sine-Sweep, X-Axis

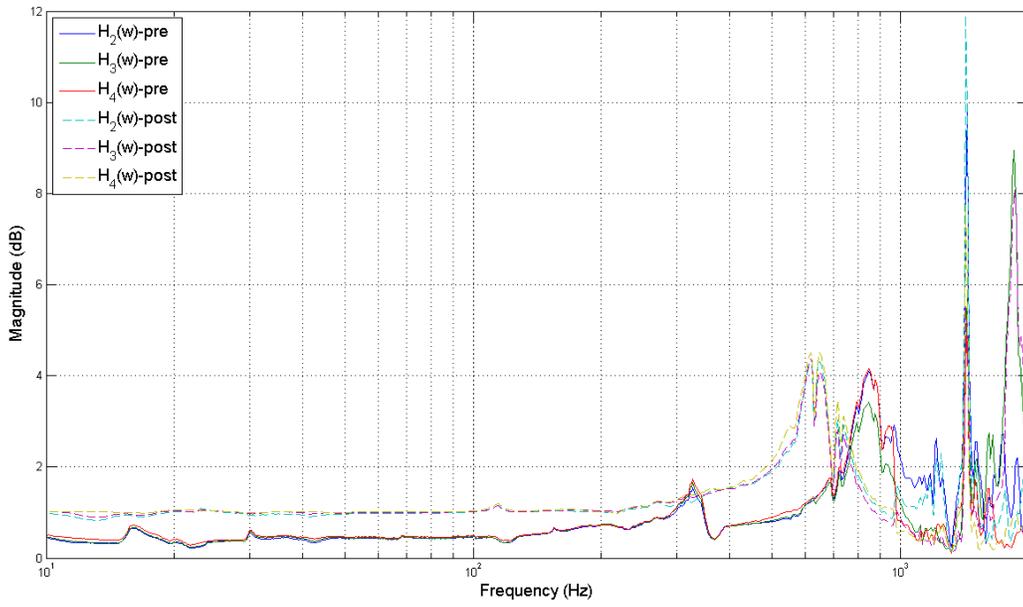


Figure 5.23: SCTEx ICU, 0.25g Sine-Sweep, Y-Axis

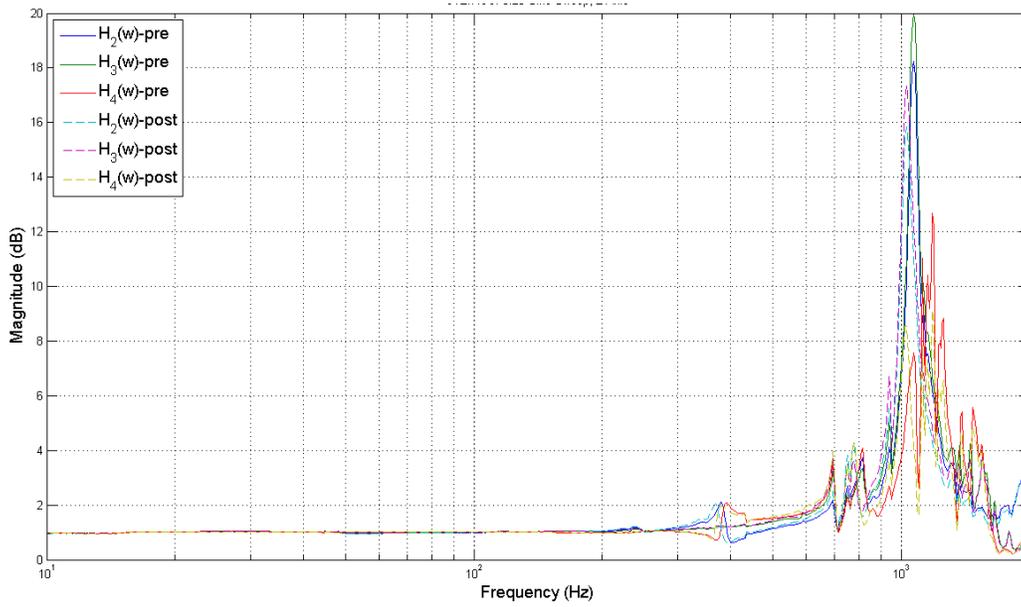


Figure 5.24: SCTEx ICU, 0.25g Sine-Sweep, Z-Axis

Finally, results from the TVAC phase exceeded expectations pertaining to the thermal modeling validation. In general, this phase of the test campaign ran as seamless as the other phases; however, there were noteworthy issues. First, and most notable, were complications relating to connectivity with the PC/104 stack. It was concluded that inexpensive electronics in the configuration were attributable to a repeated dropout problem as it was witnessed especially during periods with higher loading placed upon the ICU (both power and thermal set-points). These dropouts forced the test series to only collect data at low- and mid-range CPU power levels. Next, it was witnessed that the PC/104 weather board selected also had an issue with respect to the maximum pressure it could sense (130 kPa, or 18.85 psia). Therefore, as temperature was elevated and the pressure also increased (due to ideal gas behavior of the fluid), over-ranging values were acquired. Nevertheless, during cool-down periods of testing, pressure measurements re-entered a suitable range (and provided confidence that pressure had not been lost within the ICU). Finally, an issue was also witnessed on this weather board as gaseous-nitrogen fluid temperature measurements were acquired. The nitrogen fluid temperature was consistently measured 5-10 °C below expectations throughout the test campaign (and may be potentially coupled to the over-ranged pressure measurements). This error may have been caused by other factors, including: thermocouple calibration, the device temperature ramping up (i.e., not at steady state), and some combination of the fluid and a nearby PC/104 board, among other rationale.

Figure 5.25 shows a cold run (low TVAC temperature, -40C) and low power level (13 W) with both actual and simulated results overlaid. Figure 5.26 depicts the error (in

degrees, acquired measurements versus simulation). As noted earlier, the nitrogen temperature is offset by 4 °C; however, the measured CPU and aluminum housing temperatures match within nearly 1% that of the simulation for the duration of the nine-hour test. The model emissivity parameter is set for machined aluminum ($\epsilon=.09$).

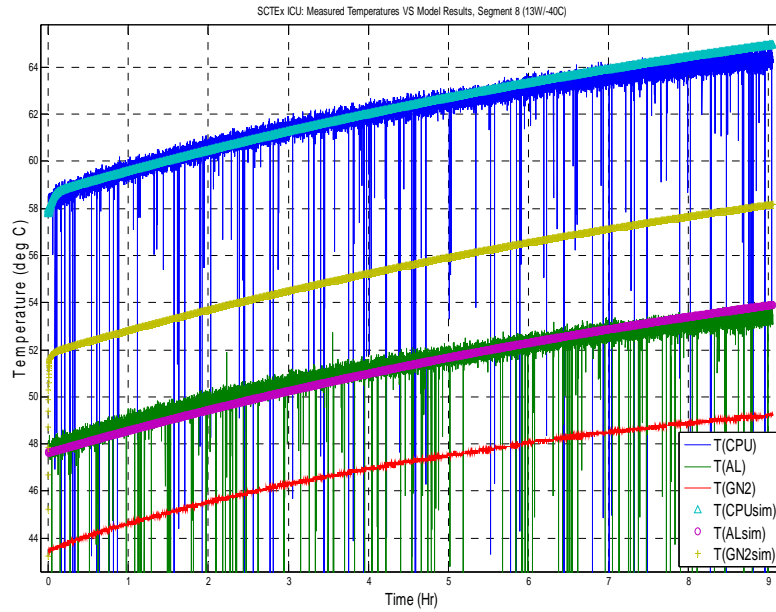


Figure 5.25: SCTEx ICU Temperature Profile, Measured Vs. Simulated, 13W/-40C

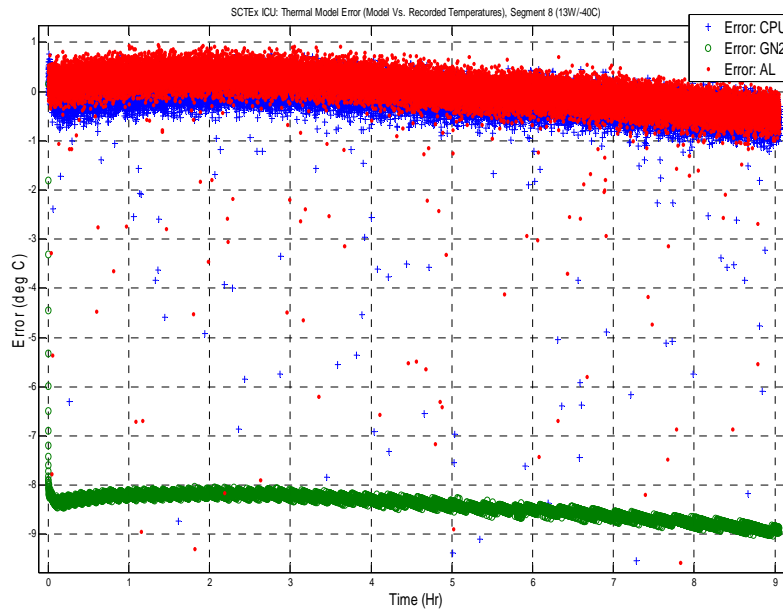


Figure 5.26: SCTEx ICU Error Profile, Measured Vs. Simulated, 13W/-40C

Figure 5.27 presents a nominal run at mid-range temperature and low-power levels (20 °C and 13 W, respectively) while Figure 5.28 shows the error (in degrees, acquired measurements versus simulation). From this data, it is again witnessed a -6 °C offset in the nitrogen temperature whereas the CPU and aluminum housing temperature offset is roughly 2 °C (negative due to the fact that the model predicts a lower temperature than what was witnessed). Although there is a noticeable offset, it should be noted that the slopes for each of these curves match very closely to one another. A general slope of +4.4 °C per hour was witnessed overall.

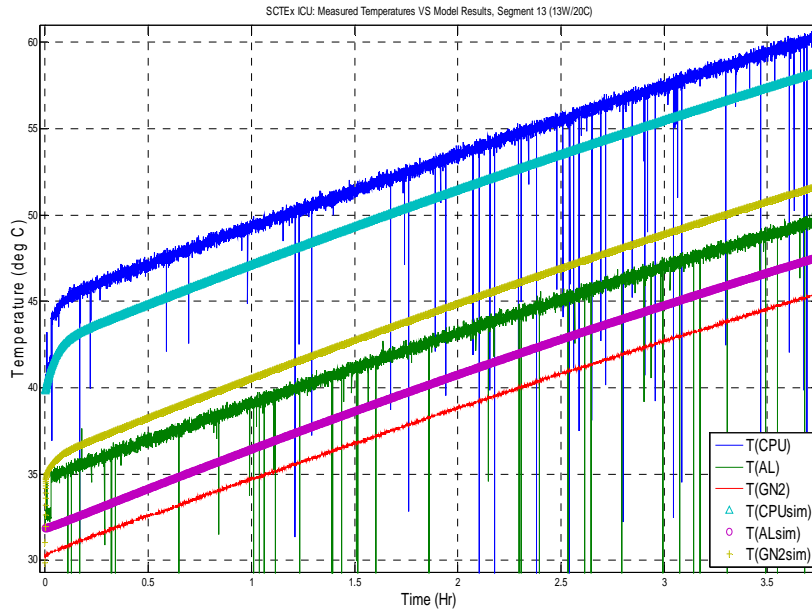


Figure 5.27: SCTEx ICU Temperature Profile, Measured Vs. Simulated, 13W/20C

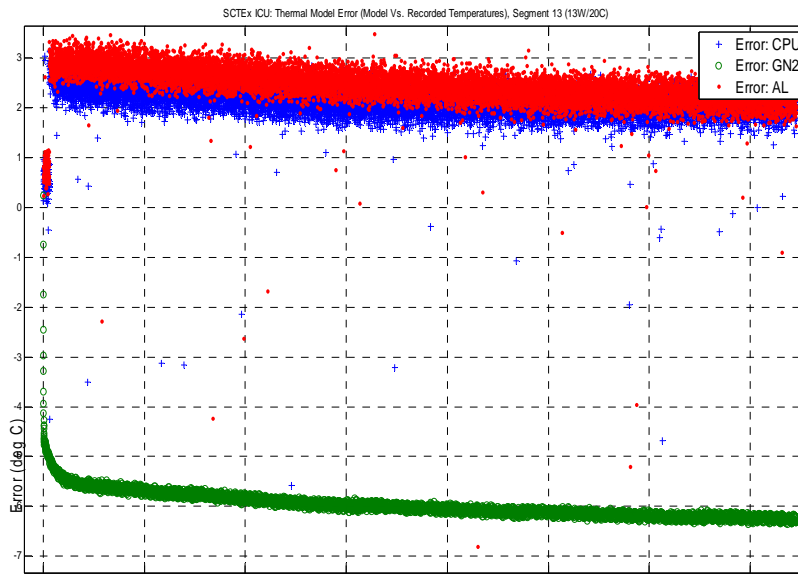


Figure 5.28: SCTEx ICU Error Profile, Measured Vs. Simulated, 13W/20C

The final run presented in Figure 5.29, corresponds to a nominal/mid-power level (27 W) and a mid-temperature setting (20 °C) while Figure 5.30 shows the error (in degrees, acquired measurements versus simulation). From this profile, again, the nitrogen average offset is -8.86 °C, CPU is -7.1 °C and Aluminum block is 2.89 °C. Some of this error is attributable to the fact that all 27 W is applied to the CPU in the mathematical model, whereas during the test run, 13 W was applied to the CPU and fan, while the remaining 14 W was applied to the resistive heater patch.

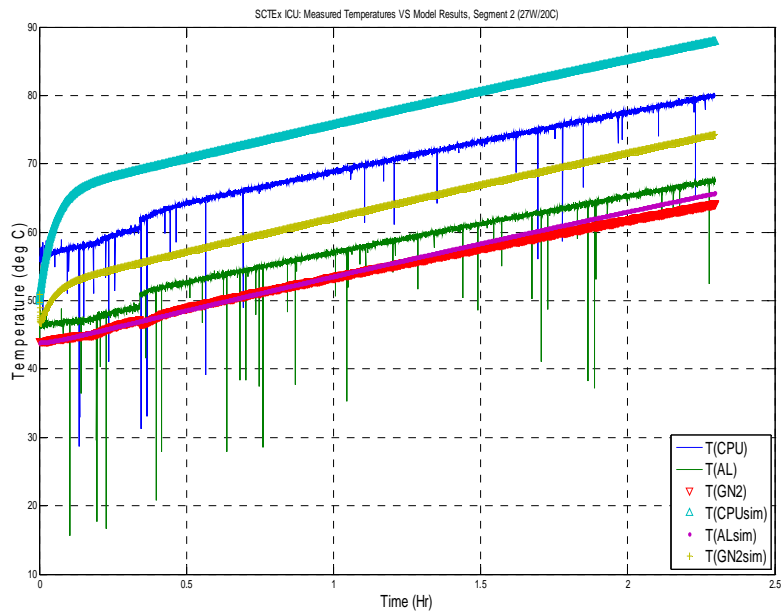


Figure 5.29: SCTEx ICU Temperature Profile, Measured Vs. Simulated, 27W/20C

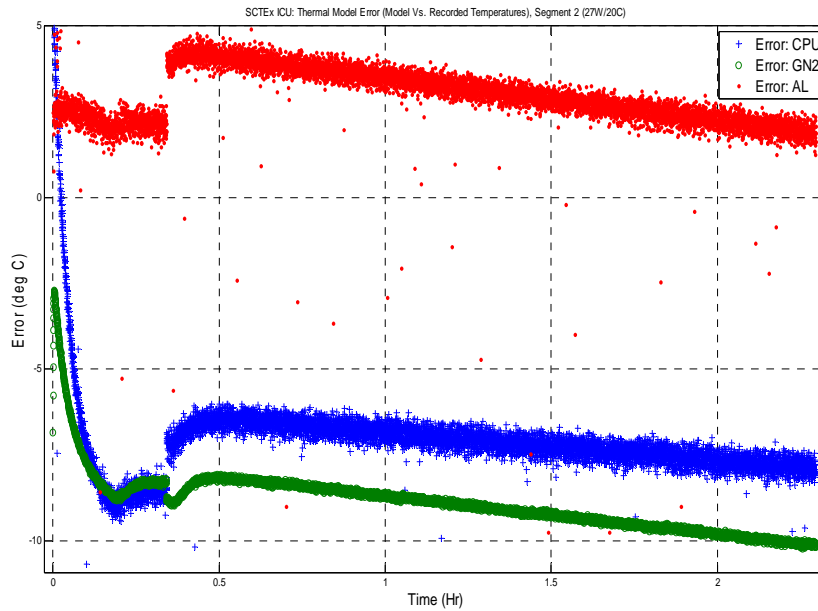


Figure 5.30: SCTEx ICU Error Profile, Measured Vs. Simulated, 27W/20C

5.4.3. *On-Orbit Predictions.* Overall, from the results gathered during the TVAC phase of testing, validation of the thermal mathematical model was determined to be successful (given, that offset factors are applied to account for minor offsets). Due to the validation of the thermal transient slopes, it is expected that steady-state conditions should be witnessed at a minimum of +/- 10% final equilibrium temperatures. Therefore, with this understanding, we may assess some of the on-orbit predicted behavior to initially map the trade-space.

To begin, we will first apply correction factors to the three cases reviewed in the previous sub-section and assess the steady-state peak temperatures. In general, roughly a positive two-degree offset was witnessed to be the worst-case differential temperature while comparing measured data from model outputs (recall that transient slopes matched

closely allowing the offset to correct for final thermal differences). Additionally, the model was reverted from the TVAC thermal case to that of the on-orbit configuration (most notably, two primary radiation faces and blackbody environmental temperatures of 293K and 3K for the Earth and deep-space, respectively). Additionally, due to the design benefits, ZOT white paint was selected as the ICU surface coating to improve thermal behavior characteristics (emissivity = .91, absorptivity = .17). [57] Results from the model corrections can be seen for ICU input-power cases of 13W and 25W in Figure 5.31 and Figure 5.32, below. As expected, the 25W load case surpasses initial thresholds (85°C) after roughly a 1.5 hour period (from an initial state of 20°C).

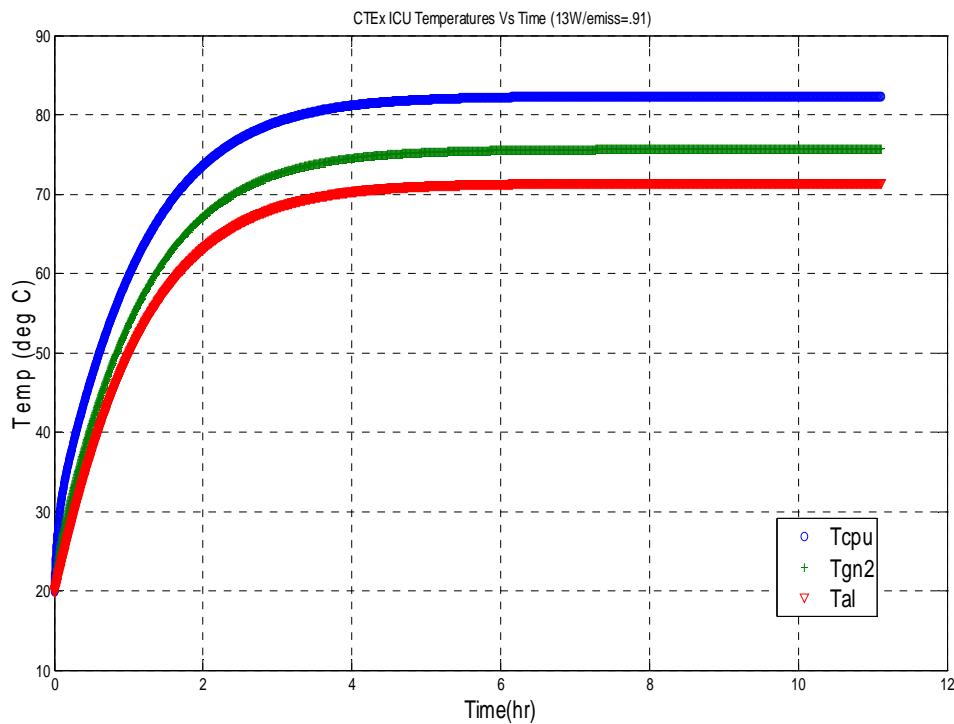


Figure 5.31: SCTEx ICU, Simulated On-Orbit Behavior (13W, Emissivity=.91)

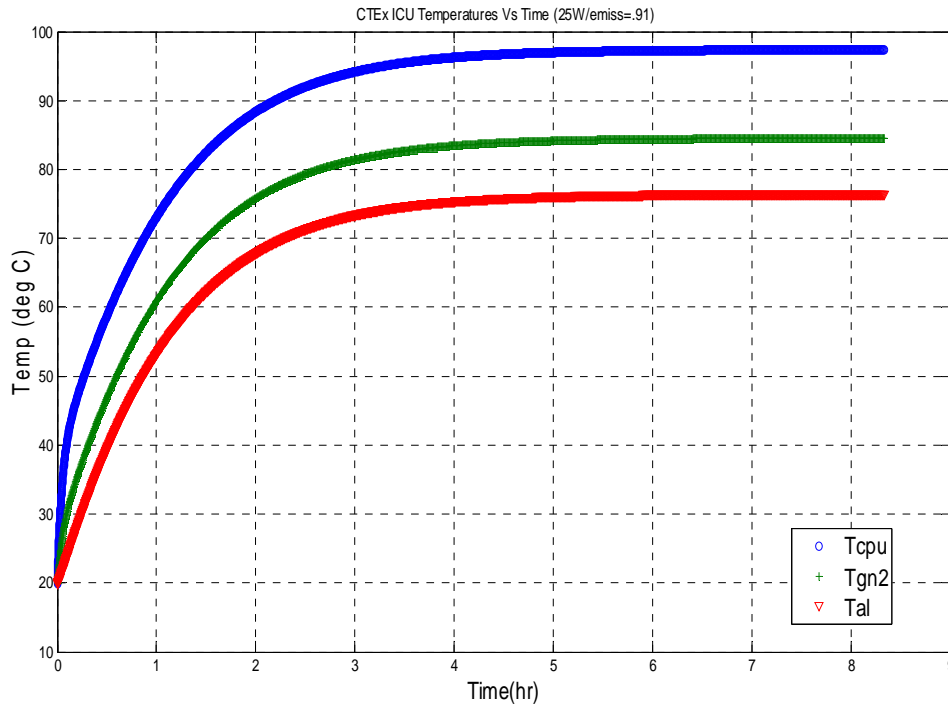


Figure 5.32: SCTEx ICU, Simulated On-Orbit Behavior (25W, Emissivity=.91)

5.5 ICU Design Summary

This chapter covered the space-based CTE_x ICU requirements, thermal model analysis, design/test methodology as well as the results and post-data analysis from the development and characterization research efforts. Overall, it was determined that the design meets minimum requirements and validates the mathematical model; however, further design and analysis will be required prior to solidifying final specifications as the current device was meant for early trade-space mapping. Conclusions from this work will be identified in Section 6.3 and future work contained in Section 6.4.

VI. Conclusions and Recommendations

This chapter presents a brief review for the research accomplished, associated resulting conclusions observed and proposed future work. Five sections constitute this chapter's makeup and include: SCTEx Design, GCTEx Design/Characterization, SCTEx ICU Design/ Characterization, Proposed Future Work, and Final Conclusions.

6.1 SCTEx Design Conclusions

Chapter Three focused on the mechanical integration and initial trade-space mapping for the space-based experiment. The overarching requirement was to meet launch and on-orbit requirements while mounting and supporting components previously selected and on-contract for the program. Engineering best-practices were adhered to in order to acquire a design meeting basic feasibility requirements. Results from this effort produced mass properties for the design and an initial assessment of the trade space associated with light-weighting the optical breadboard.

The mass properties for the design were determined to produce a space-based experiment with a mass of 250 kg while meeting envelope and center-of-gravity requirements. This reported mass assumes COTS component mass is reported accurately, structural components are isotropic, and miscellaneous hardware and wiring throughout the instrument account for roughly 10% of the overall mass. The most significant contribution to this mass is from the optical breadboard, coming in at 43.5 kg (currently specified as a COTS item which will be retrofitted to accommodate the space CTEEx configuration). Performing an eigenvalue analysis on a isogrid replacement breadboard to evaluate structural modifications shows that a potential mass reduction of

more than 75% (down to roughly 10 kg) can be realized while meeting threshold requirements. However, minimal margin is afforded for secondary payload missions. Additionally, while light-weighting the breadboard is an option, further assessment is required upon the system as a whole wherein the breadboard design is integrated with the system to assess modal, structural and thermal effects for specific design choices.

6.2 *GCTEx Design/Characterization Conclusions*

Chapter Four presented an iteration upon the ground-based CTE_x instrument as another measure of risk reduction prior to final design of the space-based experiment. The driving requirements for this effort included: implementing a design to support accommodating the redesigned/larger DVP, accommodating methods for assessing on-orbit calibration schemes, and correcting lessons-learned from previous implementations of the instrument. The design methodology capitalized on best optical-engineering practices in order to set fabrication constraints and acquire higher-fidelity precision in optical-capture results. Chapter Four detailed the philosophy and development of the linear design strategy.

Figure 6.1 is an image of the linear revision to the ground-based CTE_x instrument. The device was constructed over the period of six weeks through the support of the AFIT model shop (and other offsite fabrication resources). All mechanical assembly and electrical wiring was executed successfully according to standard operating procedures wherein discrepancies were noted and updated in the drawing and assembly packages (located in Appendix B and C as reference).



Figure 6.1: GCTEx Linear System

Results from this research exceeded expectations. Initially, all threshold requirements were met in the redesign of this instrument from those listed in Section 4.1. The test campaign also produced favorable results for the three different characterizations accomplished (deviation angle, image quality and alignment determination). Deviation angle comparisons between the previous Newtonian and updated linear revision showed a reduction in error from theoretical predictions by a minimum of 14% (attributable to an instrument with roughly 1% overall error). In context, this means that the previous instrument on average had a tolerance of ± 50 nm whereas the linear revision is ± 2 nm (i.e., confidence in instrument output wavelength was dramatically increased with the linear revision). Image quality was also witnessed to have increased as the instrument performs close to sampling limitations (in the image space). Finally, alignment characterization proved an automated algorithm developed in MATLAB could provide characterization metrics from a point source input to the system. The DVP offset

parameter was a known but relatively unquantified parameter which will require additional investigation and deliberate design choices in order to mitigate detrimental effects to performance.

6.3 *SCTEx ICU Design/Characterization Conclusions*

In Chapter Five, mathematical models were developed and an early design was built to validate the ICU which is intended to support the space-based CTE_x instrument. Requirements for this design were centered around COTS electronics in a hermetically sealed structure meeting all launch and ELC requirements. The design methodology included similar concepts currently in operation on-orbit and decisions which accommodated the current CTE_x mission CONOPS. Chapter Five reviews component design trades and operational handling of the device.

Figure 6.2 is a photo of the fabricated and assembled ICU. The aluminum housing was fabricated at the AFIT model shop requiring roughly 150 hours of machine time over the course of two months. Upon acquisition of all necessary components, the final ICU assembly was accomplished seamlessly over the course of two days and according to a standard operating procedure. Included in these assembly procedures was a leak check and purge cycle which also ran according to plan (no leaks or other significant mechanical issues were witnessed during this processing).

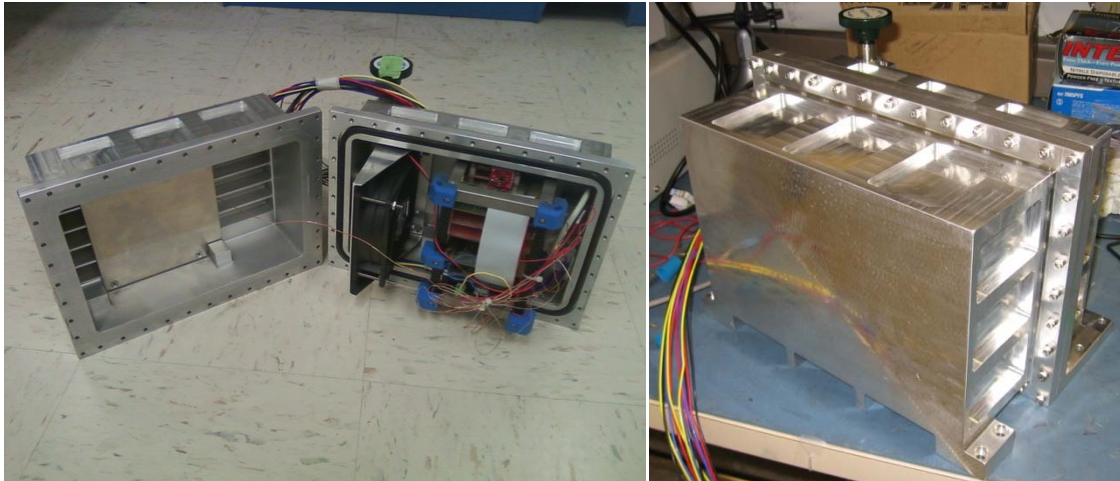


Figure 6.2: SCTEx ICU, Housing Apart (Left) and Assembled (Right)

Performance testing was accomplished after final assembly processing was finished, including operational checkout, vibe-table and thermal vacuum testing. The system operated as expected during operational checkout with no significant issues to report. Vibe-table frequency response tests resulted in validating the ICU can meet minimum threshold launch requirements (as fundamental frequencies are greater than 50 Hz). Finally, validation of the mathematical thermal model was acquired as measurements tracked to within $\pm 3^{\circ}\text{C}$ to those expected from simulations performed. Concern areas of note during this campaign include poor-performing electronics (e.g., the inexpensive “weather” board wherein multiple issues in dropouts, pressure overranging and erroneous nitrogen temperature measurements were witnessed) as well as the housing external surface coating (i.e., selection of a paint which increases emissivity and decreasing absorptivity characteristics will greatly improve expulsion of excess thermal energy through radiation to the environment). Nevertheless, with the validated thermal model, predictions could be made for on-orbit operations (having changed parameters to

include the emissivity, power input, and operating environment characteristics). The overall conclusion here is that the device may run indefinitely at a power level of 13W and should be limited to 3-4 hour segments at elevated (~25W) operating levels.

6.4 *Proposed Future Work*

This thesis research is an incremental step in the development lifecycle for the CTEEx mission. The overarching intent was to map the trade-space and iterate upon previous work accomplished in order to mature the technological readiness for space-flight operations. During this effort, several areas for follow-on research were identified (each to be detailed further below), including:

- Systems Engineering and Program Management
- CT Algorithm Development
- Optical Design Improvements
- Mechanical Development
- Avionics Development

First and foremost, one of the highest payoffs in any successful acquisition program is a strong systems engineering and program management framework. With the aid of firm mission requirements, this provides a great deal of direction for any organization. While significant technical work has been accomplished for the CTEEx program, a concerted effort needs to be placed on the mission management activities to fully realize a successful space mission. This effort needs to analyze the following overlapping areas, including:

- Mission Management: Cost, schedule (milestones, reviews, testing, etc.)

- Requirements: Key performance parameters, statutory, regulatory, certification
- Baseline Management: Traceability and related processes (e.g., specifications, configuration management, drawings, procedures, etc.)
- Technical Review Management: Milestone purpose/descriptions, chairpersons/roles, entry/exit criteria
- Integration of Systems Engineering into Program Management: Participation in risk management decisions, requirements verification/validation through test & evaluation, involvement in contracts
- Staffing: Technical and integration support

The overarching recommendation herein is to assess, write, coordinate and enforce the decisions made in the appropriate program documentation, including (but not limited to): CONOPS, Integrated Master Plan/Schedule, Test and Evaluation Master Plan, and the Systems Engineering Plan.

The second area of further development is related to the CT algorithm development. The overall issue in this area relates to confidence in the reconstruction science to achieve an accurate hypercube for further analysis. Cause for concern previously was due to hardware problems in capturing source data. The linear revision and characterization research accomplished in this thesis has provided a new level of confidence and understanding through enabling high-fidelity data acquisition. Although further effort is necessary here, an adequate level of fundamental research has been accomplished in order to support refinement of the algorithm for mission

accomplishment. Failure to attain this executable algorithm will adversely impact the space mission (either in schedule delays or potentially in mission cancellation due to the inability to perform the basic science).

Third, in conjunction with CT algorithm refinement is that of further development in the optical system. Again, though an upgrade to the ground-based system has been achieved, further work is needed on this instrument in order to reduce risk further. These areas to develop, include:

- GCTEx Upgrades/Characterization: updating the electronics/software interface to simulate the space instrument, further model/validate the new DVP, integrate the new motor/encoder/DVP into the design
- Data Collection & Review: collect additional field static and transient combustion event data, introduce potential space-based system error in the system during collection to evaluate determination and work-around schemas
- Space-Instrument Qualification & Operations Transition Plans: develop detailed procedures to characterize/trend the space instrument, design the SCTEx baffle/field stop/aperture target (characterize on GCTEx), assess potential hardware in the loop configurations

The above mentioned research would be directly traceable to developing methodologies to test a qualification version of the CTEEx instrument.

Fourth, further mechanical design is necessary in order to answer operational requirements questions. Specifically, three areas of detailed effort in this domain include:

- Structural: Complete overall mechanical integration design, assess loading on structures/mechanisms via finite element and other methods (based upon requirements detailed in the System Engineering Plan)
- Thermal: Perform detailed assessment for expected thermal input/output loading, recommend solutions, determine validation methodology and perform upon the qualification model (and/or GCTEx)
- Jitter Control: Assess optical focus response to on-board motor & ISS-induced excitation, recommend solutions, determine validation methodology and perform upon the qualification model (and/or GCTEx)

The above areas will feed into further levels of downstream mission planning as the space-instrument design matures.

Finally, the remaining element in this program relates to the avionics development. Again, a significant level of technical effort has been expended in terms of preliminary planning; however, further work needs to focus upon physically implementing the “on-paper” designs in order to integrate software and hardware into a useful form. Specifically, relating to the ICU efforts, further detailed design needs to go into the PC/104 computer stack (as the system tested in this thesis was a representative system). Considerations for operational functionality, power, thermal and reliability are but a few requirements which need to be honed. Integration of this ICU with the ground instrument may also achieve benefits relating to the future CONOPs of the experiment. Additionally, this effort needs to integrate development of the control electronics, software, and interface with the ISS/STP-provided C&DH system. The above areas will

feed into further levels of downstream mission planning as the space-instrument design matures.

6.5 *Final Conclusions*

The chromotomographic hyperspectral imaging experiment will provide another level of refinement upon current remote-sensing technologies enabling exploitation of spatial, spectral and temporal data from fast transient events. This thesis further developed the capabilities necessary to execture a space-based proof-of-concept necessary to increase the readiness of the technology. Further challenges, identified in this research, require mitigation prior to launch and on-orbit operations; nevertheless, the groundwork has been laid for a successful mission in the not-so-distant future.

Appendix A: MATLAB Analysis Code

Appendix A.1: Isogrid FEM Dat-file Rapid-Generation

```
%% CTEx Isogrid Rapid Generation Code
% Capt Jason Niederhauser
% 3 Feb 11
% Note: Code based off of original methodology from Dr. Eric Swenson,
further developed by Capt Mark Lesar, Capt Joshua Debes, and the author

% Note: This code produces isogrid *.dat files (based upon inputs
below), which can be imported into FEM software package (e.g., FEMap)
to further perform additional meshing and analysis.

close all
clear all
clc
format long

%% inputs
%constants
width = 43.5;
depth = 30;

%things to vary
iso.height=[1 1.5 2 2.5];
iso.spacing.desired=[4 6];
iso.web=[.1 .25];
iso.pocket_depth=[.1 .25];
iso.flange=[0]
iso.spacing.actual_width=[width./(floor(width./iso.spacing.desired))];
iso.spacing.actual_depth=[depth./(floor(depth./iso.spacing.desired))];
iso.rows=[depth./iso.spacing.actual_depth];
iso.cols=[width./iso.spacing.actual_width];

for mat=1:1
for web=1:size(iso.web,2)
for pd=1:size(iso.pocket_depth,2)
for h=1:size(iso.height,2)
for s=1:size(iso.spacing.desired,2)
%% output file
output_name =
['iso_grid_',num2str(iso.rows(s)),'_rows_',num2str(iso.cols(s)),'_cols_
',...

num2str(iso.spacing.desired(s)),'_spacing_',num2str(iso.height(h)),'_he
ight_',num2str(iso.pocket_depth(pd))...

'_PD_',num2str(iso.web(web)),'_web_t_', '_material_',num2str(mat),'.dat'
];
disp(' ');
disp(' ');
```



```

        fprintf(fid1, strcat('GRID, ', num2str(node_ctr), ',, ', ...
            num2str(x_loc), ', ', num2str(y_loc), ', ', num2str(z_loc)));
        fprintf(fid1, '\n');
    end
end

%% CQUAD4 CARDS
disp('element   row   col   node1   node2   node3   node4');
disp('_____');
elem_ctr = 0;
start_ctr = 0;
%Creating CQUAD4 Cards for ISO GRID (planar)
for row_ctr = 1:iso.rows(s)
    for col_ctr = 1:iso.cols(s)
        start_ctr = start_ctr + 1;
        node1 = start_ctr +(row_ctr-1)*(iso.cols(s));
        node2 = (start_ctr+1)+(row_ctr-1)*(iso.cols(s));
        node3 = (start_ctr)+(row_ctr)*(iso.cols(s))+2;
        node4 = (start_ctr)+(row_ctr)*(iso.cols(s))+1;
        elem_ctr = elem_ctr + 1;
        fprintf(fid1, strcat('CQUAD4, ', num2str(elem_ctr), ...
            ',98, ', num2str(node1), ', ', num2str(node2), ', ', num2str(node3), ', ', num2str
            (node4)));
        fprintf(fid1, '\n');
        disp(sprintf('%6d %6d %6d %6d %6d %6d %6d %6d',
            elem_ctr, row_ctr, col_ctr, node1, node2, node3, node4, start_ctr));
    end
    start_ctr=start_ctr-(iso.cols(s)-1);
end
start_ctr = 0;
%Creating CQUAD4 Cards for ISO GRID (cross pieces)
for row_ctr = 1:iso.rows(s)+1
    for col_ctr = 1:iso.cols(s)
        start_ctr = start_ctr + 1;
        node1 = start_ctr +(row_ctr-1)*(iso.cols(s));
        node2 = (start_ctr+1)+(row_ctr-1)*(iso.cols(s));
        node3 = node2+bottom_left;
        node4 = node1+bottom_left;
        elem_ctr = elem_ctr + 1;
        fprintf(fid1, strcat('CQUAD4, ', num2str(elem_ctr), ...
            ',99, ', num2str(node1), ', ', num2str(node2), ', ', num2str(node3), ', ', num2str
            (node4)));
        fprintf(fid1, '\n');
        disp(sprintf('%6d %6d %6d %6d %6d %6d %6d %6d',
            elem_ctr, row_ctr, col_ctr, node1, node2, node3, node4, start_ctr));
    end
    start_ctr=start_ctr-(iso.cols(s)-1);
end
start_ctr = 0;
top=(iso.rows(s)+1)*(iso.cols(s)+1)+1;
%Creating CQUAD4 Cards for ISO GRID (in the plane)

```

```

for row_ctr = 1:iso.rows(s)
  for col_ctr = 1:iso.cols(s)+1
    start_ctr = start_ctr + 1;
    node1 = start_ctr +(row_ctr-1)*(iso.cols(s));
    node2 = (top)+(col_ctr-1)+(row_ctr-1)*(iso.cols(s)+1);
    node3 = (top)+(col_ctr-1)+(row_ctr)*(iso.cols(s)+1);
    node4 = (start_ctr+1)+(row_ctr)*(iso.cols(s));
    elem_ctr = elem_ctr + 1;
    fprintf(fid1, strcat('CQUAD4, ', num2str(elem_ctr), ...
',99, ', num2str(node1), ', ', num2str(node2), ', ', num2str(node3), ', ', num2str
(node4)));
    fprintf(fid1, '\n');
    disp(sprintf('%6d %6d %6d %6d %6d %6d %6d %6d',
elem_ctr, row_ctr, col_ctr, node1, node2, node3, node4, start_ctr));
  end
  start_ctr=start_ctr-(iso.cols(s));
end
%fprintf(fid1, 'PSHELL      98      1    %.4f      1      1
0.\n', iso.pocket_depth(pd)); %Bottom Plates - can change thickness
%fprintf(fid1, 'PSHELL      99      1    %.4f      1      1
0.\n', iso.web(web)); %Cross Pieces - can change thickness
%if mat==1
%fprintf(fid1, 'MAT1      1      9900000.      0.33 2.539E-4
1.265E-5      70. \n');
%end
%If you have more than one material, uncomment and
%apply appropriate material card
%if mat==2
  %fprintf(fid1, 'MAT1      19900000.      0.332.539E-41.265E-
5      70. \n');
%end
fprintf(fid1, 'ENDDATA      $ End bulk data\n');
fclose(fid1);
end
end
end
end
end

```

Appendix A.2: GCTex Alignment Characterization

```
%% CTEEx Alignment Characterization
% Capt Jason Niederhauser
% 6 Apr 11

%% Step 1: Read Image
close all; clear all; clc; format compact;
[video, path] = uigetfile('C:\Users\Jason Niederhauser\Desktop\THESIS
(DOC)\4.0 DATA & FIGURES\*..*','Select .avi file to analyze'); %Prompts
user to select AVI video file for analysis.
addpath(path); %Stores the path where the AVI file is saved.
vid_in = mmreader(video); %Creates mmreader object of AVI, from which
the file will be read.
frames=1:min(250,vid_in.NumberOfFrames);
mov(1:length(frames)) = struct('cdata', zeros(vid_in.Height,
vid_in.Width, 3, 'uint8'),...
    'colormap', []);
comb = zeros(vid_in.Height,vid_in.Width);

% Read one frame at a time. (Safer for memory management)
whandle=waitbar(0);
for k = 1:numel(frames)
    mov(k).cdata = read(vid_in, frames(k)); %read frame data
    mov(k).cdata = mov(k).cdata(:,:,1);% AVI saves 3(RGB) channels,
each identical (grayscale image). Only need 1 (saves memory).
    %mov(k).cdata = mov(k).cdata.*flat_field; %Apply flat-field
correction
    comb = comb + double(mov(k).cdata); %Keep running total of frames,
will give average.
    waitbar(k/numel(frames),whandle,'loading images')
end
comb = comb./numel(frames);%Find average of all frames (potentially
useful for finding center of rotation.
close(whandle); clear whandle;

%% Step 2: Find and Create Array of X & Y points (Centroid Coordinates
of the Laser Point)
% NOTE: This Step was baselined and modified from Matlab's help
demonstration called "Identifying Round Objects" [53]

n = length(frames);
coords = zeros(n,2);
for i = 1:n
    I = mov(i).cdata;
    threshold = graythresh(I);
    bw = im2bw(I,threshold);
    bw = bwareaopen(bw,30);
    se = strel('disk',2);
    bw = imclose(bw,se);
    bw = imfill(bw,'holes');
    [B,L] = bwboundaries(bw,'noholes');
```

```

imshow(label2rgb(L, @jet, [.5 .5 .5]))
hold on
for k = 1:length(B)
    boundary = B{k};
    plot(boundary(:,2), boundary(:,1), 'w', 'LineWidth', 2)
end
stats = regionprops(L, 'Area', 'Centroid');

threshold = 0.94;

% loop over the boundaries
for k = 1:length(B)

    % obtain (X,Y) boundary coordinates corresponding to label 'k'
    boundary = B{k};

    % compute a simple estimate of the object's perimeter
    delta_sq = diff(boundary).^2;
    perimeter = sum(sqrt(sum(delta_sq,2)));

    % obtain the area calculation corresponding to label 'k'
    area = stats(k).Area;

    % compute the roundness metric
    metric = 4*pi*area/perimeter^2;

    % display the results
    metric_string = sprintf('%2.2f',metric);

    % mark objects above the threshold with a black circle
    if metric > threshold
        centroid = stats(k).Centroid;
        plot(centroid(1),centroid(2),'ko');
    end
end
coords(i,1) = stats(1,1).Centroid(1,1);
coords(i,2) = stats(1,1).Centroid(1,2);
end

%% Step 2.1: "Cleaning"/"Windowing" the data as necessary
% Note: This sub-step is meant to be used when aberations are present;
% however, **a portion** of the circle data is usable
% Note2: User should 'commented-out' this step initially in order to
% determine the appropriate window size, then un-comment this section
and
% repeat steps 2.1, 3, and 4 to find the data of interest

% Input the minimum coordinate which all centroids must be greater
than:
X_min = 138;
Y_min = 106;

```

```

X_max = 355;
Y_max = 348;

a = 0;b=0;
for count = 1:length(coords)
if coords(count,1) > X_min
    a = a+1;
    coords2(a,1) = coords(count,1);
end
end

for count = 1:length(coords)
if coords(count,2) > Y_min
    b = b+1;
    coords2(b,2) = coords(count,2);
end
end

coords = coords2;

a = 0;b=0;
for count = 1:length(coords)
if coords(count,1) < X_max
    a = a+1;
    coords2(a,1) = coords(count,1);
end
end

for count = 1:length(coords)
if coords(count,2) < Y_max
    b = b+1;
    coords2(b,2) = coords(count,2);
end
end

coords = coords2;

%% Step 3: Determine Alignment Metrics
% disp('Center of Rotation:')
[xc yx R] = try_circ_fit(coords(:,1),coords(:,2)); % [54]
x_o = xc;
y_o = yx;
% disp('Radius of Rotation:')
R_mm = R*20E-3; %deviation radius, in millimeters
R_in = R*(1/25.4)*20E-3; %deviation radius, in inches
% disp('Standard Deviation:')
R_pts = (sqrt(((x_o-coords(:,1)).^2)+((y_o-coords(:,2)).^2)));
R_std = std(R_pts);
R_var = var(R_pts);
x_std = std(coords(:,1));
y_std = std(coords(:,2));

```

```

% disp('Variance:')
x_var = var(coords(:,1));
y_var = var(coords(:,2));

Circle_Data = struct( ...
    'x_o',x_o,...
    'y_o',y_o,...
    'R',R,...
    'R_mm',R_mm,...
    'R_in',R_in,...
    'R_std',R_std,...
    'R_var',R_var);
% disp('Circle Data:')
Circle_Data

disp('Eccentricity Data:')
fit_ellipse(coords(:,1), coords(:,2)) % [55]

%% Step 4: Plot the circle coordinates on top of the traced circle
close all

figure
hold on
added_frames = zeros(512);
n = size(mov); n = n(1,2);
for i = 1:1:n
    added_frames = added_frames + double(mov(i).cdata);
    %imagesc(added_frames); %pause(.005);
end
imagesc(added_frames); colormap('gray');axis equal
plot(coords(:,1),coords(:,2),'ro')
plot(x_o,y_o,'rx')
circle([x_o,y_o],R,length(frames),'b.');
```

% Creating the circle [63]

```

legend('Laser Centroids (per Frame)', 'Center of Rotation', 'Averaged
Circle')
axis equal
hold off

%% Step 5: Determination of the Deviation Angle & Wavelength
% Deviation Curve Fit taken from Zemax data (note: lambda curve fit in
micro meters)

R; % Note: R is from the output of the circle function above(an
average), units are in pixels;
% however, we need to apply a correction offset to find the "actual"
% center of rotation and deviation angle (e.g., recall the mercury
pen
% lamp "pinwheel" -- the arm/offset of this pinwheel needs to be
accounted for and applied into
% the assessment for computing the deviation angle). Using
% trigonometry, understanding that R=hypotenuse (given above);
c=offset
```

```

    % (determine empiracally from raw data gathered and plotted)

    C = .217324; %offset angle, in degrees; empiracally determined from
    reviewing raw deviation angle vs. wavelength data

% Note: Standard curve-fit function: theta = (a*lambda^b)+c
a = .2183;
b = -3.329;
c = -1.633;
Polarity = -1; %lam>=549nm, Polarity=-1; lam<549nm, Polarity=+1
%Note: if calibration source is lambda>~550nm, then Polarity = -1;
otherwise, if lambda<~550nm, then Polarity = +1
delta_deg = Polarity*(sqrt(abs((((180/(pi))*atan2(R*20E-6,.085))^2)-
(C^2)))));
delta_pts = Polarity*(sqrt(abs((((180/(pi))*atan2(R_pts*20E-
6,.085)).^2)-(C^2)))));

delta_std = std(delta_pts);
lambda_nm = 1000 * exp((log((delta_deg-c)/a))/b); %Wavelength, in nm

Dev_angle = struct( ...
    'delta_deg',delta_deg,...
    'delta_std',delta_std,...
    'lambda_nm',lambda_nm);
Dev_angle

ans2 = [delta_deg delta_std lambda_nm]

%% Step 5.1 -- Deviation & Wavelength Computed the "NON-OFFSET(NO)" Way
theta_deg_no = Polarity*(180/(pi))*atan2(R*20E-6,.085);
theta_pts_no = Polarity*(180/(pi))*atan2(R_pts*20E-6,.085);
theta_std_no = std(theta_pts_no);
lambda_nm_no = 1000 * exp((log((theta_deg_no-c)/a))/b); %Wavelength, in
nm

Dev_angle_no = struct( ...
    'theta_deg_no',theta_deg_no,...
    'theta_std_no',theta_std_no,...
    'lambda_nm_no',lambda_nm_no);
Dev_angle_no

ans2 = [theta_deg_no theta_std_no lambda_nm_no]

```

Appendix A.3: SCTEx ICU Thermal Modeling Code

```
%CTEx ICU Thermal: Simulink Model Input File
%Model Iteration: TVAC Test Setup
%Updated: 2 Nov 10
%Capt Jason Niederhauser
% Note: this code is meant to be run as a first step to provide inputs
and initial conditions; a Simulink code will then be run followed by a
plotting program

close all; clear all; format compact; clc; ctr=0;
%% Define Constants & Initial Conditions
% INPUTS
T_TVAC = 40 + 273.15; %Temperature of the Thermal-Vacuum chamber, deg C
to Kelvin
% T_earth = T_TVAC; %Used for TVAC test runs only
% T_space = T_TVAC; %Used for TVAC test runs only
T_earth = 20+273.15; %surrounding environment temperature, K
T_space = 3; %surrounding environment temperature, K
Edot_g1 = 25; %PC/104 stack input power, watts
emiss = .91; absorp = .17; %emssivity & absorptivity for ZOT painted
surface

% ICU Physical Geometry
S1 = .75 * .0254; %Distance between channels including thickness, inches
to meters
B1 = 4 * .0254; %ICU PC/104 Card Depth, inches to meters
L1 = 4 * .0254; %ICU PC/104 Card Length, inches to meters
W1 = 6 * .0254; %ICU PC/104 Card Width, inches to meters
t1 = .060 * .0254; %PC/104 Card/Fin thickness, inches to meters

S2 = .95 * .0254; %Distance between channels including thickness, inches
to meters
B2 = 9.7 * .0254; %ICU Heat Sink Fin Depth, inches to meters
L2 = 1.3 * .0254; %ICU Heat Sink Fin Length, inches to meters
W2 = 4.65 * .0254; %ICU Heat Sink Fin Width, inches to meters
t2 = .1 * .0254; %ICU Heat Sink Fin, inches to meters

% Physical & Orbital Data
k_al = 167; %Aluminum thermal conductivity, W/m*K
Cp_al = 865; %specific heat at constant pressure, J/kg*K
L_iwall1 = .3 * .0254; %ICU Heat Sink wall thickness to space/vacuum,
inches to meters
L_icucbu = 1 * .0254; %thickness between icu & cbu, in to m
A_irad = (10.5 * 8.5) * (6.452*10^-4); %ICU Heat Sink radiation area to
space/vacuum, in^2 to m^2
A_irad2 = (((2)*(7.75*10.5))+((2)*(7*7.75))+((1)*(7*10.5))) *
(6.452*10^-4); %ICU Heat Sink radiation area (non-finned surfaces) to
space/vacuum, in^2 to m^2
sigma = 5.670*10^-8; %Stefan-Boltzmann Constant
I_EIR = 241
q_EIR = emiss * I_EIR; %Earth IR radiation, W/m^2
```

```

I_solar = 1414; %W/m^2, hot case
q_albedo = absorp * I_solar; %Earth albedo radiation, W/m^2
r_earth = 6378000; %radius of Earth, m
r_orbit = 400000 + r_earth; %radius of orbit, m
Mass_icu = (207.5 * ((.0254)^3)) * 2770; %Mass of ICU = (volume (in^3)
to m^3 ) * density_al
Mass_PCB = ((8) * (3.6*3.8*.1) * ((.0254)^3)) * 1850; %Mass of PC/104
cards = (qty)*(volume (in^3) to m^3 ) * density_al
Cp_PCB = 600; %specific heat at constant pressure, J/kg*K

%Initial Conditions
Edot_ext1 = (q_EIR) * A_irad + (q_EIR) * A_irad2 + (q_albedo) * A_irad
+ (q_albedo) * A_irad2 ;
Qin1 = Edot_g1 + Edot_ext1;
Press_icu = 18 * 6.985*10^3; %Pressure (absolute) within the ICU, psia
to Pa
R = 2.968*10^2; %GN2 Gas Constant, J/kg*K
Vdot = (108 * (.40)) * (4.719E-4); %volumetric flow rate, assume 40% of
rated fan flow rate, cfm to m^3/sec
T_card = 40 + 273.15; %Steady-state PC/104 card temperature, deg C to K
T1 = 20 + 273.15; %Inlet temp to PC/104 stack, initial guess, deg C to
K
T2 = 30 + 273.15; %Outlet temp to PC/104 stack, initial guess, deg C to
K
T3= T2; T4 = T1; Ta1 = 35 + 273.15; Ta2 = 25 + 273.15; Ta7 = T1; Ta5 =
T2; %Initial temperatures (WAG for iteration), K

% Fluid Thermophysical Data
% Fluid = GN2; Note: data below from Appendix A.4 "Fundamentals of Heat
and Mass Transfer" Fourth Edition, Incropera & DeWitt [62]
T = 20 + 273.15; %Assumed temp of the fluid
rho = Press_icu/(R * T); %mass density, kg/m^3
mu = 0.0000000455*T + 0.000004004; %viscosity, kg/s*m
k = 0.0000718*T + 0.00414; %thermal conductivity, W/m*K
Cp = -0.000000013333333*T^4 + 0.000017333333330*T^3 -
0.007966666665799*T^2 + 1.536666666650070*T + 936.99999987451000;
%specific heat at constant pressure, J/kg*K
Pr = -0.00016*T + 0.7668; %Prandtl number, unitless
mdot1 = rho*Vdot

%% Solution
%Step One: Determine Heat Capacity Parameters

MC_ci = Mass_PCB * Cp_PCB
MC_ni = ((12*8*8)* ((.0254)^3)) * rho * Cp
MC_ai = Mass_icu * Cp_al

%Step Two: Convection from PC/104 to fluid, find h1 & A1
N1 = round(W1/S1);
A_b1 = (W1-N1*t1)*B1;
A_f1 = 2*(L1/2)*B1;
A_t1 = N1*A_f1 + A_b1;

```

```

A_c1 = L1 *(S1-t1);
P1 = 2*(L1+S1-t1);
D_h1 = 4*A_c1/P1;
A1 = 2 * N1 *L1 * B1;

mdot = rho*Vdot/(N1)
Re_D1 = mdot*D_h1/(A_c1*mu)
Nu_D1 = .023*(Re_D1^.8)*(Pr^.4)
h1 = (k/D_h1) * Nu_D1
R3 = 1 / (h1 * A1)

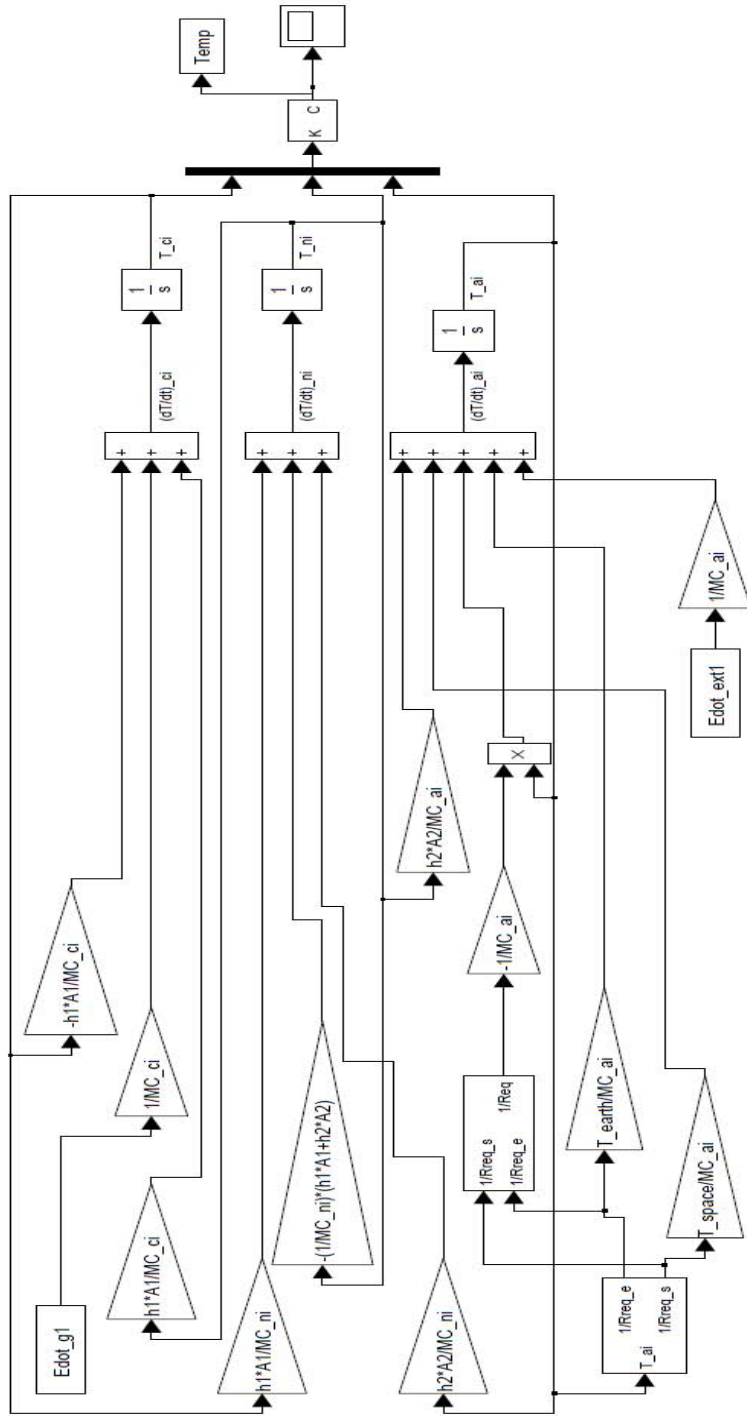
% Step Three: Convection from Fluid to Heat Sink, find h2 & A2
N2 = round(W2/S2)
A_b2 = (W2-N2*t2)*B2
A_f2 = 2*(L2/2)*B2
A_t2 = N2*A_f2 + A_b2
A_c2 = L2 *(S2-t2)
P2 = 2*(L2+S2-t2)
D_h2 = 4*A_c2/P2
A2 = 2 * N2 *L2 * B2

mdot2 = rho*Vdot/(N2)
Re_D2 = mdot2*D_h2/(A_c2*mu)
Nu_D2 = .023*(Re_D2^.8)*(Pr^.3)
h2 = (k/D_h2) * Nu_D2
R5 = 1 / (h2 * A2)

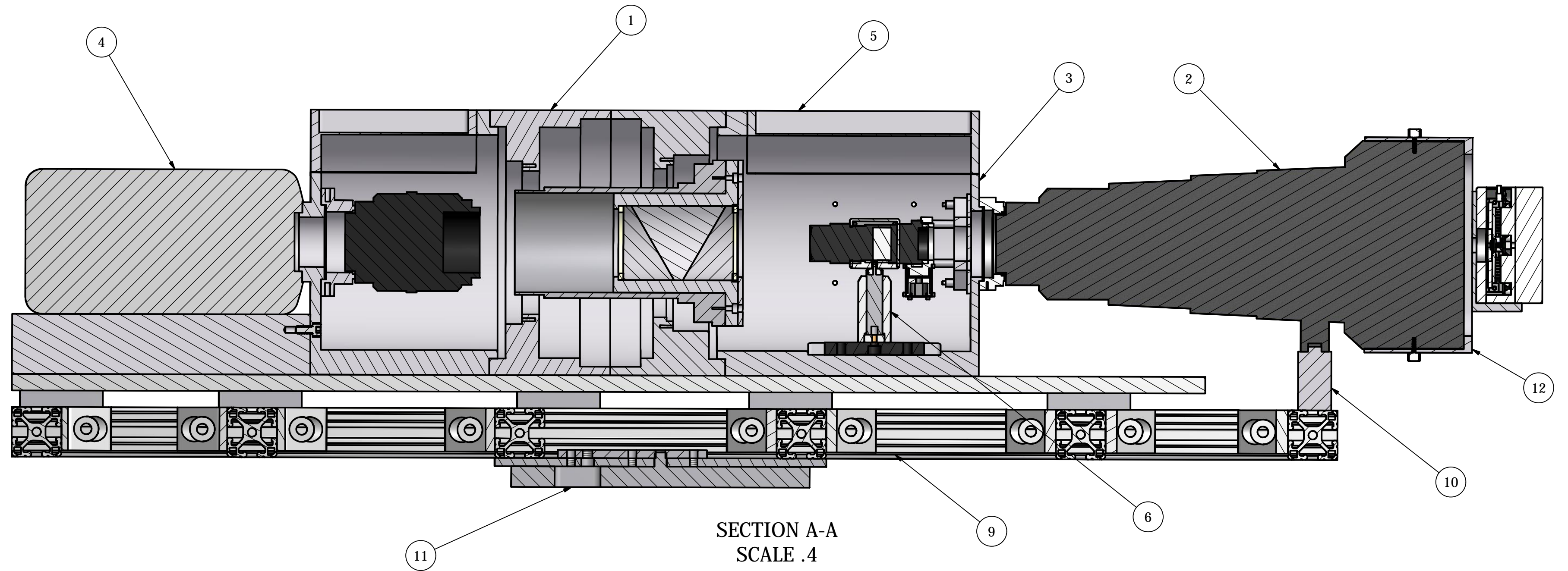
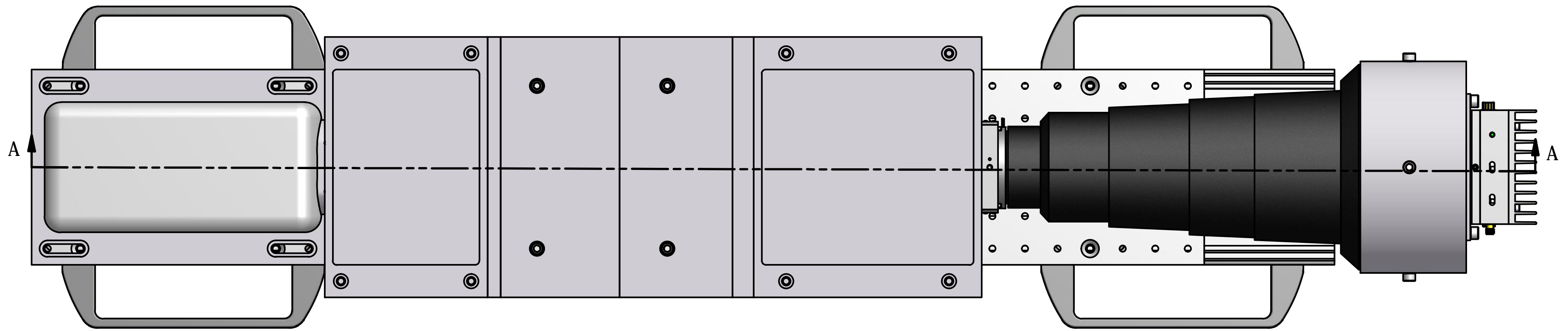
% Step Four: Conduction from space into aluminum/heat sink, find R6
R6 = L_iwall1 / (k_al * A_irad)

% Step Five: Radiation from Heat Sink surface to environment, find f
(view factor)
theta = asin(r_earth/r_orbit)
r = r_earth * cos(theta)
H = r / (tan(theta))
f = (pi*r^2) / ((pi*r^2) + (2*pi*r*H))

```



Appendix B: Mechanical Drawing Packages



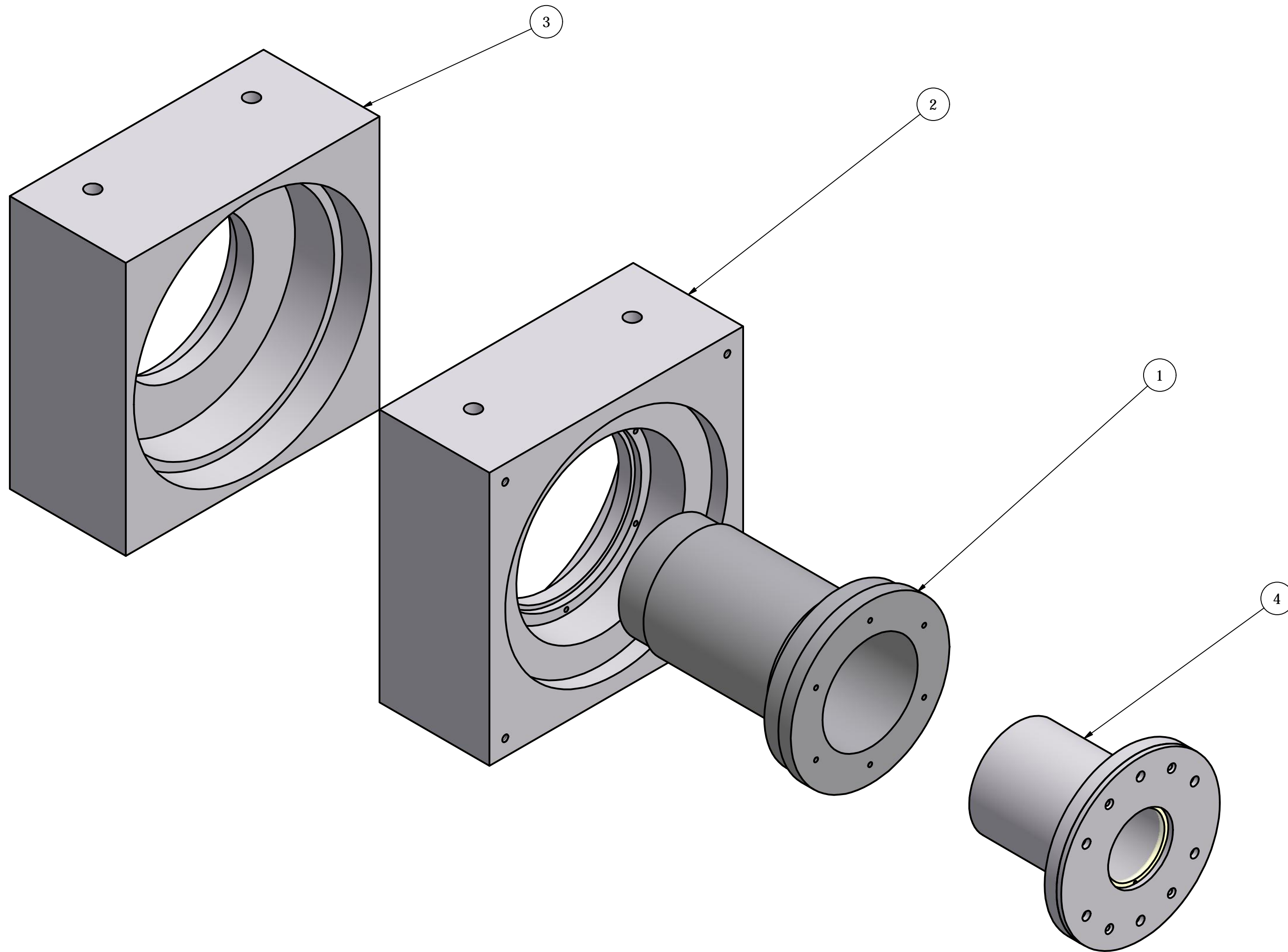
PARTS LIST		
ITEM	QTY	PART NUMBER
1	1	ASSY GCTEx Motor Encoder & Prism R2 101020
2	1	ASSY GCTEx Lens System R1 100928
3	1	Block Interface L2 R0 101111
4	1	ASSY GCTEx Camera & L1 R1 101111
5	1	Block Interface L2 ACCESS R0 101113
6	1	ASSY Mirror Turning
7	2	Cover Light L2 R0 101113
8	4	91251A923
9	1	ASSY GCTEx Structure (Linear) R2 101118
10	1	Stand Lens Nikon Telephoto R0 101118
11	1	Plate Base Tripod R0 090811
12	1	ASSY Laser Calibration Holder R0 101116

DIMENSIONS ARE IN INCHES TOLERANCES: FRACTIONAL - $\frac{1}{64}$ TWO PLACE DECIMAL - 0.010 THREE PLACE DECIMAL - 0.005	ENGINEER J. NIEDERHAUSER	11/21/2010	 UNITED STATES AIR FORCE AIR FORCE INSTITUTE OF TECHNOLOGY	
	ENGINEERING REVIEW		TITLE	
MATERIAL			ASSY GCTEx LINEAR R0 101121	
FINISH	RELEASE APPROVED		SIZE C	DWG NO GCTEX-A003
DO NOT SCALE DRAWING			SCALE	REV
FOR OFFICIAL USE ONLY				SHEET 1 OF 1

Component Listing - GCTEx Linear Revision

Updated: 18 May 11

GCTEx Part Number	Description	Material	Vendor	Vendor Part Number
GCTEX-0001	Block Mounting Camera R2 101117	Aluminum 6061-T6	NA	NA
GCTEX-0002	Block Interface L3 R0 101117	Aluminum 6061-T6	NA	NA
GCTEX-0003	Block Interface L3 ACCESS R0 101117	Stereolithography	NA	NA
GCTEX-0004	Block Interface L2 ACCESS R0 101113	Stereolithography	NA	NA
GCTEX-0005	Block Interface L2 R0 101117	Aluminum 6061-T6	NA	NA
GCTEX-0006	Stand Lens Nikon Telephoto R0 101118	Aluminum 6061-T6	NA	NA
GCTEX-0007	LCP04 Nikon Mount	Aluminum	Thorlabs, Inc.	LCP04
GCTEX-0008	NFM1 Nikon F-Mount	Aluminum	Thorlabs, Inc.	NFM1
GCTEX-0009	Plate Mounting Structural Tripod Secure R0 090811	Stainless Steel 303	NA	NA
GCTEX-0010	Plate Mounting Structural R1 101118	Stainless Steel 304	NA	NA
GCTEX-0011	Block Spacer Structure 2.5 in R0 090811	Aluminum 6061-T6	NA	NA
GCTEX-0012	Housing Mounting Motor Encoder BOTOM R2 101020	Aluminum 6061-T6	NA	NA
GCTEX-0013	Housing Mounting Motor Encoder TOP R2 101020	Aluminum 6061-T6	NA	NA
GCTEX-0014	Shaft Motor Encoder R2 101020	AISI Steel 1018	NA	NA
GCTEX-0015	Plate Mounting Optical Breadboard R1 101119	Aluminum	Newport, Inc.	SA2-06x36
GCTEX-0016	Block Interface Motor-Encoder Mockup R0 101118	Aluminum 6061-T6	NA	NA
GCTEX-0017	Block Mounting Interface Motor-Encoder R0 101116	Aluminum 6061-T6	NA	NA
GCTEX-0018	Holder Laser Telephoto Mount R0 101116	Aluminum 6061-T6	NA	NA
GCTEX-0019	Holder Laser Calibration R0 101119	Aluminum 6061-T6	NA	NA
GCTEX-0020	Cover Light L2 R0 101121	Aluminum 6061-T6	NA	NA
GCTEX-0021	Plate Mounting Prism Vibe R0 101205	Aluminum 6061-T6	NA	NA
GCTEX-0022	Plate Prism Holder HOUSING R0 100623	Aluminum 6061-T6	NA	NA
GCTEX-0023	Housing Prism Collar R0 101117	Aluminum 6061-T6	NA	NA
GCTEX-0024	Housing Prism Retainer R0 101117	Aluminum 6061-T6	NA	NA
GCTEX-0025	Ring Compression Prism Housing R0 101117	Nylon	NA	NA
GCTEX-0026	Camera HS VR	NA	Vision Research	v5.1
GCTEX-0027	Lens L3 Nikon 105mm	NA	Nikon	Nikkor, 105mm
GCTEX-0028	Lens L2 Tameron 85mm	NA	Tameron	85mm
GCTEX-0029	Lens L1 Nikon 400mm	NA	Nikon	Nikkor, 400mm
GCTEX-0030	Z-Translator, TL SM1Z	Aluminum	Thorlabs, Inc.	SM1Z
GCTEX-0031	LCP02 Mount TL	Aluminum	Thorlabs, Inc.	LCP02
GCTEX-0032	Rod Mount Optical, TL ER2	Stainless Steel	Thorlabs, Inc.	TL ER2
GCTEX-0033	Retainer Prism R0 090811	Nylon	NA	NA
GCTEX-0034	Retainer Compression Prism R0 090811	Aluminum 6061-T6	NA	NA
GCTEX-0035	Housing Prism R0 090811	Aluminum 6061-T6	NA	NA
GCTEX-0036	Prism R0 090811	Aluminum 6061-T6	NA	NA
GCTEX-0037	Holder Prism R0 090811	Aluminum 6061-T6	NA	NA
GCTEX-0038	Prism DVP Onyx R0 090811	LaSF N30; SF L6	Schott	NA
GCTEX-0039	Plate Prism Holder TOP R0 100623	Aluminum 6061-T6	NA	NA
GCTEX-0040	Plate Prism Holder BOTTOM R0 100623	Aluminum 6061-T6	NA	NA
GCTEX-0042	Plate Mounting SAM-3 Module R0 110103	Aluminum 6061-T6	NA	NA
GCTEX-0043	Bracket Connector x3 R0 110103	Aluminum 6061-T6	NA	NA
GCTEX-0044	Bracket Connector x1 R0 110103	Aluminum 6061-T6	NA	NA

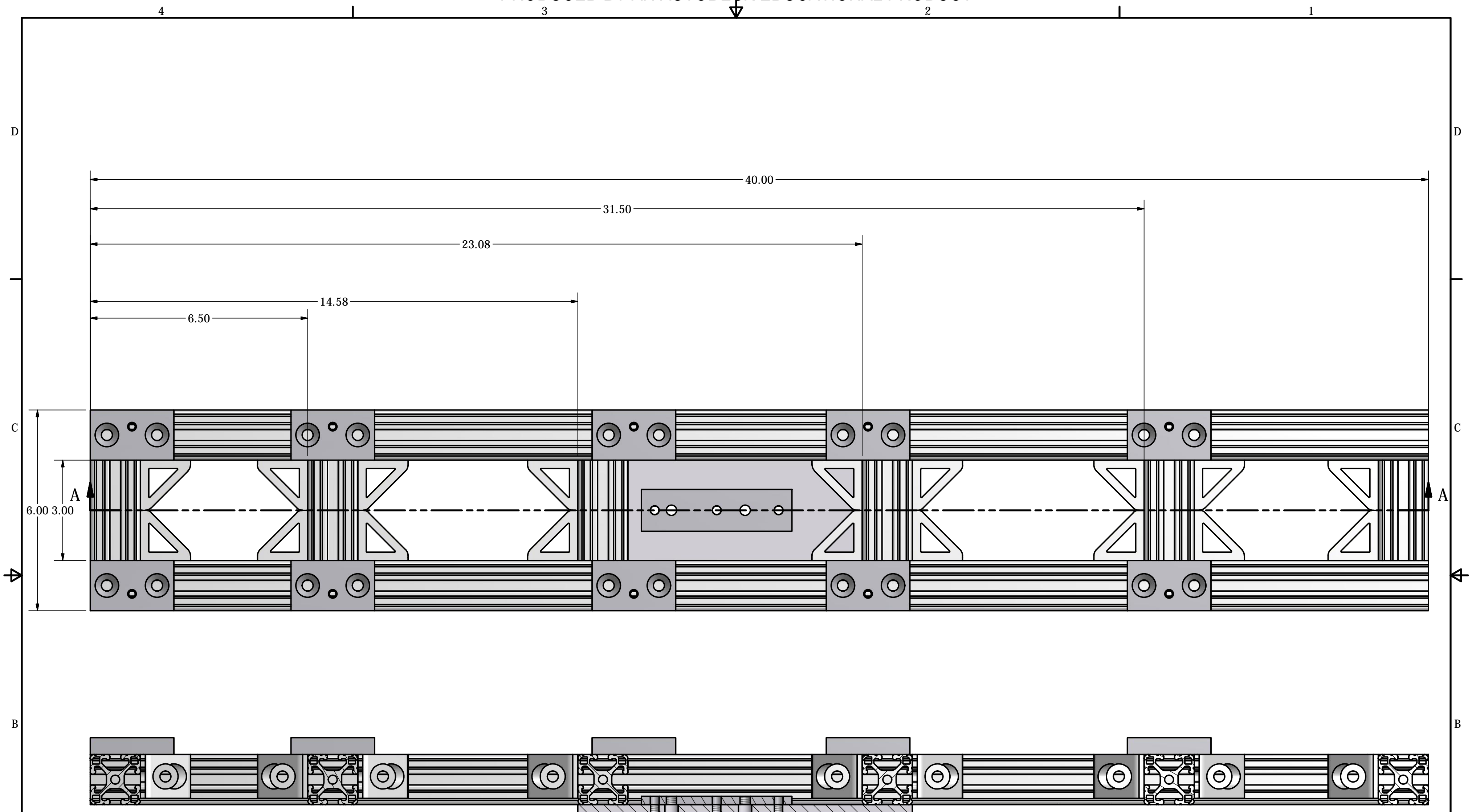


PRODUCED BY AN AUTODESK EDUCATIONAL PRODUCT

PRODUCED BY AN AUTODESK EDUCATIONAL PRODUCT

PARTS LIST			
ITEM	QTY	PART NUMBER	DESCRIPTION
1	1	Shaft Motor Encoder R2 101020	
2	1	Housing Mounting Motor Encoder TOP R2 101020	
3	1	Housing Mounting Motor Encoder BOTOM R2 101020	
4	1	ASSY GCTEx Prism & Holder R2 101020	

DIMENSIONS ARE IN INCHES TOLERANCES: FRACTIONAL - $\frac{1}{64}$ TWO PLACE DECIMAL - 0.010 THREE PLACE DECIMAL - 0.005	ENGINEER	11/18/2010	 UNITED STATES AIR FORCE AIR FORCE INSTITUTE OF TECHNOLOGY	
	J. NIEDERHAUSER ENGINEERING REVIEW			
MATERIAL			ASSY GCTEx Motor Encoder & Prism R2 101020	
FINISH	RELEASE APPROVED		SIZE	REV
DO NOT SCALE DRAWING			C	
FOR OFFICIAL USE ONLY			SCALE	DWG NO GCTEX-A001
			SHEET 1 OF 1	

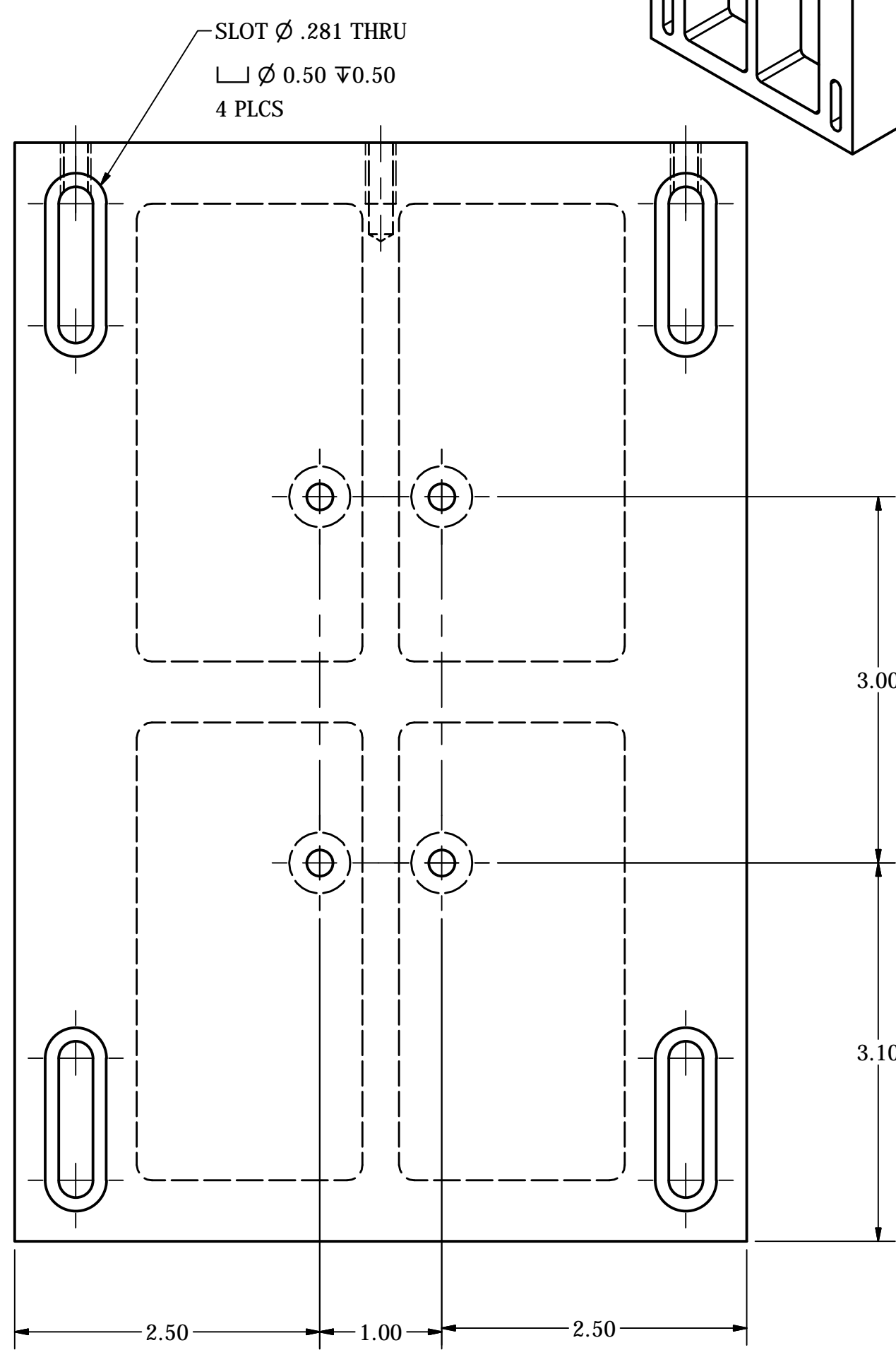
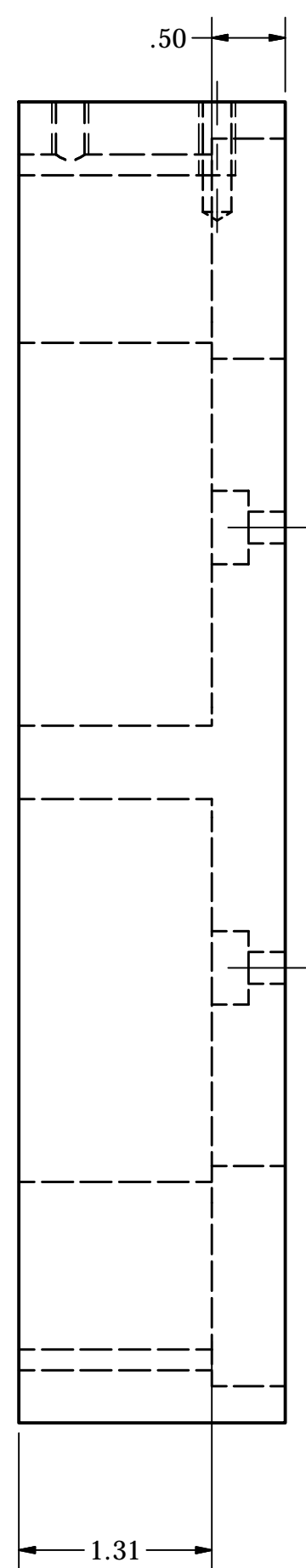
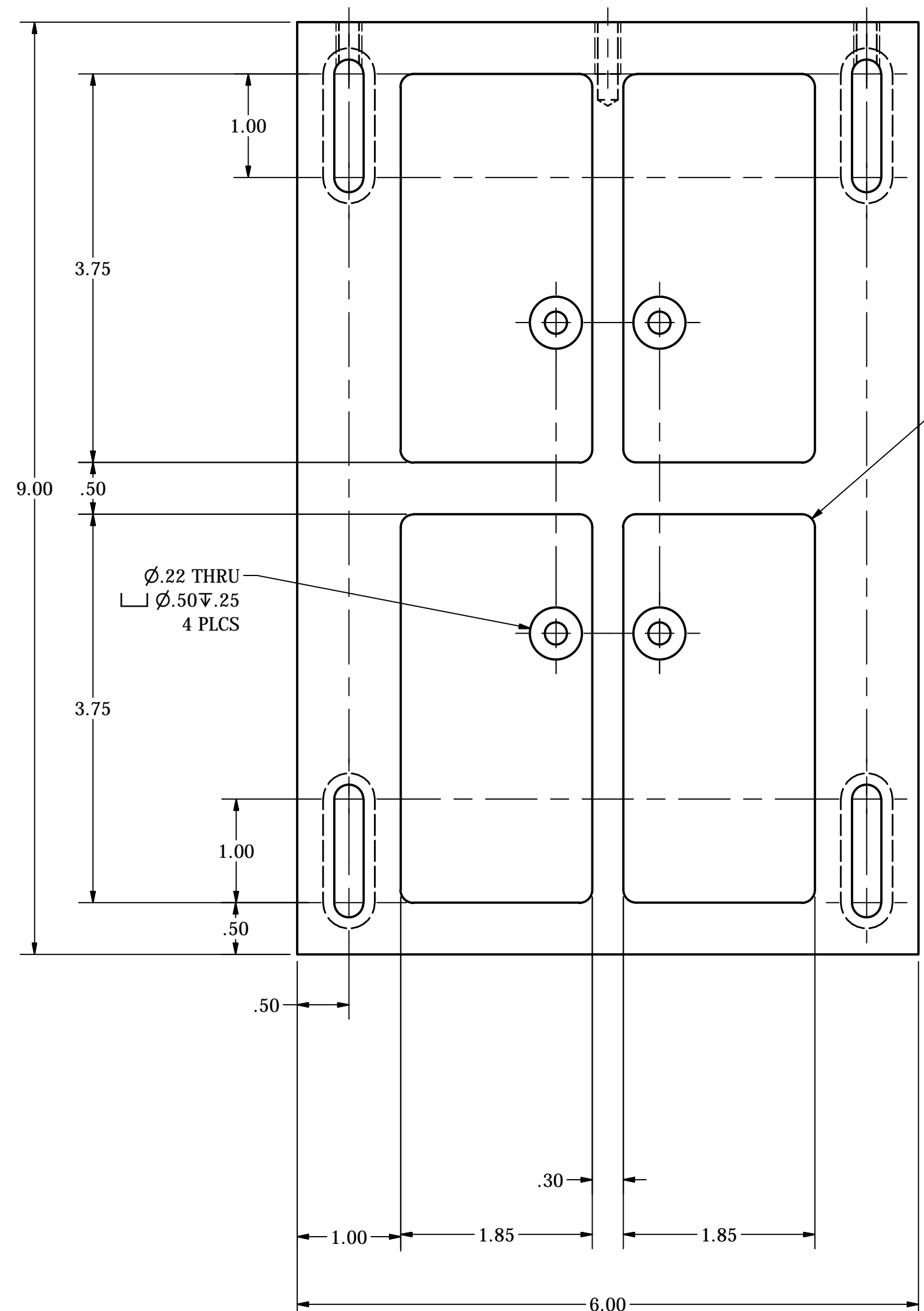
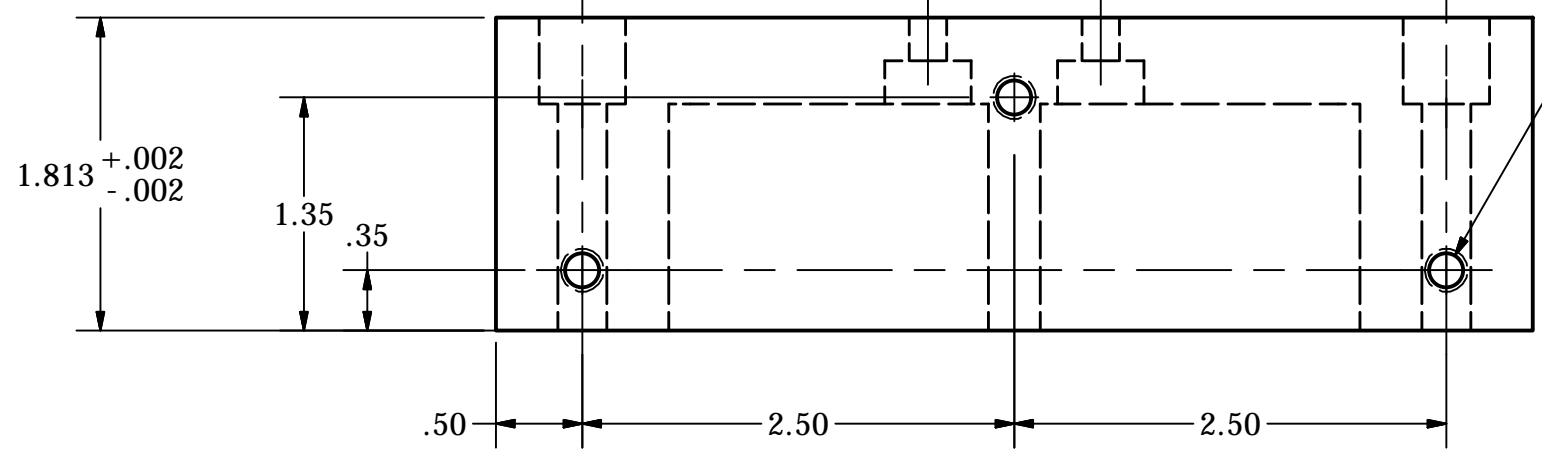
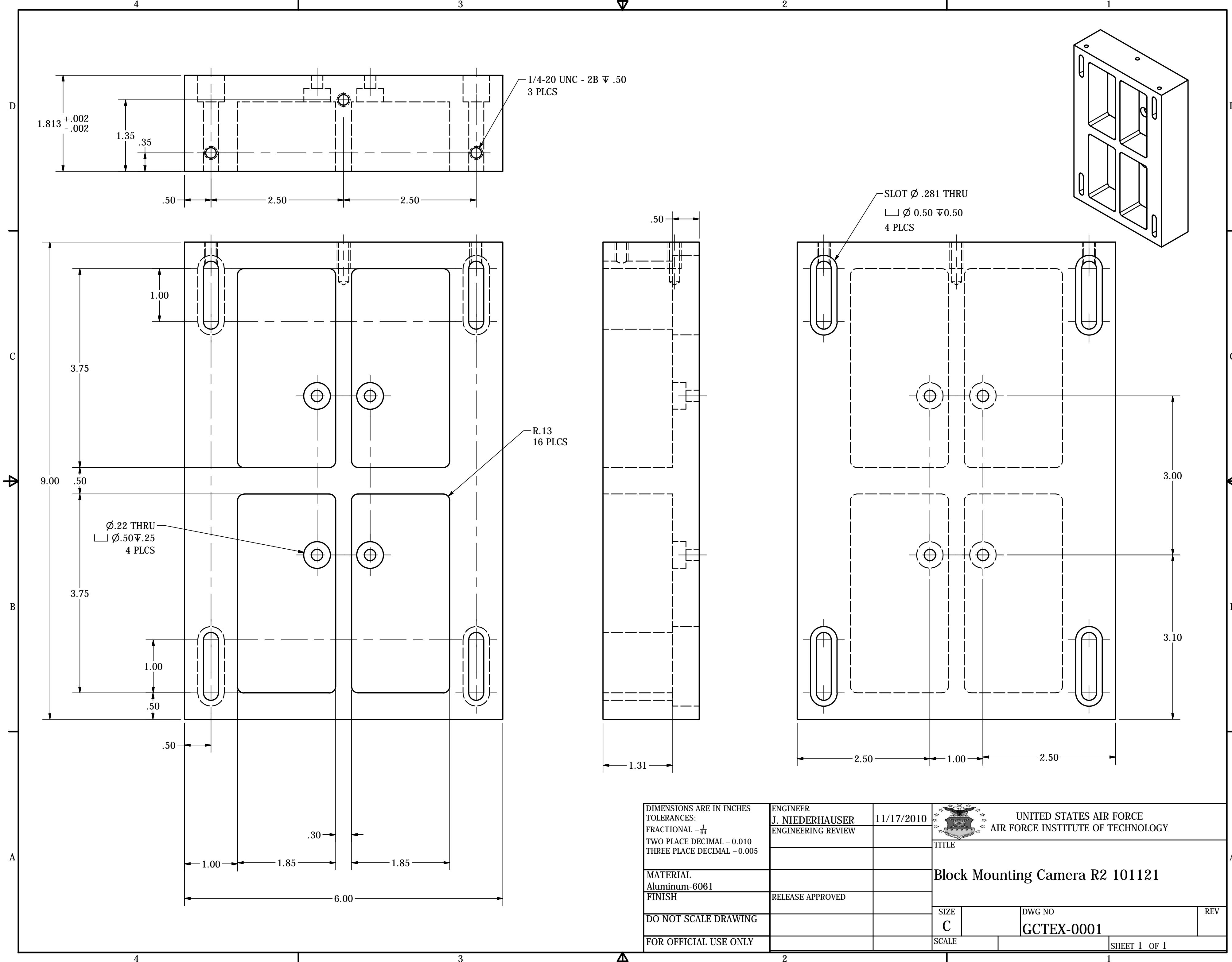
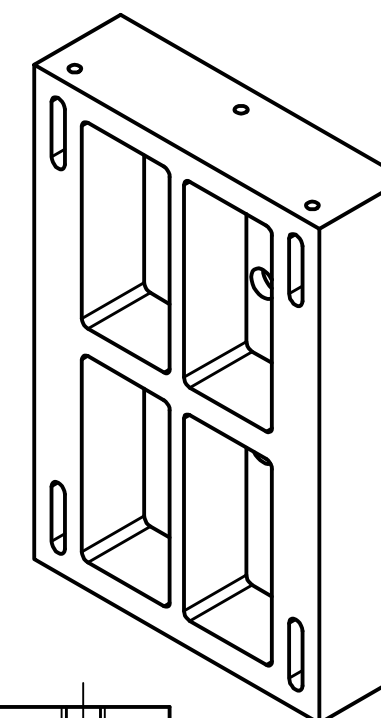


SECTION A-A
SCALE .48

DIMENSIONS ARE IN INCHES TOLERANCES: FRACTIONAL - $\frac{1}{64}$ TWO PLACE DECIMAL - 0.010 THREE PLACE DECIMAL - 0.005	ENGINEER Jason Niederhauser ENGINEERING REVIEW	11/19/2010	 UNITED STATES AIR FORCE AIR FORCE INSTITUTE OF TECHNOLOGY	
	MATERIAL		TITLE ASSY GCTEx Structure (Linear) R2 101118	
FINISH		RELEASE APPROVED		SIZE C
DO NOT SCALE DRAWING		DWG NO GCTEX-A002		REV
FOR OFFICIAL USE ONLY		SCALE		SHEET 1 OF 1

PRODUCED BY AN AUTODESK EDUCATIONAL PRODUCT

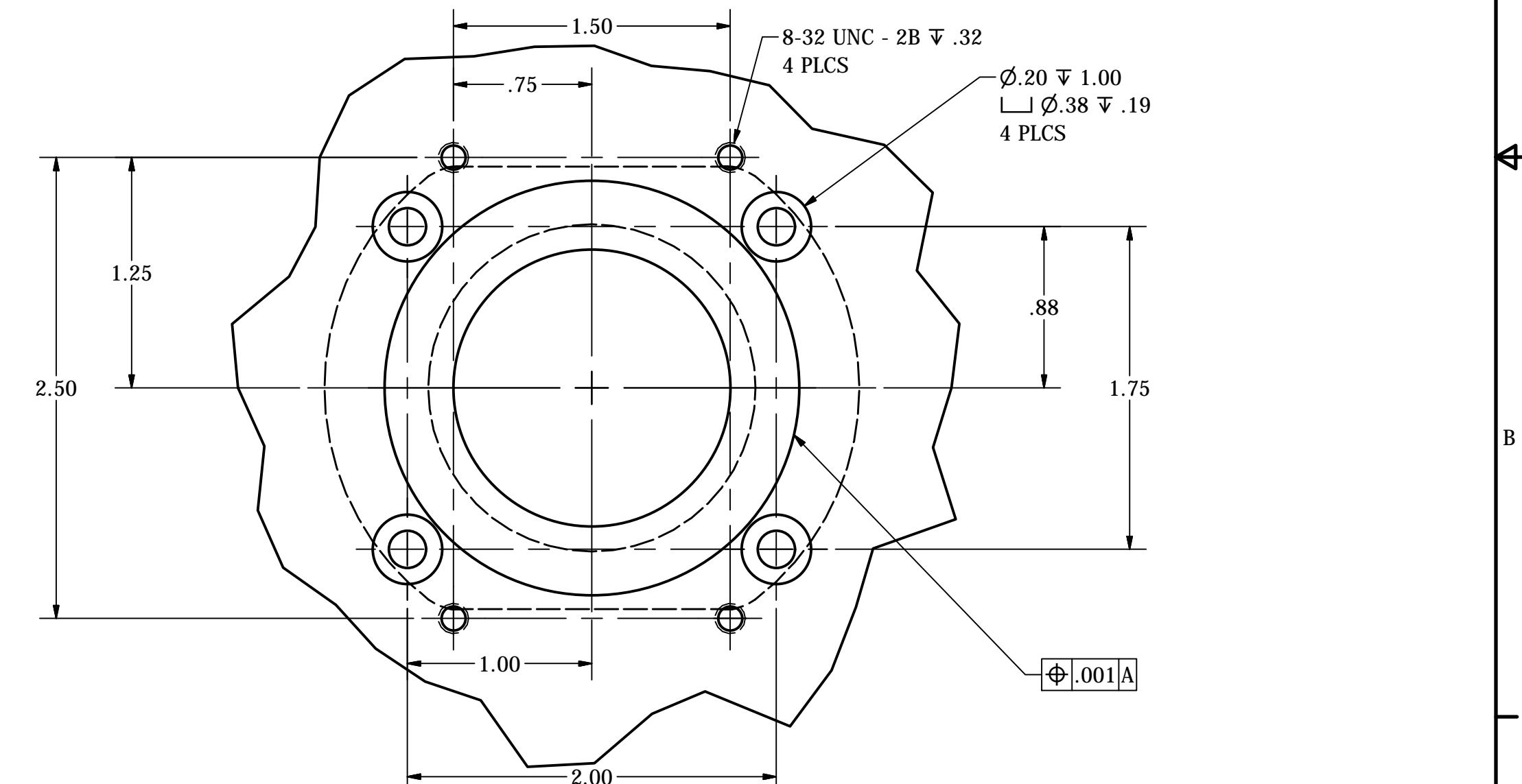
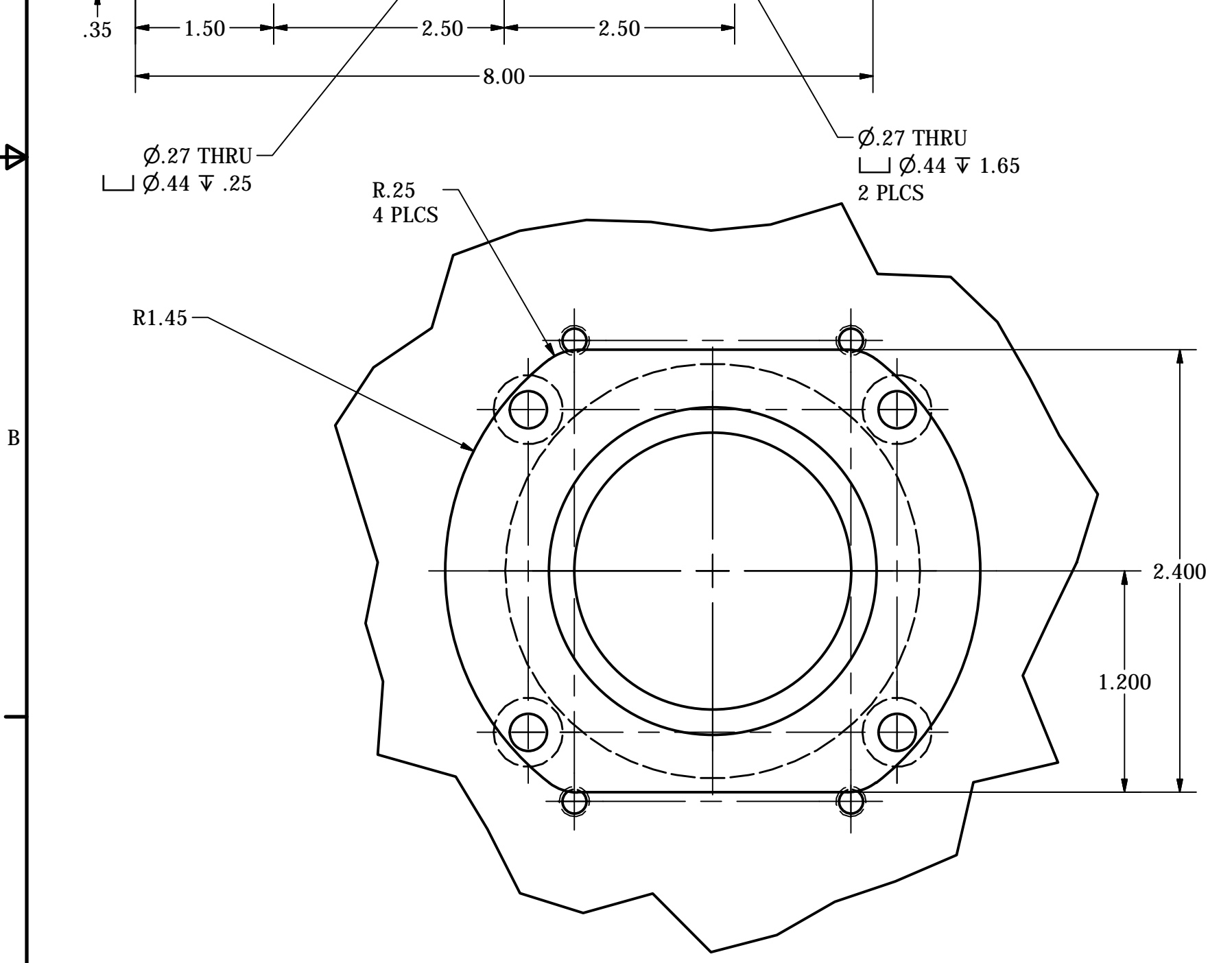
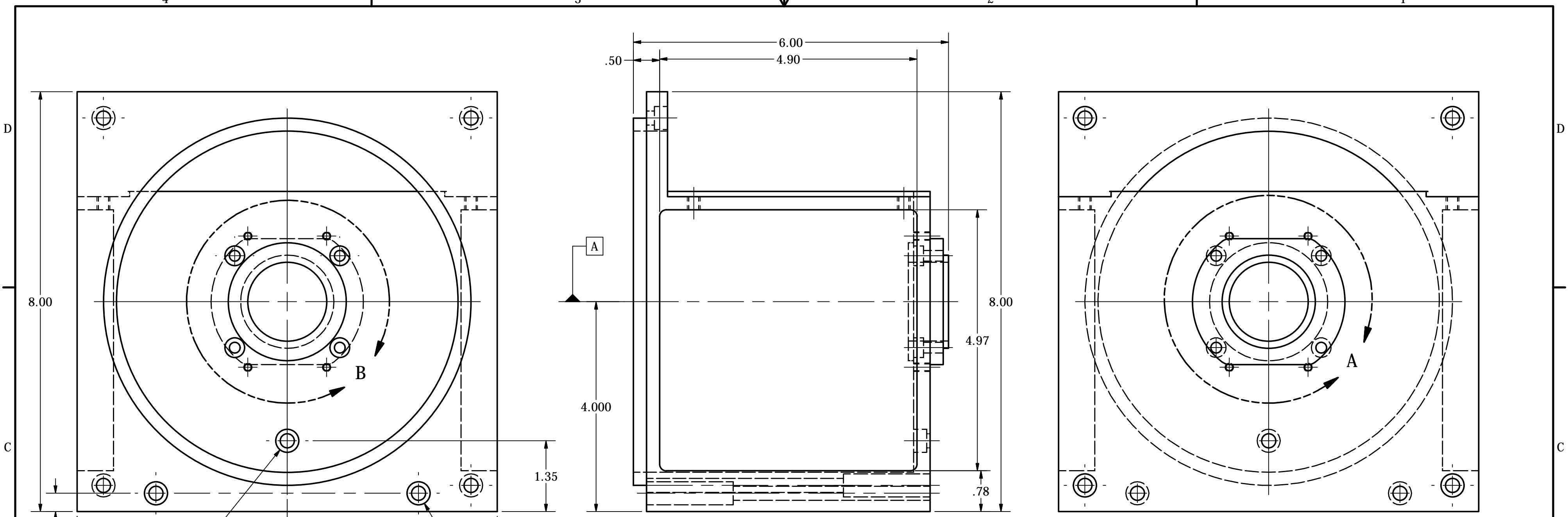
PRODUCED BY AN AUTODESK EDUCATIONAL PRODUCT



DIMENSIONS ARE IN INCHES TOLERANCES: FRACTIONAL - $\frac{1}{64}$ TWO PLACE DECIMAL - 0.010 THREE PLACE DECIMAL - 0.005	ENGINEER J. NIEDERHAUSER	11/17/2010	 UNITED STATES AIR FORCE AIR FORCE INSTITUTE OF TECHNOLOGY TITLE		
	ENGINEERING REVIEW				
MATERIAL Aluminum-6061			Block Mounting Camera R2 101121		
FINISH	RELEASE APPROVED				
DO NOT SCALE DRAWING			SIZE C	DWG NO GCTEX-0001	REV
FOR OFFICIAL USE ONLY			SCALE	SHEET 1 OF 1	

PRODUCED BY AN AUTODESK EDUCATIONAL PRODUCT

PRODUCED BY AN AUTODESK EDUCATIONAL PRODUCT



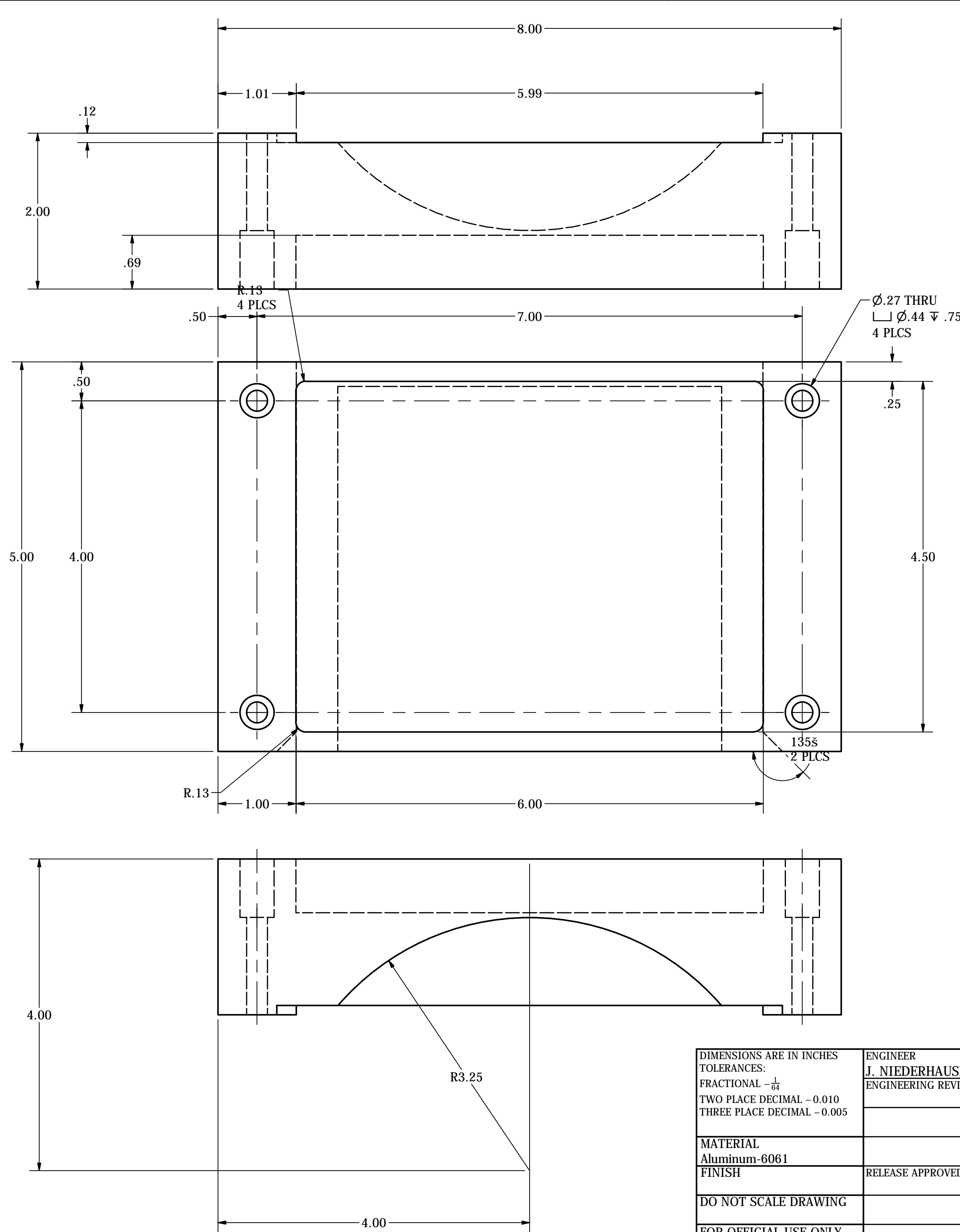
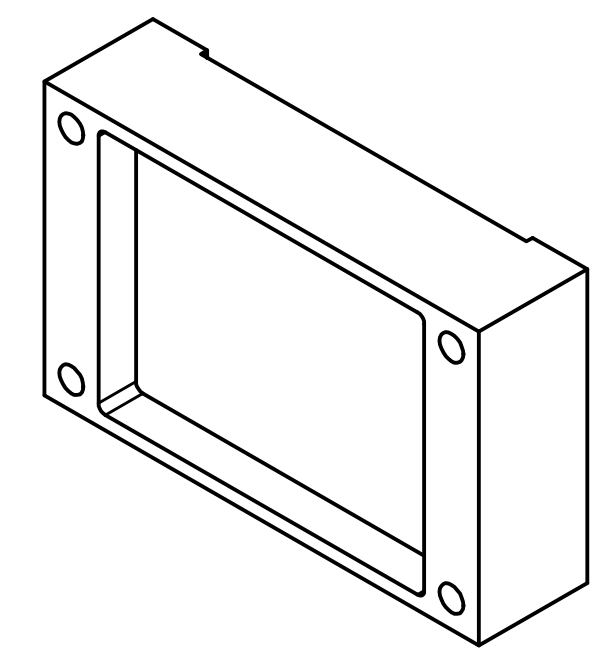
DETAIL B
SCALE 1.40 : 1

DETAIL A
SCALE 1.40 : 1

DIMENSIONS ARE IN INCHES TOLERANCES: FRACTIONAL - $\frac{1}{64}$ TWO PLACE DECIMAL - 0.010 THREE PLACE DECIMAL - 0.005	ENGINEER J. NIEDERHAUSER	DATE 11/17/2010	UNITED STATES AIR FORCE AIR FORCE INSTITUTE OF TECHNOLOGY	
	ENGINEERING REVIEW		TITLE Block Interface L3 R0 101117	
MATERIAL Aluminum-6061	FINISH RELEASE APPROVED		SIZE C	DWG NO GCTEX-0002
DO NOT SCALE DRAWING			SCALE	REV
FOR OFFICIAL USE ONLY			SHEET 2 OF 2	

PRODUCED BY AN AUTODESK EDUCATIONAL PRODUCT

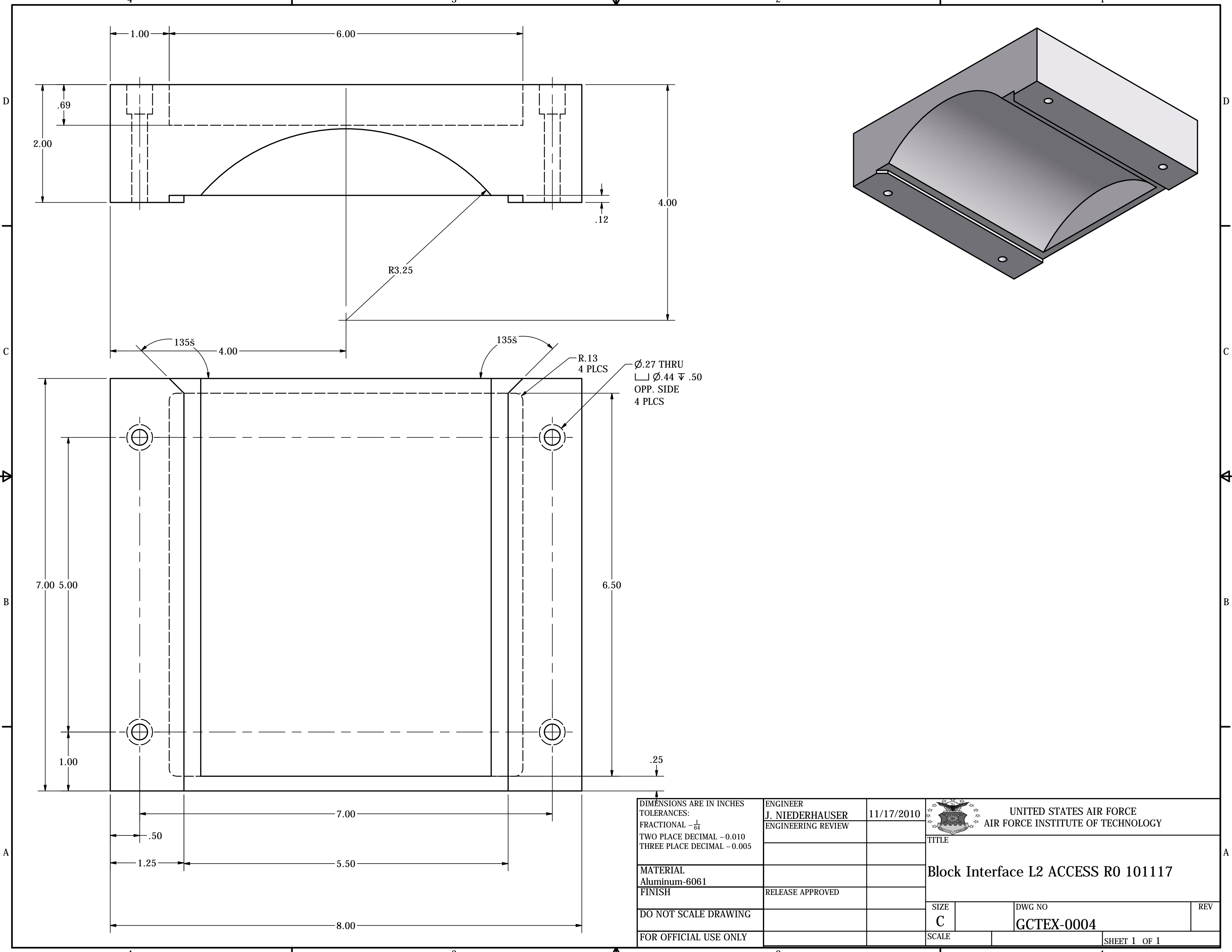
PRODUCED BY AN AUTODESK EDUCATIONAL PRODUCT



PRODUCED BY AN AUTODESK EDUCATIONAL PRODUCT

PRODUCED BY AN AUTODESK EDUCATIONAL PRODUCT

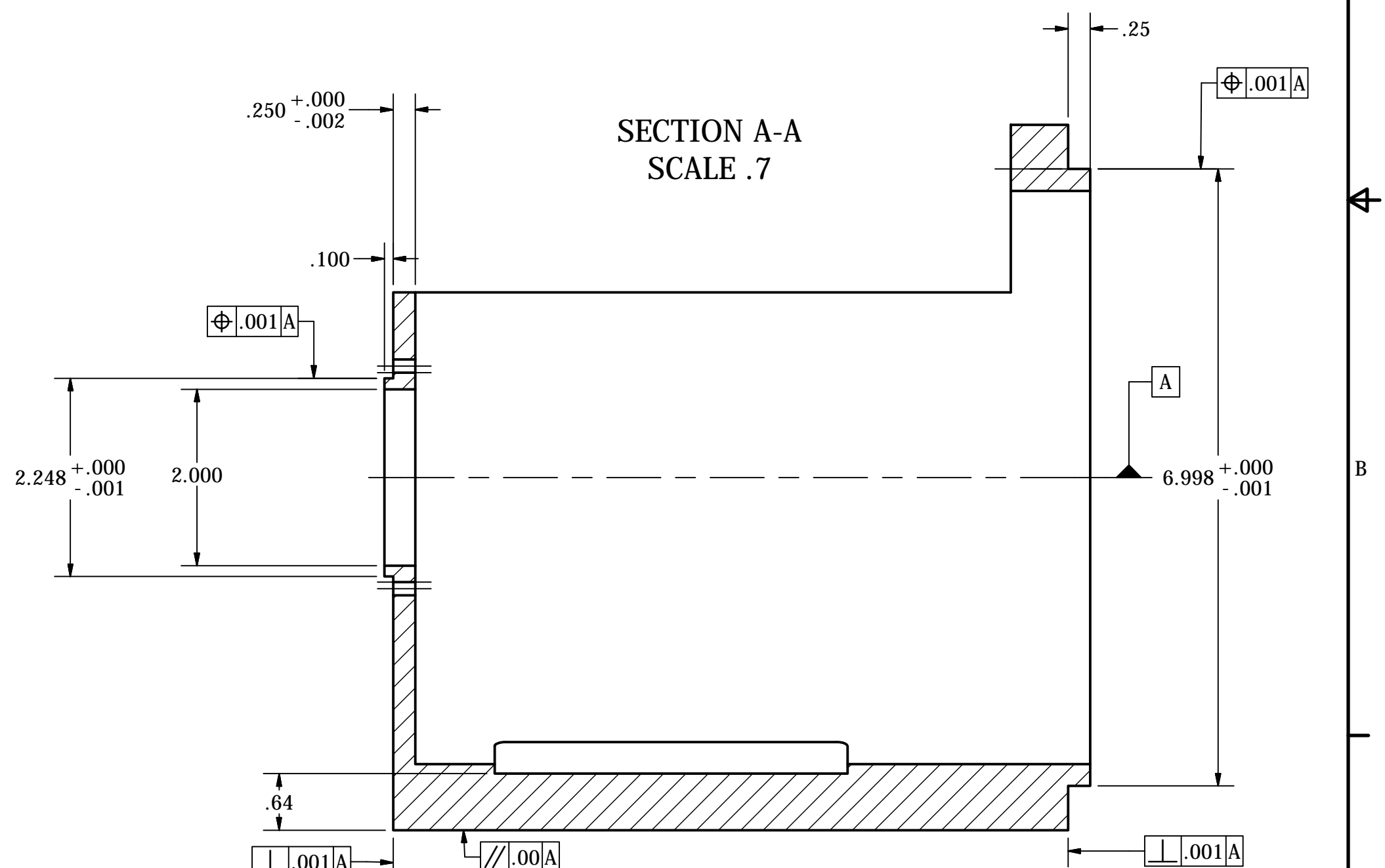
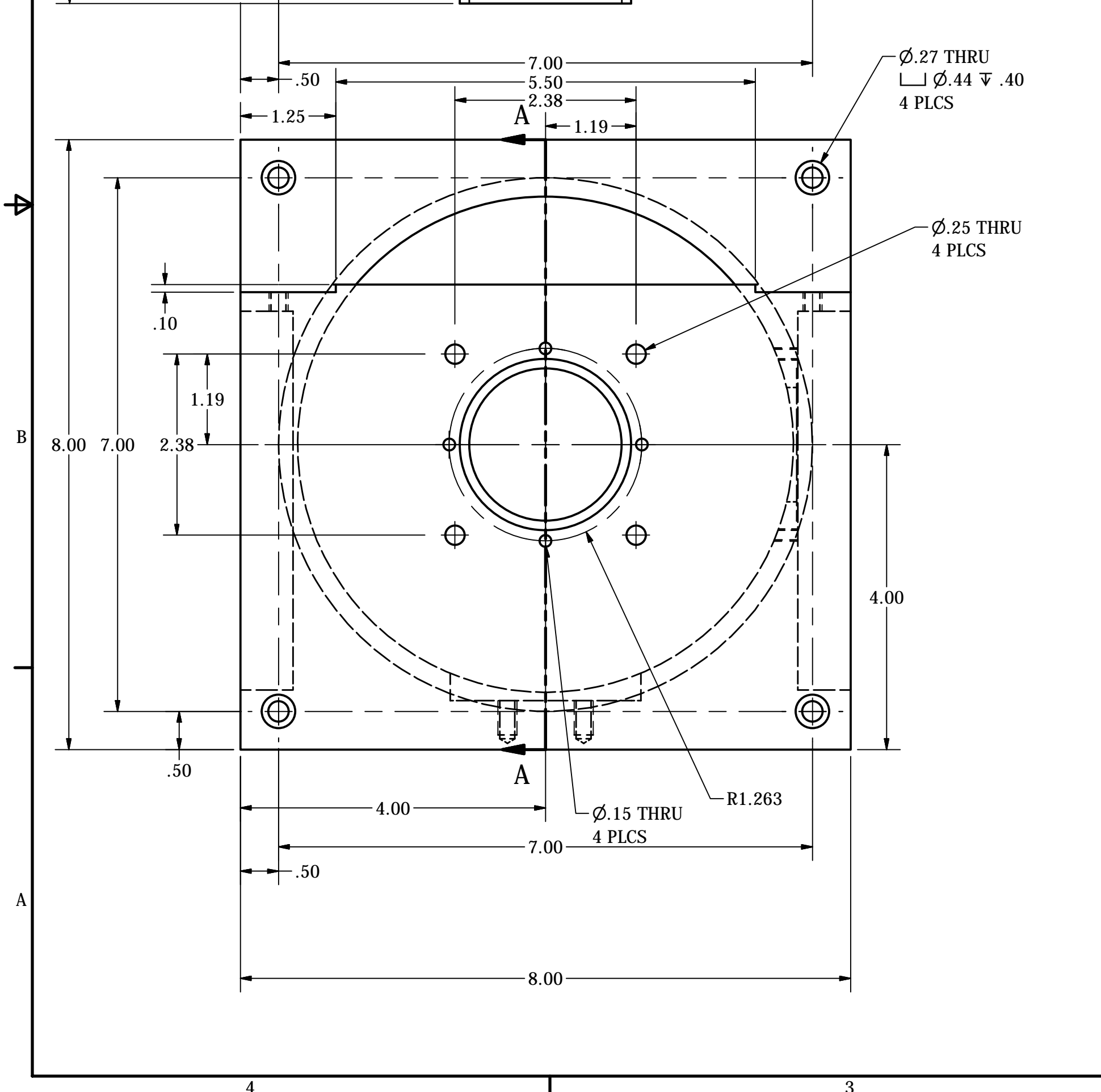
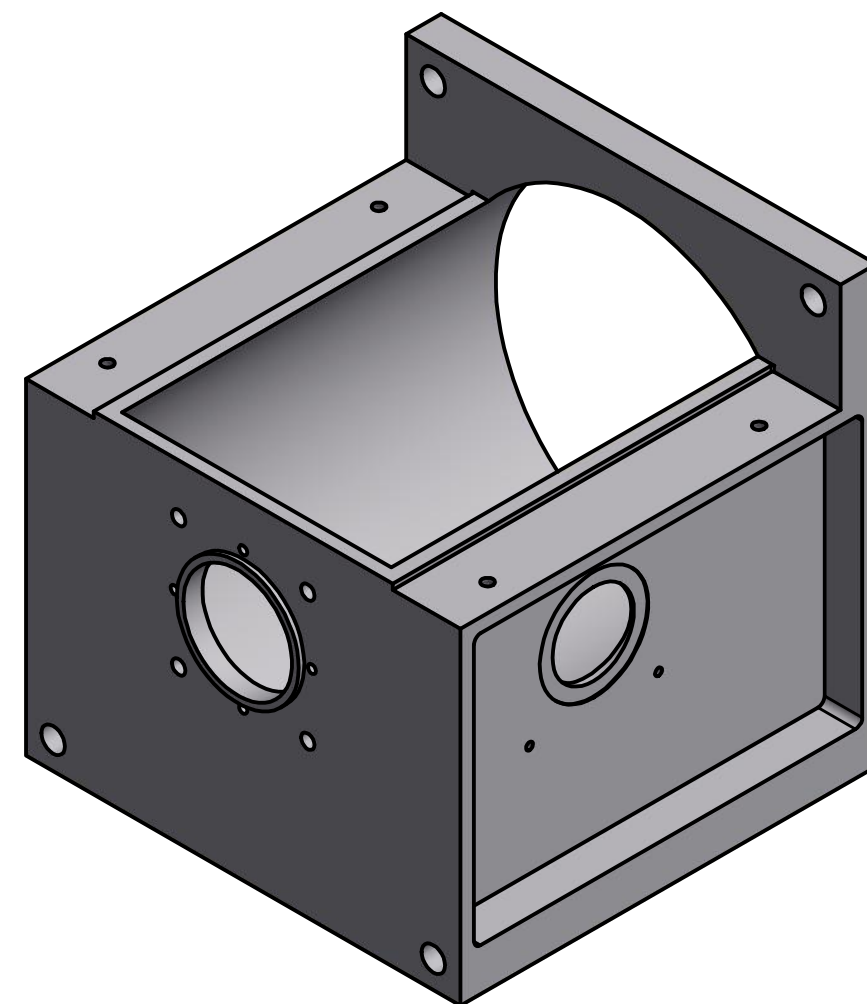
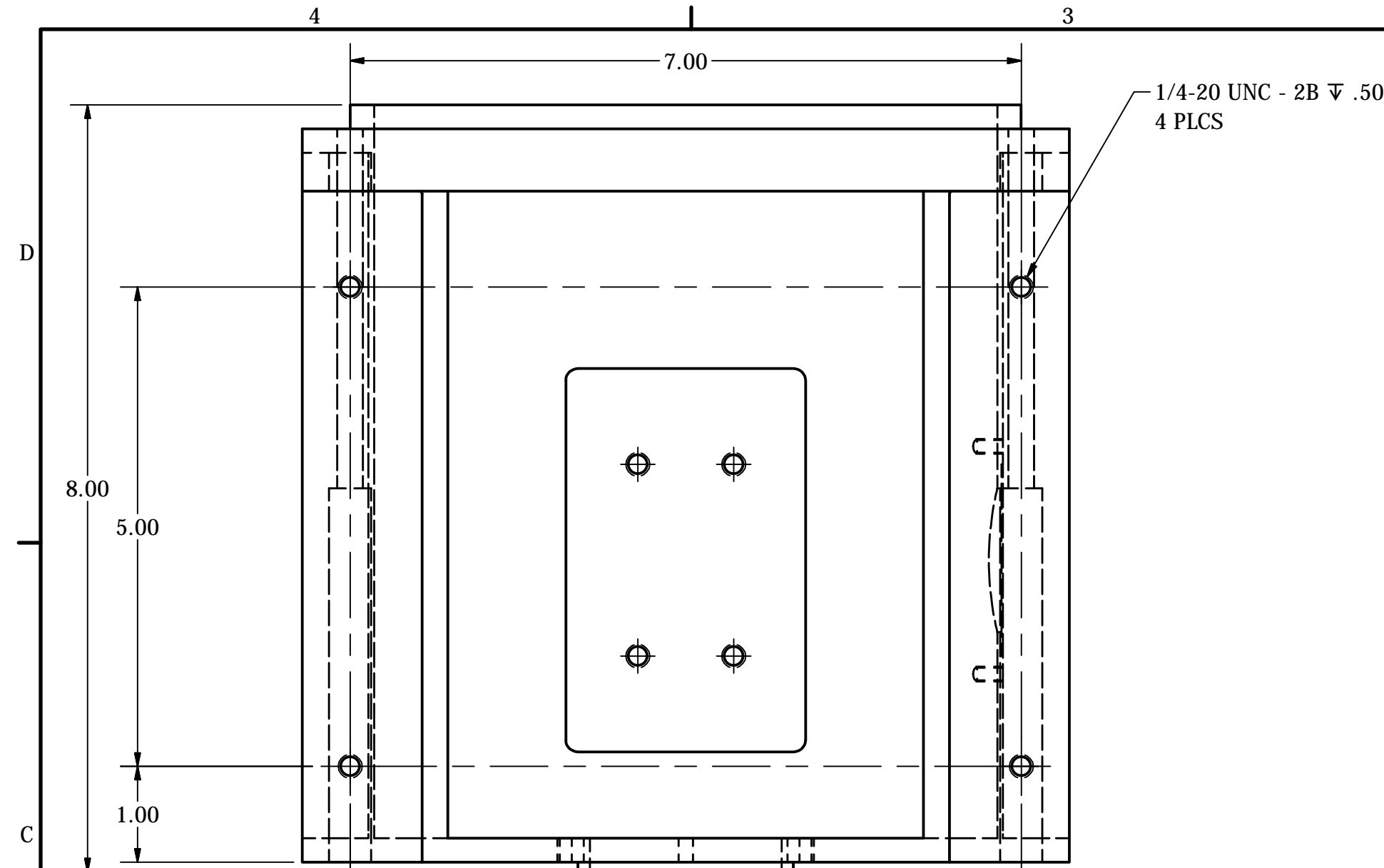
DIMENSIONS ARE IN INCHES TOLERANCES: FRACTIONAL - $\frac{1}{64}$ TWO PLACE DECIMAL - 0.010 THREE PLACE DECIMAL - 0.005	ENGINEER	11/17/2010	 UNITED STATES AIR FORCE AIR FORCE INSTITUTE OF TECHNOLOGY	
	J. NIEDERHAUSER ENGINEERING REVIEW		TITLE	
MATERIAL			Block Interface L3 ACCESS R0 101117	
Aluminum-6061			SIZE	DWG NO
FINISH	RELEASE APPROVED		C	GCTEX-0003
DO NOT SCALE DRAWING			SCALE	REV
FOR OFFICIAL USE ONLY				SHEET 1 OF 1



DIMENSIONS ARE IN INCHES TOLERANCES: FRACTIONAL - $\frac{1}{64}$ TWO PLACE DECIMAL - 0.010 THREE PLACE DECIMAL - 0.005	ENGINEER J. NIEDERHAUSER	11/17/2010	 UNITED STATES AIR FORCE AIR FORCE INSTITUTE OF TECHNOLOGY	
	MATERIAL Aluminum-6061 FINISH	ENGINEERING REVIEW		TITLE Block Interface L2 ACCESS R0 101117
DO NOT SCALE DRAWING	RELEASE APPROVED	SIZE C	DWG NO GCTEX-0004	REV
FOR OFFICIAL USE ONLY		SCALE	SHEET 1 OF 1	

PRODUCED BY AN AUTODESK EDUCATIONAL PRODUCT

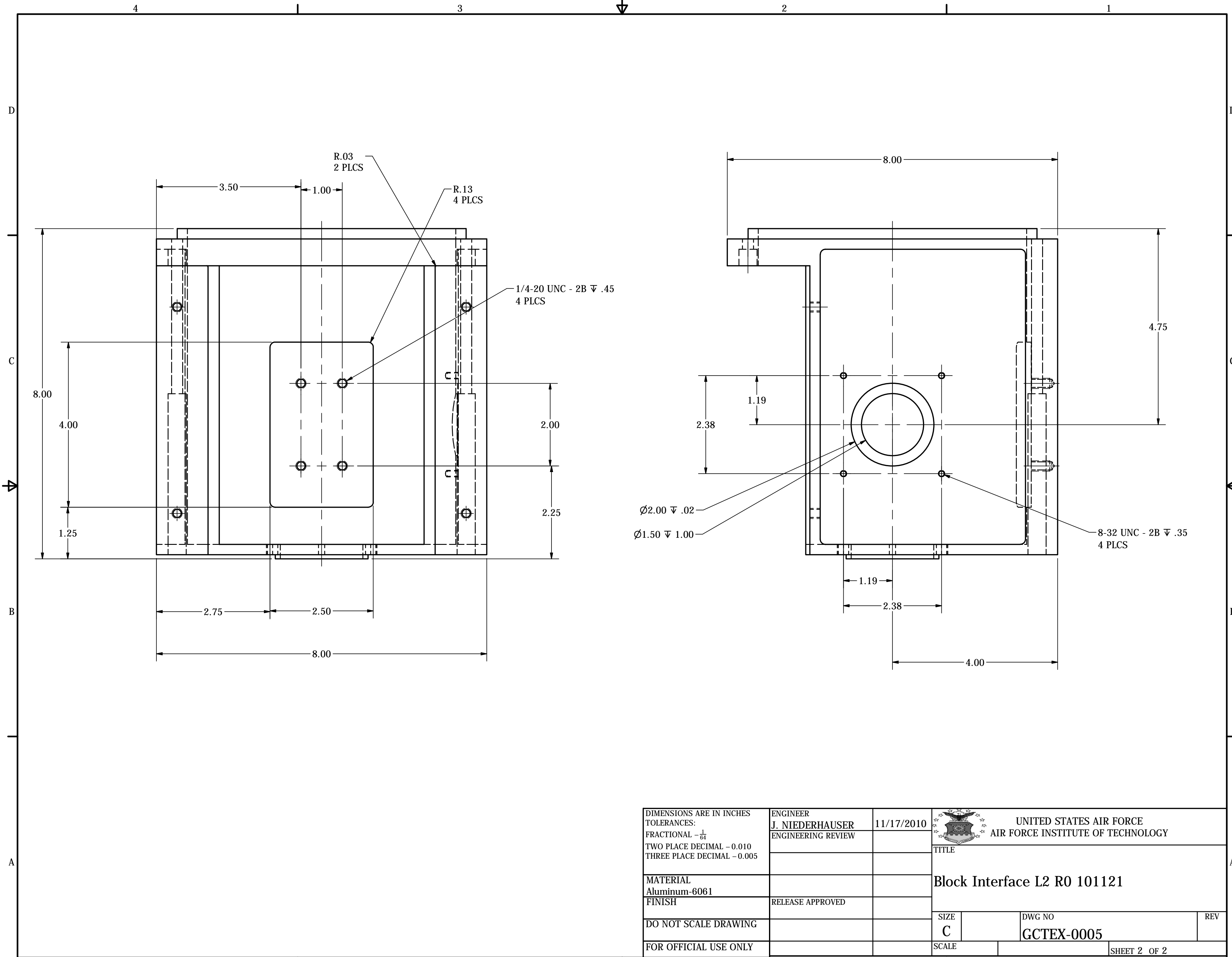
PRODUCED BY AN AUTODESK EDUCATIONAL PRODUCT



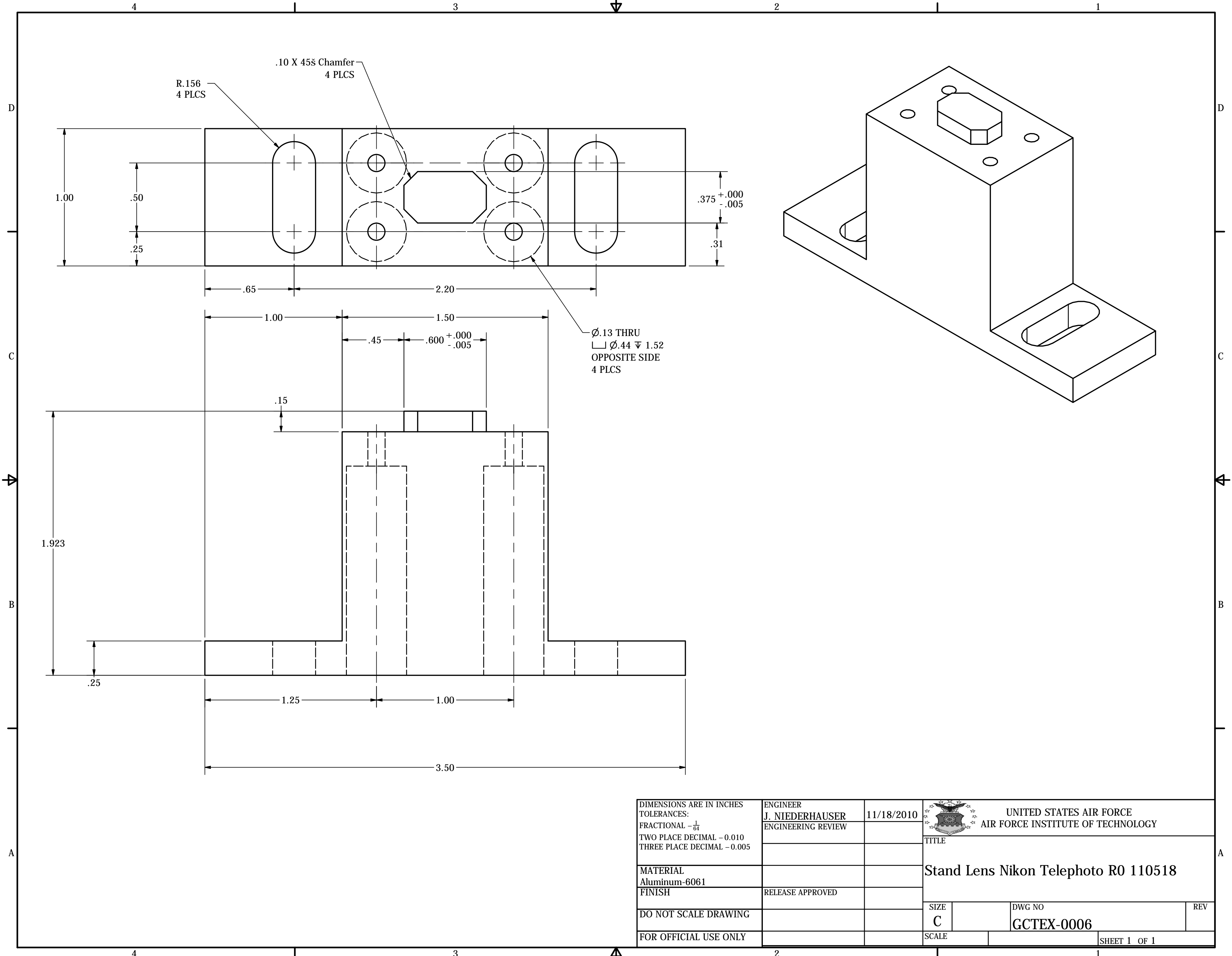
DIMENSIONS ARE IN INCHES TOLERANCES: FRACTIONAL - $\frac{1}{64}$ TWO PLACE DECIMAL - 0.010 THREE PLACE DECIMAL - 0.005	ENGINEER J. NIEDERHAUSER	11/18/2010	 UNITED STATES AIR FORCE AIR FORCE INSTITUTE OF TECHNOLOGY TITLE	
	ENGINEERING REVIEW			
MATERIAL Aluminum-6061			Block Interface L2 R0 110518	
FINISH	RELEASE APPROVED		SIZE C	DWG NO GCTEX-0005
DO NOT SCALE DRAWING			SCALE	REV
FOR OFFICIAL USE ONLY				SHEET 1 OF 2

PRODUCED BY AN AUTODESK EDUCATIONAL PRODUCT

PRODUCED BY AN AUTODESK EDUCATIONAL PRODUCT



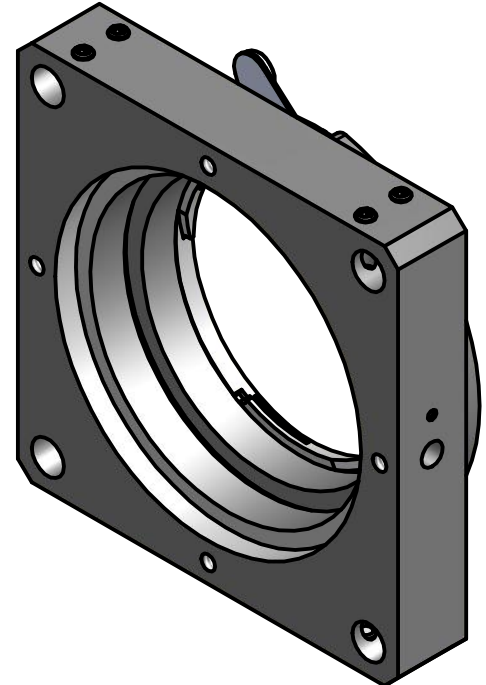
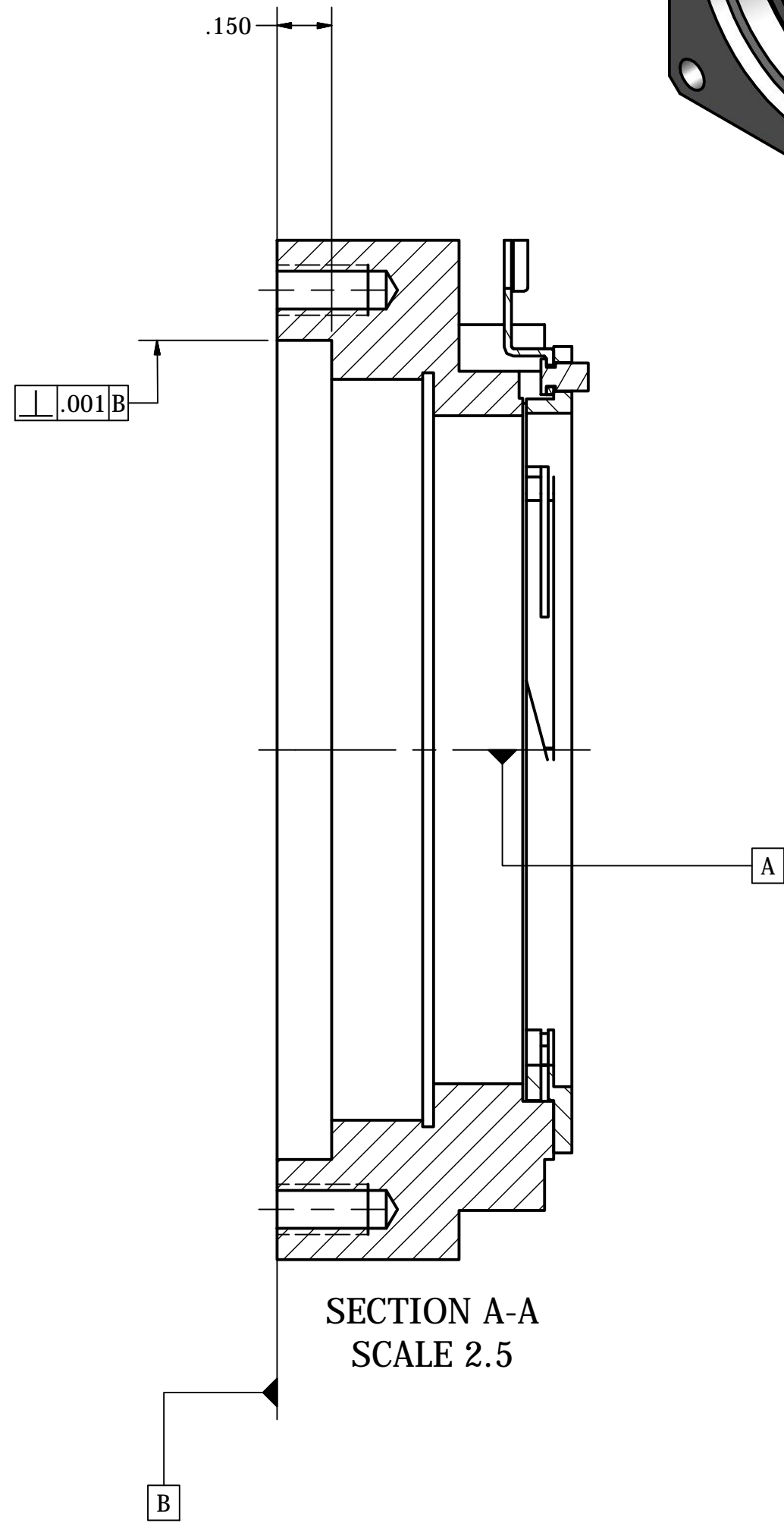
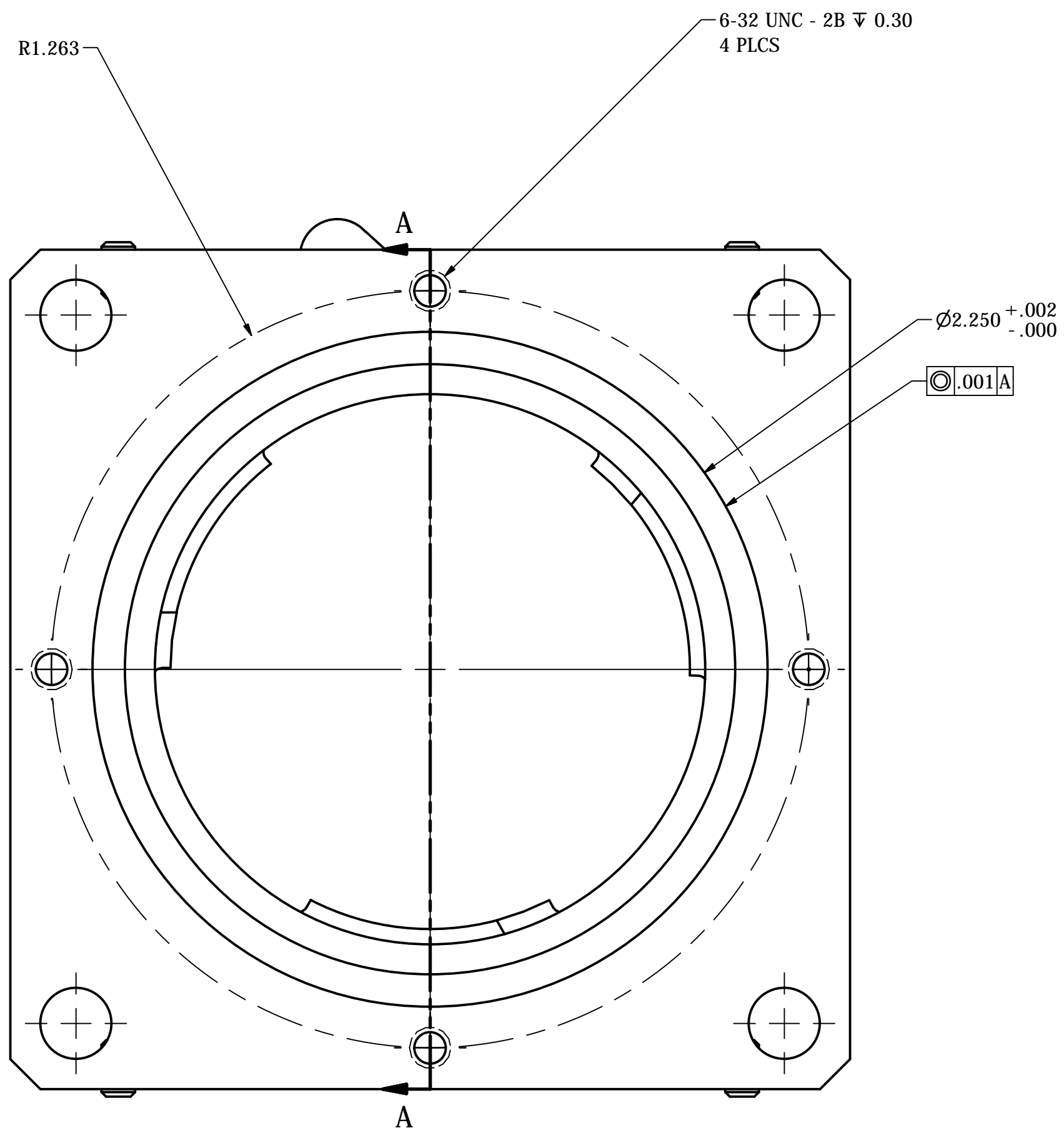
DIMENSIONS ARE IN INCHES TOLERANCES: FRACTIONAL - $\frac{1}{64}$ TWO PLACE DECIMAL - 0.010 THREE PLACE DECIMAL - 0.005	ENGINEER J. NIEDERHAUSER	DATE 11/17/2010	 UNITED STATES AIR FORCE AIR FORCE INSTITUTE OF TECHNOLOGY	
	ENGINEERING REVIEW		TITLE Block Interface L2 R0 101121	
MATERIAL Aluminum-6061			FINISH RELEASE APPROVED	
DO NOT SCALE DRAWING			SIZE C	DWG NO GCTEX-0005
FOR OFFICIAL USE ONLY			SCALE	REV SHEET 2 OF 2



DIMENSIONS ARE IN INCHES TOLERANCES: FRACTIONAL - $\frac{1}{64}$ TWO PLACE DECIMAL - 0.010 THREE PLACE DECIMAL - 0.005	ENGINEER J. NIEDERHAUSER	11/18/2010	 UNITED STATES AIR FORCE AIR FORCE INSTITUTE OF TECHNOLOGY	
	ENGINEERING REVIEW		TITLE Stand Lens Nikon Telephoto R0 110518	
MATERIAL Aluminum-6061			SIZE C	DWG NO GCTEX-0006
FINISH	RELEASE APPROVED		SCALE	REV
DO NOT SCALE DRAWING			SHEET 1 OF 1	
FOR OFFICIAL USE ONLY				

PRODUCED BY AN AUTODESK EDUCATIONAL PRODUCT

PRODUCED BY AN AUTODESK EDUCATIONAL PRODUCT



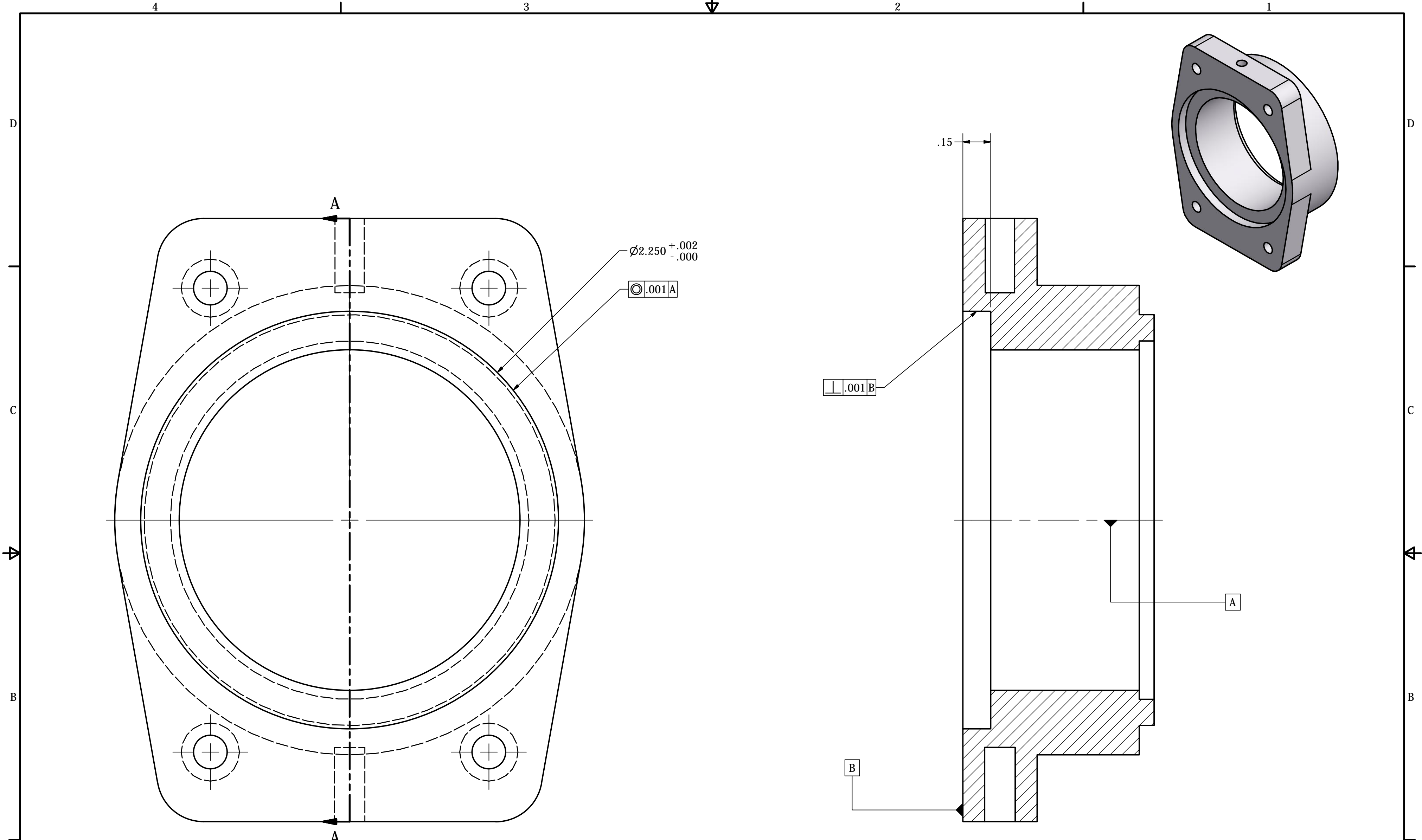
PRODUCED BY AN AUTODESK EDUCATIONAL PRODUCT

PRODUCED BY AN AUTODESK EDUCATIONAL PRODUCT

DIMENSIONS ARE IN INCHES TOLERANCES: FRACTIONAL - $\frac{1}{64}$ TWO PLACE DECIMAL - 0.010 THREE PLACE DECIMAL - 0.005	ENGINEER J. NIEDERHAUSER	11/18/2010	 UNITED STATES AIR FORCE AIR FORCE INSTITUTE OF TECHNOLOGY	
	ENGINEERING REVIEW		TITLE LCP04 Nikon Mount R0 101121	
MATERIAL Stainless Steel	FINISH RELEASE APPROVED		SIZE C	DWG NO GCTEX-0007
DO NOT SCALE DRAWING			SCALE	REV
FOR OFFICIAL USE ONLY			SHEET 1 OF 1	

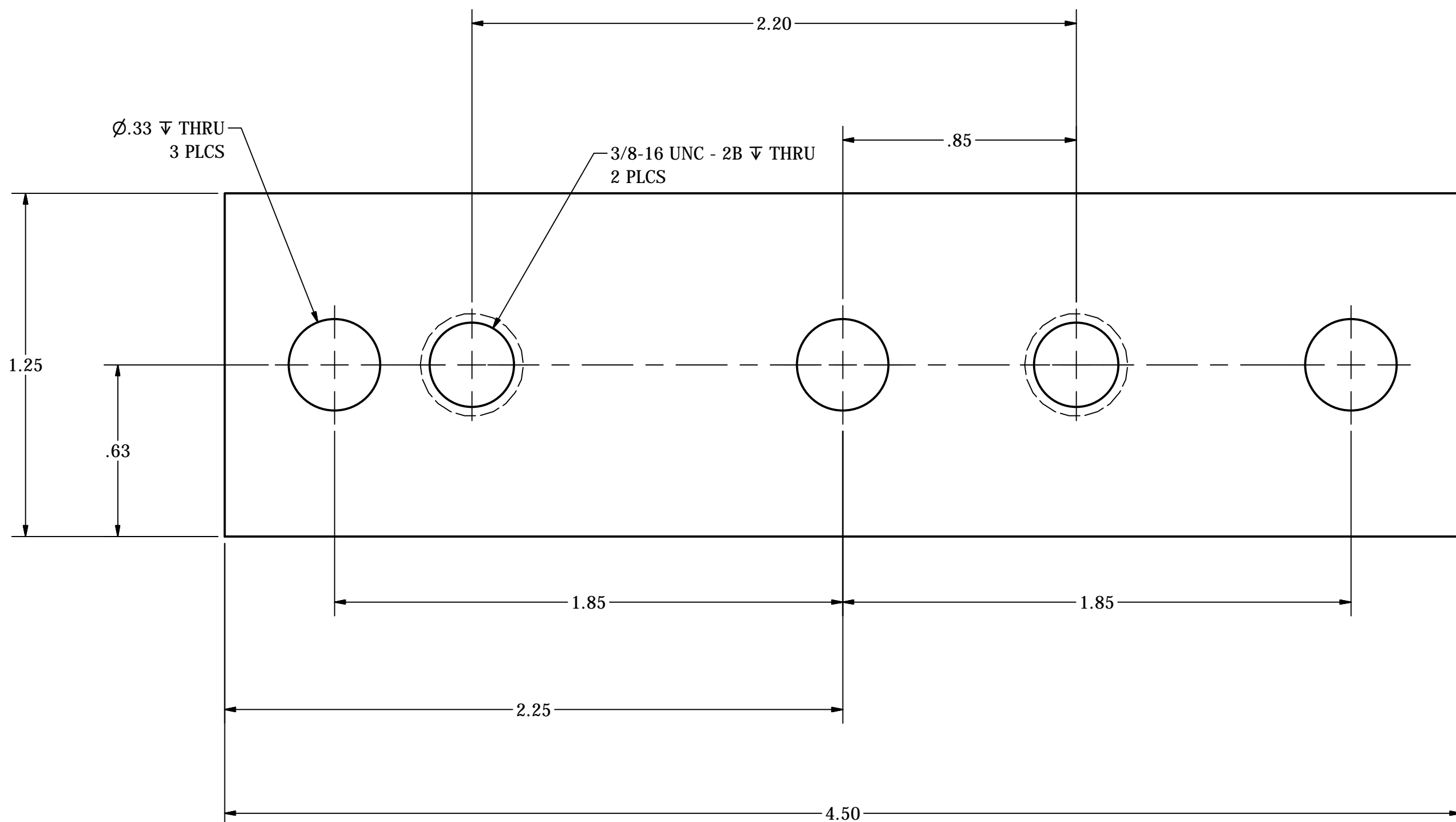
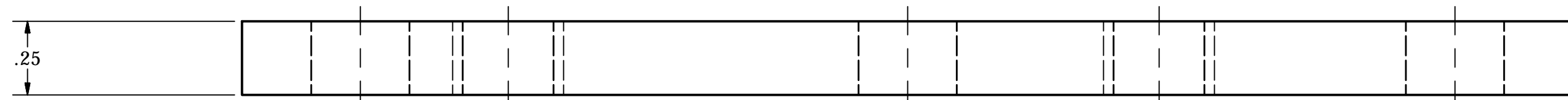
PRODUCED BY AN AUTODESK EDUCATIONAL PRODUCT

PRODUCED BY AN AUTODESK EDUCATIONAL PRODUCT



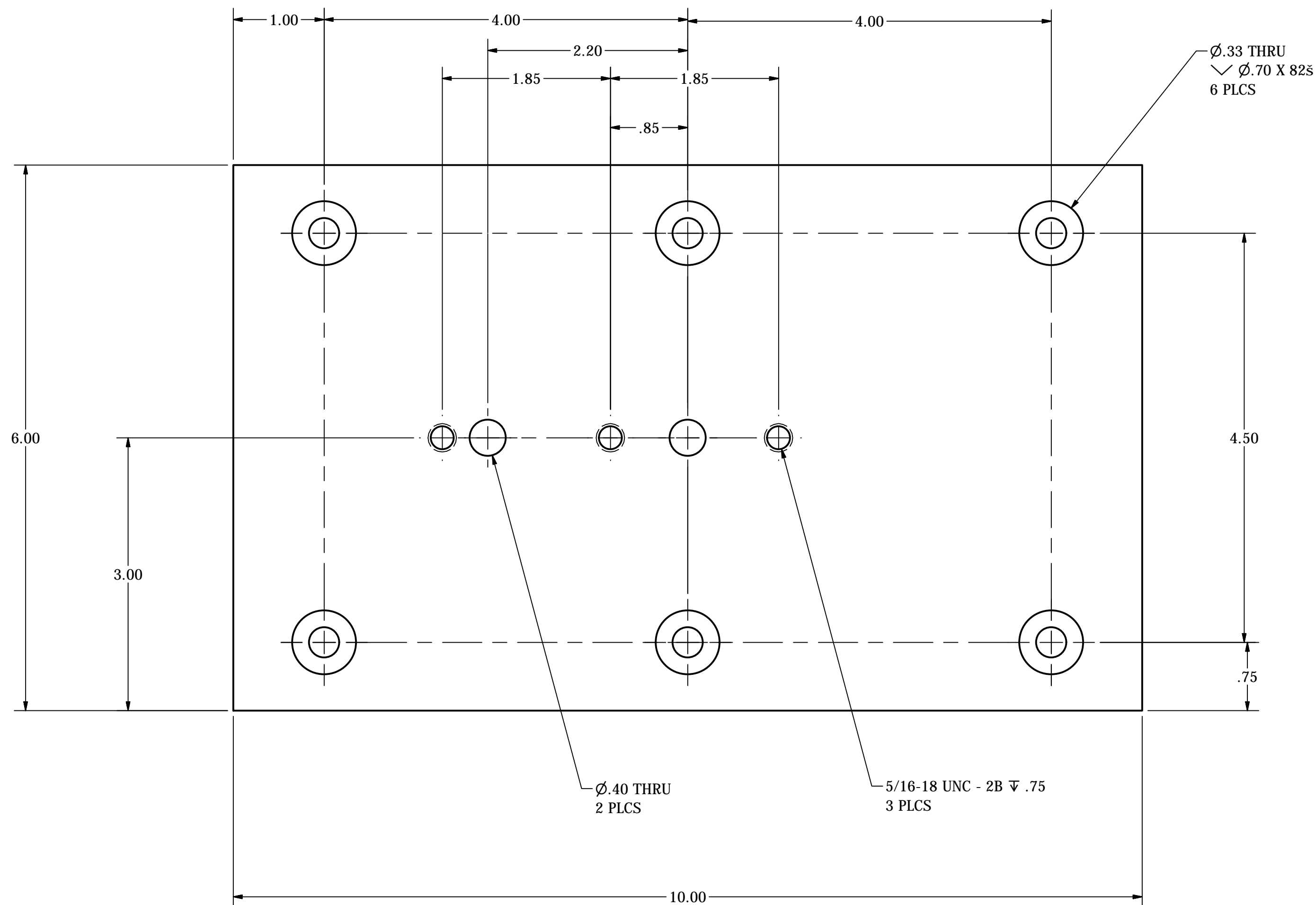
SECTION A-A
SCALE 2.75

DIMENSIONS ARE IN INCHES TOLERANCES: FRACTIONAL - $\frac{1}{64}$ TWO PLACE DECIMAL - 0.010 THREE PLACE DECIMAL - 0.005	ENGINEER J. NIEDERHAUSER	DATE 11/18/2010	 UNITED STATES AIR FORCE AIR FORCE INSTITUTE OF TECHNOLOGY	
	ENGINEERING REVIEW		TITLE NFM1 Nikon F-Mount R0 101121	
MATERIAL Aluminum-6061	FINISH RELEASE APPROVED		SIZE C	DWG NO GCTEX-0008
DO NOT SCALE DRAWING			SCALE	REV
FOR OFFICIAL USE ONLY			SHEET 1 OF 1	

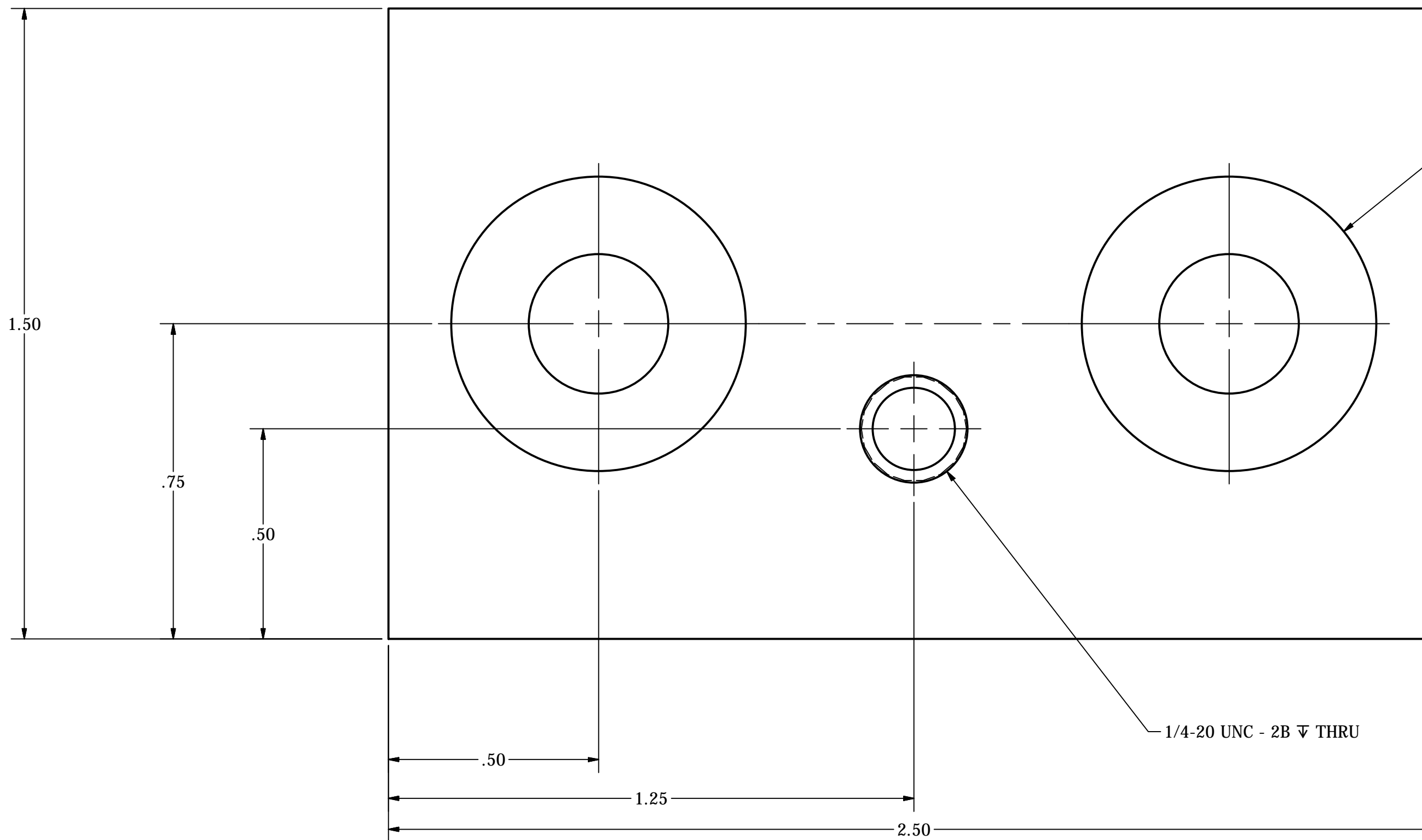
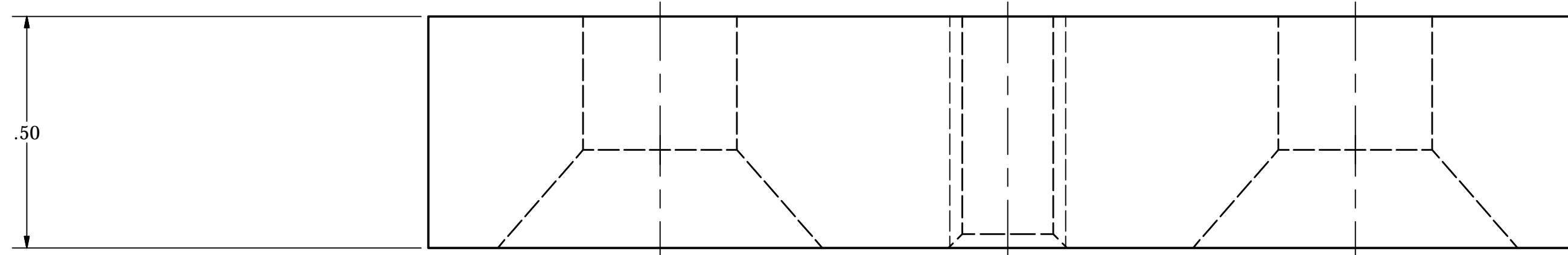


DIMENSIONS ARE IN INCHES TOLERANCES: FRACTIONAL - $\frac{1}{64}$ TWO PLACE DECIMAL - 0.010 THREE PLACE DECIMAL - 0.005	ENGINEER J. NIEDERHAUSER	11/18/2010	 UNITED STATES AIR FORCE AIR FORCE INSTITUTE OF TECHNOLOGY	
	ENGINEERING REVIEW		TITLE Plate Mounting Structural Tripod Secure R0 110518	
MATERIAL Stainless Steel			SIZE C	DWG NO GCTEX-0009
FINISH	RELEASE APPROVED		SCALE	REV
DO NOT SCALE DRAWING			SHEET 1 OF 1	
FOR OFFICIAL USE ONLY				

PRODUCED BY AN AUTODESK EDUCATIONAL PRODUCT



DIMENSIONS ARE IN INCHES TOLERANCES: FRACTIONAL - $\frac{1}{64}$ TWO PLACE DECIMAL - 0.010 THREE PLACE DECIMAL - 0.005	ENGINEER J. NIEDERHAUSER ENGINEERING REVIEW	11/18/2010	 UNITED STATES AIR FORCE AIR FORCE INSTITUTE OF TECHNOLOGY	
	MATERIAL Stainless Steel FINISH		TITLE GCTEX-0010 Plate Mounting Structural R1 101121	
DO NOT SCALE DRAWING	RELEASE APPROVED	SIZE C	DWG NO GCTEX-0010	REV
FOR OFFICIAL USE ONLY	SCALE		SHEET 1 OF 1	



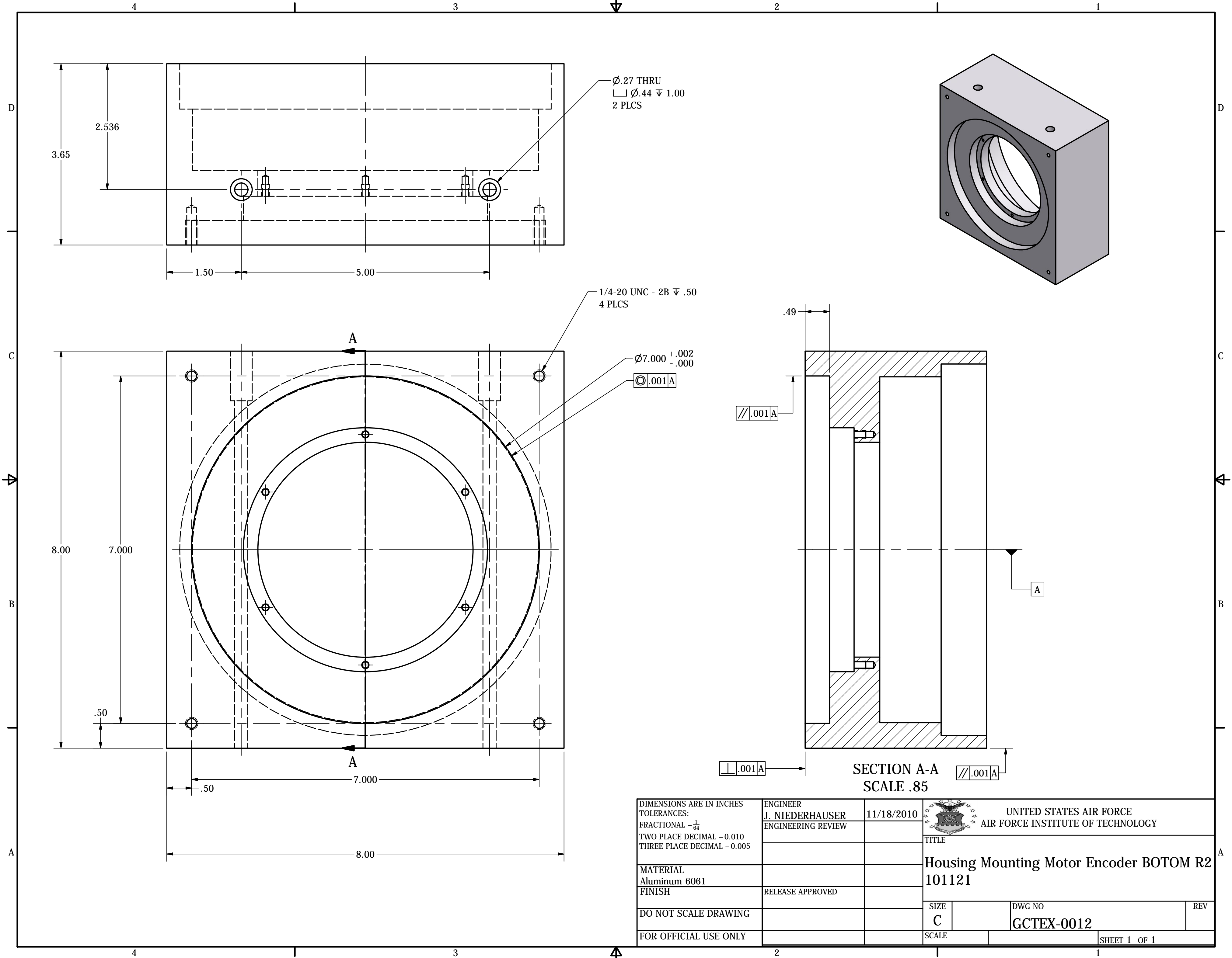
Ø.33 THRU
 ✓ Ø.70 X 825
 2 PLCS

1/4-20 UNC - 2B ✓ THRU

DIMENSIONS ARE IN INCHES TOLERANCES: FRACTIONAL - $\frac{1}{64}$ TWO PLACE DECIMAL - 0.010 THREE PLACE DECIMAL - 0.005	ENGINEER J. NIEDERHAUSER	DATE 11/18/2010	 UNITED STATES AIR FORCE AIR FORCE INSTITUTE OF TECHNOLOGY	
	ENGINEERING REVIEW		TITLE Block Spacer Structure 2.5 in R0 090811	
MATERIAL Stainless Steel			SIZE C	DWG NO GCTEX-0011
FINISH	RELEASE APPROVED			REV
DO NOT SCALE DRAWING			SCALE	SHEET 1 OF 1
FOR OFFICIAL USE ONLY				

PRODUCED BY AN AUTODESK EDUCATIONAL PRODUCT

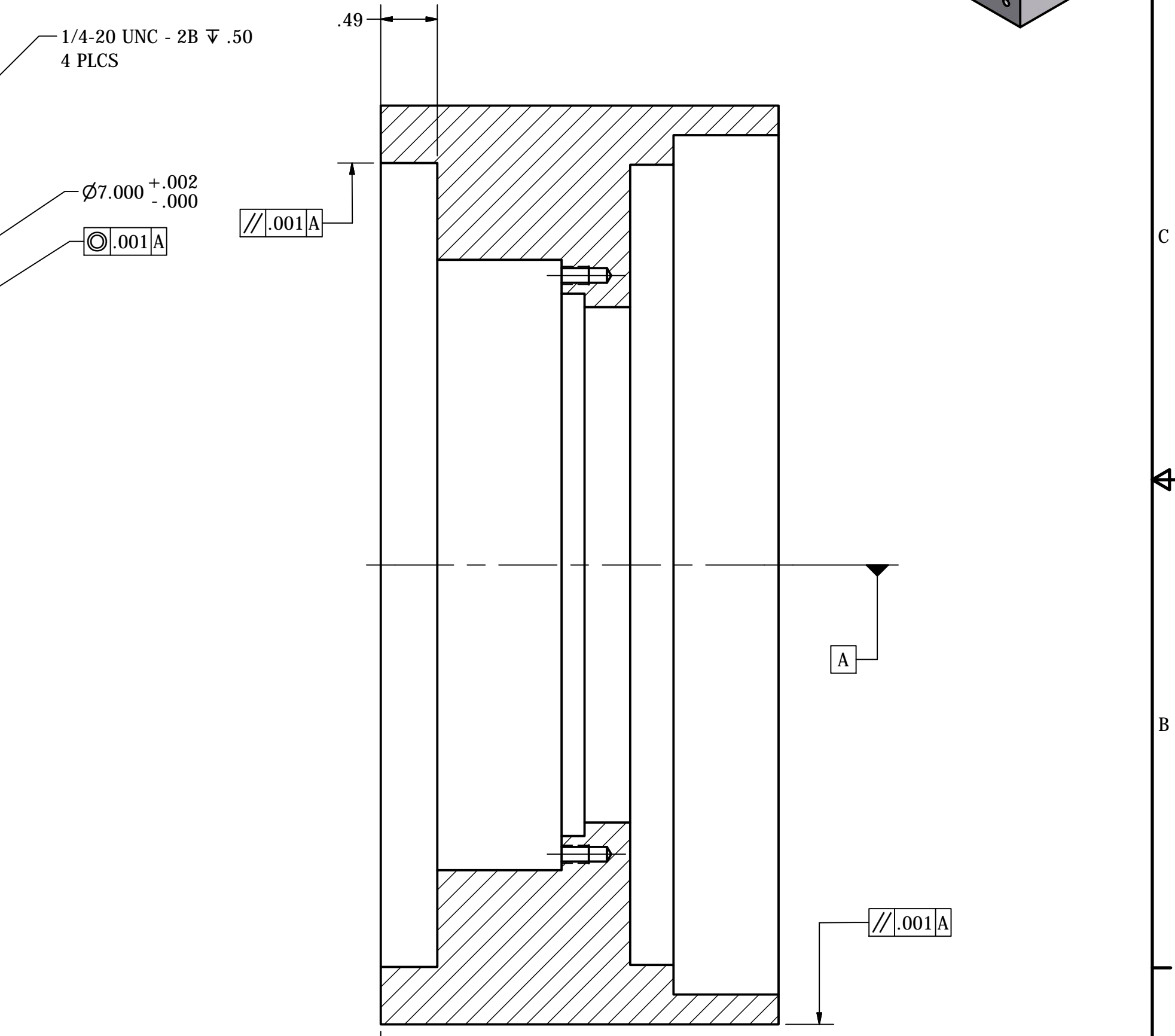
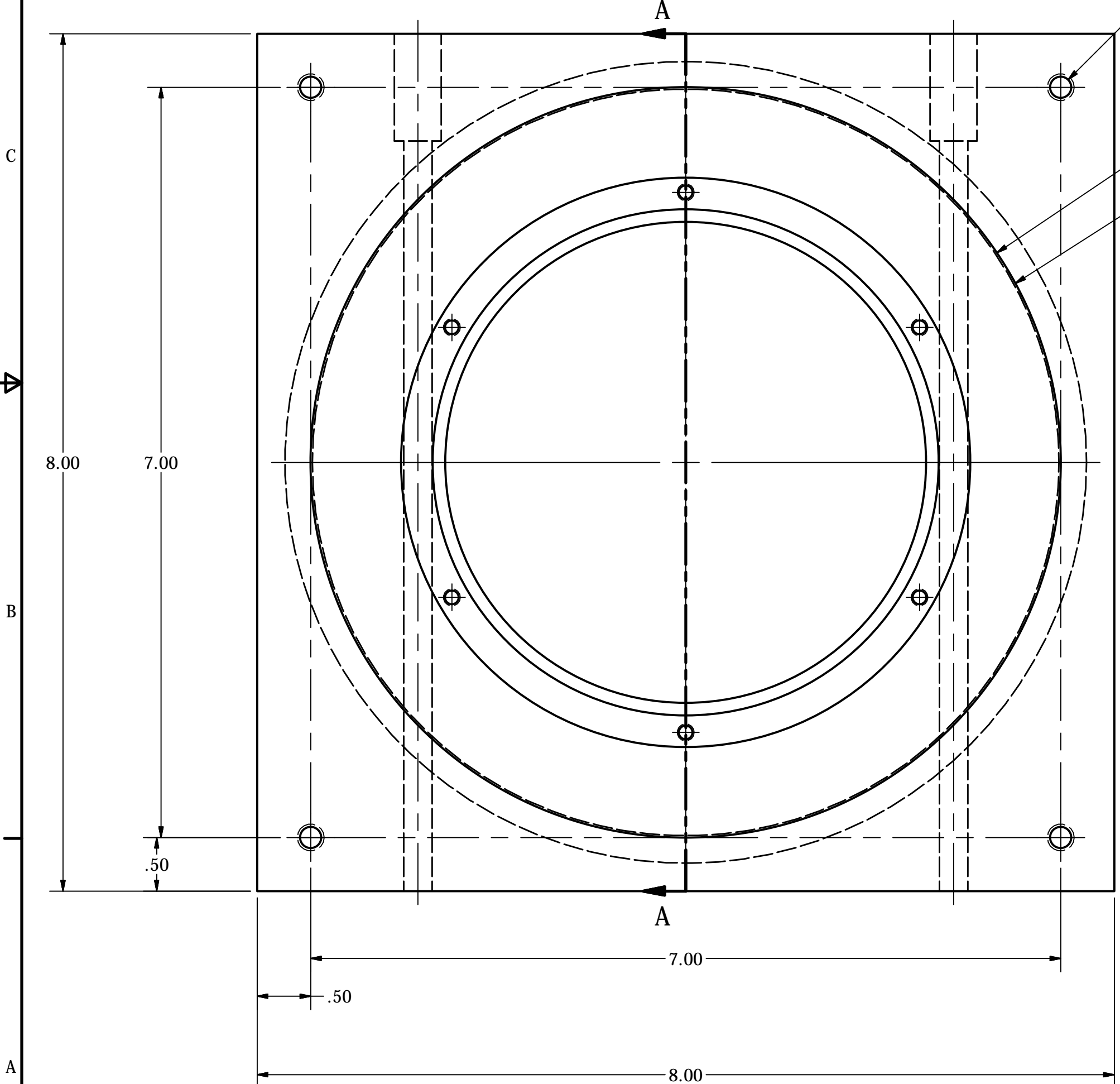
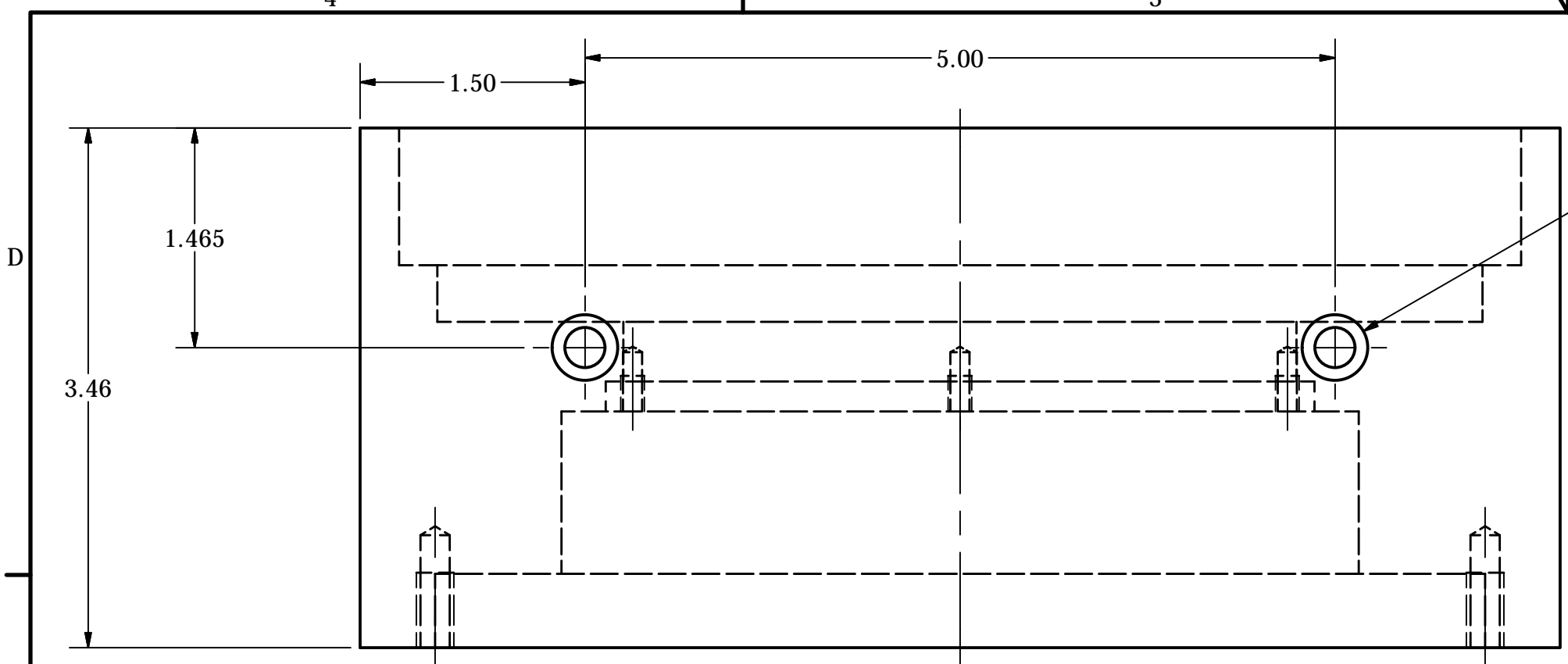
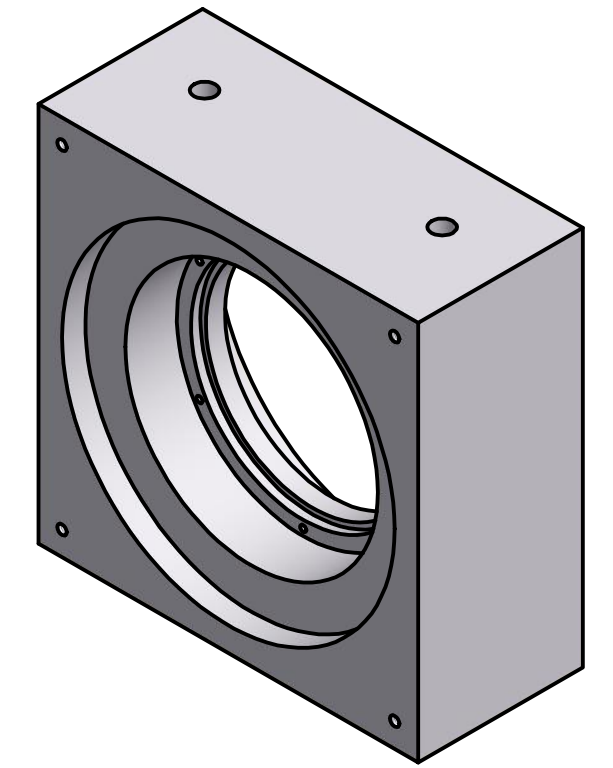
PRODUCED BY AN AUTODESK EDUCATIONAL PRODUCT



PRODUCED BY AN AUTODESK EDUCATIONAL PRODUCT

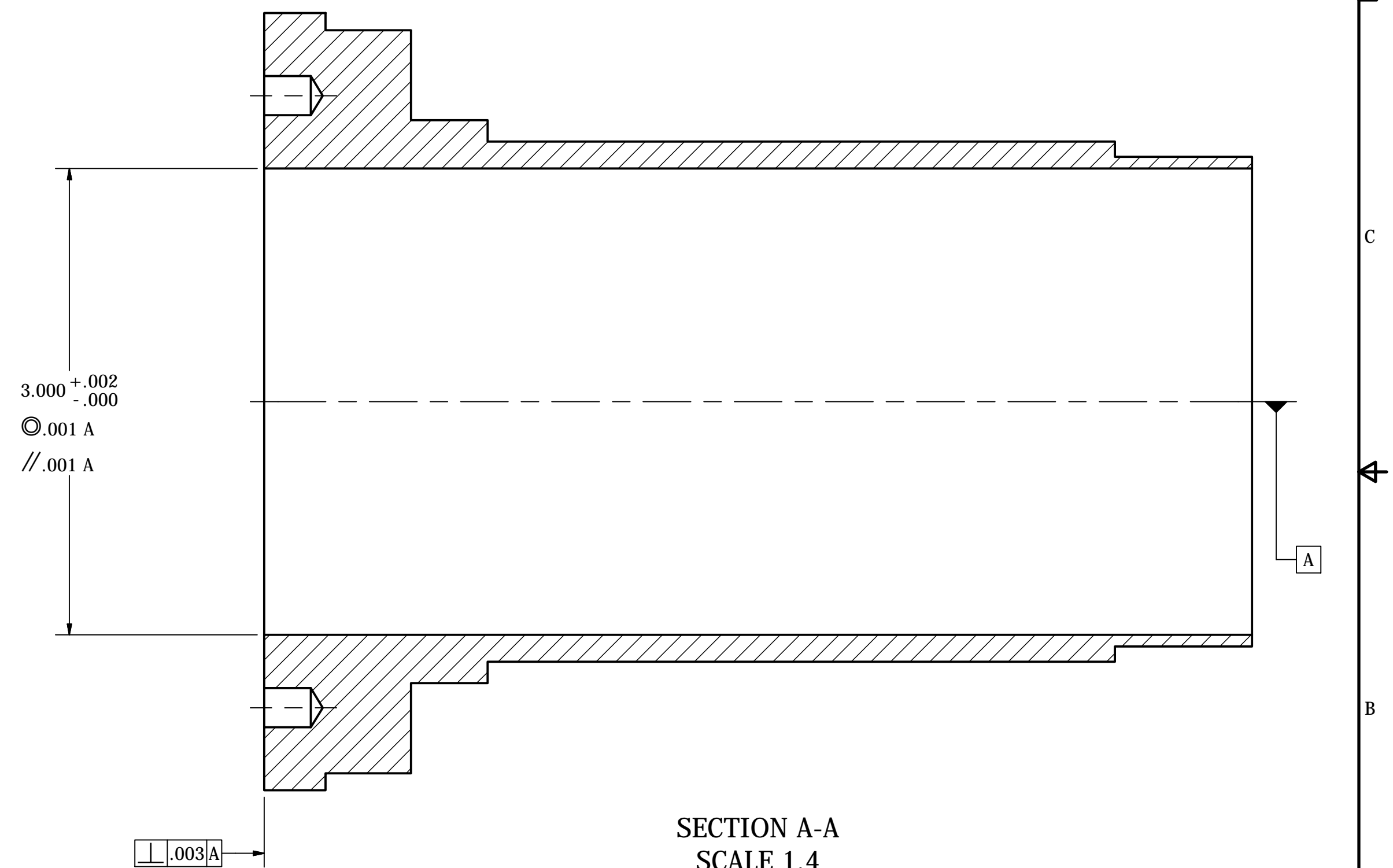
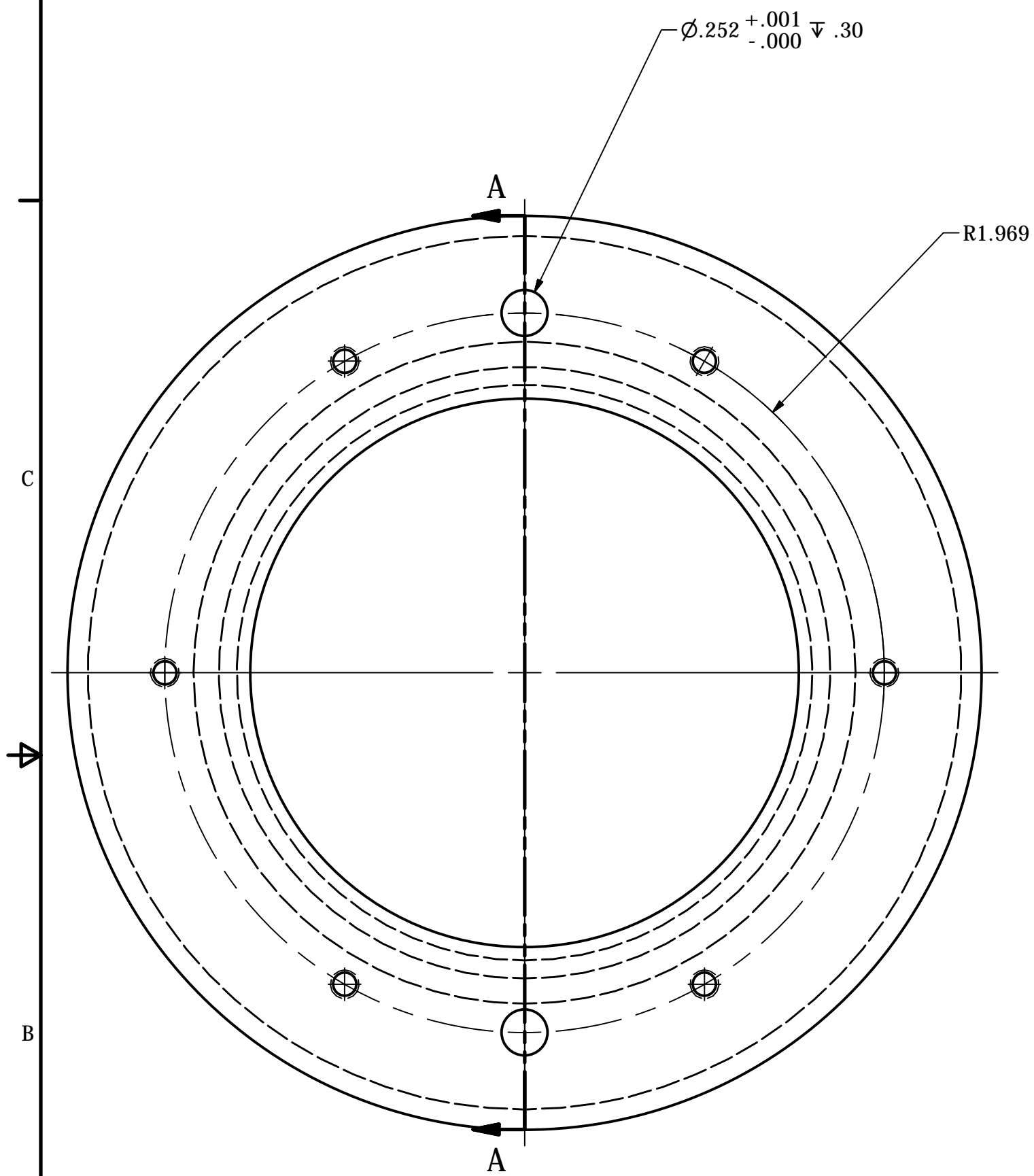
PRODUCED BY AN AUTODESK EDUCATIONAL PRODUCT

DIMENSIONS ARE IN INCHES TOLERANCES: FRACTIONAL - $\frac{1}{64}$ TWO PLACE DECIMAL - 0.010 THREE PLACE DECIMAL - 0.005	ENGINEER J. NIEDERHAUSER	11/18/2010	 UNITED STATES AIR FORCE AIR FORCE INSTITUTE OF TECHNOLOGY	
	ENGINEERING REVIEW		TITLE Housing Mounting Motor Encoder BOTOM R2 101121	
MATERIAL Aluminum-6061 FINISH	RELEASE APPROVED	SIZE C	DWG NO GCTEX-0012	REV
DO NOT SCALE DRAWING		SCALE	SHEET 1 OF 1	
FOR OFFICIAL USE ONLY				



DIMENSIONS ARE IN INCHES TOLERANCES: FRACTIONAL - $\frac{1}{64}$ TWO PLACE DECIMAL - 0.010 THREE PLACE DECIMAL - 0.005		ENGINEER J. NIEDERHAUSER ENGINEERING REVIEW	11/18/2010	 UNITED STATES AIR FORCE AIR FORCE INSTITUTE OF TECHNOLOGY	
MATERIAL Aluminum-6061 FINISH		RELEASE APPROVED	TITLE Housing Mounting Motor Encoder TOP R2 101020		
DO NOT SCALE DRAWING			SIZE C	DWG NO GCTEX-0013	REV
FOR OFFICIAL USE ONLY			SCALE	SHEET 1 OF 1	

PRODUCED BY AN AUTODESK EDUCATIONAL PRODUCT



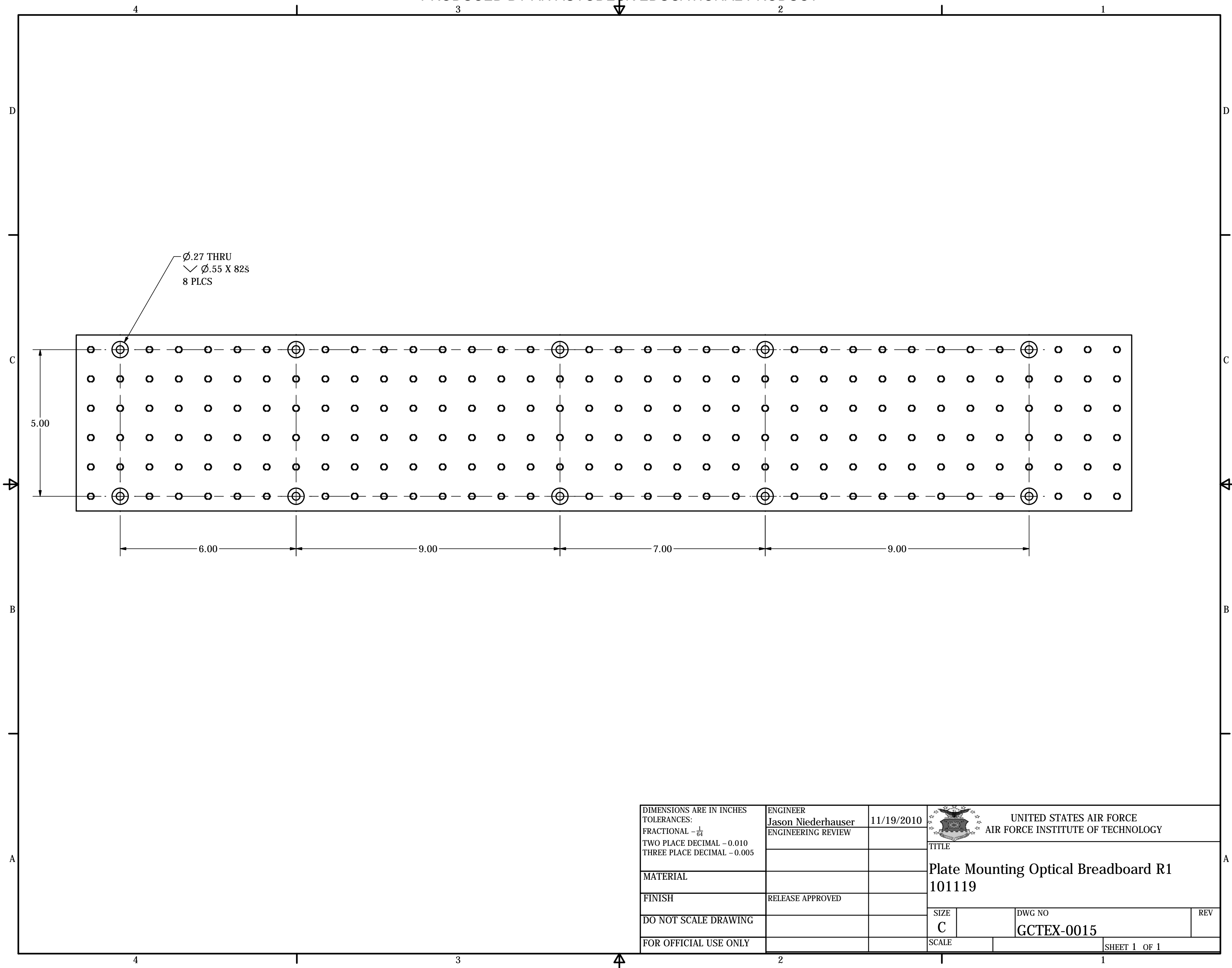
A

A

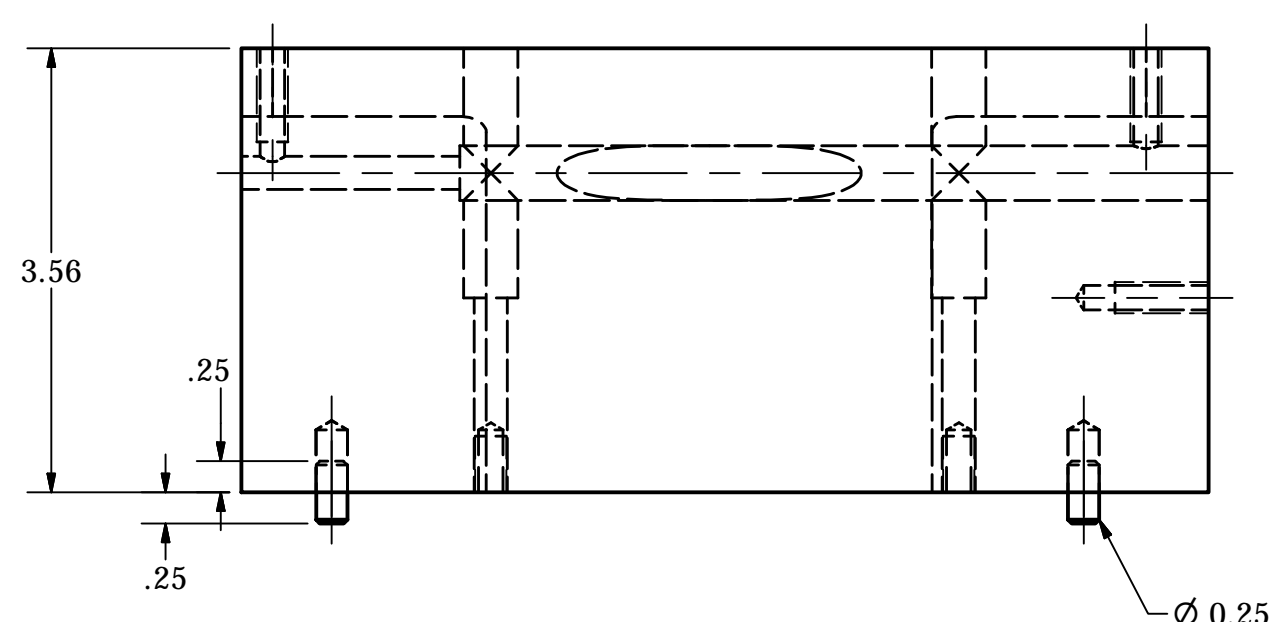
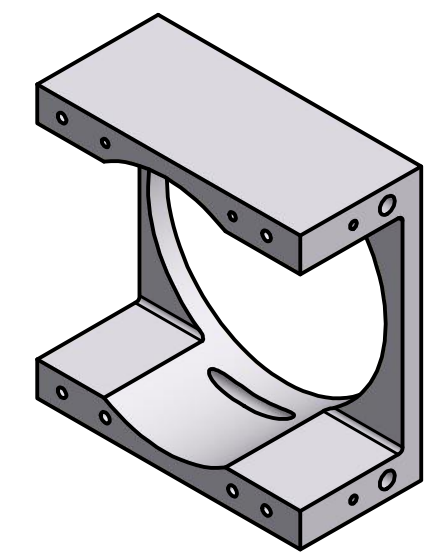
DIMENSIONS ARE IN INCHES TOLERANCES: FRACTIONAL - $\frac{1}{64}$ TWO PLACE DECIMAL - 0.010 THREE PLACE DECIMAL - 0.005	ENGINEER J. NIEDERHAUSER	DATE 11/18/2010	 UNITED STATES AIR FORCE AIR FORCE INSTITUTE OF TECHNOLOGY	
	ENGINEERING REVIEW		TITLE Shaft Motor Encoder R2 101121	
MATERIAL Steel			SIZE C	DWG NO GCTEX-0014
FINISH	RELEASE APPROVED		SCALE	REV
DO NOT SCALE DRAWING			SHEET 1 OF 1	
FOR OFFICIAL USE ONLY				

PRODUCED BY AN AUTODESK EDUCATIONAL PRODUCT

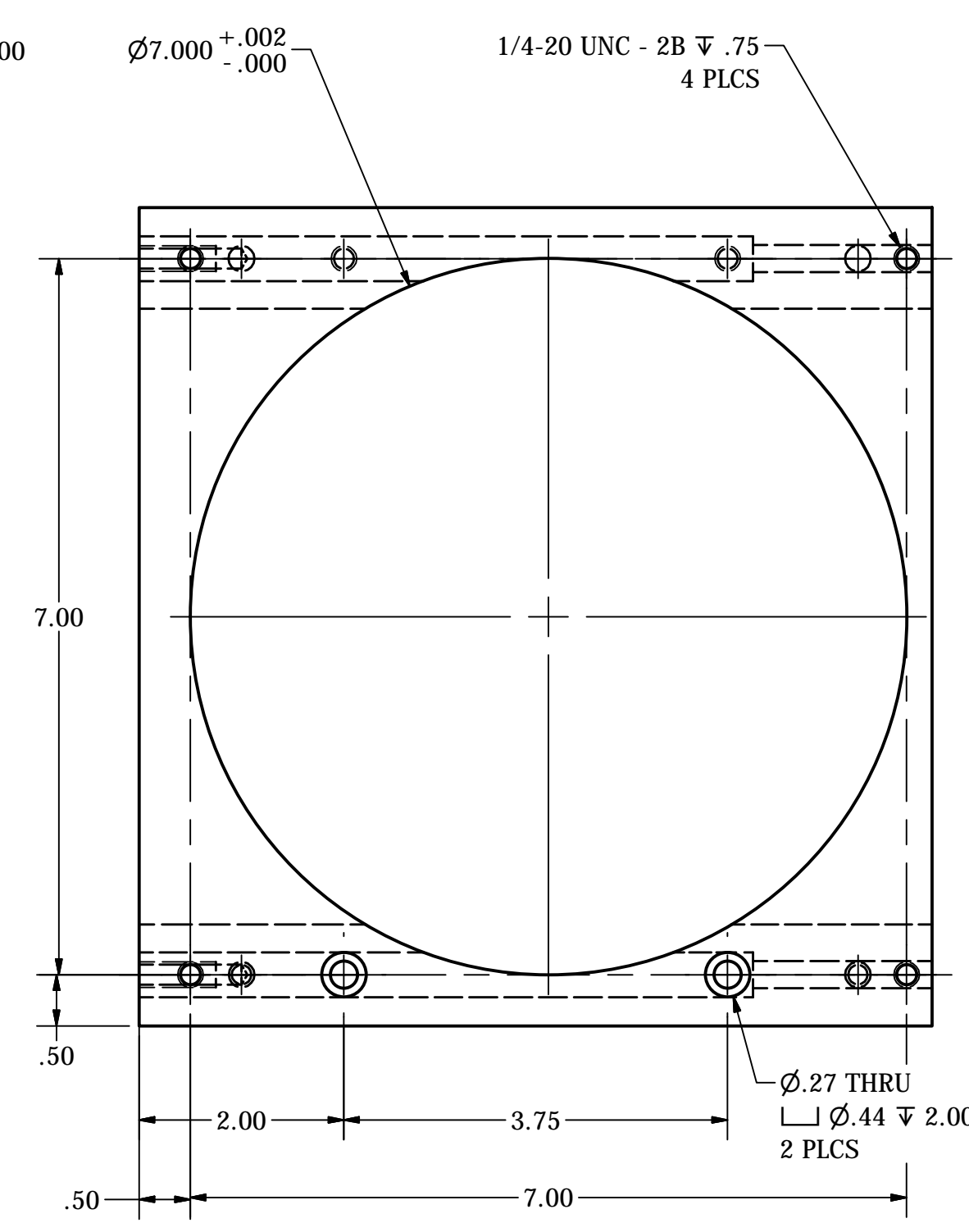
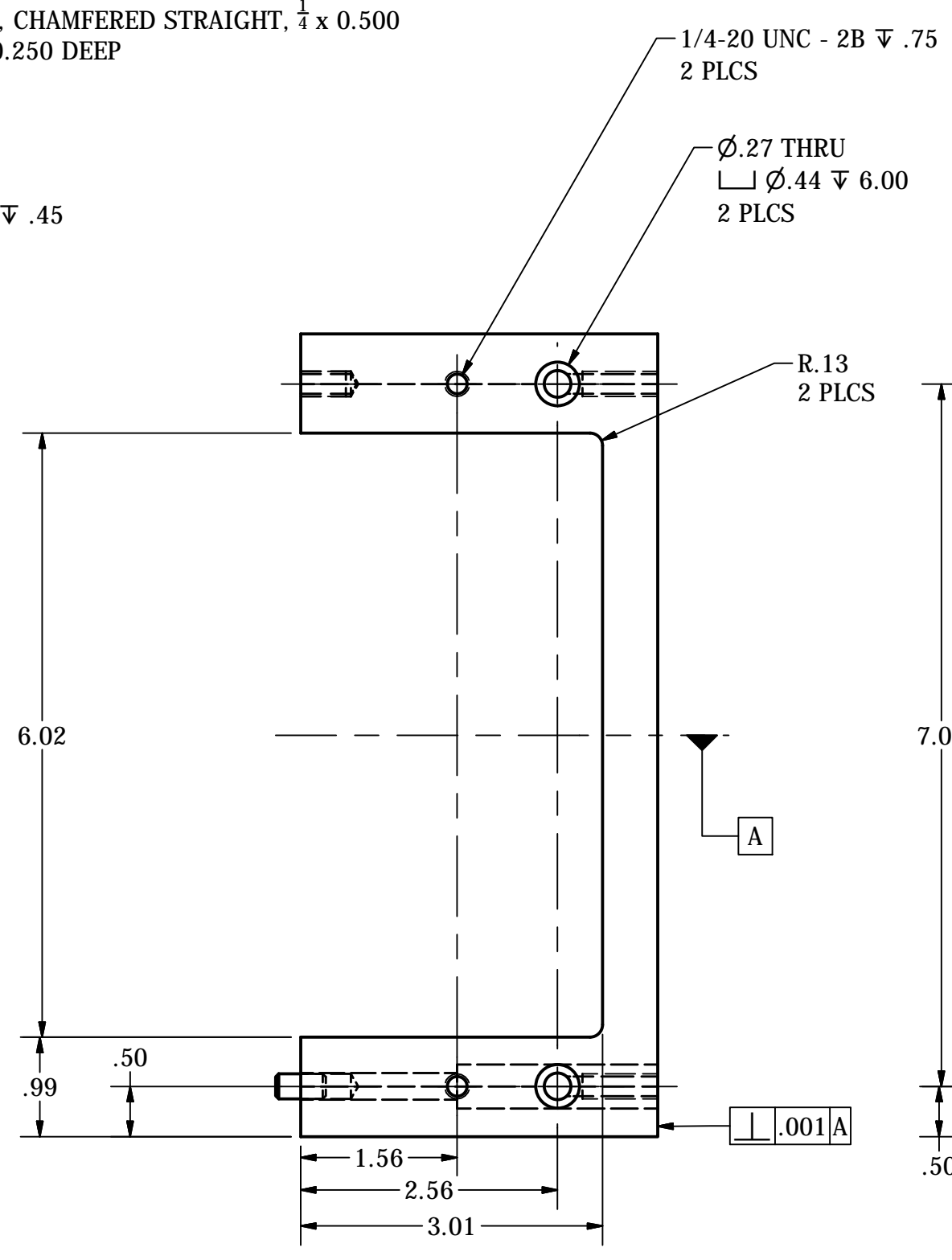
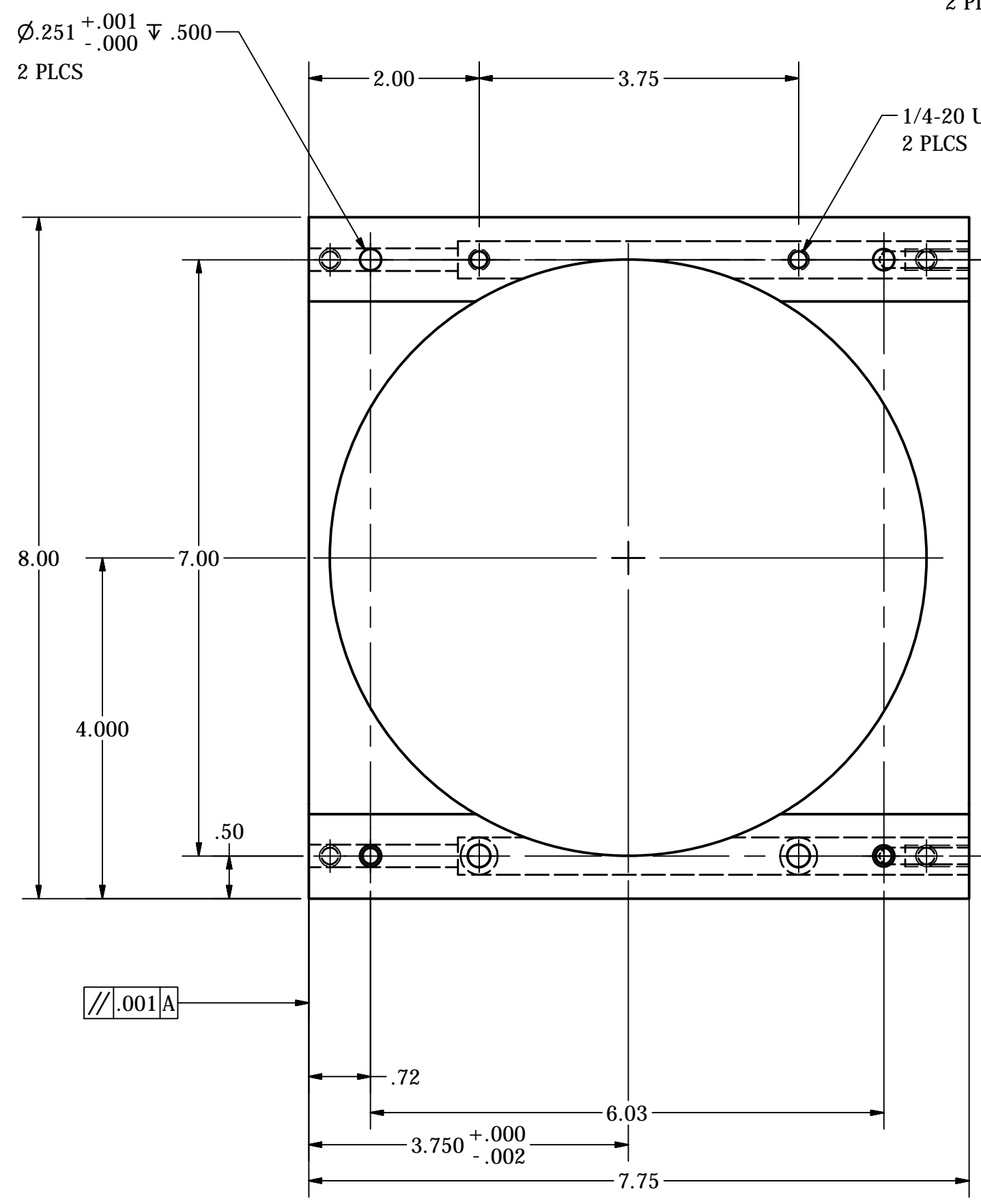
PRODUCED BY AN AUTODESK EDUCATIONAL PRODUCT



DIMENSIONS ARE IN INCHES TOLERANCES: FRACTIONAL - $\frac{1}{64}$ TWO PLACE DECIMAL - 0.010 THREE PLACE DECIMAL - 0.005	ENGINEER Jason Niederhauser	11/19/2010	 UNITED STATES AIR FORCE AIR FORCE INSTITUTE OF TECHNOLOGY	
	ENGINEERING REVIEW		TITLE Plate Mounting Optical Breadboard R1 101119	
MATERIAL			SIZE C	DWG NO GCTEX-0015
FINISH	RELEASE APPROVED		SCALE	REV
DO NOT SCALE DRAWING				
FOR OFFICIAL USE ONLY				SHEET 1 OF 1



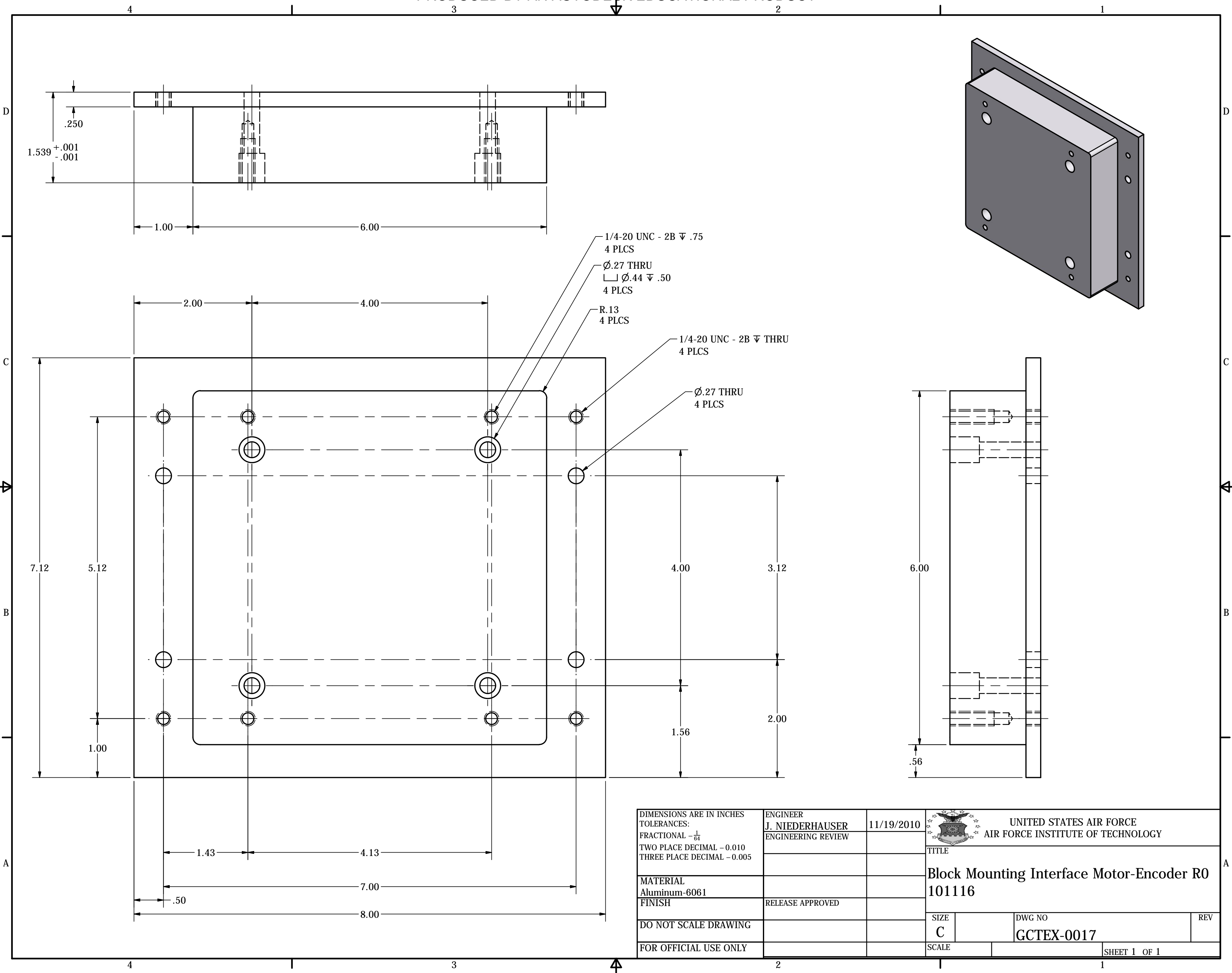
$\varnothing 0.2500/0.2495 \text{ } \nabla 0.500$
 PIN, DOWEL, CHAMFERED STRAIGHT, $\frac{1}{4} \times 0.500$
 PRESS FIT, 0.250 DEEP
 2 PLCS



DIMENSIONS ARE IN INCHES TOLERANCES: FRACTIONAL $-\frac{1}{64}$ TWO PLACE DECIMAL -0.010 THREE PLACE DECIMAL -0.005	ENGINEER Jason Niederhauser	11/19/2010	 UNITED STATES AIR FORCE AIR FORCE INSTITUTE OF TECHNOLOGY
	ENGINEERING REVIEW		
MATERIAL Aluminum-6061			SIZE C
FINISH DO NOT SCALE DRAWING	RELEASE APPROVED		DWG NO GCTEX-0016
FOR OFFICIAL USE ONLY			SCALE SHEET 1 OF 1

PRODUCED BY AN AUTODESK EDUCATIONAL PRODUCT

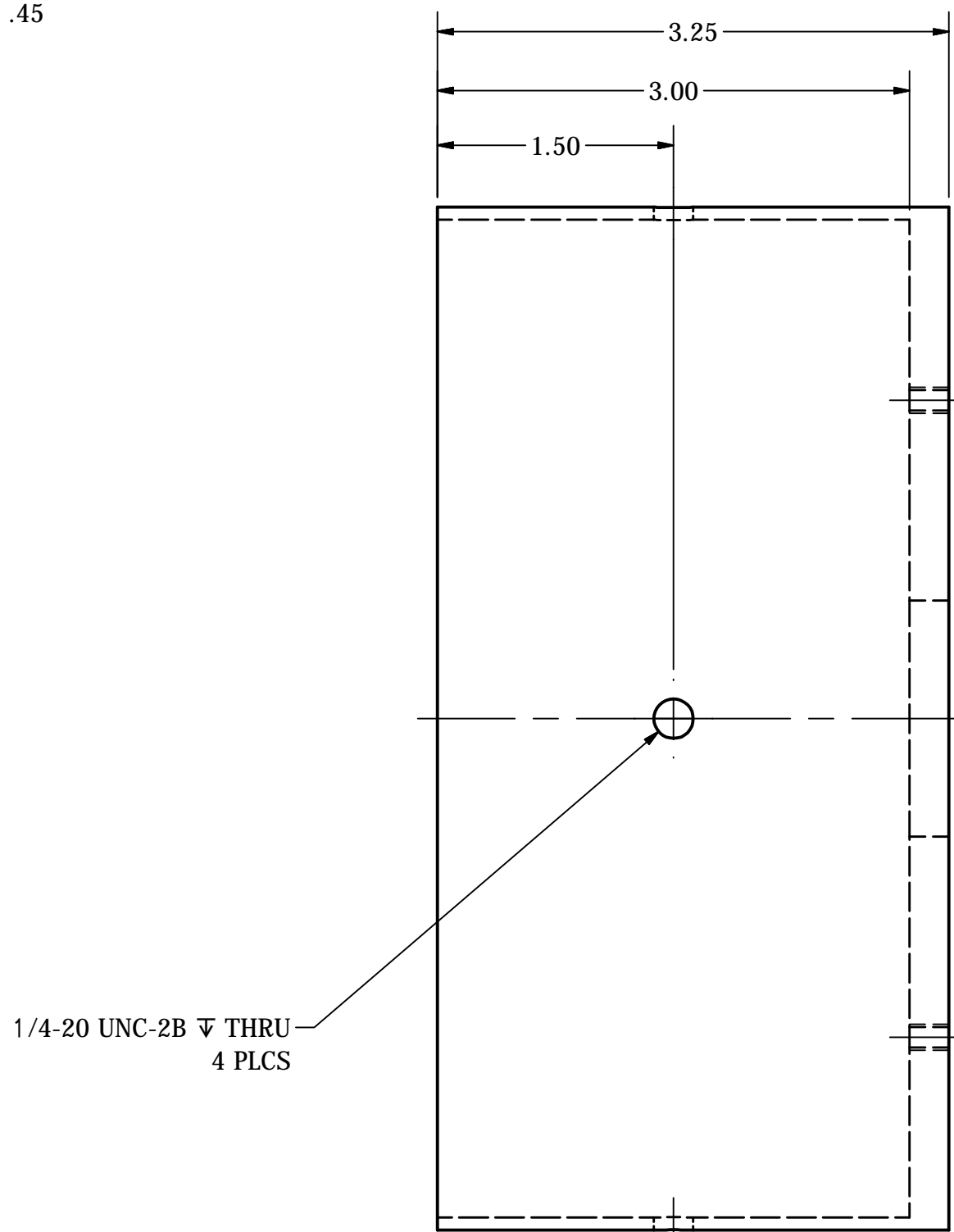
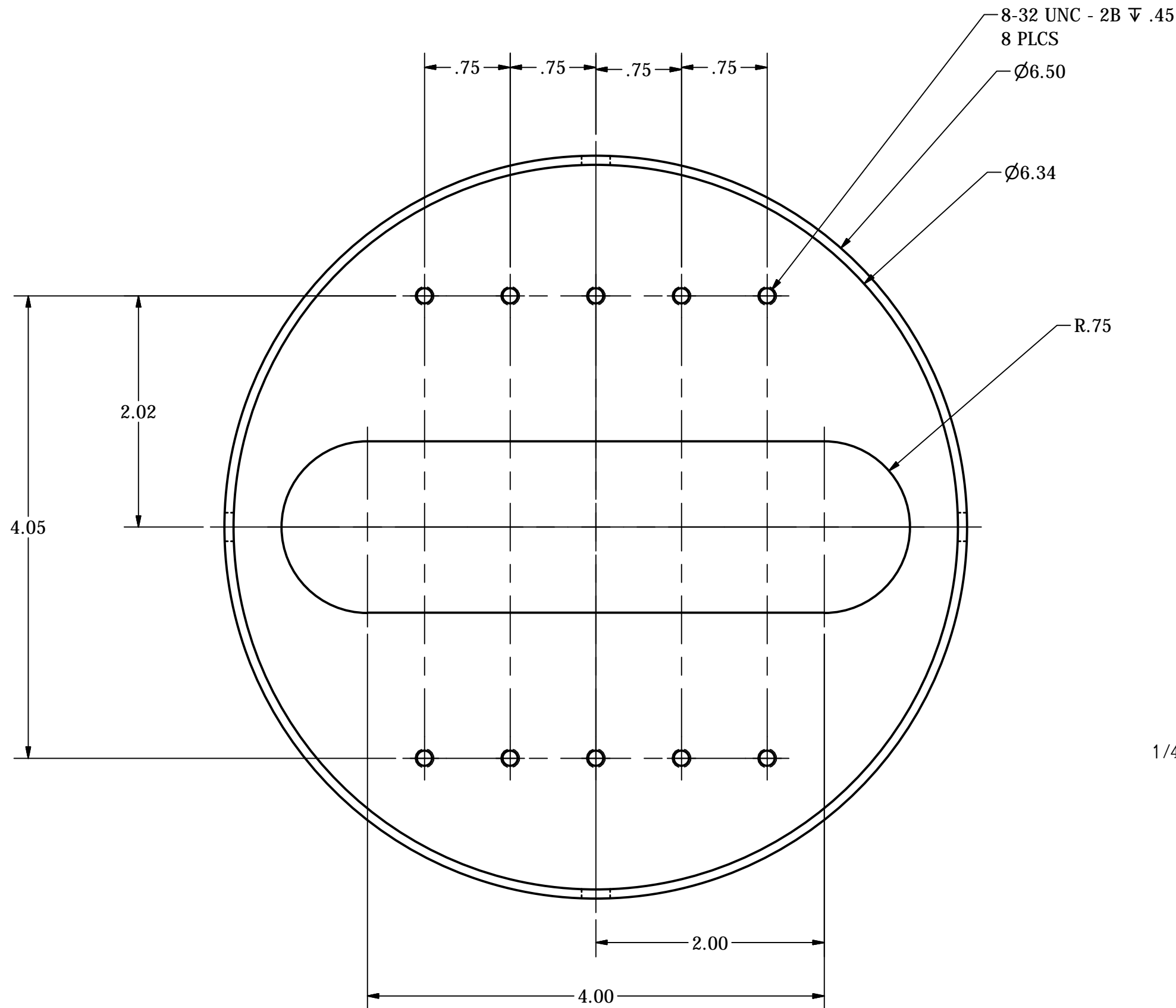
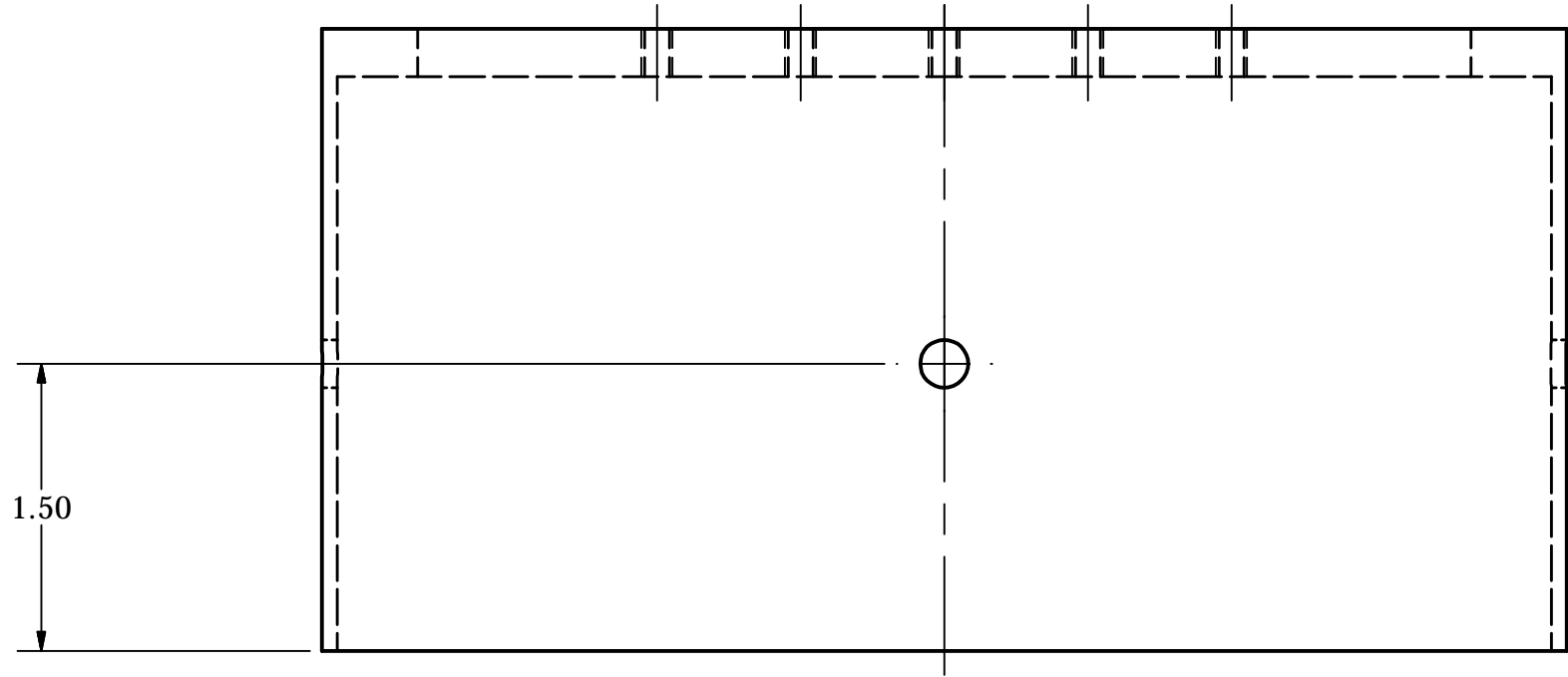
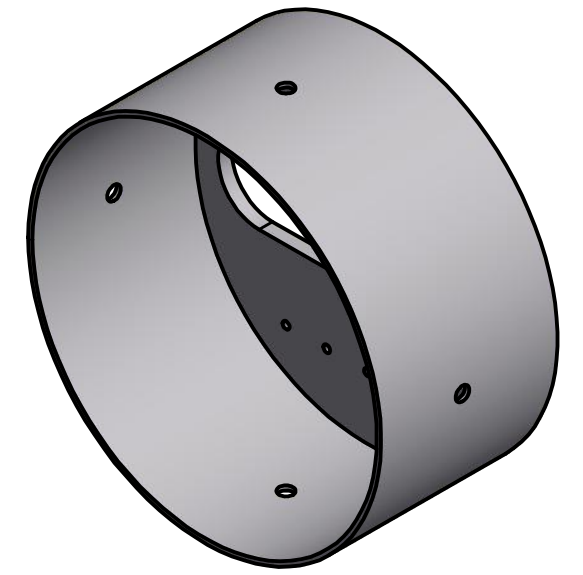
PRODUCED BY AN AUTODESK EDUCATIONAL PRODUCT



PRODUCED BY AN AUTODESK EDUCATIONAL PRODUCT

PRODUCED BY AN AUTODESK EDUCATIONAL PRODUCT

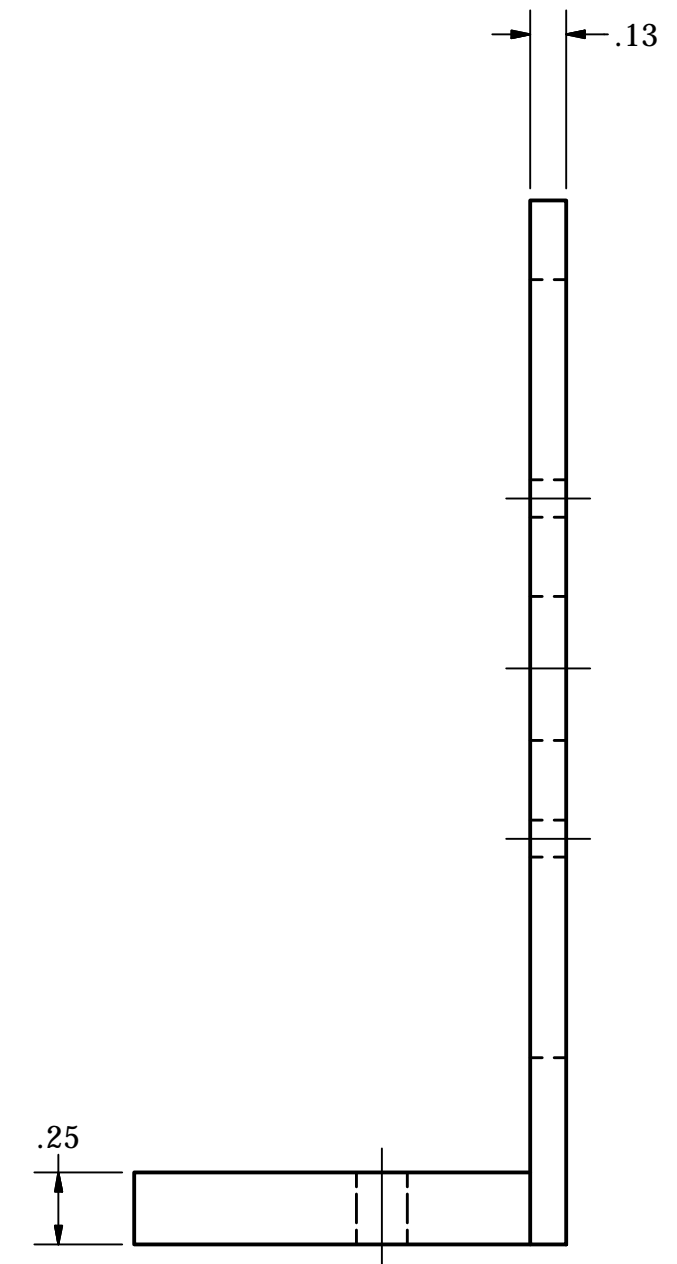
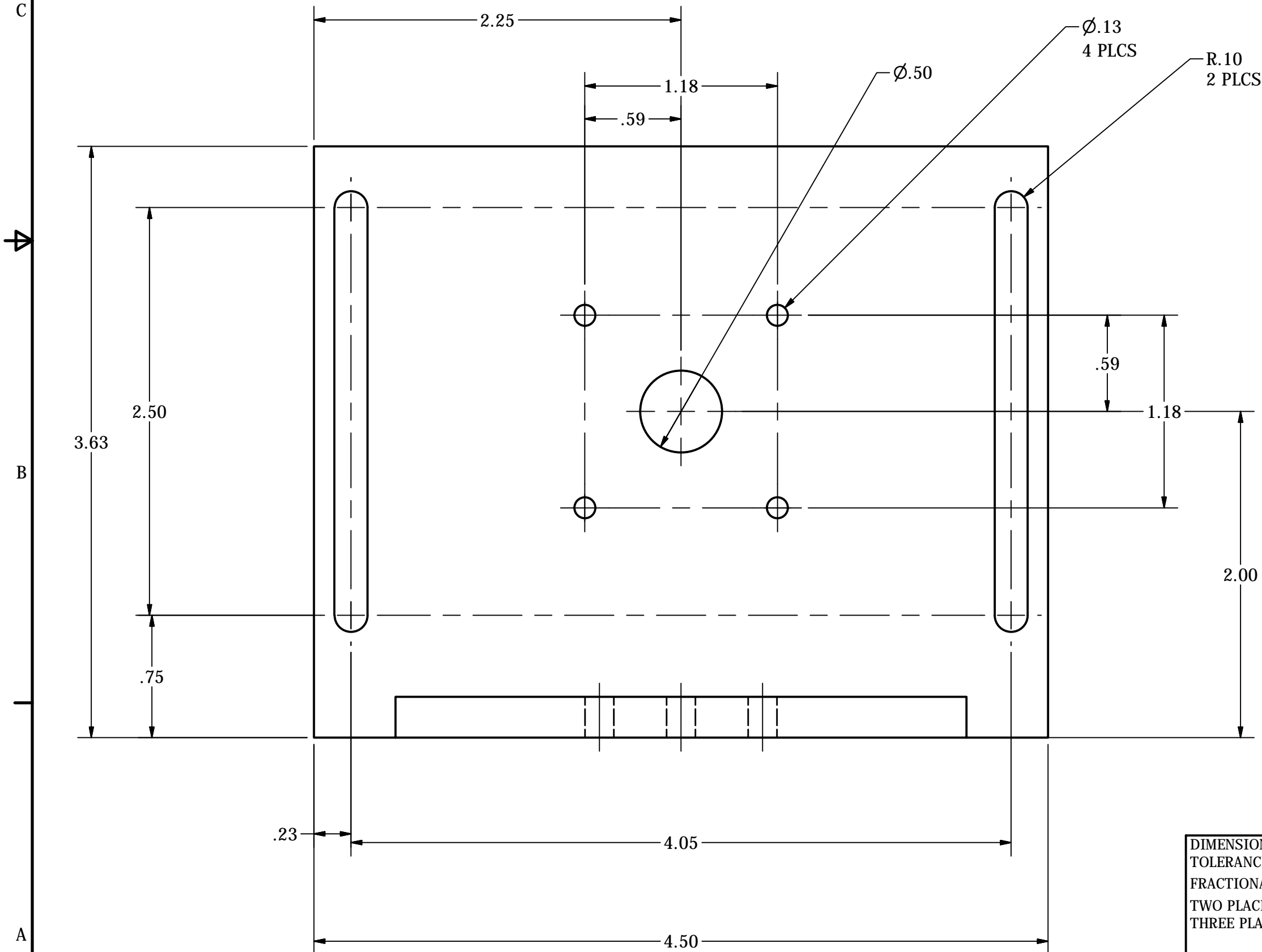
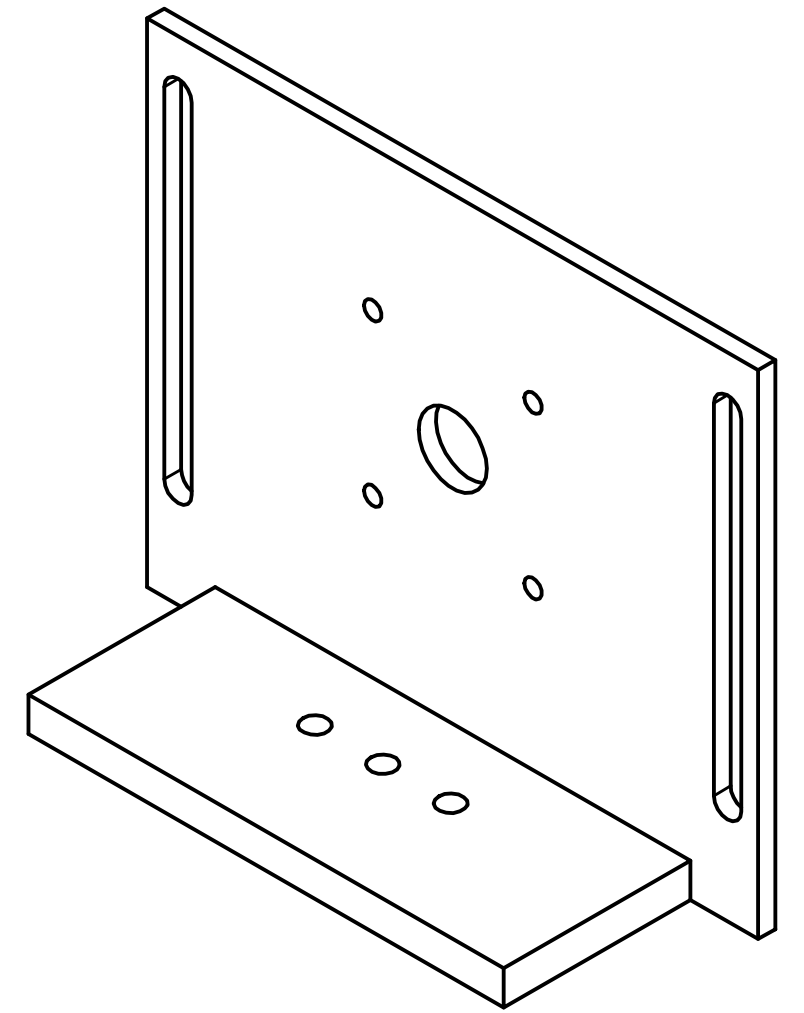
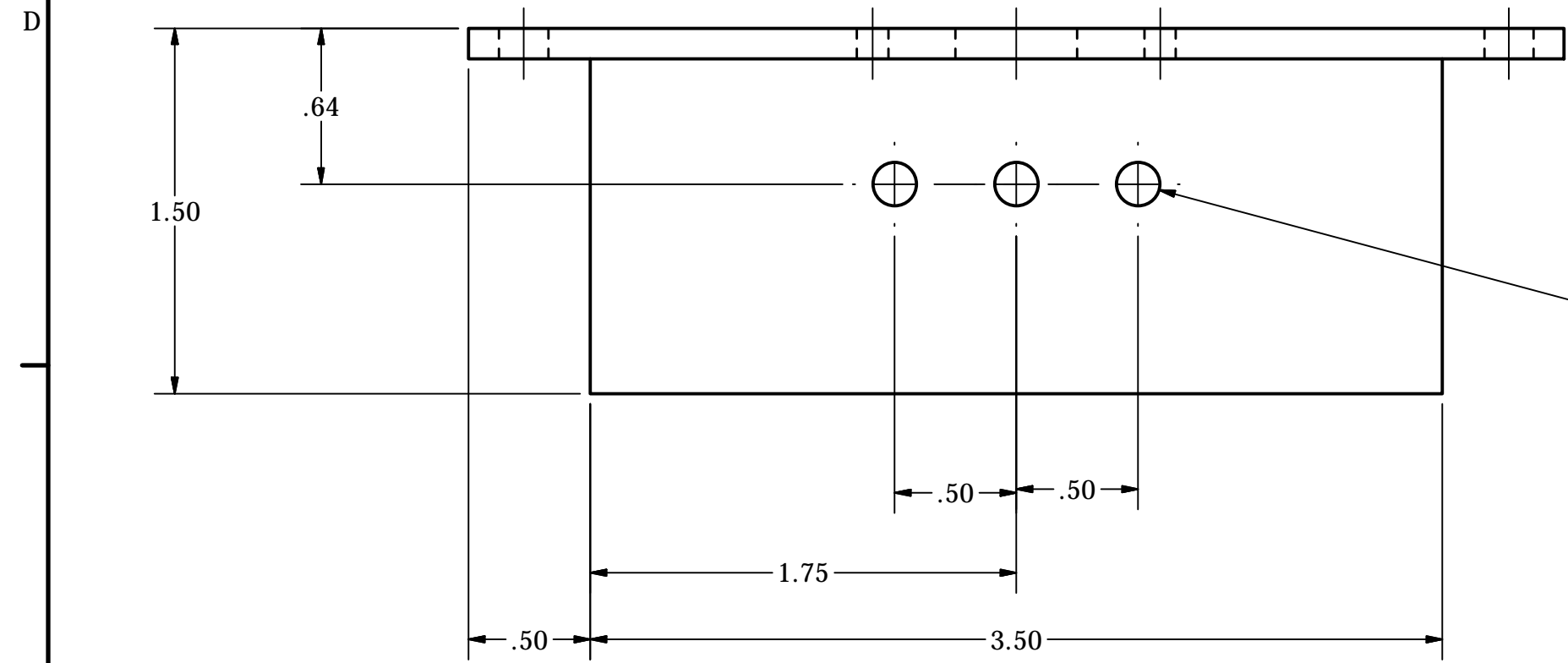
DIMENSIONS ARE IN INCHES TOLERANCES: FRACTIONAL - $\frac{1}{64}$ TWO PLACE DECIMAL - 0.010 THREE PLACE DECIMAL - 0.005	ENGINEER J. NIEDERHAUSER ENGINEERING REVIEW	11/19/2010	 UNITED STATES AIR FORCE AIR FORCE INSTITUTE OF TECHNOLOGY		
	MATERIAL Aluminum-6061 FINISH		RELEASE APPROVED	TITLE Block Mounting Interface Motor-Encoder R0 101116	
DO NOT SCALE DRAWING			SIZE C	DWG NO GCTEX-0017	REV
FOR OFFICIAL USE ONLY			SCALE	SHEET 1 OF 1	



DIMENSIONS ARE IN INCHES TOLERANCES: FRACTIONAL - $\frac{1}{64}$ TWO PLACE DECIMAL - 0.010 THREE PLACE DECIMAL - 0.005	ENGINEER J. NIEDERHAUSER	DATE 11/20/2010	 UNITED STATES AIR FORCE AIR FORCE INSTITUTE OF TECHNOLOGY	
	ENGINEERING REVIEW		TITLE Holder Laser Telephoto Mount R0 110518	
MATERIAL Aluminum-6061	FINISH RELEASE APPROVED		SIZE C	DWG NO GCTEX-0018
DO NOT SCALE DRAWING			SCALE	REV
FOR OFFICIAL USE ONLY			SHEET 1 OF 1	

PRODUCED BY AN AUTODESK EDUCATIONAL PRODUCT

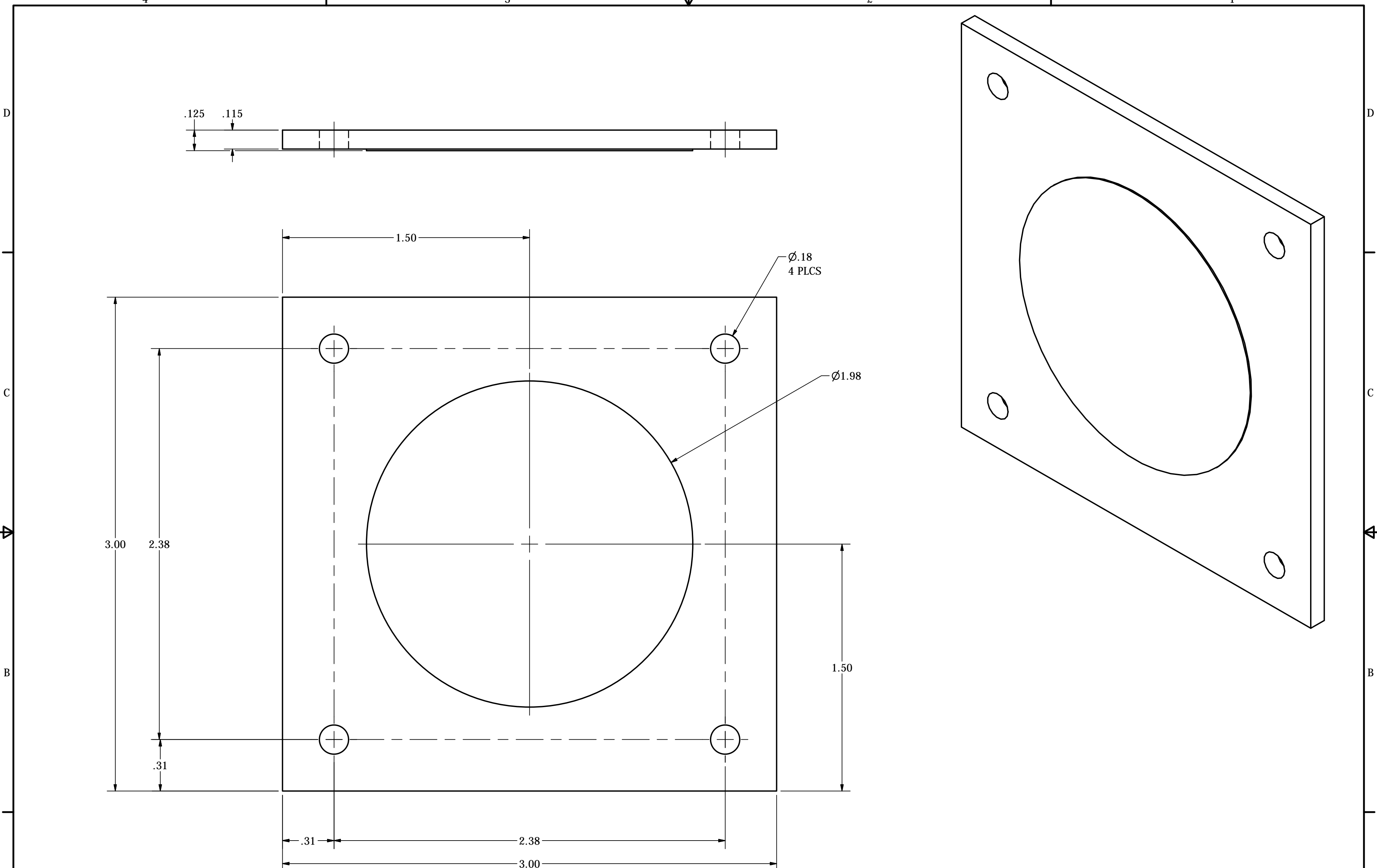
PRODUCED BY AN AUTODESK EDUCATIONAL PRODUCT



DIMENSIONS ARE IN INCHES TOLERANCES: FRACTIONAL - $\frac{1}{64}$ TWO PLACE DECIMAL - 0.010 THREE PLACE DECIMAL - 0.005	ENGINEER J. NIEDERHAUSER	11/20/2010	 UNITED STATES AIR FORCE AIR FORCE INSTITUTE OF TECHNOLOGY	
	ENGINEERING REVIEW		TITLE Holder Laser Calibration R0 101119	
MATERIAL Aluminum-6061	FINISH	RELEASE APPROVED	SIZE C	DWG NO GCTEX-0019
DO NOT SCALE DRAWING			SCALE	REV
FOR OFFICIAL USE ONLY			SHEET 1 OF 1	

PRODUCED BY AN AUTODESK EDUCATIONAL PRODUCT

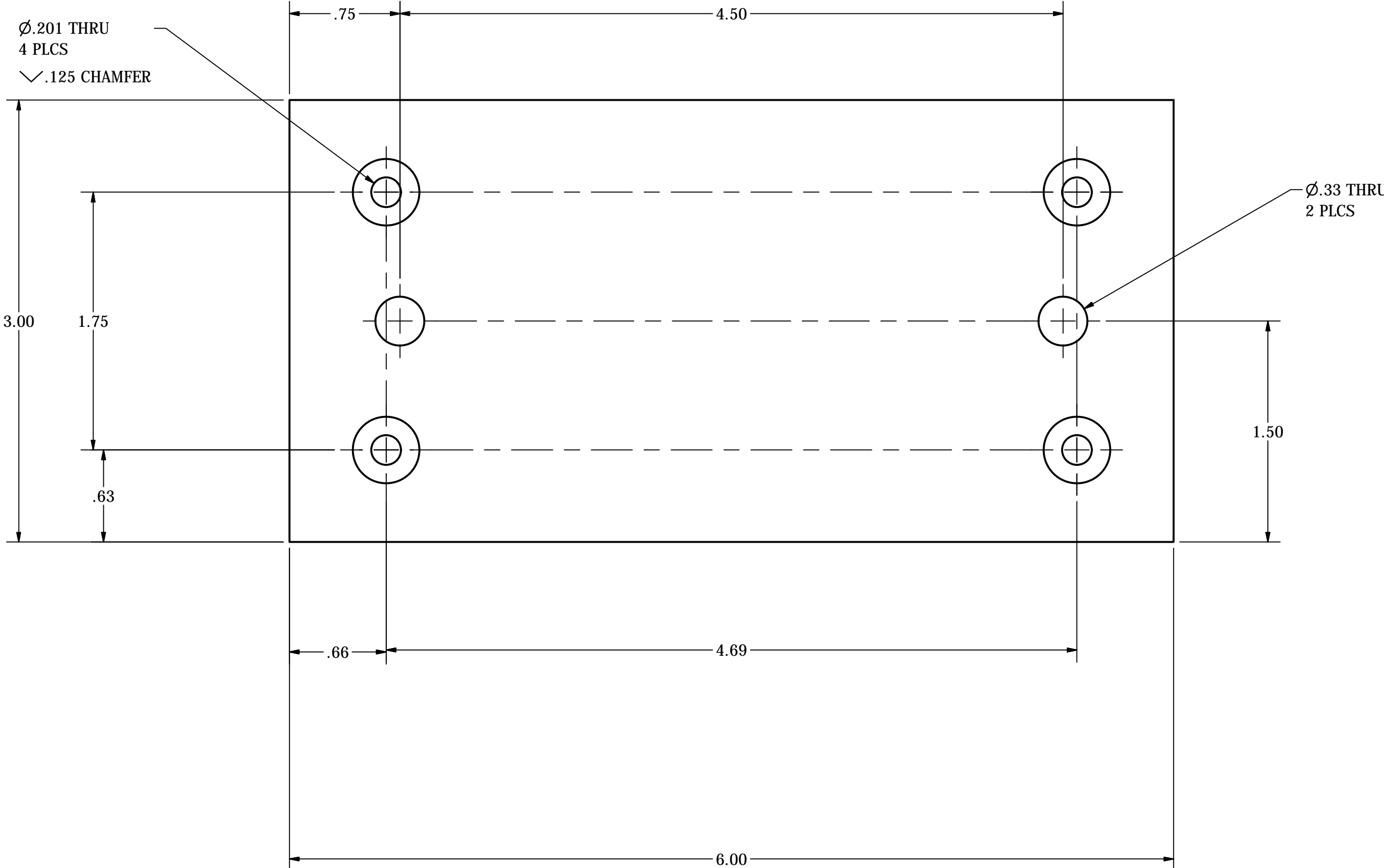
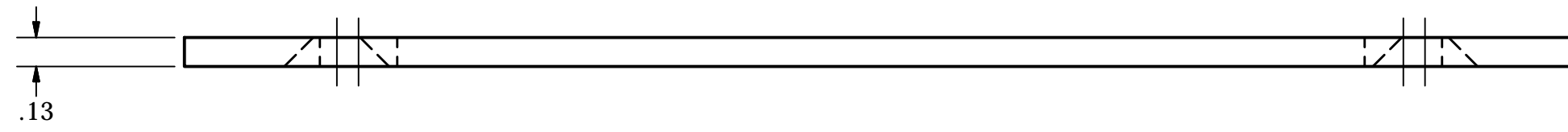
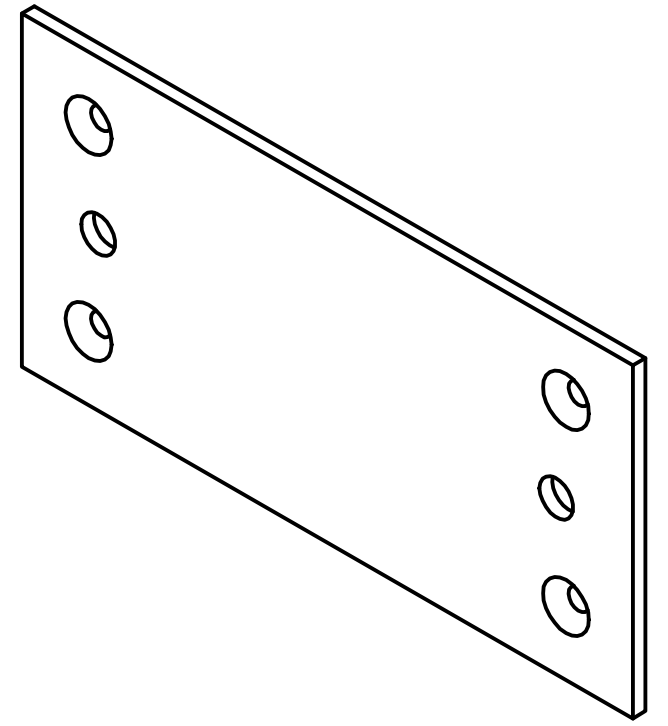
PRODUCED BY AN AUTODESK EDUCATIONAL PRODUCT



PRODUCED BY AN AUTODESK EDUCATIONAL PRODUCT

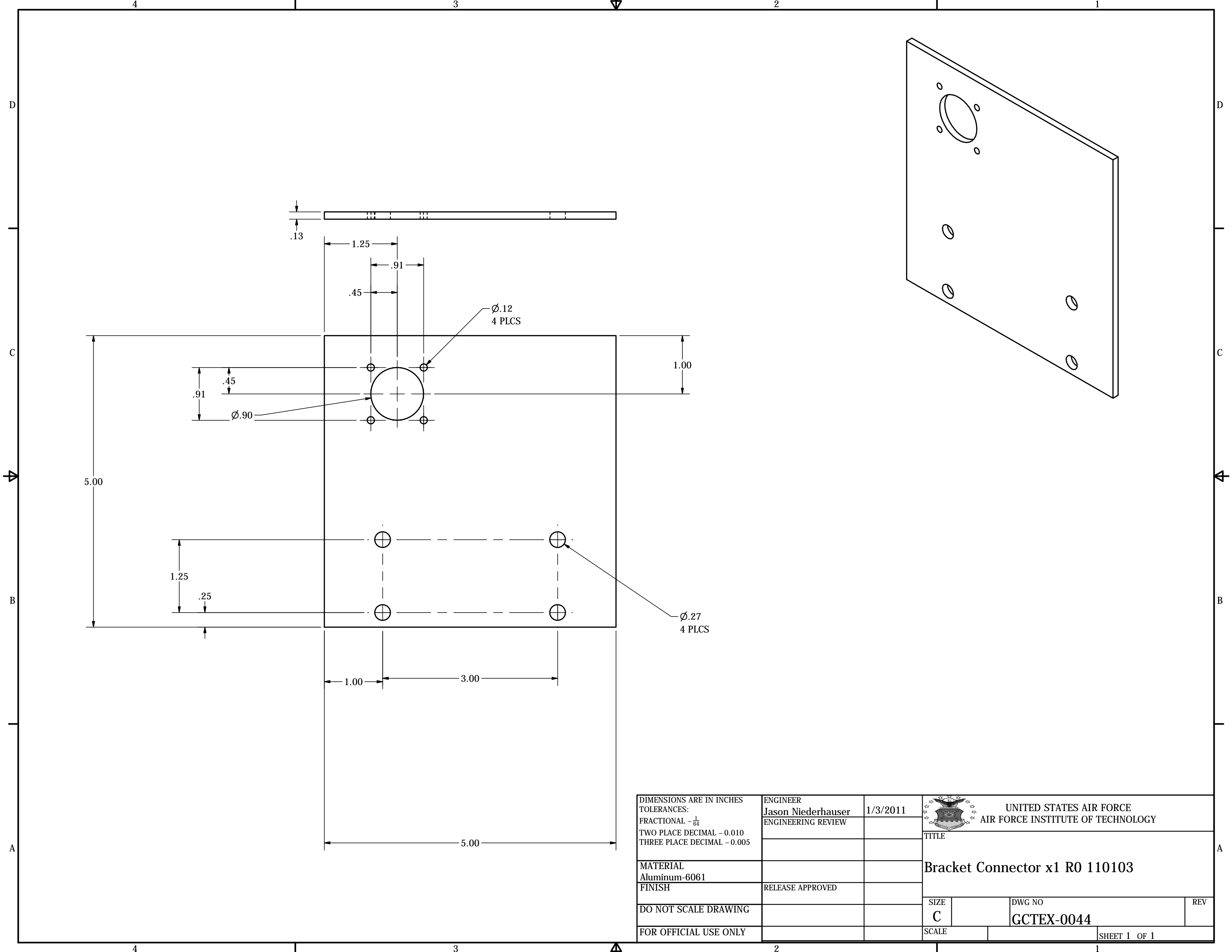
PRODUCED BY AN AUTODESK EDUCATIONAL PRODUCT

DIMENSIONS ARE IN INCHES TOLERANCES: FRACTIONAL - $\frac{1}{64}$ TWO PLACE DECIMAL - 0.010 THREE PLACE DECIMAL - 0.005	ENGINEER J. NIEDERHAUSER ENGINEERING REVIEW	11/21/2010	 UNITED STATES AIR FORCE AIR FORCE INSTITUTE OF TECHNOLOGY		
	MATERIAL Aluminum-6061 FINISH		RELEASE APPROVED	TITLE Cover Light L2 R0 101121	
DO NOT SCALE DRAWING			SIZE C	DWG NO GCTEX-0020	REV
FOR OFFICIAL USE ONLY			SCALE	SHEET 1 OF 1	



DIMENSIONS ARE IN INCHES TOLERANCES: FRACTIONAL - $\frac{1}{64}$ TWO PLACE DECIMAL - 0.010 THREE PLACE DECIMAL - 0.005	ENGINEER Jason Niederhauser ENGINEERING REVIEW	1/3/2011	UNITED STATES AIR FORCE AIR FORCE INSTITUTE OF TECHNOLOGY	
	MATERIAL		TITLE Plate Mounting SAM-3 Module R0 110103	
FINISH		RELEASE APPROVED	SIZE C	DWG NO GCTEX-0042
DO NOT SCALE DRAWING		SCALE		REV
FOR OFFICIAL USE ONLY		SHEET 1 OF 1		REV

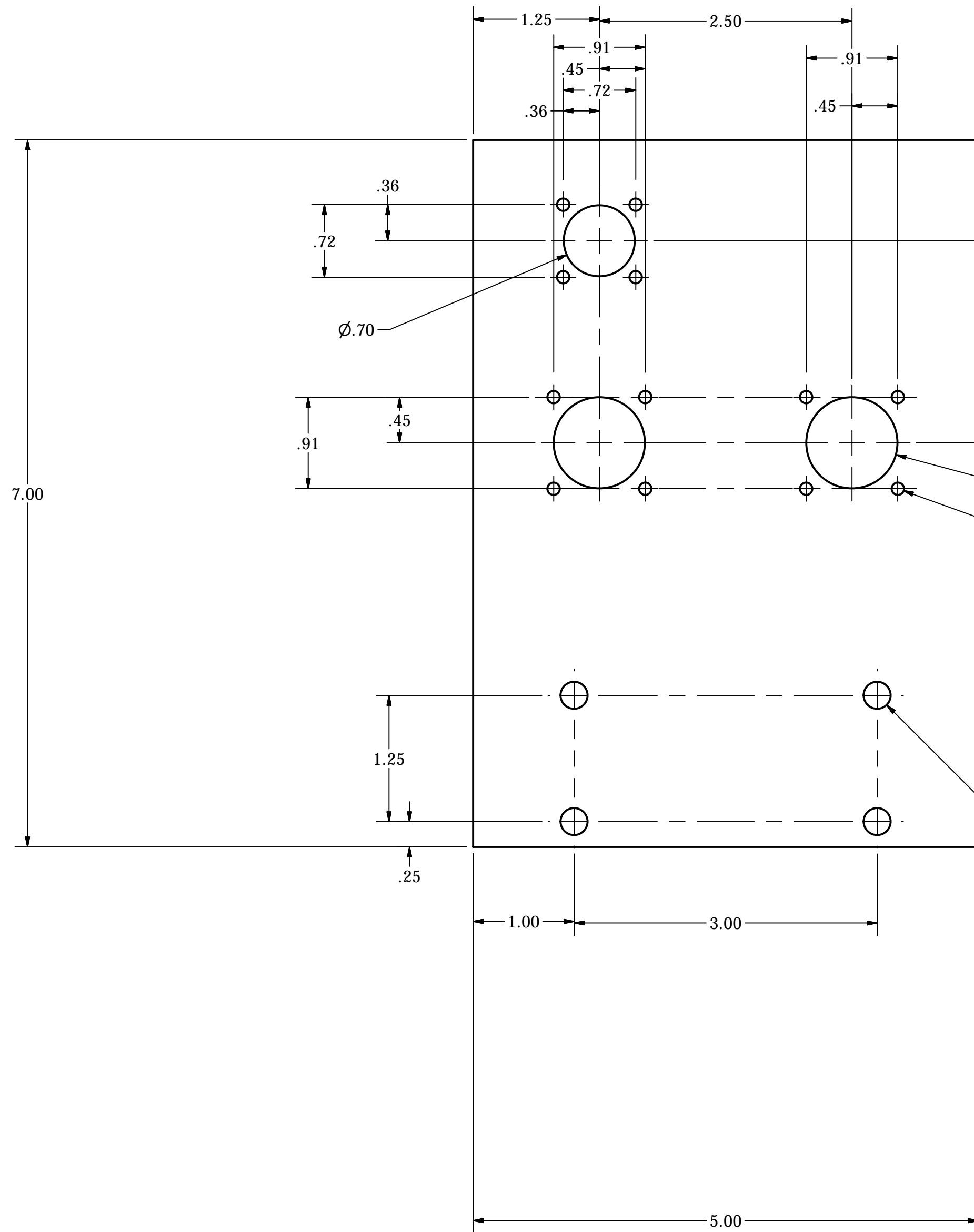
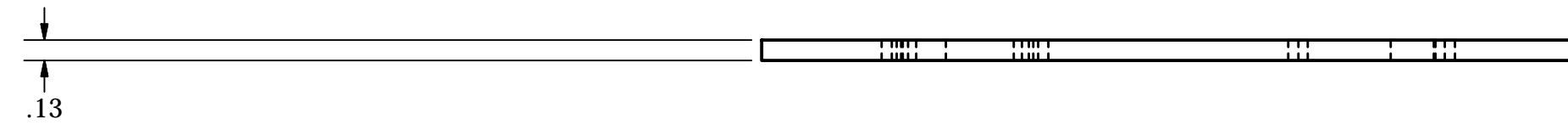
PRODUCED BY AN AUTODESK EDUCATIONAL PRODUCT



DIMENSIONS ARE IN INCHES TOLERANCES: FRACTIONAL - $\frac{1}{64}$ TWO PLACE DECIMAL - 0.010 THREE PLACE DECIMAL - 0.005	ENGINEER Jason Niederhauser	1/3/2011	 UNITED STATES AIR FORCE AIR FORCE INSTITUTE OF TECHNOLOGY	
	ENGINEERING REVIEW		TITLE Bracket Connector x1 R0 110103	
MATERIAL Aluminum-6061			SIZE C	DWG NO GCTEX-0044
FINISH	RELEASE APPROVED		SCALE	REV
DO NOT SCALE DRAWING			SHEET 1 OF 1	
FOR OFFICIAL USE ONLY				

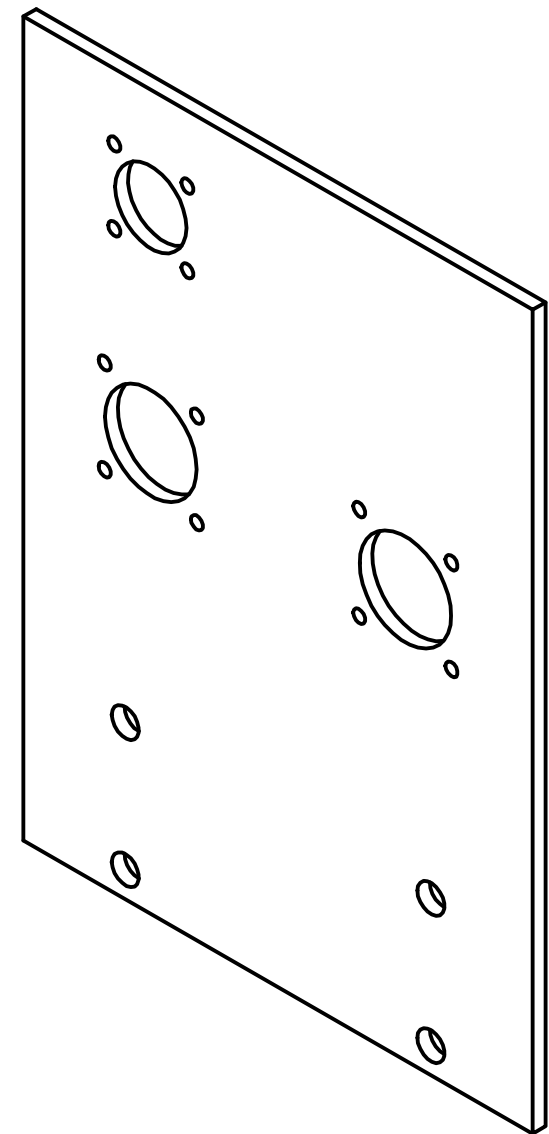
PRODUCED BY AN AUTODESK EDUCATIONAL PRODUCT

PRODUCED BY AN AUTODESK EDUCATIONAL PRODUCT

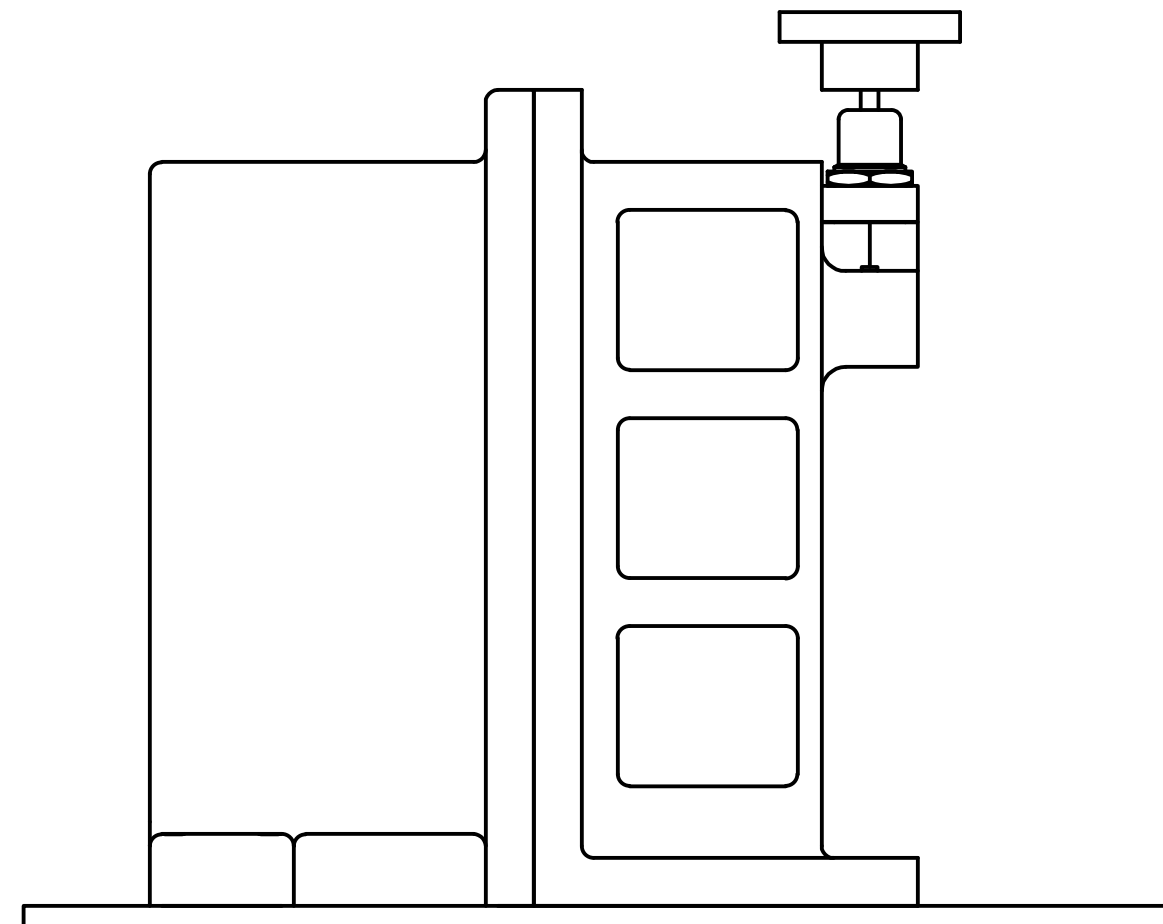
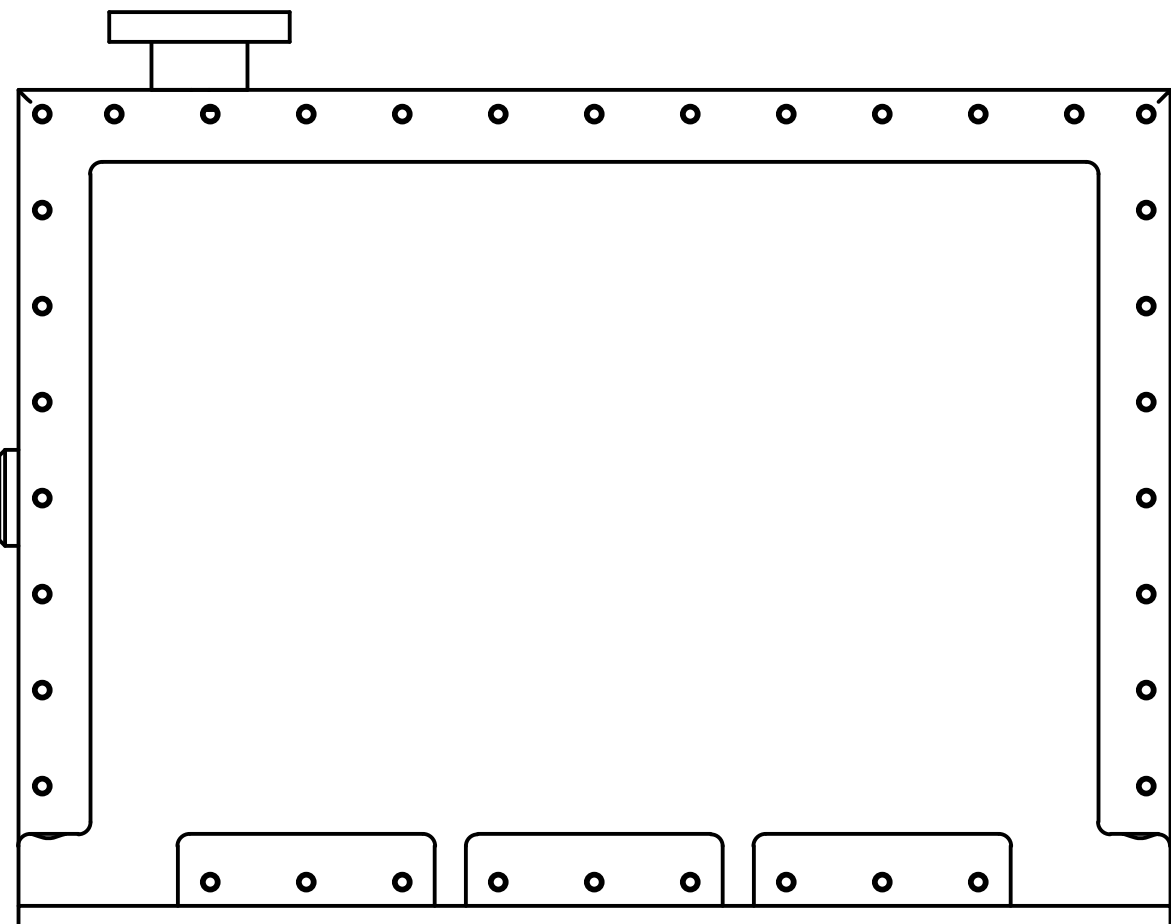
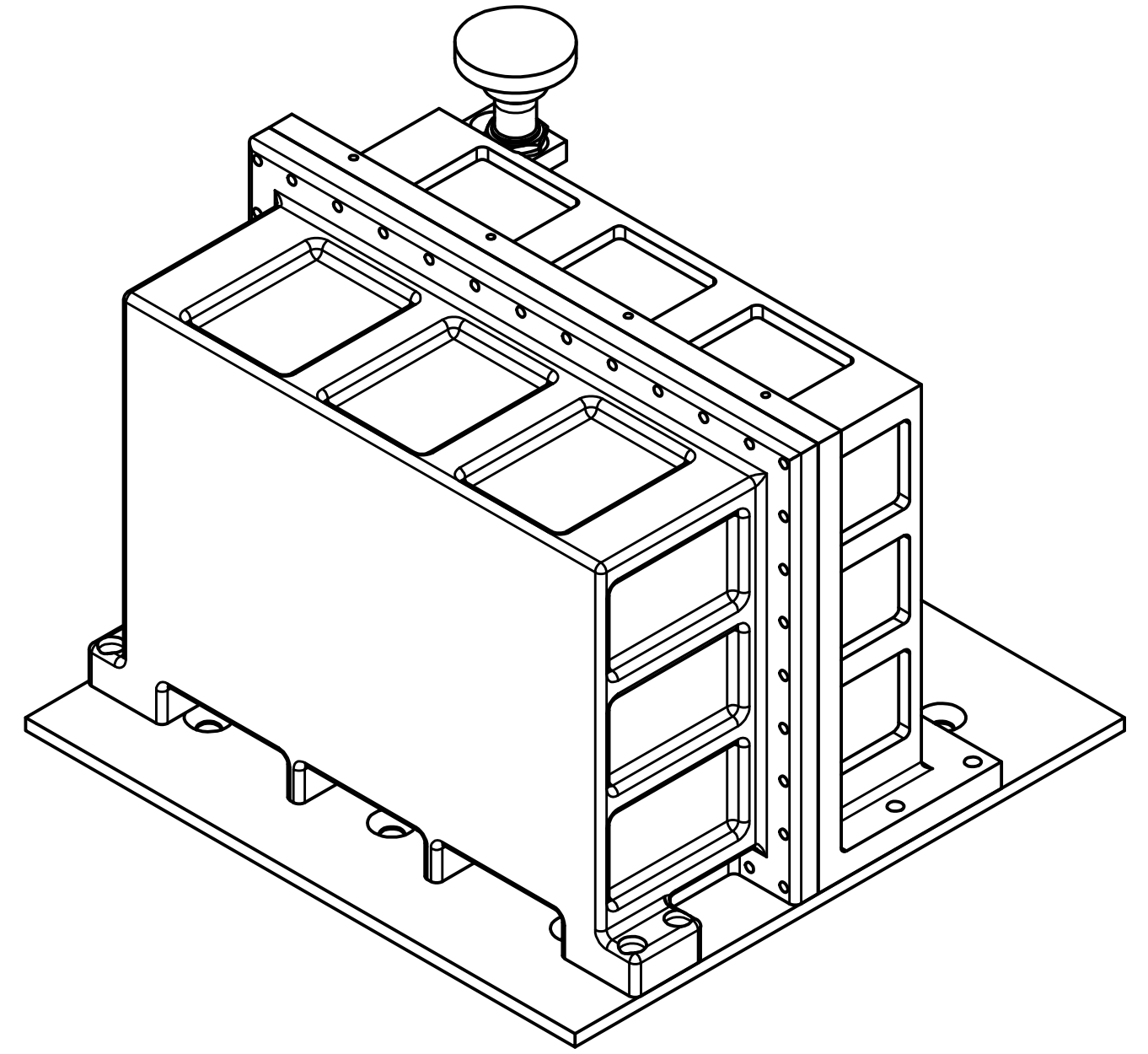
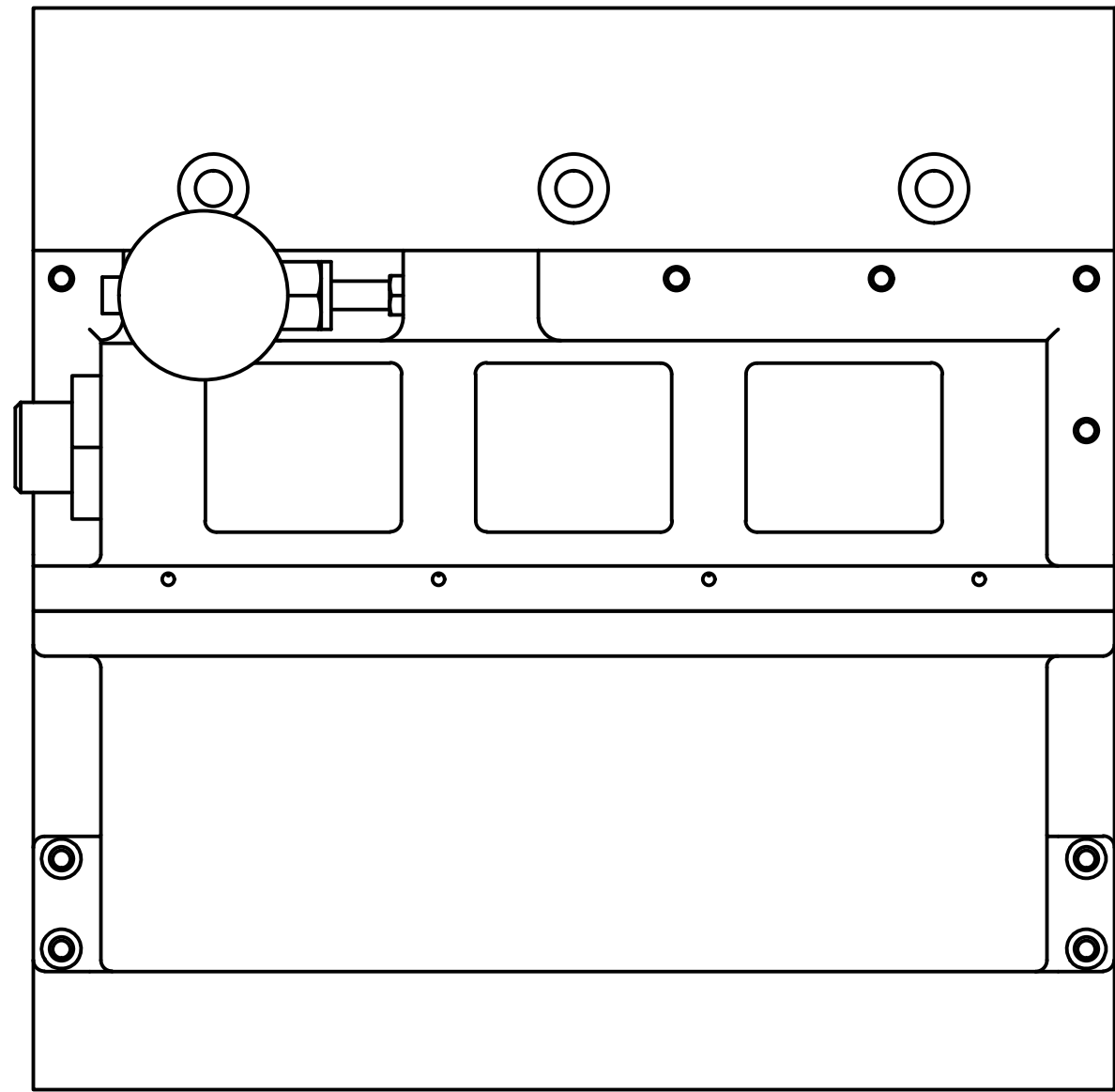


Ø.90
2 PLCS
Ø.12 ∇ THRU
12 PLCS

Ø.281
4 PLCS



DIMENSIONS ARE IN INCHES TOLERANCES: FRACTIONAL - $\frac{1}{64}$ TWO PLACE DECIMAL - 0.010 THREE PLACE DECIMAL - 0.005	ENGINEER Jason Niederhauser ENGINEERING REVIEW	1/3/2011	 UNITED STATES AIR FORCE AIR FORCE INSTITUTE OF TECHNOLOGY		
	MATERIAL Aluminum-6061 FINISH		RELEASE APPROVED	TITLE Bracket Connector x3 R0 110103	
DO NOT SCALE DRAWING			SIZE C	DWG NO GCTEX-0043	REV
FOR OFFICIAL USE ONLY			SCALE	SHEET 1 OF 1	



PRODUCED BY AN AUTODESK EDUCATIONAL PRODUCT

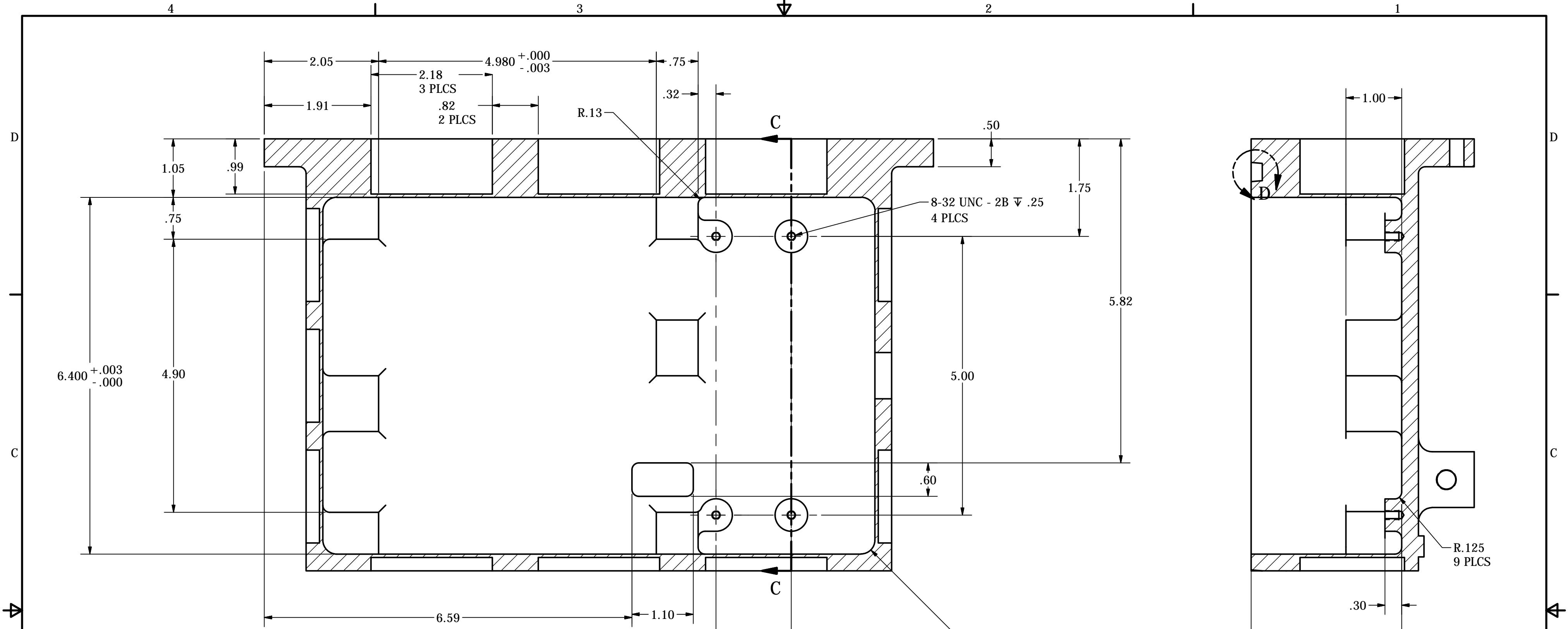
PRODUCED BY AN AUTODESK EDUCATIONAL PRODUCT

DIMENSIONS ARE IN INCHES TOLERANCES: FRACTIONAL - $\frac{1}{64}$ TWO PLACE DECIMAL - 0.010 THREE PLACE DECIMAL - 0.005	ENGINEER Jason Niederhauser	5/18/2011	 UNITED STATES AIR FORCE AIR FORCE INSTITUTE OF TECHNOLOGY	
	ENGINEERING REVIEW			TITLE ASSY SCTEx ICU R0 101008
MATERIAL			SIZE C	DWG NO ASCTEx-0001
FINISH	RELEASE APPROVED		SCALE	REV
DO NOT SCALE DRAWING				
FOR OFFICIAL USE ONLY				SHEET 1 OF 1

Component Listing - SCTEx ICU

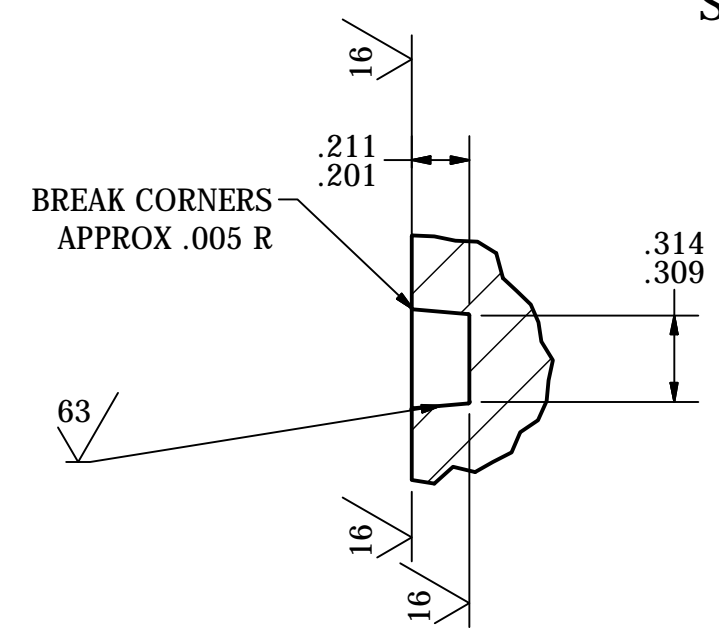
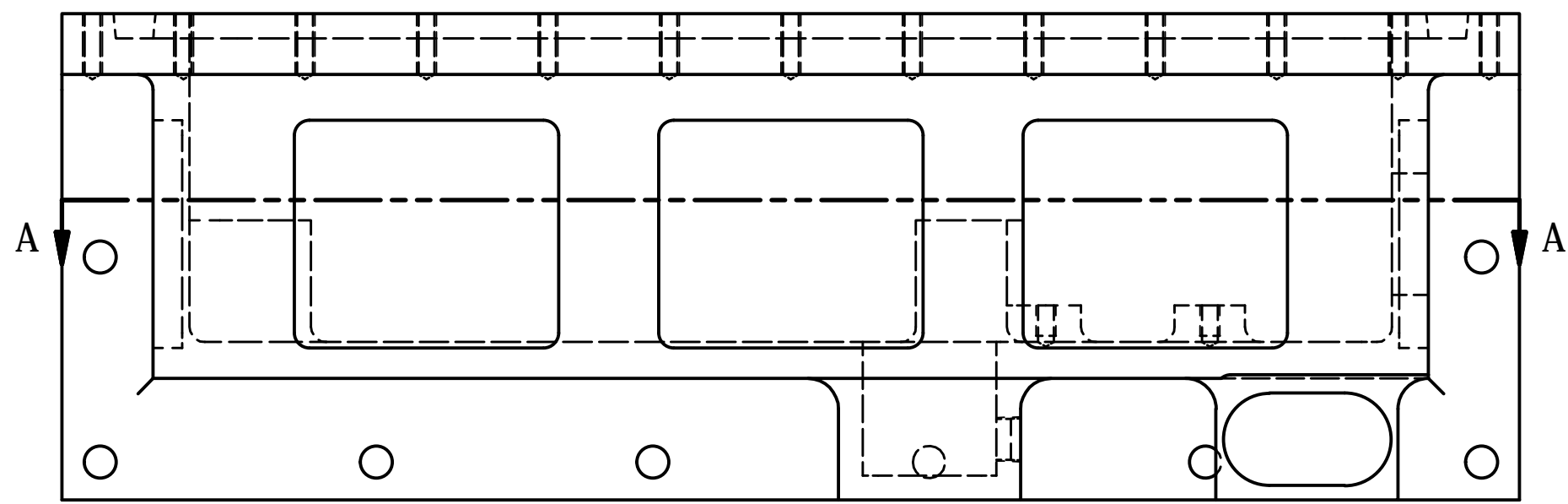
Updated: 18 May 11

SCTEx Part Number	Description	Material	Vendor	Vendor Part Number
SCTEX-0001	Housing Lower ICU R0b 101007	Aluminum 6061-T6	NA	NA
SCTEX-0002	Housing Upper ICU R0b 101007	Aluminum 6061-T6	NA	NA
SCTEX-0003	Plate Thermal Baffle ICU R0 101004	Aluminum 6061-T6	NA	NA
SCTEX-0004	Bracket Fan ICU R0 100929	Aluminum 6061-T6	NA	NA
SCTEX-0005	Plate Interface Vibe-Test R0 101106	Aluminum 6061-T6	NA	NA
SCTEX-0006	Pass-Thru Electrical Hermetic 12-Pin	Stainless Steel	PAVE Technology	1649
SCTEX-0007	O-Ring 0.25THKx10.5ID	Viton® Fluoroelastomer	Parker Hannifin	450
SCTEX-0008	Straight Fitting, WVCR Male Connector	Stainless Steel	Swagelok	SS-4-WVCR-1-2
SCTEX-0009	Bellows Valve	Stainless Steel	Swagelok	SS-4BW-VCR
SCTEX-0010	Fan DC, 12v	PBT, UL94V-O (Plastic)	Orion	OD1238-24HB
SCTEX-0011	Non-Slotted Aluminum Rail Set, 6" Length Card Cage Endcap, 4" x 4", w/3" Square Cutout Shock Rocks, Set of 12 (8 End, 4 Mid Rail Mountable)	Aluminum Aluminum Rubber	Parvus	PRV-1206-01 PRV-0439-03 PRV-0892-01



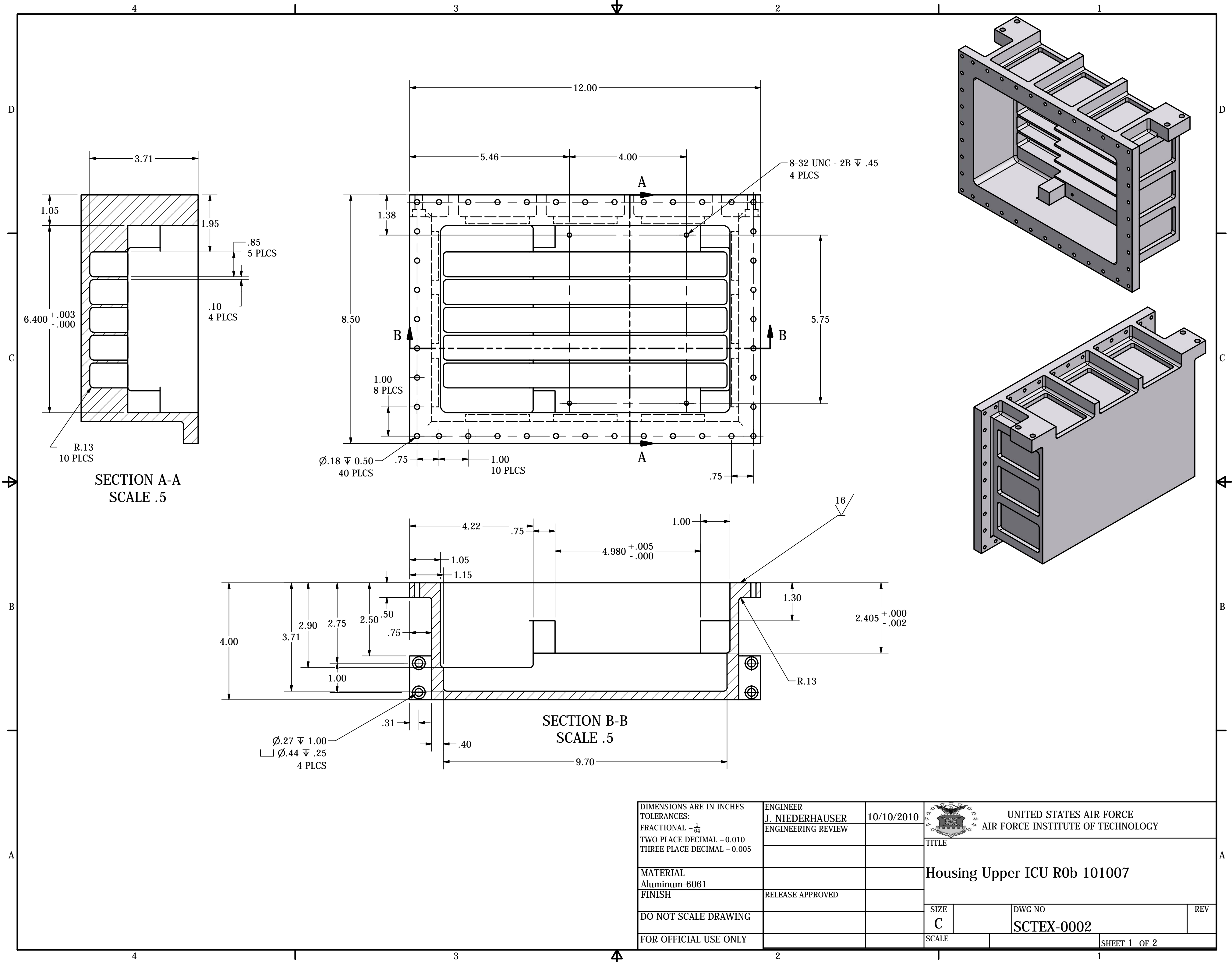
SECTION A-A
SCALE .75

SECTION C-C
SCALE .75



DETAIL D
SCALE 1.50 : 1

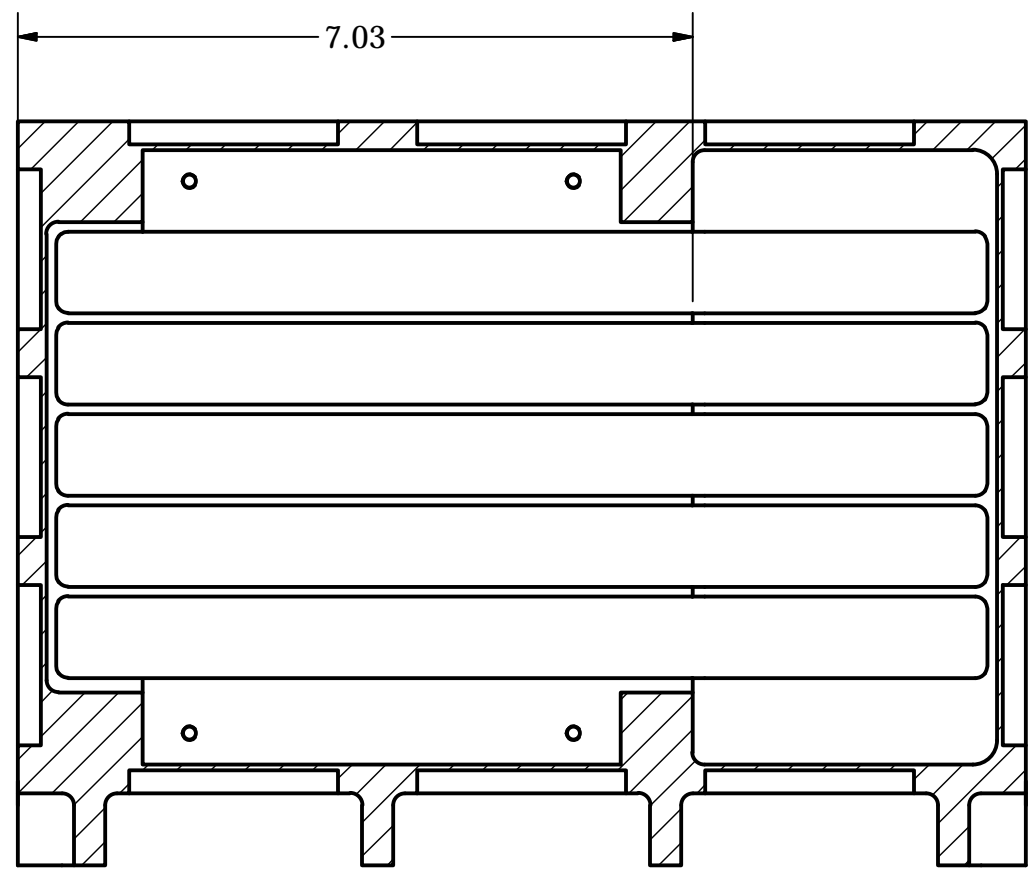
DIMENSIONS ARE IN INCHES TOLERANCES: FRACTIONAL - $\frac{1}{64}$ TWO PLACE DECIMAL - 0.010 THREE PLACE DECIMAL - 0.005	ENGINEER J. NIEDERHAUSER	10/11/2010	 UNITED STATES AIR FORCE AIR FORCE INSTITUTE OF TECHNOLOGY TITLE	
	ENGINEERING REVIEW			
MATERIAL Aluminum-6061			Housing Lower ICU R0b 101007	
FINISH	RELEASE APPROVED		SIZE C	DWG NO SCTEX-0001
DO NOT SCALE DRAWING			SCALE	REV
FOR OFFICIAL USE ONLY				SHEET 2 OF 2



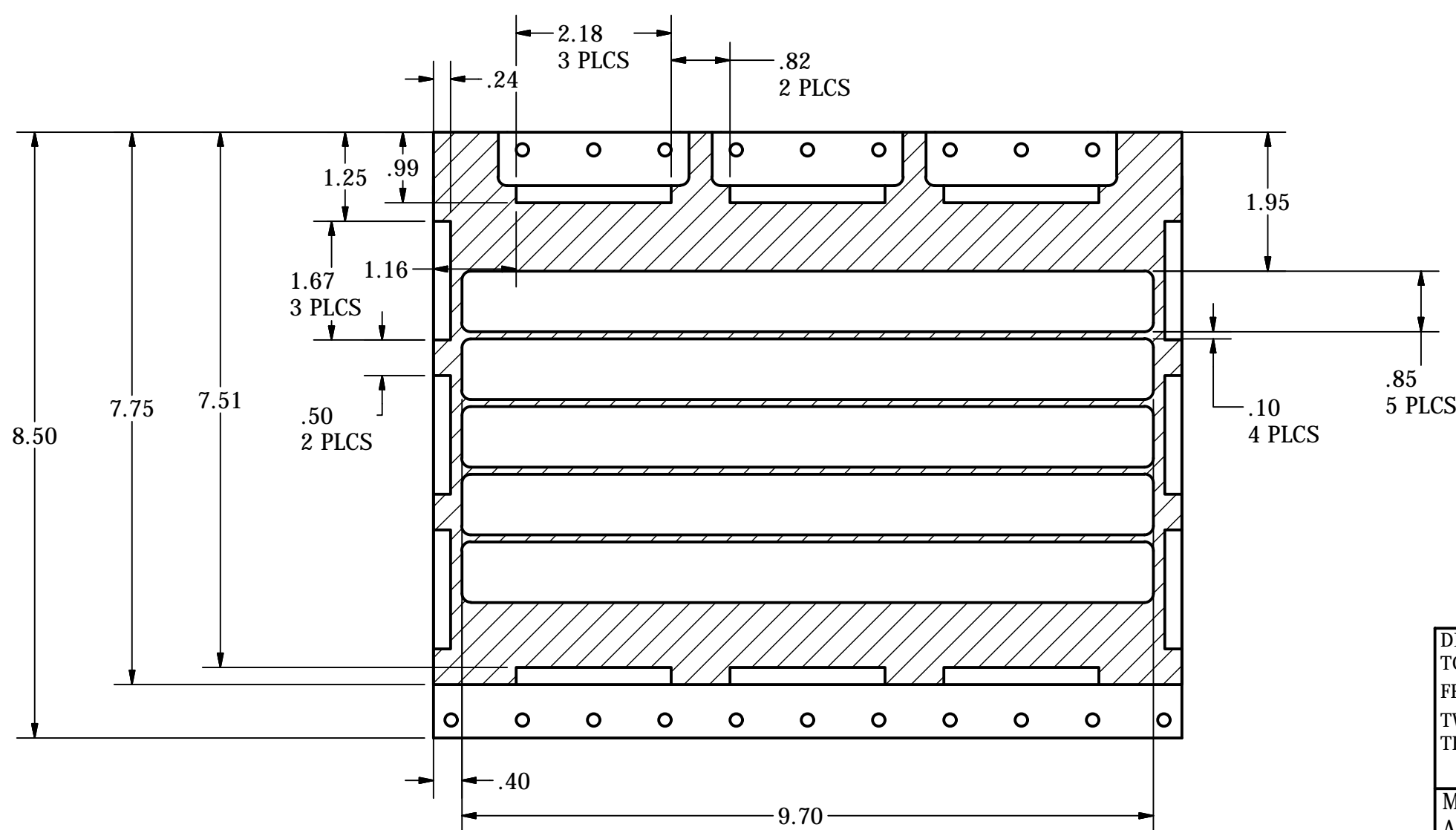
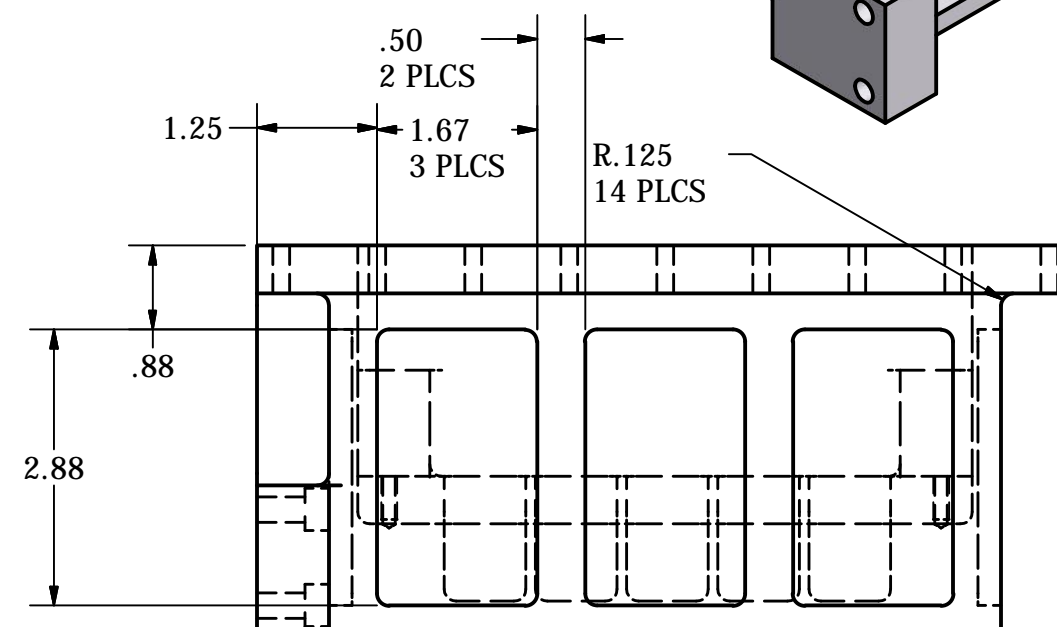
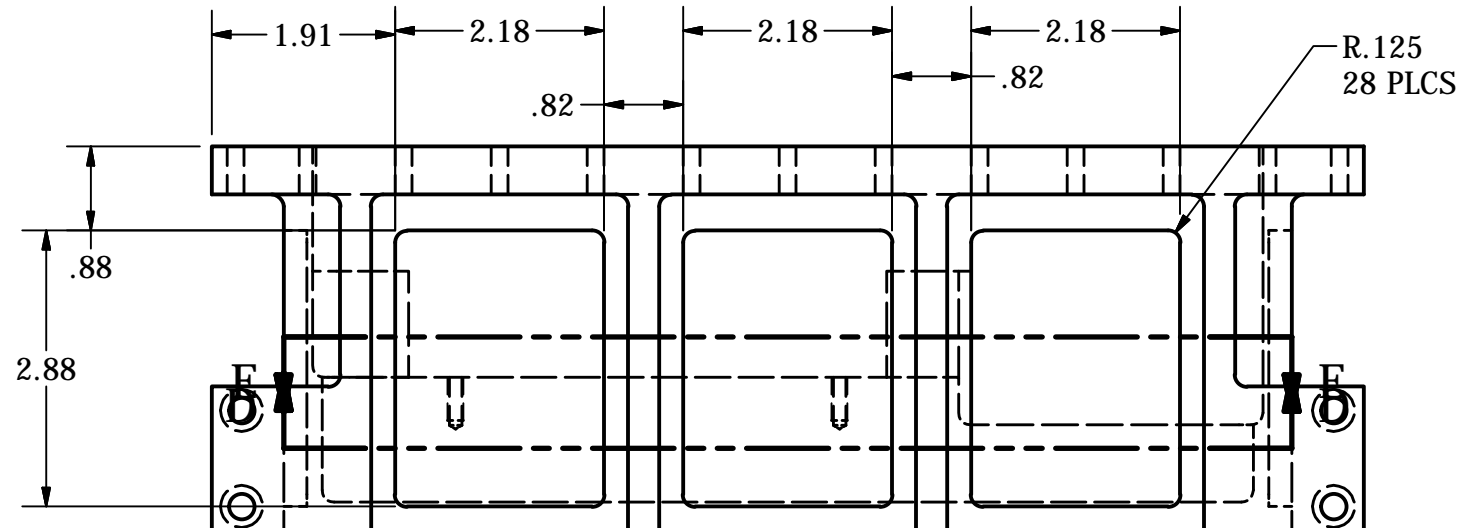
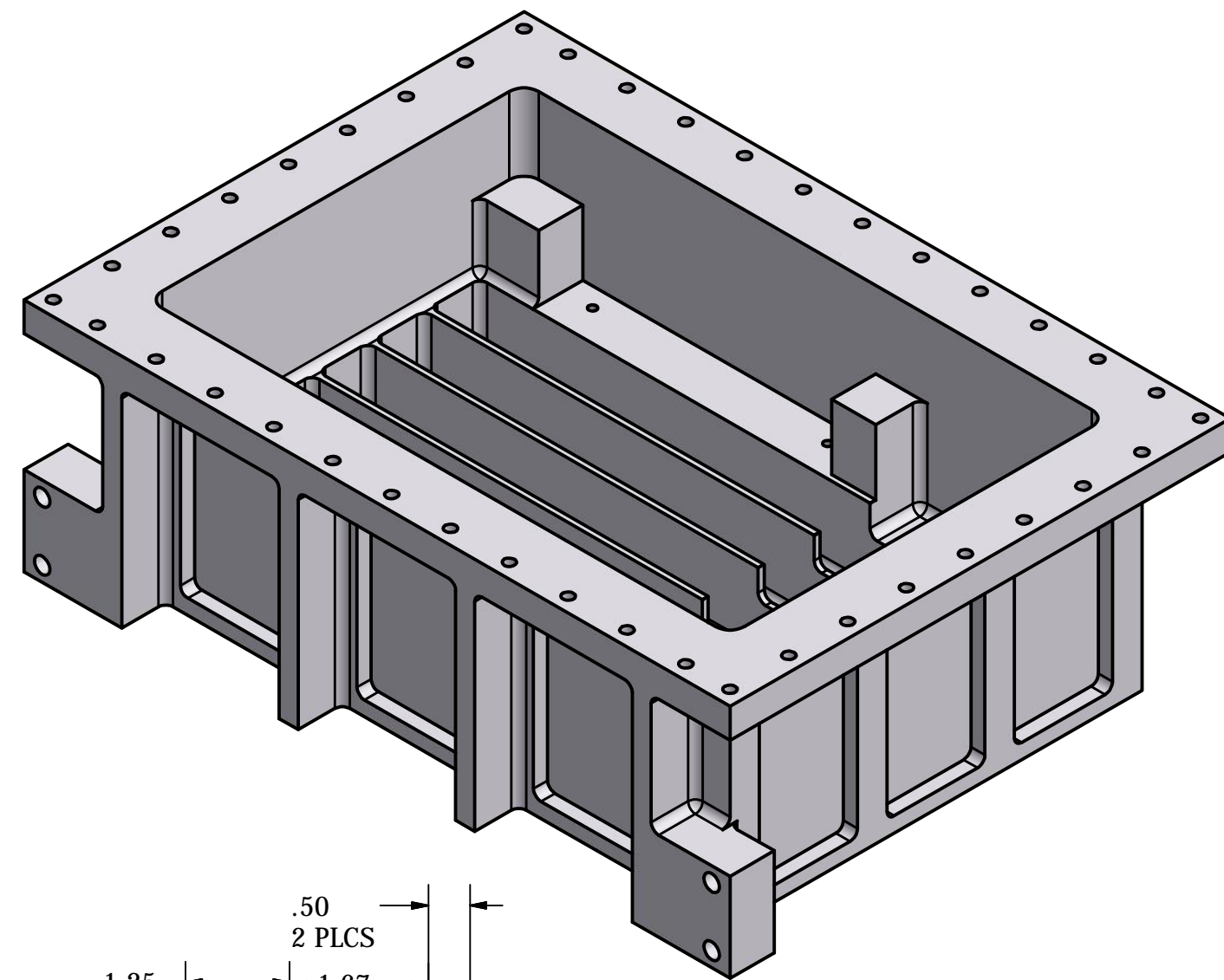
PRODUCED BY AN AUTODESK EDUCATIONAL PRODUCT

PRODUCED BY AN AUTODESK EDUCATIONAL PRODUCT

DIMENSIONS ARE IN INCHES TOLERANCES: FRACTIONAL - $\frac{1}{64}$ TWO PLACE DECIMAL - 0.010 THREE PLACE DECIMAL - 0.005		ENGINEER J. NIEDERHAUSER ENGINEERING REVIEW	10/10/2010	 UNITED STATES AIR FORCE AIR FORCE INSTITUTE OF TECHNOLOGY	
MATERIAL Aluminum-6061 FINISH		RELEASE APPROVED	TITLE Housing Upper ICU R0b 101007		
DO NOT SCALE DRAWING			SIZE C	DWG NO SCTEX-0002	REV
FOR OFFICIAL USE ONLY			SCALE	SHEET 1 OF 2	



SECTION E-E
SCALE .5

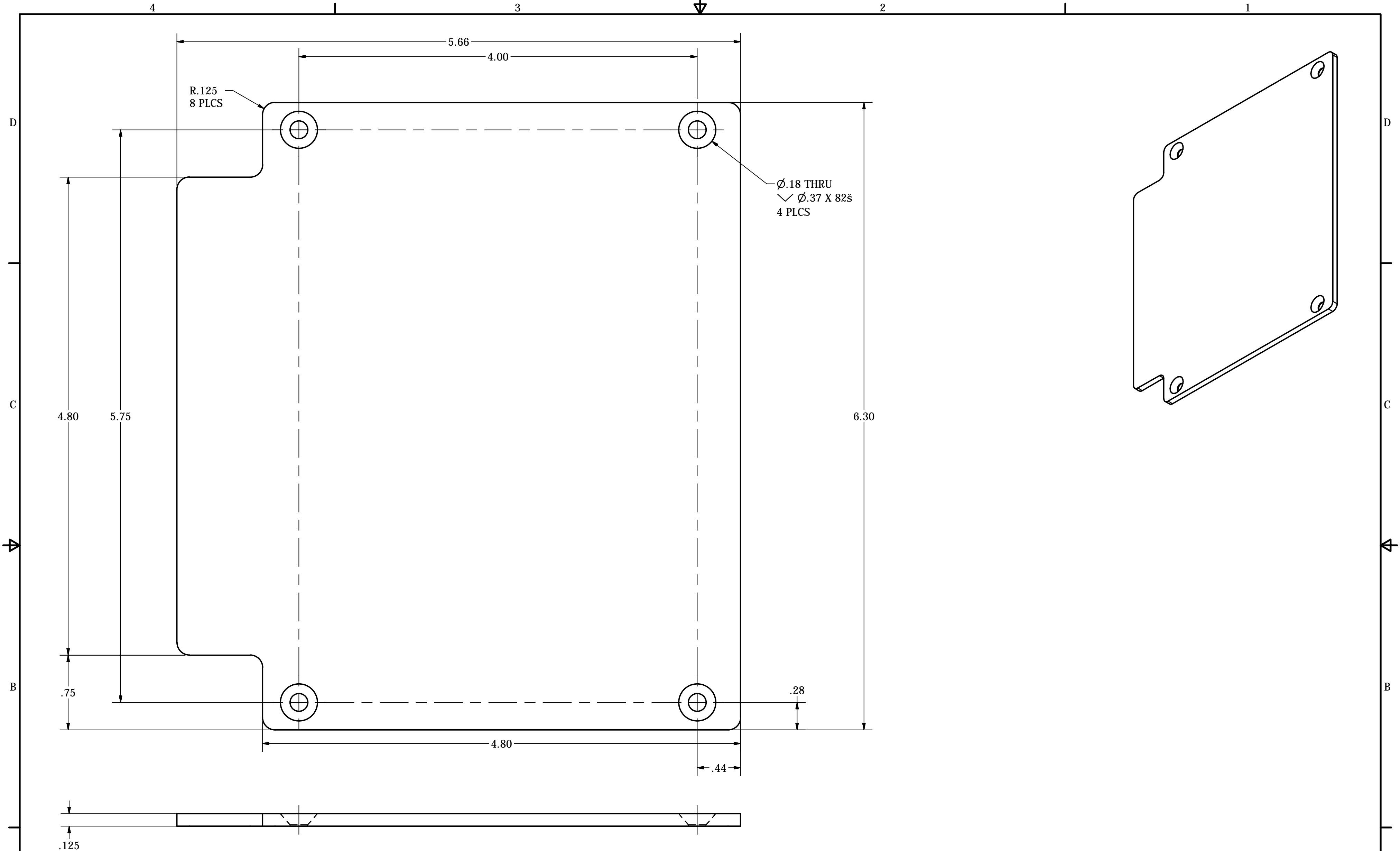


SECTION D-D
SCALE .5

DIMENSIONS ARE IN INCHES TOLERANCES: FRACTIONAL - $\frac{1}{64}$ TWO PLACE DECIMAL - 0.010 THREE PLACE DECIMAL - 0.005	ENGINEER J. NIEDERHAUSER	10/10/2010	 UNITED STATES AIR FORCE AIR FORCE INSTITUTE OF TECHNOLOGY	
	ENGINEERING REVIEW		TITLE Housing Upper ICU R0b 101007	
MATERIAL Aluminum-6061	FINISH RELEASE APPROVED	SIZE C	DWG NO SCTEX-0002	REV
DO NOT SCALE DRAWING		SCALE	SHEET 2 OF 2	
FOR OFFICIAL USE ONLY				

PRODUCED BY AN AUTODESK EDUCATIONAL PRODUCT

PRODUCED BY AN AUTODESK EDUCATIONAL PRODUCT



PRODUCED BY AN AUTODESK EDUCATIONAL PRODUCT

PRODUCED BY AN AUTODESK EDUCATIONAL PRODUCT

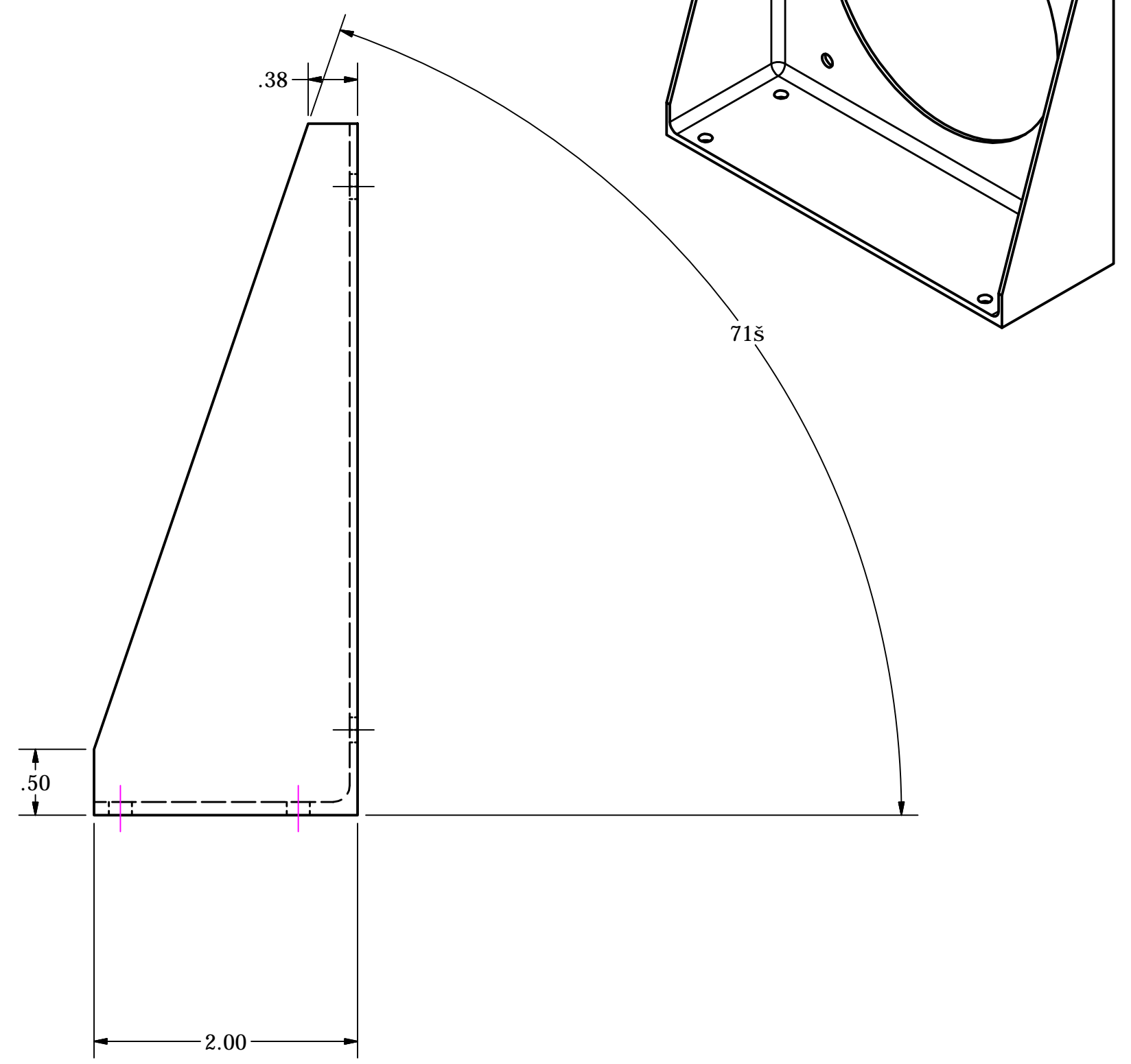
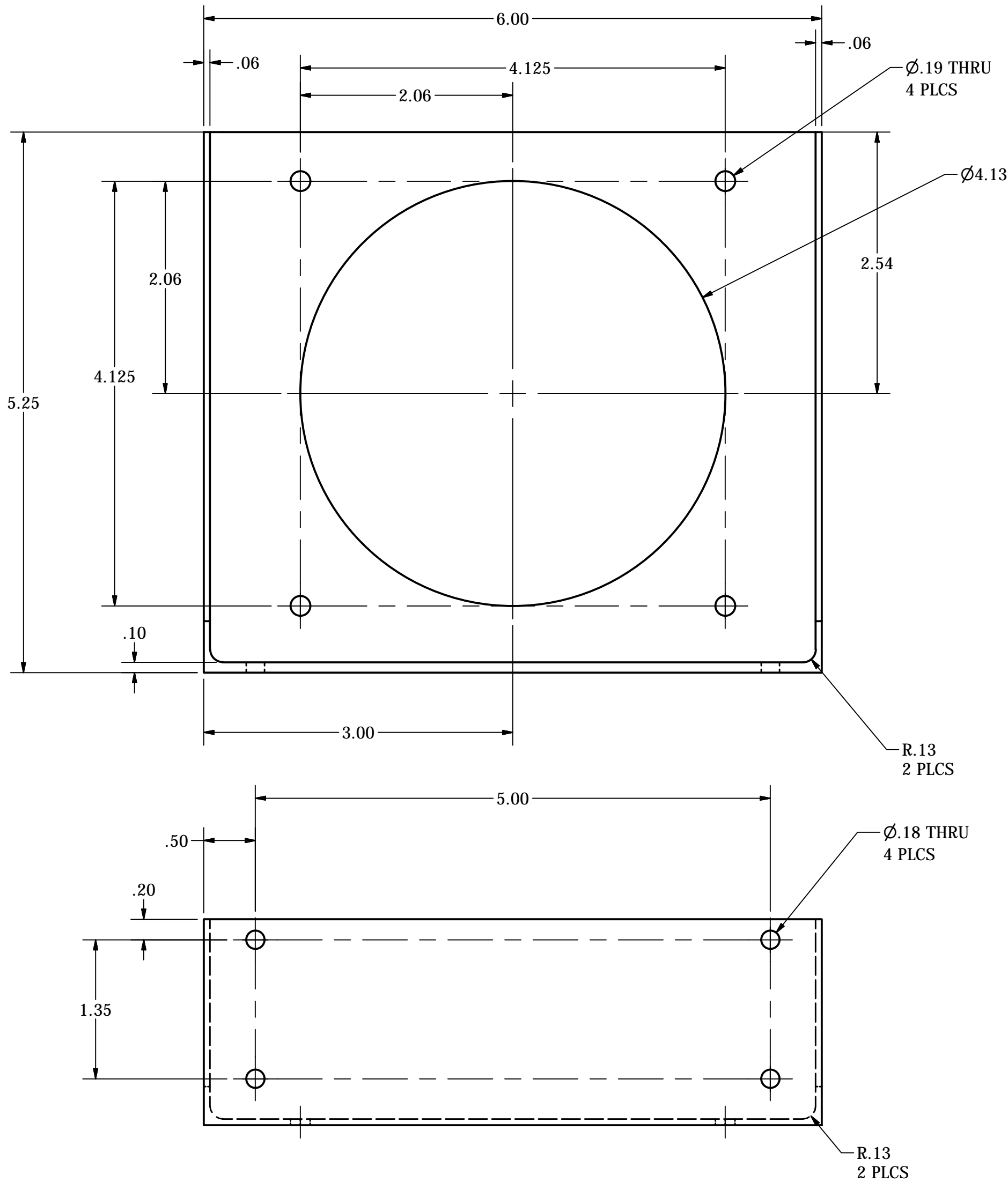
DIMENSIONS ARE IN INCHES TOLERANCES: FRACTIONAL - $\frac{1}{64}$ TWO PLACE DECIMAL - 0.010 THREE PLACE DECIMAL - 0.005	ENGINEER J. NIEDERHAUSER	10/4/2010	 UNITED STATES AIR FORCE AIR FORCE INSTITUTE OF TECHNOLOGY	
	ENGINEERING REVIEW		TITLE Plate Thermal Baffle ICU R0 101004	
MATERIAL Aluminum-6061			SIZE C	DWG NO SCTEX-0003
FINISH	RELEASE APPROVED		SCALE	REV
DO NOT SCALE DRAWING			SHEET 1 OF 1	
FOR OFFICIAL USE ONLY				

PRODUCED BY AN AUTODESK EDUCATIONAL PRODUCT

PRODUCED BY AN AUTODESK EDUCATIONAL PRODUCT

D
C
B
A

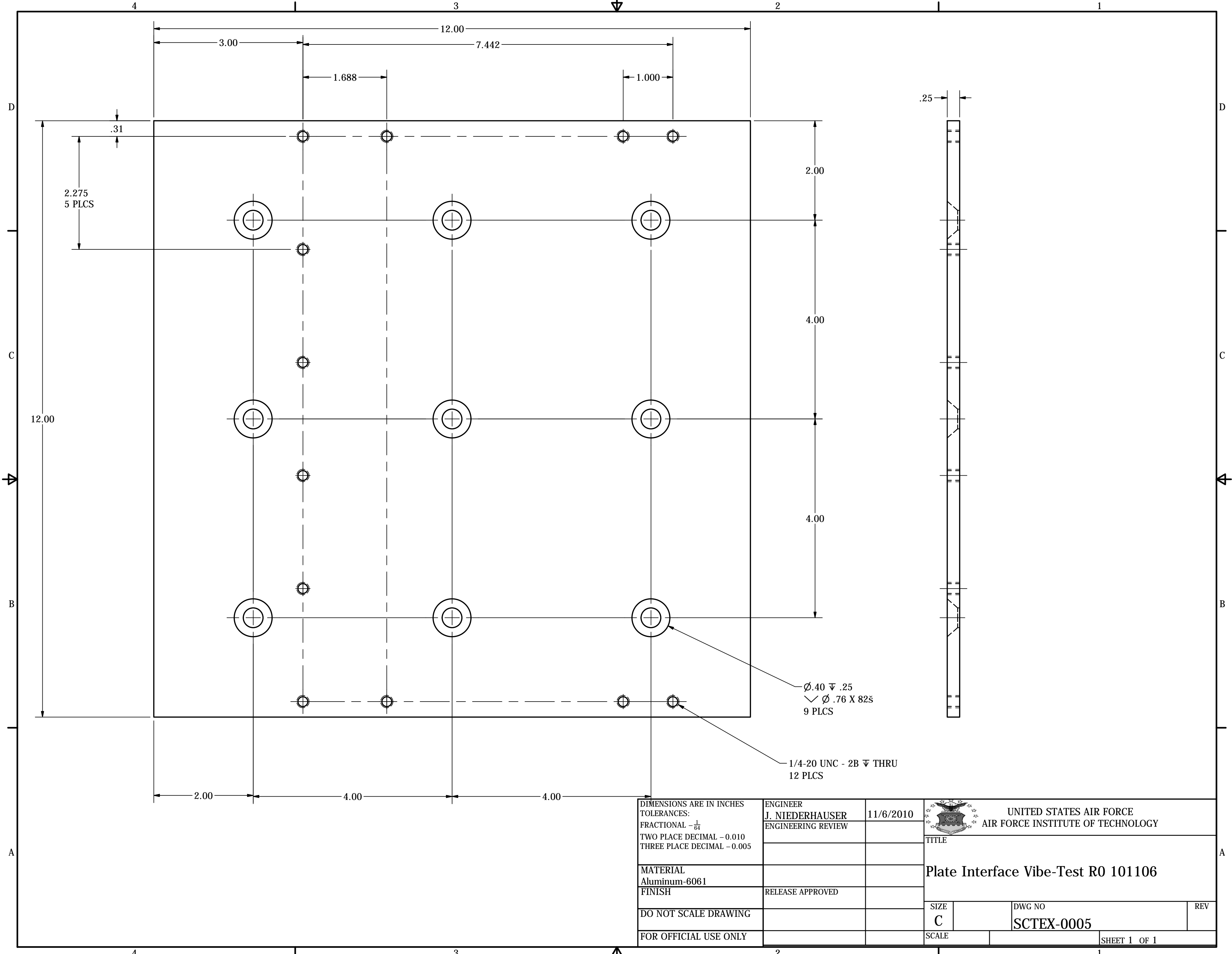
D
C
B
A



DIMENSIONS ARE IN INCHES TOLERANCES: FRACTIONAL - $\frac{1}{64}$ TWO PLACE DECIMAL - 0.010 THREE PLACE DECIMAL - 0.005	ENGINEER J. NIEDERHAUSER	10/4/2010	 UNITED STATES AIR FORCE AIR FORCE INSTITUTE OF TECHNOLOGY	
	ENGINEERING REVIEW		TITLE	
MATERIAL Aluminum-6061			Bracket Fan ICU R0 100929	
FINISH	RELEASE APPROVED		SIZE C	DWG NO SCTEX-0004
DO NOT SCALE DRAWING			SCALE	REV
FOR OFFICIAL USE ONLY			SHEET 1 OF 1	

PRODUCED BY AN AUTODESK EDUCATIONAL PRODUCT

PRODUCED BY AN AUTODESK EDUCATIONAL PRODUCT



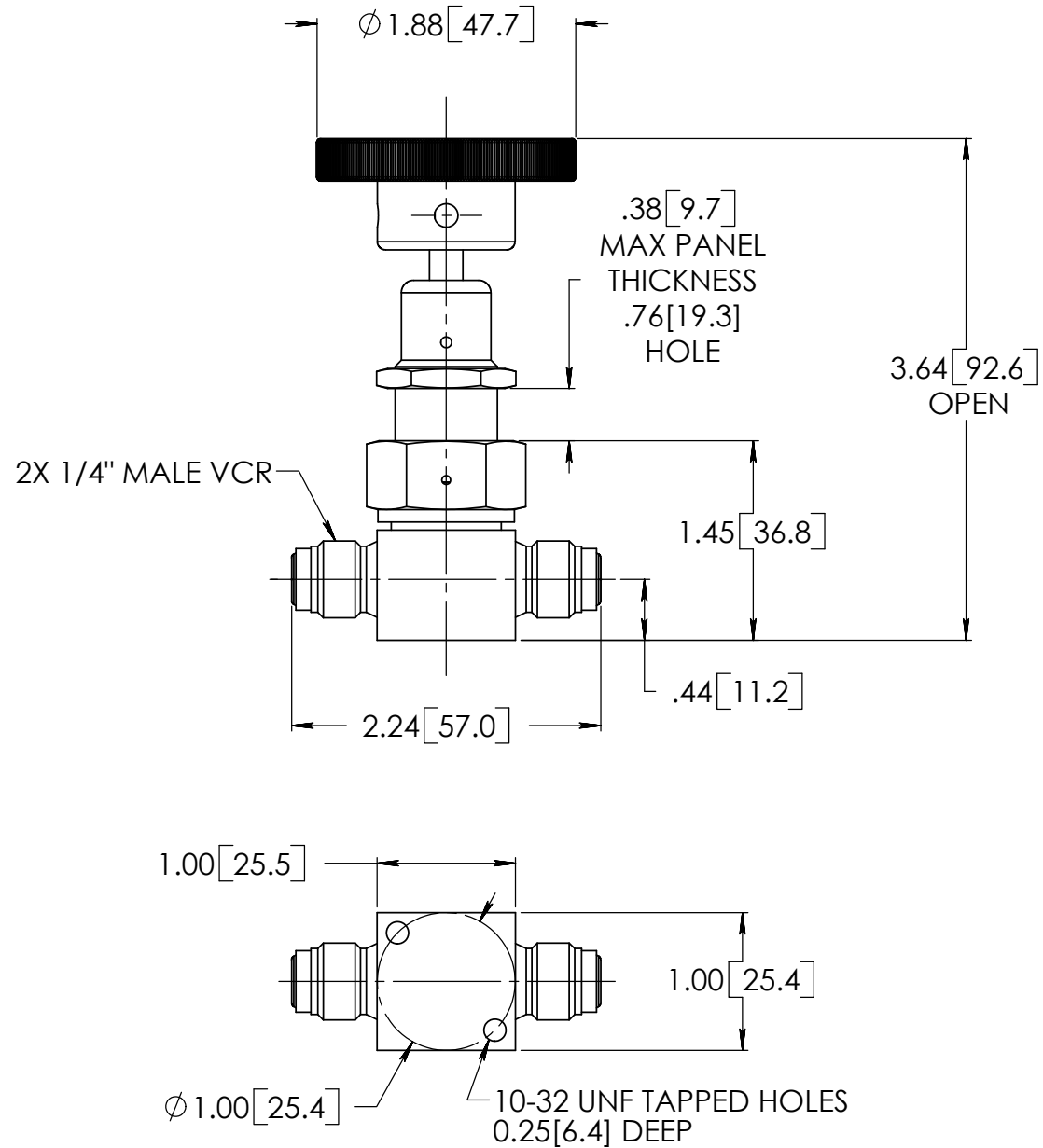
Ø.40 ∇ .25
 \surd Ø .76 X 82 \bar{s}
 9 PLCS

1/4-20 UNC - 2B ∇ THRU
 12 PLCS

DIMENSIONS ARE IN INCHES TOLERANCES: FRACTIONAL - $\frac{1}{64}$ TWO PLACE DECIMAL - 0.010 THREE PLACE DECIMAL - 0.005	ENGINEER J. NIEDERHAUSER ENGINEERING REVIEW	11/6/2010	 UNITED STATES AIR FORCE AIR FORCE INSTITUTE OF TECHNOLOGY	
	MATERIAL Aluminum-6061 FINISH	RELEASE APPROVED		TITLE Plate Interface Vibe-Test R0 101106
DO NOT SCALE DRAWING			SIZE C	DWG NO SCTEX-0005
FOR OFFICIAL USE ONLY			SCALE	REV SHEET 1 OF 1

PART NO.

SS-4BW-VCR



CUSTOMER DRAWING

Swagelok

- DRAWING NOT TO SCALE.
- DIMENSIONS ARE INCHES
NEXT TO [MILLIMETERS].
- DRAWING IS SUBJECT TO CHANGE
WITHOUT NOTICE.

DRAWN BY

MSM

6/21/2006

TITLE

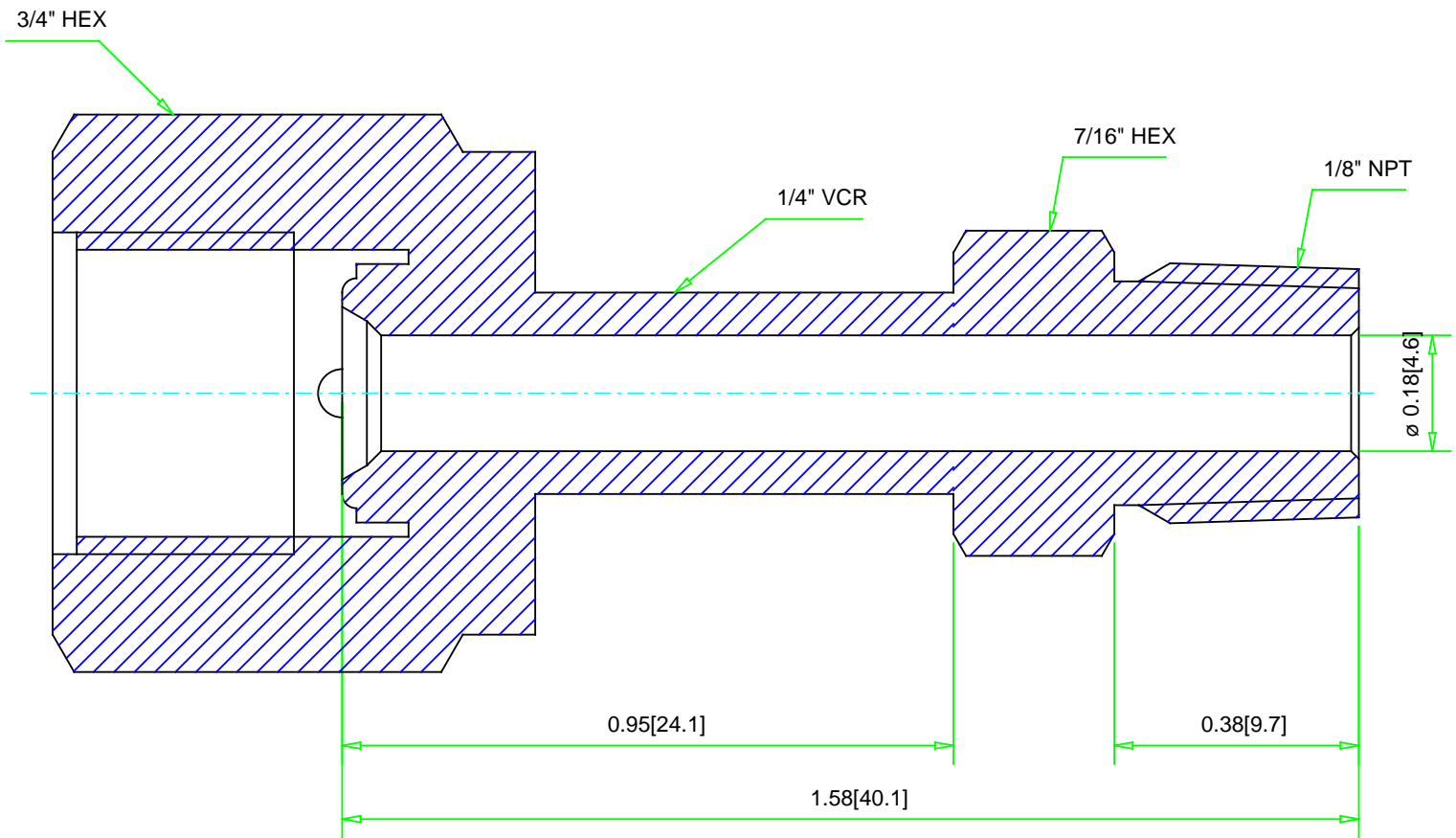
B SERIES BELLOWS VALVE

APPROVED BY

CSR-06-04087

PART NO.

SS-4BW-VCR



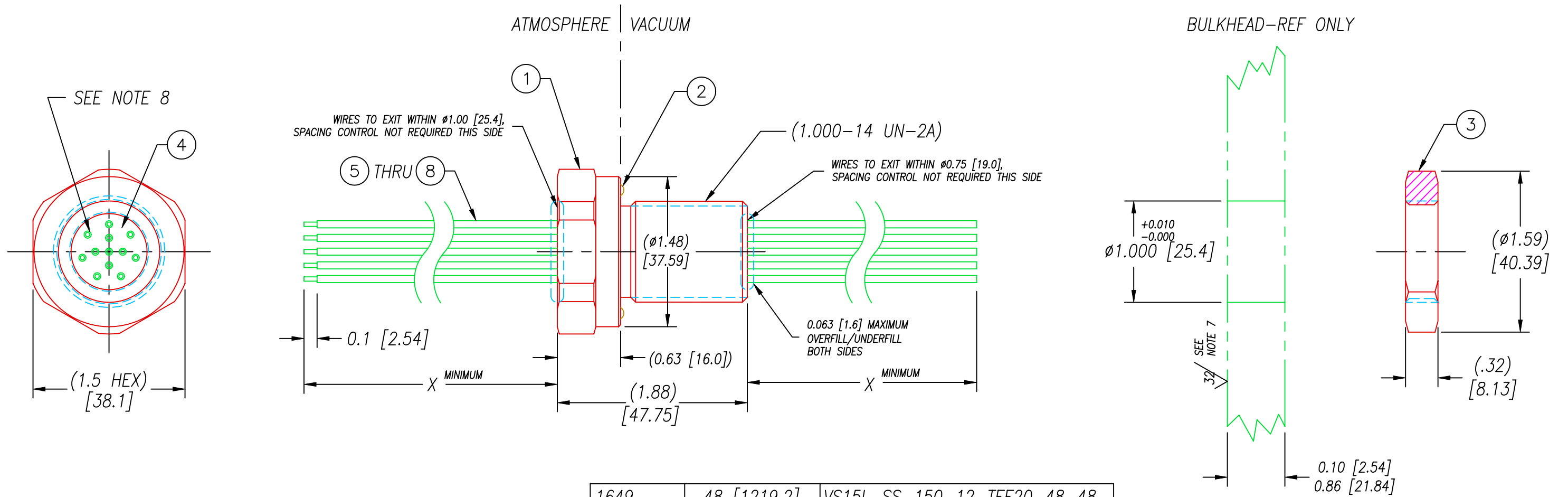
CUSTOMER DRAWING



- DRAWING NOT TO SCALE
 - DIMENSION ARE INCHES NEXT TO [MILIMETRES]
 - DRAWING IS SUBJECT TO CHANGE WITHOUT NOTICE.
 - ALL ASSEMBLED NUTS AND FERRULES ARE SHOWN AT FINGER TIGHT DIMENSIONS.
 - ALL HEX CALL-OUT ARE ACROSS FLATS.

TITLE
 Male NPT Connector

PART NO.
 SS-4-WVCR-1-2



1649	48 [1219.2]	VS15L-SS-150-12-TEE20-48-48
1649-1	196.85 [5000]	VS15L-SS-150-12-TEE20-5m-5m
PART#	X	DESCRIPTION

8	3	EE20 MIL YLW 19	WIRE 20EE MIL-W-16878/5 19 STR
7	3	EE20 MIL BLU 19	WIRE 20EE MIL-W-16878/5 19
6	3	EE20 MIL RED 19	WIRE 20EE MIL-W-16878/5 19
5	3	EE20 MIL BLK 19	WIRE 20EE MIL-W-16878/5 19
4	A/R	PAVE-Seal 150	EPOXY BLACK
3	1	0183	NUT VS15-SS
2	1	-215 VITON 75A	O-RING -215 VITON 75A
1	1	0161	HOUSING VS15L-SS
ITEM	QTY	PART NUMBER	DESCRIPTION

NOTES:

- HE LEAK TEST @1 ATM. 10×10^{-8} CC/S OR LESS.
- HYPOT 630 VDC 500 MΩ 0.01 SEC MINIMUM, WIRE TO WIRE & HOUSING.
- ALL TESTS ARE PERFORMED AT ROOM TEMPERATURE.
- ALL PARTS MUST PASS ALL TESTS.
- WIRES ARE NOT REQUIRED TO BEND SHARPLY AT EPOXY SEAL SURFACE.
- NO VOIDS LARGER THAN $\phi.035$ [.89] ARE ACCEPTABLE.
- FINISH APPLIES TO SPOTFACE FOR O-RING SEAL ONLY.
- WIRE COLOR POSITIONS ARE APPROXIMATE & VARIABLE.
- DIMENSIONS ARE IN INCHES [MILIMETERS].

ALL DIMENSIONS AND TOLERANCES APPLY TO FINISHED PART IN INCHES
 ALLOWABLE TOLERANCES UNLESS SPECIFIED OTHERWISE: NONE +/-0.5
 .X DECIMAL +/- 0.1 .XX DECIMAL +/- 0.02 .XXX DECIMAL +/-0.005
 ANGLES +/- 1 DEG SURFACE FINISH 128 microinch RMS

2751 Thunderhawk Court
 Dayton, Ohio 45414-3445
 U.S.A.
 (937)890-1100
 fax (937)890-5165
 www.pavetechnologyco.com

PAVE technology co.

DESCRIPTION PAVE-Seal Cable Harnesses
 SEE CHART

PART NUMBER 1649

REVISION LEVEL C

PROJECTION

Appendix C: Procedures

**AIR FORCE INSTITUTE OF TECH.
ENGINEERING PHYSICS DEPT.
WRIGHT-PATTERSON AFB, OH**

PROCEDURE:
REVISION:
DATE REVISED:
NUMBER OF PAGES:

SOP-GCTEx-0001
0
19 Apr 2011
13

**AFIT / ENP
REMOTE SENSING
OPERATIONS**

**Ground-Based Chromotomography
Experiment Operations**

PREPARED BY:

Test Engineer _____
Air Force Institute of Technology

DATE _____

REVIEW:

Technical Representative Review _____
Air Force Institute of Technology

DATE _____

Revision	Notes	Prepared By
0	-Initial procedure written	Capt. Niederhauser 19 Apr 11

PERSONNEL

GROUND-BASED CTE_x OPERATIONS

DATE _____

The following personnel are designated as test team members, and are chartered to perform their assignment as follows:

Test Conductor (TC) – Responsible for the timely performance of the test as written. This includes coordinating and directing the activities of the TPO and other test support teams. TC is responsible for coordinating all pretest activities and outside support required, including (but not limited to) security, fire, medical, and safety. TC is responsible for initialing completion on each step of the master test procedure.

Name _____ Signature _____

Test Director (TD) – Responsible for overall facility and test safety. Responsible for ensuring all test goals are met and all critical data is acquired. Supervises test activities to ensure procedures are followed. Has authority to perform real-time redlines on test procedures as required to ensure test requirements and goals area met.

Name _____ Signature _____

Test Panel Operator (TPO) – Responsible for operating the facility control systems during test operations as directed by TC. TPO is responsible for notifying the TC of any anomalous conditions.

Name _____ Signature _____

Instrumentation Engineer (IE) – Responsible for the operation and monitoring of all data acquisition equipment and notifying the TD and TC of any data loss or anomalies.

Name _____ Signature _____

Other Test Team Members – Responsible for performing ancillary duties in support of test, such as test stand and control room access control, support of anomaly resolution, and other necessary activities.

Name _____ Signature _____

Name _____ Signature _____

Name _____ Signature _____

Name _____ Signature _____

ALL TEST TEAM MEMBERS – Responsible for the safe performance of the test. Have read and understood all portions of the procedure. Any Test Team Member can declare an emergency or unsafe condition.

1.0**ABBREVIATIONS AND ACRYONMS**

CTE _x	Space-Based Chromotomography Experiment
FPS	Frames Per Second
IE	Instrumentation Engineer
SOP	Standard Operating Procedure
TC	Test Conductor
TD	Test Director
TPO	Test Panel Operator

2.0**TEST DESCRIPTION AND OBJECTIVES****2.1.****PURPOSE**

This procedure provides the means to perform hyperspectral data capturing for the ground-based Chromotomography Experiment (CTEx).

2.2.**SCOPE**

This procedure prepares the instrumentation and control system as well as verifies the proper mechanical configuration during the pre-test setup, Section 3.0. Section 4.0 executes the data acquisition activities, and allows for recycling, enabling multiple serial events to be captured. Finally, securing of the test equipment is carried out in Section 5.0.

3.0**PRE-TEST SETUP**

- ____ **3.1.** TC Verify all pages in this procedure are intact and complete
- ____ **3.2.** TC Go through the procedure and input any specific information required to perform operation.
- ____ **3.3.** IE **CONNECT** / Verify all necessary cables have been plugged-in:
 ___ Motor Power ___ Motor Control ___ Encoder Feedback
 ___ DAQ I/O ___ Camera I/O ___ Camera Power
 ___ SAM-3 Input (If Configured) ___ SAM-3 Output (If Configured)
- ____ **3.4.** TPO **TURN ON** laptop and instrument power
- ____ **3.5.** TPO **SELECT / OPEN** the following shortcuts:
 ___ CTE_x Encoder.vi ___ CTE_x Motor.vi ___ Phantom 630
NOTE: Each window will be henceforth called-out as *Encoder.vi* (CTE_x Encoder.vi), *Motor.vi* (CTE_x Motor.vi) or *Phantom* (Phantom 630)
- ____ **3.6.** TPO **OPEN** "CTE_x DATA" folder on the desktop
- ____ **3.7.** TPO **SELECT / CREATE** new folder, name it in format "**DDMMYY**"
NOTE: e.g., 24AUG10
- ____ **3.8.** TPO **SELECT** Phantom Window, Acquisition Menu, Setup & Recording Option
- ____ **3.9.** TC Determine whether the Phantom Camera factory reset should be accomplished (typically this should be performed); if so, continue, otherwise, skip to step 3.10
- ____ **3.9.1.** IE **CONFIGURE** Lens #3 with a lens cover/cap
- ____ **3.9.2.** TPO **SELECT** Options button on Setup & Recording window
- ____ **3.9.3.** TPO **SELECT** Black Reference, click **OK**, and **YES** on popup windows
- ____ **3.9.4.** TPO **SELECT OK** on the options window to closeout
- ____ **3.9.5.** IE **REMOVE** the Lens #3 lens cover/cap

- ____ **3.10.** TPO **CONFIGURE** camera software to the following setup parameters:
Rate: 100 fps, **Exposure Time:** 10 micro-sec, **Post Trigger:** 1 frame
NOTE: the above values may be adjusted at the discretion of the TC
- ____ **3.11.** IE **ORIENT** the GCTEx instrument at the intended source utilizing the tripod adjustment knobs
NOTE: The next step should only be performed only if absolutely required (i.e., if the source cannot be distinguished from the scene)
- ____ **3.12.** IE **REMOVE** prism assembly, as necessary
- ____ **3.13.** IE **VERIFY / ADJUST** telephoto, C-Mount and COTS camera lens (L1, L2, & L3), focal length is set to infinite
- ____ **3.14.** IE **VERIFY / ADJUST** aperture stop for the telephoto, C-Mount and COTS camera lens (L1, L2, & L3), is set to minimum f-number (or maximum diameter)
- ____ **3.15.** IE **ADJUST / FOCUS** the image utilizing the telephoto-lens for course/fine adjustment
- ____ **3.16.** IE **REPLACE** prism assembly, if necessary
- ____ **3.17.** IE **VERIFY / ADJUST** the field stop assembly as required (typically to a minimum diameter)
- ____ **3.18.** IE **REPLACE** the stray-light access cover(s)
- 4.0** **TEST ACQUISITION**
- ____ **4.1.** TPO **CONFIGURE** camera software to the following test parameters, per test plan:
Rate: ___ fps, **Exposure Time:** ___micro-sec, **Post Trigger:** 1 frame
- ____ **4.2.** TPO **SELECT / VERIFY** "Capture"
NOTE: From this point forward, the camera is acquiring data into internal on-board memory. The post-trigger (i.e., "Trigger") command must be sent to the camera to save/post-process captured data.
- ____ **4.3.** TPO **SELECT** Motor.vi Window
NOTE: the next step is N/A for a test recycle
- ____ **4.4.** TPO **SET** voltage to 1.0 volts (>0.8v to overcome motor friction)
- ____ **4.5.** TPO **RUN** Motor.vi program

_____ 4.6.	TPO	TURN ON "Read Frequency"
_____ 4.7.	TPO	SLOWLY INCREASE / DECREASE voltage to initial set point, per test plan: ____ Hz / ____ volts
_____ 4.8.	TPO	TURN OFF "Read Frequency"
_____ 4.9.		DATA CAPTURE NOTE: The following section (through 4.9.11) must be completed in quick succession.
_____ 4.9.1.	TPO	SELECT Encoder.vi Window
_____ 4.9.2.	TPO	RUN Encoder.vi program
_____ 4.9.3.	TPO	TURN ON recording
_____ 4.9.4.	TPO	SELECT Phantom Window, Acquisition Menu, Camera Clock Option
_____ 4.9.5.	TPO	SELECT "Update & Set Time" option, then "OK"
_____ 4.9.6.	TPO	SELECT Phantom Window, Acquisition Menu, Setup & Recording Option
_____ 4.9.7.	TPO	PERFORM Print-Screen (screen-capture for quick-look event capture)
_____ 4.9.8.	TC	WAIT until test / acquisition complete
_____ 4.9.9.	TPO	SELECT "Trigger" immediately after the event is complete to prevent overwriting data in the buffer
_____ 4.9.10.	TPO	SELECT Encoder.vi Window
_____ 4.9.11.	TPO	TURN OFF recording and STOP the VI
_____ 4.10.	TPO	SELECT Phantom Window
_____ 4.11.	TPO	SELECT "OK"
_____ 4.12.	TPO	SELECT "Timestamp" at the discretion of the TC

_____ 4.13.	TPO	<p>SELECT “Save” and save in format: “YYMMDD_HHMM_TestX.avi”</p> <p>where, _____ YYMMDD – Test day, two-integer/digit year, month, day (100824) _____ HHMM – 24-hour test time in hour, minute (1345) _____ TestX – test number (e.g., Test1, Test2, etc.) _____ .avi – preferred format</p> <p>NOTE: Ignore frame-rate dialog (i.e., select “OK”)</p>
_____ 4.14.	TC	LOG test run in Appendix 2.0
_____ 4.15.	TPO	SELECT Phantom Window
_____ 4.16.	TPO	SELECT “Capture”
_____ 4.17.	TPO	SELECT “Delete Cine File from Memory”
_____ 4.18.	TC	DETERMINE whether another data capture will be completed; if so, RECYCLE to Step 4.1; otherwise, continue to SECURING, Section 5.0
5.0		SECURING
_____ 5.1.	TPO	SELECT Motor.vi window
_____ 5.2.	TPO	TURN ON “Read Frequency”
_____ 5.3.	TPO	SLOWLY DECREASE voltage cease motor rotation
_____ 5.4.	TPO	STOP the motor using the “STOP” button on the VI control panel (i.e. do NOT stop the VI yet).
_____ 5.5.	TPO	SELECT Encoder.vi window
_____ 5.6.	TPO	Verify / STOP Encoder.vi program
_____ 5.7.	TPO	CLOSE all windows and dialog boxes
_____ 5.8.	TPO	SHUT-DOWN Laptop
_____ 5.9.	TPO	TURN OFF instrument and laptop power

ATTACHMENT 1.0 TEST PLAN

Date _____ Time _____

Capture Number	Date	Time	Source	Prism Rate	Resolution	FPS	Exposure Time	Notes

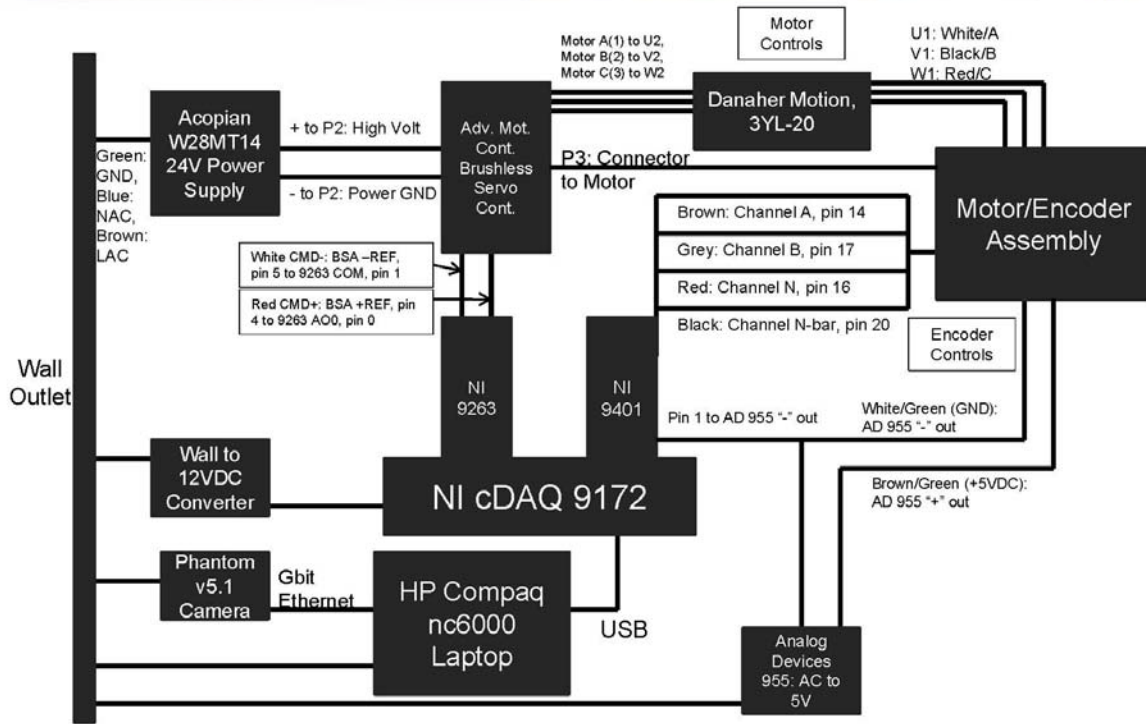
ATTACHMENT 2.0 TEST LOG

Itm	TIME	EVENT / STATUS	FILENAME
<i>(#)</i>	<i>(HHMM)</i>	<i>(Desc.)</i>	<i>(Test Data)</i>
1			
2			
3			
4			
5			
6			
7			
8			
9			
10			
11			
12			
13			
14			
15			
16			
17			
18			
19			
20			
21			
22			
23			
24			
25			
26			

ATTACHMENT 3.0 Wiring Diagram



CTEx Control System



**GCTEX OPERATIONS
AFIT/ENY**

WRIGHT-PATTERSON AFB, OH

PROCEDURE:

REVISION:

DATE REVISED:

NUMBER OF PAGES:

SOP-GCTEX-0002

0

5 Dec 2010

20

**AFIT / ENY
GCTEx
OPERATIONS**

GCTEx Assembly

PREPARED BY:

Test Engineer _____
AFIT/ENY

DATE _____

REVIEW / APPROVAL:

AF Customer _____
AFIT/ENY CTEEx Thesis Advisor

DATE _____

Revision	Notes	Prepared By
0	-Initial procedure written	Capt. Niederhauser 5 Dec 10

PERSONNEL

DATE _____

The following personnel are designated as test team members, and are chartered to perform their assignment as follows:

Test Conductor (TC) – Responsible for the timely performance of the test as written. This includes coordinating and directing the activities of the Red Crew and other test support teams. TC is responsible for coordinating all pretest activities and outside support required, including (but not limited to) security, fire, medical, and safety. TC is responsible for initialing completion on each step of the master test procedure.

Name _____ Signature _____

Test Director (TD) – Responsible for overall facility and test safety. Responsible for ensuring all test goals are met and all critical data is acquired. Supervises test activities to ensure procedures are followed. Has authority to perform real-time redlines on test procedures as required to ensure test requirements and goals area met.

Name _____ Signature _____

Red Crew Leader (RC) – Responsible for directing the activities of Red Crew members. Reports directly to the TC and ensures all Red Crew tasks are completed. Responsible for ensuring all RCM's have all required certifications and training. Responsible for ensuring all required equipment is available, accessible, and serviceable.

Name _____ Signature _____

ALL TEST TEAM MEMBERS – Responsible for the safe performance of the test. Have read and understood all portions of the test procedure. Any Test Team Member can declare an emergency or unsafe condition.

1.0**ABBREVIATIONS AND ACRYONMS**

AFIT	Air Force Institute of Technology
FOD	Foreign Object Debris
HAZCOM	Hazardous Communication
PPE	Personal Protective Equipment
RC	Red Crew
RCM	Red Crew Member
STE	Special Test Equipment
TC	Test Conductor
TD	Test Director
TPO	Test Panel Operator

2.0**TEST DESCRIPTION AND OBJECTIVES****2.1.****PURPOSE**

This procedure provides the means to perform assembly upon the AFIT Chromotomography Experiment (CTEx) Ground-Based Linear design (GCTEx) as risk-reduction for a space-based version of the instrument.

3.0**DOCUMENTATION**

The completion of each applicable event shall be verified by marking to the left of the item number. Deviations from these procedures will be coordinated with the Test Conductor

3.1.**REFERENCE DOCUMENTS**

NONE

3.2.**SPECIFICATIONS**

NONE

3.3.**DRAWINGS**

GCTEX-0001 Block Mounting Camera R2 101117
 GCTEX-0002 Block Interface L3 R0 101117
 GCTEX-0003 Block Interface L3 ACCESS R0 101117
 GCTEX-0004 Block Interface L2 ACCESS R0 101113
 GCTEX-0005 Block Interface L2 R0 101117
 GCTEX-0006 Stand Lens Nikon Telephoto R0 101118
 GCTEX-0007 LCP04 Nikon Mount
 GCTEX-0008 NFM1 Nikon F-Mount
 GCTEX-0009 Plate Mounting Structural Tripod Secure R0 090811
 GCTEX-0010 Plate Mounting Structural R1 101118
 GCTEX-0011 Block Spacer Structure 2.5 in R0 090811
 GCTEX-0012 Housing Mounting Motor Encoder BOTTOM R2 101020
 GCTEX-0013 Housing Mounting Motor Encoder TOP R2 101020
 GCTEX-0014 Shaft Motor Encoder R2 101020
 GCTEX-0015 Plate Mounting Optical Breadboard R1 101119
 GCTEX-0016 Block Interface Motor-Encoder Mockup R0 101118
 GCTEX-0017 Block Mounting Interface Motor-Encoder R0 101116
 GCTEX-0018 Holder Laser Telephoto Mount R0 101116
 GCTEX-0019 Holder Laser Calibration R0 101119
 GCTEX-0020 Cover Light L2 R0 101121
 GCTEX-A002 ASSY GCTEx Structure (Linear) R2 101118

4.0**TEST REQUIREMENTS AND RESTRICTIONS****4.1.****TRAINING**

The following training is required for personnel using these procedures:

All personnel:

Job Site HAZCOM

4.2.**LIST OF EQUIPMENT**

GCTEX-0001 Block Mounting Camera R2 101117
GCTEX-0002 Block Interface L3 R0 101117
GCTEX-0003 Block Interface L3 ACCESS R0 101117
GCTEX-0004 Block Interface L2 ACCESS R0 101113
GCTEX-0005 Block Interface L2 R0 101117
GCTEX-0006 Stand Lens Nikon Telephoto R0 101118
GCTEX-0007 LCP04 Nikon Mount
GCTEX-0008 NFM1 Nikon F-Mount
GCTEX-0009 Plate Mounting Structural Tripod Secure R0 090811
GCTEX-0010 Plate Mounting Structural R1 101118
GCTEX-0011 Block Spacer Structure 2.5 in R0 090811
GCTEX-0012 Housing Mounting Motor Encoder BOTTOM R2 101020
GCTEX-0013 Housing Mounting Motor Encoder TOP R2 101020
GCTEX-0014 Shaft Motor Encoder R2 101020
GCTEX-0015 Plate Mounting Optical Breadboard R1 101119
GCTEX-0016 Block Interface Motor-Encoder Mockup R0 101118
GCTEX-0017 Block Mounting Interface Motor-Encoder R0 101116
GCTEX-0018 Holder Laser Telephoto Mount R0 101116
GCTEX-0019 Holder Laser Calibration R0 101119
GCTEX-0020 Cover Light L2 R0 101121
GCTEX-0023 Housing Prism Collar R0 101117
GCTEX-0024 Housing Prism Retainer R0 101117
GCTEX-0025 Ring Compression Prism Housing R0 101117
GCTEX-0026 Camera HS VR
GCTEX-0027 Lens L3 Nikon 105mm
GCTEX-0028 Lens L2 Tameron 85mm
GCTEX-0029 Lens L1 Nikon 400mm
GCTEX-0030 Z-Translator, TL SM1Z
GCTEX-0031 LCP02 Mount TL
GCTEX-0032 Rod Mount Optical, TL ER2
GCTEX-A002 ASSY GCTEx Structure (Linear) R2 101118

(continued on next page)

Fasteners:

4 each M3x0.5 x 0.25"L
6 each M4x0.7 x 0.375"L
4 each M5x0.8 x .50"L
8 each 6-32 x .50"L
4 each 8-32 x .25"L
4 each 10-24 x 1.00"L
4 each ¼-20 x 7.50"L
6 each ¼-20 x 4.00"L
4 each ¼-20 x 1.75"L
27 each ¼-20 x .50"L
2 each 5-16 x .75"L

Ensure all tools associated with this experiment/test/operation are accounted for prior to initiating system/item test. Ensure all FOD is picked up from around the assembly.

5.0

SAFETY REQUIREMENTS

5.1.

PERSONNEL PROTECTIVE CLOTHING REQUIREMENTS

Standard PPE: Safety goggles or glasses (as required), hearing protection (if required), boots – soles and heels made of semi-conductive rubber containing no nails.

All jewelry will be removed by Test Crew members while working on the test assembly. No ties or other loose clothing permitted (at TC discretion).

5.2.

TEST AREA ACCESS DURING OPERATIONS

The test facility room will be limited to test personnel only. Personnel will not be allowed access to the test area unless cleared by the TC.

5.3.

EXPLOSIVE AND PERSONNEL LIMITS

NONE

5.4.

EMERGENCY PROCEDURES

In the event of an emergency that jeopardizes the safety of the operators or other personnel perform Section 9.0 emergency procedures at the end of this document.

5.5.

SPECIAL INSTRUCTIONS

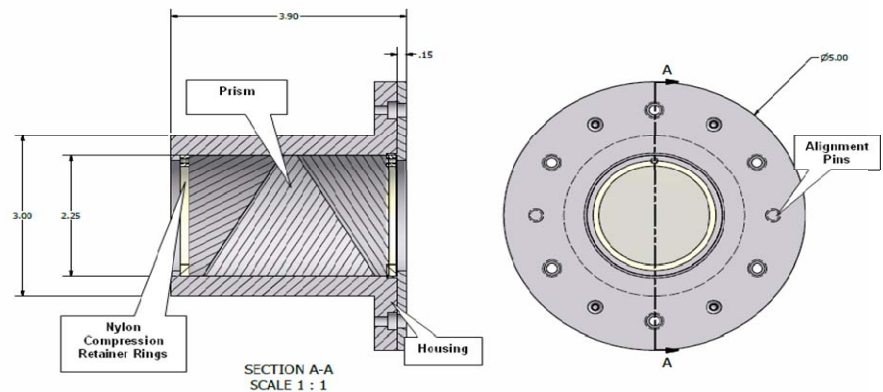
Test Crew members shall place all cellular telephones on "silent mode" or turn off prior to completing any portion of this procedure.

6.0**PRE-TEST SETUP**

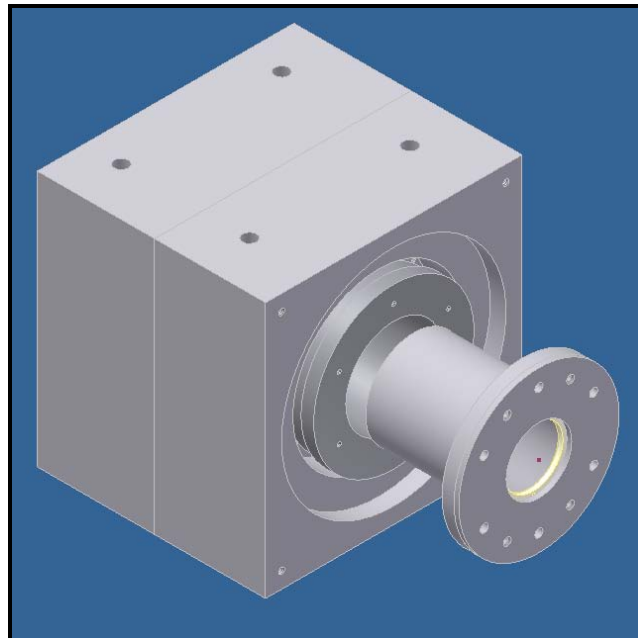
- | | | |
|-------------------|----|--|
| _____ 6.1. | TC | Verify all pages in this procedure are intact and complete |
| _____ 6.2. | TC | Go through the procedure and input any specific information required to perform operation. |
| _____ 6.3. | TC | Perform Setup Brief with Test Crew Members and note any redline changes on Attachments. |
| _____ 6.4. | TC | Verify Red Crew has donned standard PPE (and noted restrictions / special instructions). |
| _____ 6.5. | TC | Verify all personnel involved with the operation have signed this procedure. |

7.0**GCTEX ASSEMBLY****7.1.**

RC Assemble Prism into GCTEX-0023 (Housing Prism Collar R0 101117) per below drawing; Fasten/Secure GCTEX-0024 (Housing Prism Retainer R0 101117) to GCTEX-0023 (Housing Prism Collar R0 101117) with **4 each M3x0.5 x 0.25”L** fasteners and spring-washers

**7.2.**

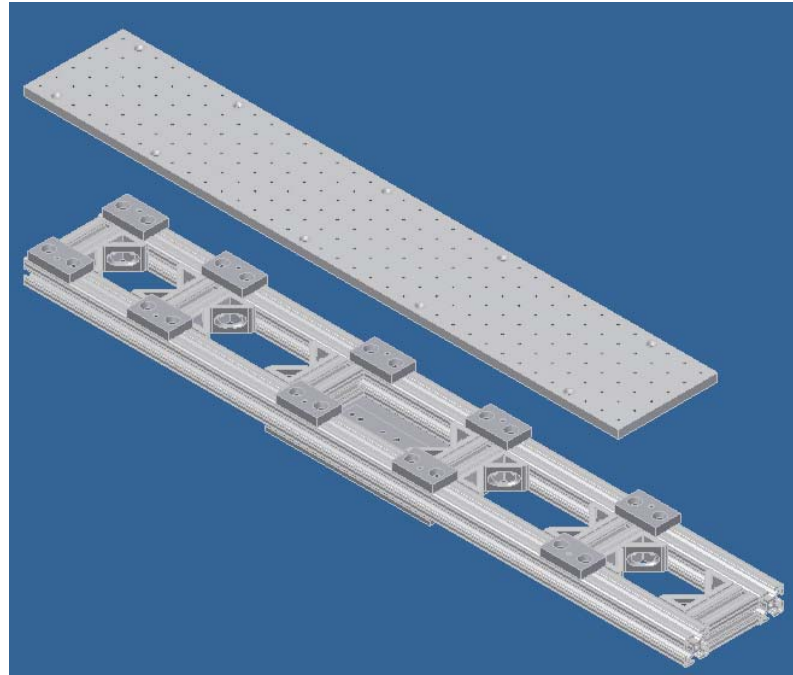
RC Fasten/Secure GCTEX-A008 (ASSY GCTEx Prism & Holder R2 101020) to GCTEX-A005 (ASSY GCTEx Motor Encoder R0 101020) with **6 each M4x0.7 x 0.375”L** fasteners and spring-washers

**7.3.**

RC Assemble GCTEX-A002 (ASSY GCTEx Structure (Linear) R2 101118) per drawing (see attachment)

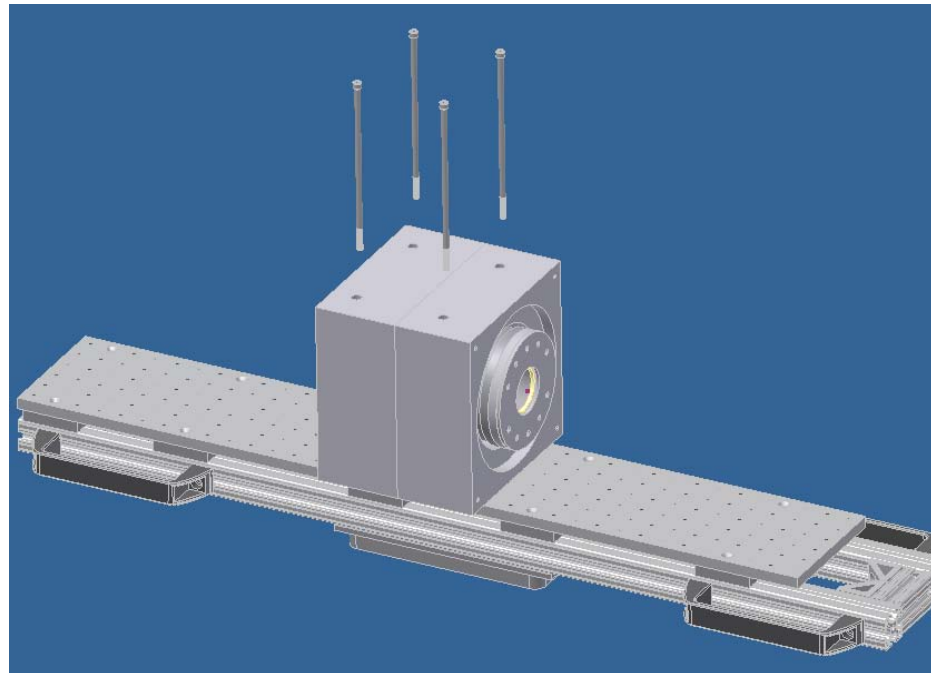
____ 7.4.

RC Fasten/Secure GCTEX-0015 (Plate Mounting Optical Breadboard R1 101119) to GCTEX-A002 (ASSY GCTEx Structure (Linear) R2 101118) with **10 each 1/4-20 x 0.50"L** fasteners



____ 7.5.

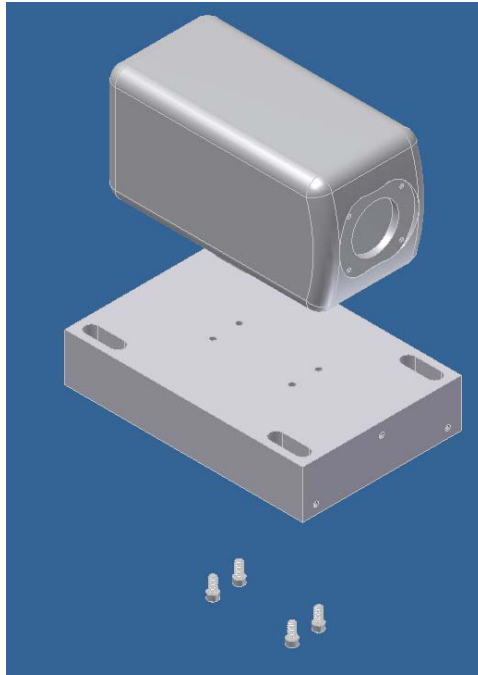
RC Fasten/Secure GCTEX-A005 (ASSY GCTEx Motor Encoder R0 101020) to GCTEX-0015 (Plate Mounting Optical Breadboard R1 101119) with **4 each 1/4-20 x 7.50"L** fasteners and spring-washers



____ 7.6.

RC

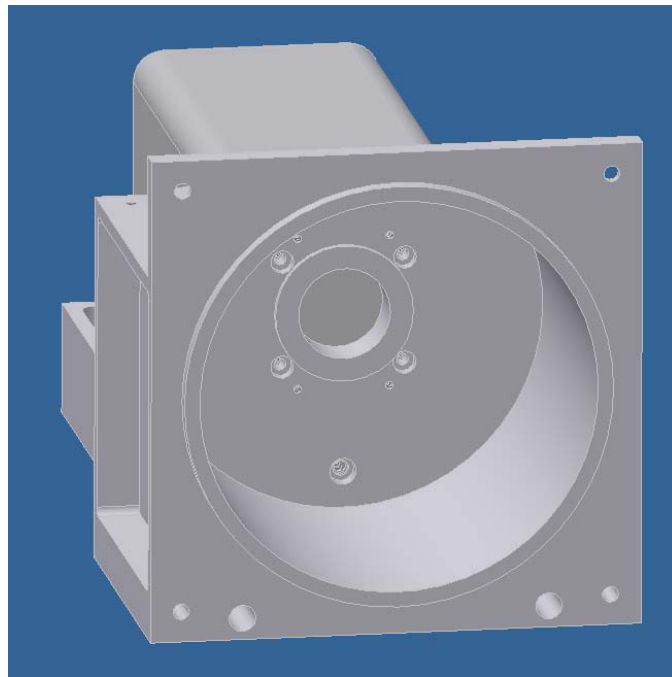
Fasten/Secure GCTEX-0026 (Camera HS VR) to GCTEX-0001 (Block Mounting Camera R2 101117) with **4 each 1/4-20 x .5"L** fasteners and spring-washers



____ 7.7.

RC

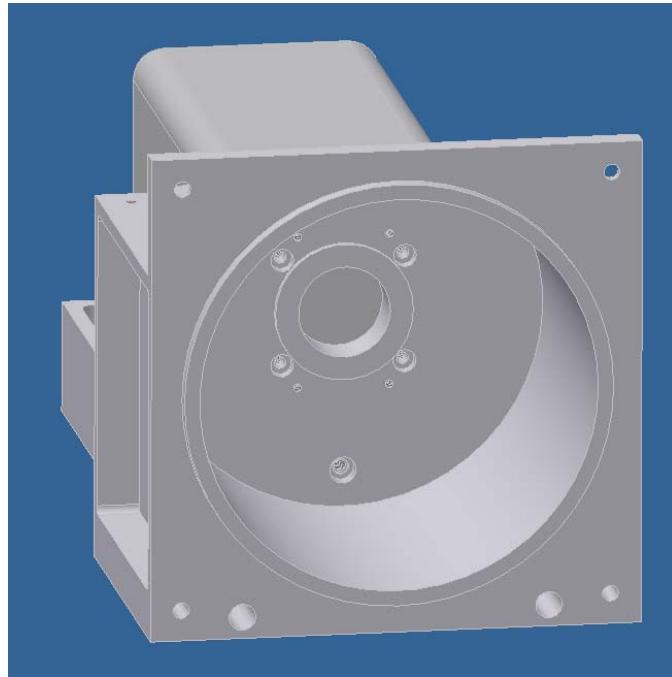
Fasten/Secure GCTEX-0002 (Block Interface L3 R0 101117) to GCTEX-0026 (Camera HS VR) with **4 each M5x0.8 x .50"L** fasteners and spring-washers



____ **7.8.**

RC

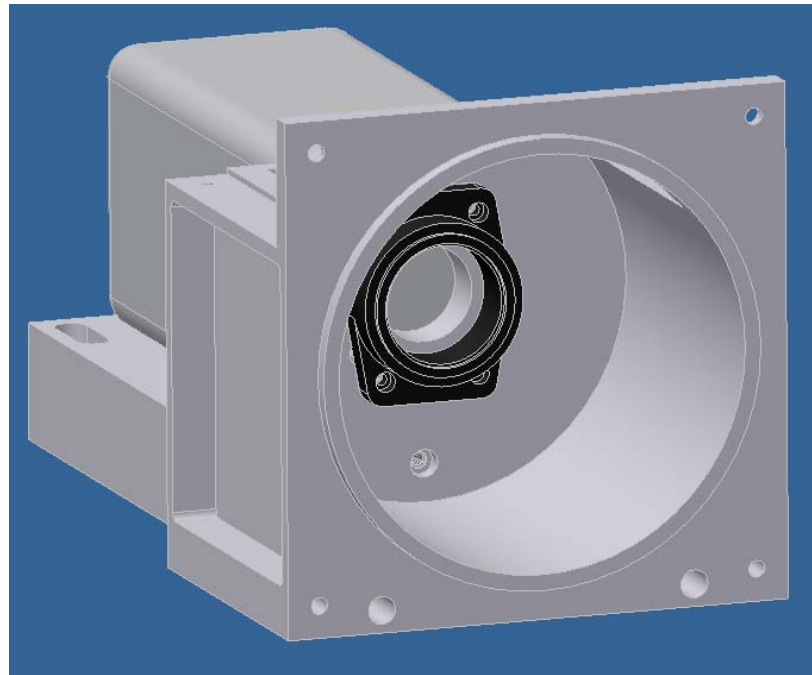
Fasten/Secure GCTEX-0002 (Block Interface L3 R0 101117) to GCTEX-0001 (Block Mounting Camera R2 101117) with **2 each 1/4-20 x 4.00"L** and **1 each 1/4-20 x .50"L** fasteners and spring-washers



____ **7.9.**

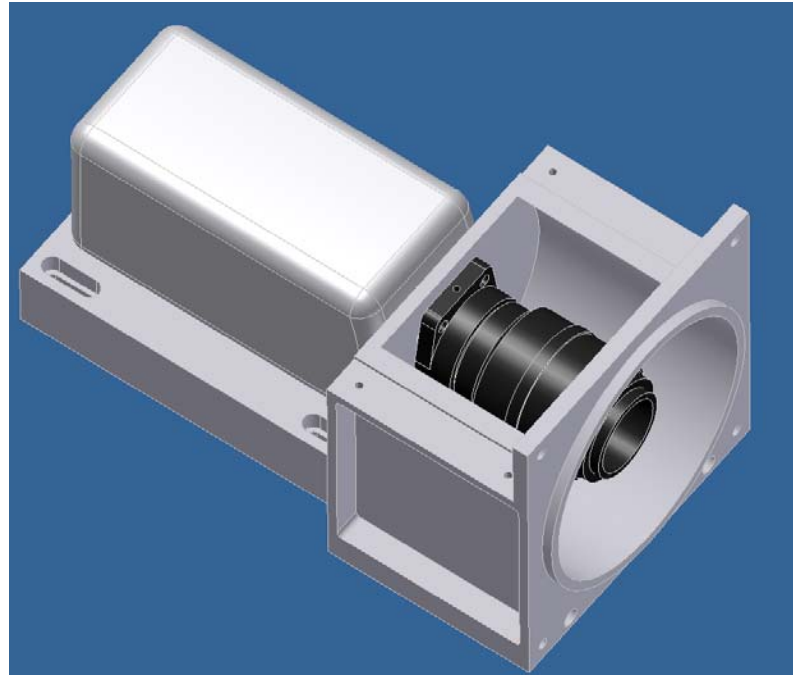
RC

Fasten/Secure GCTEX-0008 (NFM1 Nikon F-Mount) to GCTEX-0002 (Block Interface L3 R0 101117) with **4 each 10-24 x 1.00"L** fasteners and spring-washers



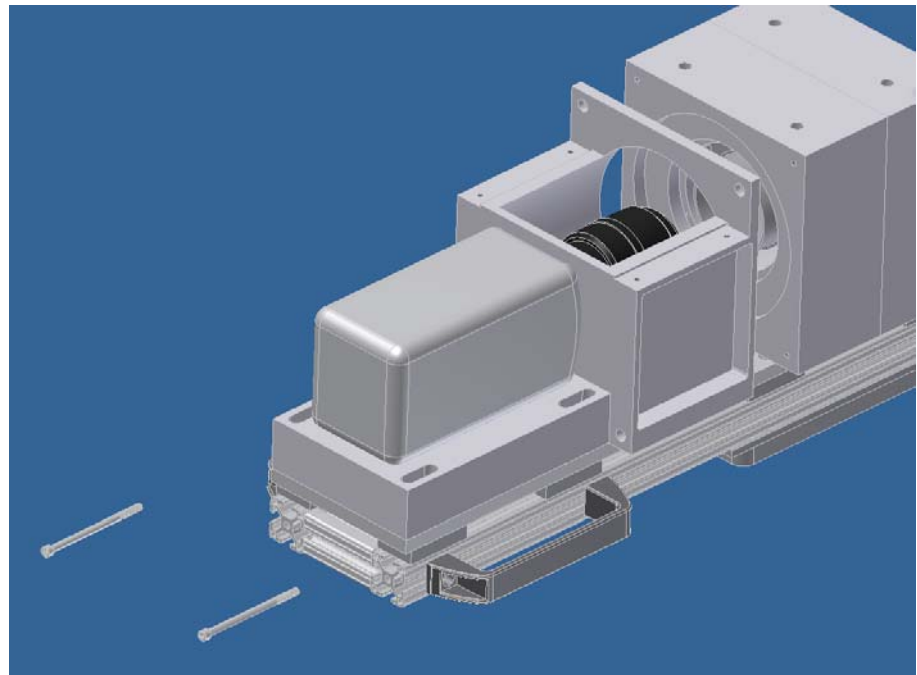
____ **7.10.**

RC Affix GCTEX-0027 (Lens L3 Nikon 105mm) to GCTEX-0008 (NFM1 Nikon F-Mount)



____ **7.11.**

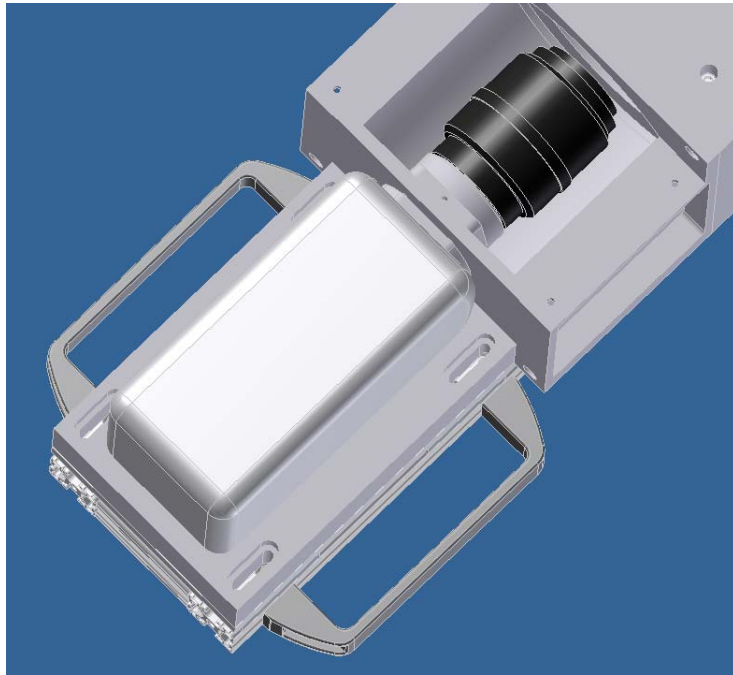
RC Fasten/Secure GCTEX-A006 (ASSY GCTEx Camera & L3 R1 101111) to GCTEX-A005 (ASSY GCTEx Motor Encoder R0 101020) with **2 each $\frac{1}{4}$ -20 x 4.00"L** and **2 each $\frac{1}{4}$ -20 x .50"L** fasteners and spring-washers



____ 7.12.

RC

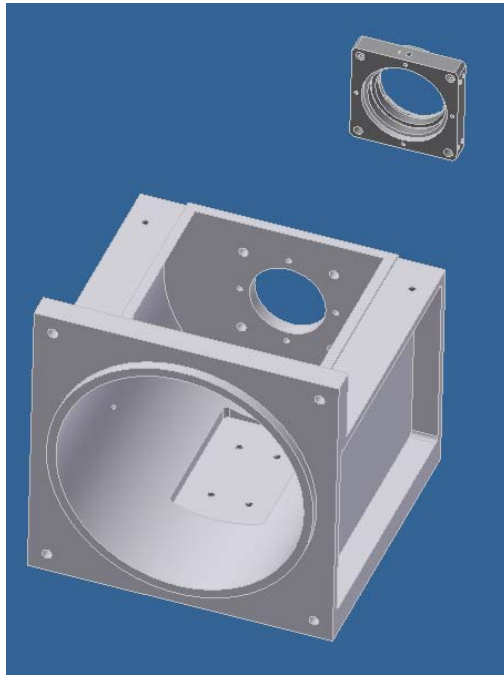
Fasten/Secure GCTEX-0001 (Block Mounting Camera R2 101117) to GCTEX-0015 (Plate Mounting Optical Breadboard R1 101119) with **4 each 1/4-20 x 1.75"L** fasteners and spring-washers



____ 7.13.

RC

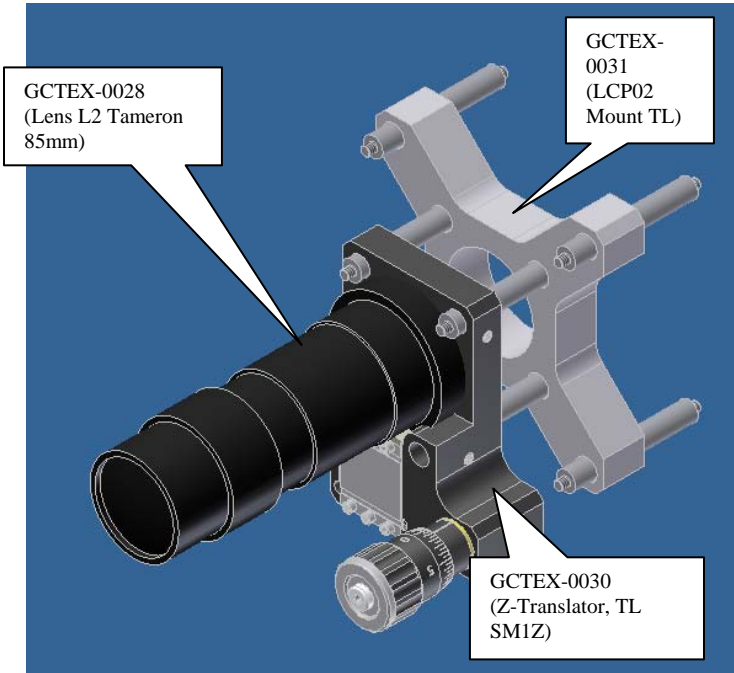
Fasten/Secure GCTEX-0007 (LCP04 Nikon Mount) to GCTEX-0005 (Block Interface L2 R0 101117) with **4 each 6-32 x .50"L** fasteners and spring-washers



7.14.

RC

Assemble GCTEX-A007 (ASSY GCTEx Lens System R1 100928)

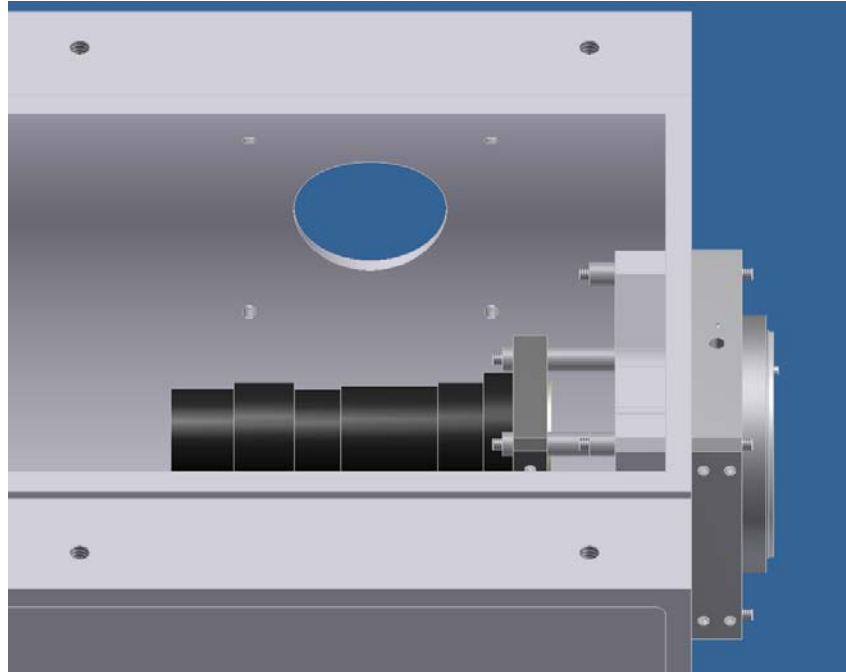


7.15.

RC

Fasten/Secure GCTEX-A007 (ASSY GCTEx Lens System R1 100928) to GCTEX-0005 (Block Interface L2 R0 101117) with **8 each GCTEX-0032 (Rod Mount Optical, TL ER2)** and **20 each 4-40 set-screws**. Note that GCTEX-0031 (LCP02 Mount TL) and GCTEX-0007 (LCP04 Nikon Mount) are mounted flush to GCTEX-0005 (Block Interface L2 R0 101117); Flange Focal Distance (FFD) must be taken into account for spacing – 64.02mm between flanges (GCTEX-0030 & GCTEX-0007).

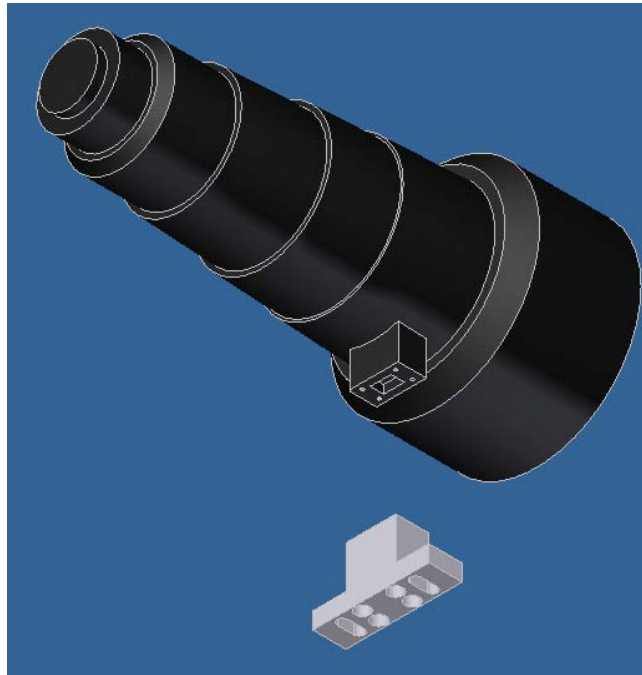
[Ref: C-Mount (17.52mm) Nikon F-Mount (46.50mm)]



____ 7.16.

RC

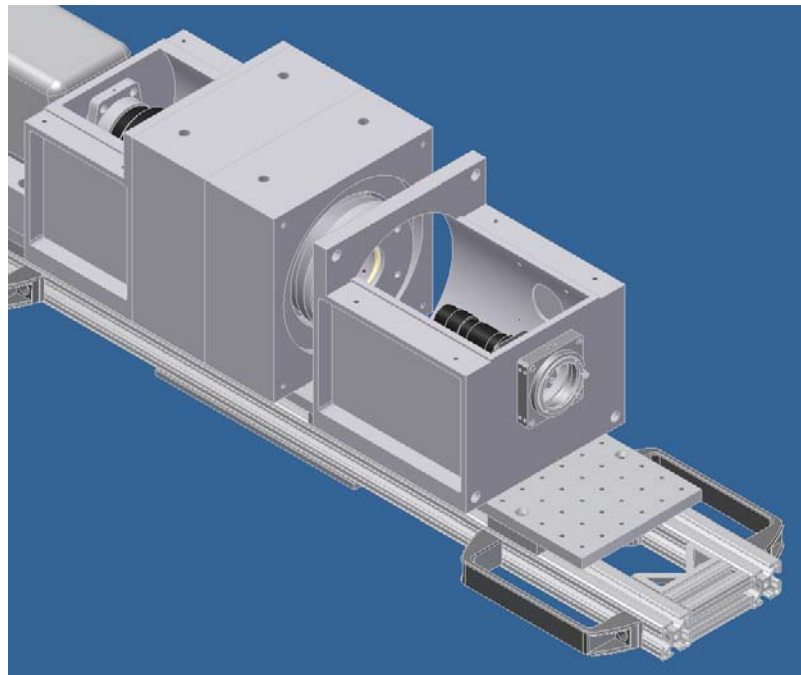
Fasten/Secure GCTEX-0006 (Stand Lens Nikon Telephoto R0 101118) to GCTEX-0029 (Lens L1 Nikon 400mm) with **4 each 6-32 x .50"L** fasteners and spring-washers



____ 7.17.

RC

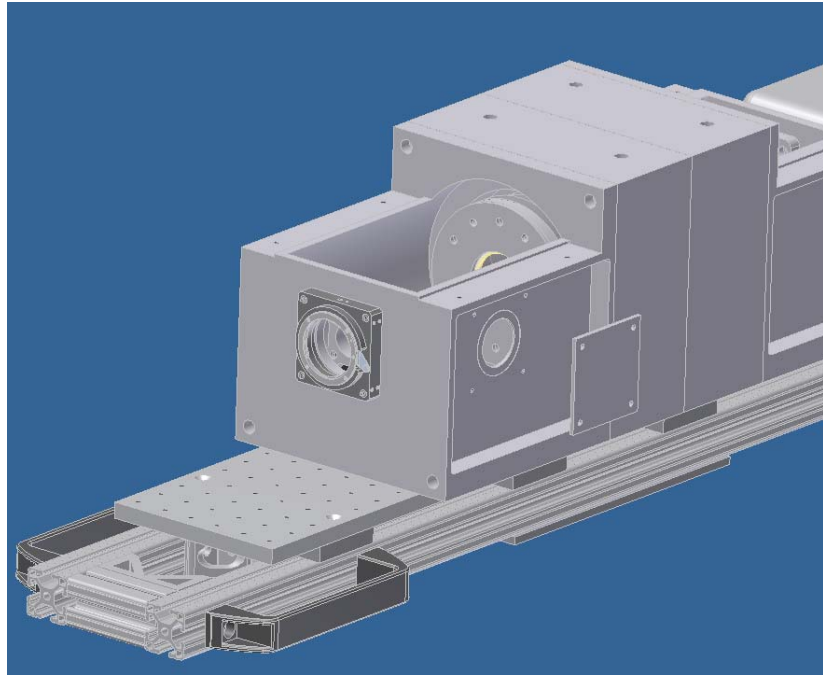
Fasten/Secure GCTEX-0005 (Block Interface L2 R0 101117) to GCTEX-A005 (ASSY GCTEx Motor Encoder R0 101020) with **2 each 1/4-20 x 4.00"L** and **2 each 1/4-20 x .50"L** fasteners and spring-washers



____ 7.18.

RC

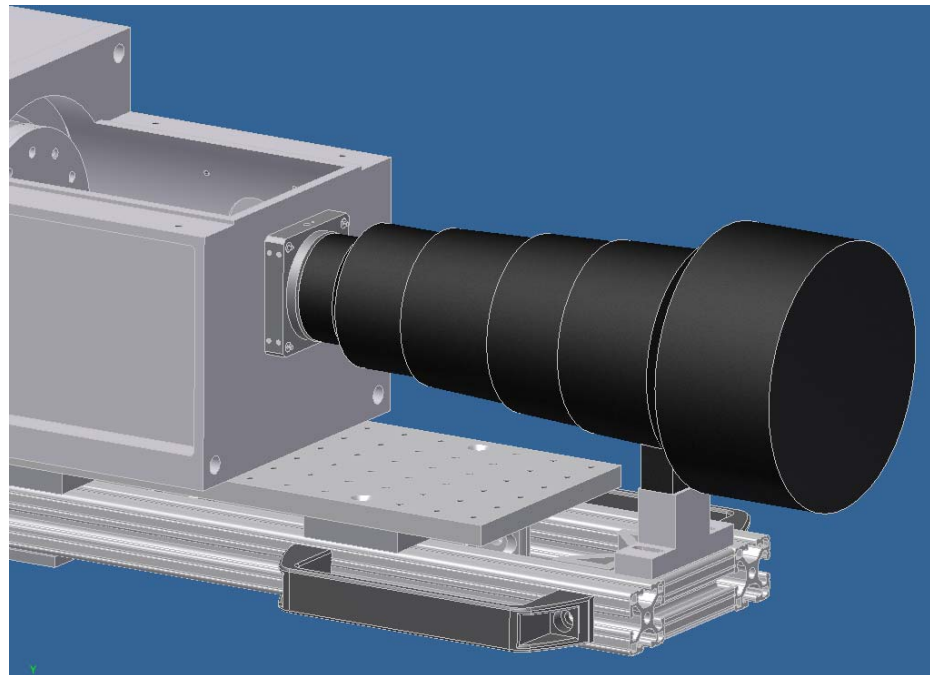
Fasten/Secure GCTEX-0020 (Cover Light L2 R0 101121) to GCTEX-0005 (Block Interface L2 R0 101117) with **4 each 8-32 x .25"L** fasteners and spring-washers



____ 7.19.

RC

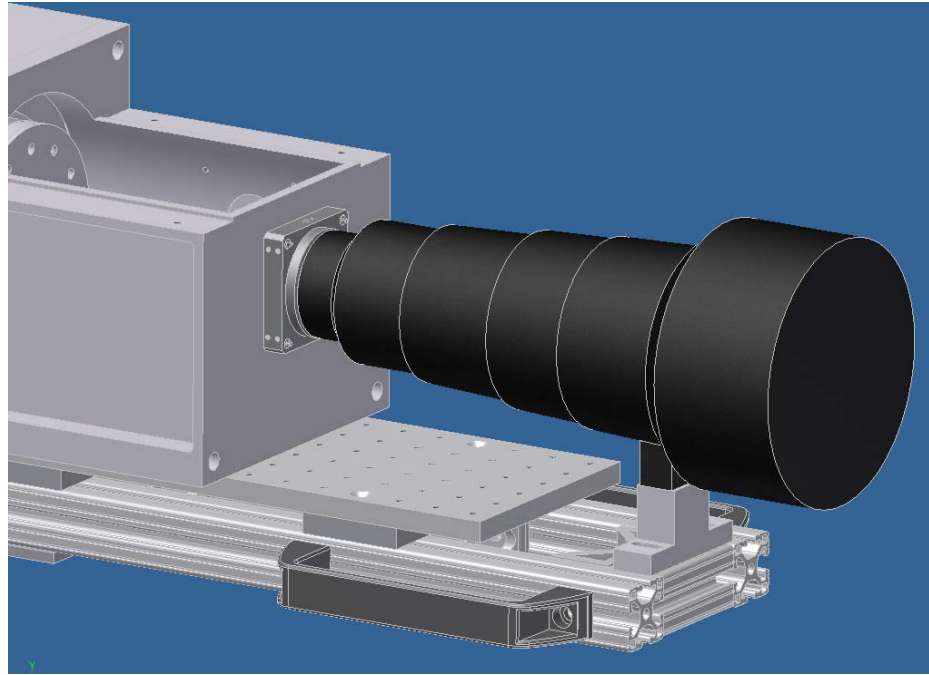
Affix GCTEX-0029 (Lens L1 Nikon 400mm) to GCTEX-0007 (LCP04 Nikon Mount)



____ **7.20.**

RC

Fasten/Secure GCTEX-0006 (Stand Lens Nikon Telephoto R0 101118) to GCTEX-A002 (ASSY GCTEx Structure (Linear) R2 101118) with **2 each 5-16 x .75"L** fasteners and spring-washers

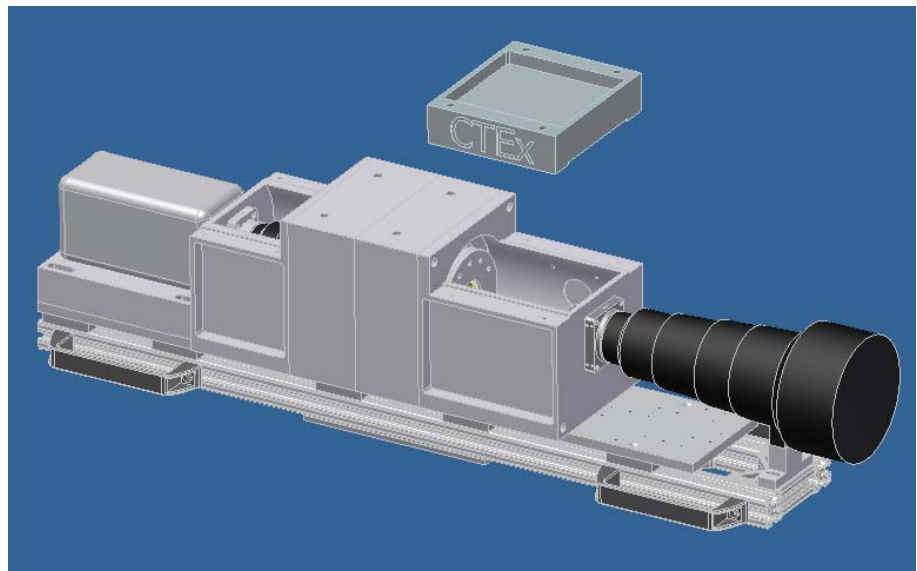


CAUTION: Do not over-torque the access-covers in the following two (2) steps

____ **7.21.**

RC

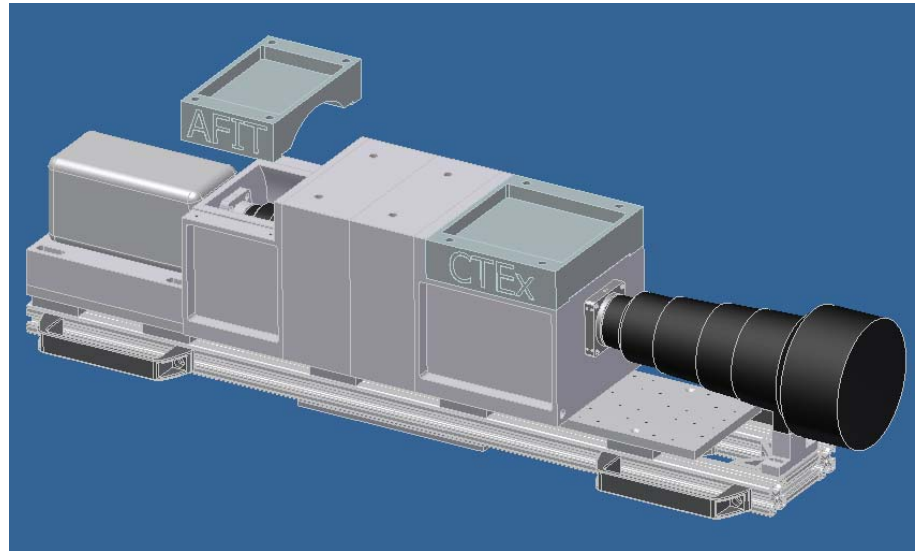
Fasten/Secure GCTEX-0004 (Block Interface L2 ACCESS R0 101113) to GCTEX-0005 (Block Interface L2 R0 101117) with **4 each 1/4-20 x .50"L** fasteners and spring-washers



____ 7.22.

RC

Fasten/Secure GCTEX-0003 (Block Interface L3 ACCESS R0 101117) to GCTEX-0002 (Block Interface L3 R0 101117) with **4 each** **1/4-20 x .50"L** fasteners and spring-washers



____ 7.23.

TC

Sign/Date to confirm assembly completion.

Procedure Completed _____ Date/Time _____

Test Conductor

END OF ASSEMBLY PROCEDURES

**GCTEX OPERATIONS
AFIT/ENY**

WRIGHT-PATTERSON AFB, OH

PROCEDURE:

REVISION:

DATE REVISED:

NUMBER OF PAGES:

SOP-GCTEX-0003

0

5 Dec 2010

22

**AFIT / ENY
GCTEx
OPERATIONS**

**GCTEx Assembly
(Motor Mock-Up)**

PREPARED BY:

Test Engineer _____
AFIT/ENY

DATE _____

REVIEW / APPROVAL:

AF Customer _____
AFIT/ENY CTEEx Thesis Advisor

DATE _____

Revision	Notes	Prepared By
0	-Initial procedure written	Capt. Niederhauser 5 Dec 10

PERSONNEL

DATE _____

The following personnel are designated as test team members, and are chartered to perform their assignment as follows:

Test Conductor (TC) – Responsible for the timely performance of the test as written. This includes coordinating and directing the activities of the Red Crew and other test support teams. TC is responsible for coordinating all pretest activities and outside support required, including (but not limited to) security, fire, medical, and safety. TC is responsible for initialing completion on each step of the master test procedure.

Name _____ Signature _____

Test Director (TD) – Responsible for overall facility and test safety. Responsible for ensuring all test goals are met and all critical data is acquired. Supervises test activities to ensure procedures are followed. Has authority to perform real-time redlines on test procedures as required to ensure test requirements and goals area met.

Name _____ Signature _____

Red Crew Leader (RC) – Responsible for directing the activities of Red Crew members. Reports directly to the TC and ensures all Red Crew tasks are completed. Responsible for ensuring all RCM's have all required certifications and training. Responsible for ensuring all required equipment is available, accessible, and serviceable.

Name _____ Signature _____

ALL TEST TEAM MEMBERS – Responsible for the safe performance of the test. Have read and understood all portions of the test procedure. Any Test Team Member can declare an emergency or unsafe condition.

1.0**ABBREVIATIONS AND ACRYONMS**

AFIT	Air Force Institute of Technology
FOD	Foreign Object Debris
HAZCOM	Hazardous Communication
PPE	Personal Protective Equipment
RC	Red Crew
RCM	Red Crew Member
STE	Special Test Equipment
TC	Test Conductor
TD	Test Director
TPO	Test Panel Operator

2.0**TEST DESCRIPTION AND OBJECTIVES****2.1.****PURPOSE**

This procedure provides the means to perform assembly upon the AFIT Chromotomography Experiment (CTEx) Ground-Based Linear design (GCTEx) as risk-reduction for a space-based version of the instrument.

3.0**DOCUMENTATION**

The completion of each applicable event shall be verified by marking to the left of the item number. Deviations from these procedures will be coordinated with the Test Conductor

3.1.**REFERENCE DOCUMENTS**

NONE

3.2.**SPECIFICATIONS**

NONE

3.3.**DRAWINGS**

GCTEX-0001 Block Mounting Camera R2 101117
 GCTEX-0002 Block Interface L3 R0 101117
 GCTEX-0003 Block Interface L3 ACCESS R0 101117
 GCTEX-0004 Block Interface L2 ACCESS R0 101113
 GCTEX-0005 Block Interface L2 R0 101117
 GCTEX-0006 Stand Lens Nikon Telephoto R0 101118
 GCTEX-0007 LCP04 Nikon Mount
 GCTEX-0008 NFM1 Nikon F-Mount
 GCTEX-0009 Plate Mounting Structural Tripod Secure R0 090811
 GCTEX-0010 Plate Mounting Structural R1 101118
 GCTEX-0011 Block Spacer Structure 2.5 in R0 090811
 GCTEX-0012 Housing Mounting Motor Encoder BOTTOM R2 101020
 GCTEX-0013 Housing Mounting Motor Encoder TOP R2 101020
 GCTEX-0014 Shaft Motor Encoder R2 101020
 GCTEX-0015 Plate Mounting Optical Breadboard R1 101119
 GCTEX-0016 Block Interface Motor-Encoder Mockup R0 101118
 GCTEX-0017 Block Mounting Interface Motor-Encoder R0 101116
 GCTEX-0018 Holder Laser Telephoto Mount R0 101116
 GCTEX-0019 Holder Laser Calibration R0 101119
 GCTEX-0020 Cover Light L2 R0 101121
 GCTEX-A002 ASSY GCTEx Structure (Linear) R2 101118

4.0**TEST REQUIREMENTS AND RESTRICTIONS****4.1.****TRAINING**

The following training is required for personnel using these procedures:

All personnel:

Job Site HAZCOM

4.2.**LIST OF EQUIPMENT**

GCTEX-0001 Block Mounting Camera R2 101117
 GCTEX-0002 Block Interface L3 R0 101117
 GCTEX-0003 Block Interface L3 ACCESS R0 101117
 GCTEX-0004 Block Interface L2 ACCESS R0 101113
 GCTEX-0005 Block Interface L2 R0 101117
 GCTEX-0006 Stand Lens Nikon Telephoto R0 101118
 GCTEX-0007 LCP04 Nikon Mount
 GCTEX-0008 NFM1 Nikon F-Mount
 GCTEX-0009 Plate Mounting Structural Tripod Secure R0 090811
 GCTEX-0010 Plate Mounting Structural R1 101118
 GCTEX-0011 Block Spacer Structure 2.5 in R0 090811
 GCTEX-0012 Housing Mounting Motor Encoder BOTTOM R2 101020
 GCTEX-0013 Housing Mounting Motor Encoder TOP R2 101020
 GCTEX-0014 Shaft Motor Encoder R2 101020
 GCTEX-0015 Plate Mounting Optical Breadboard R1 101119
 GCTEX-0016 Block Interface Motor-Encoder Mockup R0 101118
 GCTEX-0017 Block Mounting Interface Motor-Encoder R0 101116
 GCTEX-0018 Holder Laser Telephoto Mount R0 101116
 GCTEX-0019 Holder Laser Calibration R0 101119
 GCTEX-0020 Cover Light L2 R0 101121
 GCTEX-0023 Housing Prism Collar R0 101117
 GCTEX-0024 Housing Prism Retainer R0 101117
 GCTEX-0025 Ring Compression Prism Housing R0 101117
 GCTEX-0026 Camera HS VR
 GCTEX-0027 Lens L3 Nikon 105mm
 GCTEX-0028 Lens L2 Tameron 85mm
 GCTEX-0029 Lens L1 Nikon 400mm
 GCTEX-0030 Z-Translator, TL SM1Z
 GCTEX-0031 LCP02 Mount TL
 GCTEX-0032 Rod Mount Optical, TL ER2
 GCTEX-0033 Retainer Prism R0 090811
 GCTEX-0034 Retainer Compression Prism R0 090811
 GCTEX-0035 Housing Prism R0 090811
 GCTEX-0036 Prism R0 090811
 GCTEX-0037 Holder Prism R0 090811
 GCTEX-A002 ASSY GCTEx Structure (Linear) R2 101118
 GCTEX-A004 ASSY GCTEx Motor Encoder (MOCKUP) R0 101204
 GCTEX-A006 ASSY GCTEx Camera & L3 R1 101111
 GCTEX-A007 ASSY GCTEx Lens System R1 100928
 GCTEX-A008 ASSY GCTEx Prism & Holder R2 101020
 GCTEX-A009 ASSY GCTEx Prism R1 100810
 GCTEX-A010 ASSY Laser Calibration Holder R0 101116

GCTEX-A011 ASSY Mirror Turning
 GCTEX-A013 ASSY GCTEx Prism R0 090811
 GCTEX-A014 ASSY GCTEx Motor Encoder R0 090811

Fasteners:

4 each M3x0.5 x 0.25"L
 8 each M4x0.7 x 0.375"L
 4 each M5x0.8 x .50"L
 8 each 6-32 x .50"L
 4 each 8-32 x .25"L
 4 each 10-24 x 1.00"L
 4 each ¼-20 x 1.75"L
 8 each ¼-20 x 2.00"L
 4 each ¼-20 x 3.00"L
 4 each ¼-20 x 0.25"L
 6 each ¼-20 x 4.00"L
 31 each ¼-20 x .50"L
 2 each 5-16 x .75"L

Ensure all tools associated with this experiment/test/operation are accounted for prior to initiating system/item test. Ensure all FOD is picked up from around the assembly area.

5.0

SAFETY REQUIREMENTS

5.1.

PERSONNEL PROTECTIVE CLOTHING REQUIREMENTS

Standard PPE: Safety goggles or glasses (as required), hearing protection (if required), boots – soles and heels made of semi-conductive rubber containing no nails. All jewelry will be removed by Test Crew members while working on the assembly. No ties or other loose clothing permitted (at TC discretion).

5.2.

TEST AREA ACCESS DURING OPERATIONS

The test facility room will be limited to test personnel only. Personnel will not be allowed access to the test area unless cleared by the TC.

5.3.

EXPLOSIVE AND PERSONNEL LIMITS

NONE

5.4.

EMERGENCY PROCEDURES

In the event of an emergency that jeopardizes the safety of the operators or other personnel perform Section 9.0 emergency procedures at the end of this document.

5.5.

SPECIAL INSTRUCTIONS

Test Crew members shall place all cellular telephones on "silent mode" or turn off prior to completing any portion of this procedure.

6.0**PRE-TEST SETUP**

- | | | |
|-------------------|----|--|
| _____ 6.1. | TC | Verify all pages in this procedure are intact and complete |
| _____ 6.2. | TC | Go through the procedure and input any specific information required to perform operation. |
| _____ 6.3. | TC | Perform Setup Brief with Test Crew Members and note any redline changes on Attachments. |
| _____ 6.4. | TC | Verify Red Crew has donned standard PPE (and noted restrictions / special instructions). |
| _____ 6.5. | TC | Verify all personnel involved with the operation have signed this procedure. |

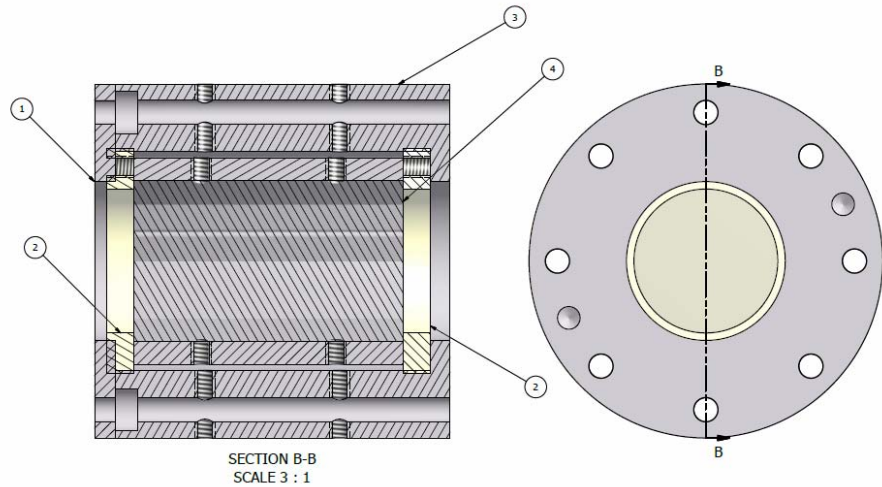
7.0

7.1.

RC

GCTEX ASSEMBLY

Assemble Prism into GCTEX-0023 (Housing Prism Collar R0 101117) per below drawing; Fasten/Secure GCTEX-0024 (Housing Prism Retainer R0 101117) to GCTEX-0023 (Housing Prism Collar R0 101117) with **4 each M3x0.5 x 0.25”L** fasteners and spring-washers



SECTION B-B
SCALE 3 : 1

PARTS LIST		
ITEM	QTY	PART NUMBER
1	1	Retainer Prism R0 090811
2	2	Retainer Compression Prism R0 090811
3	1	Housing Prism R0 090811
4	1	Prism R0 090811
5	2	Holder Prism R0 090811

7.2.

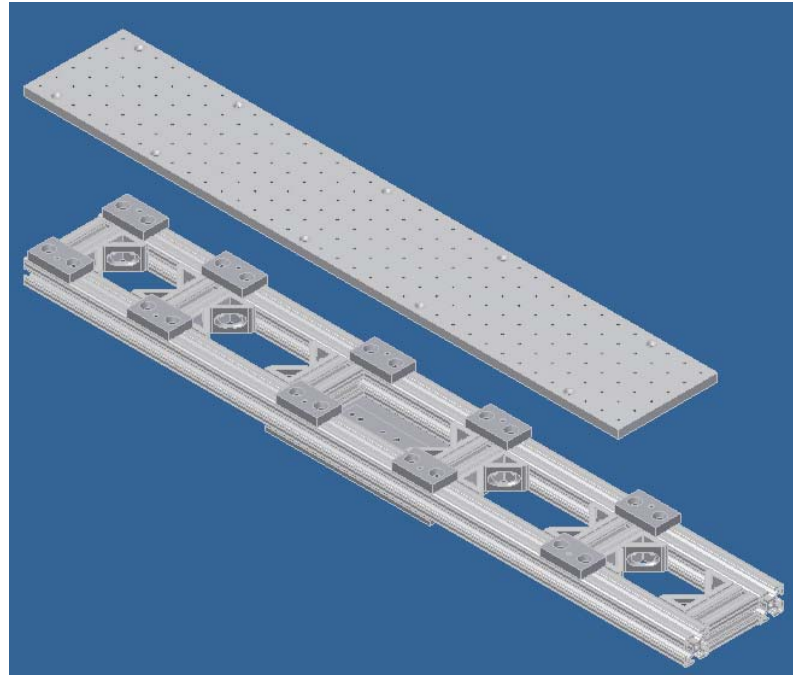
RC

Assemble GCTEX-A002 (ASSY GCTEx Structure (Linear) R2 101118) per drawing (see attachment)

____ **7.3.**

RC

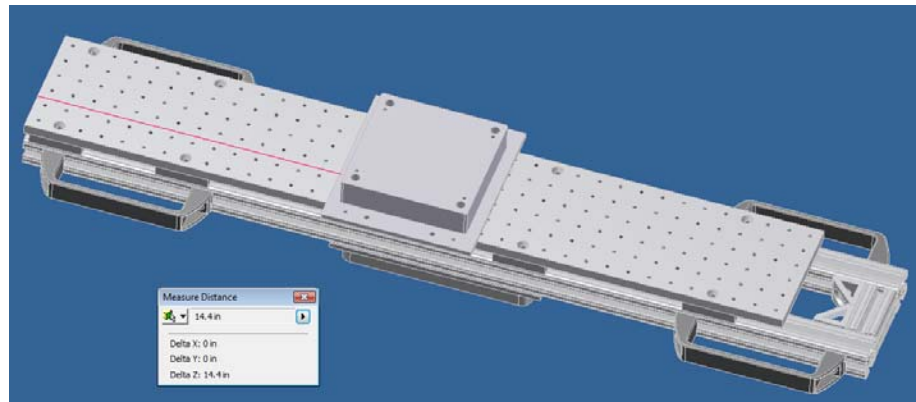
Fasten/Secure GCTEX-0015 (Plate Mounting Optical Breadboard R1 101119) to GCTEX-A002 (ASSY GCTEx Structure (Linear) R2 101118) with **10 each 1/4-20 x 0.50"L** fasteners



____ **7.4.**

RC

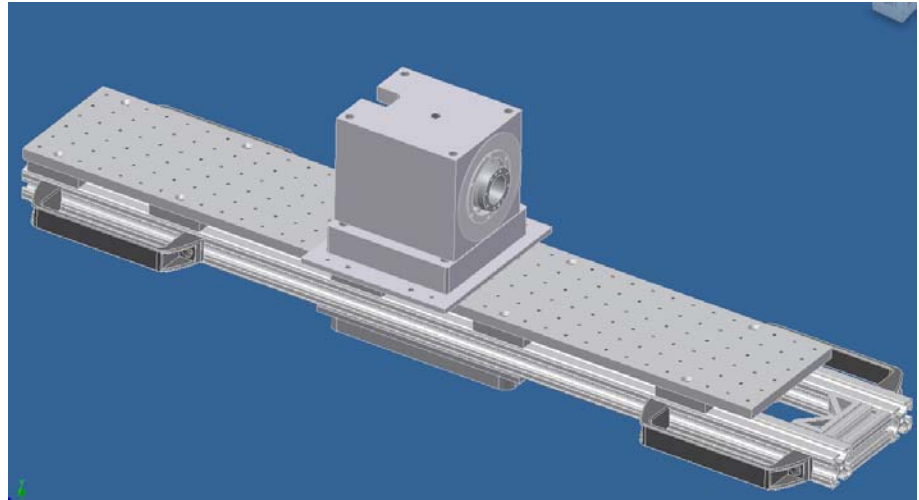
Fasten/Secure GCTEX-0017 (Block Mounting Interface Motor-Encoder R0 101116) to GCTEX-0015 (Plate Mounting Optical Breadboard R1 101119) approximately 14.4 inches from the rear of the instrument, with **4 each 1/4-20 x .50"L** fasteners and spring-washers



____ 7.5.

RC

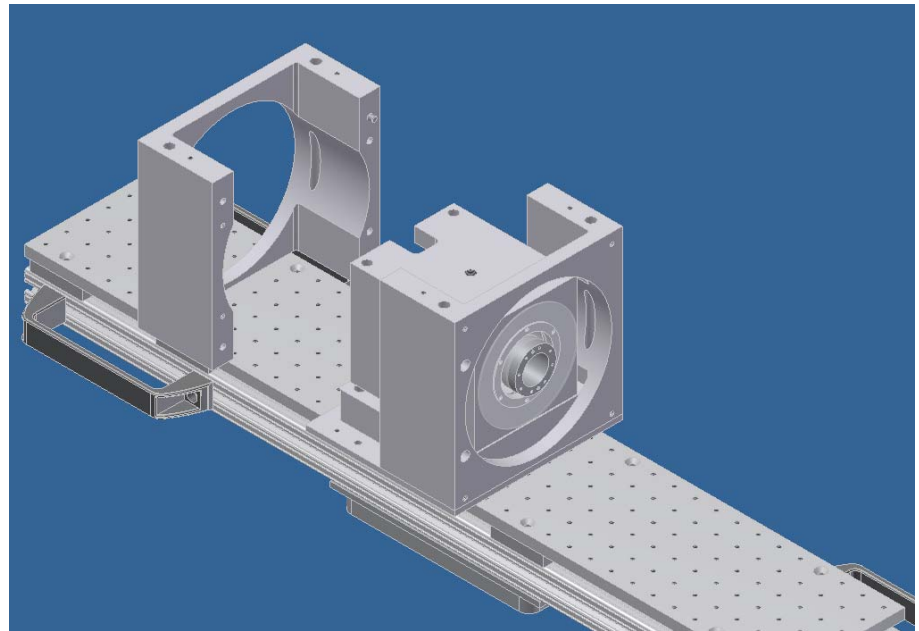
Fasten/Secure GCTEX-A014 (ASSY GCTEx Motor Encoder R0 090811) to GCTEX-0017 (Block Mounting Interface Motor-Encoder R0 101116) with **4 each 1/4-20 x 3.00"L** fasteners and spring-washers



____ 7.6.

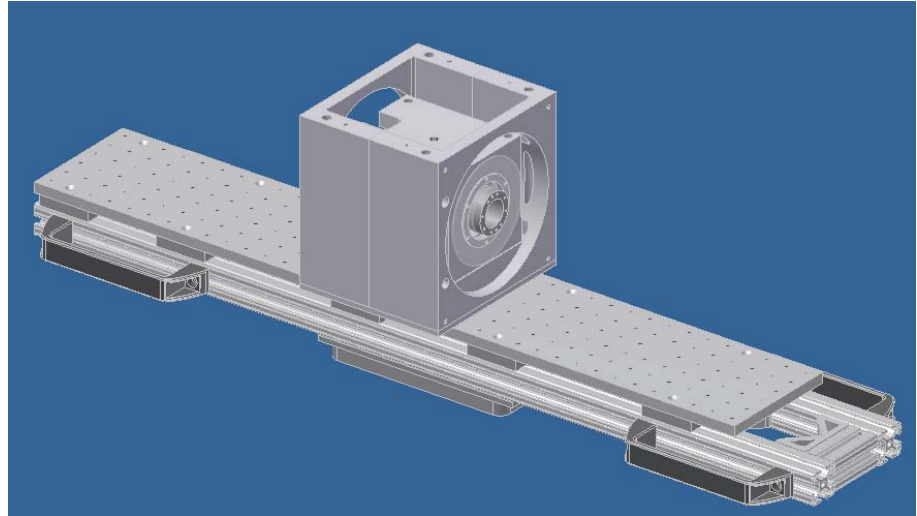
RC

Fasten/Secure GCTEX-0016 (Block Interface Motor-Encoder Mockup R0 101118) to GCTEX-0016 (Block Interface Motor-Encoder Mockup R0 101118) with **4 each 1/4-20 x 2.00"L** fasteners and spring-washers



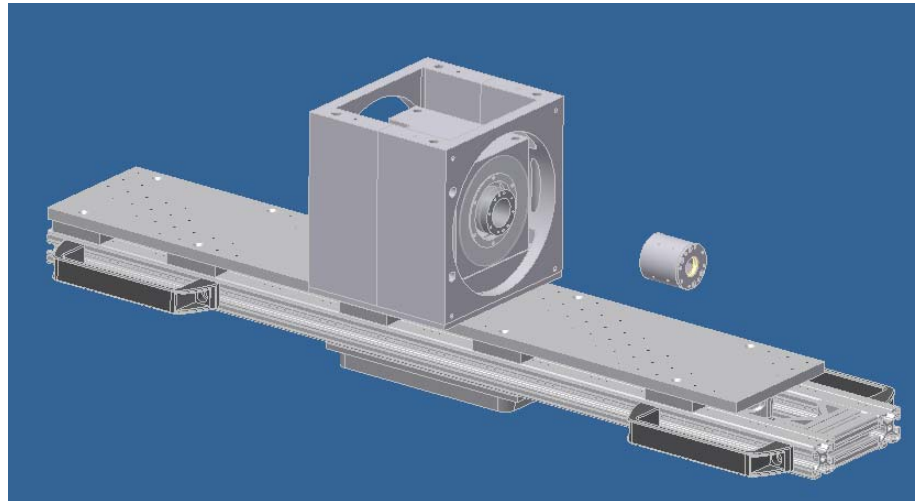
____ 7.7.

RC Fasten/Secure GCTEX-0016 (Block Interface Motor-Encoder Mockup R0 101118) to GCTEX-0015 (Plate Mounting Optical Breadboard R1 101119) with **4 each 1/4-20 x 2.00" L** fasteners and spring-washers



____ 7.8.

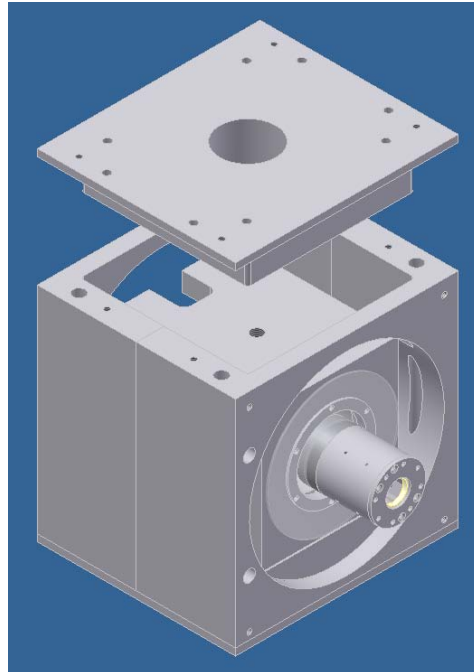
RC Fasten/Secure GCTEX-A013 (ASSY GCTEx Prism R0 090811) to GCTEX-A014 (ASSY GCTEx Motor Encoder R0 090811) with **8 each M4x0.7 x 0.375" L** fasteners and spring-washers



____ 7.9.

RC

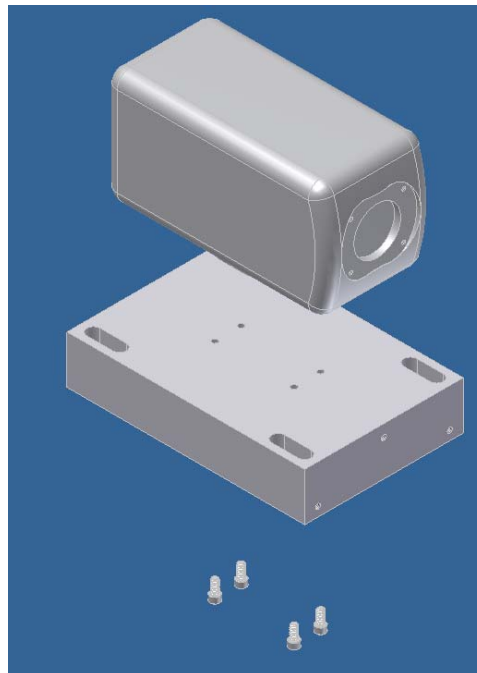
Fasten/Secure GCTEX-0041 (Block Mounting Interface Motor-Encoder R0 101116) to GCTEX-A004 (ASSY GCTEx Motor Encoder (MOCKUP) R0 101204) with **4 each 1/4-20 x 0.25"L** fasteners and spring-washers; Note that wiring for GCTEX-A014 (ASSY GCTEx Motor Encoder R0 090811) needs to be routed through the 2.00-inch port in GCTEX-0017.



____ 7.10.

RC

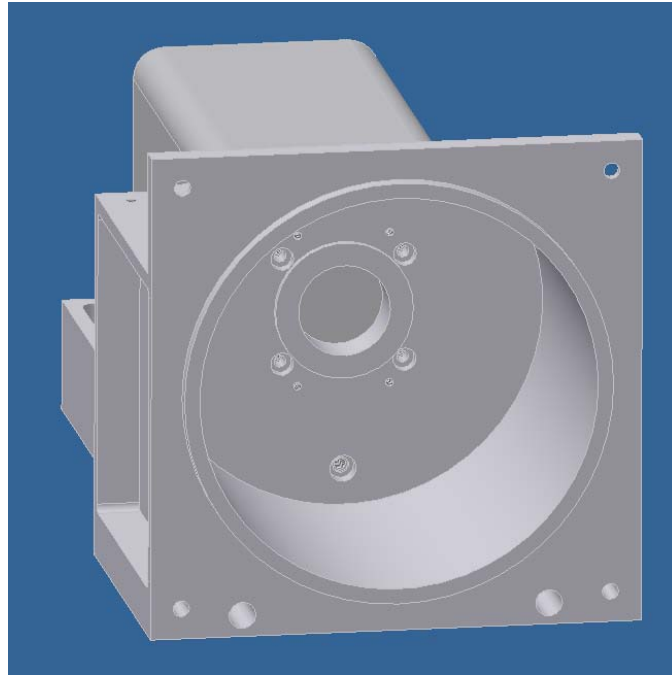
Fasten/Secure GCTEX-0026 (Camera HS VR) to GCTEX-0001 (Block Mounting Camera R2 101117) with **4 each M5x0.80x.375L"** fasteners and spring-washers



____ 7.11.

RC

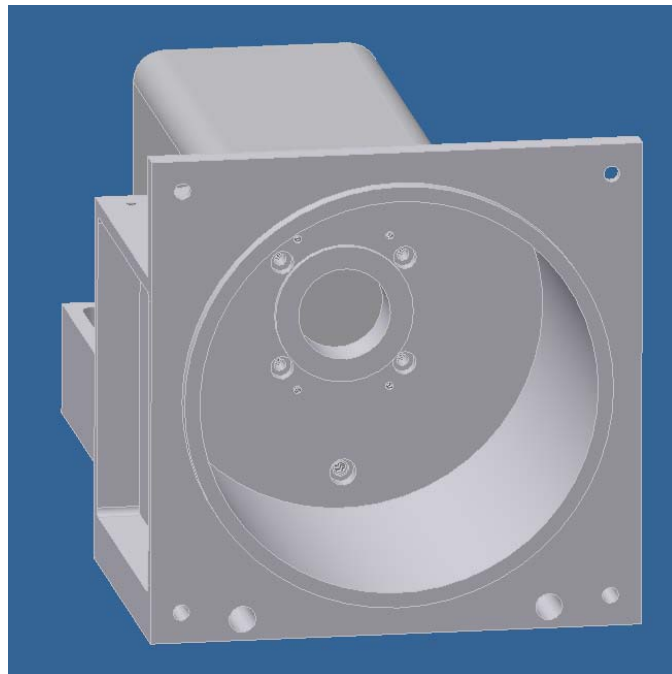
Fasten/Secure GCTEX-0002 (Block Interface L3 R0 101117) to GCTEX-0026 (Camera HS VR) with **4 each 8-32 x 0.50"L** fasteners and spring-washers



____ 7.12.

RC

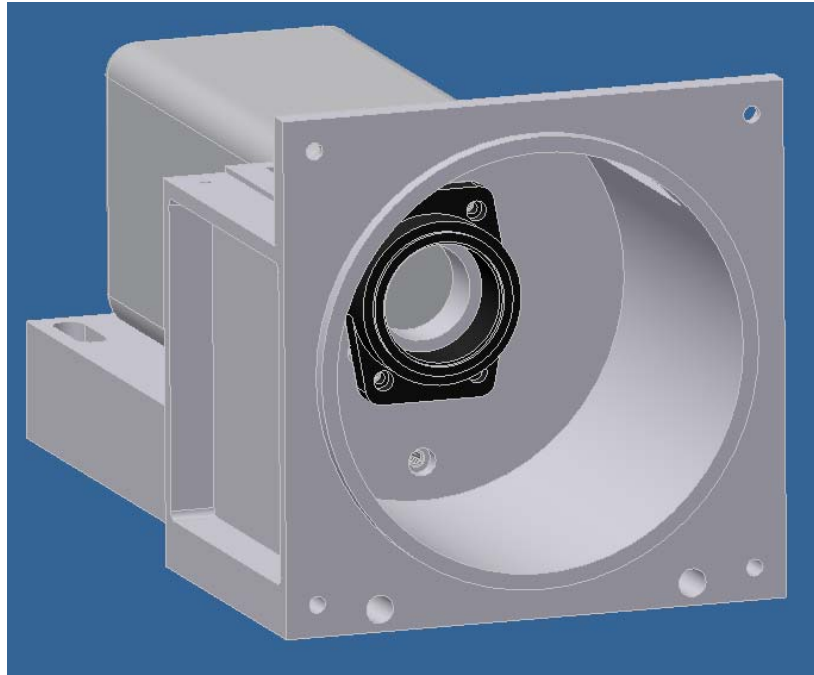
Fasten/Secure GCTEX-0002 (Block Interface L3 R0 101117) to GCTEX-0001 (Block Mounting Camera R2 101117) with **2 each 1/4-20 x 4.00"L** and **1 each 1/4-20 x .50"L** fasteners and spring-washers



____ 7.13.

RC

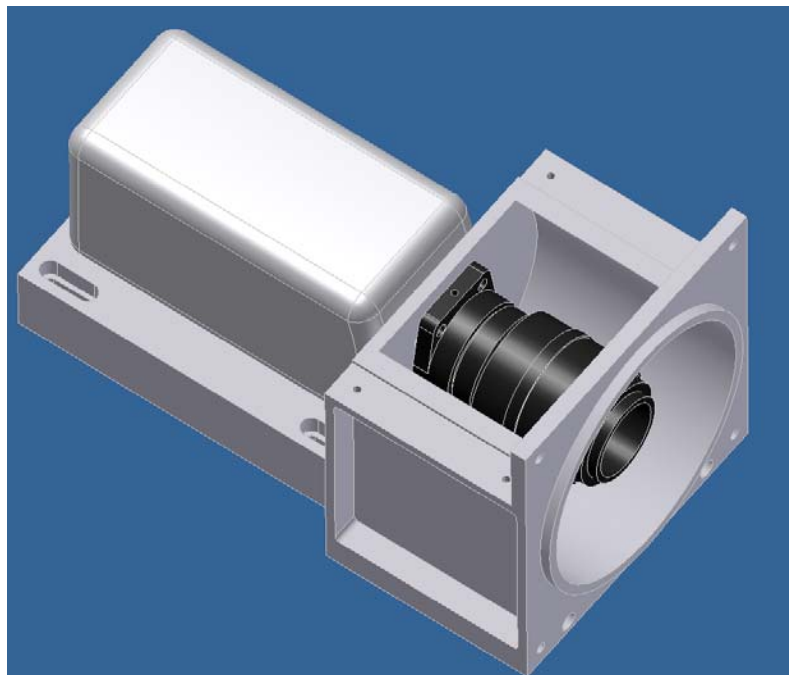
Fasten/Secure GCTEX-0008 (NFM1 Nikon F-Mount) to GCTEX-0002 (Block Interface L3 R0 101117) with **4 each 10-24 x 1.00”L** fasteners and spring-washers



____ 7.14.

RC

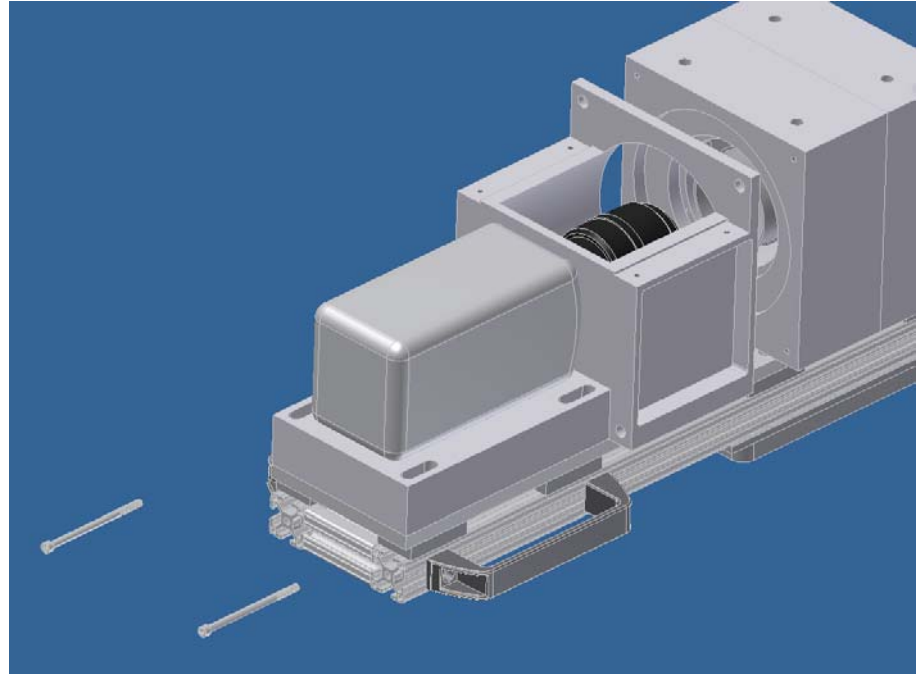
Affix GCTEX-0027 (Lens L3 Nikon 105mm) to GCTEX-0008 (NFM1 Nikon F-Mount)



____ 7.15.

RC

Fasten/Secure GCTEX-A006 (ASSY GCTEx Camera & L3 R1 101111) to GCTEX-A005 (ASSY GCTEx Motor Encoder R0 101020) with **2 each 1/4-20 x 4.00"L** and **2 each 1/4-20 x .50"L** fasteners and spring-washers



____ 7.16.

RC

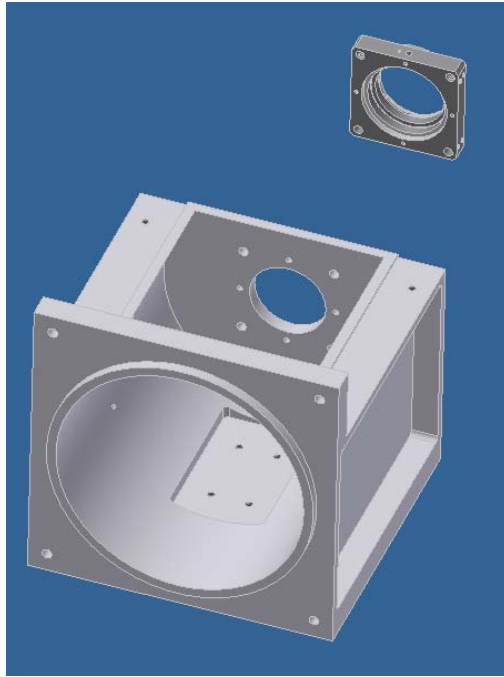
Fasten/Secure GCTEX-0001 (Block Mounting Camera R2 101117) to GCTEX-0015 (Plate Mounting Optical Breadboard R1 101119) with **4 each 1/4-20 x 1.75"L** fasteners and spring-washers



7.17.

RC

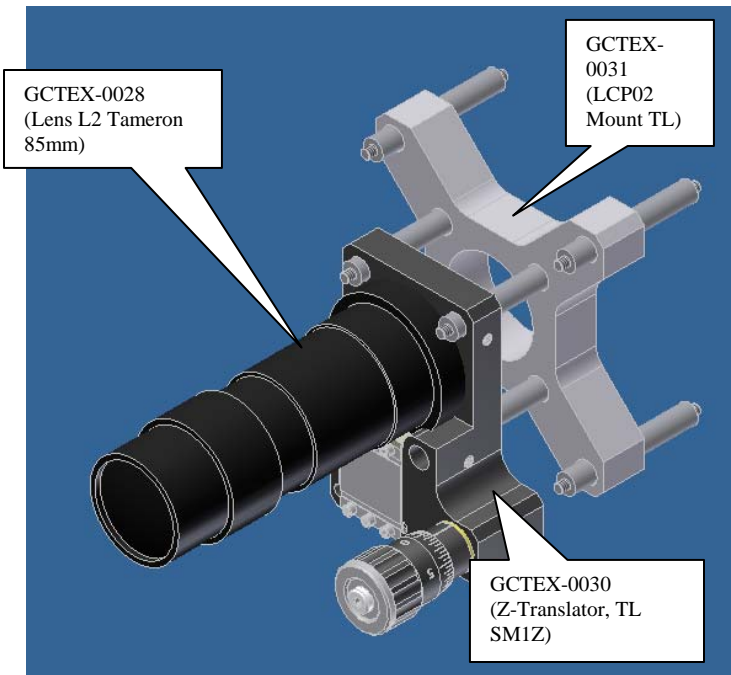
Fasten/Secure GCTEX-0007 (LCP04 Nikon Mount) to GCTEX-0005 (Block Interface L2 R0 101117) with **4 each 6-32 x .50"L** fasteners and spring-washers



7.18.

RC

Assemble GCTEX-A007 (ASSY GCTEx Lens System R1 100928)

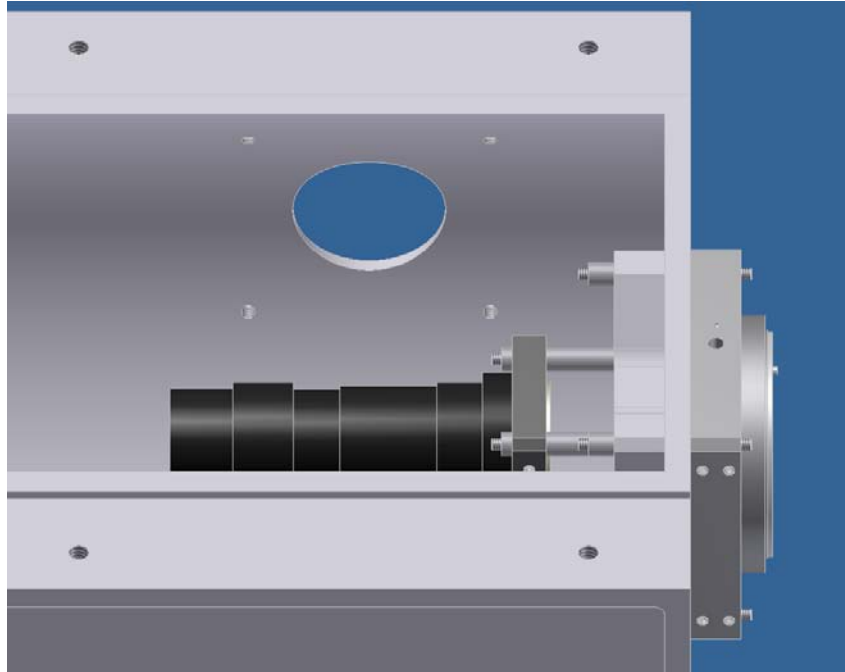


7.19.

RC

Fasten/Secure GCTEX-A007 (ASSY GCTEx Lens System R1 100928) to GCTEX-0005 (Block Interface L2 R0 101117) with **8 each GCTEX-0032 (Rod Mount Optical, TL ER2)** and **20 each 4-40 set-screws**. Note that GCTEX-0031 (LCP02 Mount TL) and GCTEX-0007 (LCP04 Nikon Mount) are mounted flush to GCTEX-0005 (Block Interface L2 R0 101117); Flange Focal Distance (FFD) must be taken into account for spacing – 64.02mm between flanges (GCTEX-0030 & GCTEX-0007).

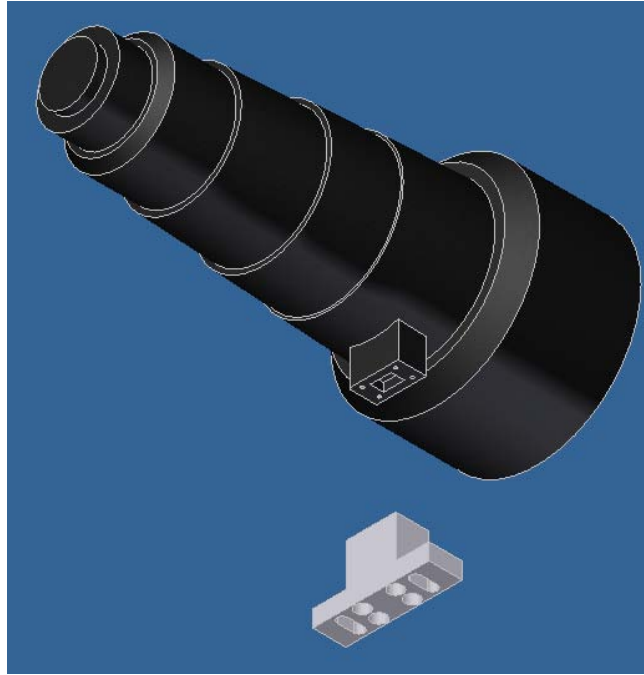
[Ref: C-Mount (17.52mm) Nikon F-Mount (46.50mm)]



____ **7.20.**

RC

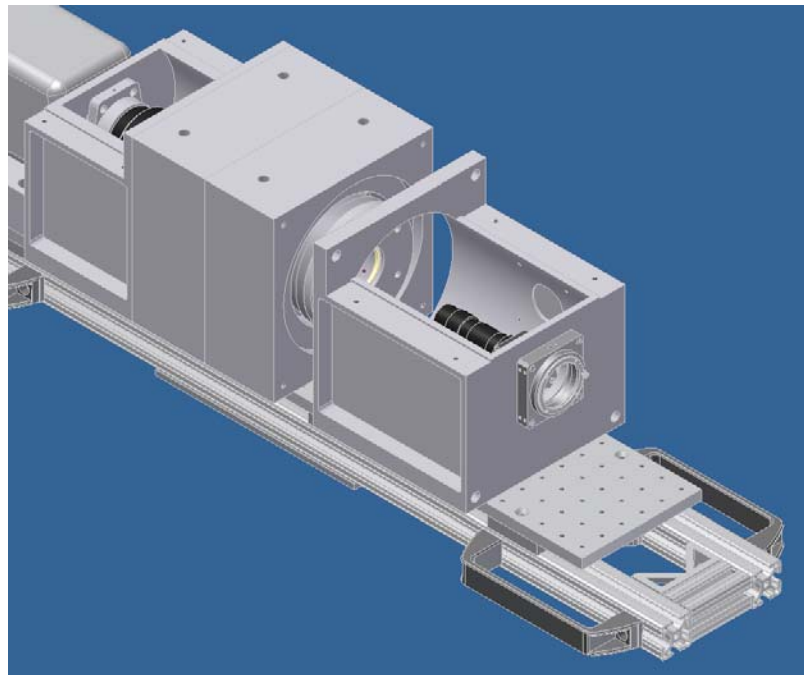
Fasten/Secure GCTEX-0006 (Stand Lens Nikon Telephoto R0 101118) to GCTEX-0029 (Lens L1 Nikon 400mm) with **4 each 6-32 x .50"L** fasteners and spring-washers



____ **7.21.**

RC

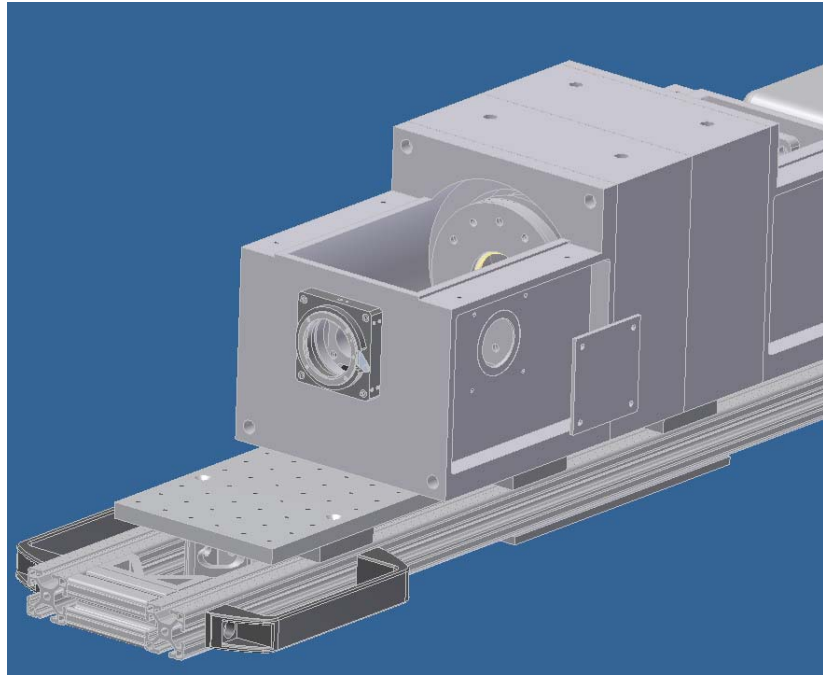
Fasten/Secure GCTEX-0005 (Block Interface L2 R0 101117) to GCTEX-A005 (ASSY GCTEx Motor Encoder R0 101020) with **2 each 1/4-20 x 4.00"L** and **2 each 1/4-20 x .50"L** fasteners and spring-washers



____ **7.22.**

RC

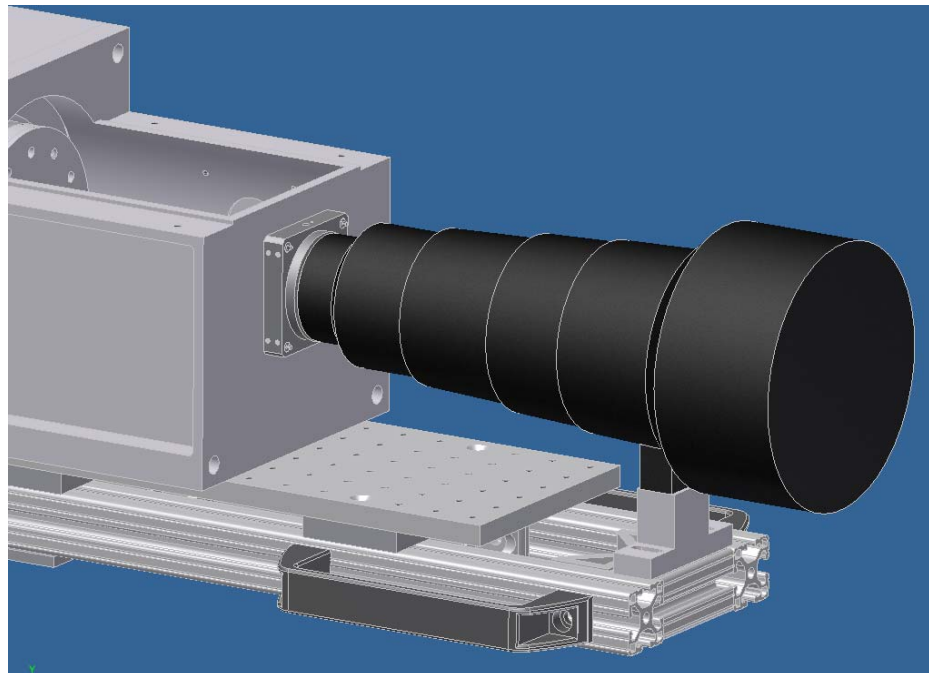
Fasten/Secure GCTEX-0020 (Cover Light L2 R0 101121) to GCTEX-0005 (Block Interface L2 R0 101117) with **4 each 8-32 x .25"L** fasteners and spring-washers



____ **7.23.**

RC

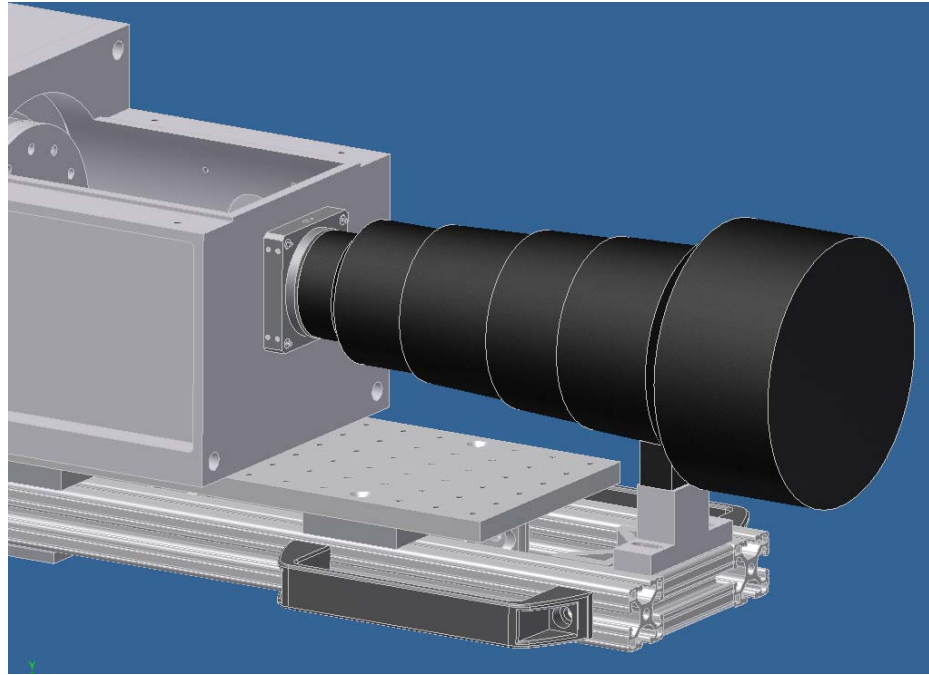
Affix GCTEX-0029 (Lens L1 Nikon 400mm) to GCTEX-0007 (LCP04 Nikon Mount)



7.24.

RC

Fasten/Secure GCTEX-0006 (Stand Lens Nikon Telephoto R0 101118) to GCTEX-A002 (ASSY GCTEx Structure (Linear) R2 101118) with **2 each 5-16 x .75"L** fasteners and spring-washers

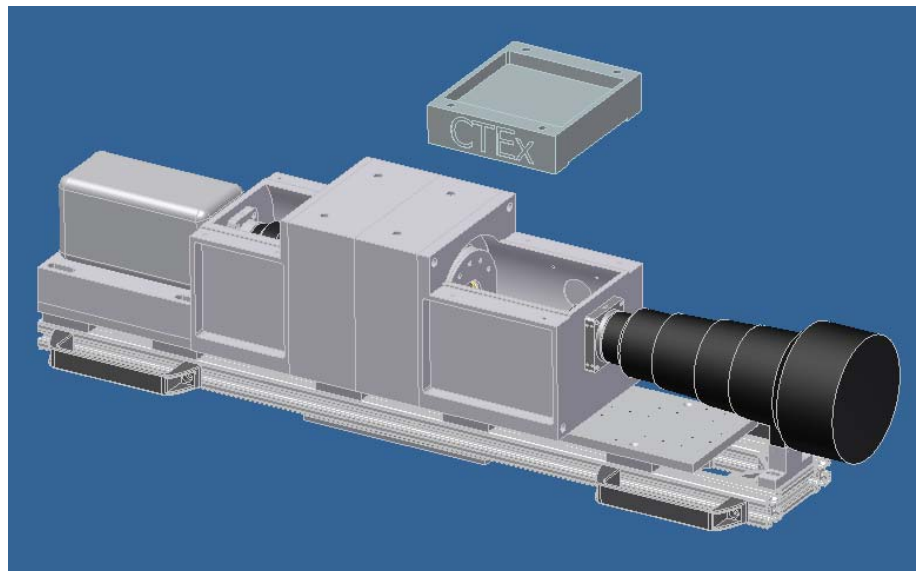


CAUTION: Do not over-torque the access-covers in the following two (2) steps

7.25.

RC

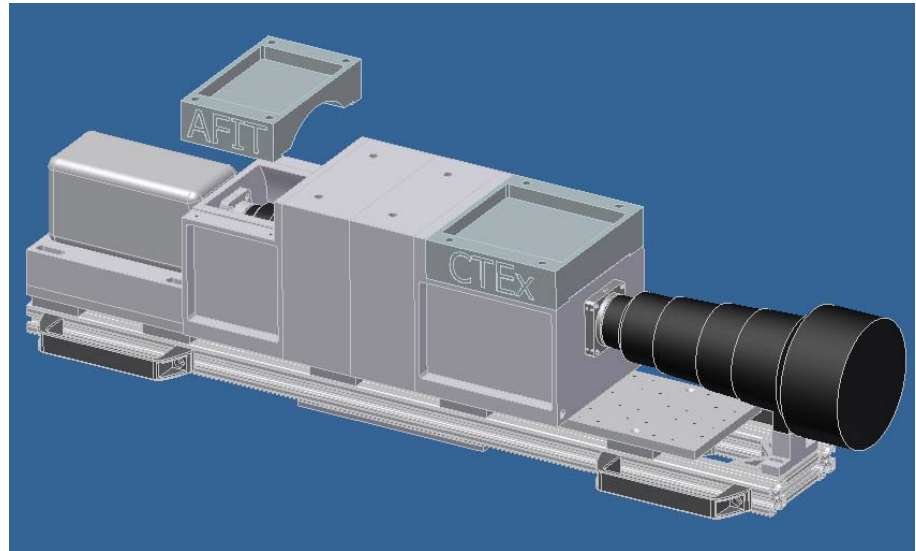
Fasten/Secure GCTEX-0004 (Block Interface L2 ACCESS R0 101113) to GCTEX-0005 (Block Interface L2 R0 101117) with **4 each 1/4-20 x .50"L** fasteners and spring-washers



____ 7.26.

RC

Fasten/Secure GCTEX-0003 (Block Interface L3 ACCESS R0 101117) to GCTEX-0002 (Block Interface L3 R0 101117) with **4 each** **1/4-20 x .50"L** fasteners and spring-washers



____ 7.27.

TC

Sign/Date to confirm assembly completion.

Procedure Completed _____ Date/Time _____

Test Conductor

END OF ASSEMBLY PROCEDURES

**AIR FORCE INSTITUTE OF TECH.
ENGINEERING PHYSICS DEPT.
WRIGHT-PATTERSON AFB, OH**

PROCEDURE:
REVISION:
DATE REVISED:
NUMBER OF PAGES:

TOP-GCTEx-0002
0
22 Dec 2010
13

**AFIT / ENP
REMOTE SENSING
OPERATIONS**

**GCTEx Instrument
Characterization
Operations**

PREPARED BY:

Test Engineer _____
Air Force Institute of Technology

DATE _____

REVIEW:

Technical Representative Review _____
Air Force Institute of Technology

DATE _____

Revision	Notes	Prepared By
0	-Initial procedure written	Capt. Niederhauser 22 Dec 10

PERSONNEL

GROUND-BASED CTE_x OPERATIONS

DATE _____

The following personnel are designated as test team members, and are chartered to perform their assignment as follows:

Test Conductor (TC) – Responsible for the timely performance of the test as written. This includes coordinating and directing the activities of the TPO and other test support teams. TC is responsible for coordinating all pretest activities and outside support required, including (but not limited to) security, fire, medical, and safety. TC is responsible for initialing completion on each step of the master test procedure.

Name _____ Signature _____

Test Director (TD) – Responsible for overall facility and test safety. Responsible for ensuring all test goals are met and all critical data is acquired. Supervises test activities to ensure procedures are followed. Has authority to perform real-time redlines on test procedures as required to ensure test requirements and goals area met.

Name _____ Signature _____

Test Panel Operator (TPO) – Responsible for operating the facility control systems during test operations as directed by TC. TPO is responsible for notifying the TC of any anomalous conditions.

Name _____ Signature _____

Instrumentation Engineer (IE) – Responsible for the operation and monitoring of all data acquisition equipment and notifying the TD and TC of any data loss or anomalies.

Name _____ Signature _____

Other Test Team Members – Responsible for performing ancillary duties in support of test, such as test stand and control room access control, support of anomaly resolution, and other necessary activities.

Name _____ Signature _____

Name _____ Signature _____

Name _____ Signature _____

Name _____ Signature _____

ALL TEST TEAM MEMBERS – Responsible for the safe performance of the test. Have read and understood all portions of the procedure. Any Test Team Member can declare an emergency or unsafe condition.

1.0**ABBREVIATIONS AND ACRYONMS**

AC	Alignment Characterization
CTEx	Chromotomography Experiment
DA	Deviation Angle
FS	Field Stop
Hg	Mercury
IE	Instrumentation Engineer
IQ	Image Quality
Mil	Military
SOP	Standard Operating Procedure
Std	Standard
TC	Test Conductor
TD	Test Director
TOP	Test Operating Procedure
TPO	Test Panel Operator
USAF	United States Air Force

2.0**TEST DESCRIPTION AND OBJECTIVES****2.1.****PURPOSE**

This procedure provides the means to perform characterization testing upon the ground-based Chromotomography Experiment (CTEx).

2.2.**SCOPE**

This procedure prepares the instrumentation and control system as well as verifies the proper mechanical configuration during the pre-test setup, Section 3.0. Section 4.0 executes the baseline system (Newtonian system) data acquisition activities, and allows for recycling, enabling multiple serial events to be captured. Finally, characterization of the updated system (linear revision) occurs in Section 5.0.

3.0

PRE-TEST SETUP

- ____ **3.1.** TC Verify all pages in this procedure are intact and complete
- ____ **3.2.** TC Go through the procedure and input any specific information required to perform operation.
- ____ **3.3.** IE **Execute** SOP GCTEX 0001 Rev 0 (Instrument Operations) Section 3.0, Pre-Test Setup

4.0

IE **BASELINE / CURRENT SYSTEM CHARACTERIZATION**

NOTE: This section performs characterization testing upon the baseline system (i.e., Vixen R200SS telescope).

- ____ **4.1.** IE Deviation Angle Characterization
- ____ **4.1.1.** IE Configure sources at a “collimated” distances (i.e., down the hall; >4m) from the instrument
 ____ Hg Pen Lamp with pinhole aperture
- ____ **4.1.2.** IE Measure the distance from instrument to source: _____
- ____ **4.1.3.** IE Reduce FS to a minimum diameter
- ____ **4.1.4.** IE Rotate the prism, by hand, to a minimum of four different positions and capture the data via SOP GCTEX 0001 Rev 0 100925 (Instrument Operations) Section 4.0, Test Acquisition
 ____ 0 Degrees, File Name: _____
 ____ 90 Degrees, File Name: _____
 ____ 180 Degrees, File Name: _____
 ____ 270 Degrees, File Name: _____

NOTE: Example filename, DA_R0_0_YYMMDD.xxx

Where:
DA: Deviation Angle
R0: Instrument Revision (R0 = Vixen, R1 = Linear/Telephoto)
0: Angle (0, 90, 180, 270, etc.)
YYMMDD: Date

- ____ **4.2.** IE Image Quality Characterization
- ____ **4.2.1.** IE Configure sources at a “collimated” distances (i.e., down the hall) from the instrument
 ____ Unilamp with USAF-1951/T-22 Mil-Std-150A (see Attachment 3.0)

- _____ **4.2.2.** IE Rotate the prism, by hand, to a minimum of four different positions and capture the data via SOP GCTEX 0001 Rev 0 100925 (Instrument Operations) Section 4.0, Test Acquisition
- _____ 0 Degrees, File Name: _____
 _____ 90 Degrees, File Name: _____
 _____ 180 Degrees, File Name: _____
 _____ 270 Degrees, File Name: _____
- NOTE:** Example filename, IQ_R0_YYMMDD.xxx
- Where:
 IQ: Image Quality
 R0: Instrument Revision (R0 = Vixen, R1 = Linear/Telephoto)
 0: Angle (0, 90, 180, 270, etc.)
 YYMMDD: Date
- _____ **4.3.** IE Real-Scene / Transient Characterization
- _____ **4.3.1.** IE Configure sources at a “collimated” distances (i.e., outside) from the instrument
- _____ Road Flares
- NOTE:** Road flares are only permitted to be initiated near Building 194
- _____ **4.3.2.** IE Rotate the prism via the motor/encoder and capture the data via SOP GCTEX 0001 Rev 0 100925 (Instrument Operations) Section 4.0, Test Acquisition
- NOTE:** Example filename, RS_R0_YYMMDD.xxx
- Where:
 RS: Real Scene
 R0: Instrument Revision (R0 = Vixen, R1 = Linear/Telephoto)
 0: Angle (0, 90, 180, 270, etc.)
 YYMMDD: Date
- 5.0** IE **UPDATED / NEW SYSTEM CHARACTERIZATION**
- NOTE:** This section performs characterization testing upon the baseline system (i.e., Vixen R200SS telescope).
- _____ **5.1.** IE Deviation Angle Characterization
- _____ **5.1.1.** IE Configure sources at a “collimated” distances (i.e., down the hall; >4m) from the instrument
- _____ Hg Pen Lamp with pinhole aperture

- | | | |
|---------------------|----|---|
| _____ 5.1.2. | IE | Measure the distance from instrument to source: _____ |
|---------------------|----|---|
- | | | |
|---------------------|----|---------------------------------|
| _____ 5.1.3. | IE | Reduce FS to a minimum diameter |
|---------------------|----|---------------------------------|
- | | | |
|---------------------|----|--|
| _____ 5.1.4. | IE | Rotate the prism, by hand, to a minimum of four different positions and capture the data via SOP GCTEX 0001 Rev 0 100925 (Instrument Operations) Section 4.0, Test Acquisition

___ 0 Degrees, File Name: _____
___ 90 Degrees, File Name: _____
___ 180 Degrees, File Name: _____
___ 270 Degrees, File Name: _____

NOTE: Example filename, DA_R0_0_YYMMDD.xxx

Where:
DA: Deviation Angle
R0: Instrument Revision (R0 = Vixen, R1 = Linear/Telephoto)
0: Angle (0, 90, 180, 270, etc.)
YYMMDD: Date |
|---------------------|----|--|
- | | | |
|-------------------|----|---------------------------------------|
| _____ 5.2. | IE | <u>Image Quality Characterization</u> |
|-------------------|----|---------------------------------------|
- | | | |
|---------------------|----|--|
| _____ 5.2.1. | IE | Configure sources at a “collimated” distances (i.e., down the hall) from the instrument

___ Unilamp with USAF-1951/T-22 Mil-Std-150A (see Attachment 3.0) |
|---------------------|----|--|
- | | | |
|---------------------|----|--|
| _____ 5.2.2. | IE | Rotate the prism, by hand, to a minimum of four different positions and capture the data via SOP GCTEX 0001 Rev 0 100925 (Instrument Operations) Section 4.0, Test Acquisition

___ 0 Degrees, File Name: _____
___ 90 Degrees, File Name: _____
___ 180 Degrees, File Name: _____
___ 270 Degrees, File Name: _____

NOTE: Example filename, IQ_R0_YYMMDD.xxx

Where:
IQ: Image Quality
R0: Instrument Revision (R0 = Vixen, R1 = Linear/Telephoto)
0: Angle (0, 90, 180, 270, etc.)
YYMMDD: Date |
|---------------------|----|--|
- | | | |
|-------------------|----|-----------------------------------|
| _____ 5.3. | IE | <u>Alignment Characterization</u> |
|-------------------|----|-----------------------------------|
- | | | |
|---------------------|----|--|
| _____ 5.3.1. | IE | Configure sources on the instrument

___ Thorlabs laser w/ mounting hardware |
|---------------------|----|--|
- | | | |
|---------------------|----|---|
| _____ 5.3.2. | IE | Reduce / Restrict the Field Stop to a minimum diameter allowing a truncated amount of incident source into the detector |
|---------------------|----|---|

_____ 5.3.3.	IE	<p>Rotate the prism, by hand, to a minimum of four different positions and capture the data via SOP GCTEX 0001 Rev 0 100925 (Instrument Operations) Section 4.0, Test Acquisition</p> <p>___ 0 Degrees, File Name: _____ ___ 90 Degrees, File Name: _____ ___ 180 Degrees, File Name: _____ ___ 270 Degrees, File Name: _____</p> <p>NOTE: Example filename, AC_R0_YYMMDD.xxx</p> <p>Where: AC: Alignment Characterization R0: Instrument Revision (R0 = Vixen, R1 = Linear/Telephoto) 0: Angle (0, 90, 180, 270, etc.) YYMMDD: Date</p>
_____ 5.4.	IE	<p><u>Real-Scene / Transient Characterization</u></p>
_____ 5.4.1.	IE	<p>Configure sources at a “collimated” distances (i.e., outside) from the instrument</p> <p>___ Road Flares</p> <p>NOTE: Road flares are only permitted to be initiated near Building 194</p>
_____ 5.4.2.	IE	<p>Setup/Record utilizing Headwall spectrometer (as baseline)</p>
_____ 5.4.3.	IE	<p>Rotate the prism via the motor/encoder and capture the data via SOP GCTEX 0001 Rev 0 100925 (Instrument Operations) Section 4.0, Test Acquisition</p> <p>NOTE: Example filename, RS_R0_YYMMDD.xxx</p> <p>Where: RS: Real Scene R0: Instrument Revision (R0 = Vixen, R1 = Linear/Telephoto) 0: Angle (0, 90, 180, 270, etc.) YYMMDD: Date</p>
_____ 5.5.	TC	<p>Sign to confirm completion, date and retain in records for future review.</p> <p>Procedure Completed _____ Date _____ _____ Test Conductor</p> <p>END OF PROCEDURE</p>

ATTACHMENT 1.0 TEST PLAN

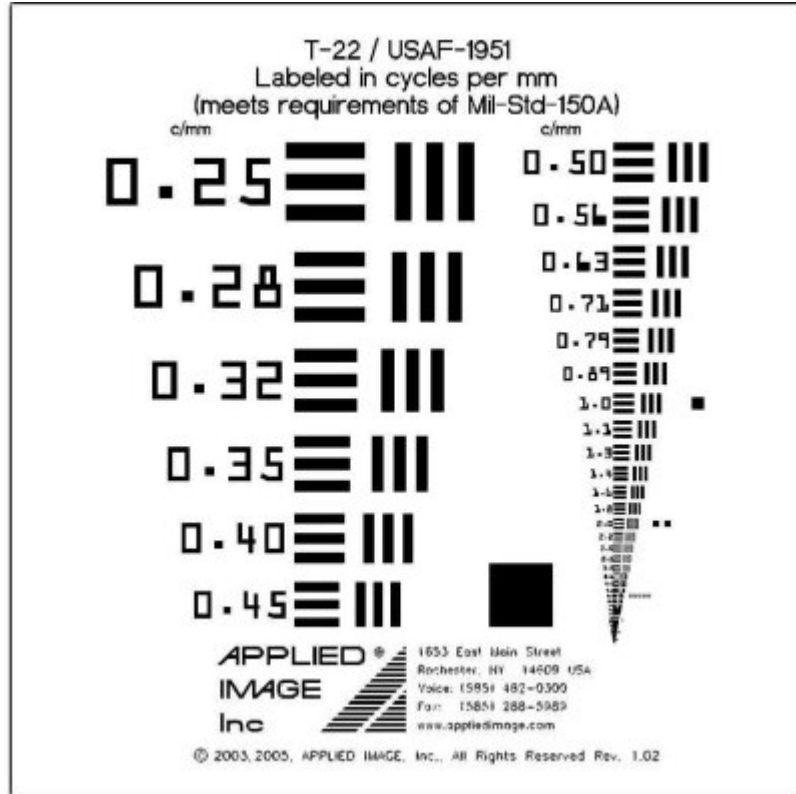
Date _____ Time _____

Capture Number	Date	Time	Source	Prism Rate	Resolution	FPS	Exposure Time	Notes

ATTACHMENT 2.0 TEST LOG

Itm	TIME	EVENT / STATUS	FILENAME
<i>(#)</i>	<i>(HHMM)</i>	<i>(Desc.)</i>	<i>(Test Data)</i>
1			
2			
3			
4			
5			
6			
7			
8			
9			
10			
11			
12			
13			
14			
15			
16			
17			
18			
19			
20			
21			
22			
23			
24			
25			
26			
27			

ATTACHMENT 3.0 IMAGE QUALITY TARGET (Reference)



**SCTEX OPERATIONS
AFIT/ENY**

WRIGHT-PATTERSON AFB, OH

PROCEDURE:

REVISION:

DATE REVISED:

NUMBER OF PAGES:

SOP-SCTEX-0001

0

12 Jan 2011

18

**AFIT / ENY
SCTEx
OPERATIONS**

ICU Assembly & Checkout

PREPARED BY:

Test Engineer _____
AFIT/ENY

DATE _____

REVIEW / APPROVAL:

AF Customer _____
AFIT/ENY CTEEx Thesis Advisor

DATE _____

Revision	Notes	Prepared By
0	-Initial procedure written	Capt. Niederhauser 12 Jan 11

PERSONNEL

DATE _____

The following personnel are designated as test team members, and are chartered to perform their assignment as follows:

Test Conductor (TC) – Responsible for the timely performance of the test as written. This includes coordinating and directing the activities of the Red Crew and other test support teams. TC is responsible for coordinating all pretest activities and outside support required, including (but not limited to) security, fire, medical, and safety. TC is responsible for initialing completion on each step of the master test procedure.

Name _____ Signature _____

Test Director (TD) – Responsible for overall facility and test safety. Responsible for ensuring all test goals are met and all critical data is acquired. Supervises test activities to ensure procedures are followed. Has authority to perform real-time redlines on test procedures as required to ensure test requirements and goals area met.

Name _____ Signature _____

Red Crew Leader (RC) – Responsible for directing the activities of Red Crew members. Reports directly to the TC and ensures all Red Crew tasks are completed. Responsible for ensuring all RCM's have all required certifications and training. Responsible for ensuring all required equipment is available, accessible, and serviceable.

Name _____ Signature _____

ALL TEST TEAM MEMBERS – Responsible for the safe performance of the test. Have read and understood all portions of the test procedure. Any Test Team Member can declare an emergency or unsafe condition.

1.0**ABBREVIATIONS AND ACRYONMS**

AFIT	Air Force Institute of Technology
FOD	Foreign Object Debris
HAZCOM	Hazardous Communication
PPE	Personal Protective Equipment
RC	Red Crew
RCM	Red Crew Member
STE	Special Test Equipment
TC	Test Conductor
TD	Test Director
TPO	Test Panel Operator

2.0**TEST DESCRIPTION AND OBJECTIVES****2.1.****PURPOSE**

This procedure provides the means to perform assembly and initial checkout upon the AFIT Space-Based Chromotomography Experiment (CTEx) Instrument Computer Unit (ICU). This procedure accomplishes the mechanical assembly, initial leak check and purge/fill operations.

3.0**DOCUMENTATION**

The completion of each applicable event shall be verified by marking to the left of the item number. Deviations from these procedures will be coordinated with the Test Conductor

3.1.**REFERENCE DOCUMENTS**

NONE

3.2.**SPECIFICATIONS**

The following list of specifications shall be used as a guide:

Gaseous Nitrogen: MILPRF27401D

3.3.**DRAWINGS**

SCTEX-0001 (Housing Lower ICU R0b)
SCTEX-0002 (Housing Upper ICU R0b)
SCTEX-0003 (Plate Thermal Baffle ICU R0)
SCTEX-0004 (Bracket Fan ICU R0)
SCTEX-0005 (Plate Interface Vibe-Test R0)
SCTEX-0006 (Pass-Thru Electrical Hermetic 12-Pin)
SCTEX-0007 (O-Ring 0.25THKx10.5ID)
SCTEX-0008 (SS-4-WVCR-1-2)
SCTEX-0009 (HV-1, Purge/Fill, SS-4BW)
SCTEX-0010 (Fan DC, 12v)
SCTEX-0011 (Card Cage, PC/104)
Attachment 1.0 Electrical Wiring

4.0**TEST REQUIREMENTS AND RESTRICTIONS****4.1.****TRAINING**

The following training is required for personnel using these procedures:

All personnel:
Job Site HAZCOM

4.2. MAXIMUM PERSONNEL:

Control Room: 15

Red Crew members will utilize the "buddy system" when performing attachments and setting up the Test Facility.

4.3. LIST OF EQUIPMENT

SCTEX-0001 (Housing Lower ICU R0b); QTY: 1EA
 SCTEX-0002 (Housing Upper ICU R0b); QTY: 1EA
 SCTEX-0003 (Plate Thermal Baffle ICU R0); QTY: 1EA
 SCTEX-0004 (Bracket Fan ICU R0); QTY: 1EA
 SCTEX-0005 (Plate Interface Vibe-Test R0); QTY: 1EA
 SCTEX-0006 (Pass-Thru Electrical Hermetic 12-Pin); QTY: 1EA
 SCTEX-0007 (O-Ring 0.25THKx10.5ID); QTY: 1EA
 SCTEX-0008 (SS-4-WVCR-1-2); QTY: 1EA
 SCTEX-0009 (HV-1, Purge/Fill, SS-4BW); QTY: 1EA
 SCTEX-0010 (Fan DC, 12v); QTY: 1EA
 SCTEX-0011 (Card Cage, PC/104); QTY: 1EA

Fasteners:

4 each 8-32 x 0.5"L
 4 each 8-32 x 2.0"L
 4 each 8-32 x 0.375"L
 40 each 8-32 x 1.0"L

Other:

Teflon Tape
 Braycote 601EF (or equivalent)
 O-Ring Lubricant (Vacuum-Compatible)

Ensure all tools associated with this experiment/test/operation are accounted for prior to initiating system/item test. Ensure all FOD is picked up from around the test facility.

5.0 SAFETY REQUIREMENTS**5.1. PERSONNEL PROTECTIVE CLOTHING REQUIREMENTS**

Standard PPE: Safety goggles or glasses (as required), hearing protection (when required), boots – soles and heels made of semi-conductive rubber containing no nails.

All jewelry will be removed by Test Crew members while working on the test facility. No ties or other loose clothing permitted (at TC discretion).

5.2. TEST AREA ACCESS DURING OPERATIONS

The test facility room will be limited to test personnel only. Personnel will not be allowed access to the test area unless cleared by the TC.

5.3.**EXPLOSIVE AND PERSONNEL LIMITS**

NONE

5.4.**EMERGENCY PROCEDURES**

In the event of an emergency that jeopardizes the safety of the operators or other personnel perform Section 9.0 emergency procedures at the end of this document.

5.5.**SPECIAL INSTRUCTIONS**

Test Crew members shall place all cellular telephones on "silent mode" or turn off prior to completing any portion of this procedure.

Test Crew Members shall notify the TC of any leaks from hydraulic system, or pneumatic system pipe or tubing connections.

6.0**PRE-TEST SETUP**

- | | | |
|-------------------|----|--|
| _____ 6.1. | TC | Verify all pages in this procedure are intact and complete |
| _____ 6.2. | TC | Go through the procedure and input any specific information required to perform operation. |
| _____ 6.3. | TC | Perform Setup Brief with Test Crew Members and note any redline changes on Attachments. |
| _____ 6.4. | TC | Verify Red Crew has donned standard PPE (and noted restrictions / special instructions). |
| _____ 6.5. | TC | Verify all personnel involved with the operation have signed this procedure. |

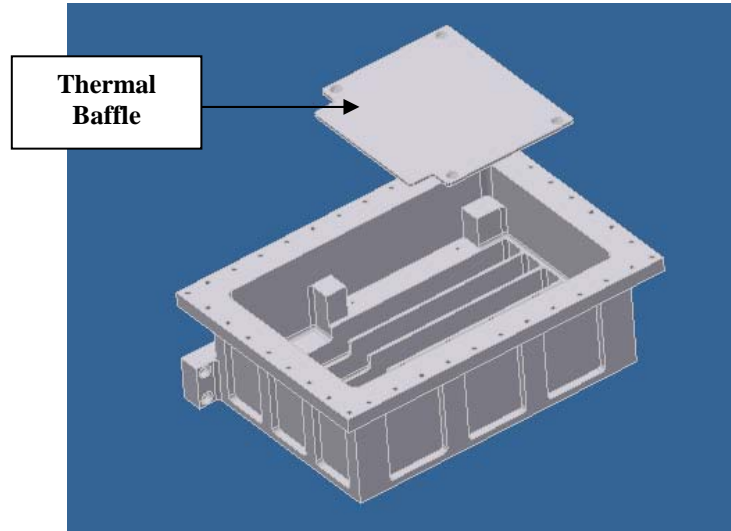
7.0

7.1.

RC

ICU ASSEMBLY

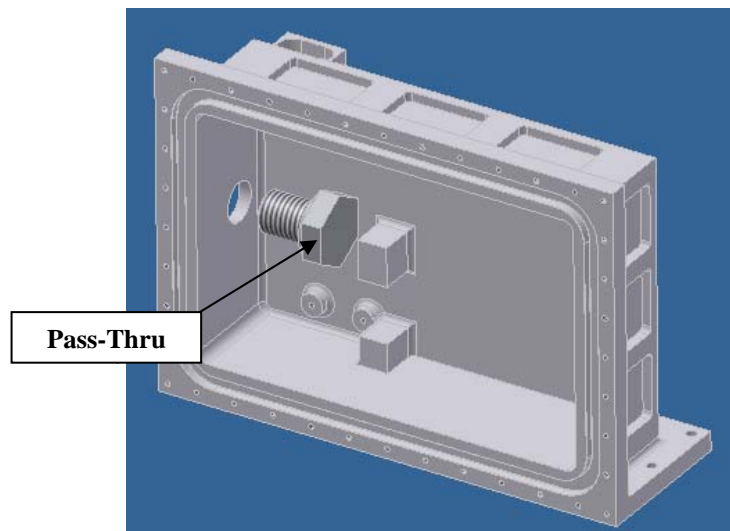
Fasten/Secure SCTEX-0003 (Plate Thermal Baffle ICU R0) to SCTEX-0002 (Housing Upper ICU R0b) with **4 each 8-32 x 0.5”L** fasteners to **10.8 in-lbs**



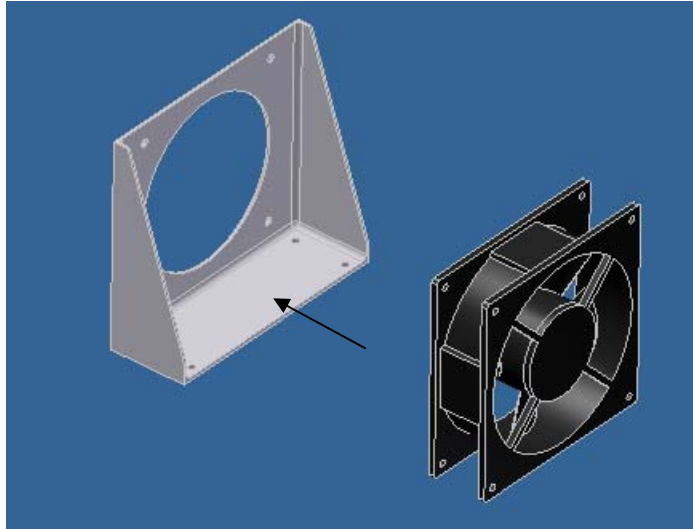
NOTE: The direction of the electrical pass-thru must be in the orientation denoted in the accompanying figure (i.e., the component o-ring must be on the interior of the enclosure).

7.2.

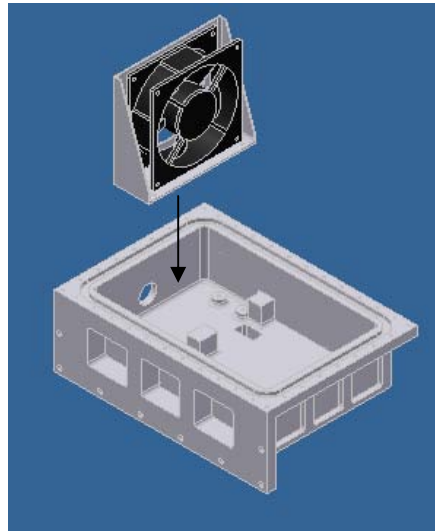
Secure/Fasten SCTEX-0006 (Pass-Thru Electrical Hermetic 12-Pin) to SCTEX-0001 (Housing Lower ICU R0b)



- ____ **7.3.** RC Fasten/Secure SCTEX-0010 (Fan DC, 12v) to SCTEX-0004 (Bracket Fan ICU R0) with **4 each 8-32 x 2.0"L** fasteners, spring washers and nuts to **15.0 in-lbs**



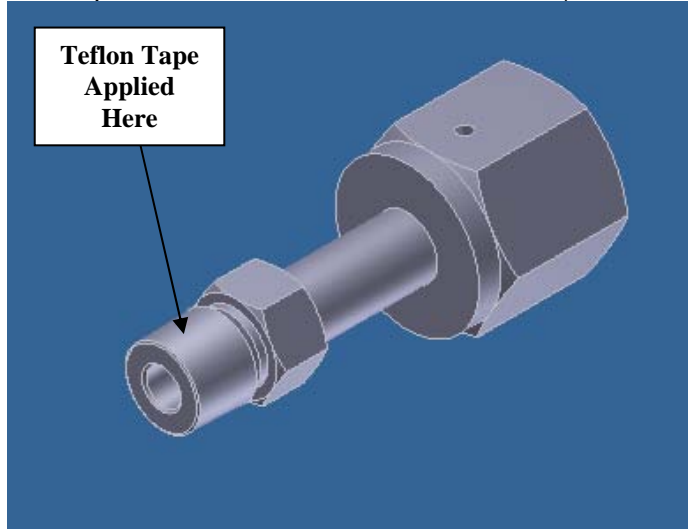
- ____ **7.4.** RC Fasten/Secure SCTEX-0004 (Bracket Fan ICU R0) to SCTEX-0001 (Housing Lower ICU R0b) with **4 each 8-32 x 0.375"L** fasteners and spring washers to **10.8 in-lbs**



- ____ **7.5.** RC Verify / **CLOSE** SCTEX-0009 (HV-1, Purge/Fill, SS-4BW)

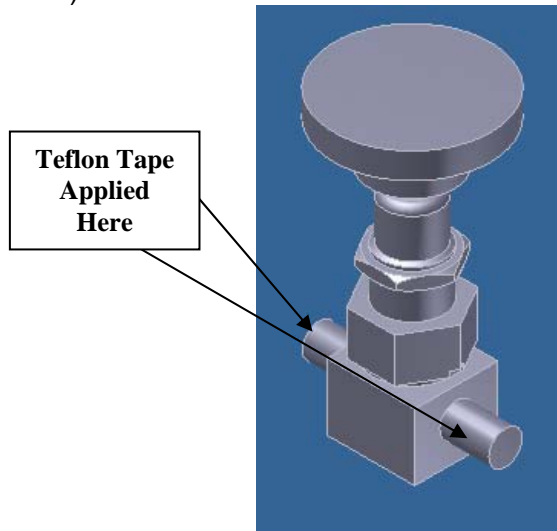
7.6.

RC Apply Teflon tape to male threads of SCTEX-0008 (SS-4-WVCR-1-2)



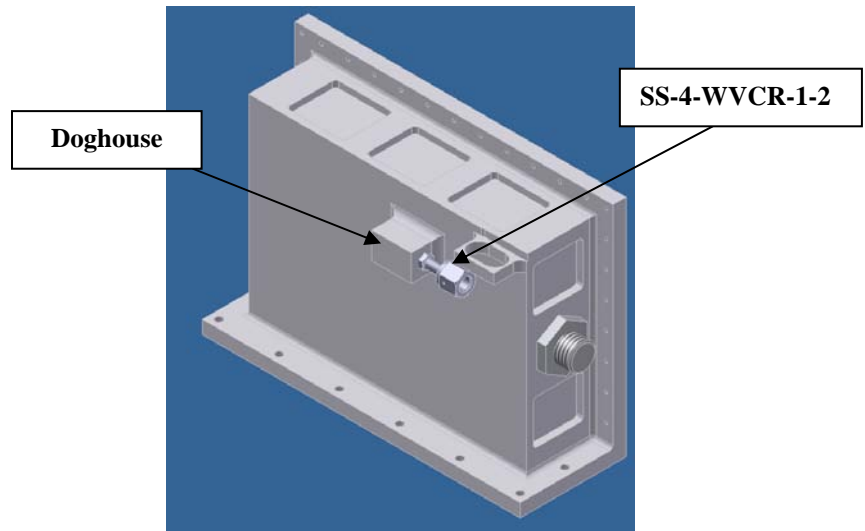
7.7.

RC Apply Teflon tape to male threads of SCTEX-0009 (HV-1, Purge/Fill, SS-4BW)



7.8.

RC Fasten/Secure SCTEX-0008 (SS-4-WVCR-1-2) to SCTEX-0001 (Housing Lower ICU R0b) 1/8-NPT doghouse

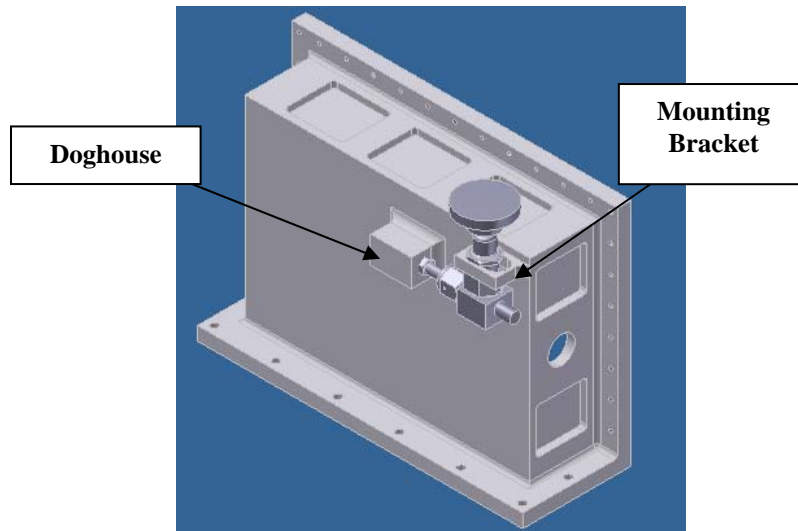


7.9.

RC Clip/Secure VCR seal to SCTEX-0009 (HV-1, Purge/Fill, SS-4BW)

7.10.

RC Fasten/Secure SCTEX-0009 (HV-1, Purge/Fill, SS-4BW) to SCTEX-0008 (SS-4-WVCR-1-2) and SCTEX-0001 (Housing Lower ICU R0b); secure valve housing via the mounting bracket.

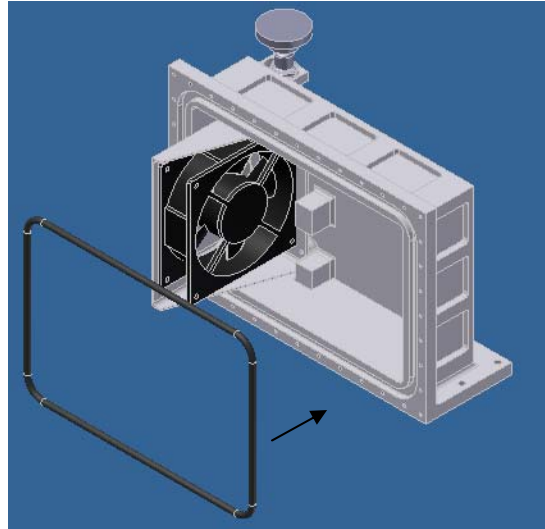


____ 7.11.

Apply a very thin amount of o-ring lubricant (vacuum compatible grease, Braycoat 601 EF or equivalent) to SCTEX-0007 (O-Ring 0.25THKx10.5ID)

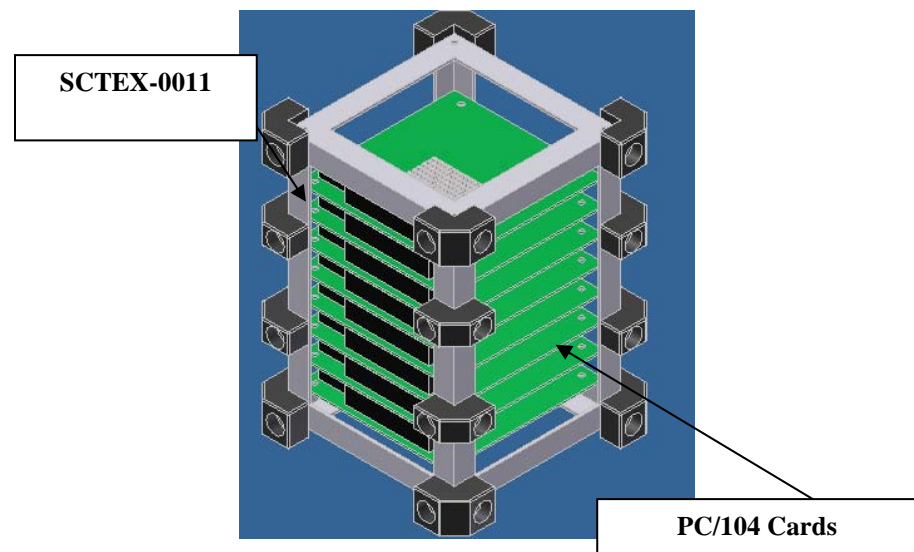
____ 7.12.

Install SCTEX-0007 (O-Ring 0.25THKx10.5ID) into SCTEX-0001 (Housing Lower ICU R0b) o-ring groove.



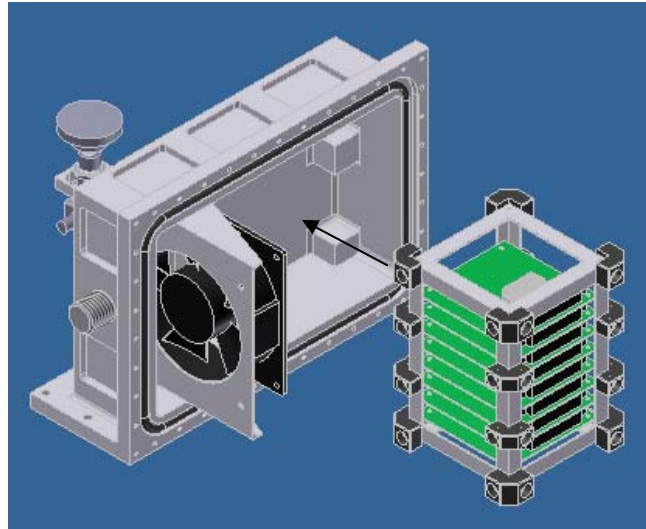
____ 7.13.

Install/Secure PC/104 computer cards into SCTEX-0011 (Card Cage, PC/104), ensure equal spacing



____ 7.14.

INSTALL SCTEX-0011 (Card Cage, PC/104) into SCTEX-0001 (Housing Lower ICU R0b)

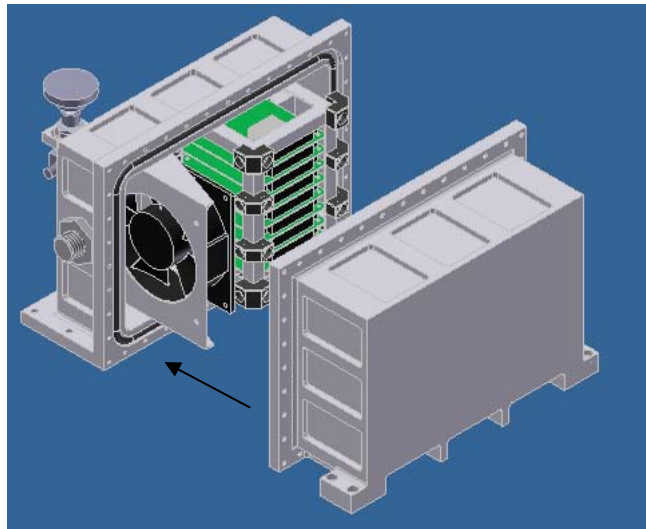


____ 7.15.

RC Solder/Wire all electrical connections per Attachment 1.0

____ 7.16.

RC Fasten/Secure SCTEX-0002 (Housing Upper ICU R0b) to SCTEX-0001 (Housing Lower ICU R0b) with **40 each 8-32 x 1.0”L** fasteners and spring washers to **10.8 in-lbs**



____ 7.17.

TC Sign/Date to confirm assembly completion.

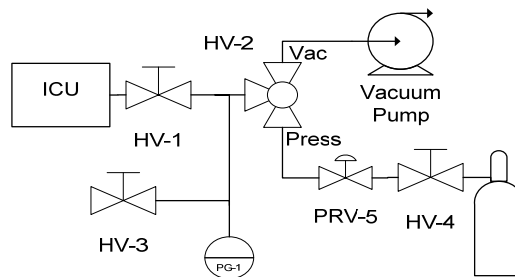
Procedure Completed _____ Date/Time _____

Test Conductor

END OF ASSEMBLY PROCEDURES

8.0**LOW-PRESSURE LEAK CHECK, FILL & PURGE**

- ____ **8.1.** RC Verify / **CLOSE** HV-1 (Purge/Fill Vlv SS-4BW)
- ____ **8.2.** RC Verify / **SET** HV-2 to **PRESS** (GN2/VAC 3WY Vlv)
- ____ **8.3.** RC Verify / **CLOSE** HV-3 (Vent Valve)
- ____ **8.4.** RC Verify / **FULLY DECREASE** PRV-5 (GN2 K-bottle regulator)
- ____ **8.5.** RC Verify / **CLOSE** HV-4 (GN2 K-bottle Isolation HV)
- ____ **8.6.** RC Verify / **OFF** Vacuum Pump
- ____ **8.7.** RC **CONFIGURE / CONNECT** ICU test setup per the following diagram:



- ____ **8.8.** RC Execute a leak-test per the following steps:
- ____ **8.8.1.** RC **OPEN** HV-4 (GN2 K-bottle Isolation HV)
- ____ **8.8.2.** RC **INCREASE** PRV-5 to 10+/- 2 psig on PG-1 (GN2 K-bottle regulator)
- ____ **8.8.3.** RC **OPEN** HV-1, allow pressure to equalize (Purge/Fill Vlv SS-4BW)
- ____ **8.8.4.** RC **FULLY DECREASE** PRV-5 (GN2 K-bottle regulator) and hold for one (1) minute minimum, assessing for leaks via leak test solution (soap & water solution; aka "snoop"). If leaks are witnessed, depressurize via opening HV-3 (Vent Valve) and correct the issue; otherwise, continue.
- ____ **8.8.5.** RC **INCREASE** PRV-5 (GN2 K-bottle regulator) to 20+/- 2 psig on PG-1, then **FULLY DECREASE** PRV-5. Hold for one (1) minute minimum, assess for leaks via leak test solution (soap & water solution; aka "snoop"). If leaks are witnessed, depressurize via opening HV-3 (Vent Valve) and correct the issue; otherwise, continue.
- ____ **8.8.6.** RC **INCREASE** PRV-5 (GN2 K-bottle regulator) to 35 +/- 2 psig on PG-1, then **FULLY DECREASE** PRV-5. Hold for five (5) minutes minimum, assess for leaks via leak test solution (soap & water solution; aka "snoop"). If leaks are witnessed, depressurize via opening HV-3 (Vent Valve) and correct the issue; otherwise, continue.

- _____ **8.8.7.** RC **CLEAN** all joints thoroughly from all snoop and other oils/solvents.
- _____ **8.9.** RC Perform fill and purge operations per the following steps, repeat ten (10) times.

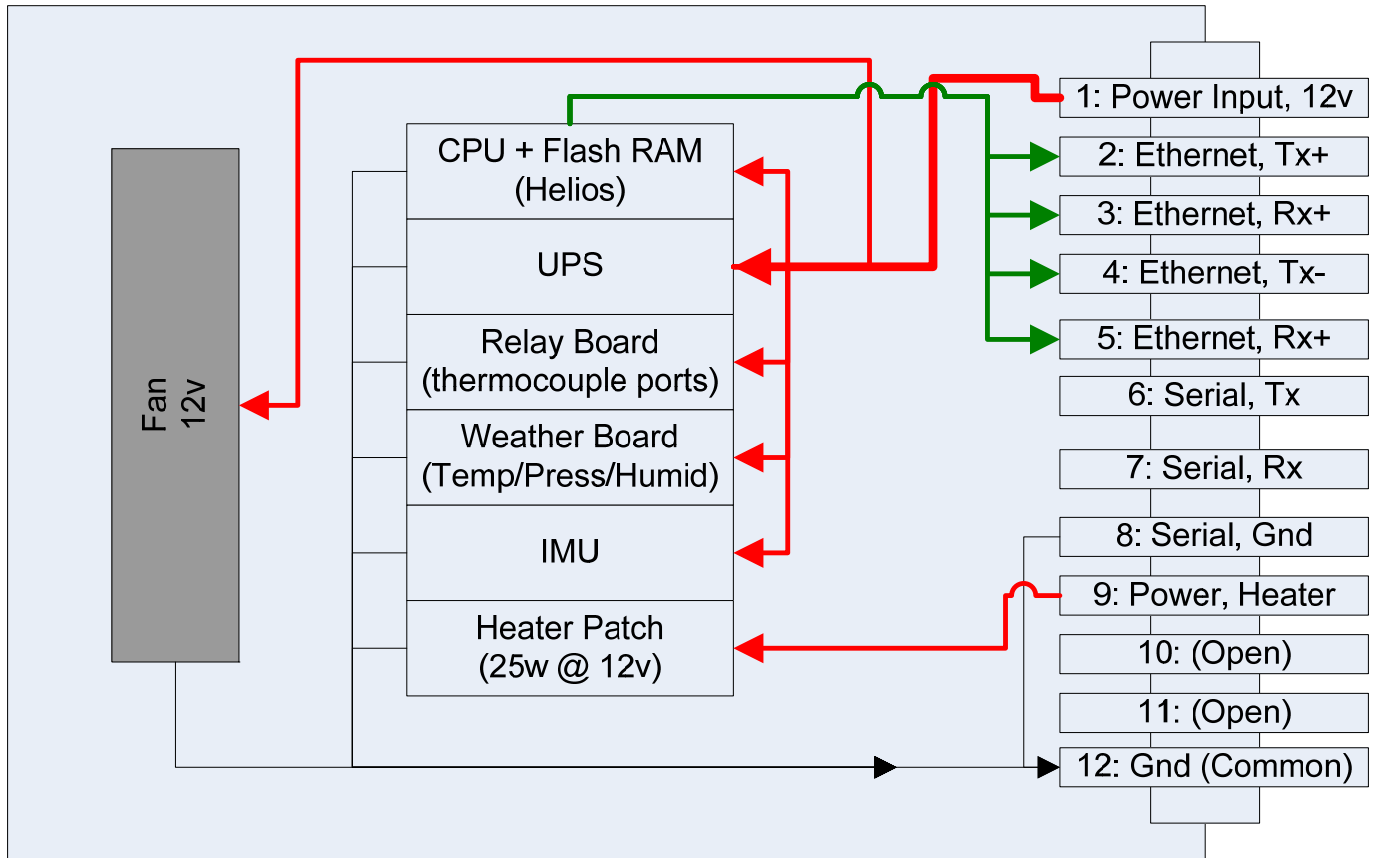
- _____ **8.9.1.** RC **OPEN** HV-3 until PG-1 reads 5 +2/-0 psig, then **CLOSE** (Vent Valve)
- _____ **8.9.2.** RC **SET** HV-2 to **VAC** (GN2/VAC 3WY Vlv)
- _____ **8.9.3.** RC **TURN ON** Vacuum Pump until PG-1 reads 26 +/- 2 inHg, then **TURN OFF.**
- _____ **8.9.4.** RC **SET** HV-2 to **PRESS** (GN2/VAC 3WY Vlv)
- _____ **8.9.5.** RC **INCREASE** PRV-5 to 30 psig, then **DECREASE FULLY** (GN2 K-bottle regulator).
- _____ **8.10.** RC **OPEN** HV-3 until PG-1 reads 3 +1/-0 psig, then **CLOSE** (Vent Valve).
- _____ **8.11.** RC **CLOSE** HV-1 (Purge/Fill Vlv SS-4BW)
- _____ **8.12.** RC **OPEN** HV-3 until PG-1 reads 0 psig then **CLOSE**
- _____ **8.13.** RC **CLOSE** HV-4 (GN2 K-bottle Isolation HV)
- _____ **8.14.** RC **DISCONNECT** all test setup hardware
- _____ **8.15.** TC Sign/Date to confirm assembly completion.

Procedure Completed _____ Date/Time _____

 Test Conductor
 END OF PROCEDURES

9.0		<u>EMERGENCY RESPONSE</u>
		NOTE: Perform the following steps in the event of a major leak, fire or other anomaly which cannot be safely managed by normal securing operations. TC shall have authority (On-Scene Command) over the situation until relieved from support organizations.
9.1	TC	If necessary, EVACUATE and/or Dial 9-911 to notify fire department of emergency
9.2	TPO	If possible/safe, ABORT any test currently in process
9.3	RCM	If possible/safe, CLOSE shop-air isolation hand-valve
9.4	ANY	If necessary, Brief fire department and medics when they arrive.
9.5	TD/T C	Continue to Monitor Facility until condition has been secured. END OF EMERGENCY PROCEDURES

ATTACHMENT 1.0 Electrical Wiring



TEST AREA B644 L125A
AFIT/ENY
SCTEx
WRIGHT-PATTERSON AFB, OH

PROCEDURE:
REVISION:
DATE REVISED:
NUMBER OF PAGES:

TOP-SCTEx-0001
0
14 Jan 2011
42

**AFIT / ENY
VIBRATION FACILITY
OPERATIONS**

ICU Vibe-Table Testing

PREPARED BY:

Test Engineer _____

DATE _____

REVIEW / APPROVAL:

AF Customer _____
Thesis Advisor

DATE _____

Revision	Notes	Prepared By
0	-Initial procedure written	Capt. Niederhauser 14 Jan 11

PERSONNEL

EXPERIMENTAL VIBRATION FACILITY

DATE _____

The following personnel are designated as test team members, and are chartered to perform their assignment as follows:

Test Conductor (TC) – Responsible for the timely performance of the test as written. This includes coordinating and directing the activities of the Red Crew and other test support teams. TC is responsible for coordinating all pretest activities and outside support required, including (but not limited to) security, fire, medical, and safety. TC is responsible for initialing completion on each step of the master test procedure.

Name _____ Signature _____

Test Director (TD) – Responsible for overall facility and test safety. Responsible for ensuring all test goals are met and all critical data is acquired. Supervises test activities to ensure procedures are followed. Has authority to perform real-time redlines on test procedures as required to ensure test requirements and goals area met.

Name _____ Signature _____

Red Crew Leader (RCL) – Responsible for directing the activities of Red Crew members. Reports directly to the TC and ensures all Red Crew tasks are completed. Responsible for ensuring all RCM's have all required certifications and training. Responsible for ensuring all required equipment is available, accessible, and serviceable.

Name _____ Signature _____

Test Panel Operator (TPO) – Responsible for operating the facility control systems during test operations as directed by TC. TPO is responsible for notifying the TC of any anomalous conditions.

Name _____ Signature _____

Red Crew Member (RCM) – Reports to the RCL. RCM is responsible for performing test-related tasks as directed by RCL.

Name _____ Signature _____

Name _____ Signature _____

Other Test Team Members – Responsible for performing ancillary duties in support of test, such as test stand and control room access control, support of anomaly resolution, and other necessary activities.

Name _____ Signature _____

Name _____ Signature _____

ALL TEST TEAM MEMBERS – Responsible for the safe performance of the test. Have read and understood all portions of the test procedure. Any Test Team Member can declare an emergency or unsafe condition.

1.0**ABBREVIATIONS AND ACRYONMS**

AFIT	Air Force Institute of Technology
DOF	Degree of Freedom
FOD	Foreign Object Debris
HAZCOM	Hazardous Communication
PPE	Personal Protective Equipment
RCL	Red Crew Leader
RCM	Red Crew Member
STE	Special Test Equipment
TC	Test Conductor
TD	Test Director
TPO	Test Panel Operator

2.0**TEST DESCRIPTION AND OBJECTIVES****2.1.****PURPOSE**

This procedure provides the means to perform vibe-table testing for test articles supplied relating to the Space-Based Chromotomography Experiment (CTEx), and more specifically, the Instrument Computer Unit (ICU). The CTEx ICU test campaign is a risk reduction ground test exercise intending to mitigate technology concerns for a future flight aboard the ISS in later years. The AFIT Vibration Facility will be configured with the proper special test equipment (STE) to direct, and measure “maximum predicted environments” associated with launching the ICU according to H-IIB Transfer Vehicle (HTV) specifications (see Attachment 5.0).

2.2.**SCOPE**

This procedure prepares the instrumentation and control system as well as verifies the proper mechanical configuration during the pre-test setup (note that the ICU will remain in the OFF/NON-POWERED position for all phases of this test series). Upon completion of the setup, appropriate levels for Sine, Random and Sine-Burst/Shock environments will be configured to test the prototype in all three axes (X, Y and Z). Rationale for each test is as follows:

Sine Sweep: The objective of the Sine sweep is to determine the fundamental and further natural frequencies, modal shapes and modal gain of the structure in the three main axis, and, by repeating this test after the high-level sine burst and random vibration, to determine whether anything in the satellite has changed/broken as a result of the tests by comparing the responses pre- and post-test. The fundamental frequency must meet launch vehicle requirements as well. This information will aid in analysis of any design changes that may be made if certain components fail.

Random Vibration: The objective of this test is to verify the capability of the satellite structure and components to withstand the fatigue introduced during launch.

Sine Burst / Shock (AS REQUIRED): The objective of this test is to check the static strength of the spacecraft structure to determine whether it can withstand the launch acceleration loads. To ensure that testing in one axis at a time will adequately stress the structure, encompassing the multi-axis design loads specified for HTV payloads, the single axis acceleration must be higher than is needed to adequately test the spacecraft.

Stand-Characterization (AS REQUIRED): The goal of the stand-characterization test is to show that the vertical acceleration of the top of the vibration stand is two orders of magnitude less than the horizontal acceleration, thereby showing that the stand can be accurately considered as a rigid-body.

2.3.

Test recycling will take place as necessary. The test facility will then be properly secured and reconfigured to a safe state for normal operations. Data will be reviewed and archived. Any facility anomalies or lessons observed will be noted in a final test report.

OBJECTIVESComplete Success

- 1) Pass all random vibration and shock tests required by HTV Req'ts/Specs (for all DOF)
- 2) No mechanical failure detected, the test occurred without any degradation
- 3) No electrical failures detected during operation/between tests

Marginal Success

- 1) Pass all random vibration and shock tests required by HTV Req'ts/Specs (for all DOF)
- 2) Minor mechanical failure detected (minor degradation; ie, non-catastrophic)
- 3) No electrical failures detected during operation/between tests

Unsuccessful

Failure of any of the above success criteria

3.0**DOCUMENTATION**

The completion of each applicable event shall be verified by marking to the left of the item number. Deviations from these procedures will be coordinated with the Test Conductor (NOTE: TC has the local authority to approve red-line revisions to this procedure).

3.1.**REFERENCE DOCUMENTS**

NONE

3.2.**SPECIFICATIONS**

The following list of specifications shall be used as a guide:

NASDA-ESPC-2857 (HTV Cargo Standard Interface Requirements Document)

3.3.**DRAWINGS**

NONE

4.0**TEST REQUIREMENTS AND RESTRICTIONS****4.1.****TRAINING**

The following training is required for personnel using these procedures:

All personnel:

Job Site HAZCOM

4.2.**MAXIMUM PERSONNEL:**

Control Room: 15

Red Crew members will utilize the "buddy system" when performing attachments and setting up the Test Facility.

4.3.**LIST OF EQUIPMENT**

Test STE (listed below), Test Article, spare tool set, fasteners, camera, computer (for functional check), spare components

SCTEX-0001 (Housing Lower ICU R0b); QTY: 1EA

SCTEX-0002 (Housing Upper ICU R0b); QTY: 1EA

SCTEX-0003 (Plate Thermal Baffle ICU R0); QTY: 1EA

SCTEX-0004 (Bracket Fan ICU R0); QTY: 1EA

SCTEX-0005 (Plate Interface Vibe-Test R0); QTY: 1EA

SCTEX-0006 (Pass-Thru Electrical Hermetic 12-Pin); QTY: 1EA

SCTEX-0007 (O-Ring 0.25THKx10.5ID); QTY: 1EA

SCTEX-0008 (SS-4-WVCR-1-2); QTY: 1EA

SCTEX-0009 (HV-1, Purge/Fill, SS-4BW); QTY: 1EA
SCTEX-0010 (Fan DC, 12v); QTY: 1EA
SCTEX-0011 (Card Cage, PC/104); QTY: 1EA

Ensure all tools associated with this experiment/test/operation are accounted for prior to initiating system/item test. Ensure all FOD is picked up from around the test facility.

5.0

SAFETY REQUIREMENTS

5.1.

PERSONNEL PROTECTIVE CLOTHING REQUIREMENTS

Standard PPE: Safety goggles or glasses (as required), hearing protection (when required), boots – soles and heels made of semi-conductive rubber containing no nails.

All jewelry will be removed by Test Crew members while working on the test facility. No ties or other loose clothing permitted (at TC discretion).

5.2.

TEST AREA ACCESS DURING OPERATIONS

The test facility room will be limited to test personnel only. Personnel will not be allowed access to the test area unless cleared by the TC.

5.3.

EXPLOSIVE AND PERSONNEL LIMITS

NONE

5.4.

EMERGENCY PROCEDURES

In the event of an emergency that jeopardizes the safety of the operators or other personnel perform Section 12.0 emergency procedures at the end of this document.

5.5.

SPECIAL INSTRUCTIONS

A qualified technician should provide orientation for operation and maintenance of the vibration table and the proper faculty member / instructor should be consulted on test-series set points prior to test operations commencing.

Test Crew members shall place all cellular telephones on “silent mode” or turn off prior to completing any portion of this procedure.

Test Crew Members shall notify the TC of any leaks from hydraulic system, or pneumatic system pipe or tubing connections.

6.0**PRE-TEST SETUP**

- | | | |
|---------------------|----|---|
| _____ 6.1. | TC | Verify all pages in this procedure are intact and complete |
| _____ 6.2. | TC | Go through the procedure and input any specific information required to perform operation. |
| _____ 6.3. | TC | Verify with Facility Management that no open Work Orders / Issues are listed for the Vibration Test Facility impeding operations. |
| _____ 6.4. | TC | Perform Setup Brief with Test Crew Members and note any redline changes on Attachments. |
| _____ 6.5. | TC | Verify Red Crew has donned standard PPE (and noted restrictions / special instructions). |
| _____ 6.6. | TC | Initiate the following Procedures/Attachment(s):

NOTE: All attachments can be completed independently from one another – there is no order to completion.

Attachment 1 – Control System Setup

Attachment 2 – Mechanical Setup |
| _____ 6.7. | TC | Verify that Attachments are complete.

_____ Attachment 1 _____ Attachment 2 |
| _____ 6.8. | TC | Perform Pre-Operation Brief with Test Crew Members

<ul style="list-style-type: none"> - Objective - Personnel and assigned roles/duties - Safety: materials, PPE, communication, etc. - Sequence of events - Emergency procedures |
| _____ 6.8.1. | TC | Pre-Test Brief Time _____ |
| _____ 6.8.2. | TC | Verify all personnel involved with the operation have signed this procedure. |

7.0		<u>TEST SERIES FLOW / PLAN</u>
____ 7.1.	TC	<u>X-AXIS [NO PRESSURE] VIBRATIONAL TESTING</u>
____ 7.1.1.	TC	RECONFIGURE Vibe-Table Mechanical Setup is Correct for X-axis test, per Attachment 6.0
____ 7.1.2.	TC	EXECUTE Sine Sweep Test, Section 8.0
____ 7.1.3.	TC	EXECUTE Random Vibe Test, Section 9.0
____ 7.1.4.	TC	EXECUTE Sine Sweep Test, Section 8.0
____ 7.1.5.	TC	EXECUTE a functional checkout upon the system
____ 7.1.6.	TC	Log data/results in Appendix 4.0
____ 7.2.	TC	<u>Y-AXIS [NO PRESSURE] VIBRATIONAL TESTING</u>
____ 7.2.1.	TC	EXECUTE Sine Sweep Test, Section 8.0
____ 7.2.2.	TC	EXECUTE Random Vibe Test, Section 9.0
____ 7.2.3.	TC	EXECUTE Sine Sweep Test, Section 8.0
____ 7.2.4.	TC	EXECUTE a functional checkout upon the system
____ 7.2.5.	TC	Log data/results in Appendix 4.0
____ 7.3.	TC	<u>Z-AXIS [NO PRESSURE] VIBRATIONAL TESTING</u>
____ 7.3.1.	TC	Verify Vibe-Table Mechanical Setup for Z-axis test, per Attachment 6.0
____ 7.3.2.	TC	EXECUTE Sine Sweep Test, Section 8.0
____ 7.3.3.	TC	EXECUTE Random Vibe Test, Section 9.0
____ 7.3.4.	TC	EXECUTE Sine Sweep Test, Section 8.0
____ 7.3.5.	TC	EXECUTE a functional checkout upon the system
____ 7.3.6.	TC	Log data/results in Appendix 4.0
____ 7.4.	TC	<u>X-AXIS [LOW PRESSURE] VIBRATIONAL TESTING</u>
____ 7.4.1.	TC	RECONFIGURE Vibe-Table Mechanical Setup is Correct for X-axis test, per Attachment 6.0
____ 7.4.2.	TC	EXECUTE SOP SCTEX 0001 Rev 0 101130 (ICU Assembly & Checkout).doc

____ 7.4.3.	TC	EXECUTE Sine Sweep Test, Section 8.0
____ 7.4.4.	TC	EXECUTE Random Vibe Test, Section 9.0
____ 7.4.5.	TC	EXECUTE Sine Sweep Test, Section 8.0
____ 7.4.6.	TC	EXECUTE a functional checkout upon the system
____ 7.4.7.	TC	Log data/results in Appendix 4.0
____ 7.5.	TC	<u>Y-AXIS [LOW PRESSURE] VIBRATIONAL TESTING</u>
____ 7.5.1.	TC	RECONFIGURE Vibe-Table Mechanical Setup for Y-axis test, per Attachment 6.0
____ 7.5.2.	TC	EXECUTE SOP SCTEX 0001 Rev 0 101130 (ICU Assembly & Checkout).doc
____ 7.5.3.	TC	EXECUTE Sine Sweep Test, Section 8.0
____ 7.5.4.	TC	EXECUTE Random Vibe Test, Section 9.0
____ 7.5.5.	TC	EXECUTE Sine Sweep Test, Section 8.0
____ 7.5.6.	TC	EXECUTE a functional checkout upon the system
____ 7.5.7.	TC	Log data/results in Appendix 4.0
____ 7.6.	TC	<u>Z-AXIS [LOW PRESSURE] VIBRATIONAL TESTING</u>
____ 7.6.1.	TC	REORIENT shaker IAW Attachment 7.
____ 7.6.2.	TC	RECONFIGURE Vibe-Table Mechanical Setup for Z-axis test, per Attachment 6.0
____ 7.6.3.	TC	EXECUTE SOP SCTEX 0001 Rev 0 101130 (ICU Assembly & Checkout).doc
____ 7.6.4.	TC	EXECUTE Sine Sweep Test, Section 8.0
____ 7.6.5.	TC	EXECUTE Random Vibe Test, Section 9.0
____ 7.6.6.	TC	EXECUTE Sine Sweep Test, Section 8.0
____ 7.6.7.	TC	EXECUTE a functional checkout upon the system
____ 7.6.8.	TC	Log data/results in Appendix 4.0
____ 7.7.	TC	EXECUTE recycle to previous test (as req'd) or proceed to Shut-Down, Section 10.0

8.0

SINE-SWEEP TEST

NOTE: It is critical that the following file be the proper file according to the configuration intended to be tested (i.e., X&Y-Axis vs Z-axis).

8.1.

TPO Open "CTEX_HTV_SineSweep_XXX-Axis.sin" file

8.2.

TPO Click "SETUP > PROFILES..." and verify/enter the following parameters IAW ATTACHMENT 5.0, HTV MAXIMUM PREDICTED ENVIRONMENTAL LEVELS (MPEL)::

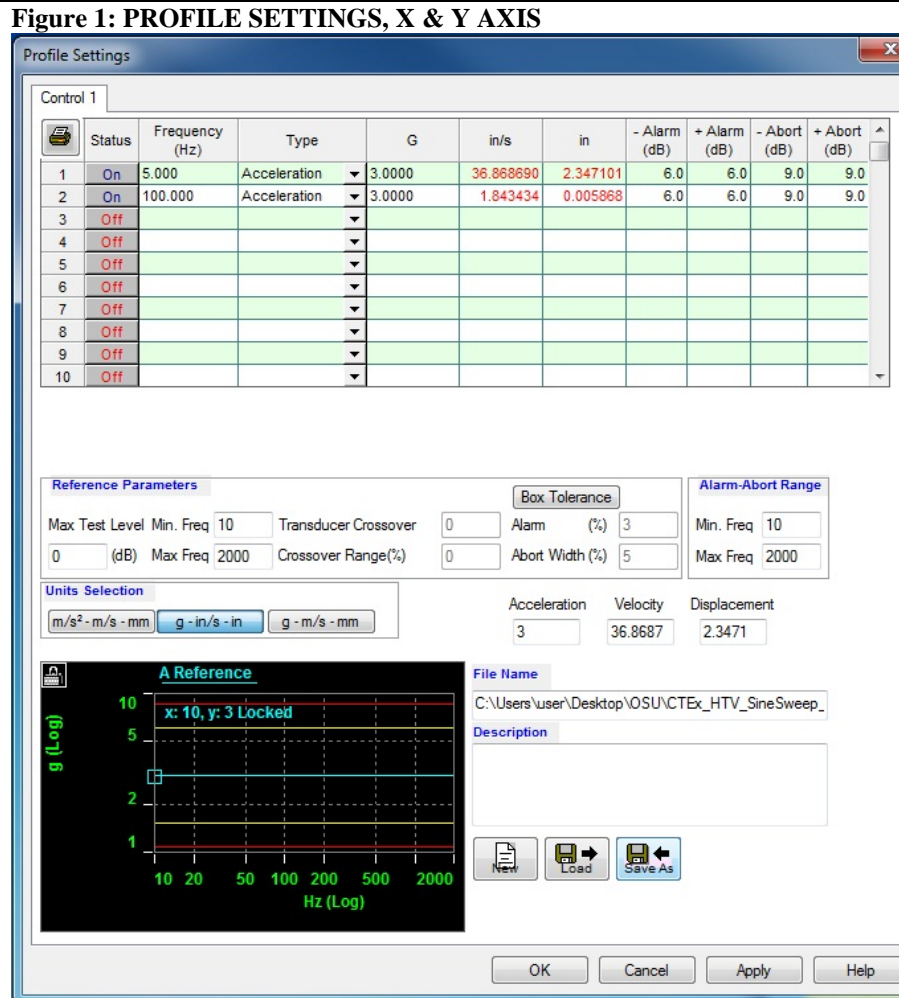
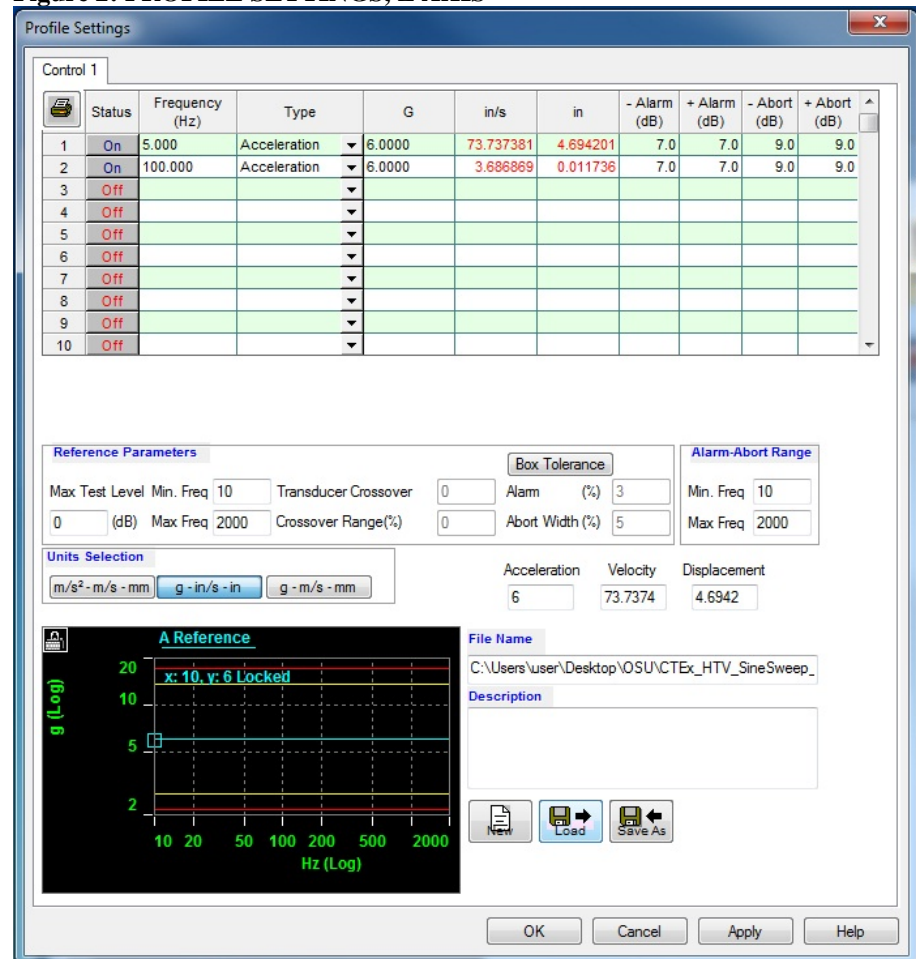


Figure 2: PROFILE SETTINGS, Z AXIS



8.3.

RCL Verify all test personnel are clear of the test facility

CAUTION: Test to commence with the completion of the next step. Anomalous conditions witnessed by ANY test team member are to be reported to TC immediately for command decision (unity of command). TPO to be ready to initiate an ABORT command if directed by TC.

8.4.

TPO Select "RUN TEST" menu and "START TEST" option

8.5.

RCL Upon completion of test, initiate quick visual inspection for post-test anomalous conditions. Take photo.

_____ 8.6.	TPO	Select "Post Analysis" menu, "Save Plot to ASCII file" save file in format: <u>Sx_r1_MMDD_HHMM.xxx</u> Where, S := Type of Test (S ine-Sweep; R andom; B urst) x := Test Axis (x-Axis; y-Axis; z-axis) r1 := Run number (r1, r2, r3, etc.) MM := Two-digit month DD := Two-digit day HH := Two-digit hour (24-hour time) MM := Two-digit minute
_____ 8.7.	TPO	Log Test / Initial Results in Data Log, Appendix 4
_____ 8.8.	TC	Return to next process flow, Section 7.0
END OF SINE-SWEEP TEST		

9.0

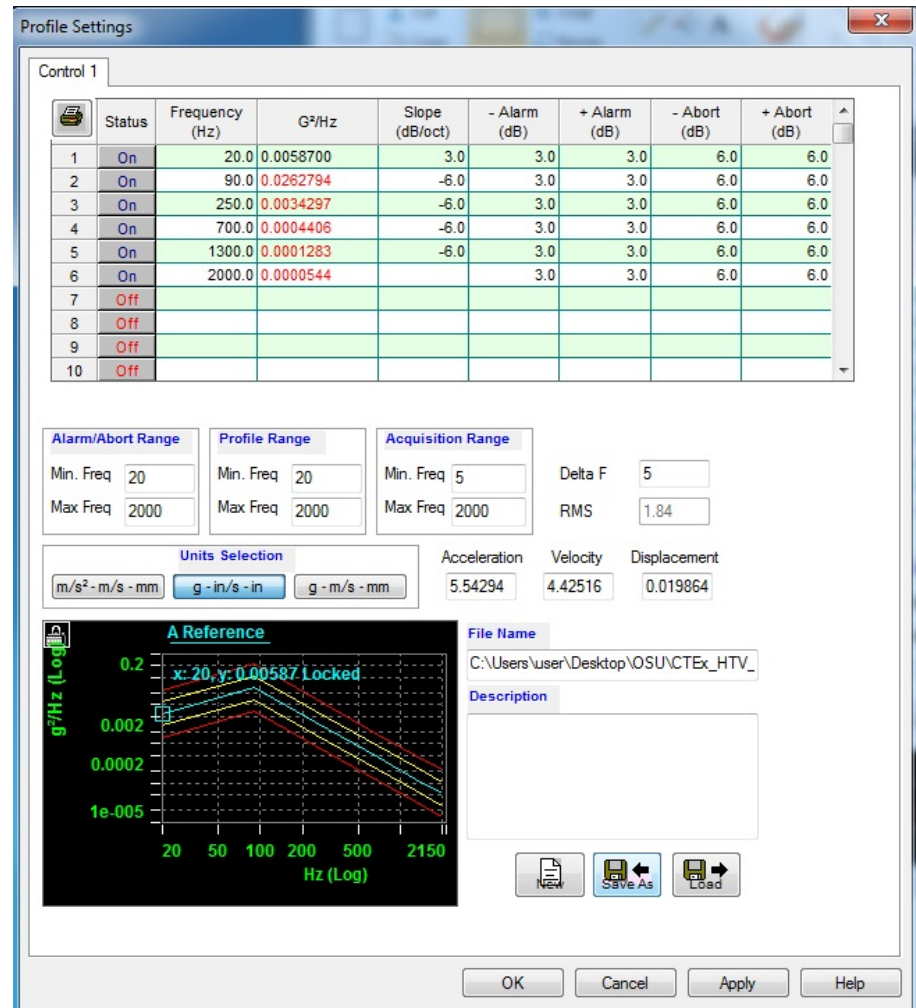
RANDOM-VIBE TEST

____ **9.1.**

TPO Open “CTEx_HTV_RandomVibe.ran” file

____ **9.2.**

TPO Click “**SETUP > PROFILES...**” and verify/enter the following parameters IAW ATTACHMENT 5.0, HTV MAXIMUM PREDICTED ENVIRONMENTAL LEVELS (MPEL):



____ **9.3.**

RCL Verify all test personnel are clear of the test facility

CAUTION: Test to commence with the completion of the next step. Anomalous conditions witnessed by ANY test team member are to be reported to TC immediately for command decision (unity of command). TPO to be ready to initiate an ABORT command if directed by TC.

____ **9.4.**

TPO Select “RUN TEST” menu and “START TEST” option

____ **9.5.**

RCL Upon completion of test, initiate quick visual inspection for post-test anomalous conditions. Take photo.

_____ 9.6.	TPO	Select "Post Analysis" menu, "Save Plot to ASCII file" save file in format: <u>Rx r1 MMDD HHMM.xxx</u> Where, S := Type of Test (S ine-Sweep; R andom; B urst) x := Test Axis (x-Axis; y-Axis; z-axis) r1 := Run number (r1, r2, r3, etc.) MM := Two-digit month DD := Two-digit day HH := Two-digit hour (24-hour time) MM := Two-digit minute
_____ 9.7.	TPO	Log Test / Initial Results in Data Log, Appendix 4
_____ 9.8.	TC	Return to next process flow, Section 7.0
END OF RANDOM VIBE TEST		

10.0

SHAKER-TABLE SHUT-DOWN

- ____ **10.1.** RCM **PRESS STOP** on cooling system M-Series Control Panel and **WAIT** until the STOP button turns red (~3-5 minutes), then **PROCEED**.
- ____ **10.2.** RCM **CLOSE** shop-air isolation hand-valve
- ____ **10.3.** RCM **DISCONNECT** shop-air line to shaker-table inlet
- ____ **10.4.** RCM **TURN OFF** Vibe-slip table
- ____ **10.5.** RCM **TURN OFF** Circuit Breaker No. 7 (Power Station 480V, 3-Phase, 3W)
- ____ **10.6.** TC Sign to confirm completion, date and archive for reporting.

Procedure Completed _____ **Date** _____

Test Conductor

END OF PROCEDURES

12.0		<u>EMERGENCY RESPONSE</u>
		NOTE: Perform the following steps in the event of a major leak, fire or other anomaly which cannot be safely managed by normal securing operations. TC shall have authority (On-Scene Command) over the situation until relieved from support organizations.
12.1	TC	If necessary, EVACUATE and/or Dial 9-911 to notify fire department of emergency
12.2	TPO	If possible/safe, ABORT any test currently in process
12.3	RCM	If possible/safe, CLOSE shop-air isolation hand-valve
12.4	RCM	If possible/safe, TURN OFF Circuit Breaker No. 7 (Power Station 480V, 3-Phase, 3W)
12.5	ANY	If necessary, Brief fire department and medics when they arrive.
12.6	TD/T C	Continue to Monitor Facility until condition has been secured.
		END OF EMERGENCY PROCEDURES

ATTACHMENT 1.0 Control System Setup

Date _____ Time _____

NOTE: If there are any deviations to the verification steps below, note these exceptions and report them to the TC.

1.0

____ 1.1

TPO **TURN ON** Spectral Dynamics control system computer

____ 1.2

TPO **SELECT** "Puma" shortcut on desktop

____ 1.3

TPO **SELECT** "SETUP > CHANNELS" Definition Menu

NOTE: Ensure the accelerometer serial number, sensitivity and other data below matches – annotate if different.

____ 1.4

TPO **Verify / Enter** the following parameters:

Figure 3: PUMA channel definition (Sine Sweep)

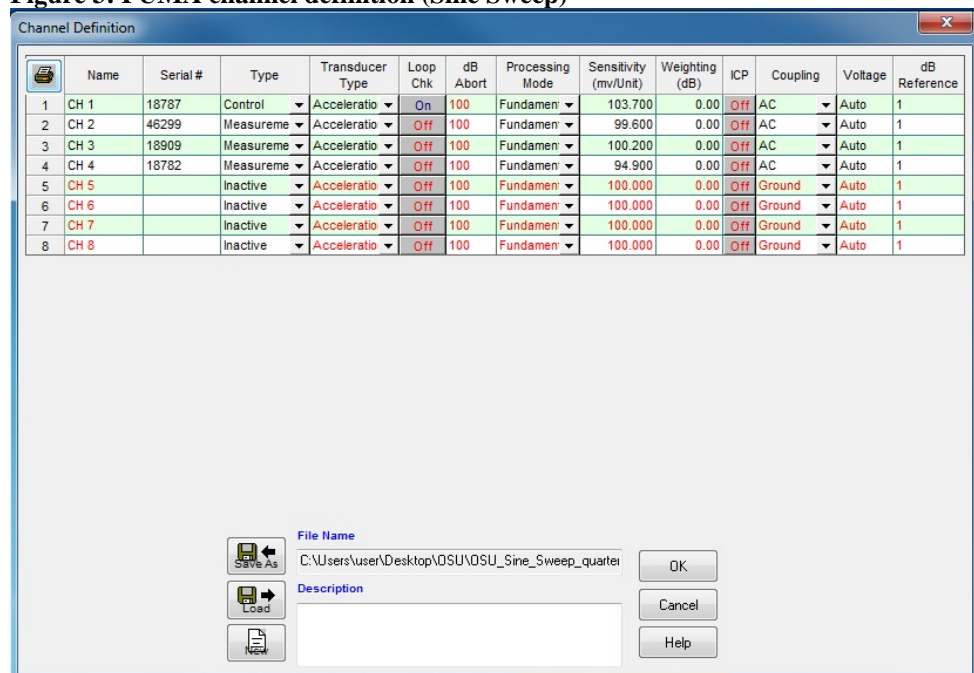


Figure 4: PUMA channel definition (Random Vibe)

	Name	Serial #	Type	Engineering Units	Loop Chk	Sensitivity (mv/Unit)	Transducer Units	Weighting (dB)	RMS Abort	ICP	Coupling	dB Reference	Reference Chans
1	CH 1	18787	Control	No EU's - g's or	On	103.700	g	0.00	30.0000	Off	AC	1	NONE
2	CH 2	46299	Measure	g (in/sec, in)	Off	99.600	g	0.00	30.0000	Off	AC	1	1
3	CH 3	18909	Measure	g (in/sec, in)	Off	100.200	g	0.00	30.0000	Off	AC	1	1
4	CH 4	18782	Measure	g (in/sec, in)	Off	94.900	g	0.00	30.0000	Off	AC	1	1
5	CH 5		Inactive	g	Off	100.000	g	0.00	30.0000	Off	Ground	1	NONE
6	CH 6		Inactive	g	Off	100.000	g	0.00	30.0000	Off	Ground	1	NONE
7	CH 7		Inactive	g	Off	100.000	g	0.00	30.0000	Off	Ground	1	NONE
8	CH 8		Inactive	g	Off	100.000	g	0.00	30.0000	Off	Ground	1	NONE

File Name: C:\Users\user\Desktop\OSU\OSU_Random_Vibe.chn
Description:
Buttons: Save As, Load, New, OK, Cancel, Help

____ 1.5

TPO Sign and Return to TC upon completion of Attachment

TPO Signature _____

END OF ATTACHMENT 1

ATTACHMENT 2.0 Mechanical Setup

Date _____ Time _____

NOTE: During the mechanical set up, perform a visual inspection of connections and components and notify TC of any discrepancies.

1.0

STE SETUP

- | | | |
|------------|-----|--|
| _____ 1.1. | RCL | Verify Red Crew has donned Standard PPE and has hearing protection ready/available |
| _____ 1.2. | RCM | SECURE into STE fixture (thumb-screws hand-tight) |
| _____ 1.3. | RCM | AFFIX accelerometers per Attachment 6.0 |

2.0

SHAKER-TABLE SETUP

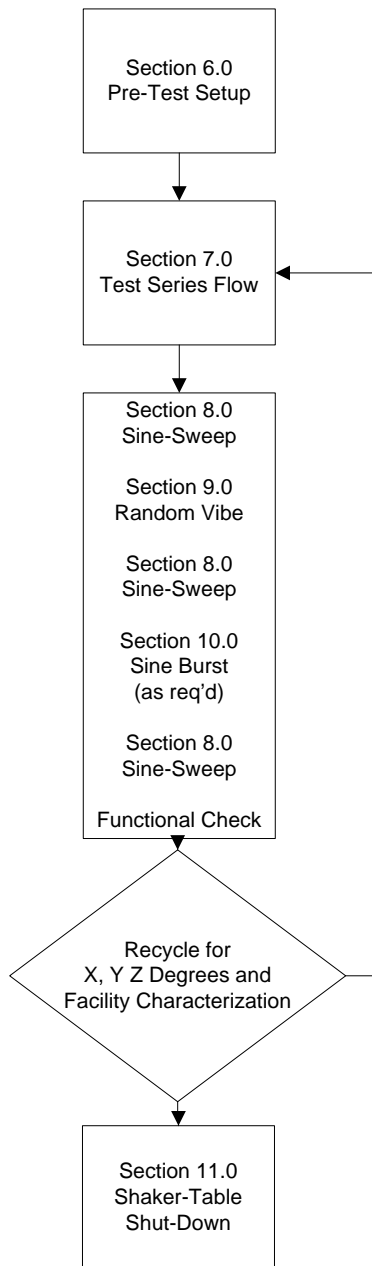
NOTE: The next several steps remove water from the facility shop-air system.

- | | | |
|-------------|-----|--|
| _____ 2.1. | RCM | Verify / CLOSE shop-air isolation hand-valve |
| _____ 2.2. | RCM | DISCONNECT fitting at shop-air isolation hand-valve |
| _____ 2.3. | RCM | POSITION bucket under nozzle |
| _____ 2.4. | RCM | SLOWLY OPEN shop-air isolation hand-valve and allow condensed moisture to exit line; CLOSE shop-air isolation hand-valve when moisture in the line has been minimized. |
| _____ 2.5. | RCM | CONNECT shop-air line to shaker-table inlet |
| _____ 2.6. | RCM | SLOWLY OPEN shop-air isolation hand-valve to roughly 10-20% OPEN |
| _____ 2.7. | RCM | Verify >90 psig on shaker-table inlet gage |
| _____ 2.8. | RCM | TURN ON Circuit Breaker No. 7 (Power Station 480V, 3-Phase, 3W) |
| | | NOTE: The next step only pertains to operations utilizing the slip table (if not to be used, skip to the following step) |
| _____ 2.9. | RCM | PRESS START on Vibe-Slip Table and WAIT until oil emanates from the sides/edges of the slip table, then PROCEED . |
| _____ 2.10. | RCM | PRESS START on cooling system M-Series Control Panel |
| _____ 2.11. | RCM | VERIFY all lights are GREEN on Control Panel and GAIN is set to 3.0 |
| _____ 2.12. | RCL | Sign and Return to TC upon completion of Attachment. |

RCL Signature _____

END OF ATTACHMENT 2

ATTACHMENT 3.0 TOP Process Flow Diagram



ATTACHMENT 4.0 TEST LOG

Itm	TIME	EVENT / STATUS	FILENAME
<i>(#)</i>	<i>(HHMM)</i>	<i>(Desc.)</i>	<i>(SxMMDDr1)</i>
1			
2			
3			
4			
5			
6			
7			
8			
9			
10			
11			
12			
13			
14			
15			
16			
17			
18			
19			
20			
21			
22			
23			
24			
25			
26			
27			

ATTACHMENT 5.0

HTV MAXIMUM PREDICTED ENVIRONMENTAL LEVELS (MPEL)

(Excerpt from NASDA-ESPC-2857, Rev C, 26 JUL 10)

NASDA-ESPC-2857 Rev.C
Part 2 Volume 2

3.4.5. Safety

The cargo shall meet the safety requirement specified in JSX-2001015 for phases 3) and 4) of section 3.3.5.1 and NSTS1700.7B ISS Addendum (for ISS Payloads) or SSP50021 (for ISS system equipments) for phases 5) ~ 7) of section 3.3.5.1.

3.4.6. Environmental Conditions

The unpressurized cargo shall satisfy required performance and functions after exposure to or under the environmental condition defined below. Environmental conditions not defined in this document shall be as specified in section 3.2.6 of SSP50273 "Segment Specification for HTV".

3.4.6.1. Launch Conditions

3.4.6.1.1. Acoustic

Acoustic environment is shown in Table 3.4.6.1.1-1.

3.4.6.1.2. Sinusoidal Vibration

Sinusoidal vibration environment (Maximum Predicted Environment Level, MPEL) when the cargo is fixed with the launch structural support interface (HCAM/HCAM-P) defined in section 3.3.1.1.1 is as follows. Verification approach of equipment within the unpressurized cargo is shown in Fig. 3.4.6.1.2-1.

Z_{PL} Direction: 6.0 Go-p (5 ~ 100 Hz)

X_{PL} , Y_{PL} Direction: 3.0 Go-p (5 ~ 100 Hz)

[Note] Above conditions are derived from H-IIB CLA #4 results.

3.4.6.1.3. Random Vibration

Random vibration environment when the cargo is fixed rigidly with the launch structural support interface (HCAM/HCAM-P) defined in section 3.3.1.1.1 is shown in Table 3.4.6.1.3-1.

3.4.6.1.4. Acceleration

Quasi-static acceleration environment at the center of mass of the unpressurized cargo when the cargo is fixed rigidly with the launch structural support interface (HCAM/HCAM-P) defined in section 3.3.1.1.1 is shown in Table 3.4.6.1.4-1.

3.4.6.1.5. Shock

Shock environment for HCAM/HCSM separation on HCAM-P mounting surfaces and HCSM-P mounting surface are shown in Fig. 3.4.6.1.5-1.

3.4.6.1.6. Load Spectrum

H-IIB load spectrum applied to the center of mass of the unpressurized cargo is shown in Table 3.4.6.1.6-1.

3.4.6.1.7. Ambient Pressure Change

Maximum ambient pressure change rate is 4520 Pa/sec.
(Refer to NASDA-ESPC-2602 HTV/H-IIB Rocket ICD, section 3.2.2.15.1)

3.4.6.1.8. Thermal Condition

Thermal conditions during launch phases are as shown in Table 3.4.6.1.8-1.

3.4.6.1.9. Contamination

(1) During the phases before the HTV is separated from the H-IIB
Amount of the contamination accumulation on the exposed surfaces due to the ullage motor of the H-IIB is less than 10 A (design target value).

(2) During the phases after the HTV is separated from the H-IIB
Contamination environment is specified in SSP 30426, section 3.4 and 3.5.

Table 3.4.6.1.1-1 Acoustic Environment for Launch (Maximum Predicted Environment Level)

1/1 Octave Band Center Frequency (Hz)	Acoustic Level (dB)
31.5	132.2
63	136.3
125	133.4
250	135.4
500	127.5
1000	121.3
2000	116.3
4000	113
8000	114.2
O.A.	140.9
Duration	60 s Max

(This requirement is applied to the equipment installed in the unpressurized cargo)

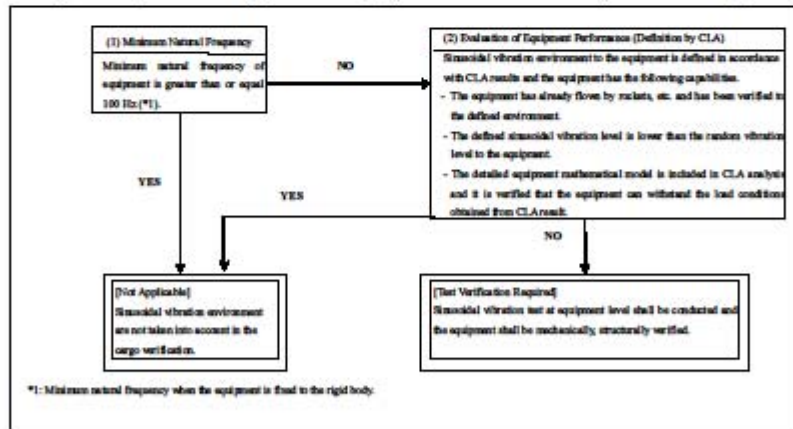


Fig. 3.4.6.1.2-1 Verification Approach of Equipment inside of Unpressurized Cargo to Sinusoidal Vibration Environment (Flow Chart)

Table 3.4.6.1.3-1 Random Vibration Environment for Launch (Maximum Predicted Environment Level)

	Frequency [Hz]	Flight Acceptance Level $\times 9.8^2 [(m/s^2)^2/Hz]$
HTV Cargo (300 kg \geq Mass > 100 kg)	20	0.00587
	20-90	(+3.0 dB/oct)
	90-250	0.02626
	250-700	(-6.0 dB/oct)
	700-1300	0.00337
	1300-2000	(-6.0 dB/oct)
	2000	0.00143
Overall	3.62 $\times 9.8 [m/s^2 rms]$	
HTV Cargo (500 kg \geq Mass > 300 kg)	20	0.00205
	20-90	(+3.0 dB/oct)
	90-250	0.00918
	250-700	(-6.0 dB/oct)
	700-1300	0.00118
	1300-2000	(-6 dB/oct)
	2000	0.00050
Overall	2.14 $\times 9.8 [m/s^2 rms]$	
Duration		60 s Max

Note: This environment is derived from the acoustic test results of HTV System STM (H-IIB acoustic environment including rocket fairing fill effects)

Table 3.4.6.1.4-1 Quasi-Static Acceleration Environment at the Center of Mass of Unpressurized Cargo (Maximum Predicted Environment Level)

	X_{PL} $\times 9.8$ m^2/sec	Y_{PL} $\times 9.8$ m^2/sec	Z_{PL} $\times 9.8$ m^2/sec	RX_{PL} rad/s^2	RY_{PL} rad/s^2	RZ_{PL} rad/s^2
MAX	3.0	3.0	6.0	30.0	15.0	15.0
MIN	-3.0	-3.0	-1.5	-30.0	-15.0	-15.0

[Note] – Accelerations are defined in payload coordinate system.

- 6 components of accelerations are applied simultaneously.
- This environment is derived from the results of HTV/H-IIB CLA (HTV CLA cycle03).
- Reduced load condition will be defined considering Flight specific CLA result reflecting flight configuration and cargo structural math models.

NASDA-ESPC-2857 Rev.C
Part 2 Volume 2

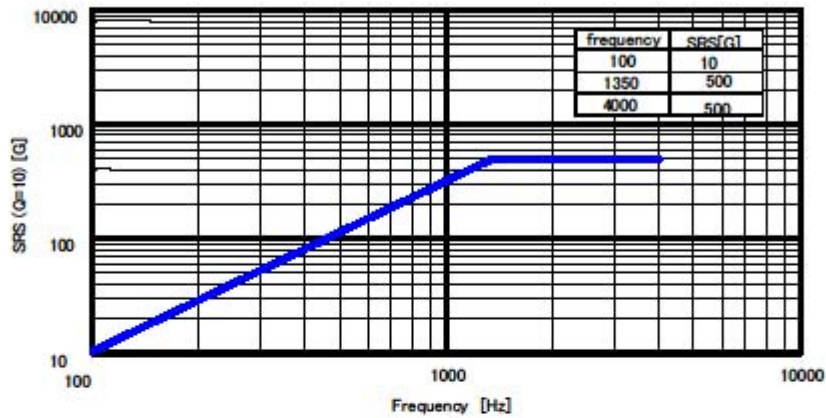


Fig. 3.4.6.1.5-1 Shock Environment for HCAM/HCSM Separation

Table 3.4.6.1.6-1 H-IIB Launch Load Spectrum

Load Step Number	Cycles/Flight		Total	Cyclic Stress (% limit value)	
	Launch	Landing		Minimum	Maximum
1	3	N/A	3	-100	100
2	2		2	-90	90
3	3		3	-80	80
4	3		3	-70	70
5	3		3	-60	60
6	9		9	-50	50
7	17		17	-40	40
8	540		540	-30	30
9	1050		1050	-20	20
10	9420		9420	-10	10

Note: This condition is derived from the results of HTV/H-IIB CLA (CLA#2, CLA#4). (Random vibration due to the acoustic environment inside of H-IIB fairing are not considered)

ATTACHMENT 6.0 Accelerometer Positioning

1.0

X-AXIS (AT LOW PRESSURE)SETUP

NOTE: All accelerometers need to be positioned in-line with the shaker-axis

1.1.

RCL

POSITION accelerometers in the following locations:

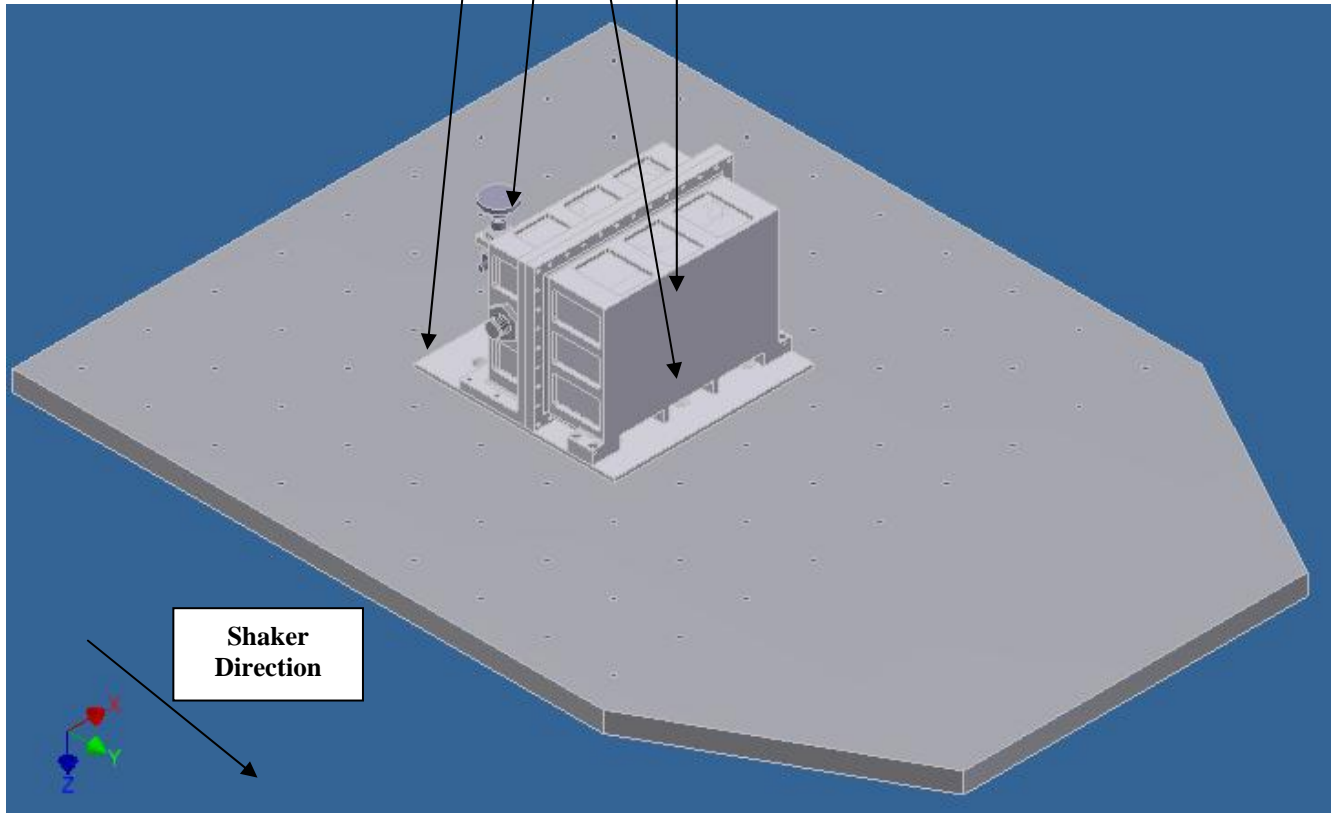
Accelerometer Placement (X-AXIS)

Channel 1: Control, along interface base-plate

Channel 2: Measurement, Place on valve handle

Channel 3: Measurement, Place on SCTEX-0002, Lower portion of housing

Channel 4: Measurement, Place on SCTEX-0002, Upper portion of housing



2.0

Y-AXIS (AT LOW PRESSURE)SETUP

NOTE: All accelerometers need to be positioned in-line with the shaker-axis

2.1.

RCL

POSITION accelerometers in the following locations:

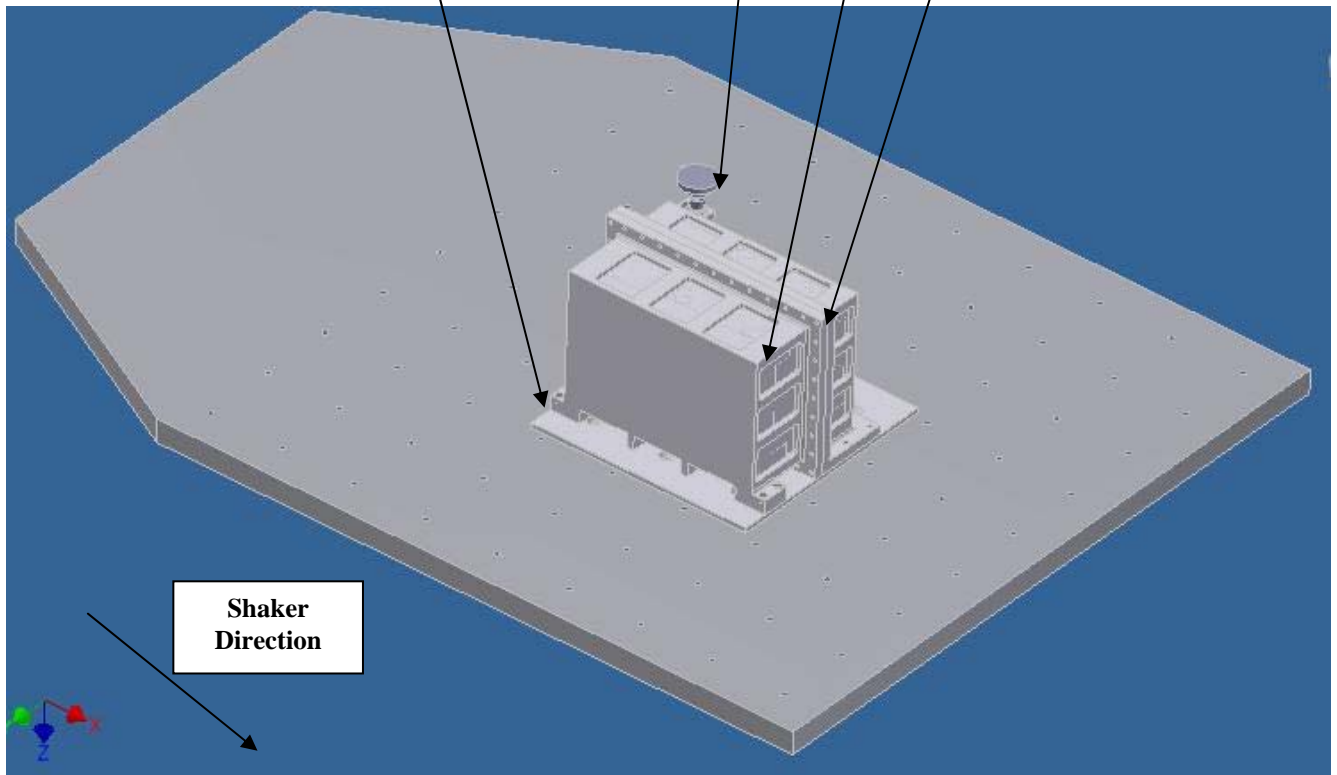
Accelerometer Placement (Y-AXIS)

Channel 1: Control, along interface base-plate

Channel 2: Measurement, Place on valve handle

Channel 3: Measurement, Place on SCTEX-0001, Upper portion of housing

Channel 4: Measurement, Place on SCTEX-0002, Upper portion of housing



3.0

Z-AXIS (AT LOW PRESSURE) SETUP

NOTE: All accelerometers need to be positioned in-line with the shaker-axis

3.1.

RCL

POSITION accelerometers in the following locations:

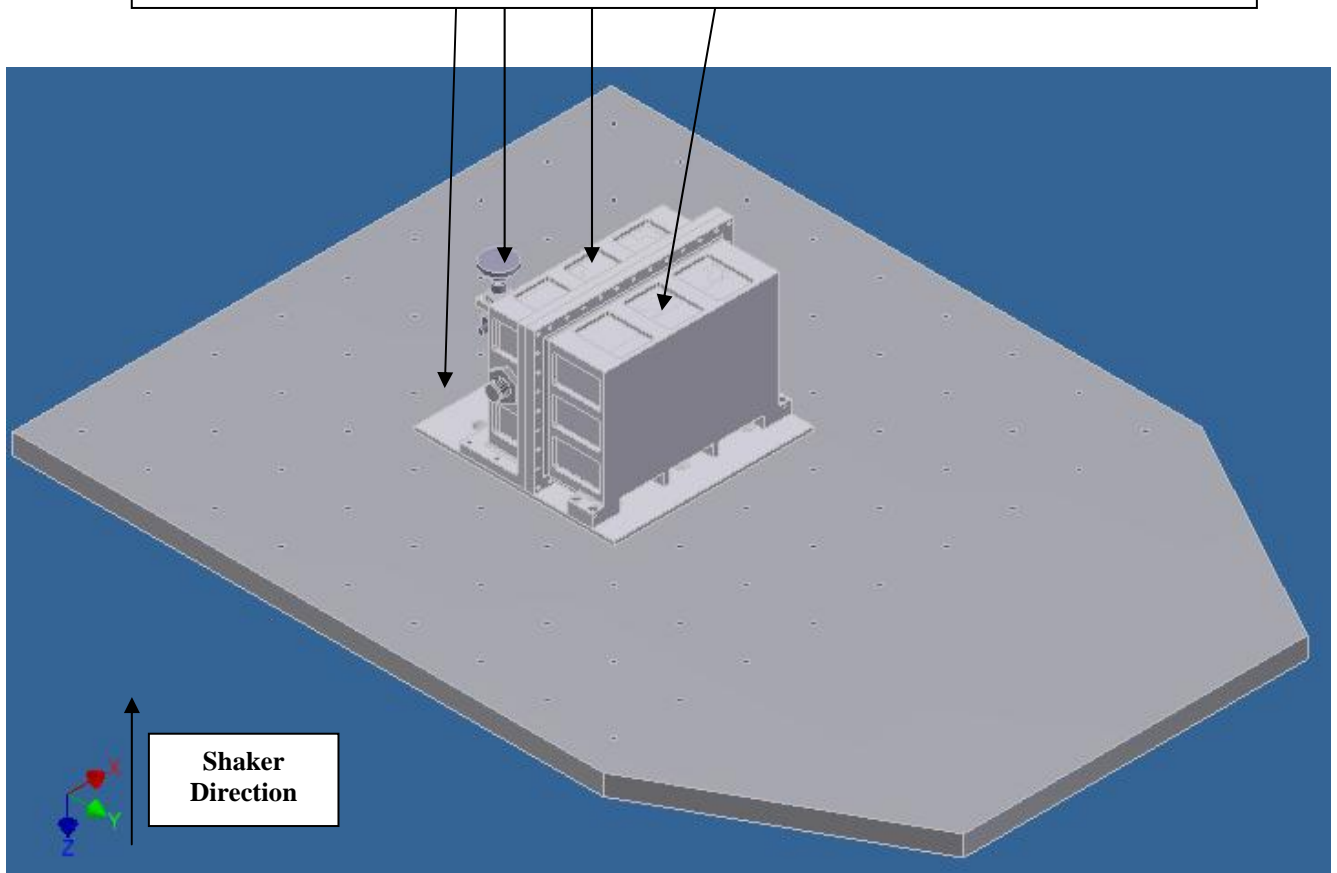
Accelerometer Placement (Z-AXIS)

Channel 1: Control, along interface base-plate (or on shaker plate)

Channel 2: Measurement, Place on valve handle

Channel 3: Measurement, Place on SCTEX-0001, Upper portion of housing

Channel 4: Measurement, Place on SCTEX-0002, Upper portion of housing



4.0

X-AXIS (NO PRESSURE) SETUP

NOTE: All accelerometers need to be positioned in-line with the shaker-axis

NOTE: The electrical feed-through will be removed to pass accelerometers within the housing

4.1.

RCL **POSITION** accelerometers in the following locations:

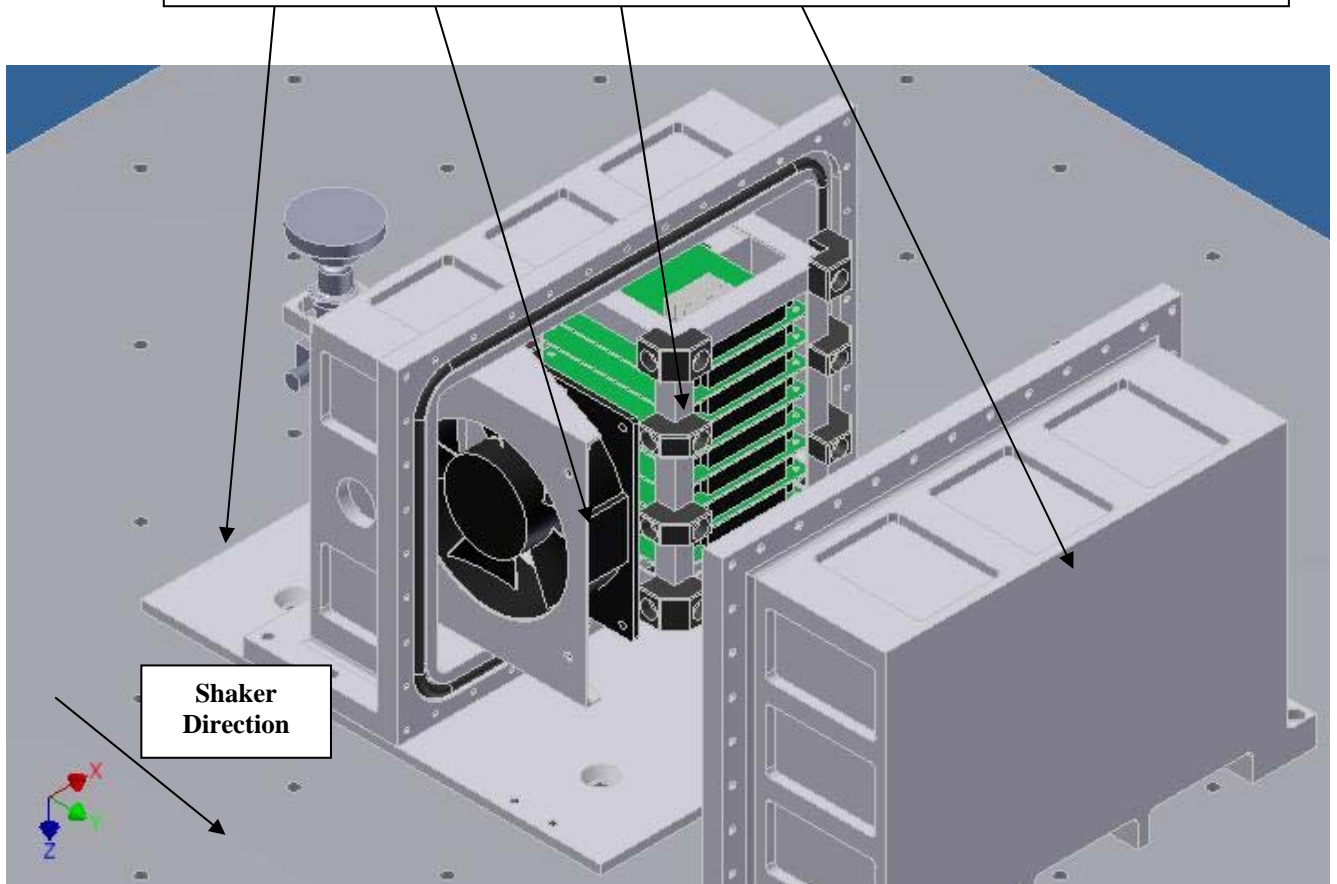
Accelerometer Placement (X-AXIS)

Channel 1: Control, along interface base-plate

Channel 2: Measurement, Place on DC Fan

Channel 3: Measurement, Place on Parvus Card Cage

Channel 4: Measurement, Place on SCTEX-0003 (thermal baffle) –or– SCTEX-0002 (ICU upper housing)



5.0

Y-AXIS (NO PRESSURE) SETUP

NOTE: All accelerometers need to be positioned in-line with the shaker-axis

NOTE: The electrical feed-through will be removed to pass accelerometers within the housing

5.1.

RCL

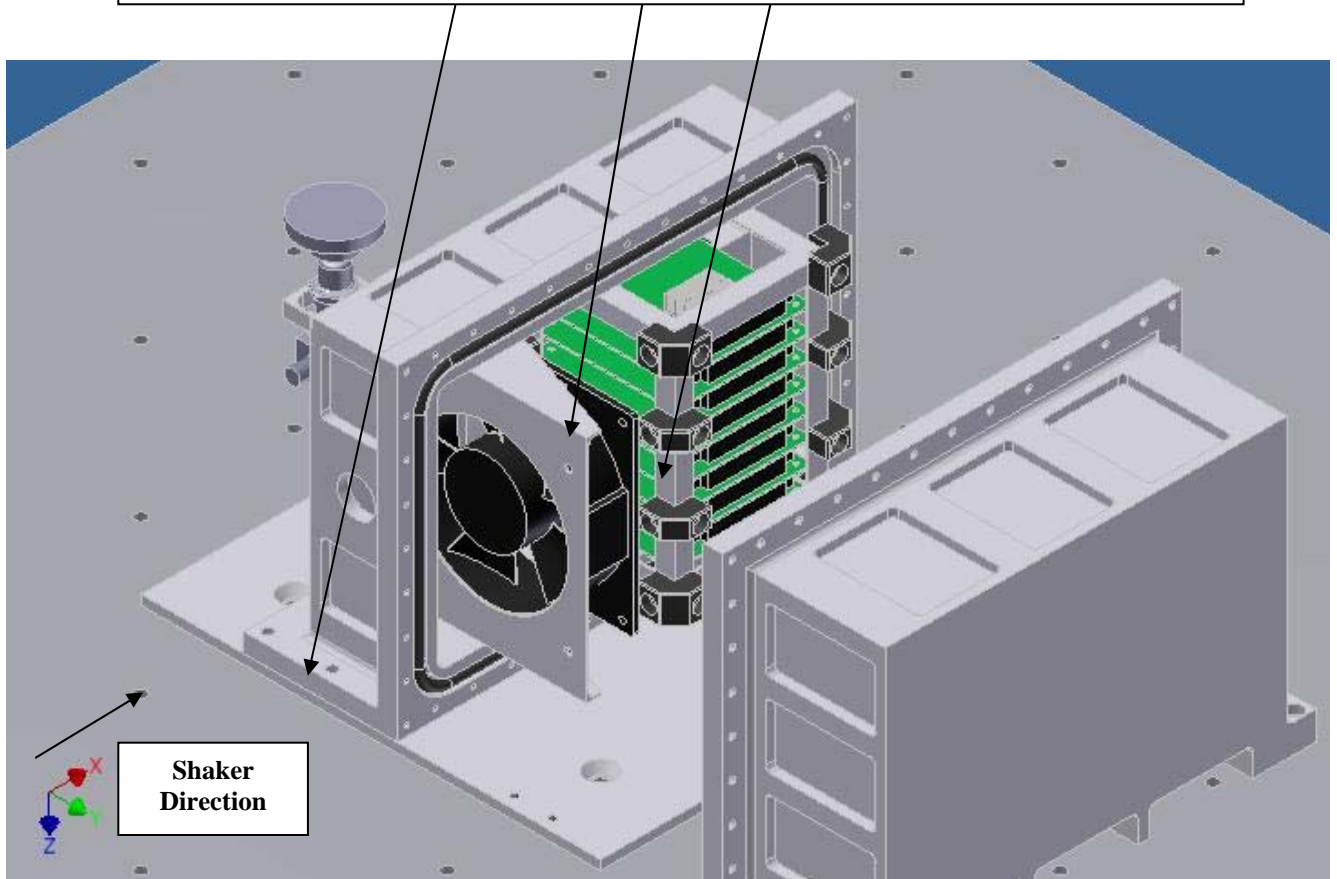
POSITION accelerometers in the following locations:

Accelerometer Placement (Y-AXIS)

Channel 1: Control, along interface base-plate

Channel 2: Measurement, Place on DC Fan

Channel 3: Measurement, Place on Parvus Card Cage



6.0

Z-AXIS (NO PRESSURE) SETUP

NOTE: All accelerometers need to be positioned in-line with the shaker-axis

NOTE: The electrical feed-through will be removed to pass accelerometers within the housing

6.1.

RCL

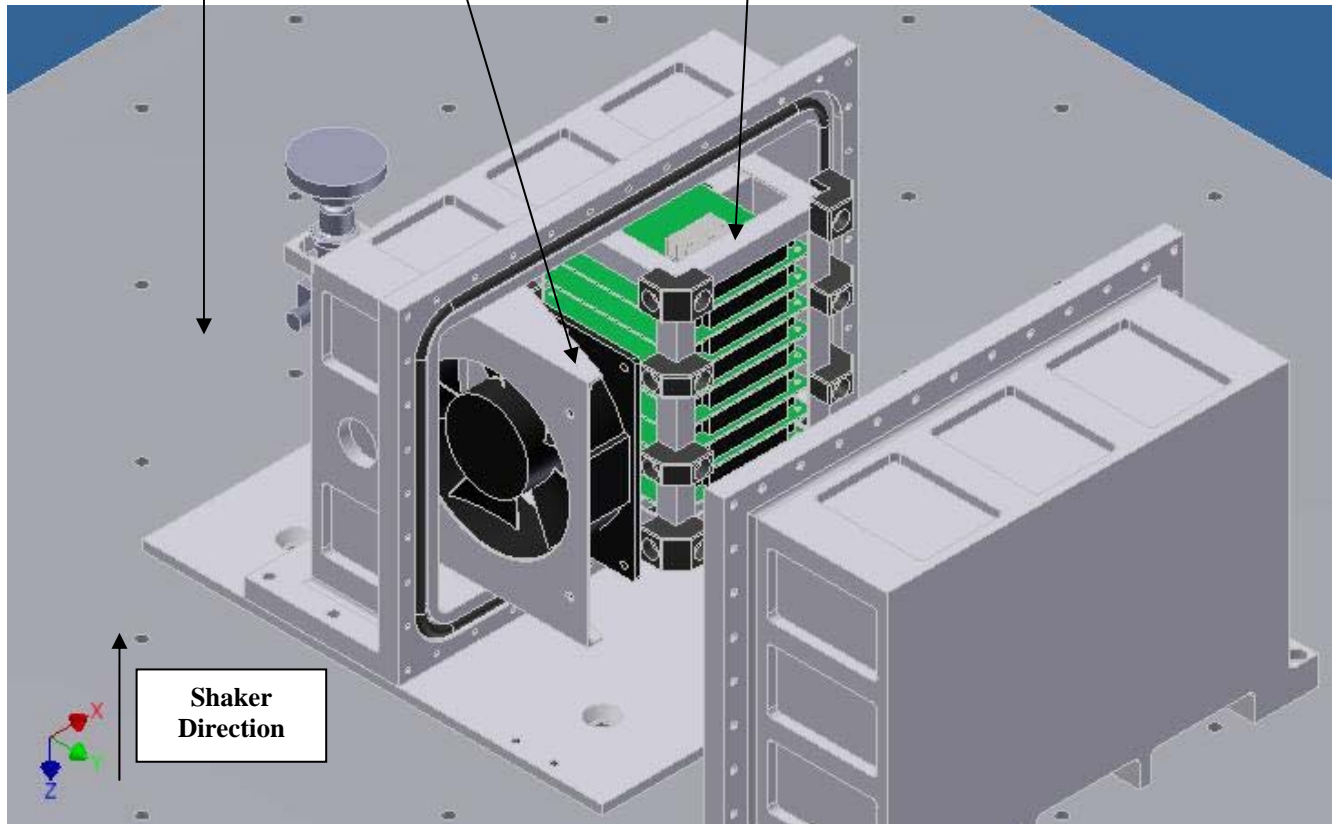
POSITION accelerometers in the following locations:

Accelerometer Placement (Z-AXIS)

Channel 1: Control, along interface base-plate

Channel 2: Measurement, Place on DC Fan

Channel 3: Measurement, Place on Parvus Card Cage



ATTACHMENT 7.0 Vibe Table Reorientation

Date _____ Time _____

NOTE: During reorientation perform a visual inspection of connections and components and notify TC of any discrepancies.

1.0

PREPARATION

- ____ 1.1. RCL Verify Red Crew has donned Standard PPE and has hearing protection ready/available

NOTE: If air system has not already been purged of water today, continue with steps 1.2-1.5. If the system has already been purged, skip to step 1.6.
- ____ 1.2. RCM **Verify / CLOSE** shop-air isolation hand-valve
- ____ 1.3. RCM **DISCONNECT** fitting at shop-air isolation hand-valve
- ____ 1.4. RCM **POSITION** bucket under nozzle
- ____ 1.5. RCM **SLOWLY OPEN** shop-air isolation hand-valve and allow condensed moisture to exit line; **CLOSE** shop-air isolation hand-valve when moisture in the line has been minimized.
- ____ 1.6. RCM **Verify / CLOSE** shop-air isolation hand-valve
- ____ 1.7. RCM **REMOVE** all Test Equipment from the slip table or adapter.
Based on the current and desired configurations follow the section as specified below:

 - Section 2.0: From Slip Table to Adapter on Shaker (Horizontal to Vertical)
 - Section 3.0: From Adapter on Shaker to Slip Table (Vertical to Horizontal)

2.0

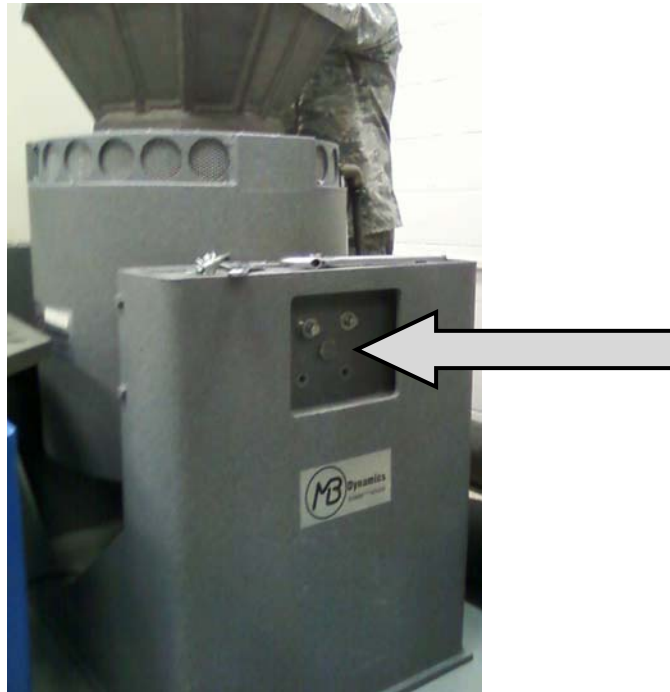
REORIENTING FROM HORIZONTAL TO VERTICAL

- ____ 2.1. RCM **DISCONNECT** air supply from shaker assembly. Black material around shaker head should deflate.

NOTE: The slip table is attached to the shaker via 5 threaded rods as pictured below. The next several steps allow for removal of the threaded rods so that the shaker head can be rotated to the vertical position.

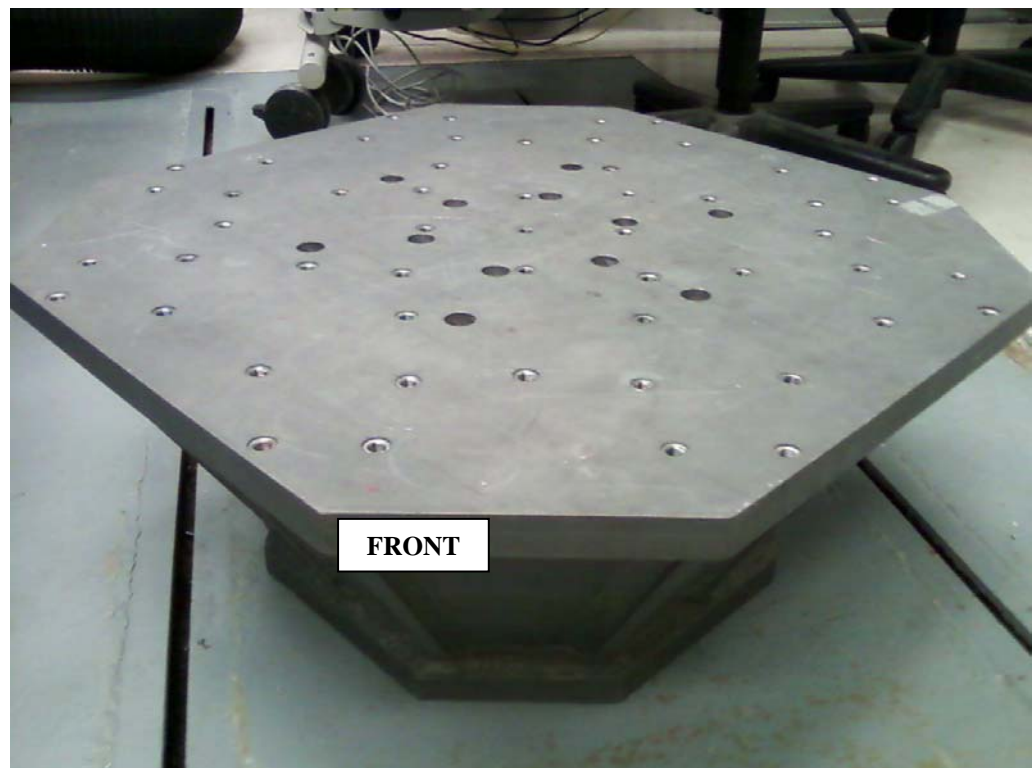


- ____ **2.2.** RCM **REMOVE** the nut from the end of each threaded rod with appropriate closed end wrench.
- ____ **2.3.** RCM **REMOVE** the metal spacer from each threaded rod.
- ____ **2.4.** RCM Slide the slip table off the threaded rods. This may require some slight rotation of the shaker head.
- ____ **2.5.** RCM **REMOVE** black spacers and unscrew each threaded rod.
- NOTE:** Rotating the shaker is a two-person job as described below:
- Person 1:** Slide the slip table away from the shaker. Be careful as the bottom of the table is oily and oil will drip on the floor if it overhangs too far/too long.
- Person 2:** Carefully, but quickly rotate the shaker 90 degrees away from the slip table and towards the back wall.
- Person 1:** Once the shaker has been rotated, safely slide the slip table back towards the shaker.
- ____ **2.6.** RCM **ROTATE** the shaker.
- NOTE:** In the next two steps use 2 small open-ended adjustable wrenches and 1 large open-ended adjustable wrench to secure the 4 small and 1 large bolt on each side of the shaker as shown below:



- ____ **2.7.** RCM **TIGHTEN** the 4 small bolts on each side of the shaker assembly
- ____ **2.8.** RCM **TIGHTEN** the large bolt in the center of each side of the shaker assembly
- ____ **2.9.** RCM **TURN OFF** slip table if done with testing on slip table.

NOTE: The adapter is heavy and moving it requires two people. There should be one side of the adapter that has a faint marking that says "**FRONT**" which should face towards the slip table.



____ **2.10.** RCM **PLACE** the adapter on the shaker head:

NOTE: The Allen Tool used in the following step should be located in the tool box.

____ **2.11.** RCM **DROP** the 12 bolts into the appropriate holes and using the Allen Tool, **TIGHTEN** all bolts to secure the adapter to the shaker head.

NOTE: On both sides of the shaker there are two sets of airbags. Underneath the side fixtures are two valves on each side of the shaker assembly which will be used during the next step to inflate all 4 airbags.

Watch closely to observe the side panels rise as the airbag inflates. Stop inflating when the panel is level with the side walls. Then proceed to the next valve until both side panels are as close to level with the side walls as possible.

Inflate until these panels are level with the sides

Valves are located underneath the side fixtures



____ **2.12.** RCM **CONNECT** the adapter to the hose and **INFLATE** all 4 airbags.

____ **2.13.** RCM **CONNECT** the air supply to the shaker assembly. **TURN ON** air supply and **WATCH** to ensure the black material around the shaker head inflates.

____ **2.14.** RCM **PROCEED** to Step 4.0

3.0 **REORIENTING FROM VERTICAL TO HORIZONTAL**

NOTE: The slip table takes 5-10 minutes before it is completely covered by the oil. Performing the next step allows adequate time for the slip table to fill with oil while the rest of the procedure is followed.

____ **3.1.** RCM **VERIFY / TURN ON** Vibe-Slip Table.

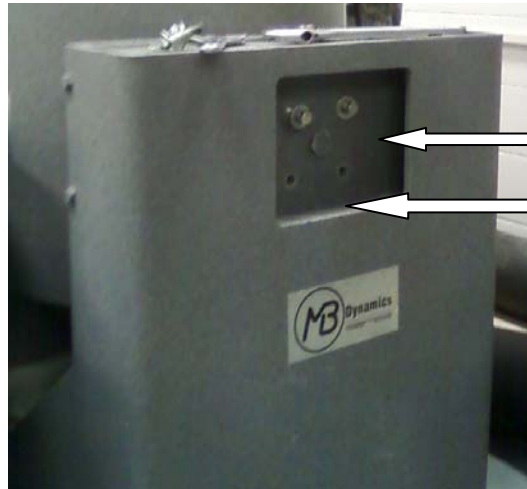
____ **3.2.** RCM **TURN OFF** air supply and disconnect hose from the shaker assembly.

NOTE: On both sides of the shaker there are two sets of airbags. Underneath the side fixtures are two valves on each side of the shaker assembly which will be used during the next step to deflate all 4 airbags.

When deflating, use the valves found underneath the side fixtures



When deflating, look to the side panel cutout and you should see the shaker is now resting on the fixture as depicted below.



This panel should be resting on

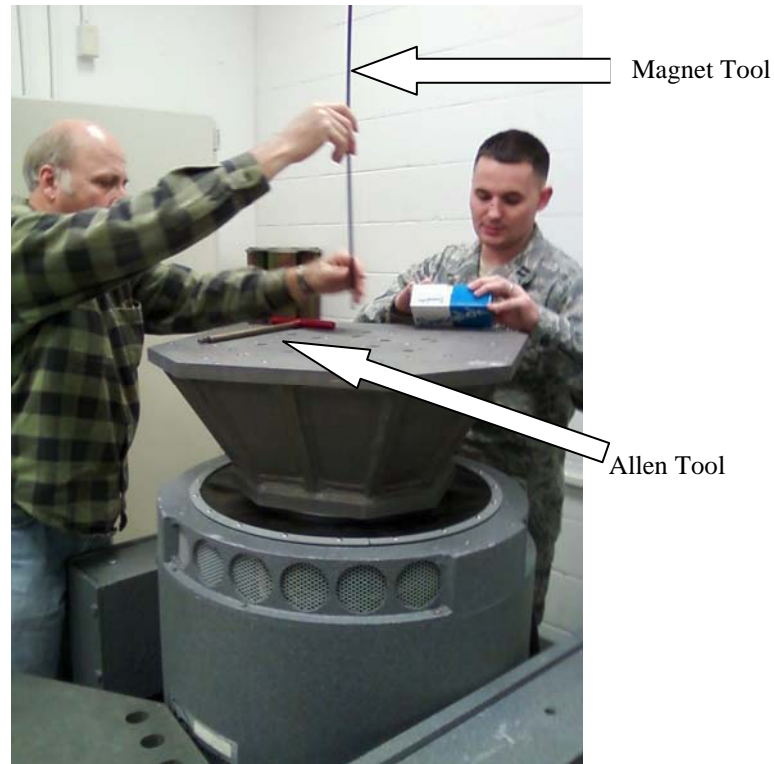
this part of the shaker assembly.

3.3.

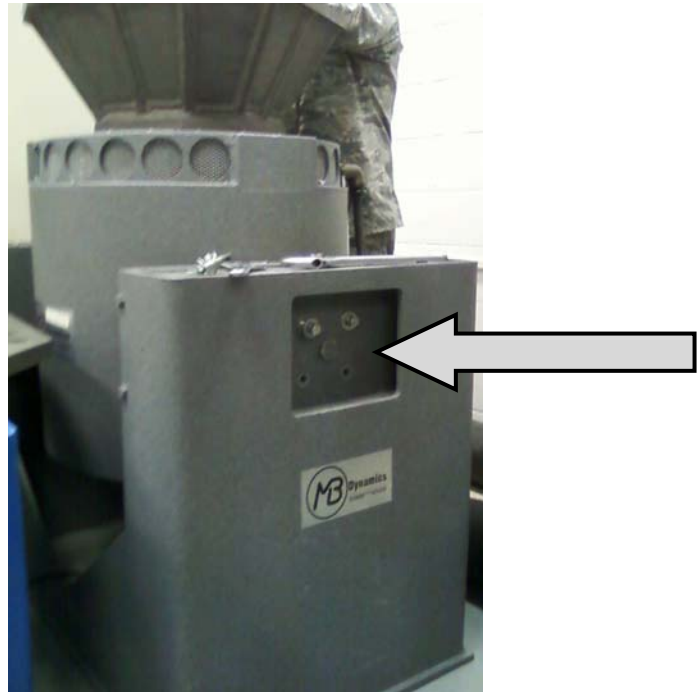
RCM

Using the adapter from the hose, **DEFLATE** all 4 airbags.

NOTE: The Allen Tool and Magnet Tool used in the following two steps should be located in the tool box.



- ___ **3.4.** RCM Using the Allen Tool, **LOOSEN** the 12 bolts that secure the adapter to the shaker head.
- ___ **3.5.** RCM Using the Magnet Tool, **REMOVE** the bolts.
- NOTE:** The adapter is heavy and moving it requires two people.
- ___ **3.6.** RCM **REMOVE** the adapter from the shaker and set it aside.
- NOTE:** In the next two steps use 2 small open-ended adjustable wrenches and 1 large open-ended adjustable wrench to remove the 4 small bolts and loosen the 1 large bolt on each side of the shaker as shown below:
- DO NOT LOSE THE BOLTS – SET ASIDE IN A SAFE PLACE**



- ____ **3.7.** RCM **REMOVE** the 4 smaller bolts from each side of the shaker..
- ____ **3.8.** RCM **LOOSEN** (DO NOT REMOVE) the large bolt in the center of each side of the shaker.
- NOTE:** Ensure the entire slip table surface is covered in oil before proceeding. If required, spread some of the oil over any corners that may still be dry. Check to ensure the slip table is easily moveable on the surface and then proceed to the next step.
- NOTE:** Rotating the shaker is a two-person job as described below:
- Person 1:** Slide the slip table away from the shaker. Be careful as the bottom of the table is now oily and oil will drip on the floor if it overhangs too far/too long.
- Person 2:** Carefully, but quickly rotate the shaker 90 degrees towards the slip table.
- Person 1:** Once the shaker has been rotated, safely slide the slip table back towards the shaker.
- ____ **3.9.** RCM **ROTATE** the shaker.
- ____ **3.10.** RCM **REATTACH** the air supply hose. Watch to ensure the black material around the shaker head inflates.
- NOTE:** The next several steps attach the slip table to the shaker head. Each attachment point has:
- 1) 1 x Threaded rod
 - 2) 1 x Convex black plastic spacer
 - 3) 1 x Concave black plastic spacer

- 4) 1 x Metal convex spacer
- 5) 1 x Nut

There are 5 attachment points and below is a picture of the completed configuration for your reference:



- ____ **3.11.** RCM Screw in the 5 threaded rods into the shaker head.

NOTE: The next step required one convex and one concave black plastic spacer. It does not matter which side goes towards the shaker, just be consistent for each rod.
- ____ **3.12.** RCM **PLACE** spacers on all 5 threaded rods.
- ____ **3.13.** RCM **SLIDE** the slip table onto the threaded rods. This may require some slight rotation of the shaker head to ensure all threaded rods line up correctly.
- ____ **3.14.** RCM Slide the metal spacer onto each threaded rod with the **convex** part towards the shaker
- ____ **3.15.** RCM **AFFIX** a nut onto the end of each threaded rod and tighten with appropriate closed end wrench.
- 4.0** RCL Sign and Return to TC upon completion of Attachment.

RCL Signature _____
END OF ATTACHMENT 7

**TEST AREA B644 L125A
AFIT/ENY**

WRIGHT-PATTERSON AFB, OH

PROCEDURE:

REVISION:

DATE REVISED:

NUMBER OF PAGES:

TOP-SCTEX-0002

0

4 Jan 2011

31

**AFIT / ENY
SPACE SIMULATOR VACUUM FACILITY
OPERATIONS**

SCTE_x ICU Thermal-Vacuum (TVac) Testing

PREPARED BY:

Test Engineer _____

DATE _____

APPROVAL:

AF Customer _____
Thesis Advisor

DATE _____

Revision	Notes	Prepared By
0	-Initial procedure written	Capt. Niederhauser 3 Jan 11

PERSONNEL

EXPERIMENTAL VIBRATION FACILITY

DATE _____

The following personnel are designated as test team members, and are chartered to perform their assignment as follows:

Test Conductor (TC) – Responsible for the timely performance of the test as written. This includes coordinating and directing the activities of the Red Crew and other test support teams. TC is responsible for coordinating all pretest activities and outside support required, including (but not limited to) security, fire, medical, and safety. TC is responsible for initialing completion on each step of the master test procedure.

Name _____ Signature _____

Test Director (TD) – Responsible for overall facility and test safety. Responsible for ensuring all test goals are met and all critical data is acquired. Supervises test activities to ensure procedures are followed. Has authority to perform real-time redlines on test procedures as required to ensure test requirements and goals area met.

Name _____ Signature _____

Red Crew Leader (RCL) – Responsible for directing the activities of Red Crew members. Reports directly to the TC and ensures all Red Crew tasks are completed. Responsible for ensuring all RCM's have all required certifications and training. Responsible for ensuring all required equipment is available, accessible, and serviceable.

Name _____ Signature _____

Test Panel Operator (TPO) – Responsible for operating the facility control systems during test operations as directed by TC. TPO is responsible for notifying the TC of any anomalous conditions.

Name _____ Signature _____

Red Crew Member (RCM) – Reports to the RCL. RCM is responsible for performing test-related tasks as directed by RCL.

Name _____ Signature _____

Other Test Team Members – Responsible for performing ancillary duties in support of test, such as test stand and control room access control, support of anomaly resolution, ground station operation and other necessary activities.

Name _____ Signature _____

Name _____ Signature _____

Name _____ Signature _____

Name _____ Signature _____

ALL TEST TEAM MEMBERS – Responsible for the safe performance of the test. Have read and understood all portions of the test procedure. Any Test Team Member can declare an emergency or unsafe condition.

1.0**ABBREVIATIONS AND ACRYONMS**

CTEx	Space-Based Chromotomography Experiment
DAQ	Data Acquisition
FCV	Fluid Control Valve
FV	Fluid Valve
HPU	Hydraulic Power Unit
HV	Hand Valve
ICU	Instrument Computer Unit
PI	Pressure Indicator
PPE	Personal Protective Equipment
RCL	Red Crew Leader
RCM	Red Crew Member
STE	Special Test Equipment
TC	Test Conductor
TD	Test Director
TP	Turbo Pump
TPO	Test Panel Operator
TVAC	Thermal Vacuum Chamber
VP	Vacuum Pump

2.0**TEST DESCRIPTION AND OBJECTIVES****2.1.****PURPOSE**

This procedure provides the means to perform thermal-vacuum (TVac) testing for test articles relating to the Space-Based Chromotomography Experiment (CTEx), and more specifically, the Instrument Computer Unit (ICU). A simulated space environment (vacuum and temperature gradients) will be utilized in order to characterize this prototype design (in order to acquire lessons learned for a flight design). The CTEx ICU test campaign is a risk reduction ground test exercise intending to mitigate technology concerns for a future ISS mission in later years. The AFIT TVac Facility will be configured with the proper special test equipment (STE) to direct, and measure "maximum predicted environments" associated with operating a SCTEx ICU vehicle in the space environment.

2.2.**SCOPE**

This procedure prepares the instrumentation and control system as well as verifies the proper mechanical configuration during the pre-test setup. Vacuum levels in excess of 1×10^{-5} torr (1×10^{-6} torr desired) are expected to be reached with accompanying temperature profiles of -40 to +40 degrees Celsius. Test recycling will take place as necessary. The test facility will then be properly secured and reconfigured to a safe state for normal operations. Data will be reviewed and achieved. Any facility anomalies or lessons learned will be noted in a final test report.

2.3.**OBJECTIVES**Complete Success

- 1) Temperature profiles do not exceed the device's ability to dissipate the thermal input loading (25W and 40 W expected).
- 2) Mechanical & Electrical functionality during all phases of T-Vac

Marginal Success

Mechanical & Electrical functionality during all phases of T-Vac

Unsuccessful

Failure of any one or more of the success criteria

3.0**DOCUMENTATION**

The completion of each applicable event shall be verified by marking to the left of the item number. Deviations from these procedures will be coordinated with the Test Conductor (NOTE: TC has the local authority to approve red-line revisions to this procedure).

3.1.**REFERENCE DOCUMENTS**

PHPK Thermal Vacuum Operations and Maintenance Guidebook

3.2.**SPECIFICATIONS**

The following list of regulatory documents shall be used as a guide:

NASDA-ESPC-2857 (HTV Cargo Standard Interface Requirements Document)

3.3.**DRAWINGS**

SCTEX-0001 (Housing Lower ICU R0b)
SCTEX-0002 (Housing Upper ICU R0b)
SCTEX-0003 (Plate Thermal Baffle ICU R0)
SCTEX-0004 (Bracket Fan ICU R0)
SCTEX-0005 (Plate Interface Vibe-Test R0)
SCTEX-0006 (Pass-Thru Electrical Hermetic 12-Pin)
SCTEX-0007 (O-Ring 0.25THKx10.5ID)
SCTEX-0008 (SS-4-WVCR-1-2)
SCTEX-0009 (HV-1, Purge/Fill, SS-4BW)
SCTEX-0010 (Fan DC, 12v)
SCTEX-0011 (Card Cage, PC/104)
Attachment 1.0 Electrical Wiring

4.0**TEST REQUIREMENTS AND RESTRICTIONS****4.1.****TRAINING**

The following training is required for personnel using these procedures:

All personnel:

Job Site HAZCOM

Cryogenic Safety Training (Minimum: one operator per team)

4.2.**MAXIMUM PERSONNEL:**

Control Room: 15

Red Crew members will utilize the "buddy system" when performing attachments and setting up the Test Facility and will also work in shifts in order to complete the entire test.

4.3.**LIST OF EQUIPMENT**

SCTEX-0001 (Housing Lower ICU R0b); QTY: 1EA
SCTEX-0002 (Housing Upper ICU R0b); QTY: 1EA
SCTEX-0003 (Plate Thermal Baffle ICU R0); QTY: 1EA
SCTEX-0004 (Bracket Fan ICU R0); QTY: 1EA
SCTEX-0005 (Plate Interface Vibe-Test R0); QTY: 1EA
SCTEX-0006 (Pass-Thru Electrical Hermetic 12-Pin); QTY: 1EA
SCTEX-0007 (O-Ring 0.25THKx10.5ID); QTY: 1EA
SCTEX-0008 (SS-4-WVCR-1-2); QTY: 1EA
SCTEX-0009 (HV-1, Purge/Fill, SS-4BW); QTY: 1EA
SCTEX-0010 (Fan DC, 12v); QTY: 1EA
SCTEX-0011 (Card Cage, PC/104); QTY: 1EA

Fasteners:

4 each 8-32 x 0.5"L
4 each 8-32 x 2.0"L
4 each 8-32 x 0.375"L
40 each 8-32 x 1.0"L

Other:

Teflon Tape
O-Ring Lubricant (Vacuum-Compatible)

Test Pod Fixture STE, Camera, SCTEx ICU Test Article, Ground Station Computer, Light Meter

Ensure all tools associated with this experiment/test/operation are accounted for prior to initiating system/item test. Assure all trash, debris, and FOD is picked up from around the test facility.

5.0**SAFETY REQUIREMENTS****5.1.****PERSONNEL PROTECTIVE CLOTHING REQUIREMENTS**

Standard PPE: Safety goggles or glasses (as required), hearing protection (when required), safety-toe boots – soles and heels made of semi-conductive rubber containing no nails.

Cryogenic PPE: Have the following available as required: cryogenic gloves with long cuffs, face shield or hood, and safety goggles.

All jewelry will be removed by Test Crew members while working on the test facility. No ties or other loose clothing permitted (at TC discretion).

5.2.**TEST AREA ACCESS DURING OPERATIONS**

The test facility room will be limited to test personnel only. Personnel will not be allowed access to the test area unless cleared by the TC.

5.3.**EXPLOSIVE AND PERSONNEL LIMITS**

NONE

5.4.**EMERGENCY PROCEDURES**

In the event of an emergency that jeopardizes the safety of the operators or other personnel perform Section XX emergency procedures at the end of this document.

5.5.**SPECIAL INSTRUCTIONS**

Test Crew members shall place all cellular telephones on “silent mode” or turn off prior to completing any portion of this procedure.

Test Crew Members shall notify the TC of any leaks from HPU, hydraulic system, or pneumatic system pipe or tubing connections.

6.0		<u>PRE-TEST SETUP</u>
____ 6.1.	TC	Verify all pages in this procedure are intact and complete
____ 6.2.	TC	Go through the procedure and input any specific information required to perform operation.
____ 6.3.	TC	Verify with Facility Management that no open Work Orders / Issues are listed for the TVac Test Facility, impeding operations.
____ 6.4.	TC	Perform Setup Brief with Test Crew Members and note any redline changes on Attachments.
____ 6.5.	TC	Verify Red Crew has donned standard PPE (and noted restrictions).
____ 6.6.	TC	Initiate the following Procedures/Attachment(s): NOTE: All attachments can be completed independently from one another – there is no order to completion. Attachment 1 – Control System Setup Attachment 2 – Mechanical Setup
____ 6.7.	TC	Verify that Attachments are complete. ____ Attachment 1 ____ Attachment 2
____ 6.8.	TC	Perform Pre-Operation Brief with Test Crew Members - Objective - Personnel and assigned roles/duties - Safety: materials, PPE, communication, etc. - Sequence of events - Emergency procedures
____ 6.8.1.	TC	Pre-Test Brief Time _____
____ 6.8.2.	TC	Verify all personnel involved with the operation have signed this procedure.

7.0

VACUUM PUMP OPERATION

____ **7.1.**

IE Verify data recording started for:

____ ICU P/C-104 Stack

____ Thermocouple & Electrical Power Recording Station

____ **7.2.**

TPO Record CC-10: _____ torr (TVAC Vac Level)

____ **7.3.**

TC Verify GO/NO-GO status with test team to begin vacuum pump ops:

____ TD ____ TC ____ IE ____ TPO ____ RCL

NOTE: The vacuum roughing pump will begin operation with the completion of the next step. On the back of the roughing pump, the oil you can see through the glass panel may foam and it may start to smell in the room a little. That is normal -- if foaming doesn't go down after 45-60 seconds, alert TVAC support personnel.

____ **7.4.**

TPO **START** VP-03 (VAC ROUGHING PUMP).

____ **7.5.**

TPO **OPEN** FV-06 (VAC ROUGHING ISO)

____ **7.6.**

TPO Record CC-10 every ten (10) minutes (or at TC discretion):

Time (hhmm)	Vacuum Level (Torr)

NOTE: Roughing takes approximately less than one hour to achieve

____ **7.7.**

TC When CC-10 reads 5×10^{-2} torr (or less), **proceed**.

____ **7.8.**

RCM Verify / **OPEN** HV-12 (H2O COOLING SUPPLY)

____ **7.9.**

TPO **START** TP-01 (VAC TURBO PUMP)

____ **7.10.**

TPO **CLOSE** FV-06 (VAC ROUGHING ISO)

____ 7.11. TPO **OPEN** FV-02 (Vacuum Fore-Line Iso)

____ 7.12. TPO Record CC-10 every ten (10) minutes:

Time (hhmm)	Vacuum Level (Torr)

____ 7.13. TC When CC-10 reads $<1 \times 10^{-6}$ torr –or– suitable vacuum level as deemed by TC, **proceed**.

____ 7.14. RCM Verify / **CONNECT** LN2 Supply lines as needed

____ 7.15. RCM Verify / **OPEN** LN2 Supply Tank

____ 7.16. TPO Select “Enclosure OV” screen

____ 7.17. TPO **START** P-104 (FLU THERMAL XFER PUMP)

____ 7.18. TPO Verify and record fluoroinert fluid flow on FE-105 is 23 +/- 5 gpm and allow to flow for at least one (1) minute prior to proceeding:

_____ gpm

____ 7.19. TPO Select “Seg Temp Entry” screen

____ 7.20. IE Verify data recording operating nominally, or as expected for:

_____ ICU P/C-104 Stack

_____ Thermocouple & Electrical Power Recording Station

____ 7.21. TPO Record CC-10: _____ torr (TVAC Vac Level)

____ 7.22. TC Verify GO/NO-GO status with test team to begin thermal cycling:

_____ TD _____ TC _____ IE _____ TPO _____ RCL

NOTE: Thermal cycling will commence with the completion of the next step. A RCM needs to monitor the LN2 dewar supply/level to perform a change-over when necessary (note that typically three dewars are required to acquire -24/-40 deg C TVAC temperatures from ambient). Additionally, all test team members need to watch for leaks in this area during the operation.

____ 7.23.

TPO

START Segment Cycling, note the amount of LN2 dewars utilized:

Dewar No.	Time	TVAC Temp		Dewar No.	Time	TVAC Temp
1				15		
2				16		
3				17		
4				18		
5				19		
6				20		
7				21		
8				22		
9				23		
10				24		
11				25		
12				26		
13				27		
14				28		

____ 7.24.

TC

Determine whether tests accomplished are adequate; if so, skip to TVAC shutdown, Section 8.0; otherwise, proceed.

____ 7.25.

TPO

START Segment Cycling

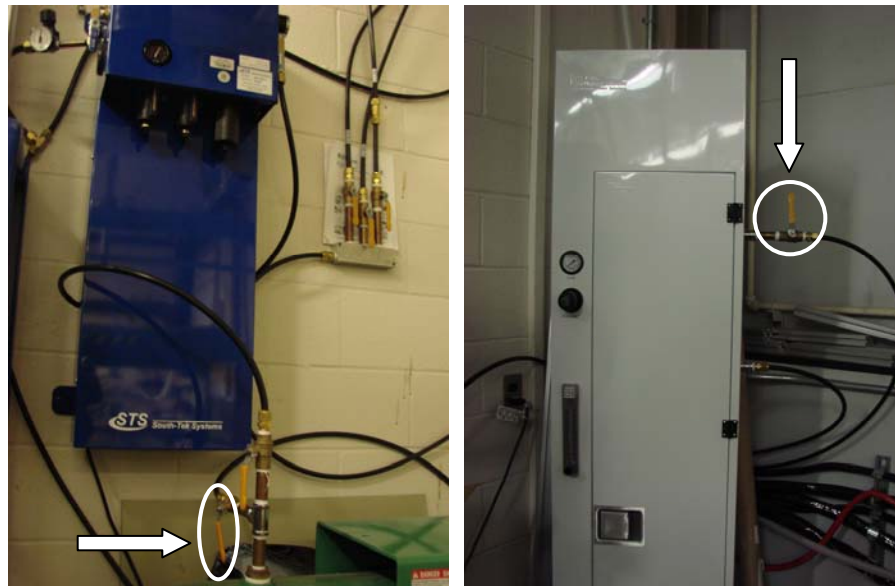
8.0**TVAC SHUT-DOWN**

- ____ **8.1.** TPO Select "Enclosure OV" screen
- ____ **8.2.** TPO Verify / **STOP** P-104 (FLU THERMAL XFER PUMP)
- ____ **8.3.** TPO **Select** "Vac Chamber OV" Screen
- ____ **8.4.** TPO **Verify / CLOSE** FV-02 (Vacuum Fore-Line Iso)
- ____ **8.5.** TPO **Verify / STOP** TP-01 (VAC TURBO PUMP)
- ____ **8.6.** TPO **Verify / STOP** VP-03 (VAC ROUGHING PUMP)
- ____ **8.7.** TPO **Verify / CLOSE** FV-06 (VAC ROUGHING ISO)

WARNING: Failure to disengage the door clamps in the next step prior to commencing further shutdown (via loosening the threaded rods and moving the C-clamps out of the path of the door) can lead to personnel injury.

- ____ **8.8.** RCM **DISENGAGE** door clamps.

NOTE: TVAC GN2 back-filling will commence with the completion of the next two steps. HV-160 & HV-161 can be found in the back of the lab in Bldg 640, Rm 273 and are pictured below. While FV-10 is open, flow may be verified via adjusting the purge flow-meter to a set-point between 2-3 gpm.



- ____ **8.9.** RCM Verify / **OPEN** HV-160 & HV-161 (GN2 Supply / Purge 1)
- ____ **8.10.** TPO **OPEN** FV-10 until CC-10 reads 760 torr, then **CLOSE** (GN2 TVAC FILL ISO).
- ____ **8.11.** RCM **CLOSE** HV-115 (Fluoroinert Tank Ullage Pressure Iso)

____ 8.12.	RCM	CLOSE HV-160 & HV-161 that were opened in step 8.9.
____ 8.13.	RCM	OPEN chamber door.
____ 8.14.	RCM	CLOSE Facility Soft Water Hand-Valve (HV-12)
<p>NOTE: If deemed prudent by TVAC facility personnel, upon completion of TVAC tests, the TVAC door may be closed and VP-03 may remain on as “a happy roughing pump is a running roughing pump” (WL).</p>		
____ 8.15.	TC	Sign to confirm completion, date and archive for reporting.
<p>Procedure Completed _____ Date _____</p>		
<p style="text-align: center;">Test Conductor</p>		
<p>END OF PROCEDURES</p>		

12.0		<u>EMERGENCY RESPONSE</u>
12.1	TC	NOTE: Perform the following steps in the event of a major leak, fire or other anomaly which cannot be safely managed by normal securing operations.
12.2	TPO RCL	Monitor the test stand situation using remote cameras, and system instrumentation.
12.3	TPO / TC / RCM	If necessary, Brief fire department and medics when they arrive.
12.4	TPO	Continue to Monitor Facility until condition has been secured.
		END OF EMERGENCY PROCEDURES

ATTACHMENT 1.0 Control System Setup

Date _____ Time _____

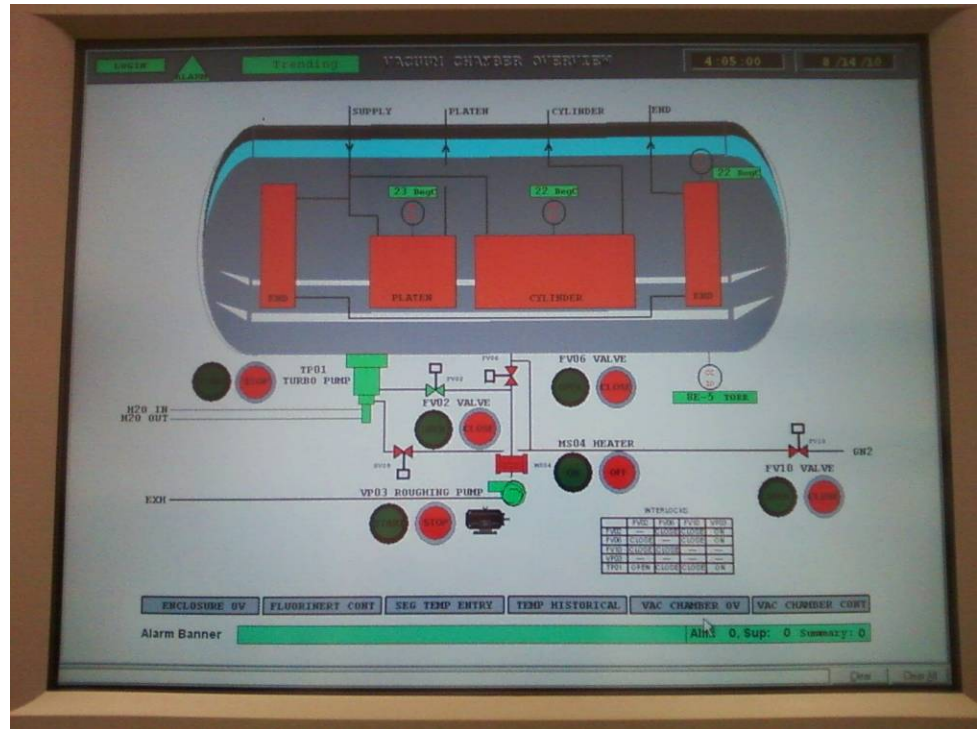
NOTE: If there are any deviations to the verification steps below, note these exceptions and report them to the TC.

1.0

TVAC CONTROL SYSTEM SETUP

____ 1.1 TPO **VERIFY / TURN ON TVAC control system**

____ 1.2 TPO **SELECT "VAC CHAMBER OV"**



____ 1.3 TPO **VERIFY / STOP TP-01**

____ 1.4 TPO **VERIFY / STOP VP-03**

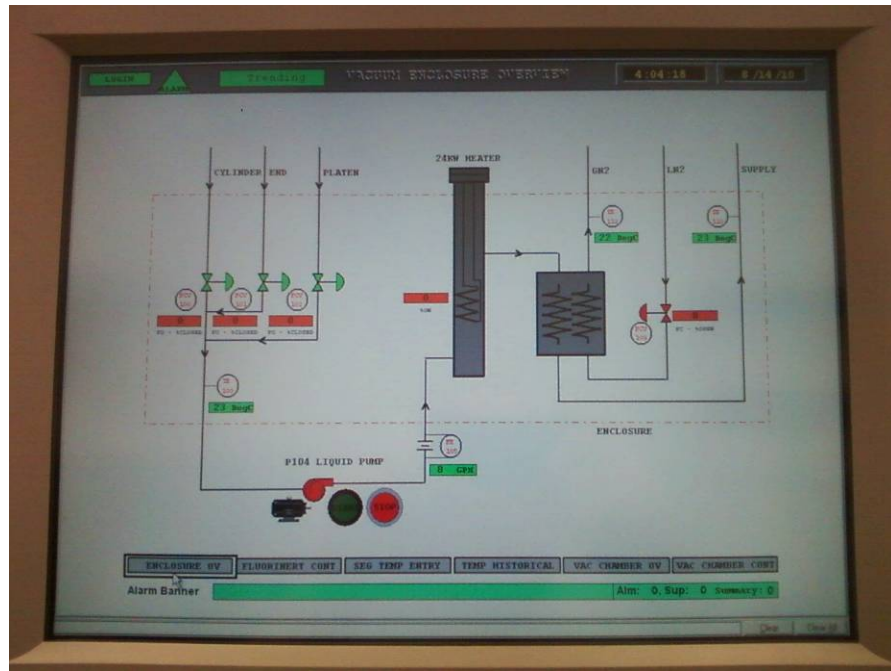
____ 1.5 TPO **VERIFY / CLOSE FV-02**

____ 1.6 TPO **VERIFY / CLOSE FV-06**

____ 1.7 TPO **VERIFY / CLOSE FV-10**

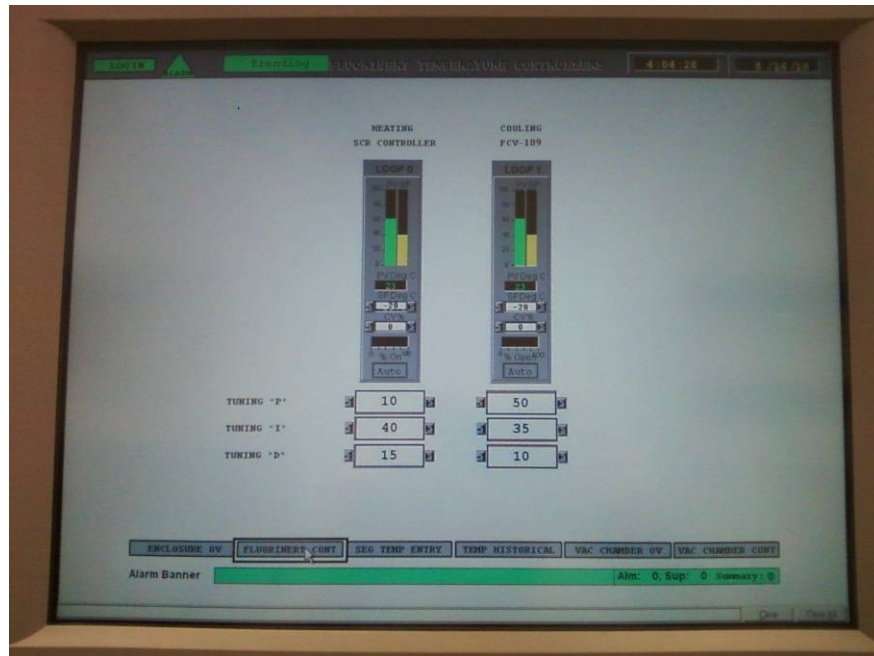
____ 1.8 TPO **VERIFY / OFF MS-04**

____ 1.9 TPO **SELECT "ENCLOSURE OV"**



____ 1.10 TPO **VERIFY / STOP P-104**

____ 1.11 TPO **SELECT "FLUORINERT CONT"**

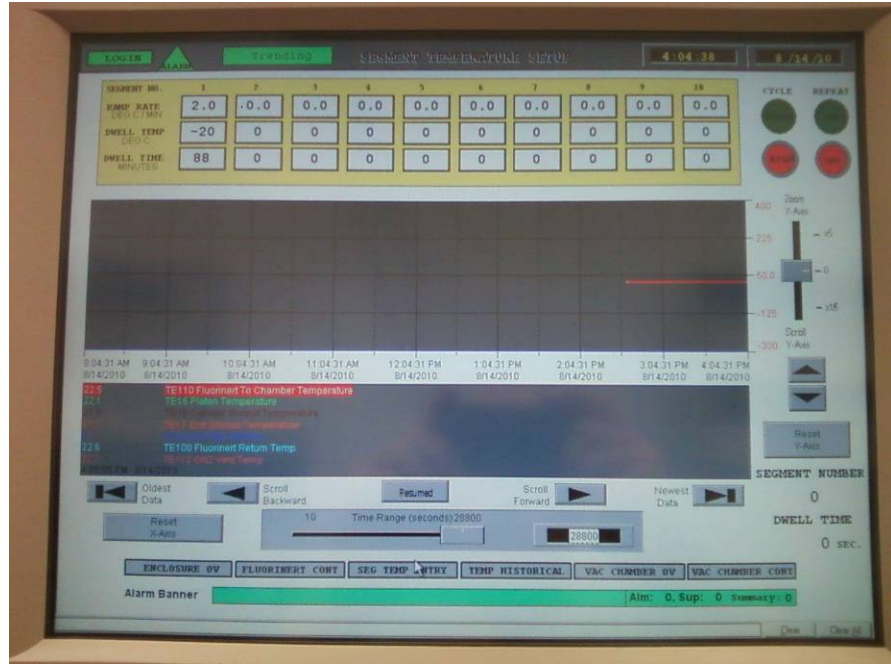


____ 1.12 TPO **Verify / Enter the following parameters:**

	Heating/SCR Contrlr	Cooling/FCV-109
Proportional (P)	10	50
Integral (I)	40	35
Derivative (D)	15	10

1.13

TPO **SELECT "SEG TEMP ENTRY"**



1.14

TPO Verify / **STOP** Segment Cycle (Temp Cycle Ctrl)

1.15

TPO Verify / **OFF** Repeat (Temp Repeat Ctrl)

1.16

TPO **Verify / Enter** the following parameters:

Segment No.	1	2	3	4	5	6	7	8	9	10
Ramp Rate (deg C/Min)										
Dwell Temp (Deg C)										
Dwell Time (Min)										

1.17

TPO Sign and Return to TC upon completion of Attachment

TPO Signature _____

END OF ATTACHMENT 1

ATTACHMENT 2.0 Mechanical Setup

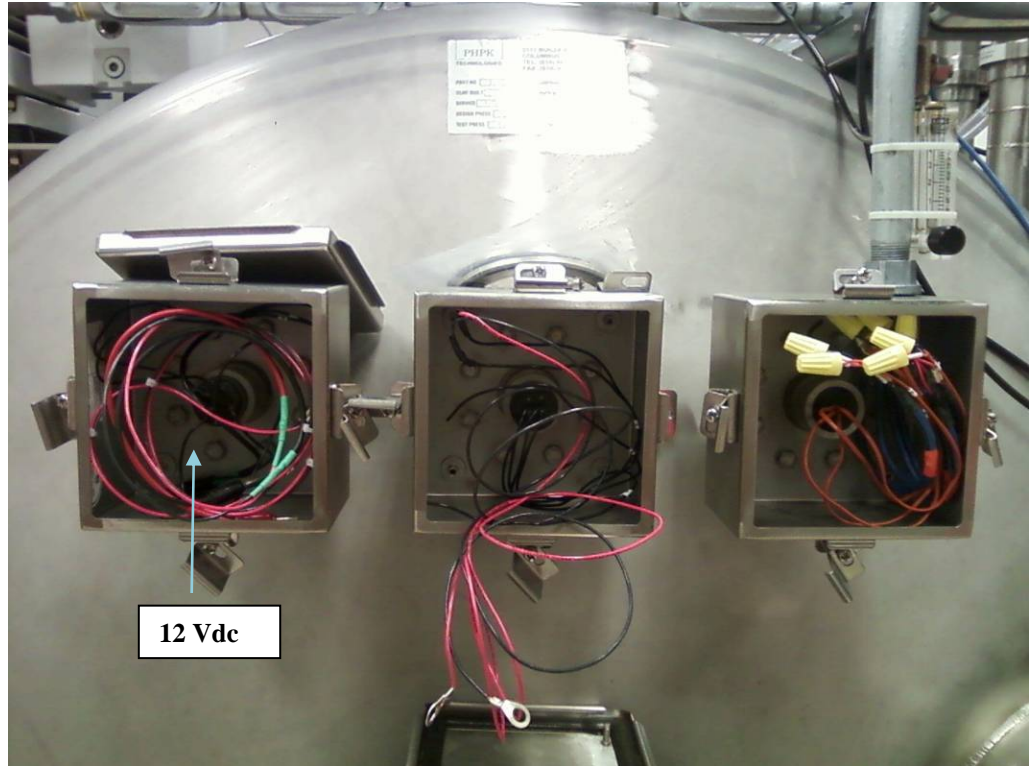
Date _____ Time _____

NOTE: During the mechanical set up, perform a visual inspection of connections and components and notify TC of any discrepancies.

1.0

STE SETUP

- ____ 1.1. RCL Verify Red Crew has donned Standard PPE
- ____ 1.2. RCM **SECURE** SCTEx ICU into STE fixture (and any additional Test Articles)
- ____ 1.3. IE **CONNECT** electrical power input to SCTEx ICU per Attachment 6.0
 ____ Heater Patch ____ ICU PC/104



- ____ 1.4. IE **CONNECT** ground station I/O data lines to SCTEX ICU per Attachment 6.0
- ____ 1.5. IE **CONNECT** all voltage and current monitoring lines per Attachment 6.0
- ____ 1.6. IE **AFFIX** all thermocouples per Attachment 3.0
- ____ 1.7. IE **START** ICU PC/104 DAQ data recording, verify nominal readings

____ 1.8. IE **START** Thermocouple / Electrical Power DAQ data recording, verify nominal readings

____ 1.9. RCM **CLOSE TVAC** access door

NOTE: Securing of the TVAC door commences with the next step – ensure that the fasteners are not over-torqued, as damage can result (“snugging” them is acceptable)

____ 1.10. RCM **SECURE** TVAC access door with the threaded-rod clamps

2.0 **TVAC SETUP**

NOTE: The following step (Step 2.1) verifies the current and nominal state of the TVAC facility (i.e., it should not reconfigure the facility). If a valve is found out of this nominal position, contact TVAC support personnel for assistance prior to proceeding.

____ 2.1. RCM **VERIFY / CONFIGURE** the following facility valves:

OPEN	CLOSED
__ FCV-100*	__ HV-107
__ FCV-101*	__ HV-108
__ FCV-102*	__ FCV-109
__ HV-114	__ HV-113
__ HV-121	__ HV-115
__ HV-103	__ HV-116
__ HV-105	__ HV-117
__ HV-110	__ HV-118
	__ HV-119
	__ HV-120

NOTE: Valves marked above with an asterisk (*) are open unless heating/cooling operations are invoked.

NOTE: Completion of the next three steps is only required if heating/cooling operations are to be accomplished during this test.

- ____ **2.2.** RCM **OPEN** HV-115 (Fluoroinert Tank Ullage Pressure Iso).
- ____ **2.3.** RCM Verify and record 20-35 psig on PI-111: _____ psig (Fluoroinert Tank Ullage Pressure).
- ____ **2.4.** RCM If necessary, **ADJUST** PCV-111 to read 30-35 psig on PI-111
- ____ **2.5.** RCM **SLIGHTLY OPEN** Facility Soft Water Hand-Valve (HV-12)
- ____ **2.6.** RCM **CONNECT** LN2 flex hose to dewar and configure hand-valves and regulators per manufacturer specification.
- ____ **2.7.** RCM Verify / **OPEN** HV-150 (GN2 Scanning Electron Microscope Purge Iso)
- ____ **2.8.** RCM Verify / **OPEN** HV-151 (GN2 Supply Tank to Fluorocarbon Tank Iso)
- ____ **2.9.** RCM **TURN ON** PI-152 and verify 80 +/- 10 psig: _____ psig
- ____ **2.10.** RCL Sign and Return to TC upon completion of Attachment.

RCL Signature _____

END OF ATTACHMENT 2

ATTACHMENT 3.0 EXTERNAL THERMOCOUPLE PLACEMENT

1.0

EXTERNAL THERMOCOUPLE PLACEMENT

1.1.

RCL

POSITION thermocouples in the following locations:

Thermocouple Placement

Channel 1: Control, on the Platen

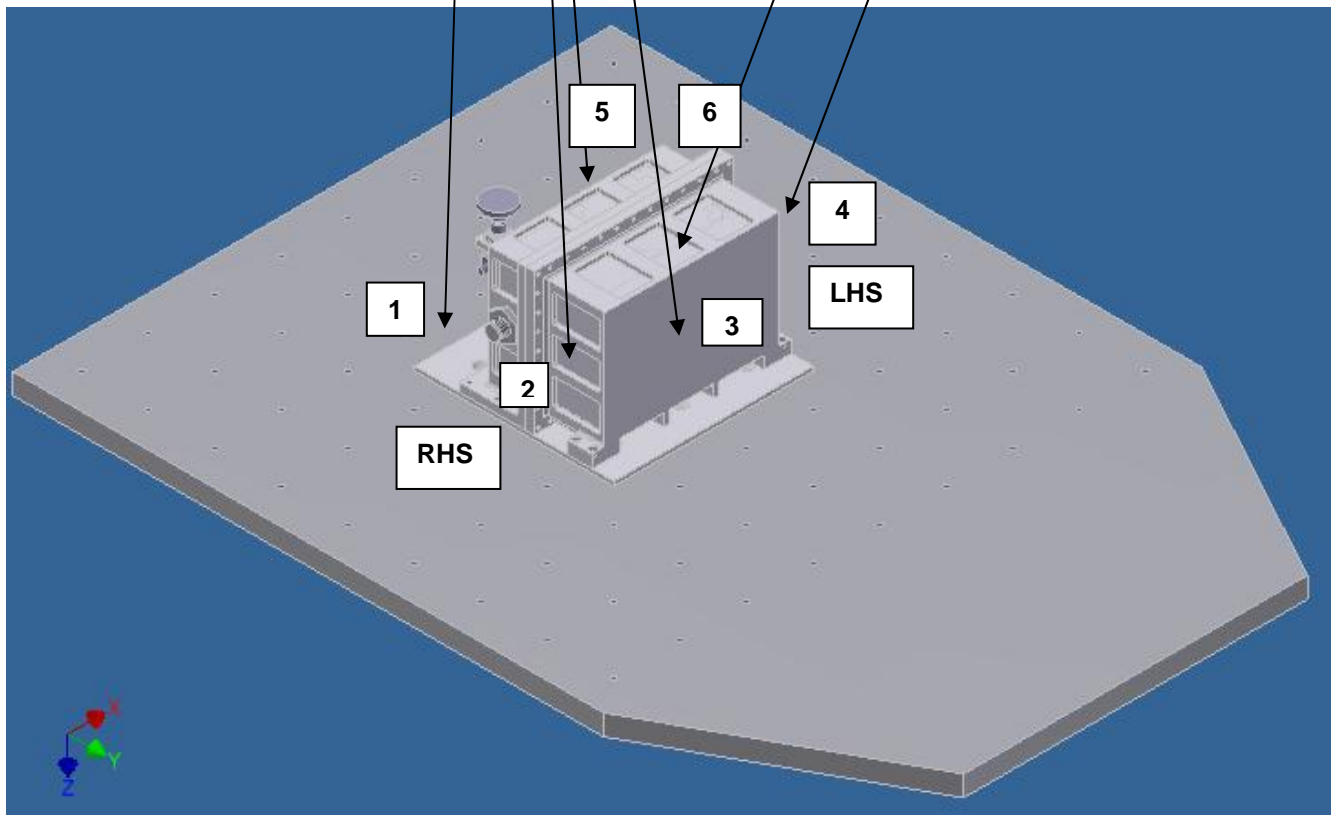
Channel 2: Measurement, Place on SCTEX-0002, RHS (middle) portion of ass'y

Channel 3: Measurement, Place on SCTEX-0002, Front portion of ass'y

Channel 4: Measurement, Place on SCTEX-0001, LHS (middle) portion of ass'y

Channel 5: Measurement, Place on SCTEX-0001, Rear portion of ass'y

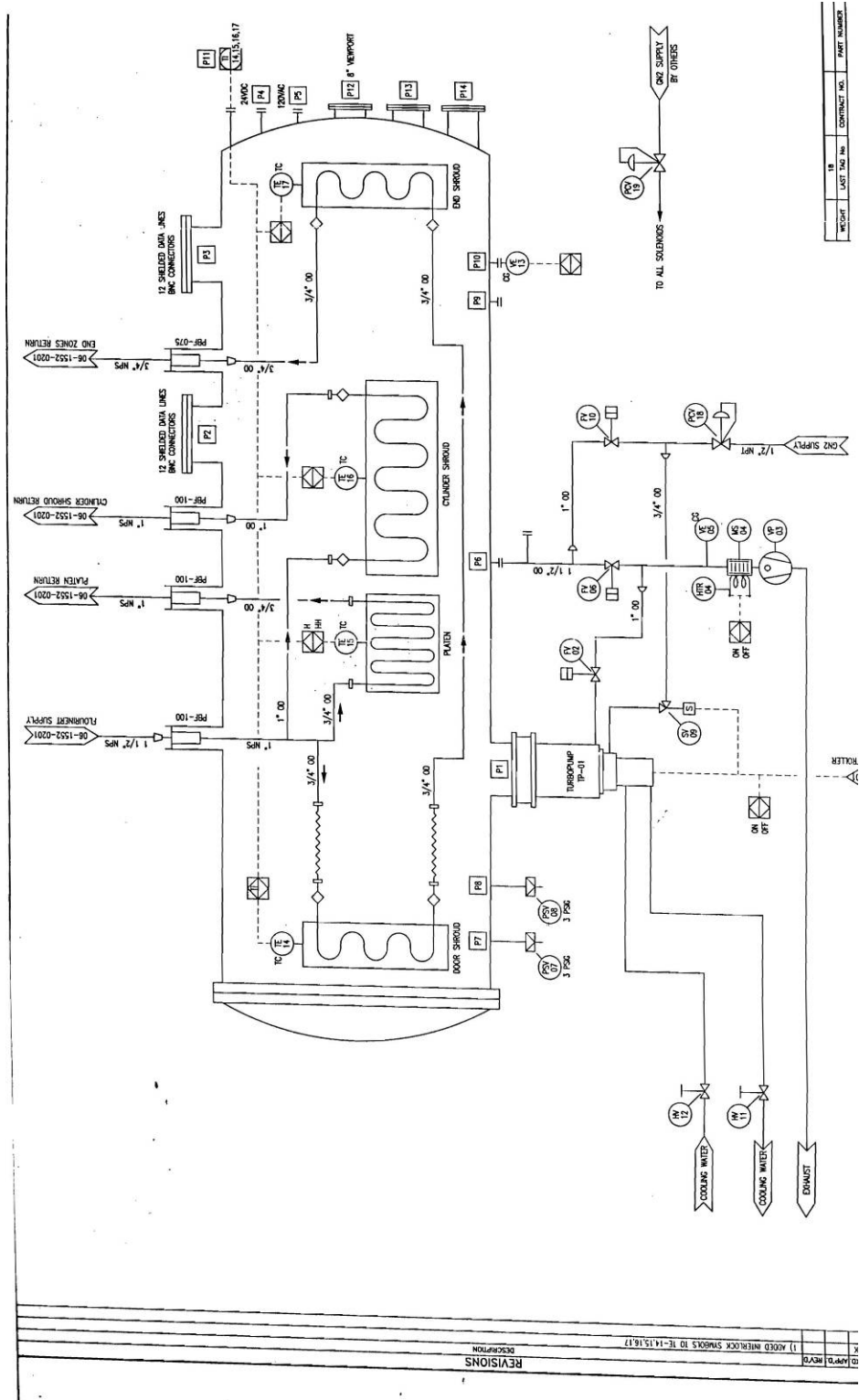
Channel 6: Measurement, Place on SCTEX-0002, Upper portion of ass'y



**ATTACHMENT 4.0
MULTIPURPOSE TEST LOG**

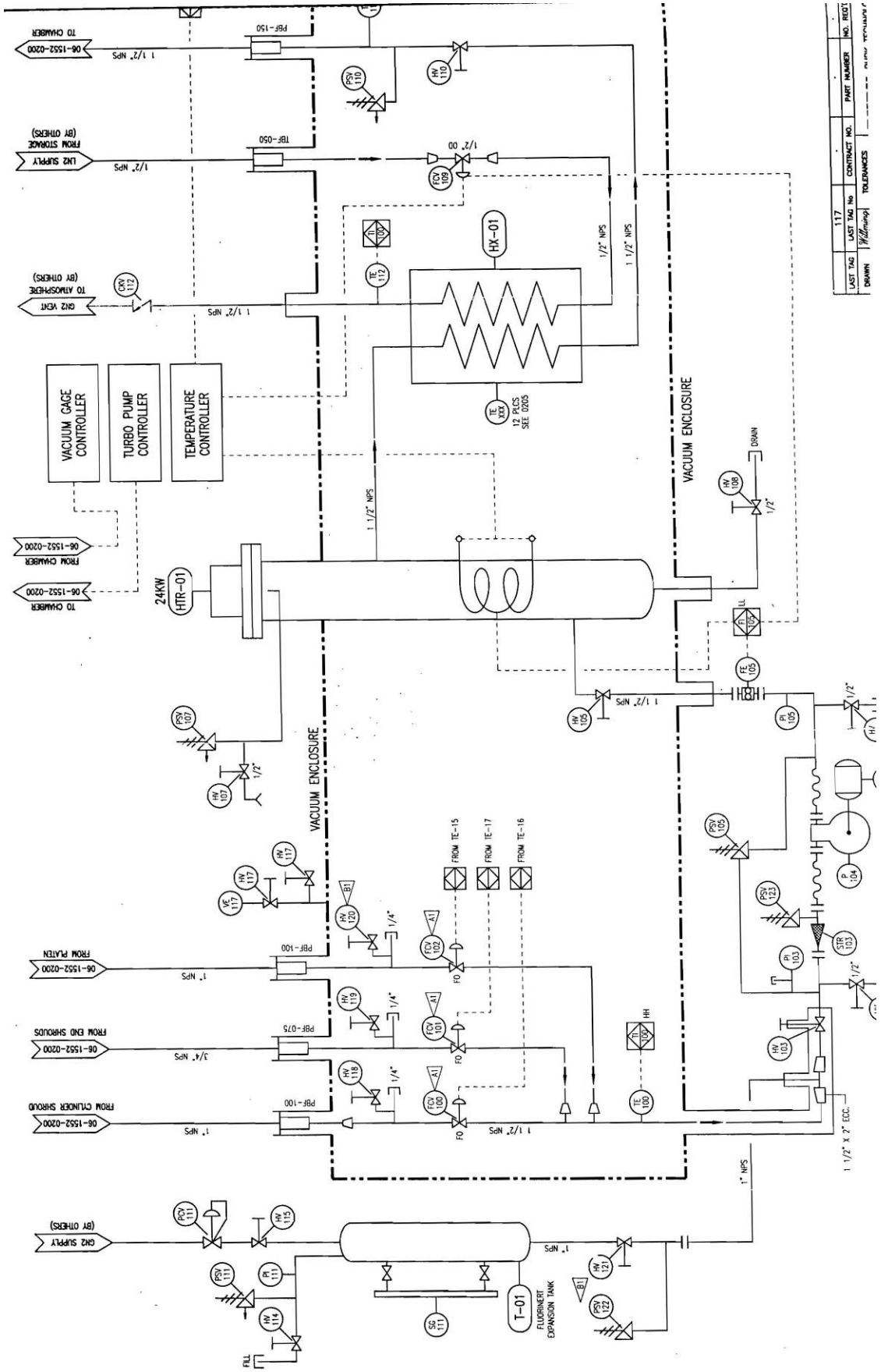
Itm	TIME	EVENT / STATUS	FILENAME
<i>(#)</i>	<i>(HHMM)</i>	<i>(Desc.)</i>	<i>(SxMMDDr1)</i>
1			
2			
3			
4			
5			
6			
7			
8			
9			
10			
11			
12			
13			
14			
15			
16			
17			
18			
19			
20			
21			
22			
23			
24			
25			
26			
27			

ATTACHMENT 5.0 Facility Drawings



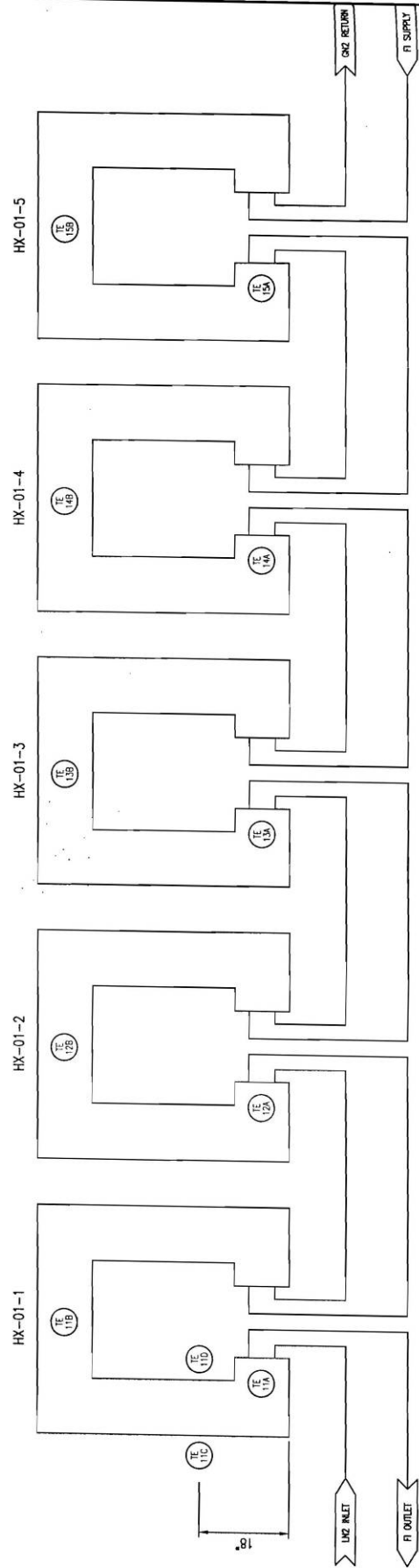
REV	DATE	BY	CHKD	DESCRIPTION
18				CONTRACT NO. PART NUMBER

NO.	DATE	BY	DESCRIPTION
1	11-15-12		1) ADDED INTERLOCK SYMBOLS TO 1E-14, 15, 16, 17



LAST TAG	117	CONTRACT NO.		PART NUMBER	NO. REV.
DRAWN		TOLERANCES			

1) CHANGED HCV-100, 102 & 102 TO REMOVE FLOW CONTROL VALVES
 2) ADDED HW118, 119, 120, 121, & PSY122, 123
 M4 01 1107/6/5



LAST TAG	LAST TAG No	CONTRACT NO.	PART NUMBER	NO. RECD	NEXT
	116				

ATTACHMENT 6.0 SCTEx ICU Wiring Diagram

Figure 1: ICU Internal Wiring Flow Diagram

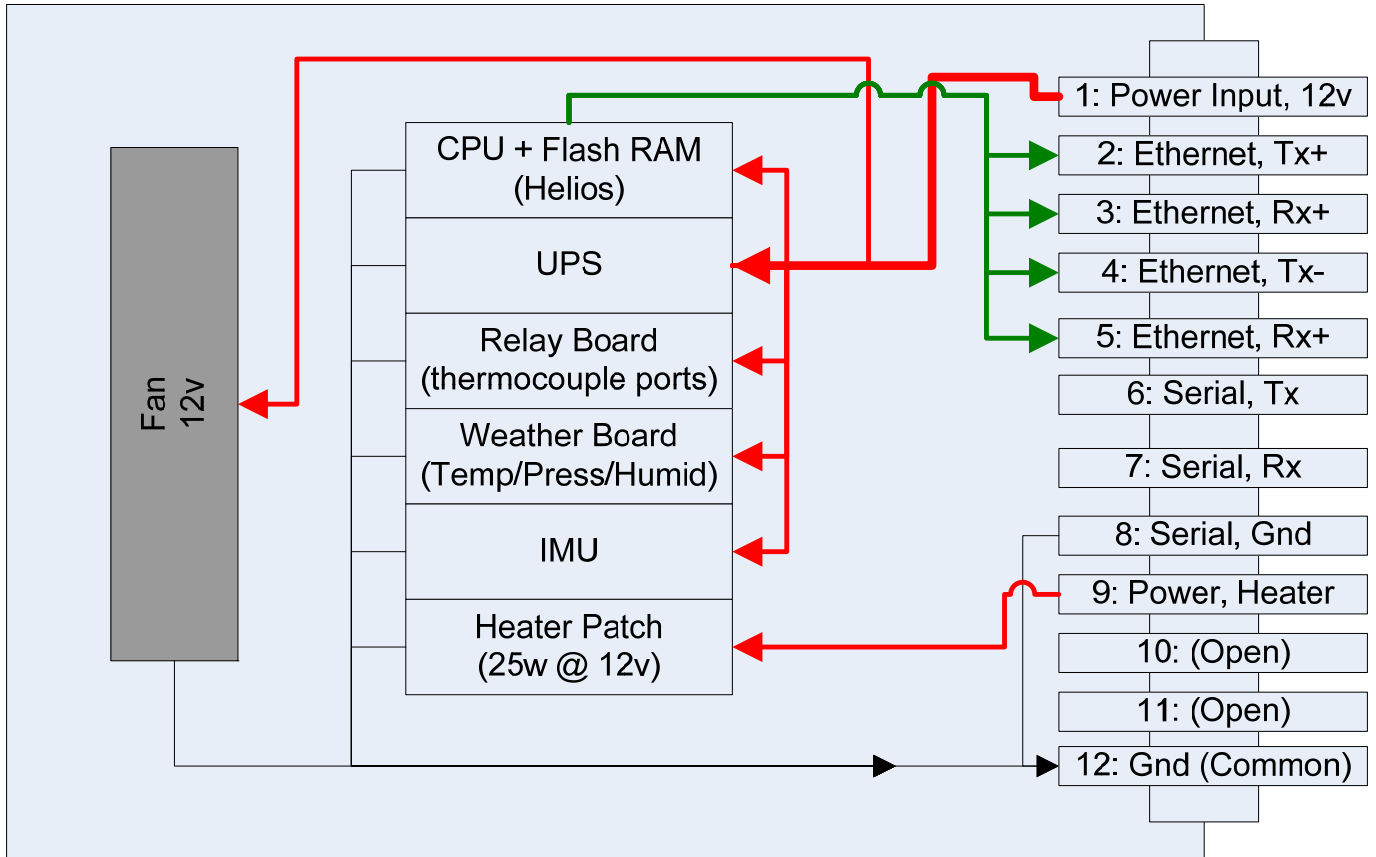
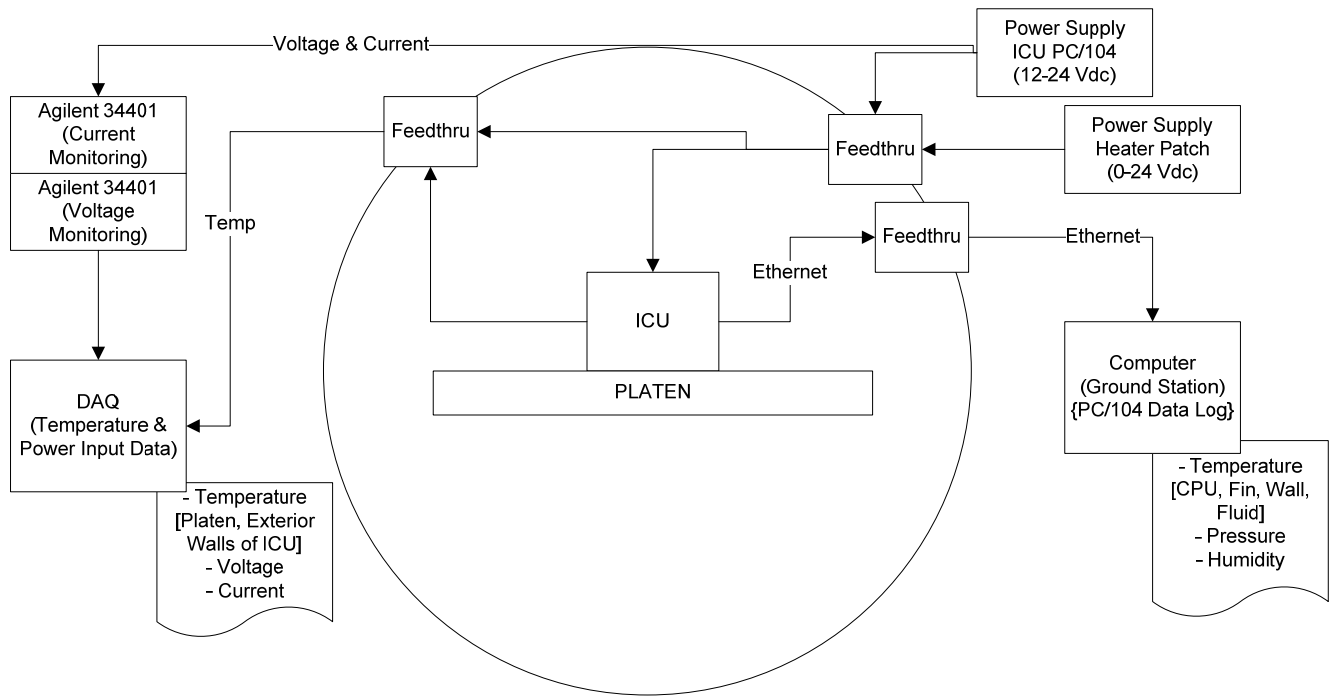


Figure 2: TVAC Internal / External Wiring Diagram



Bibliography

- [1] Fabrizio Vagni, "Survey of Hyperspectral and Multispectral Imaging Technologies," North Atlantic Treaty Organization, TR-SET-065-P3, May 2007.

- [2] Department of Defense, *Multispectral Users Guide.*, August, 1995.

- [3] Britannica Online Encyclopedia. (2011, April) Spectroscopy. [Online].
<http://www.britannica.com/EBchecked/topic/558901/spectroscopy?sections=558901TOC>

- [4] William J. Starr, *ANALYSIS OF SLEWING AND ATTITUDE DETERMINATION REQUIREMENTS FOR CTE_x*. Wright-Patterson AFB: Air Force Institute of Technology, 2010, Master's Thesis.

- [5] N. M. Short. (2010, December) The Remote Sensing Tutorial. [Online].
<http://rst.gsfc.nasa.gov/Front/overview.html>

- [6] Daniel O'Dell, *DEVELOPMENT AND DEMONSTRATION OF A FIELD-DEPLOYABLE FAST CHROMOTOMOGRAPHIC IMAGER*. Wright-Patterson AFB: Air Force Institute of Technology, 2010, Master's Thesis.

- [7] Opto-Knowledge Systems Inc. (2010, December) Why Spectral Imaging? [Online]. http://www.techexpo.com/WWW/opto-knowledge/why_spectral.html

- [8] Global Security. (2010, December) Hyperspectral Imaging. [Online].
<http://www.globalsecurity.org/intell/library/imint/hyper.htm>

- [9] Richard Cobb and Jonathan Black, "Space Chromotomography Experiment (CTEx)," in *2009 DOD Space Experiments Review Board Brief*, September 2009.

- [10] Glen P. Perram, and Ronald F. Tuttle Randall L. Bostick, "Instrumental Systematic Errors in a Chromotomographic Hyperspectral Imaging System," in *Aerospace Conference, 2010 IEEE* , Wright-Patterson AFB, 2010, pp. 1-15.

- [11] RANDALL L. BOSTICK and GLEN P. PERRAM, "HYPER SPECTRAL IMAGING USING CHROMOTOMOGRAPHY: A FIELDABLE VISIBLE INSTRUMENT FOR TRANSIENT EVENTS," in *International Journal of High Speed Electronics and Systems*, vol. 18, No. 3, Wright-Patterson AFB, 2008, pp. 519-529.
- [12] Glen P. Perram, Ronald Tuttle Randall L. Bostick, "Characterization of spatial and spectral resolution of a rotating prism chromotomographic hyperspectral imager," in *Next-Generation Spectroscopic Technologies II, SPIE*, vol. 7319, Wright-Patterson AFB, 2009, pp. 731903-1 - 731903-13.
- [13] Todd A. Book, *DESIGN ANALYSIS OF A SPACE BASED CHROMOTOMOGRAPHIC HYPER SPECTRAL IMAGING EXPERIMENT*. Wright-Patterson AFB: Air Force Institute of Technology, 2010, Master's Thesis.
- [14] NASA. (2011, January) Japanese Experiment Module - Exposed Facility. [Online]. http://www.nasa.gov/images/content/393013main_JEM-EF2.jpg
- [15] Jay Pearlman, Lushalan Liao, and Peter Jarecke Mark Folkman, "EO-1/Hyperion hyperspectral imager design, development, characterization, and calibration," in *SPIE*, vol. 4151, 2001, pp. 40-51.
- [16] Jay S. Pearlman, Jeffrey A. Mendenhall, and Dennis Reuter Stephen G. Ungar, "Overview of the Earth Observing One (EO-1) Mission," in *IEEE*, vol. 41, No. 6, 2003, pp. 1149-1159.
- [17] SATNEWS.com. (2010, November) ATK. Ten Years Of Observation (Satellite). [Online]. <http://www.satnews.com/cgi-bin/story.cgi?number=1271859338>
- [18] NASA's Goddard Space Flight Center. (2010, Dec) Earth Observing 1. [Online]. <http://eo1.gsfc.nasa.gov/Technology/Hyperion.html>
- [19] NASA. (2010, December) EO-1 Firsts: Hyperion Science Validation. [Online]. <http://eo1.gsfc.nasa.gov/new/general/firsts/hyperion.html>
- [20] Pamela S. Barry, Carol C. Segal, John Shepanski, Debra Beiso, and Stephen L. Carman Jay S. Pearlman, "Hyperion, a Space-Based Imaging Spectrometer," in *IEEE TRANSACTIONS ON GEOSCIENCE AND REMOTE SENSING*, vol. 41,

No. 6, 2003, pp. 1160-1173.

- [21] Greg Glaros, Patrick Stadter, Cheryl Reed, and Eric Finnegan, Michael Hurley, Charlie Merk, Tom Kawecki, Chris Garner, and Paul Jaffe Jay Raymond, "A TACSAT UPDATE AND THE ORS/JWS STANDARDIZED BUS," in *3rd Responsive Space Conference*, Los Angeles, 2005.
- [22] AFRL. (2010, Dec) Tactical Satellite 3 Fact Sheet. [Online].
http://www.kirtland.af.mil/library/factsheets/factsheet_print.asp?fsID=12887&page=1
- [23] Thomas W. Cooley, Richard M. Nadile, James A. Gardner, Peter S. Armstrong, Abraham M. Payton, Thom M. Davis, Stanley D. Straight Ronald B. Lockwood, "Advanced responsive tactically-effective military imaging spectrometer (ARTEMIS) system overview and objectives," in *Imaging Spectrometry XII, SPIE*, vol. 6661, Kirtland AFB, 2007, pp. 666102-1 - 666102-6.
- [24] R. Lockwood, S. Biggar, N. Anderson, J. Czapla-Myers, S. Miller, T. Chrien, S. Schiller, J. Silny, M. Glennon and T. Cooley K. Thome, "PREFLIGHT AND VICARIOUS CALIBRATION OF ARTEMIS," in *Geoscience and Remote Sensing Symposium, 2008. IGARSS 2008. IEEE International*, vol. I, 2008, pp. I-249 - I-252.
- [25] USAF. (2010, December) Wright-Patterson AFB - Media Gallery. [Online].
<http://www.wpafb.af.mil/shared/media/ggallery/hires/AFG-100610-060.jpg>
- [26] T. Cooleya, R. Nadilea, J. Gardnera, P. Armstronga, T. Davisa, S. Straighta, T. Chrienb, E. Gussinb, and D. Makowskib R. Lockwooda, "ADVANCED RESPONSIVE TACTICALLY-EFFECTIVE MILITARY IMAGING SPECTROMETER (ARTEMIS) DEVELOPMENT AND ON-ORBIT FOCUS," in *Geoscience and Remote Sensing Symposium, 2008. IGARSS 2008. IEEE International*, vol. 4, 2008, pp. IV-251 - IV254.
- [27] Daniel R. Korwan, Robert L. Lucke, William A. Snyder, Curtiss O. Davis Michael R. Corson, "THE HYPERSPECTRAL IMAGER FOR THE COASTAL OCEAN (HICO) ON THE INTERNATIONAL SPACE STATION," in *IEEE International*, vol. 4, 2008, pp. IV-101 - IV-104.

- [28] Michael R. Corson and Curtiss O. Davis. (2010, Dec) HICO Science Mission Overview. [Online]. <http://www.ioccg.org/sensors/HICO-IOCCG13.pdf>
- [29] R. Gould, R. Arnone, P. Lyon, P. Martinolich, R. Vaughan, A. Lawson, T. Scardino, W. Hou, W. Snyder, R. Lucke, M. Corson, M. Montes, C. Davis M. Lewis, "The Hyperspectral Imager for the Coastal Ocean (HICO): Sensor and Data Processing Overview," in *NRL SSC HICO Article for Oceans 09 Conference*, 2009, pp. 1-9.
- [30] Naval Research Laboratory. (2010, December) RAIDS - Remote Atmospheric and Ionospheric Detection System. [Online]. <http://www.nrl.navy.mil/tira/Projects/raids/>
- [31] Herbert J. Kramer. (2002) ISS Utilization: JEM/Kibo-EF (Exposed Facility) experiments of USA. [Online]. <https://directory.eoportal.org/presentations/330/10001432.html>
- [32] Jonathan M. Mooney, "Angularly Multiplexed Spectral Imager," in *SPIE*, vol. 2480, 1994, pp. 65-77.
- [33] Toby D. Reeves, Jonathan M. Mooney, William S. Ewing, Freeman D. Shepherd, Andrzej Brodzik James E. Murguia, "A Compact Visible/Near Infrared Hyperspectral Imager," in *SPIE*, vol. 4028, 2000, pp. 457-468.
- [34] Jonathan M. Mooney, "Spectral Imaging Via Computed Tomography," in *IRIS Passive Sensors*, vol. 1, Hanscom AFB, 1994, pp. 203-215.
- [35] Samuel Mantravadi, "Spatial and Spectral Resolution Limits of Hyperspectral Imagers Using Computed Tomography: A Comparison," in *Aerospace Conference, 2007 IEEE*, Wright-Patterson AFB, 2007.
- [36] Anthony J. Dearing, *SIMULATING A CHROMOTOMOGRAPHIC SENSOR FOR HYPERSPECTRAL IMAGING IN THE INFRARED*. Wright-Patterson AFB: Air Force Institute of Technology, 2004, Master's Thesis.
- [37] Kevin C. Gustke, *RECONSTRUCTION ALGORITHM CHARACTERIZATION AND PERFORMANCE MONITORING IN LIMITED-ANGLE CHROMOTOMOGRAPHY*. Wright-Patterson AFB: Air Force Institute of

Technology, 2004, Master's Thesis.

- [38] Daniel A. LeMaster, *DESIGN AND MODEL VERIFICATION OF AN INFRARED CHROMOTOMOGRAPHIC IMAGING SYSTEM*. Wright-Patterson AFB: Air Force Institute of Technology, 2004, Master's Thesis.
- [39] Malcolm G. Gould, *RECONSTRUCTION OF CHROMOTOMOGRAPHIC IMAGING SYSTEM INFRARED HYPERSPECTRAL SCENES*. Wright-Patterson AFB: Air Force Institute of Technology, 2005, Master's Thesis.
- [40] Phillip Sheirich, *An Engineering Trade Space Analysis for a Space-Based Hyperspectral Chromotomographic Scanner*. Wright-Patterson AFB: Air Force Institute of Technology, 2009, Master's Thesis.
- [41] Steven D. Miller, *INVESTIGATION OF A NOVEL COMPACT VIBRATION ISOLATION SYSTEM FOR SPACE APPLICATIONS*. Wright-Patterson AFB: Air Force Institute of Technology, 2010, Master's Thesis.
- [42] Arthur L. Morse, *PRELIMINARY ELECTRICAL DESIGNS FOR CTEX AND AFIT SATELLITE GROUND STATION*. Wright-Patterson AFB: Air Force Institute of Technology, 2010, Master's Thesis.
- [43] Johnson Space Center, "International Space Station," NASA, Johnson Space Center, Fact Sheet FS-2009-01-002-JSC, 2009.
- [44] Julie A. Robinson, "ISS External Accommodations & Manifest Opportunities," NASA, Briefing 2010.
- [45] Parker Hannifiin Corporation, "Parker O-Ring Handbook," Cleveland, Data Sheet ORD 5700, 2007.
- [46] RC Optical Systems, "AFIT CTS Platform Update," Teleconference between AFIT and RC Optical Systems with associated slides. December 2009.
- [47] TiNi Aerospace, Inc, "EJECTOR RELEASE MECHANISM SELECTION GUIDE," San Leandro, Data Sheet 2010.

- [48] McDonnell Douglas Astronautics Company, *Isogrid Design Handbook*. Huntington Beach, CA: NASA - Marshall Space Flight Center, February 1973. [Online]. http://femci.gsfc.nasa.gov/Isogrid/NASA-CR-124075_Isogrid_Design.pdf
- [49] idigitalphoto.com. (2010, November) flange focal distance. [Online]. http://www.idigitalphoto.com/dictionary/flange_focal_distance
- [50] Markerink. (2010, November) Camera mounts & registers. [Online]. <http://www.markerink.org/WJM/HTML/mounts.htm>
- [51] Quickset International. (2010, December) Hercules Tripod Specifications. [Online]. <http://www.quickset.com/products-technologies/durable-tripods/hercules/>
- [52] Applied Image Inc. (2010, December) USAF 1951 Resolution Test Chart| Mil-Std-150A| Improved Layout| T-22. [Online]. http://www.aig-imaging.com/mm5/merchant.mvc?Screen=PROD&Store_Code=AIPI&Product_Code=T-22&Category_Code=
- [53] Eugene Hecht, *Optics*, 4th ed., Adam Black, Ed. San Francisco, United States of America: Pearson Education, Inc., 2002.
- [54] Vision Research. (2007, October) Phantom v5.1. [Online]. http://www.visionresearch.com/uploads/docs/Discontinued/V5/DS_v51.pdf
- [55] MathWorks. (2010, December) Examples and Webinars - Identifying Round Objects. [Online]. <http://www.mathworks.com/products/image/demos.html?file=/products/demos/shipping/images/ipexroundness.html>
- [56] Izhak Bucher. (2010, December) MATLAB Central - try_circ_fit.m. [Online]. http://www.mathworks.com/matlabcentral/fileexchange/5557-circle-fit/content/try_circ_fit.m
- [57] Ohad Gal. (2003, March) MATLAB Central - fit_ellipse.m. [Online]. <http://www.mathworks.com/matlabcentral/fileexchange/3215>

- [58] Frank P. Incropera and David P. DeWitt, *Fundamentals of Heat and Mass Transfer*, 4th ed. New York, United States: John Wiley and Sons, 1996.
- [59] Wiley J. Larson and James R. Wertz, Ed., *Space Mission Analysis and Design III*, Third Edition ed. El Segundo, CA: Microcosm Press, 2005.
- [60] Parvus Corporation. (2010, August) Shock Rocks. [Online].
<http://www.parvus.com/product/overview.aspx?prod=ShockRocks>
- [61] Orion Fans, "OD1238 - 'VA Series'," Knight Electronics, Inc., Dallas, Data Sheet 2010.
- [62] PAVE Technology Co., "PAVE-Seal (R) Cable Harnesses," Dayton, Data Sheet PN 1649, 2010.
- [63] Swagelok Company, "Bellows-Sealed Valves," Data Sheet MS-01-22, 2008.
- [64] Castrol, "Castrol Braycote® 600EF," Naperville, Data Sheet 04.11.2008, Version Number 3.0, 2008.
- [65] Japan Aerospace Exploration Agency, "HTV Cargo Standard Interface ," JAXA, Requirements Document NASDA-ESPC-2857 Rev.C, 2010.
- [66] Johnson Space Center, "Qualification and Acceptance Environmental Test Requirements," NASA, Houston, SSP 41172 Rev U, 28 March 2003.
- [67] Zhihua He. (2002, December) Draw a circle. [Online].
<http://www.mathworks.com/matlabcentral/fileexchange/2876-draw-a-circle>

Vita

Capt Jason D. Niederhauser graduated from Lapeer East High School, Lapeer Michigan in June of 1998. Later that fall, he entered undergraduate studies at Western Michigan University (WMU) in Kalamazoo, Michigan wherein he graduated in April, 2002 with a Bachelors of Science in Engineering (Mechanical). In his final year at WMU and through December, 2002, he worked as a cooperative-education mechanical engineer at the LECO Corporation, located in Saint Joseph, Michigan. In January, 2003 he entered the United States Air Force through attending Officer Training School at Maxwell AFB, Montgomery, Alabama and was commissioned a Second Lieutenant later that April. His first assignment was to the Propulsion Directorate, Air Force Research Laboratory, Edwards AFB, California where he was a test conductor performing small and large-scale liquid rocket engine research and development test activities. In 2006, he was reassigned to the 1st Air and Space Test Squadron, 30th Space Wing, Vandenberg AFB, California where he was a Launch Mission Manager and Flight Commander for Minotaur launch vehicle system bed-down and operations. In 2009, Capt Niederhauser was selected by the Vigilant Scholar program through Air Force Space Command to attend the Air Force Institute of Technology (AFIT) at Wright Patterson AFB, Ohio, culminating in a Master's of Science in Astronautical Engineering.

After graduation from AFIT in June, 2011, Capt Niederhauser will be reassigned to the Air Force Tactical Exploitation of National Capabilities (TENCAP), Space Innovation and Development Center, Schriever AFB, Colorado.

REPORT DOCUMENTATION PAGE			<i>Form Approved</i> <i>OMB No. 0704-0188</i>	
The public reporting burden for this collection of information is estimated to average 1 hour per response, including the time for reviewing instructions, searching existing data sources, gathering and maintaining the data needed, and completing and reviewing the collection of information. Send comments regarding this burden estimate or any other aspect of this collection of information, including suggestions for reducing this burden to Department of Defense, Washington Headquarters Services, Directorate for Information Operations and Reports (0704-0188), 1215 Jefferson Davis Highway, Suite 1204, Arlington, VA 22202-4302. Respondents should be aware that notwithstanding any other provision of law, no person shall be subject to any penalty for failing to comply with a collection of information if it does not display a currently valid OMB control number. PLEASE DO NOT RETURN YOUR FORM TO THE ABOVE ADDRESS.				
1. REPORT DATE (DD-MM-YYYY) 16-06-2011		2. REPORT TYPE Master's Thesis	3. DATES COVERED (From — To) Aug 2009 – Jun 2011	
4. TITLE AND SUBTITLE Design and Characterization of a Space Based Chromotomographic Hyperspectral Imaging Experiment			5a. CONTRACT NUMBER	
			5b. GRANT NUMBER	
			5c. PROGRAM ELEMENT NUMBER	
6. AUTHOR(S) Niederhauser, Jason D., Capt, USAF			5d. PROJECT NUMBER	
			5e. TASK NUMBER	
			5f. WORK UNIT NUMBER	
7. PERFORMING ORGANIZATION NAME(S) AND ADDRESS(ES) Air Force Institute of Technology Graduate School of Engineering and Management (AFIT/ENY) 2950 Hobson Way WPAFB OH 45433-7765			8. PERFORMING ORGANIZATION REPORT NUMBER AFIT/GA/ENY/11-J02	
9. SPONSORING / MONITORING AGENCY NAME(S) AND ADDRESS(ES) Undisclosed Sponsor			10. SPONSOR/MONITOR'S ACRONYM(S) Undisclosed Sponsor	
			11. SPONSOR/MONITOR'S REPORT NUMBER(S) Undisclosed Sponsor	
12. DISTRIBUTION / AVAILABILITY STATEMENT DISTRIBUTION STATEMENT A. UNLIMITED DISTRIBUTION				
13. SUPPLEMENTARY NOTES This material is declared a work of the U.S. Government and is not subject to copyright protection in the United States.				
14. ABSTRACT (U) This research focuses upon the design, analysis and characterization of several systems related to a space-based chromotomographic experiment (CTEx), a hyperspectral imager, currently in development at the Air Force Institute of Technology. Three interrelated subject-areas were developed. The initial focal point was a generic, system-level mechanical layout and integration analysis of the space-based instrument. The scope of this work was intended to baseline the space-based system design in order to allow for further trade-space refinement and requirements development. Second, development of an iteration upon the ground-based version of CTEx was accomplished in an effort to support higher-fidelity field data-collection. This effort encompassed both the engineering design process as well as a system-level characterization test series to validate the enhancements to deviation angle, image quality, and alignment characterization methodologies. Finally, the third effort in this thesis related to the design, analysis, and characterization test campaign encompassing the space-based CTEx instrument computer unit (ICU). This activity produced an experimentally validated thermal mathematical model supporting further trade-space refinement and operational planning aspects for this device. Results from all three of the above focus areas support the transition of this next-generation technology from the laboratory to a fully-realized, space-readied platform achieving intelligence preparation of the battlespace for the warfighter.				
15. SUBJECT TERMS Hyperspectral, Chromotomography, CTEx				
16. SECURITY CLASSIFICATION OF:		17. LIMITATION OF ABSTRACT UU	18. NUMBER OF PAGES 384	19a. NAME OF RESPONSIBLE PERSON Dr. Jonathan T. Black
a. REPORT U	b. ABSTRACT U			c. THIS PAGE U

Standard Form 298 (Rev. 8-98)
Prescribed by ANSI Std. Z39.18